

AN ABSTRACT OF THE DISSERTATION OF

Corey Brumsted for the degree of Doctor of Philosophy in Chemistry presented on November 14, 2017.

Title: Pactamycin Inspired Drug Discovery: A Synthetic and Chemoenzymatic Approach

Abstract approved: _____

Taifo Mahmud

Pactamycin, first reported in 1962, is a potent antitumor antibiotic produced by the soil bacterium *Streptomyces pactum*. Structurally, it contains a cyclopentitol core unit, a 3-aminoacetophenone (3AAP), a 6-methylsalicylic acid (6-MSA), and a *N,N*-dimethyl urea. The aminocyclopentitol ring is derived from glucose, possibly via *N*-acetyl glucosamine (GlcNAc), the 3-aminoacetophenone (3AAP) moiety is derived from 3-aminobenzoic acid (3ABA), and the 6-MSA moiety is produced from acetate by an iterative type I polyketide synthase. Despite some knowledge of its biosynthetic origin, details of the mode of formation of this unique natural product are still elusive.

Using genetic, chemical complementation, and biochemical studies we demonstrate that 3ABA is processed by a set of discrete polyketide synthase proteins, i.e. an AMP-forming acyl-CoA synthetase (PtmS), an acyl carrier protein (ACP) (PtmI), and a β -ketoacyl-ACP synthase (PtmK), to give 3-[3-aminophenyl]3-oxopropionyl-ACP, which is then glycosylated by a broad spectrum *N*-glycosyltransferase, PtmJ (Chapter 2). This is

the first example of glycosylation of an ACP-bound polyketide intermediate in natural product biosynthesis. Additionally, we demonstrate that PtmO is a hydrolase that is responsible for the release of the glycosylated β -ketoacid product from the ACP, and the free β -ketoacid product subsequently undergoes non-enzymatic decarboxylation.

In addition to the β -ketoacyl-ACP synthase gene *ptmK*, the pactamycin biosynthetic gene cluster also contains a gene (*ptmR*) that encodes a β -ketoacyl-acyl carrier protein (β -ketoacyl-ACP) synthase (KAS) III. KAS III catalyzes the first step in fatty acid biosynthesis, involving a Claisen condensation of the acetyl-CoA starter unit with the first extender unit, malonyl-ACP, to form acetoacetyl-ACP. KAS III-like proteins have also been reported to catalyze acyltransferase reactions using coenzyme A esters or discrete ACP-bound substrates. Through in vivo and in vitro characterizations of the KAS III-like protein PtmR, we discovered that this enzyme directly transfers a 6-methylsalicylyl moiety from an iterative type I polyketide synthase (PtmQ) to the aminocyclopentitol unit in pactamycin biosynthesis (Chapter 3). PtmR is highly promiscuous, recognizing a wide array of *S*-acyl-*N*-acetylcysteamines as substrates to produce a suite of pactamycin derivatives with diverse alkyl and aromatic features. The results suggest that KAS III-like proteins may be used as versatile tools for modifications of complex natural products for drug discovery.

The pronounced biological activity displayed by pactamycin spans across all three phylogenetic domains. Unfortunately the indiscriminate cytotoxicity of pactamycin towards mammalian cells has suppressed its development toward therapeutic appli-

cation. Nevertheless, we believe pactamycin is a wellspring of promising biological activity that is waiting to be harnessed. Our previous work demonstrated, through biosynthetic manipulations, production of new pactamycin analogs with pronounced antimalarial activity, lacking significant antibacterial activity, and are about 10–30 times less toxic than pactamycin toward mammalian cells. Furthermore, we have developed a chemoenzymatic process using the promiscuous KAS III-like protein PtmR to produce new pactamycin analogs.

Continuing our efforts to draw further on the bountiful activity of the aminocyclitol core of pactamycin, we have taken a third approach by synthesizing the core aminocyclopentitol ring which could open up a diverse library of biologically active compounds. In Chapter 4, we describe an efficient, modular, and asymmetric synthesis of several aminocyclopentitol compounds resembling the pactamycin pharmacophore believed responsible for its biological activity. The outlined synthesis work has generated four promising biologically active compounds, two of which display modest activity against Gram-positive bacteria, whereas the other two compounds exhibit potent anticancer activity against A375 melanoma cells.

©Copyright by Corey Brumsted
November 14, 2017
All Rights Reserved

Pactamycin Inspired Drug Discovery: A Synthetic and Chemoenzymatic Approach

by
Corey Brumsted

A DISSERTATION

submitted to

Oregon State University

in partial fulfillment of
the requirements for the
degree of

Doctor of Philosophy

Presented November 14, 2017
Commencement June, 2018

Doctor of Philosophy dissertation of Corey Brumsted presented on November 14, 2017

APPROVED:

Major Professor, representing Chemistry

Chair of the Department of Chemistry

Dean of the Graduate School

I understand that my dissertation will become part of the permanent collection of Oregon State University libraries. My signature below authorizes release of my dissertation to any reader upon request.

Corey Brumsted, Author

ACKNOWLEDGEMENTS

I would like to express my sincerest gratitude to my grandmother, Rachael, for her love, inspiration and for her unwavering encouragement throughout my studies. Our conversations and friendship have been the foundation for my success. I want to thank my mother, for nurturing my education early-on and helping to set me on this path, and later for her encouragement to pursue my goals. I would like to thank my grandmother, Carolyn, who has been a continued source of love and support. I want to thank my Dad and my siblings and the rest of my family for their emotional sustenance. I want to thank Mani Mahjouri for the unrelenting inspiration.

I want to thank my advisor, Professor Taifo Mahmud, for giving me opportunity and guidance to pursue ideas. I am grateful for his unwavering support. He has provided guidance in my scientific research and taught me the value of collaboration in science.

I want to thank my friend and colleague, Adam Barsamian, for the endless miles of invaluable and insightful conversations that carried me through my research and the program. I would also like to thank Andrew Osborne and Edward Fynn for their friendship and support. I also want to thank the chemistry and pharmacy students for their friendship over the years.

Lastly, I would like to thank my committee for their guidance, encouragement and support. I am also grateful to the school of pharmacy and the chemistry department for financial support and the opportunity to work with and learn from exceptional instructors and faculty.

CONTRIBUTION OF AUTHORS

Chapter 2. Akane Hirayama (Kudo and Eguchi Lab) and Mostafa Abugrain (Mahmud lab) performed the genetic and biochemical experiments. Professors Kudo and Eguchi assisted in the preparation of the manuscript.

Chapter 3. Andrew Osborn (Mahmud Lab) performed the phylogenetic analysis (figure S19) and assisted in the purification of TM-025. Mostafa Abugrain performed the genetic and biochemical experiments. Professor Philmus assisted in the purification of PtmR and editing the manuscript.

Chapter 4. Evan Carpenter (Indra Lab) performed the anticancer assays.

TABLE OF CONTENTS

	<u>Page</u>
Chapter 1. Introduction	1
1.1 Natural Products.....	1
1.2 The Importance of Natural Products	2
1.3 Classes of Natural Products	5
1.3.1 Isoprenoids.....	5
1.3.2 Alkaloids.....	7
1.3.3 Ribosomal and Non-Ribosomal Peptides	7
1.3.4 Polyketides.....	9
1.3.5 Aminocyclitols.....	11
1.4 Pactamycin.....	12
1.4.1 Background.....	12
1.4.2 Total Syntheses of Pactamycin.....	15
1.4.3 Analogs of Pactamycin.....	17
1.4.4 Pactamycin biosynthesis.....	18
1.4.5 Research objectives.....	22
1.5 References.....	23
Chapter 2. Formation of 3-Aminoacetophenone Moiety and Evidence for Glycosylation of An Acyl Carrier Protein-bound Polyketide Intermediate in Pactamycin Biosynthesis.....	27
2.1 Introduction.....	28
2.2 Results.....	31
2.2.1 Involvement of the discrete PKS proteins in 3AAP formation.....	31
2.2.2 Synthesis and evaluation of N-acetylcysteamine thioesters of 3ABA and 3-[3-aminophenyl]3-oxopropionate.....	32
2.2.3 Isolation of GlcNAc-3AAP in culture broths of mutants incubated with 3AP-3OP-SNAC.....	35
2.2.4 Characterization of the hydrolase PtmO.	37
2.2.5 PtmJ is a promiscuous glycosyltransferase.....	38

TABLE OF CONTENTS (Continued)

	<u>Page</u>
2.2.6 The proposed timing of glycosylation in pactamycin biosynthesis.....	40
2.3 Discussion.....	41
2.4 Experimental.....	45
2.5 Supporting information.....	56
 Chapter 3. A Highly Promiscuous β -Ketoacyl-ACP Synthase (KAS) III-like Protein Is Involved in Pactamycin Biosynthesis.....	 74
3.1 Introduction.....	75
3.2 Results.....	77
3.3 Methods.....	84
3.3.1 Feeding Experiments with 6-MSA.....	86
3.3.2 Production of PtmR.....	86
3.3.3 Acyltransferase Assay.....	87
3.3.4 Scaled-up Enzymatic Reaction and Isolation of TM-107.....	87
3.4 Supporting information.....	91
 Chapter 4. Asymmetric Total Synthesis of a Pactamycin-Inspired Amino-cyclopentitol Utilizing a Sml ₂ Mediated Imino-Pinacol Coupling Strategy.....	 132
4.1 Introduction.....	133
4.2 Synthesis goals for this study.....	135
4.3 Retrosynthetic analysis.....	135
4.4 Imino pinacol coupling reactions with oxime ethers.....	136
4.5 Stereochemical analysis.....	137
4.6 Forward synthesis: 1 st Generation route.....	138
4.7 Byproduct formation and investigation towards an alternate route.....	142
4.8 Forward synthesis: 3 rd generation route and total synthesis of TM-118.....	145
4.8.1 Stereochemical rationalization of imino pinacol product.....	147
4.8.1 Endgame synthesis to TM-118.....	148
4.9 Biological activity.....	149
4.10 Supporting Information.....	152

TABLE OF CONTENTS (Continued)

	<u>Page</u>
Chapter 5. Conclusion.....	183
Bibliography.....	186
Chapter 1 References.....	187
Chapter 2 References.....	190
Chapter 3 References.....	191
Chapter 4 References.....	192
Appendix A. NMR Data Chapter 2.....	195
Appendix B. NMR Data Chapter 3.....	211
Appendix C. NMR Data Chapter 4.....	239

LIST OF FIGURES

<u>Figure</u>	<u>Page</u>
Figure 1.1. Examples of natural products with functional roles in nature	2
Figure 1.2. Medicinally important natural products	5
Figure 1.3. Notable terpenoid natural products and starter units IPP and DMAPP	6
Figure 1.4. Examples of some alkaloids of interest.....	7
Figure 1.5 A. Small molecule ribosomal peptides.....	8
Figure 1.5 B. Structures of some important natural products from NRPS	9
Figure 1.6. Examples of some important polyketides.....	11
Figure 1.7. Bioactive aminocyclopentitol (blue) units and clinically used drugs.....	12
Figure 1.8. Pactamycin and some biosynthetically derived bioactive analogs.....	13
Figure 1.9. Summary of the Hanessian synthesis of pactamycin	15
Figure 1.10. Summary of the Johnson synthesis of pactamycin.....	16
Figure 1.11. Early ¹³ C-labeling experiments detailing the biosynthetic origin of pactamycin.....	19
Figure 1.12. Pactamycin biosynthesis pathways.....	20
Figure 1.13. Radical SAM mediated carbocyclization of an aminosugar.....	21
Figure 2.1. Biosynthetic origin of pactamycin.....	28
Figure 2.2. Proposed pathways from 3ABA to 3AAP	29
Figure 2.3. Synthesis of ABA-SNAC and 3AP-OP-SNAC.....	33
Figure 2.4. Proposed Pathway to pactamycin.....	34

LIST OF FIGURES (Continued)

<u>Figure</u>	<u>Page</u>
Figure 2.5. Synthesis of [¹³ C]GlcNAc-[¹³ C]3ABA and feeding $\Delta ptmH/\Delta ptmT$	36
Figure 2.6. MS result of feeding [¹³ C]GlcNAc-[¹³ C]3ABA to $\Delta ptmH/\Delta ptmT$	37
Figure 3.1. Pactamycin and derivatives obtained from biosynthetic manipulations.....	76
Figure 3.2. HPLC analyses of PtmR reactions using de-6-MSA pactamycin.....	77
Figure 3.3. Proposed catalytic activity of PtmR.....	80
Figure 4.1. Bioactive aminocyclopentitol (blue) units in natural products and clinically used drugs.....	133
Figure 4.2. Biosynthetically modified pactamycin congeners.....	134
Figure 4.3. Retrosynthesis of TM-118.....	135
Figure 4.4. First reported keto aldoxime pinacol coupling.....	136
Figure 4.5. Imino pinacol coupling from carbohydrate precursors.....	136
Figure 4.6. Substrate configurations that are expected to effect diastereoselection.....	137
Figure 4.7. Synthesis scheme to aminocyclopentitols and deoxyaminocyclopentitols.....	139
Figure 4.8. Synthesis scheme towards aminocyclopentitols via oxazolidinone route.....	143
Figure 4.9. Summary of conditions and results for the oxazolidinone pinacol coupling	144
Figure 4.10. Total synthesis of aminocyclopentitol TM118.....	146
Figure 4.11: Key NOE correlations of the imino-pinacol products	147

LIST OF FIGURES (Continued)

<u>Figure</u>	<u>Page</u>
<p>Figure 4.12. Antibacterial testing of pactamycin analogs. Agar diffusion assay of pactamycin analogs against <i>P. aeruginosa</i> (A) and <i>S. aureus</i> (B). PCT = pactamycin; Amp = ampicillin; Apra = apramycin; DMSO; 10 μL of 10 mM each. Microdilution assay of TM-117 against <i>S. aureus</i> (C-G). (C) TM-117 (1 mM to 1 nM); (D) pactamycin (1 mM to 1 nM); (E) ampicillin (1 mM to 1 nM); (F) apramycin (1 mM to 1 nM); (G) DMSO; (H) cells.....</p>	150
<p>Figure 4.13. Antitumor activity of pactamycin analogs. Dose response curve (above) and structures of synthetic pactamycin analogs (below) screened against melanoma A375 cells.....</p>	151
<p>Figure 4.14. ^1H NMR data for TM-118 (D_2O).....</p>	178
<p>Figure 4.15. ^{13}C NMR of TM-118 (D_2O).....</p>	179

LIST OF TABLES

<u>Table</u>	<u>Page</u>
Table 3.1. Conversion of TM-025 to various pactamycin analogs.....	82
Table 3.2. ^1H NMR and ^{13}C NMR shifts for TM107.....	88

LIST OF APPENDIX A FIGURES

<u>Figure</u>	<u>Page</u>
Appendix Figure 6.1. ^1H NMR (CDCl_3) spectrum of 3ABA-SNAC.....	196
Appendix Figure 6.2. ^{13}C NMR (CDCl_3) spectrum of 3ABA-SNAC.....	197
Appendix Figure 6.3. ^1H NMR (CDCl_3) spectrum of 3AP-3OP-SNAC.....	198
Appendix Figure 6.4. ^{13}C NMR (CDCl_3) spectrum of 3AP-3OP-SNAC.....	199
Appendix Figure 6.5. ^1H NMR (CDCl_3) spectrum of BOC-3ABA-SNAC.....	200
Appendix Figure 6.6. ^{13}C NMR (CDCl_3) spectrum of BOC ABA-SNAC.....	201
Appendix Figure 6.7. ^1H NMR (CDCl_3) spectrum of Meldrum's adduct SI-2	202
Appendix Figure 6.8. ^{13}C NMR (CDCl_3) spectrum of Meldrum's adduct SI-2	203
Appendix Figure 6.9. ^{13}C NMR (MeOD) spectrum of Meldrum's adduct SI-2	204
Appendix Figure 6.10. ^1H NMR (CDCl_3) spectrum of BOC-3AP-3OP-SNAC.....	205
Appendix Figure 6.11. ^{13}C NMR (CDCl_3) spectrum of 3AP-3OP-SNAC.....	206
Appendix Figure 6.12. ^1H NMR (D_2O - MeOD) spectrum of [^{13}C]GlcNAc-[^{13}C]3ABA.....	207
Appendix Figure 6.13. ^{13}C NMR (D_2O - MeOD) spectrum of [^{13}C]GlcNAc-[^{13}C]3ABA.....	208
Appendix Figure 6.14. ^{13}C NMR (D_2O - MeOD) spectrum of [^{13}C]GlcNAc-[^{13}C]3ABA.....	209

LIST OF APPENDIX B FIGURES

<u>Figure</u>	<u>Page</u>
Appendix Figure 6.15. ^1H NMR (CDCl_3) spectrum of 6-MSA-SNAC.....	211
Appendix Figure 6.16. ^{13}C NMR (CDCl_3) spectrum of 6-MSA-SNAC.....	212
Appendix Figure 6.17. ^1H NMR (CDCl_3) spectrum of acetyl-SNAC.....	213
Appendix Figure 6.18. ^{13}C NMR (CDCl_3) spectrum of acetyl-SNAC.....	214
Appendix Figure 6.19. ^1H NMR (CDCl_3) spectrum of propionyl-SNAC.....	215
Appendix Figure 6.20. ^{13}C NMR (CDCl_3) spectrum of propionyl-SNAC.....	216
Appendix Figure 6.21. ^1H NMR (CDCl_3) spectrum of butyryl-SNAC.....	217
Appendix Figure 6.22. ^{13}C NMR (CDCl_3) spectrum of butyryl-SNAC.....	218
Appendix Figure 6.23. ^1H NMR (CDCl_3) spectrum of 4-chlorobutyryl-SNAC.....	219
Appendix Figure 6.24. ^{13}C NMR (CDCl_3) spectrum of 4-chlorobutyryl-SNAC.....	220
Appendix Figure 6.25. ^1H NMR (CDCl_3) spectrum of isobutyryl-SNAC.....	221
Appendix Figure 6.26. ^{13}C NMR (CDCl_3) spectrum of isobutyryl-SNAC.....	222
Appendix Figure 6.27. ^1H NMR (CDCl_3) spectrum of isovaleryl-SNAC.....	223
Appendix Figure 6.28. ^{13}C NMR (CDCl_3) spectrum of isovaleryl-SNAC.....	224
Appendix Figure 6.29. ^1H NMR (CDCl_3) spectrum of 2,4-dimethyl- 2-pentenoyl-SNAC.....	225
Appendix Figure 6.30. ^{13}C NMR (CDCl_3) spectrum of 2,4-dimethyl-2- pentenoyl-SNAC.....	226
Appendix Figure 6.31. ^1H NMR (CDCl_3) spectrum of 2-methylbutyryl-SNAC	227
Appendix Figure 6.32. ^{13}C NMR (CDCl_3) spectrum of 2-methylbutyryl-SNAC.....	228

LIST OF APPENDIX B FIGURES (Continued)

<u>Figure</u>	<u>Page</u>
Appendix Figure 6.33. ^1H NMR (CDCl_3) spectrum of benzoyl-SNAC.....	229
Appendix Figure 6.34. ^{13}C NMR (CDCl_3) spectrum of benzoyl-SNAC.....	230
Appendix Figure 6.35. ^1H NMR (CDCl_3) spectrum of 3-aminobenzoyl-SNAC.....	231
Appendix Figure 6.36. ^{13}C NMR (CDCl_3) spectrum of 3-aminobenzoyl-SNAC.....	232
Appendix Figure 6.37. ^1H NMR (CDCl_3) spectrum of phenylacetyl-SNAC.....	233
Appendix Figure 6.38. ^{13}C NMR (CDCl_3) spectrum of phenylacetyl-SNAC.....	234
Appendix Figure 6.39. ^1H NMR (CDCl_3) spectrum of cyclohexanecarbonyl-SNAC.....	235
Appendix Figure 6.40. ^{13}C NMR (CDCl_3) spectrum of cyclohexanecarbonyl-SNAC.....	236
Appendix Figure 6.41. ^1H NMR (CDCl_3) spectrum of cycloheptanecarbonyl-SNAC.....	237
Appendix Figure 6.42. ^{13}C NMR (CDCl_3) spectrum of cycloheptanecarbonyl-SNAC.....	238

LIST OF APPENDIX C FIGURES

<u>Figure</u>	<u>Page</u>
Appendix Figure 6.43: ^1H NMR (CDCl_3) spectrum of 4	240
Appendix Figure 6.44: ^{13}C NMR (CDCl_3) spectrum of compound 4	241
Appendix Figure 6.45: HSQC (CDCl_3) spectrum of compound 4	242
Appendix Figure 6.46: HMBC (CDCl_3) spectrum of compound 4	243
Appendix Figure 6.47: COSY (CDCl_3) spectrum of compound 4	244
Appendix Figure 6.48: NOESY (CDCl_3) spectrum of compound 4	245
Appendix Figure 6.49: ^1H NMR (CDCl_3) spectrum of 6	246
Appendix Figure 6.50: ^{13}C NMR (CDCl_3) spectrum of 6	247
Appendix Figure 6.51: HSQC (CDCl_3) spectrum of 6	248
Appendix Figure 6.52: COSY (CDCl_3) spectrum of 6	249
Appendix Figure 6.53: ^1H NMR (CDCl_3) spectrum of 7	250
Appendix Figure 6.54: ^{13}C NMR (CDCl_3) spectrum of 7	251
Appendix Figure 6.55: HSQC (CDCl_3) spectrum of 7	252
Appendix Figure 6.56: HMBC (CDCl_3) spectrum of 7	253
Appendix Figure 6.57: ^1H NMR (CDCl_3) spectrum of lactol SI-2	254
Appendix Figure 6.58: ^{13}C NMR (CDCl_3) spectrum of lactol SI-2	255
Appendix Figure 6.59: HSQC (CDCl_3) spectrum of lactol SI-2	256
Appendix Figure 6.60: COSY (CDCl_3) spectrum of lactol SI-2	257
Appendix Figure 6.61: ^1H NMR (CDCl_3) spectrum of 8	258

LIST OF APPENDIX C FIGURES (Continued)

<u>Figure</u>	<u>Page</u>
Appendix Figure 6.62: ^{13}C NMR (CDCl_3) spectrum of 8	259
Appendix Figure 6.63: HSQC (CDCl_3) spectrum of 8	260
Appendix Figure 6.64: COSY (CDCl_3) spectrum of 8	261
Appendix Figure 6.65: ^1H NMR (CDCl_3) spectrum of TM-122.....	262
Appendix Figure 6.66: ^{13}C NMR (CDCl_3) spectrum of TM-122.....	263
Appendix Figure 6.67: HSQC (CDCl_3) spectrum of TM-122.....	264
Appendix Figure 6.68: HMBC (CDCl_3) spectrum of TM-122.....	265
Appendix Figure 6.69: COSY (CDCl_3) spectrum of TM-122.....	266
Appendix Figure 6.70: NOESY (CDCl_3) spectrum of TM-122.....	267
Appendix Figure 6.71: ^1H NMR (CDCl_3) spectrum of TM-121.....	268
Appendix Figure 6.72: ^{13}C NMR (CDCl_3) spectrum of TM-121.....	269
Appendix Figure 6.73: HSQC (CDCl_3) spectrum of TM-121.....	270
Appendix Figure 6.74: HMBC (CDCl_3) spectrum of TM-121.....	271
Appendix Figure 6.75: COSY (CDCl_3) spectrum of TM-121.....	272
Appendix Figure 6.76: NOESY (CDCl_3) spectrum of TM-121.....	273
Appendix Figure 6.77: ^1H NMR (CDCl_3) spectrum of 12	274
Appendix Figure 6.78: ^{13}C NMR (CDCl_3) spectrum of 12	275
Appendix Figure 6.79: HSQC (CDCl_3) spectrum of 12	276
Appendix Figure 6.80: COSY (CDCl_3) spectrum of 12	277

LIST OF APPENDIX C FIGURES (Continued)

<u>Figure</u>	<u>Page</u>
Appendix Figure 6.81: ^1H NMR (CDCl_3) spectrum of 17	278
Appendix Figure 6.82: ^{13}C NMR (CDCl_3) spectrum of 17	279
Appendix Figure 6.83: HSQC (CDCl_3) spectrum of 17	280
Appendix Figure 6.84: HMBC (CDCl_3) spectrum of 17	281
Appendix Figure 6.85: COSY (CDCl_3) spectrum of 17	282
Appendix Figure 6.86: ^1H NMR (CDCl_3) spectrum of E-19	283
Appendix Figure 6.87: ^{13}C NMR (CDCl_3) spectrum of E-19	284
Appendix Figure 6.88: HSQC (CDCl_3) spectrum of E-19	285
Appendix Figure 6.89: COSY (CDCl_3) spectrum of E-19	286
Appendix Figure 6.90: HMBC (CDCl_3) spectrum of E-19	287
Appendix Figure 6.91: ^1H NMR (CDCl_3) spectrum of Z-19	288
Appendix Figure 6.92: ^{13}C NMR (CDCl_3) spectrum of Z-19	289
Appendix Figure 6.93: HSQC (CDCl_3) spectrum of Z-19	290
Appendix Figure 6.94: HMBC (CDCl_3) spectrum of Z-19	291
Appendix Figure 6.95: COSY (CDCl_3) spectrum of Z-19	292

LIST OF APPENDIX C FIGURES (Continued)

<u>Figure</u>	<u>Page</u>
Appendix Figure 6.96: ^1H NMR (CDCl_3) spectrum of 5S-E-19	293
Appendix Figure 6.97: ^{13}C NMR (CDCl_3) spectrum of 5S-E-19	294
Appendix Figure 6.98: ^1H NMR (CDCl_3) spectrum of 15	295
Appendix Figure 6.99: ^{13}C NMR (CDCl_3) spectrum of 15	296
Appendix Figure 6.100: COSY (CDCl_3) spectrum of 15	297
Appendix Figure 6.101: ^1H NMR (CDCl_3) spectrum of 20	298
Appendix Figure 6.102: ^{13}C NMR (CDCl_3) spectrum of 20	299
Appendix Figure 6.103: DEPT135 (CDCl_3) spectrum of 20	300
Appendix Figure 6.104: HMBC (CDCl_3) spectrum of 20	301
Appendix Figure 6.105: COSY (CDCl_3) spectrum of 20	302
Appendix Figure 6.106 ^1H NMR (CDCl_3) spectrum of 5	303
Appendix Figure 6.107: ^{13}C NMR (CDCl_3) spectrum of 5	304
Appendix Figure 6.108: ^1H NMR (CDCl_3) spectrum of 14	305
Appendix Figure 6.109: ^{13}C NMR (CDCl_3) spectrum of 14	306
Appendix Figure 6.110: ^1H NMR (CDCl_3) spectrum lactol SI-3	307
Appendix Figure 6.111: ^{13}C NMR (CDCl_3) spectrum of lactol SI-3	308
Appendix Figure 6.112: COSY (CDCl_3) spectrum of lactol SI-3	309
Appendix Figure 6.113: HSQC (CDCl_3) spectrum of lactol SI-3	310
Appendix Figure 6.114: HMBC (CDCl_3) spectrum of lactol SI-3	311

LIST OF APPENDIX C FIGURES (Continued)

<u>Figure</u>	<u>Page</u>
Appendix Figure 6.115: ^1H NMR (CDCl_3) spectrum of 21	312
Appendix Figure 6.116: ^{13}C NMR (CDCl_3) spectrum of 21	313
Appendix Figure 6.117: HSQC (CDCl_3) spectrum of 21	314
Appendix Figure 6.118: ^1H NMR (CDCl_3) spectrum of TM-120.....	315
Appendix Figure 6.119: ^{13}C NMR (CDCl_3) spectrum of TM-120.....	316
Appendix Figure 6.120: HSQC (CDCl_3) spectrum of TM-120.....	317
Appendix Figure 6.121: HMBC (CDCl_3) spectrum of TM-120.....	318
Appendix Figure 6.122: COSY (CDCl_3) spectrum of TM-120.....	319
Appendix Figure 6.123: NOESY (CDCl_3) spectrum of TM-120.....	320
Appendix Figure 6.124: ^1H NMR (CDCl_3) spectrum of TM-119.....	321
Appendix Figure 6.125: ^{13}C NMR (CDCl_3) spectrum of TM-119.....	322
Appendix Figure 6.126: COSY (CDCl_3) spectrum of TM-119.....	323
Appendix Figure 6.127: HSQC (CDCl_3) spectrum of TM-119.....	324
Appendix Figure 6.128: HMBC (CDCl_3) spectrum of TM-119.....	325
Appendix Figure 6.129: HMBC (CDCl_3) spectrum of TM-119.....	326
Appendix Figure 6.130: NOESY (CDCl_3) spectrum of TM-119.....	327
Appendix Figure 6.131: ^1H NMR (D_2O -MeOD) spectrum of TM-117.....	328
Appendix Figure 6.132: ^{13}C NMR (D_2O -MeOD) spectrum of TM-117.....	329
Appendix Figure 6.133: HMBC (D_2O -MeOD) spectrum of TM-117.....	330

LIST OF APPENDIX C FIGURES (Continued)

<u>Figure</u>	<u>Page</u>
Appendix Figure 6.134: HSQC (D ₂ O-MeOD) spectrum of TM-117.....	331
Appendix Figure 6.135: HMBC (D ₂ O-MeOD) spectrum of TM-117.....	332
Appendix Figure 6.136: HMBC (D ₂ O-MeOD) spectrum of TM-117.....	333
Appendix Figure 6.137: NOESY (D ₂ O-MeOD) spectrum of TM-117.....	334
Appendix Figure 6.138: ¹ H NMR (D ₂ O) spectrum of TM-118.....	335
Appendix Figure 6.139: ¹³ C NMR (D ₂ O) spectrum of TM-118.....	336
Appendix Figure 6.140: COSY (D ₂ O) spectrum of TM-118.....	337
Appendix Figure 6.141: HSQC (D ₂ O) spectrum of TM-118.....	338
Appendix Figure 6.142: HMBC (D ₂ O) spectrum of TM-118.....	339
Appendix Figure 6.143: NOESY (D ₂ O) spectrum of TM-118.....	340

Chapter 1. Introduction

1.1 Natural Products

All organisms utilize a vast network of processes known as primary metabolism to interconvert organic compounds into energy and to support other essential life functions. Secondary metabolism comprises the processes responsible for the synthesis of chemical compounds within an organism that are generally *non-essential* to the day-to-day survival of the organism, though these compounds can offer distinct evolutionary advantages to the organism. The building blocks for secondary metabolites, or natural products, come from primary metabolism, which therefore provides the templates for these structurally diverse compounds. As such, the chemical structures produced vary significantly from organism to organism, and the actual function of the compound and/or its relationship to the organism is often unknown or poorly understood.¹ Natural products are sometimes utilized by the producing organism or sequestered from dietary sources and used as a defense tool against predators, such as the case of the potent sodium ion channel disrupter batrachotoxin from the dendrobatidae family of poison dart frogs.^{2,3} Additionally, natural products may provide protection from other environmental hazards like ultraviolet radiation as is likely the case for the natural sunscreen compounds gadusol and the related mycosporin-like amino acids found in marine animals.⁴ Some organisms utilize natural products to attract their mates. For instance, the American Cockroach produces the secondary metabolite, periplanone B, as a sex attractant.^{5,6,7,8} Male Cardinal birds (*Cardinalis cardinalis*) use the red pigment canthaxanthin (Figure 1.1), one of the many highly colored carotenoids, in their plumage

to attract females for mating.⁹ Since evolution has favored functional roles for secondary metabolites in nature, they are predisposed to be biologically active compounds, and as such they have historically occupied a considerable role in modern medicine.

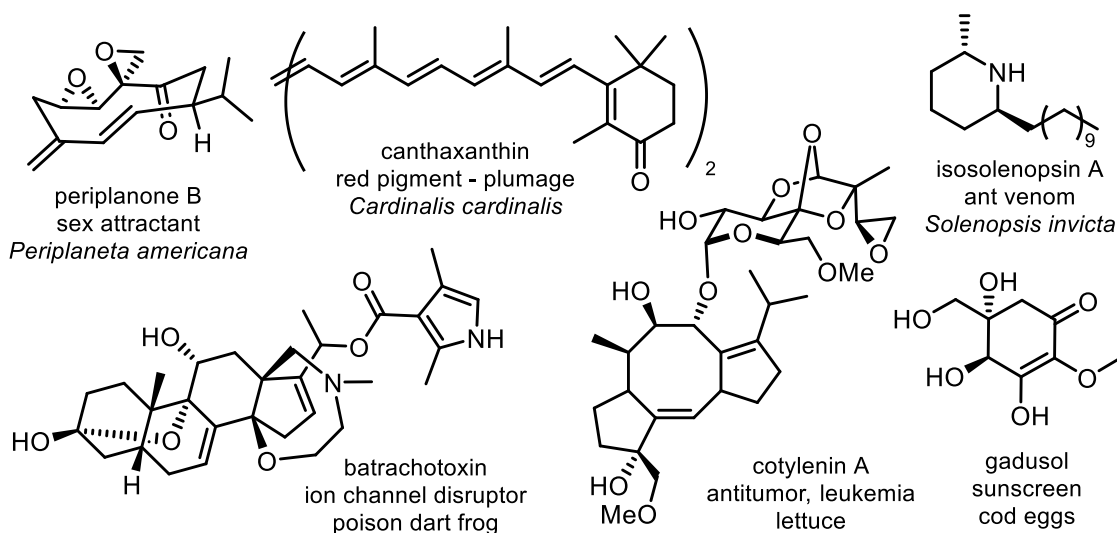


Figure 1.1. Examples of natural products with functional roles in nature

1.2 The Importance of Natural Products

Natural products have been the lifeblood of drug discovery for decades and their role is especially prominent in the areas of infectious disease and cancer chemotherapy. These compounds have served as the structural scaffolds that medicinal chemistry has exploited for the development of new pharmaceutical therapies over the years. In fact a large portion of drugs to date are either unaltered natural products themselves or inspired by natural product motifs.^{10,11,12,13} Additionally they have been the inspiration that has driven advancements in other fields, especially synthetic organic chemistry.

The isolation of the secondary metabolite morphine from the opium poppy *Papaver somniferum* over 200 years ago, initiated the modern era of drug discovery. Despite the current disturbing state of the opioid epidemic, morphine and its analogs have saved countless lives in relieving acute and chronic pain from surgery, life-threatening injuries, car accidents, cancer, etc. It is inconceivable in modern times to undergo major surgery without morphine or its analogs.^{14,15} The cinchona alkaloid quinine, isolated in 1820, was one of the only effective treatments for malaria following World War II and continues to remain on the World Health Organization's "List of Essential Medicines that satisfy the priority healthcare needs of the population of a country".¹⁶ Prior to the age of antibiotics initiated by Alexander Fleming's discovery of the beta-lactam natural product penicillin, people were literally dying in hospitals from cuts and scratches. The introduction of penicillin not only revolutionized drug discovery but revolutionized human existence on this planet, saving an immeasurable amount of lives.¹⁷ In fact, life expectancy around the world has nearly *doubled* from 40 years, in the 20th century, to 77 years now.¹⁰ Until the 1990s, roughly 80% of all drugs were natural products or natural product inspired compounds. Although, the percentage of natural product drugs or natural product inspired derivatives dropped between 1990 and 2000, this is largely credited to the pharmaceutical industry's overestimation of, and consequently over-reliance on combinatorial approaches to bringing new non-natural product derived drugs to market. Despite this heavy investment in combinatorial approaches, as of 2014, only three de novo combinatorial sourced drugs (sorafenib,

atuluren and vemurafenib) were approved.^{6,18,19} The overall trend, as noted in numerous detailed reviews, suggests that natural products will remain at the forefront of drug discovery for the foreseeable future.⁶⁻¹⁰ Moreover, the importance of natural products and their vital role in modern medicine was recently underscored in awarding the 2015 Nobel Prize in Physiology and Medicine for the discovery of two classes of natural products, the avermectins and separately artemisinin. The avermectins have nearly eradicated river blindness and elephantitis, two parasitic scourges that plagued some of the poorest countries in the world, while the discovery of artemisinin is credited with the sweeping reduction in malaria patient mortality rates.^{20,21} The meaningful impact of natural products on human health and society is great and the importance is fundamental.

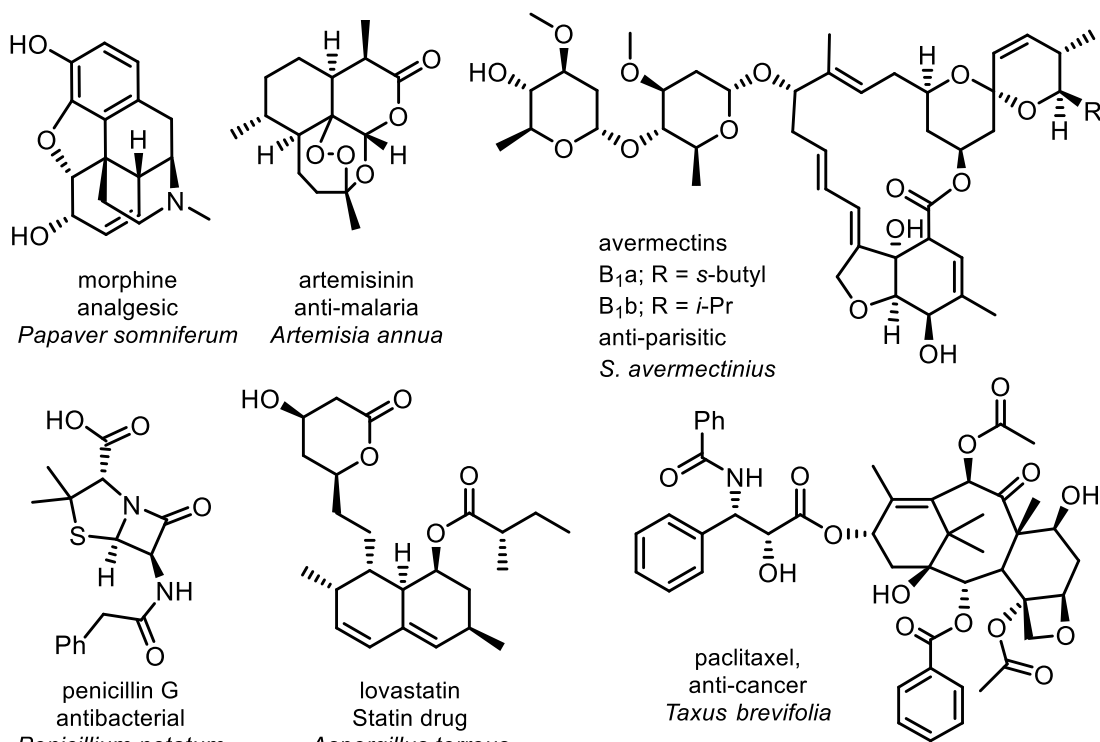


Figure 1.2. Medicinally important natural products

1.3 Classes of Natural Products

Natural products can be loosely categorized by characteristic biosynthetic machinery and/or intermediates. Some important natural products classified generally by their biosynthesis are isoprenoids, alkaloids, ribosomal and non-ribosomal peptides, polyketides, and aminocyclitols. There is however much overlap as secondary metabolites are often the result of a biosynthetic intermediate(s) entering multiple pathways.

1.3.1 Isoprenoids

Isoprenoids, also known as terpenoids, are found in all organisms and make up a structurally diverse collection of natural products. Some notable examples of terpenoid natural products include the anticancer drugs paclitaxel and ingenol, as well as the important terpenoids cholesterol, vitamin A, and menthol. Terpenoids consist of iterations of 5-carbon building blocks of isoprene units formed from the condensation of isopentenyl diphosphate (IPP) or its isomer, dimethylallyl diphosphate (DMAPP). The condensation products often re-arrange and cyclize through carbocation rearrangements, resulting in the tremendous structural diversity of isoprenoids. Terpenoids are categorized by the number of C₅ subunits that they are made of: monoterpenes (C₁₀) consist of two C₅ units, sesquiterpenes (C₁₅) contain three C₅ units, diterpenes (C₂₀) contain four C₅ units, sesterterpenes (C₂₅) contain five C₅ units, triterpenes (C₃₀) contain six C₅ units and tetraterpenes (C₄₀) eight C₅ units. Both monomers, IPP and DMAPP, are products of the mevalonate pathway (MVA) found in mammals, plants, bacteria and fungi or the methylerythritol phosphate pathway (MEP), which is not found in mammals but present in many pathogenic bacteria, plants, and malaria parasites.^{22,23}

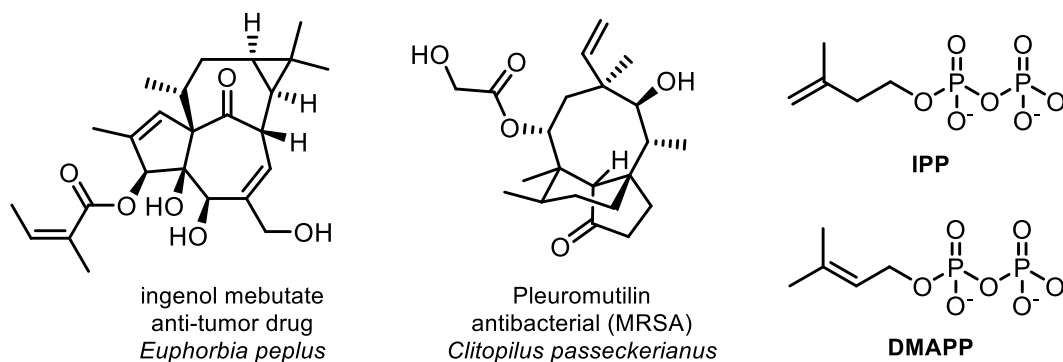


Figure 1.3. Notable terpenoid natural products and starter units IPP and DMAPP

1.3.2 Alkaloids

Alkaloids are organic amines, containing at least one nitrogen and often multiple. They have historically been found in plants and are biosynthetically derived from amino acids. The alkaloid carbon skeleton can be formed or acquired through other secondary metabolic processes while one or more of the incorporated nitrogen atoms comes from one or multiple amino acids.¹ For example, the steroidal backbone of cyclopamine (Figure 1.4) is biosynthesized through the typical terpene pathway via a series of head-to-tail combinations of DMAPP and IPP units forming the intermediate cholesterol, which gets oxidized, followed by a transamination from gamma-aminobutyric acid, then cyclization to the final compound.²⁴ The majority of alkaloids come from a small number of amino acid building blocks. Nitrogen incorporation can occur through many different processes but imine formation/transamination and Mannich reactions are used frequently in the biosynthesis of alkaloids.¹

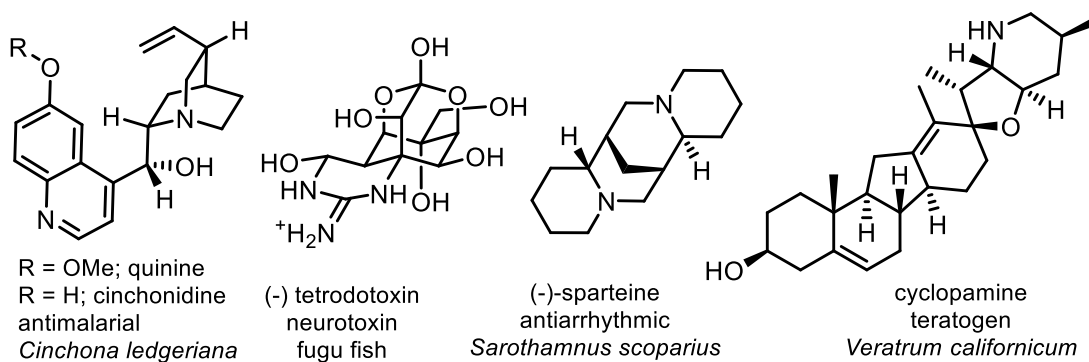


Figure 1.4. Examples of some alkaloids of interest

1.3.3 Ribosomal and Non-ribosomal Peptides

While peptides hold tremendous potential for therapeutic applications, a major obstacle is that oral administration is often not feasible due to inactivation or degradation of the peptide by enzymes in the GI tract, thereby requiring injection. Developments in drug delivery, however, hold some promise to overcoming this hurdle. The opioid peptide, β -endorphin, is a ribosomal peptide produced in the pituitary gland, and is several times more potent than morphine at pain relief, though addiction and withdrawal symptoms are still an issue. Pyrroloquinoline quinone (Figure 1.5) is a biologically important antioxidant and ribosomal peptide found in soil, human breast milk, plants and interstellar dust.^{1,25,26,27} The prenylated small molecule and ribosomal peptide, ComX, is an extra-cellular signaling molecule isolated from *B. subtilis*.^{28,29}

Ribosomal peptides constitute proteins and polypeptides synthesized on the ribosome. The biosynthesis of ribosomal peptides occurs using genes of DNA that encode the construction of a precursor peptide. After the precursor peptide is synthesized, it is hydrolytically cleaved followed by post translational modifications that allow the formation of peptides that are not encoded by DNA.¹

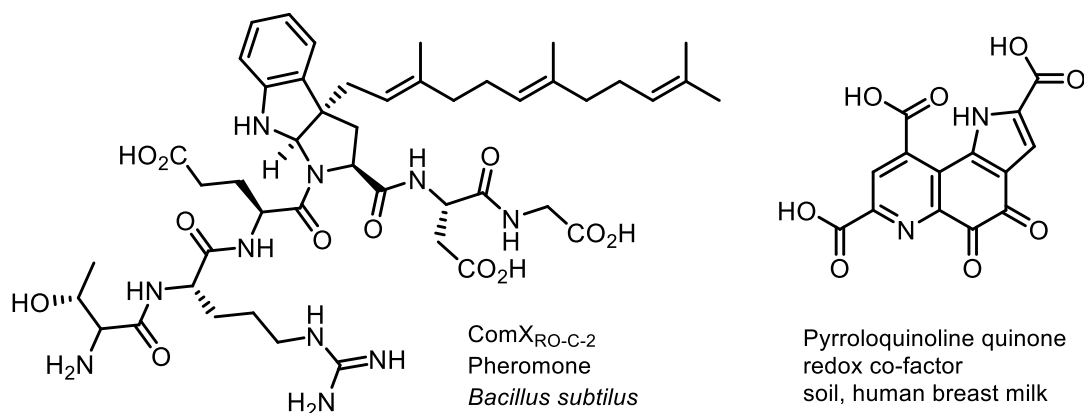


Figure 1.5 A. Small molecule ribosomal peptides

Non-ribosomal peptides are comprised of proteinogenic and non-proteinogenic peptides and typically biosynthesized by an array of modular enzymes known as non-ribosomal peptide synthase enzymes (NRPS). A starter unit amino acid is loaded, and the peptidyl backbone is built up iteratively in an assembly line like, building-block fashion, then hydrolyzed or cyclized by a terminal thioesterase to form either linear or macrocyclic peptides. Though this description is overly simplistic, the assembly line logic can be used to predict the structure of non-ribosomal peptides from a biosynthetic gene cluster with a high degree of accuracy. Some medicinally significant natural products from NRPS's include the beta-lactam antibiotics like penicillin G, the cephalosporins, and nocardicin A, the macrocyclic peptides including the arylomycins (Figure 1.5) and the important anticancer agents vinblastine and vincristine.^{1,30,31,32,33,34}

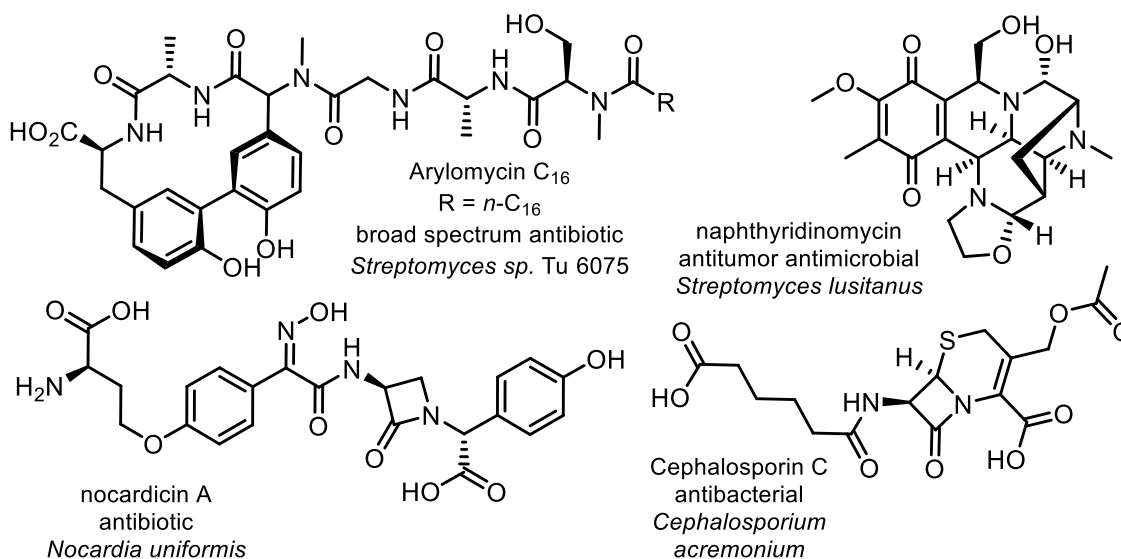


Figure 1.5 B. Structures of some important natural products from NRPSs

1.3.4 Polyketides

Polyketides and fatty acids derive from the acetate pathway and encompass an enormous array of natural products, many of which are biologically active and medically useful compounds. For instance, the prostaglandins are modified fatty acids that are distributed throughout different tissues of humans and animals in minute concentrations as chemical messengers and effect different functions of the body.¹ As such the prostaglandins have considerable potential as therapeutics like the prostaglandin prostacyclin, which is used for pulmonary hypertension (Figure 1.6). Other important polyketides include the erythromycin antibiotics or the carcinogenic fungal toxins, the aflatoxins, which are a serious contaminant commonly found in apples and peanuts. Additionally the statins and previously mentioned avermectins (Figure 1.2) are considerably noteworthy pharmaceutically relevant polyketides.^{14, 15}

Polyketides are derived biosynthetically from starter units of acetyl/propionyl/benzoyl thioester (CoA) building blocks and extended through a series of Claisen condensation reactions with substituted or unsubstituted malonyl thioesters (CoAs) similar to fatty acids. These building blocks are loaded by an acyl transferase (AT) onto an acyl carrier protein (ACP) or to a beta keto-acyl synthase (KS) which catalyzes the decarboxylative condensation between the malonate thioester and the acetyl group in the chain elongation step.^{35,36}

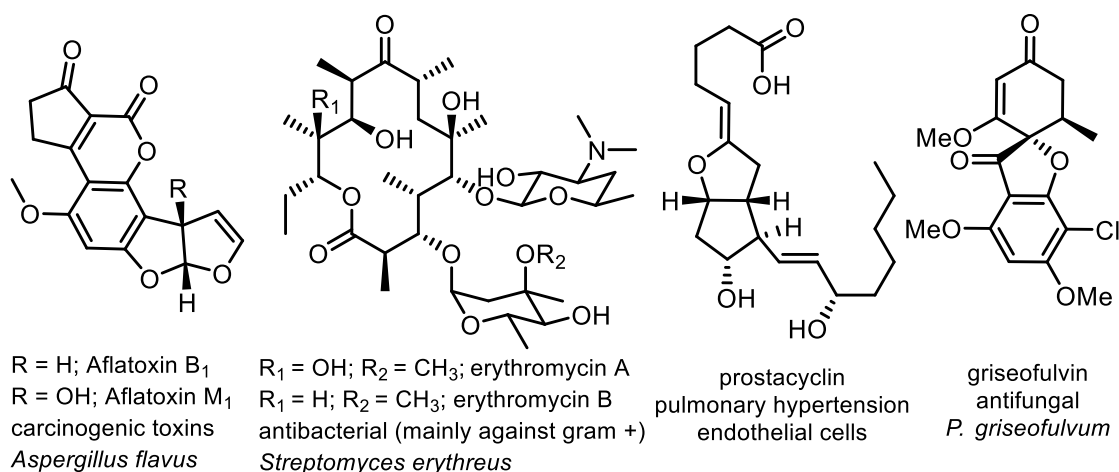


Figure 1.6. Examples of some important polyketides

1.3.5 Aminocyclitols

Aminocyclitols are a subclass of cyclitols, 5 or 6-membered polyhydroxylated carbon rings or carbasugars, containing an amine functionality and are generally microbial in origin. Aminocyclopentitols, the 5-membered ring variants of aminocyclitols, are a small but important class of pharmaceutically active natural products.^{37,38} Some relevant natural or nature inspired aminocyclopentitols include the antiviral carbocyclic nu-

cleosides such as neplanocin A and Baraclude[®], the neuramidase inhibitor and influenza drug Rapivab[®], the anticancer and antidiabetic glycosidase inhibitors trehazolin and mannostatins, as well as the interleukin-1 receptor associated kinase 4 (IRAK4) inhibitors that can be used to treat chronic inflammatory diseases such as rheumatoid arthritis and inflammatory bowel disease (Figure 1.7).^{39,40,41} Some aminocyclitols are also active insecticides and fungicides with agricultural applications. Pactamycin (**1**, Figure 1.7) is an antitumor antibiotic aminocyclopentitol with pronounced cytotoxicity that spans across all three phylogenetic domains.^{42,43,44}

Biosynthetically, aminocyclitols are made from simple carbohydrates via sugar phosphate cyclase enzymes, with the exception of aminocyclopentitols. The 5-membered ring formation of aminocyclopentitols is less understood, but cyclization is expected to occur through radical SAM mediated processes on amino-sugar derived substrates as evident by the biosynthetic genes encoding their involvement.^{45,46,47,48,49} However, direct evidence of such processes has yet to be fully elucidated.

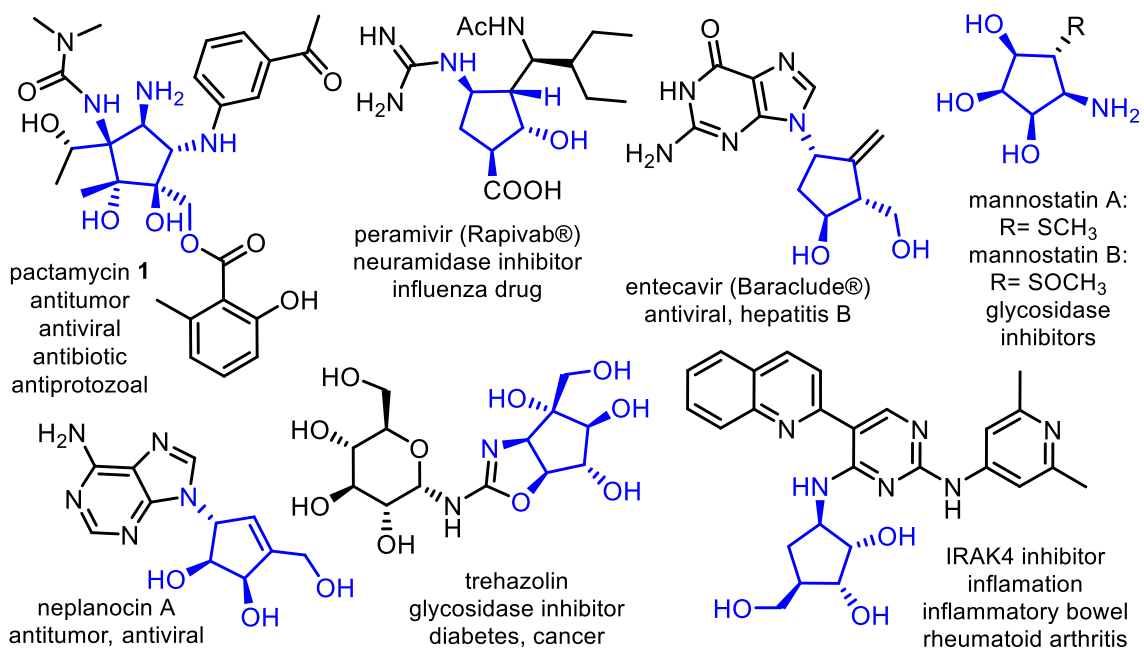


Figure 1.7 Bioactive aminocyclopentitol (blue) units and clinically used drugs

1.4 Pactamycin

1.4.1 Background

Pactamycin (**1**) is an aminocyclopentitol natural product that was first isolated from the culture broth of *Streptomyces pactum* in the 1960's at the former Upjohn Chemical Company.³¹ In the ensuing time since its discovery, pactamycin attracted the attention of generations of biologists and chemists alike due to its rich bioactivity profile and complex chemical structure. Nearly a decade after its discovery, a remarkable structure elucidation study of pactamycin involving chemical degradation and spectroscopic data resulted in a proposed structure in 1970, which was corrected in 1972 by X-ray crystallography.^{50,51,52}

Pactamycin was first reported as a potential antitumor antimicrobial therapeutic displaying significant cytotoxicity *in vitro* and *in vivo* activity but development has been hampered due to its indiscriminate toxicity towards mammalian cells and its structural complexity.³¹ It was later found to strongly inhibit protein synthesis by binding to the

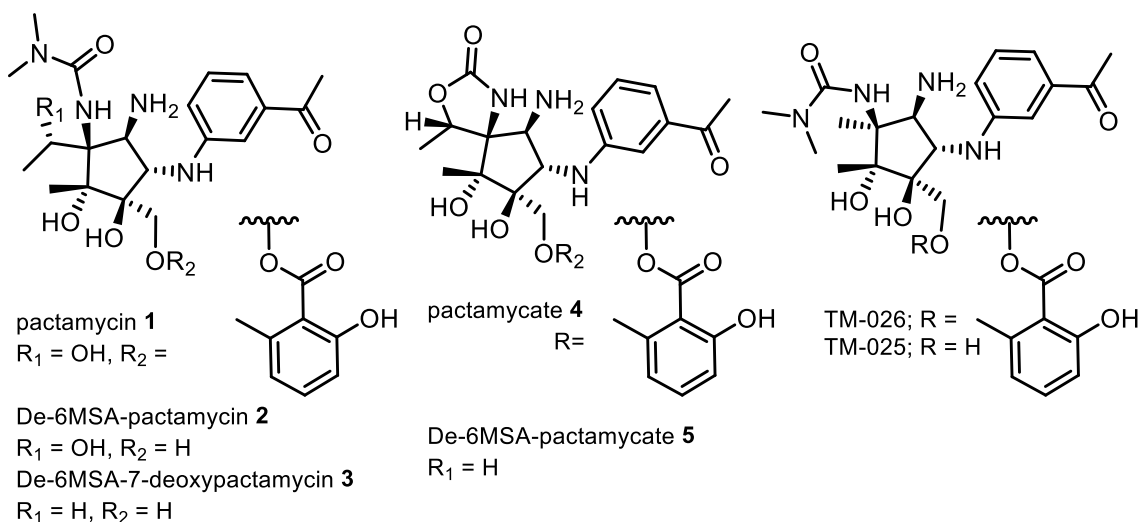


Figure 1.8. Pactamycin and some biosynthetically derived bioactive analogs

30S ribosomal subunit of most organisms.^{53,54} Hanessian recently demonstrated that the pactamycin derivative, de-6-MSA-pactamycin shares the same ribosomal binding site as pactamycin, using x-ray crystallography.⁵⁵ Interestingly, de-6-MSA-pactamycin and derivatives of de-6-MSA-pactamycin however do *not* share the same universal cytotoxicity profile as pactamycin, and in fact display diminished toxicity towards mammalian cells and selectivity over pactamycin towards malaria parasites.^{56,57} This suggests that an interaction of the 6-MSA portion of pactamycin within the binding site is at least in part responsible for its broad toxicity. This could be tremendously useful in designing biologically active de-6-MSA-pactamycin analogs and selectively curtailing the non-specific tox-

icity displayed by pactamycin itself. However, based on work from the Mahmud lab, other structural features also appear to play a significant role in moderating the cytotoxicity and selectivity of pactamycin analogs, such as the 2°-hydroxyethyl side chain or lack thereof in pactamycin or derivative TM-026 (Figure 1.8).⁵⁸ For instance, TM-026 has the 6-MSA moiety intact yet retains none or reduced antibacterial activity and lacks the broad cytotoxicity of pactamycin.⁴⁴ To address the structure activity relationships (SARs) involved in the toxicity associated with pactamycin as well as to prepare new bioactive analogs, several research groups have undertaken different approaches toward this end.^{44,59,60,61,62,63,64}

1.4.2 Total Syntheses of Pactamycin

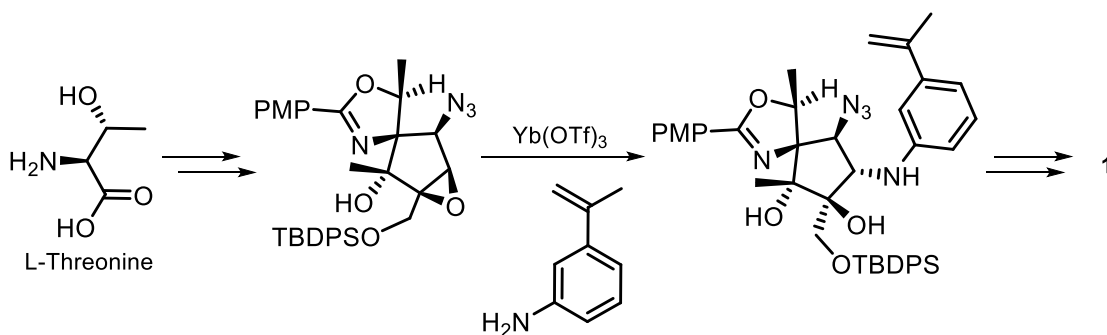


Figure 1.9. Summary of the Hanessian synthesis of **1**

The challenging aminocyclopentitol core of pactamycin (**1**) has been the target of numerous synthetic attempts towards pactamycin over the years.^{65,66,67,68,69,70,71} In 2011, Hanessian reported the first total synthesis of pactamycin, providing remarkable closure to a longstanding synthetic challenge.^{72,73} Utilizing L-threonine as a strategic synthetic

chiron containing carbons C1, C2, C7 and C8, as well as the hydroxyethyl sidechain and the C1 nitrogen, they obtained pactamycin in 29-steps and 3% yield, despite a number of unforeseen and taxing setbacks (Figure 1.9).⁶² They reached the cyclopentane ring through a series of well documented transformations. They performed a number of functional group transformations and stereochemical inversions providing their key intermediate epoxide in 21-steps (Figure 1.9). A stereoselective epoxide ring opening appended the aniline portion to the aminocyclopentitol ring which completed the entire carbon skeleton of pactamycin. After a number of challenging functional group inter-conversions on the highly substituted aminocyclopentitol ring which presented further inopportune setbacks, they delivered both pactamycin and separately pactamycate. Notably, the 1st total synthesis of pactamycin was reported 50 - years after its discovery, which speaks volumes to the structural complexity of this molecule.

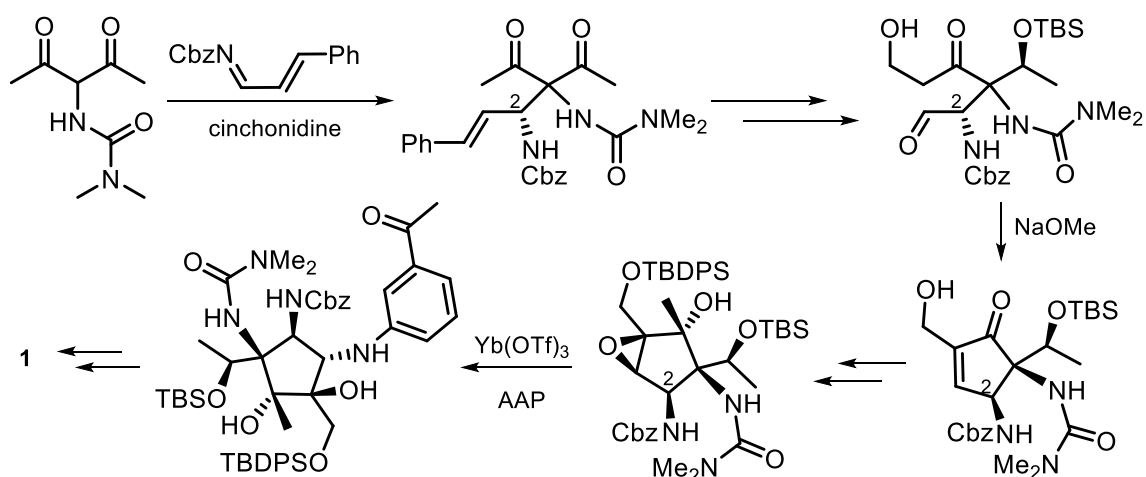


Figure 1.10. Summary of the Johnson synthesis of pactamycin (**1**)

In 2013, Johnson reported their own total synthesis of pactamycin, enantioselectively from acetyl acetone in an astonishing 15 steps (1.9% overall yield).^{74,75} Johnson's

strategy relied on setting the C2 stereocenter early, albeit with incorrect stereochemical configuration which turned out beneficial as it aided diastereoselection later on and was easily epimerized to the correct one. An asymmetric Mannich addition of a urea malonate nucleophile onto the Cbz-protected cinnamaldehyde imine (Figure 1.10) appended the remaining carbons for the aminocyclitol ring and set the (incorrect) C2 stereocenter. Utilizing the urea early in the synthesis obviated some of the issues faced by Hanessian when installing the urea on the condensed aminocyclopentitol ring later on. A desymmetrizing reduction set the hydroxyethyl stereocenter on the sidechain, and later corrected their C2 stereocenter in a base mediated epimerizing intramolecular aldol condensation forming the cyclopentenone ring. Several functional group transformations brought them to an epoxide similar to Hanessian's late stage intermediate, similarity that was then exploited in a familiar asymmetric epoxide ring opening, this time however with unprotected 3AAP which formed the entire pactamycin skeleton. Following deprotection and appendage of the 6-MSA moiety, Johnson's expeditious total synthesis of pactamycin was complete. Both Hanessian and Johnson have since prepared a number of novel and biologically active pactamycin derivatives with improved therapeutic application.

1.4.3 Analogs of Pactamycin

As previously mentioned, one of the major hurdles in developing therapeutic applications for pactamycin is its structural complexity. While the Hanessian group and

separately the Johnson group significantly advanced the challenge utilizing a traditional tactic, by first obtaining pactamycin by total synthesis, then preparing derivatives from the final product and synthetic intermediates; the Mahmud group has employed a multi-pronged, and somewhat less conventional strategy in obtaining novel pactamycin derivatives.^{45-47, 49, 51-53, 61-64}

The approaches taken by the Mahmud group rely on biosynthetic manipulations as well as chemoenzymatic and synthetic approaches. Accordingly, by utilizing this multi-faceted strategy, the Mahmud group has produced numerous highly potent biologically active pactamycin derivatives. Through biosynthetic manipulations, the Mahmud group has demonstrated the production of new pactamycin analogs with pronounced antimalarial activity, lacking significant antibacterial activity, which are about 10–30 times less toxic than pactamycin toward mammalian cells (Figure 1.8). Additionally pactamycin derivatives TM-101 and TM-102 displayed nanomolar activity against *P. falciparum*, no antibacterial activity and reduced cancer cytotoxicity versus pactamycin, resulting in an improved selectivity index.⁵² Furthermore, we recently discovered that an acyltransferase (PtmR), used by *S. pactum* in the biosynthesis of pactamycin is capable of accepting a variety of substrates and developed a chemoenzymatic process to produce novel pactamycin analogs.⁵³ Continuing our efforts to draw further on the bountiful activity of the aminocyclitol core of pactamycin, we have taken a third approach by synthesizing the core aminocyclopentitol ring believed responsible for much of pactamycin's bioactivity. This synthesis work has since generated four new biologically active

aminocyclitols, two of which display modest inhibitory activity against Gram-positive bacteria. Importantly, these synthesis efforts have also produced two novel and promising aminocyclopentitols, both of which display potent activity against melanoma (A375 cells), on par with pactamycin derivative TM-026.

1.4.4 Pactamycin biosynthesis

In *S. pactum*, pactamycin is derived from three major metabolic pathways: 1) the shikimate pathway delivers dehydroshikimic acid (DHS), the precursor of the 3-aminobenzoic acid that leads to the 3-aminoacetophenone moiety; 2) the amino sugar metabolic pathway supplies the precursor for the aminocyclopentitol moiety; and 3) the acetate pathway produces 6-methylsalicylic acid by iterative type I polyketide synthase. Early feeding studies by Rinehart and Weller using isotopically labeled precursors had established glucose, methionine and acetate as critical starting units in pactamycin bio

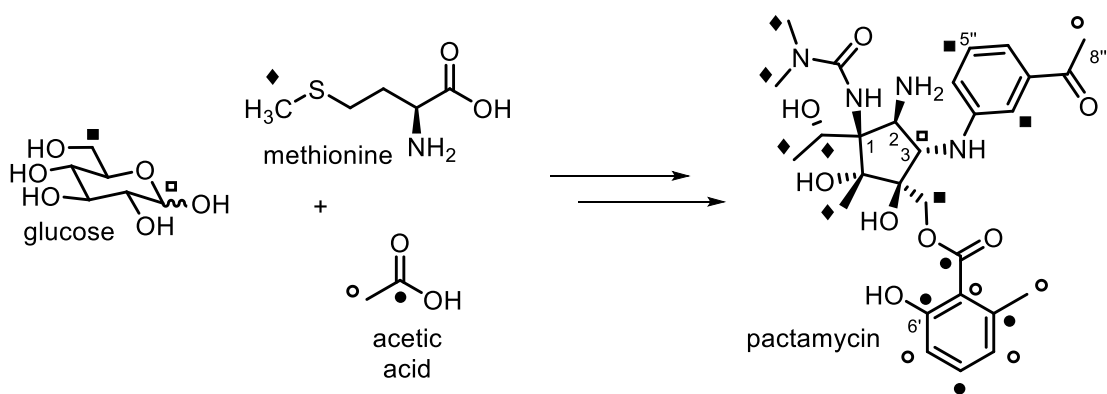


Figure 1.11. Early ^{13}C -labeling experiments detailing the biosynthetic origin of pactamycin

synthesis (Figure 1.11).^{76,77} This pioneering work demonstrated that both the *N*- and *C*-

methyl groups on the *N,N*-dimethyl urea and on the aminocyclitol ring come from methionine (presumably via SAM-dependent methylations) and remarkably, the hydroxymethine carbon and the methyl group attached are formed via two-iterative C-methylations. Additionally this established the origin of the 6-MSA portion of the molecule as coming from a polyketide pathway. Furthermore, the carbons C-5'' and C-3'' of the aminoacetophenone (AAP) moiety came from C-6 of glucose. The 3AAP unit is derived from 3-aminobenzoic acid, a shunt product of dehydroshikimic acid (DHS). Several years later, Rinehart and coworkers again employed feeding experiments, this time using ^{13}C -labeled 3-aminobenzoic acid, demonstrated that ABA is in fact a direct precursor while the C-8'' methyl of the AAP moiety is derived from acetate which sug

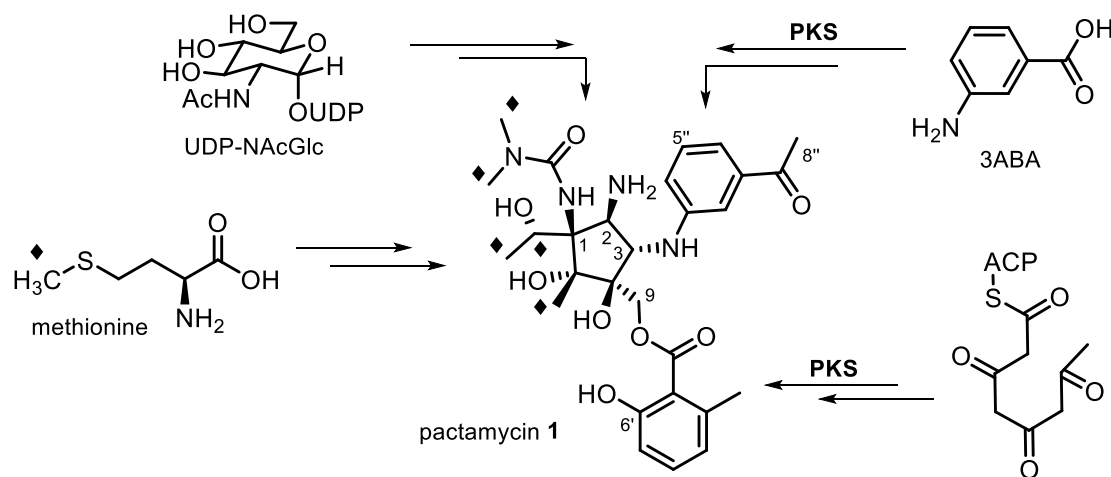


Figure 1.12. Pactamycin biosynthesis pathways

gests a polyketide origin.⁷⁸ Decades later, after discovery of the biosynthetic gene cluster responsible for the production of pactamycin, more detailed knowledge of the biosynthesis has started to emerge.^{79,80} Conversion of DHS to 3ABA was shown to be cata-

lyzed by PtmT (or PctV), a unique PLP-dependent aminotransferase-aromatase enzyme.^{81,82} Further, Kudo has shown that a glycosyltransferase, PctL (or PtmJ), is able to catalyze, although at a low rate, the coupling between 3-aminoacetophenone and UDP-*N*-acetyl- α -D-glucosamine; this reaction was proposed to occur prior to formation of the cyclopentane ring. The mode of formation of the cyclopentitol ring in pactamycin is not yet determined. However, the early incorporation studies by Rinehart indicated that this portion of the molecule is derived from glucose, presumably via *N*-acetylglucosamine (GlcNAc). Analysis of the biosynthetic gene cluster reveals that a radical SAM enzyme (PtmC) is likely responsible for the ring formation, however, there is no direct evidence of such a process to date. Interestingly, radical carbocyclizations forming 5-membered

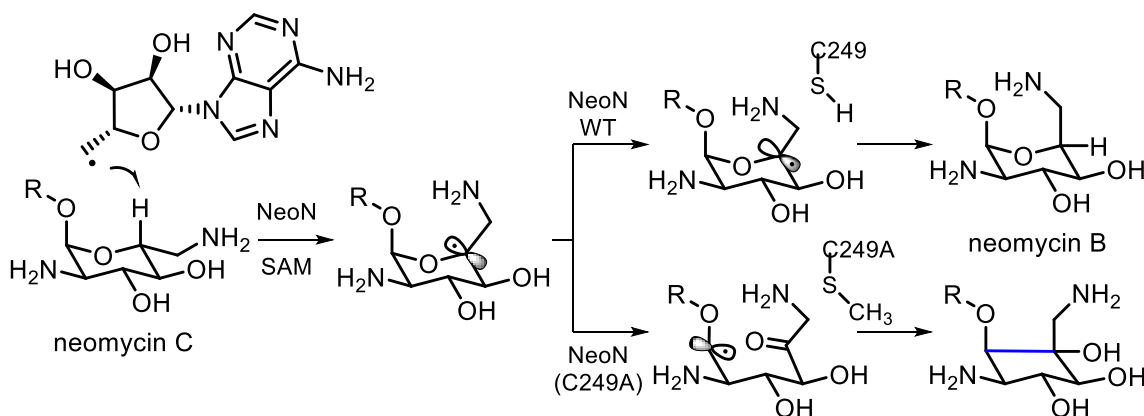


Figure 1.13. Radical SAM mediated carbocyclization of an aminosugar

rings using synthetic iron-sulfur clusters similar to those found in radical SAM enzymes were demonstrated in the late 1970s.^{83,84,85} Although not until recently has such a transformation been demonstrated enzymatically. A recently disclosed result from the Kudo lab revealed that a point mutant (but not the wild-type) of the radical SAM epimerase

from neomycin B biosynthesis, NeoN (C249), mediates the direct conversion of an aminopyranoside in neomycin C to an aminocyclopentitol (Figure 1.13).⁸⁶ The putative radical SAM-mediated carbocyclization (by PtmC) in pactamycin biosynthesis in addition to the radical SAM point mutant NeoN (C249A) mediated cyclization motivated our bioinspired radical cyclization approach to the synthesis of a pactamycin inspired aminocyclopentitol. In addition to the 5-membered ring formation in pactamycin biosynthesis, a number of transformations are unknown. Specifically, the timing, conversion and glycosylation of 3AAP prior to cyclization of the aminosugar is yet to be determined. Some of the tailoring steps that are used to decorate the aminocyclopentitol ring, such as C-methylation of C-7 (by PtmH) and *N*-methylation of the urea (by ptmD) have been elucidated. Others processes such as carbamoylation of the primary amine at C-1 to form the urea, C-methylation of the ring, hydroxylation, deacetylation, hydrolysis and appendage of the 6-MSA unit to the C-9 primary alcohol have yet to be determined.^{52,53,68,69}

1.4.5 Research Objectives

To decipher the biosynthetic pathway to pactamycin in *S. pactum* and to produce new analogs of pactamycin, we pursued the following research objectives:

1. Elucidate details and timing of the formation of the 3AAP moiety in the biosynthesis of pactamycin in relation to glycosylation of ABA and formation of the aminocyclopentitol ring using chemical complementation and isotopic labeling experiments.

2. Synthesize [^{13}C]GlcNAc-[^{13}C]3ABA and appropriate *N*-acetylcysteamine (NAC) thioester as mimics of the acyl-carrier protein-bound substrates for chemical complementation studies.
3. Synthesize 6-MSA-SNAC to determine whether PtmR is responsible for attaching the 6-MSA unit to pactamycin and prepare other NAC compounds to exploit the relaxed substrate specificity of PtmR to obtain novel pactamycin derivatives.
4. Synthesize aminocyclopentitol compounds as potential surrogates for the pactamycin pharmacophore, and test their antibacterial and anticancer activities.

1.5 Reference

- 1 Dewick, P.M., *Medicinal Natural Products*. 2002 John Wiley & Sons, Chichester, W. Sussex, England.
- 2 Albuquerque, E.X.; Daly, J.W.; Witkop, B.; *Science*, **1971**, 172, 995.
- 3 Daly, J. W. *Proc. Natl. Acad. Sci. USA*, **1995**, 92, 9-13.
- 4 Osborn, A. R.; Amabruk, K. H.; Holzwarth, G.; Asamizu, S.; LaDu, J.; Kean, K. M.; Karlplus, A.; Tanguay, R. L.; Bakalinsky, A. T.; Mahmud, T. *eLife*, **2015**;4:e05919.
- 5 Chow, Y. S.; Wang, S. F. *J Chem Ecol* **1981**, 7, 265–272.
- 6 Bell, W.J., Vuturo, S.B., Robinson, S., Hawkins, W.A., *J. Kans. Entomol. Soc.* **1977**, 50, 503
- 7 Boeckh, J., Sass, H., Wharton, D.R.A. *Science* **1970**, 168, 589
- 8 Still, W. C. *J. Am. Chem. Soc.* **1979**, 101, 2493–2495.
- 9 McGraw, K. J.; Hill, G. E.; Stradi, R.; Parker, R. S. *Physiol. Biochem. Zoo.* **2001**, 74, 843.
- 10 Butler, S. M. *J. Nat. Prod.* **2004**, 67, 2141-2153.
- 11 Newman, D. J.; Cragg, G. M. *J. Nat. Prod.* **2016**, 79, 629–661.
- 12 Ojima, I. *J. Med. Chem.* **2008**, 51, 2587–2588.
- 13 Newman, D. J. *J. Med. Chem.* **2008**, 51, 2589.
- 14 Li, J. W.-H.; Vederas, J. C. *Science* **2009**, 325, 161–165.
- 15 Wiffen, P. J.; Wee, B.; Moore, R. A., *Cochrane Database of Systematic Reviews*; John Wiley & Sons, **2016**.
- 16 *WHO Model List of Essential Medicines* (19th List). World Health Organization. **2015**.
- 17 American Chemical Society International Historic Chemical Landmarks. Discovery and Development of Penicillin. <http://www.acs.org/content/acs/en/education/whatischemistry/landmarks/flemingpenicillin.html> (accessed May 27, 2017).
- 18 Hoelder, S.; Clarke, P. A.; Workman, P. *Mol. Onc.* **2012**, 6, 155–176.
- 19 Brumsted, C. J.; Moorlag, H.; Radinov, R. N.; Ren, Y.; Waldmeier, P. (Hoffmann-La Roche, Inc., Nutley, NJ, U.S.A.) U.S. Patent 9,556,172 B2, Jan. 31, 2017.
- 20 Shen, B. *Cell* **2015**, 163, 1297.
- 21 The Nobel Prize in Physiology or Medicine 2015. *Nobelprize.org*. Nobel Media AB 2014. Web.(Accessed July 3 2017)http://www.nobelprize.org/nobel_prizes/medicine/laureates/2015/
- 22 Rohmer, M.; Seemann, M.; Horbach, S.; Bringer-Meyer, S.; Sahm, H. *J. Am. Chem. Soc.* **1996**, 118, 2564.
- 23 Kuzuyama, T.; Seto, H. *Proc. Jpn. Acad., Ser. B* **88**, **2012**.
- 24 Augustin, M. M.; Ruzicka, D. R.; Shukla, A. K.; Augustin, J. M.; Starks, C. M.; O’Neil-Johnson, M.; McKain, M. R.; Evans, B. S.; Barrett, M. D.; Smithson, A.; Wong, G. K.-S.; Deyholos, M. K.; Edger, P. P.; Pires, J. C.; Leebens-Mack, J. H.; Mann, D. A.; Kutchan, T. M. *Plant J* **2015**, 82, 991–1003.
- 25 Killgore, J., Smidt, C., Duich, L., Romero-Chapman, N., Tinker, D., Reiser, K., Melko, M., Hyde, D., Rucker, R. B. **1989**, *Science*, 245, 850–852

-
- 26 Steinberg, F., Stites, T. E., Anderson, P., Storms, D., Chan, I., Eghbali, S., Rucker, R. *Exp. Biol. Med. (Maywood)* **2003**, 228, 160–166
 - 27 Jonscher, K. R.; Stewart, M. S.; Alfonso-Garcia, A.; DeFelice, B. C.; Wang, X. X.; Luo, Y.; Levi, M.; Heerwagen, M. J. R.; Janssen, R. C.; Houssaye, B. A. de la; Wiitala, E.; Florey, G.; Jonscher, R. L.; Potma, E. O.; Fiehn, O.; Friedman, J. E. *FASEB J* **2017**, 31, 1434–1448.
 - 28 Okada, M.; Sato, I.; Cho, S. J.; Iwata, H.; Nishio, T.; Dubnau, D.; Sakagami, Y. *Nat Chem Biol* **2005**, 1, 23–24.
 - 29 McIntosh, J. A.; Donia, M. S.; Schmidt, E. W. *Nat. Prod. Rep.* **2009**, 26 (4), 537–559.
 - 30 Pu, J.-Y.; Peng, C.; Tang, M.-C.; Zhang, Y.; Guo, J.-P.; Song, L.-Q.; Hua, Q.; Tang, G.-L. *Org. Lett.* **2013**, 15 (14), 3674–3677.
 - 31 Payne, J. A. E.; Schoppet, M.; Hansen, M. H.; Cryle, M. J. *Mol. BioSyst.* **2016**, 13, 9–22.
 - 32 Fischbach, M. A.; Walsh, C. T. *Chem. Rev.* **2006**, 106, 3468–3496.
 - 33 Izumikawa, M.; Cheng, Q.; Moore, B. S. *J. Am. Chem. Soc.* **2006**, 128, 1428–1429.
 - 34 Felnagle, E. A.; Jackson, E. E.; Chan, Y. A.; Podevels, A. M.; Berti, A. D.; McMahon, M. D.; Thomas, M. G. *Mol. Pharmaceutics* **2008**, 5, 191–211.
 - 35 Gay, D., You, Y.-k, Keatinge-Clay, A., Cane D.E.; *Biochemistry* **2013**, 52, 8916–8928.
 - 36 Hopwood, D.A. *Chem. Rev.* **1997**, 97, 2465–2497.
 - 37 Mahmud, T. *Nat. Prod. Rep.* **2003**, 20, 137–166.
 - 38 Mahmud, T.; Flatt, P. M.; Wu, X. J. *Nat. Prod.* **2007**, 70, 1384–1391.
 - 39 Blaser, A., Reymond, J.L. *Org. Lett.* **2000**, 2, 1733.
 - 40 Smith, B. J.; McKimm-Breshkin, J. L.; McDonald, M.; Fernley, R. T.; Varghese, J. N.; Colman, P. M. *J. Med. Chem.* **2002**, 45, 2207–2212.
 - 41 McElroy, W. T.; Seganish, W.M.; Herr, J.R.; Harding, J.; Yang, J.; Yet, L.; Komanduri, V.; Prakash, K. C.; Lavey, B.; Tulshian, D.; Greenlee, W. J.; Sondey, C.; Fischmann, T. O.; Niu, X. *Bioorg & Med Chem Lett* **2015**, 25, 1836–1841.
 - 42 Bhuyan, B. K., Dietz, A. & Smith, C. G. *Antimicrob. Agents Chemother.* **1961**, 184, 1050–1056.
 - 43 Taber, R., Rekosh, D., Baltimore, D. *J Virol* **1971**, 8, 395–401
 - 44 Otoguro, K., Iwatsuki, M., Ishiyama, A., Namatame, M., Nishihara-Tukashima, A., Shibahara, S., Kondo, S., Yamada, H., and Omura, S. *The Journal of Antibiotics* **2010**, 63, 381–384.
 - 45 Sakuda, S.; Sugiyama, Y.; Zhou, Z.-Y.; Takao, H.; Ikeda, H.; Kakinuma, K.; Yamada, Y.; Nagasawa, H. *J. Org. Chem.* **2001**, 66, 3356–3361.
 - 46 Kudo F, Kasama Y, Hirayama T, Eguchi T *J Antibiot (Tokyo)* **2007**, 60, 492–503.
 - 47 Kudo, F.; Hoshi, S.; Kawashima, T.; Kamachi, T.; Eguchi, T. *J. Am. Chem. Soc.* **2014**, 136, 13909–13915.
 - 48 Sakuda, S.; Sugiyama, Y.; Zhou, Z.-Y.; Takao, H.; Ikeda, H.; Kakinuma, K.; Yamada, Y.; Nagasawa, H. *J. Org. Chem.* **2001**, 66, 3356–3361.
 - 49 Ito, T.; Roongsawang, N.; Shirasaka, N.; Lu, W.; Flatt, P. M.; Kasanah, N.; Miranda, C.; Mahmud, T. *ChemBioChem* **2009**, 10, 2253–2265.

-
- 50 P. F. Wiley, H. K. Jahnke, F. MacKellar, R. B. Kelly, A. D. Argoudelis, *J. Org. Chem.* **1970**, 35, 1420 – 1425.
- 51 D. J. Duchamp, Abstracts *J. Am. Crystal. Assoc.* Winter Meeting. Albuquerque, **1972**, April, 23.
- 52 D. D. Weller, A. Haber, K. L. Rinehart, Jr., P. F. Wiley, *J. Antibiot.* **1978**, 31, 997 – 1006.
- 53 Egebjerg, J.; Garrett, R. A. *Biochimie* **1991**, 73, 1145–1149.
- 54 G. Dinos, D. N. Wilson, Y. Teraoka, W. Szaflarski, P. Fucini, D. Kalpaxis, K. H. Nierhaus, *Mol. Cell* **2004**, 13, 113
- 55 Tourigny, D. S.; Fernández, I. S.; Kelley, A. C.; Vakiti, R. R.; Chattopadhyay, A. K.; Dorich, S.; Hanessian, S.; Ramakrishnan, V. *J. Mol. Biol.* **2013**, 425, 3907–3910.
- 56 Lu, W.; Roongsawang, N.; Mahmud, T. *Chemistry & Biology* **2011**, 18, 425–431.
- 57 Hanessian, S.; Vakiti, R. R.; Chattopadhyay, A. K.; Dorich, S.; Lavallée, C. *Bioorg. Med. Chem.* **2013**, 21, 1775–1786.
- 58 Ito, T.; Roongsawang, N.; Shirasaka, N.; Lu, W.; Flatt, P. M.; Kasanah, N.; Miranda, C.; Mahmud, T. *ChemBioChem* **2009**, 10 (13), 2253–2265.
- 59 Otoguro, K.; Iwatsuki, M.; Ishiyama, A.; Namatame, M.; Nishihara-Tukashima, A.; Shibahara, S.; Kondo, S.; Yamada, H.; Ōmura, S. *J. Antibiot.* **2010**, 63, 381–384.
- 60 Almabruk, K. H.; Lu, W.; Li, Y.; Abugreen, M.; Kelly, J. X.; Mahmud, T. *Org. Lett.* **2013**, 15, 1678–1681.
- 61 Sharpe, R. J.; Malinowski, J. T.; Johnson, J. S. *J. Am. Chem. Soc.* **2013**, 135, 17990.
- 62 Sharpe, R. J.; Malinowski, J. T.; Sorana, F.; Luft, J. C.; Bowerman, C. J.; DeSimone, J. M.; Johnson, J. S. *Bioorg. Med. Chem.* **2015**, 23, 1849–1857.
- 63 Abugrain, M. E.; Lu, W.; Li, Y.; Serrill, J. D.; Brumsted, C. J.; Osborn, A. R.; Alani, A.; Ishmael, J. E.; Kelly, J. X.; Mahmud, T. *ChemBioChem* **2016**, 17, 1585–1588.
- 64 Abugrain, M. E.; Brumsted, C. J.; Osborn, A. R.; Philmus, B.; Mahmud, T. *ACS Chem. Biol.* **2017**, 12, 362–366.
- 65 Tsujimoto, T., Nishikawa, T., Urabe, D., Isobe, M. *Synlett* **2005**, 2005, 433.
- 66 Knapp, S., Yu, Y. *Org. Lett.* **2007**, 9, 1359.
- 67 Haussener, T. J., Looper, R. E. *Org. Lett.* **2012**, 14, 3632.
- 68 Malinowski, J. T., McCarver, S. J., Johnson, J. S. *Org. Lett.* **2012**, 14, 2878.
- 69 Matsumoto, N., Tsujimoto, T., Nakazaki, A. Isobe, M. Nishikawa, T. *RSC Adv.* **2012**, 2, 9448.
- 70 Yamaguchi, M., Hayashi, M. Hamada, Y. Nemoto, T. *Org. Lett.* **2016**, 18, 2347
- 71 Gerstner, N. C., Adams, C. S., Grigg, R. D., Tretbar, M., Rigoli, J. W. Schomaker, J. M. *Org. Lett.* **2016**, 18, 284
- 72 Hanessian, S.; Vakiti, R. R.; Dorich, S.; Banerjee, S.; Lecomte, F.; DelValle, J. R.; Zhang, J.; Deschênes-Simard, B. *Angew. Chem. Int. Ed.* **2011**, 50, 3497.
- 73 Hanessian, S. Vakiti, R. R., Dorich, S., Banerjee, S. Deschênes-Simard, B. *J. Org. Chem.* **2012**, 77, 9458.
- 74 Malinowski, J. T., Sharpe, R. J., Johnson, J. S. *Science* **2013**, 340, 180.
- 75 Sharpe, R. J., Malinowski, J. T., Johnson, J. S. *J. Am. Chem. Soc.* **2013**, 135, 17990.

-
- 76 Weller, D. D.; Rinehart, K. L. *J. Am. Chem. Soc.* **1978**, *100*, 6757–6760.
- 77 Rinehart, K. L., Jr.; Weller, D. D.; Pearce, C. J. *J. Nat. Prod.* **1980**, *43*, 1-20.
- 78 Rinehart, K. L.; Potgieter, M.; Delaware, D. L.; Seto, H. *J. Am. Chem. Soc.* **1981**, *103*, 2099–2101.
- 79 Kudo, F.; Kasama, Y.; Hirayama, T.; Eguchi, T. *J Antibiot (Tokyo)* **2007**, *60*, 492-503.
- 80 Ito, T.; Roongsawang, N.; Shirasaka, N.; Lu, W.; Flatt, P. M.; Kasanah, N.; Miranda, C.; Mahmud, T. *Chembiochem* **2009**, *10*, 2253-2265.
- 81 Hirayama, A.; Eguchi, T.; Kudo, F. *Chembiochem* **2013**, *14*, 1198-1203.
- 82 Rinehart, K. L., Jr. *Jpn J Antibiot* **1979**, *32 Suppl*, S32-46
- 83 Averill, B. A.; Herskovitz, T.; Holm, R. H.; Ibers, J. A. *J. Am. Chem. Soc.* **1973**, *95*, 3523.
- 84 Inoue, H.; Fujimoto, N.; Imoto, E. *J. Chem. Soc., Chem. Commun.* **1977**, *0*, 412–413.
- 85 Inoue, H.; Suzuki, M.; Fujimoto, N. *J. Org. Chem.* **1979**, *44*, 1722–1724.
- 86 Kudo, F.; Hoshi, S.; Kawashima, T.; Kamachi, T.; Eguchi, T. *J. Am. Chem. Soc.* **2014**, *136*, 13909–13915

**Chapter 2. Formation of 3-Aminoacetophenone Moiety and Evidence for
Glycosylation of An Acyl Carrier Protein-bound Polyketide Intermediate in
Pactamycin Biosynthesis**

Since its discovery more than 50 years ago, pactamycin (**1**) has attracted considerable attention from chemists and biologists alike due to its unique chemical structure and potent biological activity. Its chemical structure consists of a highly decorated cyclopentitol core unit, a 3-aminoacetophenone (3AAP), a 6-methylsalicylic acid (6-MSA), and a *N,N*-dimethylurea (Figure 2.1). It has been proposed that the core cyclopentitol unit is derived from glucose (Glc) or *N*-acetylglucosamine (GlcNAc).¹ The 3AAP moiety is derived from 3-aminobenzoic acid (3ABA), a shunt product of dehydroshikimic acid (DHS). Conversion of DHS to 3ABA is catalyzed by PtmT (or PctV), a unique PLP-dependent aminotransferase-aromatase enzyme.²⁻⁴ The 6-MSA moiety is produced by the iterative type

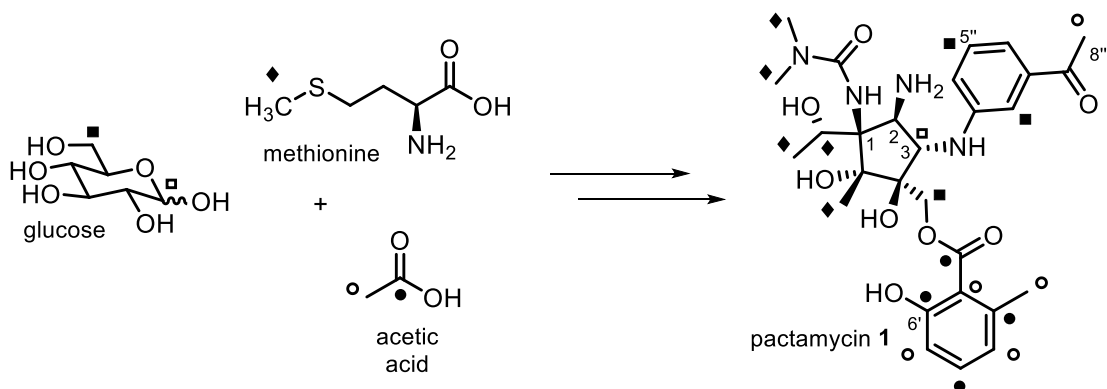


Figure 2.1. Biosynthetic origin of pactamycin

polyketide synthase PtmQ (PctS).⁵ A number of tailoring processes, e.g., amination, carbamoylation (urea formation), *C*- and *N*-methylations, and hydroxylation, are involved in the pathway prior to the attachment of the 6-MSA unit by PtmR in the last step, resulting in a highly decorated aminocyclopentitol unit that is rich in stereocenters (Figure 2.1)

Although direct involvement of 3ABA in pactamycin biosynthesis had been established,^{2,3} the process underlying its conversion to the 3AAP moiety was not well understood. On the basis of the putative functions of genes within the pactamycin cluster, two plausible pathways have been proposed for the formation of the 3AAP moiety. The first one involves the putative AMP-forming acyl-CoA synthetase PtmS (PctU), which may convert 3ABA to 3ABA-AMP, followed by coupling between 3ABA-AMP and acetyl-CoA to give β -ketoacyl CoA ester.⁶ Hydrolysis of the β -ketoacyl-CoA by the putative hydrolase PtmO (PctQ) followed by a decarboxylation reaction would give 3AAP (Figure 2.2, path A).⁶

The other pathway involves PtmS and discrete polyketide enzymes, PtmI (PctK) (an acyl carrier protein, ACP), and PtmK (PctM) (a β -ketoacyl-ACP synthase, KAS) (Figure 2.2, path B).⁵ PtmK is similar to KAS I/II, which is responsible for the elongation steps in fatty acid biosynthesis.^{7,8} In this scenario, PtmS is proposed to activate 3ABA and load it to the ACP PtmI (PctK), whereas PtmK is proposed to catalyze condensation between 3ABA-ACP and malonyl-ACP. PtmO is proposed to act as a hydrolase, which cleaves the PKS product from the ACP (PtmI), or as an acyltransferase, which is involved in the loading of malonyl-CoA to the ACP. However, no experimental evidence is available to support any of these pathways or to determine the mode of formation of the 3AAP moiety. The mode of formation of the cyclopentitol unit in pactamycin is also unknown. Through incorporation studies using isotopically labeled precursors, Rinehart and co-workers have shown that this portion of the molecule is derived from glucose, presumably via *N*-

acetylglucosamine (GlcNAc). More recently, following the identifica-

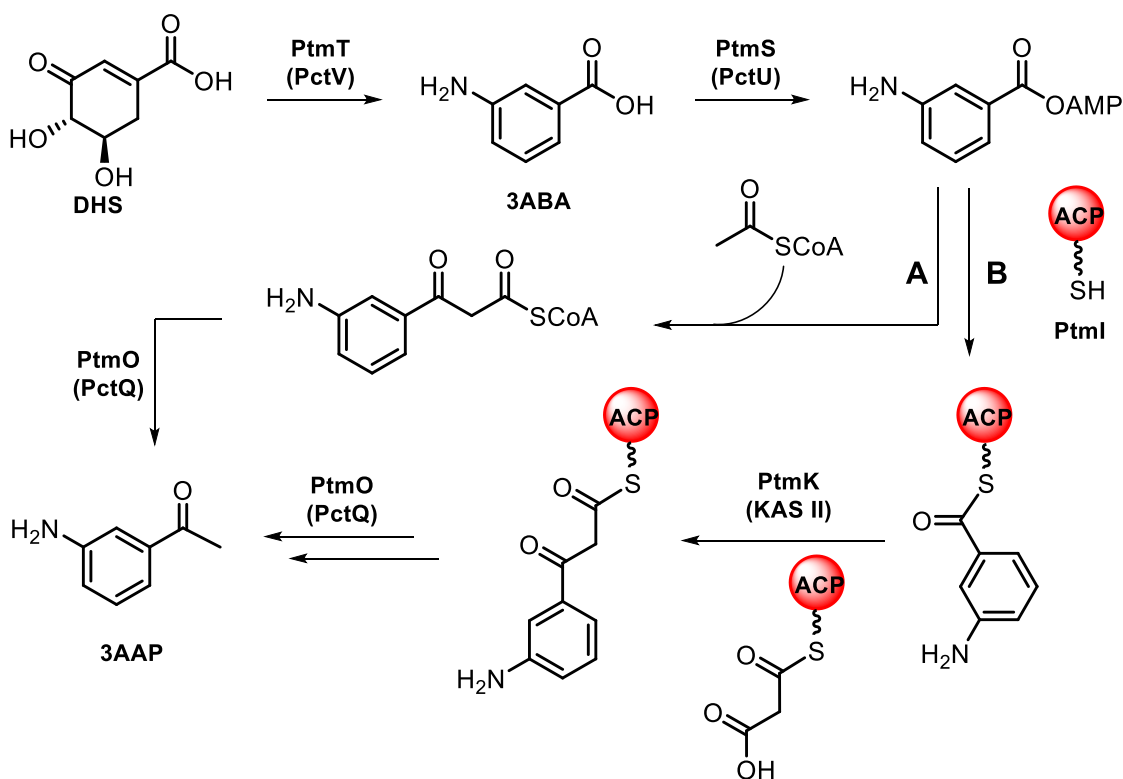


Figure 2.2. Proposed pathways from 3ABA to 3AAP

tion of the pactamycin biosynthetic gene clusters in *Streptomyces pactum*, it was proposed that a radical SAM-dependent enzyme (PtmC or PctE), a putative glycosyltransferase (PtmJ or PctL), and a putative deacetylase (PtmG or PctI) are involved in the formation of the cyclopentitol core, and that this process is similar to the formation of the mitosane core structure during mitomycin biosynthesis.^{5,6,9} In mitomycin biosynthesis, however, D-glucosamine (or its derivative) is assembled into the mitosane unit through condensation with 3-amino-5-hydroxybenzoic acid (AHBA). Although details for this reaction are not available, it was proposed that a PtmJ (PctL) homologue, MitB, mediates

the condensation reaction, followed by an unknown mechanism to complete the C-C bond formation.¹⁰ In fact, the glycosyltransferase PtmJ (PctL) from *S. pactum* has been shown to catalyze a coupling reaction between UDP-*N*-acetyl- α -D-glucosamine and 3AAP.⁶ The product would then need to undergo deacetylation, possibly by the *N*-deacetylase homologue PtmG (PctI) followed by radical-mediated rearrangement by PtmC (PctE) to form the cyclopentitol ring structure. Inactivation of the *ptmC* and *ptmJ* genes indeed abolished the production of pactamycin.⁵

Despite the ability of PtmJ (PctL) to glycosylate 3AAP, our incorporation studies showed that 3AAP is not able to rescue the production of pactamycin in the $\Delta ptmT$ mutant strain of *S. pactum*, which lacks the ability to produce 3ABA,² suggesting that 3AAP is not an intermediate in the pactamycin pathway (data not shown).³ These results prompted us to investigate the mode of formation of the 3AAP unit in pactamycin biosynthesis and the timing of the glycosylation reaction catalyzed by PtmJ. In the present study, we used genetic, chemical complementation, and biochemical approaches to interrogate the formation of the 3AAP unit of pactamycin and the timing of the glycosylation reaction. The results revealed the involvement of discrete polyketide synthase proteins in the formation of the 3AAP unit and an unprecedented glycosylation of an ACP-bound polyketide intermediate.

RESULTS:

Involvement of the discrete polyketide synthase proteins in 3AAP formation.

During our recent study on the tailoring processes in pactamycin biosynthesis, we discovered that *ptmS* (*PctU*), *ptmI* (*PctK*), *ptmK* (*PctM*), and *ptmO* (*PctQ*) are not involved in the transfer of 6-MSA to the aminocyclopentitol unit, but they seem to play a critical role in the early steps of the pathway.¹¹ To confirm that result and to explore the role of these genes in pactamycin biosynthesis, in this study we inactivated the *ptmI*, *ptmK*, or *ptmO* genes in $\Delta ptmH$ mutant strain, which produces pactamycin analogues, TM-025 and TM-026 (Figure S1). The $\Delta ptmH$ mutant was used because the products are chemically more stable and produced in higher yields than pactamycin. The mutants were constructed by in-frame deletion strategy, except for $\Delta ptmH/ptmK::aac(3)IV$, which was generated using a gene disruption method, as attempts to obtain in-frame deletion mutants of *ptmK* were unsuccessful. The resulting $\Delta ptmH/\Delta ptmI$, $\Delta ptmH/ptmK::aac(3)IV$, and $\Delta ptmH/\Delta ptmO$ mutants were cultured and the products were analyzed by ESI-MS. As expected, the results showed that inactivation of *ptmI*, *ptmK*, or *ptmO* in the $\Delta ptmH$ mutant entirely abolished the production of TM-025/TM-026 (Figure S2a-c). In addition, the mutants did not give any detectable intermediates, which based on our observation with other *S. pactum* mutants, indicates that the gene products are involved early in the pathway.^{5,12} Chemical incorporation experiments with 3-ABA in these mutants did not give any products, consistent with the notion that these discrete polyketide synthase enzymes play a role in the conversion of 3ABA to the 3AAP moiety.

Synthesis and evaluation of N-acetylcysteamine (NAC) thioesters of 3ABA and 3-[3-aminophenyl]3-oxopropionate (3AP-3OP).

Based on the above results, we hypothesized that 3ABA is activated by PtmS and loaded onto the acyl carrier protein PtmI. Claisen condensation between 3ABA-ACP and malonyl-ACP catalyzed by PtmK would give 3-[3-aminophenyl]3-oxopropionyl-ACP. To test this hypothesis, we synthesized *N*-acetylcysteamine (NAC) thioesters of 3ABA and 3-[3-

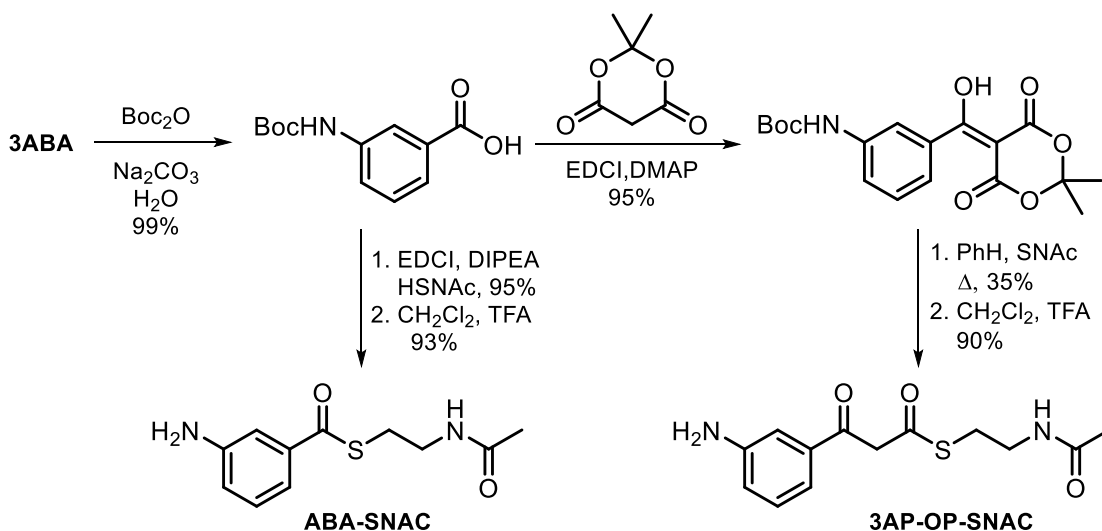
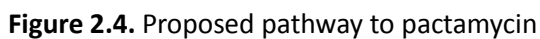


Figure 2.3. Synthesis of ABA-SNAC and 3AP-OP-SNAC

aminophenyl]3-oxopropionate (3AP-3OP), which mimics the β -ketoacyl-ACP. 3ABA-SNAC was synthesized from Boc-protected 3ABA and NAC in the presence of 1-ethyl-3-(3-dimethylaminopropyl)carbodiimide (EDCI) and 4-dimethylaminopyridine (DMAP) followed by Boc removal using trifluoroacetic acid (TFA) (Figure 2.3). 3AP-3OP-SNAC was also synthesized from Boc-protected 3ABA employing a dehydrative coupling reaction with Meldrum's acid (Figure 2.3). Thermal decarboxylation and *in situ* trapping of the



3AP-3OP-SNAC was also added to cultures of *ΔptmS*, *ΔptmI*, *ΔptmK*, *ΔptmH/ΔptmI*, and *ΔptmH/ptmK::aac(3)IV* mutants. Interestingly, the compound was unable to rescue the production of pactamycin or TM-025/TM-026 in these mutants. However, as discrete polyketide and fatty acid synthases usually work in concert, this result is not entirely unexpected. We propose that PtmS, PtmI, and PtmK need to form a suitable complex to function properly and that the synthetic β -ketoacyl intermediate has to be loaded initially onto PtmI, presumably through the ketosynthase. (Figure 2.4).

Isolation of GlcNAc-3AAP in culture broths of mutants incubated with 3AP-3OP-SNAC.

Whereas the *ΔptmS*, *ΔptmI*, *ΔptmK*, *ΔptmH/ΔptmI*, and *ΔptmH/ptmK::aac(3)IV* mutants incubated with 3AP-3OP-SNAC did not produce pactamycin or TM-025/TM-026, they produced a new product with a molecular formula of $C_{16}H_{22}N_2O_6$ (m/z 361.1370 $[M+Na]^+$, Figure S2d-e). Further analysis of the product by MS/MS and direct comparisons of the product with synthetically prepared authentic compound confirmed the identity of the product to be GlcNAc-3AAP. This product may be due to unspecific hydrolysis of the NAC thioester by the putative hydrolase PtmO. The resulting β -ketoacid would then undergo non-enzymatic decarboxylation to give 3AAP, which is subsequently glycosylated by the glycosyltransferase PtmJ to give GlcNAc-3AAP (Figure 2.4, dashed arrows). The latter compound, however, is accumulated in the culture, suggesting that it is not an intermediate in pactamycin biosynthesis as previously suggested.⁶

To confirm that GlcNAc-3AAP is not involved in the pathway, the compound was chemically synthesized and added to cultures of the $\Delta ptmH/\Delta ptmT$ and $\Delta ptmJ$ mutants. Since PtmT is an aminotransferase responsible for the synthesis of 3ABA, the $\Delta ptmH/\Delta ptmT$ mutant lacks the ability to produce any pactamycin analogs. If GlcNAc-3AAP is involved in the pathway, it should be able to rescue the production of TM-025/TM-026 and pactamycin in $\Delta ptmH/\Delta ptmT$ and $\Delta ptmJ$, respectively. As expected, analysis of the extracts by ESI-MS showed that GlcNAc-3AAP did not give any products in these mutants. Similarly, incorporation experiments with 3AAP in cultures of $\Delta ptmH/\Delta ptmT$ and $\Delta ptmJ$ mutants also did not give any pactamycin products, confirm

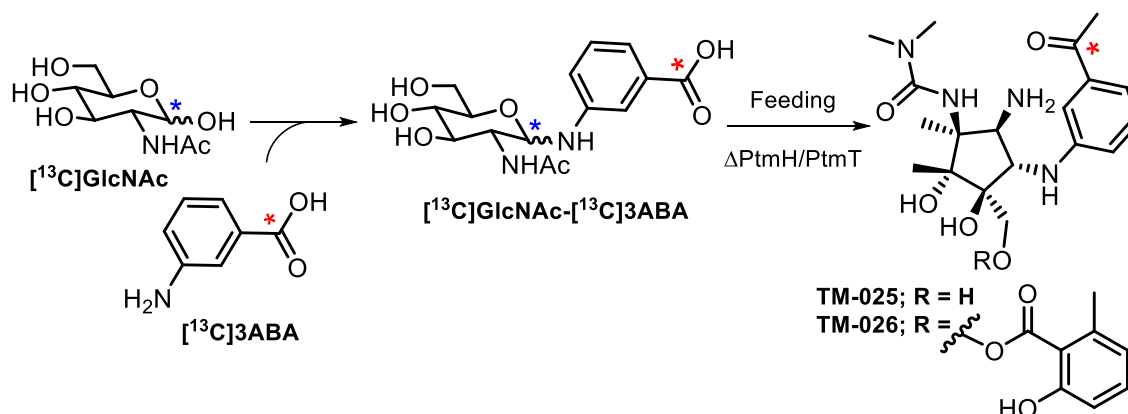


Figure 2.5 Synthesis of $[^{13}\text{C}]\text{GlcNAc}-[^{13}\text{C}]\text{3ABA}$ and feeding $\Delta ptmH/\Delta ptmT$

ing that 3AAP is not involved in the pathway. Further, GlcNAc-3ABA was synthesized and added to cultures of the same mutants. Surprisingly, this compound was able to rescue the production of TM-025/TM-026 in the $\Delta ptmH/\Delta ptmT$ mutant but not in the $\Delta ptmJ$ mutant (figures S4 and S5). The results raised a question whether the compound was incorporated into the pathway intact or underwent hydrolysis (of the sugar) to give

3ABA, which is a natural precursor of pactamycin. To address this question, we synthesized doubly ^{13}C -labeled $[^{13}\text{C}]\text{GlcNAc}-[^{13}\text{C}]\text{3ABA}$ by coupling of *N*-acetyl- $[1-^{13}\text{C}]\text{glucosamine}$ and 3-amino- $[1-^{13}\text{C}]\text{benzoic acid}$ and added the compound into the cultures of $\Delta\text{ptmH}/\Delta\text{ptmT}$ mutant (Figure 2.5). MS analysis of the products (TM-025 and TM-026) showed *m/z* values of 396.19 and 530.23, respectively (Figure 2.6 and Figure S5), which indicate the products only bear single isotope enrichment, indicating that the compound undergoes hydrolysis to $[^{13}\text{C}]\text{3ABA}$.

Characterization of the hydrolase PtmO.

The formation of GlcNAc-3AAP from 3AP-3OP-SNAC in cultures of ΔptmS , ΔptmI , ΔptmK , $\Delta\text{ptmH}/\Delta\text{ptmI}$, and $\Delta\text{ptmH}/\text{ptmK}::\text{aac}(3)/\text{IV}$ mutants is believed to be due to unspecific hydrolysis of the NAC thioester by the putative hydrolase PtmO, followed by non-enzymatic decarboxylation and glycosylation by PtmJ. To confirm that PtmO is responsible for the hydrolysis of 3AP-3OP-SNAC, the compound was added to cultures of the ΔptmO mutant. As expected, the mutant neither produced pactamycin nor GlcNAc-3AAP, suggesting the hydrolytic activity of PtmO and its important role in pactamycin biosynthesis. This was subsequently biochemically confirmed by incubating 3AP-3OP-SNAC with purified recombinant PtmO, which gave 3AAP as product (figure S9). No product was observed when boiled PtmO was used. The results confirm the activity of PtmO as a hydrolase, and also indicate that the β -ketoacid product can indeed undergo a spontaneous decarboxylation reaction.

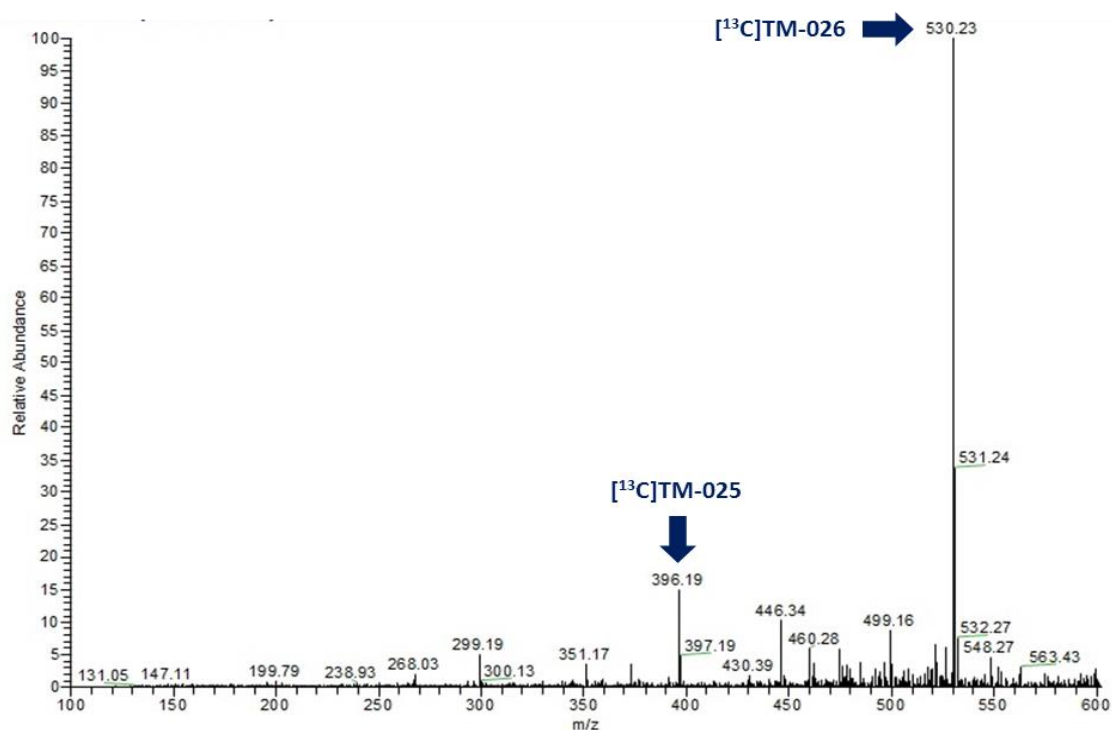


Figure 2.6. MS result of feeding [^{13}C]GlcNAc-[^{13}C]3ABA to $\Delta ptmH/\Delta ptmT$

PtmJ is a promiscuous glycosyltransferase.

Although GlcNAc-3AAP is not an intermediate in the pactamycin pathway, its production by the *S. pactum* strains when incubated with 3AAP indicates the relaxed substrate specificity of PtmJ. To explore the extent of the promiscuity of PtmJ, we tested a number of phenylamines, i.e. aniline (AN), 3-fluoroaniline (3FAN), and 4-fluoroaniline (4FAN), by incorporating the compounds individually to the cultures of $\Delta ptmH/\Delta ptmT$ mutant. Analysis of the extracts of the culture broths by ESI-MS revealed the ability of the mutant to glycosylate the phenylamines to give GlcNAc-AN, GlcNAc-3FAN, and GlcNAc-4FAN (Figure S5). The products were isolated chromatographically and their chemical structures were characterized by NMR. Interestingly, besides the GlcNAc products, glucosyl

aniline (Glc-AN), Glc-3FAN, and Glc-4FAN were also produced, suggesting that PtmJ not only recognizes NDP-GlcNAc, but also NDP-glucose, as donor sugar. To rule out the possibility that other glycosyltransferases are involved in this reaction, we added 3AAP, AN, 3FAN, and 4FAN individually to cultures of the $\Delta ptmJ$ mutant.⁵ Analysis of the extracts by ESI-MS did not show any glycosylated 3AAP or ANs, confirming that PtmJ is the sole enzyme responsible for the formation of the glycosylated phenylamines in *S. pactum*.

To confirm the activity of PtmJ and its promiscuity *in vitro*, we cloned the gene in the expression vector pRSET B and transferred the plasmid into *E. coli* BL21 $\Delta DE3$ pLysS. The expression of the gene was induced by isopropyl β -D-thiogalactopyranoside (IPTG) to give a high amount of recombinant protein. However, the PtmJ protein was mostly produced in insoluble form. Attempts to obtain more soluble protein by modifying growth and induction conditions, e.g., varying growth temperature, time of induction, and/or IPTG concentration as well as by using an alternative expression vector (pET20b) were not successful. We subsequently carried out enzymatic reactions using whole cell extracts. These extracts were incubated with 3AAP, AN, 3FAN, 4FAN, and 3ABA individually in the presence of UDP-GlcNAc and Mg^{2+} . The reaction mixtures were incubated for 4 h at 28 °C and the products were analyzed by ESI-MS. The results showed the formation of GlcNAc-3AAP, GlcNAc-AN, and GlcNAc-3FAN in these reactions, whereas those using extracts of *E. coli* harboring empty vector did not give any products (Figure S6). Parallel experiments using cell-free extract (soluble portion only) also gave similar results, suggesting that PtmJ was actually produced in soluble form, albeit in a low quanti-

ty. Interestingly, despite its structure similarity to 3AAP, 3ABA was not processed by PtmJ (Figure S7). In addition to the above *in vitro* experiments, we carried out *in vivo* enzymatic reactions by adding the individual substrates directly to the cultures of *E. coli* harboring the gene 2 h after IPTG induction. The cultures were agitated in an incubator shaker for 16 h, and the products were extracted with EtOAc and *n*-BuOH. Analysis of the products by ESI-MS revealed the production of GlcNAc-3AAP, GlcNAc-AN, GlcNAc-3FAN but not GlcNAc-3ABA, which is consistent with the results of the *in vitro* assays. None of these products were observed in cultures of *E. coli* harboring empty pRSET B fed with the substrates, indicating that their formation is catalyzed solely by PtmJ.

The proposed timing of glycosylation in pactamycin biosynthesis.

The above results unambiguously showed that neither 3ABA nor 3AAP is the natural substrate for PtmJ. The data also ruled out the possibility of free 3AAP and GlcNAc-3AAP as intermediates in the pathway, suggesting that the glycosylation reaction must take place during the conversion from 3ABA to the 3AAP moiety, which is catalyzed by discrete polyketide synthase enzymes (Figure 2.4). Therefore, it may be proposed that the substrate for PtmJ is an ACP-bound polyketide intermediate. Although both 3ABA-SNAC and 3AP-3OP-SNAC, which mimics the β -ketoacyl-ACP, can rescue the production of TM-025/TM-026 in $\Delta ptmH/\Delta ptmT$ mutant, by default the latter intermediate is a more likely substrate for PtmJ.

DISCUSSION:

3-Aminobenzoic acid (3ABA) is a common small molecule used in synthetic organic chemistry, but its occurrence in nature is rare. Consequently, its biosynthesis has only been established very recently.^{2,3} In pactamycin biosynthesis, 3ABA has been shown to be the precursor of the 3AAP moiety.^{1,2,13} In this study, we showed that the conversion of 3ABA to 3AAP moiety is catalyzed by a set of discrete polyketide synthase enzymes, PtmS, Ptml, and PtmK. PtmS is a putative AMP-forming acyl-CoA synthetase, which is postulated to convert 3ABA to 3ABA-AMP and then load it to the ACP Ptml. PtmK is similar to β -ketoacyl-ACP synthases (KAS) I/II, which are responsible for the elongation steps in fatty acid biosynthesis.^{7,8} Another stand-alone KAS protein (PtmR) in the pathway was also considered as a candidate enzyme involved in 3AAP formation; however, we recently identified that this protein catalyzes the transfer of 6-MSA from the iterative type I PKS, PtmQ, to an aminocyclopentitol unit.¹¹ The putative hydrolase PtmO is proposed to catalyze the cleavage of the PKS product from Ptml. Inactivation of *ptmS*, *ptml*, *ptmK*, or *ptmO* in *S. pactum* or Δ *ptmH* entirely abolished the production of pactamycin, TM-025/TM-026, or any other intermediates, indicating that the gene products are necessary for pactamycin biosynthesis, and are most likely involved early in the pathway. As observed in many discrete polyketide and fatty acid synthases, PtmS, Ptml, and PtmK may be produced as a multi-protein complex that works in concert. PtmS shares high sequence similarity with the adenylation domains in the loading modules of the rifamycin and ansamitocin PKSs (RifA and AsmA, respectively).^{14,15} The latter pro-

teins are part of multifunctional multimodular type I polyketide synthases that convert 3-amino-5-hydroxybenzoic acid (AHBA) to AHBA-AMP, which is then loaded onto an acyl carrier protein (ACP).^{15,16} The ability of 3AP-3OP-SNAC to rescue the production of TM-026 in $\Delta ptmH/\Delta ptmT$ (which contains a complete set of *ptmS*, *ptmI*, and *ptmK*) but not in mutant strains lacking either one of these genes supports this notion. However, further detailed studies are necessary to illuminate the nature of interactions between these discrete polyketide proteins.

Although 3AAP and GlcNAc-3AAP have been proposed to be part of pactamycin biosynthesis, these compounds appeared to have no direct involvement in the pathway. In addition, incorporation experiments and biochemical studies have also ruled out the possibility of glycosylation of 3ABA. While PtmJ can glycosylate 3AAP, this enzyme does not process 3ABA. Interestingly, GlcNAc-3ABA was able to rescue the production of TM-025/TM-026 when fed to $\Delta ptmH/\Delta ptmT$. However, incorporation studies using [¹³C]GlcNAc-[¹³C]3ABA revealed that this compound was first hydrolyzed to 3ABA before being incorporated into the pathway. On the other hand, 3ABA-SNAC and 3-[3-aminophenyl]3-oxopropionyl-SNAC, which resembles ACP-bound non-glycosylated polyketide extension of 3ABA, were both able to rescue the production of TM-025/TM-026 in $\Delta ptmH/\Delta ptmT$. These results not only confirmed the role of PKS in 3AAP formation but also indicated that glycosylation takes place after the formation of 3-[3-aminophenyl]3-oxopropionyl-ACP. While it is possible that 3ABA-SNAC is hydrolyzed to 3ABA prior to incorporation into the pathway, hydrolysis of 3AP-3OP-SNAC and sponta-

neous decarboxylation will result in 3AAP, which is not involved in the pactamycin biosynthesis. Therefore, the production of TM-026 by $\Delta ptmH/\Delta ptmT$ when incubated with 3AP-3OP-SNAC strongly suggests that 3AP-3OP-ACP is indeed involved in the pathway. Also, since 3AAP is not involved in the pathway, the glycosylation reaction should take place prior to PKS product hydrolysis, i.e., on an ACP-bound polyketide intermediate. Previously, Liu and coworkers reported the ability of the methymycin glycosyltransferase DesVII to process a NAC thioester of synthetically prepared linear polyketide chains.¹⁷ The result demonstrated the ability of a glycosyltransferase to process a linear polyketide intermediate, albeit less efficiently in comparison to when the natural substrate (a 12 membered ring methymycin aglycone) was used.¹⁷ Furthermore, the fact that GlcNAc-3AAP is not directly involved in pactamycin biosynthesis also suggests that additional modifications of the sugar moiety are required before the glycosylated β -ketoacyl product is cleaved from the ACP. These may include deacetylation of the GlcNAc moiety by the deacetylase PtmG, urea formation by the carbamoyltransferase PtmB, and/or rearrangement and cyclization to an aminocyclopentitol intermediate by the radical SAM protein PtmC. On the other hand, although UDP-GlcNAc has been proposed to be the sugar donor for the PtmJ reaction, the use of other activated sugars (e.g., modified UDP-GlcNAc) has not been ruled out. It is entirely possible considering the highly broad-spectrum nature of PtmJ. There are a number of enzymes within the pathway that have been proposed to be involved in the modifications of the cyclopentitol unit, such as the oxidoreductase PtmN, the aminotransferase PtmA, the carbamoyltransferase PtmB, and

the deacetylase PtmG.^{5,6} However, their functions have not been biochemically characterized. In fact, inactivation of these genes in *S. pactum* completely abolished the production of pactamycin with no intermediate compounds detected, suggesting that they are involved in the early steps of the biosynthetic pathway (unpublished data). Therefore, instead of modifying the cyclopentitol unit, several of these proteins may function as UDP-GlcNAc modifying enzymes. A similar set of enzymes have been reported in the biosynthesis of 2,3-diamino-2,3-dideoxy- α -D-glucopyranose (UDP-GlcN3N), which is part of lipid A variants found in certain Gram-negative bacteria, e.g., *Acidithiobacillus ferrooxidans*, *Leptospira interrogans*, and *Legionella pneumophila*.¹⁸

In conclusion, this study reveals new insights into the formation of 3AAP moiety of pactamycin, involving a set of discrete polyketide synthase proteins, and provides compelling evidence for the glycosylation of an ACP-bound polyketide intermediate by a highly broad-spectrum glycosyltransferase, PtmJ. In addition, we show that PtmO is a hydrolase enzyme that is responsible for the release of the glycosylated β -ketoacid product from the ACP, and the free β -ketoacid subsequently undergoes non-enzymatic decarboxylation. However, whether the oxidoreductase PtmN, the aminotransferase PtmA, the carbamoyltransferase PtmB, the deacetylase PtmG, and/or the radical SAM enzyme PtmC function before or after the release of the glycosylated polyketide intermediate remain to be determined. Further investigations on the unique biotransformation from a sugar molecule to a cyclopentitol (ribomimetic) are warranted, and will significantly advance our knowledge of how such transformations occurs in nature.

EXPERIMENTAL:

General: All chemical reactions were performed under an argon or nitrogen atmosphere employing oven-dried glassware. Analytical thin-layer chromatography (TLC) was performed using silica plates (60 Å) with a fluorescent indicator (254 nm), which were visualized with a UV lamp and ceric ammonium molybdate (CAM) solution. Chromatographic purification of products was performed on silica gel (60 Å, 72–230 mesh). Proton NMR spectra were recorded on Bruker 400, 500 or 700 MHz spectrometers. Proton chemical shifts are reported in ppm (δ) relative to the residual solvent signals as the internal standard (CDCl_3 : δ_{H} 7.26; D_2O : δ_{H} 4.79). Multiplicities in the ^1H NMR spectra are described as follows: s = singlet, bs = broad singlet, d = doublet, bd = broad doublet, t = triplet, bt = broad triplet, q = quartet, m = multiplet; coupling constants are reported in Hz. Carbon NMR spectra were recorded on a Bruker 300 (75 MHz) spectrometer with complete proton decoupling. Carbon chemical shifts are reported in ppm (δ) relative to the residual solvent signal as the internal standard (CDCl_3 : δ 77.16), or with sodium 2,2-dimethylsilapentane-5-sulphonate (DSS) (δ 0.0) as an external standard. Low-resolution electrospray ionization (ESI) mass spectra were recorded on a ThermoFinnigan liquid chromatograph-ion trap mass spectrometer, and high-resolution electrospray mass spectra were recorded on a Waters/Micromass LCT spectrometer. Size exclusion chromatography was done on Sephadex LH-20 (Pharmacia).

Construction of $\Delta ptmH/\Delta ptmI$, $\Delta ptmH/ptmK::aac(3)IV$, and $\Delta ptmH/\Delta ptmO$ mutants (Figure S1). The target genes were inactivated using gene in-frame deletion strategy. Two ~1 kb PCR fragments upstream (HindIII/EcoRI) and downstream (EcoRI/XbaI), of the *ptmI* and *ptmO* genes were fused and cloned into the HindIII/XbaI sites of pBluescript II SK(-) vector. The PCR products of *ptmI* and *ptmO* were excised and cloned into the HindIII/XbaI sites of pTMN002 to generate pTMM052 and pTMM08, respectively. All plasmids were then individually introduced into the $\Delta ptmH$ mutant strain of *S. pactum* by conjugation using the *E. coli* donor strain ET12567/pUZ8002. Apramycin resistant strains representing single crossover mutants were obtained and subsequently grown on BTT agar plates containing apramycin (50 μ g/mL). Apramycin sensitive colonies were counter-selected by replica plating on BTT agar with and without apramycin (50 μ g/mL). The resulting double-crossover candidate strains were confirmed by PCR amplification with F1 and R2 primers flanking the respective targeted gene.

Construction of $\Delta ptmH/ptmK::aac(3)IV$ (figure S1): The *ptmK* gene (1.7 kb) was inactivated using a gene disruption strategy. The internal fragment (0.88 kb) of *ptmK* was generated by PCR using a forward primer containing a HindIII site and a reverse primer containing a XbaI site, and *S. pactum* genomic DNA as a template. The PCR product was cloned into the HindIII/XbaI sites of pTMN002 to generate pTMM055. Plasmid pTMM055 was introduced into the *S. pactum* $\Delta ptmH$ strain by conjugation, as described by Kieser et al.¹ The freshly harvested spores and the overnight-grown *E. coli* ET12567/pUZ8002 containing plasmid pTMM055 were mixed and plated onto MS agar

plates containing MgCl_2 (10 mM). After incubation at 30 °C for 18 h, the plates were overlaid with sterile water (1 mL) containing nalidixic acid (1 mg/mL) and apramycin (1 mg/mL) and incubated at 30 °C for 5-7 days. The exconjugant (single crossover) colonies were purified by plating onto BTT agar plates supplemented with apramycin (50 $\mu\text{g/mL}$). Disruption of *ptmK* was confirmed by PCR amplification.

Synthesis of ABA-SNAC:

Synthesis of 3-((*tert*-butoxycarbonyl)amino)benzoic acid: 3-aminobenzoic acid: 3-aminobenzoic acid (1 g, 7.29 mmol) was added to an aqueous 1M solution of Na_2CO_3 (16 mL, 16 mmol, 2.2 eq.) and 0.025 mL of MeOH was added, followed by Boc-anhydride (1.67 g, 7.65 mmol, 1.05 eq) and the reaction stirred 12 h at room temperature. After reaching completion, the reaction was diluted with water and the pH was adjusted to pH 9 with 1M NaOH, washed with EtOAc (3 x 20 mL), the aqueous acidified with 1M HCl to pH 4 and extracted with EtOAc (3 x 30 mL), dried over Na_2SO_4 , filtered and volatiles removed in vacuo. 1.71 g, 99 %.²²

Synthesis of *S*-(2-acetamidoethyl) 3-((*tert*-butoxycarbonyl)amino)benzothioate: 3-((*tert*-butoxycarbonyl)amino) benzoic acid (237 mg, 1 mmol) was added under argon to a solution of Et_3N (0.288 mL, 2.07 mmol, 2.07 eq) in anhydrous CH_2Cl_2 (7.4 mL) and successively added EDCI-HCl (197.5 mg, 1.03 mmol, 1.03 eq) *N*-hydroxybenzotriazole (135.12 mg, 1.03 mmol, 1.03 eq) and *N*-acetylcysteamine (166.9 mg, 1.4 mmol, 1.4 eq.). The reaction was stirred at room temperature for 25 minutes when TLC indicated reac-

tion completion, then diluted with CH_2Cl_2 (3 mL), washed successively with saturated NaHCO_3 solution (1 x 5 mL), H_2O (1 x 10 mL), 1M HCl (1x 15 mL), and brine (1 x 5 mL), dried over Na_2SO_4 , filtered and volatiles removed in vacuo. The colorless residue was dissolved in EtOAc (10 mL) and added CuSO_4 -impregnated silica gel ($\text{CuSO}_4\text{-SiO}_2$, 2.4 g)¹⁹ and stirred 10 minutes to remove excess thiol, then passed through a small silica gel column to provide 217 mg (64% yield) of the title compound as a sticky foam. ^1H NMR (300 MHz, CDCl_3) δ 7.94 (s, 1H), 7.63 (t, J = 9 Hz, 2H), 7.37 (t, J = 8 Hz, 1H), 6.72 (br s, 1H), 5.95 (br s, 1H), 3.53 (dd, J = 6 Hz, 2H), 3.22 (t, J = 6 Hz, 2H), 1.97 (s, 3H), 1.53 (s, 9H). HR-ESI-MS: observed m/z 361.12061 $[\text{M}+\text{Na}]^+$, calculated. for $\text{C}_{16}\text{H}_{22}\text{N}_2\text{O}_4\text{SNa}$ m/z 361.11925 $[\text{M}+\text{Na}]^+$.

Synthesis of *S*-(2-acetamidoethyl) 3-aminobenzothioate (**3-ABA-SNAC**): Compound **5** (0.420 mmol, 100 mg) was dissolved in CH_2Cl_2 (0.320 mL, 1.31 M) under N_2 , then cooled in an ice bath. TFA (0.320 mL, 7.4 eq.) was added dropwise at 0 °C and stirred for 10 h at 0-10 °C when TLC indicated reaction completion. The mixture was diluted with CH_2Cl_2 (10 mL) and the reaction quenched at 0 °C by dropwise addition of NaHCO_3 -phosphate buffer solution (300 mg NaHCO_3 in 10 mL of pH 7 phosphate buffer), then extracted with CH_2Cl_2 (5 x 10 mL) and dried over MgSO_4 , filtered and volatiles removed *in vacuo*. Preparative TLC (Et_2O -MeOH = 200:10) provided analytically pure material. ^1H NMR (500 MHz, CDCl_3) δ = 7.38 (d, J = 8, 1H), 7.25 (m, 2H), 6.91 (d, J = 8, 1H), 5.98 (brs, 1H), 4.21-3.50 (brs, 1H), 3.55 (q, J = 6, 2H), 3.23 (t, J = 6, 2H), 1.99 (s, 3H). ^{13}C NMR (125 MHz, CDCl_3) δ = 192.5, 170.4, 146.8, 137.8, 129.6, 120.1, 117.6, 113.0, 77.3,

77.0, 76.8, 39.8, 28.6, 23.3 ppm. HR-ESI-MS: observed m/z 261.06675 $[M+Na]^+$; calculated for $C_{11}H_{14}N_2O_2SNa$ m/z 261.06682 $[M+Na]^+$.

Synthesis of 3AP-OP-SNAC:

Synthesis of *tert*-butyl(3-((2,2-dimethyl-4,6-dioxo-1,3-dioxan-5-ylidene) (hydroxy) methyl)phenyl) carbamate (**SI-2**): Under an atmosphere of nitrogen, Boc-ABA (4.21 mmol, 1 g), was suspended in CH_2Cl_2 (21 mL, 0.2 M) and added *N,N'*-dimethylaminopyridine (DMAP) (5.47 mmol, 669 mg, 1.3 eq.) followed by EDCI-HCl (4.84 mmol, 929 mg, 1.15 eq.). Meldrum's acid (4.42 mmol, 637 mg, 1.05 eq.) was then added at room temperature and the reaction was stirred at this temperature for 14 h until the reaction was complete as indicated by TLC ($Et_2O-EtOAc = 1: 2$, vanillin stain). The reaction was diluted with CH_2Cl_2 (20 mL), washed with 0.5 M HCl (3 x 20 mL), then H_2O (1 x 100 mL) and brine (1 x 50 mL). The organics were dried over Na_2SO_4 , filtered and volatiles were removed *in vacuo* to yield the title compound (1.47 g, 96%) as an orange foam which was used in the next step without further purification. 1H NMR (300 MHz, $CDCl_3$) δ 15.39 (s, 1H), 7.68 (s, 1H), 7.58 (d, $J = 8$ Hz, 1H), 7.47-7.27 (m, 2H), 6.59 (s, 1H), 1.84 (s, 6H), 1.51 (s, 9H). LRMS ESI-(+) found m/z 364.2 $[M+H]^+$; m/z 386.2 $[M+Na]^+$. HR-ESI-MS: observed m/z 386.12136 $[M+Na]^+$, calculated. for $C_{18}H_{21}NO_7Na$ m/z 386.12102 $[M+Na]^+$. ^{13}C NMR (75 MHz, $CDCl_3$) δ 189.3, 152.6, 138.6, 133.9, 128.9, 124.0, 123.1, 119.0, 105.1, 91.2, 81.1, 28.4, 27.0 ppm; IR data (cm^{-1}): 3333, 2981, 1727, 1673, 1559, 1397, 1289, 1236, 1159, 460.

Synthesis of *S*-(2-acetamidoethyl) 3-(3-((*tert*-butoxycarbonyl)amino)phenyl)-3-oxopropanethioate (**Boc-3AP-OP-SNAC**): Meldrum's adduct (**SI-2**, 0.949 mmol, 345 mg) was added to a solution of *N*-acetylcysteamine (1.72 mmol, 102 mg) in benzene (9.5 mL, 0.1 M) under argon. The mixture was placed in a 90 °C oil bath and stirred 12 h at this temperature until the reaction was complete by consumption of starting material by TLC. The reaction mixture was cooled to room temperature and concentrated to a low volume under vacuum, then diluted with EtOAc (25 mL). The resulting solution was added CuSO₄-SiO₂ (1 g) and stirred at room temperature for 1 h under N₂, and added CuSO₄-impregnated silica gel (CuSO₄-SiO₂, 1 g)²⁰ and stirred for 10 min to remove excess thiol, then passed through a small silica gel column to provide a mixture of **Boc-3AP-OP-SNAC** and its enol tautomer in a ratio of 3:2 (116 mg, 32%). ¹H NMR (300 MHz, CDCl₃) δ 12.99 (s, 1H), 7.90 (s, 1H), 7.80 (s, 1H), 7.63 (d, *J* = 8 Hz, 1H), 7.52 (d, *J* = 8 Hz, 1H), 7.45 (d, *J* = 8 Hz, 1H), 7.41-7.39 (m, 3H), 6.94 (s, 1H), 6.23 (s, 2H), 6.03 (s, 1H), 4.15 (s, 2H), 3.42 (m, 4H), 3.05 (m, 4H), 1.92 (s, 3H), 1.89 (s, 3H), 1.46 (s, 18H). ¹³C NMR (75 MHz, CDCl₃) δ 194.8, 192.7, 192.2, 170.9, 170.7, 169.3, 153.0, 152.9, 139.6, 139.2, 136.6, 133.5, 129.5, 129.4, 124.0, 122.9, 122.0, 121.0, 118.6, 116.5, 97.3, 80.9, 77.6, 77.2, 76.7, 60.5, 53.9, 39.9, 39.2, 29.5, 28.4, 28.3, 23.3, 23.1, 21.1, 14.3 ppm. IR data (cm⁻¹): 3320, 3077, 2978, 1702, 1608, 1588, 1544, 1240, 1160. HR-ESI-MS: observed *m/z* 403.13066 [M+Na]⁺, calculated. for C₁₈H₂₄N₂O₅SNa *m/z* 403.12981 [M+Na]⁺.

Synthesis of *S*-(2-Acetamidoethyl)3-(3-Aminophenyl)-3-Oxopropanethioate (**3AP-OP-SNAC**): Boc-3AP-OP-SNAC (0.263 mmol, 100 mg) was dissolved in CH₂Cl₂ (0.2 mL,

1.78 M) under N₂, then cooled in an ice bath. TFA was added dropwise at 0 °C and stirred for 8 h at a temperature range of 0 to 10 °C until the reaction was completed by TLC. The mixture was diluted with CH₂Cl₂ (10 mL) and the reaction was quenched at 0 °C by dropwise addition of NaHCO₃-phosphate buffer solution (300 mg NaHCO₃ in 10 mL, pH 7, phosphate buffer), then extracted with CH₂Cl₂ (5 x 10 mL) and dried over Na₂SO₄, filtered and volatiles removed in vacuo. After chromatography (Et₂O–MeOH = 100:5 to 50:5), the title compound was obtained as a yellow oil (59 mg, 80%). ¹H NMR (300 MHz, DMSO-*d*₆) δ 13.34 – 12.70 (m, 1H), 8.03 (m, 2H), 7.28 – 6.93 (m, 6H), δ 6.84 (d, *J* = 8 Hz, 1H), 6.74 (d, *J* = 8 Hz, 1H), 6.26 (s, 1H), 5.36 (s, 1H), 4.33 (s, 2H), 3.42 (m, 4H), 3.04 (t, *J* = 6.5 Hz, 2H), 2.94 (t, *J* = 6.5 Hz, 2H), 1.80 (s, 3H), 1.79 (s, 3H). ¹³C NMR (75 MHz, DMSO-*d*₆) δ 193.9, 192.9, 192.6, 169.2, 169.1, 149.1, 149.0, 136.6, 132.6, 129.2, 129.2, 119.2, 117.5, 116.4, 113.9, 112.7, 111.3, 96.5, 53.5, 40.4, 40.1, 39.8, 39.5, 39.2, 39.0, 38.7, 38.3, 38.0, 28.5, 27.7, 27.0, 22.5 ppm. LR-ESI-MS: found *m/z* 281 [M+H]⁺; *m/z* 303.1 [M+Na]⁺. IR data (cm⁻¹): 3409, 3005, 2918, 1658, 1435, 1022, 953, 706. HR-ESI-MS: observed *m/z* 303.07806 [M+Na]⁺, calculated. for C₁₃H₁₆N₂O₃SNa *m/z* 303.07738 [M+Na]⁺.

Synthesis of *N*-Acetyl-*D*-glucosaminy-1-aminoacetophenone (GlcNAc-1-AAP).

N-acetyl-*D*-glucosamine (GlcNAc) (2.0 mmol, 442 mg) and 3AAP (2.0 mmol, 135 mg) were added 15 mL MeOH followed by 5.0 mL of acetic acid, and the mixture was stirred at room temperature 18h. After removal of the solvent, the residue was directly purified by silica-gel chromatography using CHCl₃–CH₃OH (20:1 to 6:3). The glycosylated product was recrystallized from the MeOH solution to give a yellow compound (50 mg). ¹H NMR

(500 MHz, CD₃OD) δ 7.34 (d, J = 8 Hz, 1H), 7.26 (dd, J = 14, 6 Hz, 2H), 6.93 (dd, J = 8, 2 Hz, 1H), 4.86 (s, 10H), 4.63 (d, J = 9 Hz, 1H), 3.86 (dd, J = 20, 11 Hz, 2H), 3.71 (d, J = 5 Hz, 1H), 3.55 (d, J = 10 Hz, 1H), 3.40 (d, J = 7 Hz, 2H), 3.33 (d, J = 19 Hz, 3H), 2.55 (d, J = 6 Hz, 3H), 1.98 (d, J = 5 Hz, 3H).

Synthesis of [¹³C]GlcNAc-[¹³C]3ABA. *N*-acetyl-D-[1-¹³C]glucosamine ([¹³C]GlcNAc) (0.146 mmol, 20.1 mg) and [1'-¹³C] 3-aminobenzoic acid ([¹³C]3ABA) (0.146 mmol, 32.4 mg) were mixed with 2.18 mL of MeOH and 0.73 mL of AcOH, and the mixture was stirred 18h at room temperature. The reaction was concentrated *in vacuo* and applied to a column of silica-gel (CH₂Cl₂-CH₃OH, 80:20 to 0:100) to give the title compound as a mixture of both alpha and beta anomers (7.5 mg, ¹H NMR (300 MHz, D₂O–MeOD) δ 7.33 (br s, 2H), 7.12 (t, J = 8 Hz, 1H), 6.74 (d, J = 9 Hz, 1H), 4.88 (d, J = 10 Hz, 1H), 4.37 (d, J = 9 Hz, 1H), 3.86–3.41 (m, 6H), 1.98 (s, 3H). ¹³C NMR (75 MHz, D₂O–MeOD) δ 175.8, 147.4, 147.5, 129.5, 129.4, 126.0, 120.8, 117.3, 115.3, 104.3, 86.9, 82.4, 78.3, 76.6, 72.3, 62.8, 56.5, 22.8 ppm. HR-ESI-MS: observed m/z 365.12301 [M+Na]⁺, calculated. for C₁₃¹³C₂H₂₀N₂O₇Na m/z 365.12298 [M+Na]⁺.

Incorporation experiments. $\Delta ptmH/\Delta ptmI$, $\Delta ptmH/\Delta ptmO$, and $\Delta ptmH/\Delta ptmK::aprR$ mutant strains were streaked on BTT agar [glucose (1%), yeast extract (0.1%), beef extract (0.1%), casein hydrolysate (0.2%), agar (1.5%), pH 7.4] and incubated at 30 °C for 3 days. Spores of the mutant strains were grown in Erlenmeyer flasks (125 mL) each containing 30 mL seed medium [glucose (1%), yeast extract (0.1%), beef extract (0.1%), casein hydrolysate (0.2%), pH 7.4] for 3 days at 28°C and 200 rpm.

The seed cultures of each strain (1 mL each) were used to inoculate 2 x 50 mL Erlenmeyer flasks containing production medium, modified Bennett medium [glucose (1%), yeast extract (0.1%), beef extract (0.1%), soytone (0.2%), pH 7.4] (10 mL in each flask). After incubation for 16 h under the same condition, each mutant strain was fed with 3.0 mM of 3AP-3OP-SNAC and the last flask of each strain was used as a control (No feeding). The feeding was repeated every 12 h for 2 days. After 5 days of incubation, the cultures were centrifuged and the metabolites of each group were extracted twice with equal volume of EtOAc and once with 1.5 volume of *n*-BuOH. The organic solvent was evaporated in vacuo. The residues were dissolved in MeOH and were analyzed by MS and HPLC.

Cloning and construction of expression plasmids of *ptmO* and *ptmJ*. The *ptmO* gene was amplified using the primers ptmO-BglII and ptmO-EcoRI, and *ptmJ* gene was amplified using the primers ptmJ-EcoRI and ptmJ-HindIII. The PCR products were respectively cloned into BamHI and EcoRI sites and EcoRI and HindIII sites of the pRSET B to generate the expression vector pTMM080 (pRSET B-ptmO) and pTMM067 (pRSET B-ptmJ) and were introduced into the *E. coli* BL21 (DE3) pLysS (Invitrogen). The empty vector pRSET B was introduced into the *E. coli* BL21 (DE3) pLysS to be used as a control. Additionally, ptmJ was also cloned into NdeI and EcoRI sites of the pET-28b and was subsequently transformed to *E. coli* BL21 (DE3) pLysS. For protein expression of *ptmJ* and *ptmO*, the bacteria were grown in LB medium supplemented with chloramphenicol (50 µg/mL) and ampicillin (100 µg/mL) at 37 °C for 16 h. An aliquot (1 mL) of overnight

grown culture was used to inoculate a fresh LB medium (100 mL in 500 mL flask), supplemented with the same antibiotics, at a temperature of 37 °C under shaking of 230 rpm and was grown until an OD₆₀₀ of 0.6 was reached. Recombinant protein expression was induced with isopropyl β-D-thiogalactopyranoside (IPTG) to a final concentration of 0.1 mM and cultivated further. Fifteen milliliters of culture were harvested from the induced culture by centrifugation at 5000 rpm at 4 °C for 20 min.

Enzyme assay of PtmO. Enzyme assays (100 μL) were performed at 30 °C for 6 h in 25 mM phosphate buffer (pH 7.5) containing recombinant PtmO (50 μL) or boiled PtmO (50 μL) with 3AP-3OP-SNAC (2 mM). After incubation for 5 h at 30 °C, the reaction was quenched with 100 μL MeOH and analyzed by ESI-MS and HPLC.

Enzyme assay of PtmJ (PctL). The PtmJ reaction (100 μL) was performed using 40 μL of the whole cells or 40 μL of the cell free extract and 60 μL solution containing 2 mM substrate (aniline, 3-fluoroaniline, 4-fluoroaniline, 3-aminoacetophenone, or 3-aminobenzoic acid) and 2 mM UDP-*N*-Acetylglucosamine. The reactions were performed at 28 °C for 6 hours. The whole cells and cell-free extract of the empty vector were used as control. The reaction was quenched by addition of 100 μL methanol and the precipitated protein was removed by centrifugation. The resultant supernatants were used for mass spectrometry analyses.

Biotransformation (PtmJ) assay

E. coli (BL21) harboring *ptmJ* in pRSETB was grown as described above (5 x 150ml flasks containing 50ml LB medium). Two hours after induction with IPTG, the substrate, (ani-

line, 3-fluoroaniline, 3-aminoacetophenone or 3-aminobenzoic acid) at a final concentration of 2 mM, was added to the broth culture. The reaction mixture was incubated at 16 °C on a rotary shaker (200 rpm) overnight. the *E. coli* (BL21) strain containing pRSETB alone was employed as a negative control. The reaction was quenched by centrifugation to obtain the supernatant. The supernatant was extracted twice with ethyl acetate (1:1) and once with *n*-butanol (1:1). The *n*-butanol extract was evaporated to dryness and dissolved in 5 mL methanol and used for monitoring glycosylated products by ESI-MS.

SUPPORTING INFORMATION

Formation of 3-Aminoacetophenone Moiety and Evidence for Glycosylation of An Acyl Carrier Protein-bound Polyketide Intermediate in Pacitamicin Biosynthesis

Corey J. Brumsted,[¶] Mostafa E. Abugrain,[§] Wanli Lu,[§] and Taifo Mahmud^{*,§,¶} (Akane Hirayama,[†] Fumitaka Kudo,[†] Tadashi Eguchi)

[¶]Department of Chemistry and [§]Department of Pharmaceutical Sciences, Oregon State University, Corvallis, OR 97331-3507 (USA)

[†]Department of Chemistry, Tokyo Institute of Technology, 2-12-1 O-Okayama, Meguro-ku, Tokyo 152-8551, Japan

Supporting Figures

Figure S1. PCR analysis of **a)** $\Delta ptmH/\Delta ptmI$, **b)** $\Delta ptmH/ptmK::aac(3)IV$, and **c)** $\Delta ptmH/\Delta ptmO$.

Figure S2. ESI-MS (+) analysis of **a)** $\Delta ptmH/\Delta ptmI$, **b)** $\Delta ptmH/ptmK::aac(3)IV$, **c)** $\Delta ptmH/\Delta ptmO$, chemical complementation of **d)** $\Delta ptmH/\Delta ptmI$, **e)** $\Delta ptmH/ptmK::aac(3)IV$, and **f)** $\Delta ptmH/\Delta ptmO$ with 3AP-3OP-SNAC.

Figure S3. ESI-MS (+) analysis of $\Delta ptmH/\Delta ptmT$ mutant fed with 3AP-3OP-SNAC.

Figure S4. ESI-MS (+) analysis of $\Delta ptmJ$ mutant fed with NAcGlc-3ABA

Figure S5. ESI-MS analysis of $\Delta ptmH/\Delta ptmT$ mutant fed with **a)** GlcNAc-3ABA, and **b)** [¹³C]GlcNAc-[¹³C]3ABA.

Figure S6. ESI-MS (+) analysis of $\Delta ptmH/\Delta ptmT$ mutant fed with phenylamines. **a)** control, **b)** aniline (AN), **c)** 3-fluoroaniline (3FAN), **d)** 4-fluoroaniline (4FAN).

Figure S7. ESI-MS (+) analysis of glycosylation of 3AAP, AN, and 3FAN by cell-free extracts of *Escherichia coli* containing PtmJ.

Figure S8. ESI-MS (+) analysis of glycosylation of 3ABA by cell-free extracts of *Escherichia coli* containing PtmJ.

Figure S9. HPLC analysis (215 nm) of the hydrolase activity of PtmO

NMR data of all synthetic compounds used in this study can be found in Appendix A

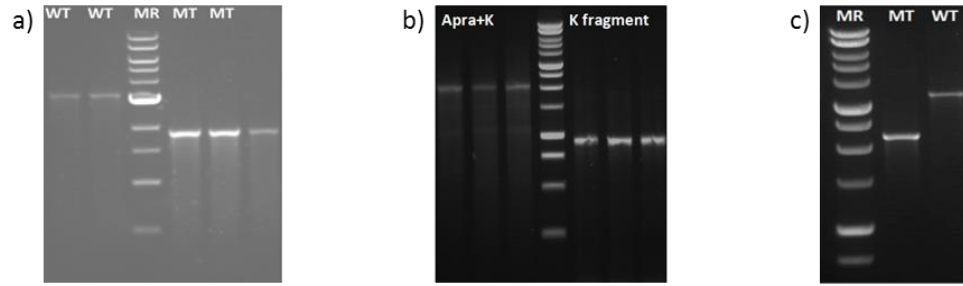


Figure S1. PCR analysis of a) $\Delta ptmH/\Delta ptmI$, b) $\Delta ptmH/ptmK::aac(3)IV$, and c) $\Delta ptmH/\Delta ptmO$.

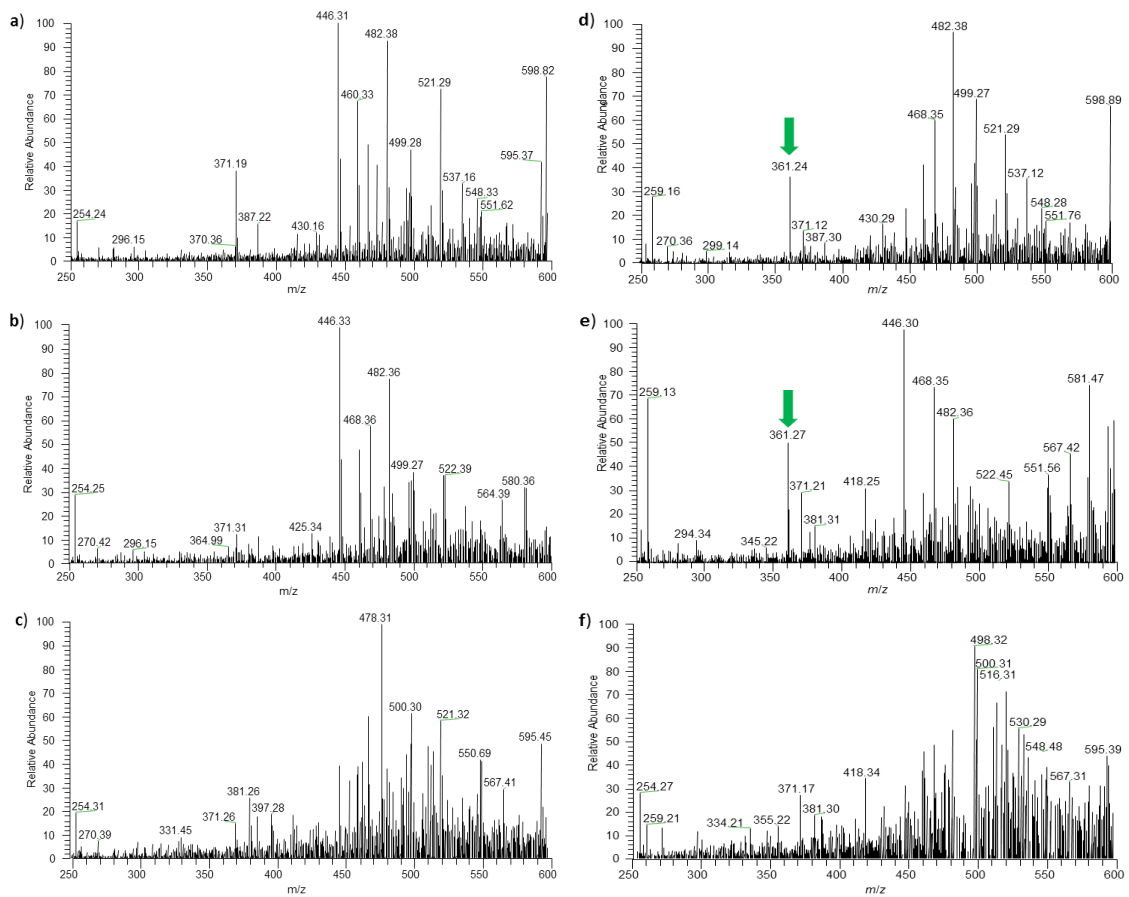


Figure S2. ESI-MS (+) analysis of a) $\Delta ptmH/\Delta ptmI$, b) $\Delta ptmH/ptmK::aac(3)IV$, c) $\Delta ptmH/\Delta ptmO$, chemical complementation of d) $\Delta ptmH/\Delta ptmI$, e) $\Delta ptmH/ptmK::aac(3)IV$, and f) $\Delta ptmH/\Delta ptmO$ with 3AP-3OP-SNAC.

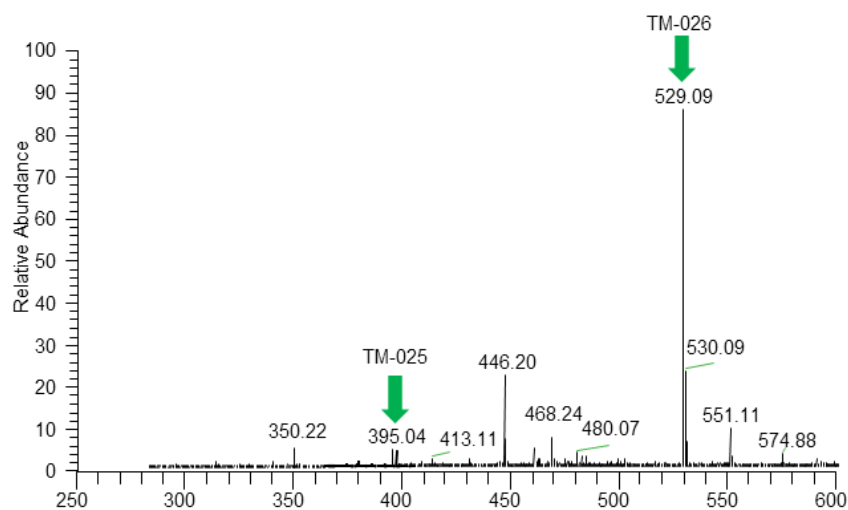


Figure S3. ESI-MS (+) analysis of $\Delta ptmH/\Delta ptmT$ mutant fed with 3AP-3OP-SNAC.

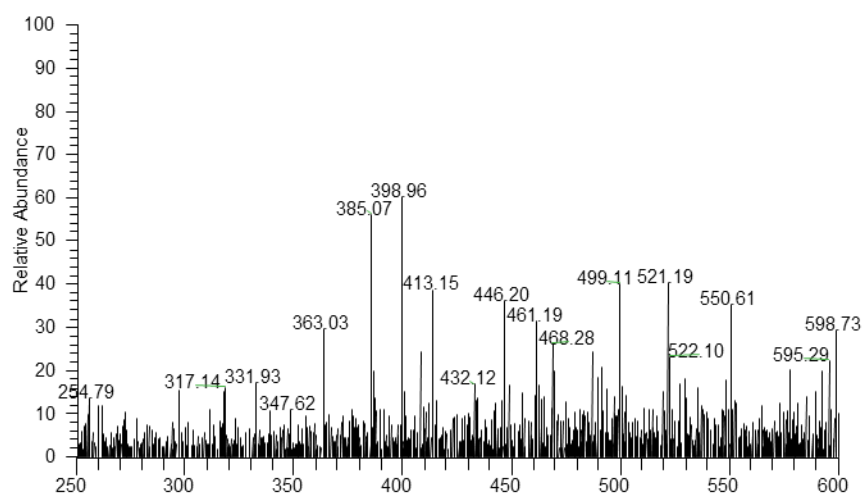


Figure S4. ESI-MS (+) analysis of $\Delta ptmJ$ mutant fed with NAcGlc-3ABA

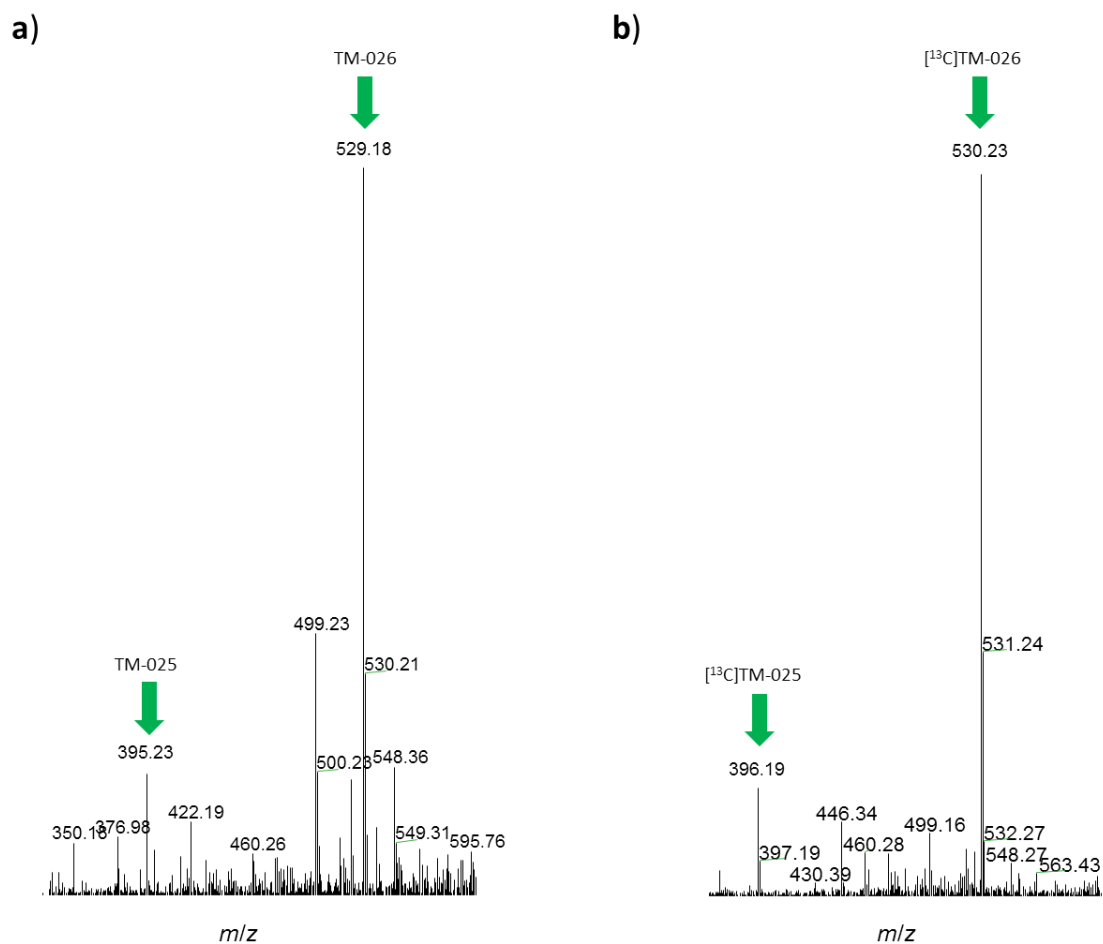


Figure S5. ESI-MS analysis of $\Delta ptmH/\Delta ptmT$ mutant fed with **a)** GlcNAc-3ABA, and **b)** $[^{13}\text{C}]\text{GlcNAc}-[^{13}\text{C}]\text{3ABA}$.

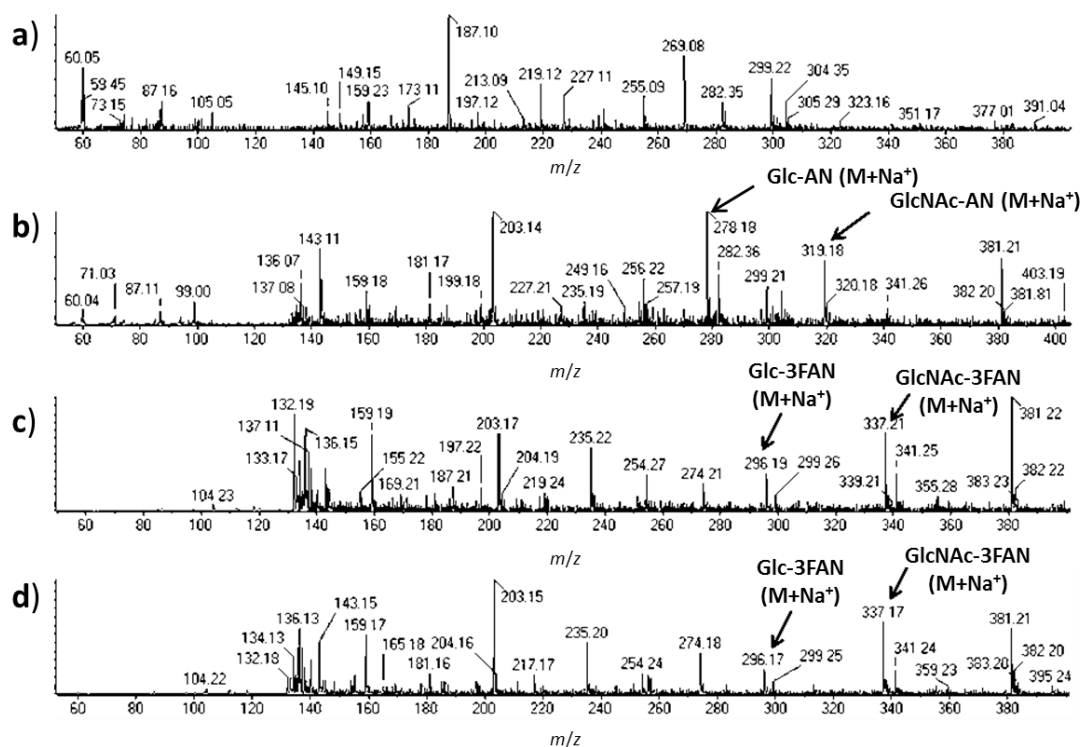


Figure S6. ESI-MS (+) analysis of $\Delta ptmH/\Delta ptmT$ mutant fed with phenylamines. **a)** control, **b)** aniline (AN), **c)** 3-fluoroaniline (3FAN), **d)** 4-fluoroaniline (4FAN).

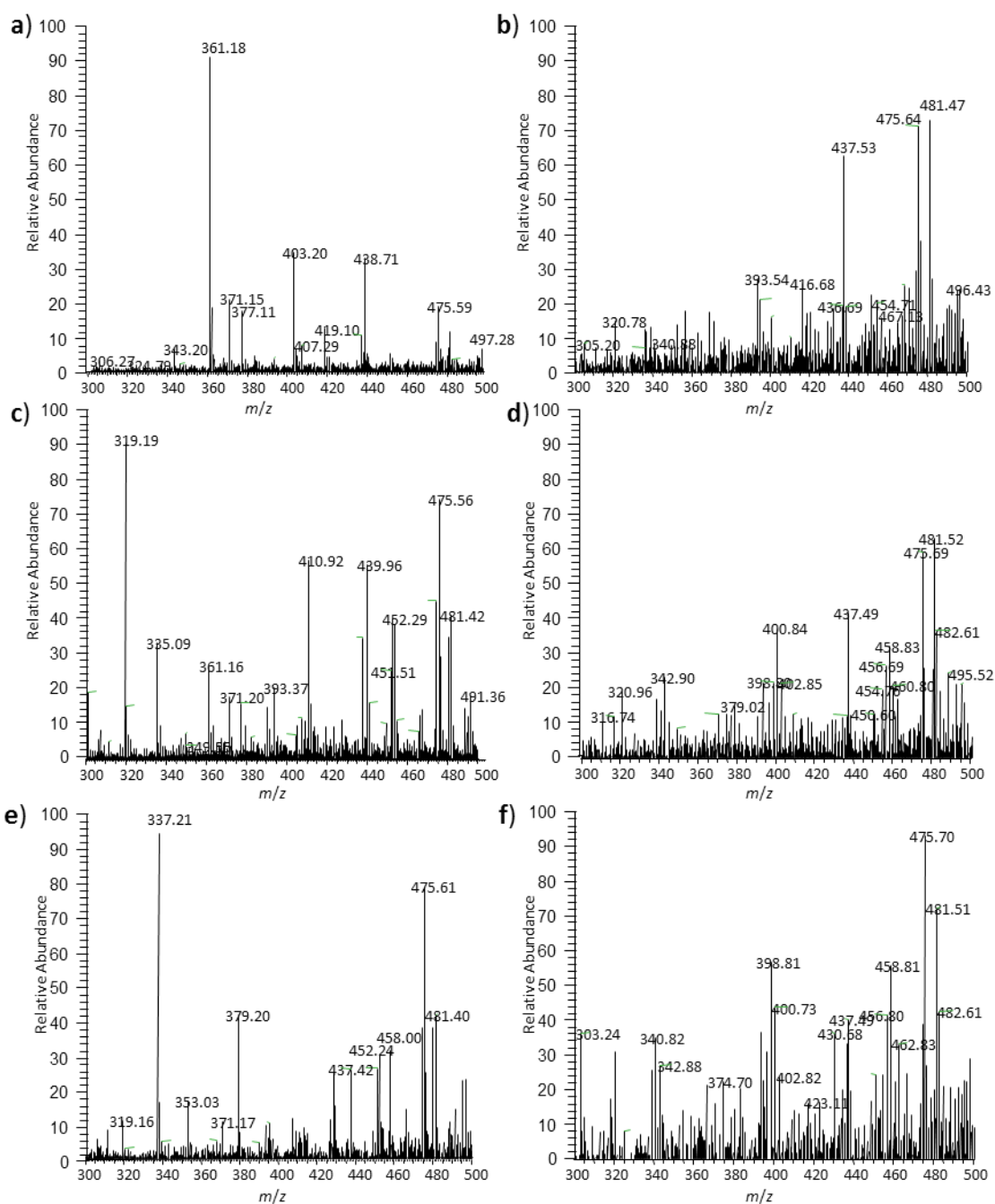


Figure S7. ESI-MS (+) analysis of glycosylation of 3AAP, AN, and 3FAN by cell-free extracts of *Escherichia coli* containing PtmJ.

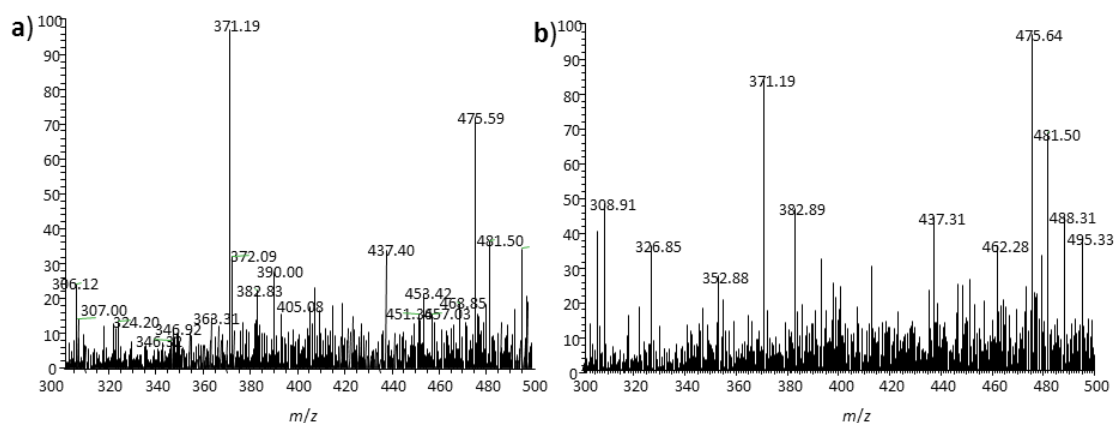


Figure S8. ESI-MS (+) analysis of glycosylation of 3ABA by cell-free extracts of *Escherichia coli* containing PtmJ.

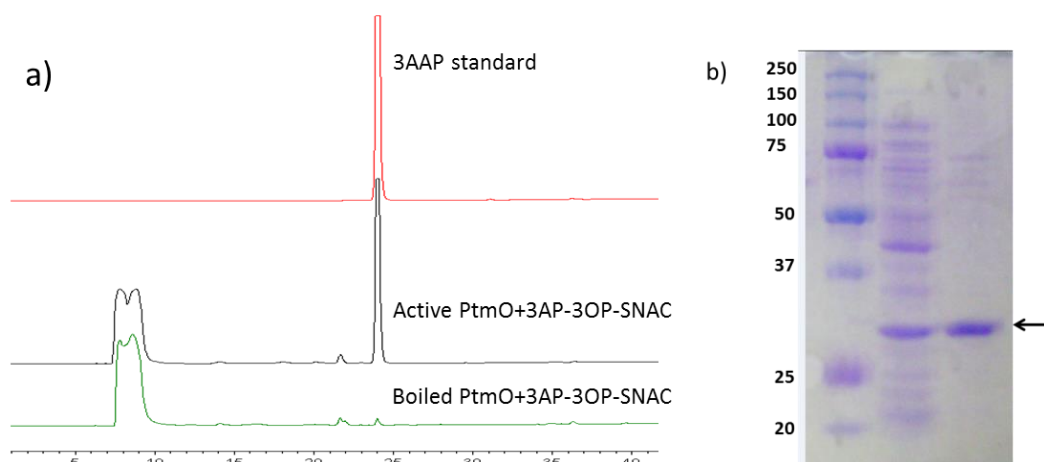
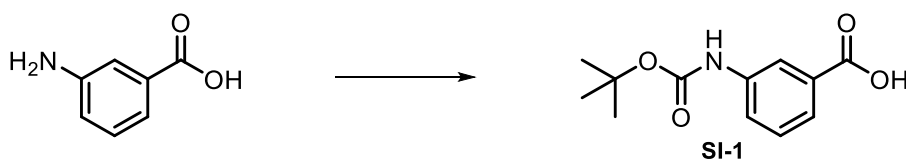


Figure S9. a) HPLC analysis (215 nm) of the hydrolase activity of PtmO, and b) SDS-page gel of purified PtmO protein.

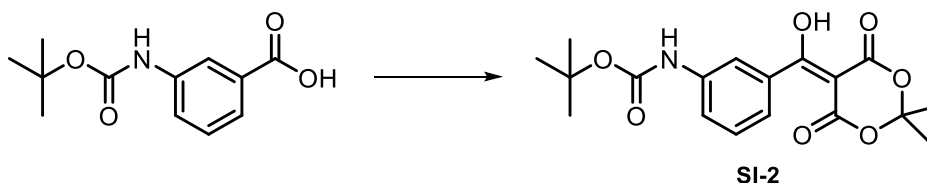
General Experimental conditions:

All reactions were carried out under an inert, argon atmosphere in oven-dried glassware at 170°C unless indicated otherwise. Flash column chromatography was carried out with SiliaFlash P60, 60 Å silica gel. Reactions and column chromatography were monitored with EMD silica gel 60 F254 plates and visualized with potassium permanganate, ceric

ammonium molybdate, iodine, or vanillin stains. Benzene (PhH), methylene chloride (DCM), and triethylamine (Et₃N) were distilled over calcium hydride prior to use. All other reagents and solvents were used without further purification from commercial sources. Instrumentation: FT-IR spectra were obtained on NaCl plates with a PerkinElmer Spectrum Vision spectrometer. Proton and carbon NMR spectra (¹H NMR and ¹³C NMR) were recorded in deuterated chloroform (CDCl₃) unless otherwise noted on a Bruker 700 MHz Avance III Spectrometer with carbon-optimized cryoprobe and Bruker 400 MHz DPX-400 spectrometer and calibrated to residual solvent peaks. Multiplicities are abbreviated as follows: s = singlet, d = doublet, t = triplet, q = quartet, sept = septet, br = broad, m = multiplet.

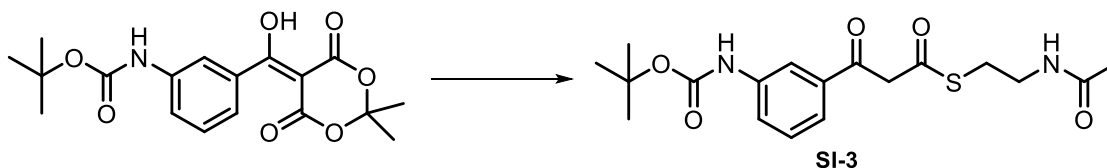


Synthesis of 3-((*tert*-butoxycarbonyl)amino)benzoic acid (**SI-1**): 3-aminobenzoic acid (1 g, 7.29 mmol) was added to a 1M aqueous solution of Na₂CO₃ (16.05 mL, 16.05 mmol, 2.2 eq) and 25 μ L of methanol was added, followed by boc-anhydride (1.67 g, 7.65 mmol, 1.05 eq) and the reaction stirred 12 h at room temperature. After reaching completion, the reaction was diluted with water and the pH was adjusted to pH 9 with 1M NaOH, washed with EtOAc (3 x 20 mL), and the aqueous was added 1M HCl until pH = 4 was achieved and extracted with EtOAc (3 x 30 mL), dried over Na₂SO₄, filtered and volatiles were removed *in vacuo* (1.71g, 99 %). Analytical data matched reported data.²²



Synthesis of *tert*-butyl (3-((2,2-dimethyl-4,6-dioxo-1,3-dioxan-5-ylidene)(hydroxy) methyl) phenyl) carbamate (**SI-2**): Under an atmosphere of nitrogen **SI-1** (4.21mmol, 1 g), was suspended in DCM (21 mL, 0.2M) and added *N, N'*-dimethylaminopyridine (DMAP) (5.47 mmol, 669 mg, 1.3 eq) followed by EDCI-HCl (4.84 mmol, 929 mg, 1.15 eq). Meldrum's acid²¹ (4.42 mmol, 637 mg, 1.05eq) was added at room temperature and the reaction was stirred at this temperature for 14 h until the reaction was complete as indicated by TLC (EtOAc-Et₂O = 2:1, vanillin stain). The reaction was diluted with DCM (20 mL), washed with 0.5M HCl (20 mL x 3), then H₂O (100 mL), and brine (50 mL). The organics were dried over Na₂SO₄, filtered and solvent removed *in vacuo* to yield **SI-2** (1.47 g, 96%) as an orange foam which was used in the next step without further purification.

¹H NMR (300 MHz, CDCl₃) δ 15.39 (s, 1H), 7.68 (s, 1H), 7.58 (d, *J* = 7.7 Hz, 1H), 7.47-7.27 (m, 2H), 6.59 (s, 1H), 1.84 (s, 6H), 1.51 (s, 9H). ¹³C NMR (75 MHz, CDCl₃) δ 189.27, 152.60, 138.57, 133.90, 128.85, 124.04, 123.05, 119.00, 105.13, 91.20, 81.14, 28.44, 26.98; IR data (cm⁻¹): 3333, 2981, 1727, 1673, 1559, 1397, 1289, 1236, 1159, 460. HR-ESI-MS Theoretical [M+Na]⁺: 386.12102 *m/z*, Observed [M+Na]⁺: 386.12136 *m/z*. LRMS (ESI+) found 364.2 *m/z* = [M+H], 386.2 *m/z* = [M+Na].



Synthesis of S-(2-acetamidoethyl) 3-(3-((tert-butoxycarbonyl)amino)phenyl)-3-

oxopropanethioate (SI-3): The meldrums adduct **SI-2** (0.949mmol, 345mg) was added to

a solution of *N*-Acetylcysteamine (1.72 mmol, 102 mg) in benzene (9.5 mL, 0.1M) under argon. The mixture was placed in a 90°C oil bath and stirred 12h at this temperature un-

til the reaction was complete by consumption of starting material on TLC. The reaction

mixture was cooled to room temperature and concentrated to a low volume under vac-

uum, then diluted with EtOAc (25mL). The resulting solution was added CuSO₄-SiO₂

(1g)²¹ and stirred at room temperature for 1 h under N₂, and passed through a small

column of SiO₂ to provide **SI-3** as mixture of its keto and enol tautomers in a ratio of 3:2

(116 mg, 32%). LRMS (ESI+) found: 403 *m/z* = M+Na. ¹H NMR (300 MHz, CDCl₃) δ 12.99

(s, 1H), 7.90 (s, 1H), 7.80 (s, 1H), 7.63 (d, *J* = 8.0 Hz, 1H), 7.52 (d, *J* = 7.7 Hz, 1H), 7.45 (d, *J*

= 7.8 Hz, 1H), 7.41-7.39 (m, 3H), 6.94 (s, 1H), 6.23 (s, 2H), 6.03 (s, 1H), 4.15 (s, 2H), 3.42

(m, 4H), 3.05 (m, 4H), 1.92 (s, 3H), 1.89 (s, 3H), 1.46 (s, 18H). ¹³C NMR (75 MHz, CDCl₃) δ

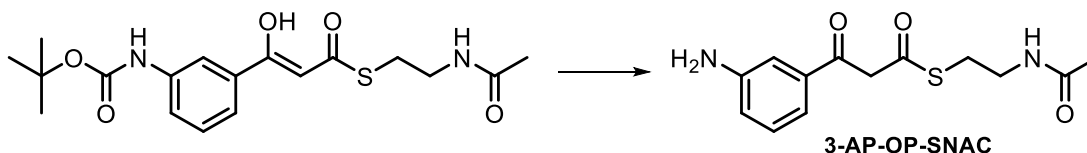
194.81, 192.73, 192.17, 170.88, 170.66, 169.27, 152.97, 152.88, 139.56, 139.22, 136.55,

133.49, 129.54, 129.36, 124.01, 122.94, 121.99, 121.03, 118.62, 116.47, 97.32, 80.96,

77.58, 77.16, 76.74, 60.48, 53.88, 39.88, 39.19, 29.52, 28.41, 28.26, 23.26, 23.14, 21.11,

14.27; IR data (cm⁻¹): 3320, 3077, 2978, 1702, 1608, 1588, 1544, 1240, 1160. HR-ESI-MS

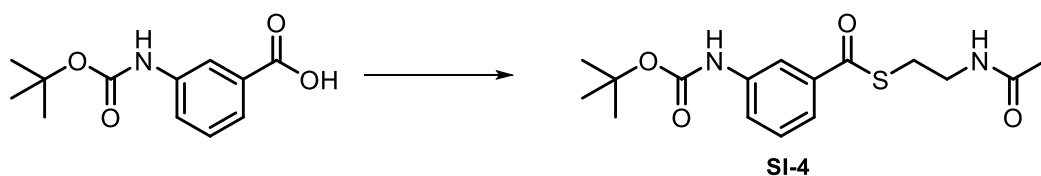
Observed [M+Na]⁺: 403.13066 *m/z*, Theoretical [M+Na]⁺: *m/z* 403.12981.



Synthesis of *S*-(2-acetamidoethyl) 3-(3-aminophenyl)-3-oxopropanethioate (3-AP-OP-

SNAC): **SI-3** (0.263 mmol, 100 mg) was dissolved in DCM (0.200 mL, 1.31M) under N₂, then cooled in an ice bath. TFA (0.200 mL, 7.4eq) was added dropwise at 0°C and stirred for 8h at 0-10°C when TLC indicated reaction completion. The mixture was diluted with DCM (10 mL) and the reaction quenched at 0 °C by dropwise addition of NaHCO₃-phosphate buffer solution (300 mg NaHCO₃ in 10 mL of pH 7 phosphate buffer), then extracted with DCM (5x10 mL) and dried over Na₂SO₄, filtered and volatiles removed *in vacuo*. After chromatography (Et₂O-MeOH =100:5 to 50:5) the title compound was obtained as a yellow oil (59 mg, 80%). ¹H NMR (300 MHz, *d*₆-DMSO) δ 13.34 – 12.70 (m, 1H), 8.03 (m, 2H), 7.28 – 6.93 (m, H), δ 6.84 (d, *J* = 7.8 Hz, 1H), 6.74 (d, *J* = 7.7 Hz, 1H), 6.26 (s, 1H), 5.36 (s, 1H), 4.33 (s, 2H), 3.42 (m, 4H), 3.04 (t, *J* = 6.6 Hz, 2H), 2.94 (t, *J* = 6.8 Hz, 2H), 1.80 (s, 3H), 1.79 (s, 3H). ¹³C NMR (75 MHz, *d*₆-DMSO) δ 193.92, 192.94, 192.56, 169.22, 169.12, 149.06, 148.99, 136.63, 132.56, 129.23, 129.17, 119.18, 117.53, 116.39, 113.85, 112.67, 111.27, 96.51, 53.52, 40.35, 40.08, 39.80, 39.52, 39.24, 38.96, 38.69, 38.29, 38.00, 28.49, 27.73, 27.02, 22.45. Enol-tautomer: ¹H NMR (500 MHz, CDCl₃) δ = 13.08 (s, 1H), 7.40 – 7.04 (m, 3H), 6.83 (d, *J* = 8, 1H), 6.10 (s, 1H), 6.07-5.92 (m, 1H), 4.01-3.75 (m, 2H), 3.54 (dd, *J* = 13, 7 Hz, 2H), 3.17 (t, *J* = 6 Hz, 2H), 2.01 (s, 3H). Keto-

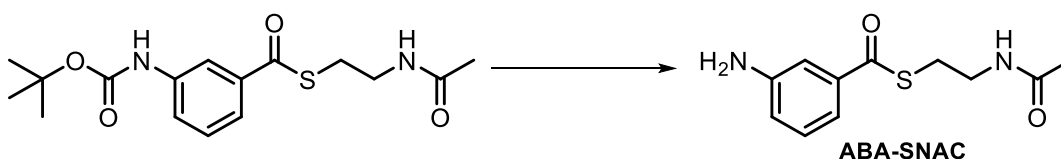
tautomer: ^1H NMR (500 MHz, CDCl_3) δ = 7.40 – 7.04 (m, 3H), 6.93 (d, J = 7 Hz, 1H), 6.00 (brm, 2H), 4.23 (s, 2H), 4.01-3.75 (brm, 2H), 3.50 (dd, J = 13, 7 Hz, 2H), 3.14 (t, J = 6 Hz, 2H), 1.97 (s, 3H). ^{13}C NMR (126 MHz, CDCl_3) δ = 194.7, 192.9, 192.3, 169.9, 147.1, 146.8, 136.9, 133.6, 129.8, 129.6, 120.5, 118.9, 118.5, 116.7, 114.2, 112.7, 97.0, 53.8, 39.9, 39.2, 29.3, 28.1, 23.3 ppm. HRMS-ESI(+): Theoretical $[\text{M}+\text{Na}]^+$: 303.07738 m/z ; observed $[\text{M}+\text{Na}]^+$: 303.07806 m/z ; IR data (cm^{-1}): 3409, 3005, 2918, 1658, 1435, 1022, 953, 706.



Synthesis of S-(2-acetamidoethyl) 3-((tert-butoxycarbonyl)amino)benzothioate (SI-4):

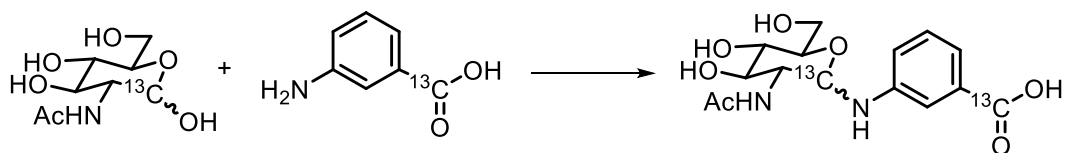
Boc-ABA (**SI-1**, 237 mg, 1 mmol) was added under argon to a solution of Et_3N (0.288 mL, 2.07 mmol, 2.07 eq) in anhydrous DCM (7.4 mL) and successively added EDCI-HCl (197.5 mg, 1.03 mmol, 1.03 eq) *N*-hydroxybenzotriazole (135.12 mg, 1.03 mmol, 1.03 eq) and *N*-Acetylcysteamine (166.85 mg, 1.4 mmol, 1.4 eq). The reaction was stirred at room temperature for 25 minutes when TLC indicated reaction completion, then diluted with DCM (3 mL), washed successively with saturated NaHCO_3 solution (5 mL), H_2O (10 mL), 1M HCl (15 mL), and brine (5 mL), dried over Na_2SO_4 , filtered and volatiles removed *in vacuo*. The colorless residue was dissolved in EtOAc (10mL) and added CuSO_4 - impregnated silica gel (CuSO_4 - SiO_2 , 2.4g)¹ and stirred 10 minutes to remove excess thiol, then passed through a small silica gel column to provide 217 mg (64% yield) of the

title compound as a sticky foam. ^1H NMR (300 MHz, CDCl_3) δ 7.94 (s, 1H), 7.63 (t, J = 9 Hz, 2H), 7.37 (t, J = 8 Hz, 1H), 6.72 (br s, 1H), 5.95 (br s, 1H), 3.53 (dd, J = 6 Hz, 2H), 3.22 (t, J = 6 Hz, 2H), 1.97 (s, 3H), 1.53 (s, 9H). Theoretical $[\text{M}+\text{Na}]^+$: m/z 361.11925, observed $[\text{M}+\text{Na}]^+$: m/z 361.12061.



Synthesis of *S*-(2-acetamidoethyl) 3-aminobenzothioate (3-ABA-SNAC): Boc-3-ABA-SNAC

(0.420 mmol, 100 mg) was dissolved in DCM (0.320 mL, 1.31 M) under N_2 , then cooled in an ice bath. TFA (0.320 mL, 7.4eq) was added dropwise at 0°C and stirred for 10h at $0-10^\circ\text{C}$ when TLC indicated reaction completion. The mixture was diluted with DCM (10 mL) and the reaction quenched at 0°C by dropwise addition of NaHCO_3 -phosphate buffer solution (300 mg NaHCO_3 in 10 mL of pH 7 phosphate buffer), then extracted with DCM (5x10 mL) and dried over MgSO_4 , filtered and volatiles removed *in vacuo*. Preparative TLC (Et_2O -MeOH =200:10) provided analytically pure material. ^1H NMR (500 MHz, CDCl_3) δ = 7.38 (d, J = 8 Hz, 1H), 7.25 (m, 2H), 6.91 (d, J = 8 Hz, 1H), 5.98 (brs, 1H), 4.21-3.50 (brs, 1H), 3.55 (q, J = 6 Hz, 2H), 3.23 (t, J = 6 Hz, 2H), 1.99 (s, 3H). ^{13}C NMR (126 MHz, CDCl_3) δ = 192.51, 170.35, 146.82, 137.76, 129.62, 120.09, 117.57, 113.03, 77.29, 77.04, 76.79, 39.75, 28.58, 23.27. HR-ESI-MS: calculated for $\text{C}_{11}\text{H}_{14}\text{N}_2\text{O}_2\text{SNa}$, $[\text{M}+\text{Na}]^+$: m/z 261.06682, observed $[\text{M}+\text{Na}]^+$: m/z 261.06675.



Synthesis of *N*-acetyl-D-glucosaminyl-1-aminobenzoic acid ($[^{13}\text{C}]\text{GlcNAc}-[^{13}\text{C}]\text{3ABA}$): *N*-acetyl-D- $[1\text{-}^{13}\text{C}]\text{glucosamine}$ ($[^{13}\text{C}]\text{GlcNAc}$) (0.146 mmol, 20.1 mg) and $[1'\text{-}^{13}\text{C}]$ 3-aminobenzoic acid ($[^{13}\text{C}]\text{3ABA}$) (0.146 mmol, 32.4 mg) were suspended in methanol (2.18 mL) and acetic acid (0.73 mL), and the mixture was stirred 18 h at room temperature. The reaction was concentrated *in vacuo* and applied to column of silica-gel (CH_2Cl_2 - CH_3OH , 80:20 to 0:100) to give the title compound as a mixture of both anomers (7.5 mg, ^1H NMR (300 MHz, D_2O -MeOD = 3:1) δ 7.33 (br s, 2H), 7.12 (t, J = 8 Hz, 1H), 6.74 (d, J = 9 Hz, 1H), 4.88 (d, J = 10 Hz, 1H), 4.37 (d, J = 9 Hz, 1H), 3.86 -3.41 (m, 6H), 1.98 (s, 3H). ^{13}C NMR (75 MHz, D_2O -MeOD) δ 175.8, 147.4, 147.5, 129.5, 129.4, 126.0, 120.80, 117.30, 115.3, 104.3, 86.9, 82.4, 78.3, 76.6, 72.3, 62.8, 56.5, 22.8. HR-ESI-MS(+): Observed $[\text{M}+\text{Na}]^+$: m/z 365.12301. Theoretical $[\text{M}+\text{Na}]^+$: m/z 365.12298.

References:

1. Rinehart, K. L., Jr.; Weller, D. D.; Pearce, C. J. *J. Nat. Prod.* **1980**, 43, 1-20.
2. Almabruk, K. H.; Lu, W.; Li, Y.; Abugreen, M.; Kelly, J. X.; Mahmud, T. *Org Lett* **2013**, 15, 1678-1681.
3. Hirayama, A.; Eguchi, T.; Kudo, F. *Chembiochem* **2013**, 14, 1198-1203.
4. Rinehart, K. L., Jr. *Jpn J Antibiot* **1979**, 32 Suppl, S32-46.
5. Ito, T.; Roongsawang, N.; Shirasaka, N.; Lu, W.; Flatt, P. M.; Kasanah, N.; Miranda, C.; Mahmud, T. *Chembiochem* **2009**, 10, 2253-2265.
6. Kudo, F.; Kasama, Y.; Hirayama, T.; Eguchi, T. *J Antibiot (Tokyo)* **2007**, 60, 492-503.
7. Bibb, M. J.; Sherman, D. H.; Omura, S.; Hopwood, D. A. *Gene* **1994**, 142, 31-39.
8. Ahlert, J.; Shepard, E.; Lomovskaya, N.; Zazopoulos, E.; Staffa, A.; Bachmann, B. O.; Huang, K.; Fonstein, L.; Czisny, A.; Whitwam, R. E.; Farnet, C. M.; Thorson, J. S. *Science* **2002**, 297, 1173-1176.
9. Mao, Y.; Varoglu, M.; Sherman, D. H. *Chem Biol* **1999**, 6, 251-263.
10. Mao, Y.; Varoglu, M.; Sherman, D. H. *J Bacteriol* **1999**, 181, 2199-2208.
11. Abugrain, M. E.; Brumsted, C. J.; Osborn, A. R.; Philmus, B.; Mahmud, T. *ACS Chem Biol* **2017**, 12, 362-366.
12. Lu, W.; Roongsawang, N.; Mahmud, T. *Chem Biol* **2011**, 18, 425-431.
13. Adams, E. S.; Rinehart, K. L. *J Antibiot (Tokyo)* **1994**, 47, 1456-1465.
14. August, P. R.; Tang, L.; Yoon, Y. J.; Ning, S.; Muller, R.; Yu, T. W.; Taylor, M.; Hoffmann, D.; Kim, C. G.; Zhang, X.; Hutchinson, C. R.; Floss, H. G. *Chem Biol* **1998**, 5, 69-79.
15. Yu, T. W.; Bai, L.; Clade, D.; Hoffmann, D.; Toelzer, S.; Trinh, K. Q.; Xu, J.; Moss, S. J.; Leistner, E.; Floss, H. G. *Proc Natl Acad Sci U S A* **2002**, 99, 7968-7973.
16. Admiraal, S. J.; Khosla, C.; Walsh, C. T. *J Am Chem Soc* **2003**, 125, 13664-13665.
17. Kao, C. L.; Borisova, S. A.; Kim, H. J.; Liu, H. W. *J Am Chem Soc* **2006**, 128, 5606-5607.
18. Sweet, C. R.; Ribeiro, A. A.; Raetz, C. R. *J Biol Chem* **2004**, 279, 25400-25410.
19. Gilbert, I. H.; Ginty, M.; O'Neill, J. A.; Simpson, T. J.; Staunton, J.; Willis, C. L. *Bioorg. Med. Chem. Lett.* **1995**, 5, 1587-1590.
20. Gilbert, I. H.; Ginty, M.; O'Neill, J. A.; Simpson, T. J.; Staunton, J.; Willis, C. L. *Bioorganic & Medicinal Chemistry Letters* **1995**, 5, 1587-1590.
21. Higher yields were obtained when Meldrum's acid was recrystallized (acetone-water) immediately prior to use.
22. Ferdani, R.; Pajewski, R.; Djedović, N.; Pajewska, J.; Schlesinger, P. H.; Gokel, G. W. *New J. Chem.* **2005**, 29, 673-680.

A Highly Promiscuous β -Ketoacyl-ACP Synthase (KAS) III-like Protein Is
Involved in Pactamycin Biosynthesis

Mostafa E. Abugrain,[†] Corey J. Brumsted,[‡] Andrew R. Osborn,[†] Benjamin
Philmus,[†] and Taifo Mahmud^{†,‡,*}

[†]Department of Pharmaceutical Sciences, Oregon State University Corvallis, Oregon
97331, United States

[‡]Department of Chemistry, Oregon State University, Corvallis, Oregon 97331, United
States

Chapter 3. A Highly Promiscuous β -Ketoacyl-ACP Synthase (KAS) III-like Protein Is Involved in Pactamycin Biosynthesis

β -Ketoacyl-acyl carrier protein synthase (KAS) enzymes play a central role in type I (modular) and type II (dissociable) fatty acid synthases (FASs) and polyketide synthases (PKSs), as well as in chalcone synthases.¹ In the type II dissociable FASs, three types of KAS enzymes are known: KAS I (FabB) and KAS II (FabF) are responsible for the elongation steps, whereas KAS III (FabH) catalyzes the initiation step, involving a Claisen condensation of the acetyl-CoA starter unit with the first extender unit, malonyl-ACP, to form acetoacetyl-ACP (Figure S1a).¹ In *Streptomyces*, KAS III can also recruit alternative starter units, such as isobutyryl-CoA and methylbutyryl-CoA, to form branched chain fatty acids. Less efficiently, it can also catalyze acyl-CoA:ACP transacylase (ACAT) reactions.²

Over the past decade, a number of KAS III-like enzymes have been reported to have unusual catalytic functions. The *cln2* gene of the clorobiocin cluster in *Streptomyces roseochromogenes* var. *oscitans* has been found through a gene inactivation study to be responsible for the transfer of the pyrrolylcarbonyl unit to the sugar moiety of clorobiocin.³ The KAS III-like protein CerJ uses malonyl-CoA analogs to form sugar esters in cervimycin biosynthesis (Figure S1b),⁴ whereas ChlB6 from the chlorothricin pathway transfers a 3-chloro-6-methoxy-2-methylbenzoyl moiety from a discrete ACP, ChlB2, to a sugar moiety of chlorothricin (Figure S1c).⁵ The 3-chloro-6-methoxy-2-methylbenzoyl unit is derived from a 6-methylsalicylyl (6-MSA) unit, a product of an iterative type I PKS (ChlB1). Incorporation of this PKS product to the sugar moiety of chlorothricin requires

multiple intermediary acyl transfer reactions involving two discrete KAS III-like proteins (ChlB3 and ChlB6) and a discrete ACP (ChlB2; Figure S1c).⁵

Genes encoding proteins homologous to ChlB6 have been found in a number of natural products biosynthetic gene clusters, such as *aviN* of the avilamycin A cluster in *Streptomyces viridochromogenes* Tü57,⁶ *evrI* of the evernimicin cluster in *Micromonospora carbonacea* var. *africana* ATCC 39149,⁷ *calO4* of the calicheamicin cluster in *Micromonospora echinospora* subsp. *calichensis*,⁸ *pokM2* of the polyketomycin cluster in *Streptomyces diastatochromogenes* Tü6028,⁹ *tiaF* of the tiacumicin cluster in *Dactylosporangium aurantiacum* subsp. *hamdenensis* NRRL 18085,¹⁰ and *esmD1* of the esmeraldin pathway in *Streptomyces* antibiotics Tü 2706.¹¹ Except esmeraldin, all of these natural products contain one or more sugar moieties decorated by 6-MSA or orsellinic acid derivatives. However, in contrast to the chlorothricin pathway, they lack the genes that code for the second KAS III and the discrete ACP in their clusters.

A gene encoding a protein homologous to KAS III was also found in the pactamycin cluster in *Streptomyces pactum* (Figure S2).¹² This gene (*ptmR*) may be involved in the attachment of 6-MSA, which is synthesized by the iterative type I PKS PtmQ,¹² to the aminocyclopentitol core unit in pactamycin biosynthesis. Also present in the cluster are genes that code for a KAS I protein (PtmK), a discrete ACP (PtmI), and a putative hydrolase/acyltransferase (PtmO). The roles of these genes in pactamycin biosynthesis are currently unknown, but their possible involvement in the attachment of 6-MSA cannot be ruled out.

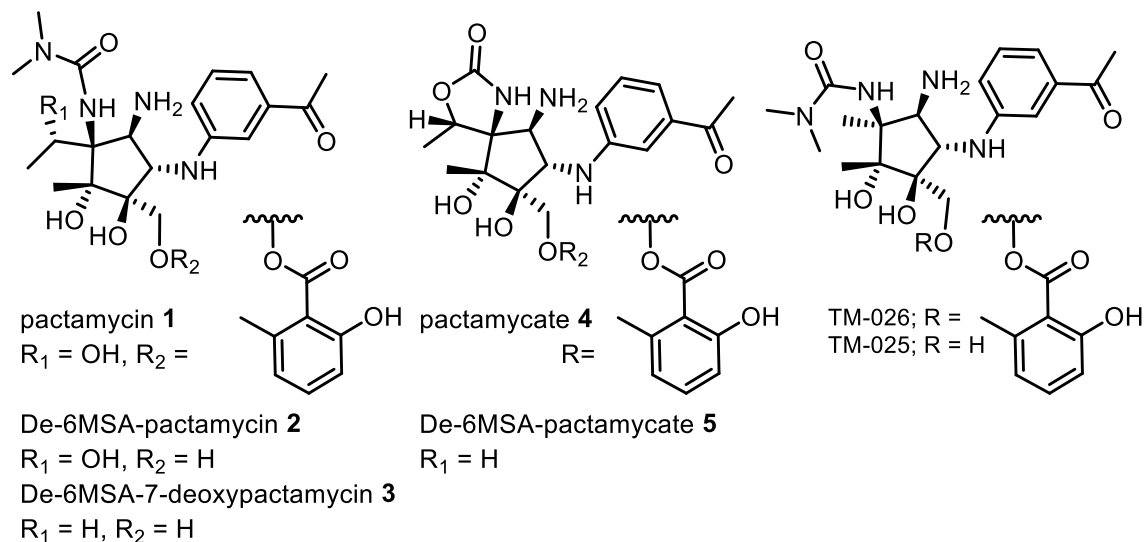


Figure 3.1. Pactamycin (1) and derivatives obtained from biosynthetic manipulations

To investigate the involvement of *ptmI*, *ptmK*, *ptmO*, and *ptmR* in the transfer of the 6-MSA moiety, we generated mutant strains of *S. pactum* by either in-frame deletion or gene disruption with *aac(3)IV* (Figures S3 and S4) and characterized their products by ESI-MS and HPLC. Inactivation of *ptmI*, *ptmK*, or *ptmO* completely abrogated the production of pactamycin and its analogs (Figure S5),¹² suggesting that these genes are involved in the early steps of the pathway, not in the attachment of 6-MSA, which occurs later in the pathway.^{12,13} On the other hand, the $\Delta ptmR$ mutant produced de-6-MSA-pactamycin (2) and its degradation product, de-6-MSA-pactamycate (5; Figures 2.1, S6a, and S7), consistent with the absence of 6-MSA-transferase activity in this mutant. Furthermore, we inactivated *ptmR* in a mutant strain of *S. pactum*, $\Delta ptmH$, which produces 7-deoxy-7-demethylpactamycin (TM-026, 6).¹⁴ The double gene knockout mutant, $\Delta ptmH/\Delta ptmR$, produces de-6-MSA-7-deoxy-7-demethylpactamycin (TM-025, 7; Figures

S6g and S8), confirming the function of PtmR as a 6-MSA-transferase. These results were further corroborated by a gene complementation experiment, in which an integrative plasmid harboring intact *ptmR* was introduced into $\Delta ptmH/\Delta ptmR$. As expected, the resulting conjugants were able to produce TM-026 (Figure S6f).

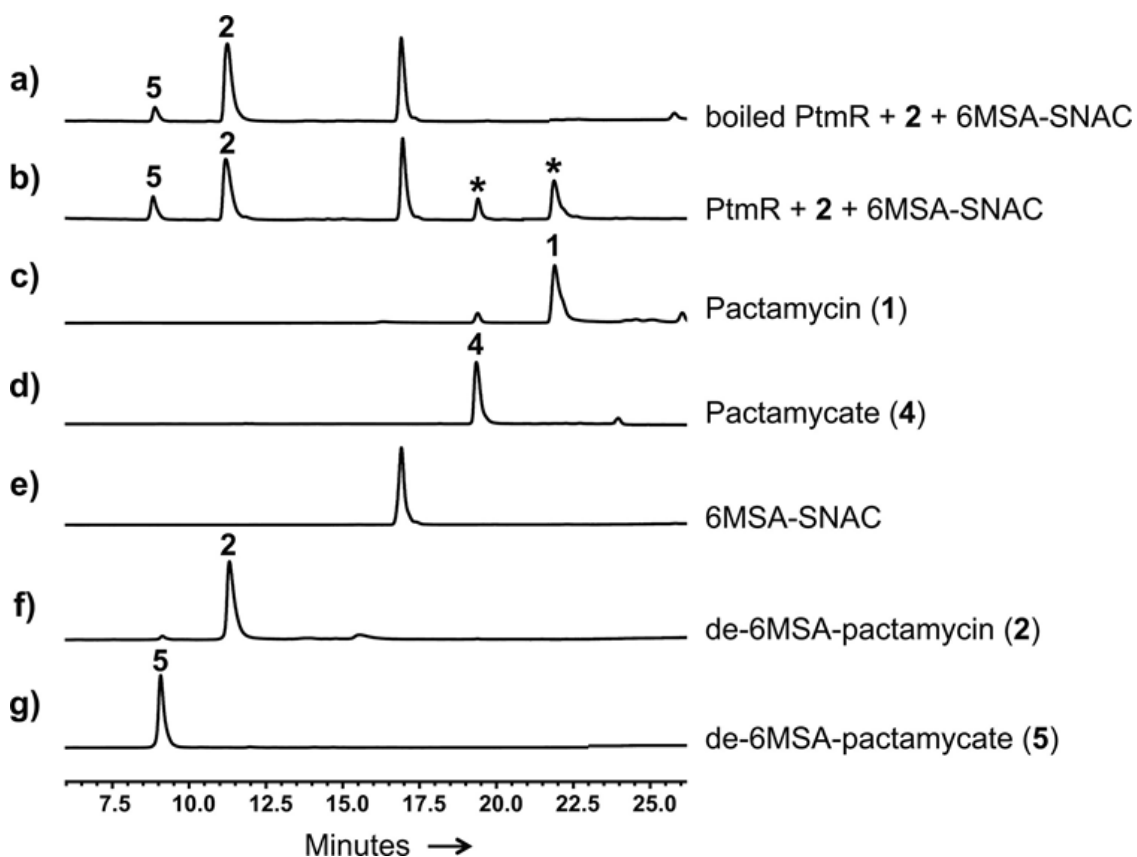


Figure 3.2. HPLC analyses of PtmR reactions using de-6-MSApactamycin

To characterize the catalytic function of PtmR *in vitro*, we cloned the gene in the expression vector pET-20b(+) and heterologously expressed it in *Escherichia coli* BL21(DE3) pLysS to give a 39-kDa C-terminal His₆-tagged protein (Figure S9). Initial enzymatic experiments were carried out using cell-free extracts of *E. coli* containing PtmR,

with de-6-MSApactamycin (**2**), de-6-MSA-7-deoxypactamycin (**3**), de-6-MSApactamycate (**5**), or TM-025 (**7**) as substrates. The synthetically prepared *N*-acetylcysteamine (NAC) thioester of 6-MSA, which mimics an ACP-bound substrate, was used as a model acyl donor substrate. ESI-MS and HPLC analyses of the reaction products revealed the conversion of the de-6-MSA analogs to their corresponding 6-MSA esters (Figures S10 and S11). Similar experiments using purified PtmR protein and de-6-MSA-pactamycin also gave pactamycin and its degradation product, pactamycate (Figure 3.2), which unambiguously confirm the 6-MSA-transferase activity of PtmR. Incubations of the enzyme and TM-025 with 6-MSA free acid as a substrate did not give any products, indicating PtmR only recognizes an activated substrate (data not shown). Moreover, addition of 6-MSA to $\Delta ptmQ$ and $\Delta ptmQ/\Delta ptmH$ cultures did not give pactamycin or TM-026 (Figure S12), suggesting that free 6-MSA is not involved in the pathway.

However, in saphenamycin biosynthesis, it is proposed that 6-MSA is first activated by a 6-MSA adenylase (EsmD2) to its AMP derivative and loaded onto a carrier protein (EsmD3) before being transferred to saphenic acid by EsmD1, a ChlB6 homologue.¹¹ In fact, a gene encoding a putative AMP-forming acyl-CoA synthetase is present in the pactamycin cluster. The gene product (PtmS) has been proposed to catalyze the activation of 3-aminobenzoic acid (3ABA), the precursor of the 3-aminoacetophenone moiety of pactamycin.^{12,15} However, its role in the pactamycin pathway has yet to be experimentally established.

To investigate the possible involvement of PtmS in the 6-MSA transfer, we inac-

tivated the gene in *S. pactum* by in frame-deletion and analyzed the products by ESI-MS. Similar to the $\Delta ptmI$, $\Delta ptmK$, and $\Delta ptmO$ mutants, $\Delta ptmS$ was not able to produce pactamycin or its analogs (Figure S13), suggesting that it is involved in an early step of the pathway. However, the results cannot rule out the possibility of PtmS playing a dual role in the pathway that is activating both 3ABA and 6-MSA. This may also be the case with the discrete ACP PtmI. To test this possibility, we carried out coculture experiments using $\Delta ptmQ/\Delta ptmH + \Delta ptmI$ and $\Delta ptmQ/\Delta ptmH + \Delta ptmS$. Cocultures of $\Delta ptmQ/\Delta ptmH + \Delta ptmJ$ (which lacks the glycosyltransferase activity)¹² were used as a positive control. It is expected that the $\Delta ptmQ/\Delta ptmH$ mutant product (TM-025) will be taken up by $\Delta ptmJ$ and converted to TM-026. A similar phenomenon should occur in the $\Delta ptmQ/\Delta ptmH + \Delta ptmI$ and $\Delta ptmQ/\Delta ptmH + \Delta ptmS$ cultures. However, if PtmI and PtmS are involved in the 6-MSA attachment, no conversion from TM-025 to TM-026 should be observed. As expected, the $\Delta ptmQ/\Delta ptmH + \Delta ptmJ$ cultures produced TM-026 as a major metabolite (Figure S14). The same result was also observed in the cultures of $\Delta ptmQ/\Delta ptmH + \Delta ptmI$ and $\Delta ptmQ/\Delta ptmH + \Delta ptmS$, indicating that both PtmI and PtmS do not play a role in 6-MSA attachment. Altogether, the results show that PtmR is responsible for a direct transfer of the 6-MSA moiety from the iterative type I PKS PtmQ to the aminocyclopentitol unit in pactamycin biosynthesis (Figure 3.3).

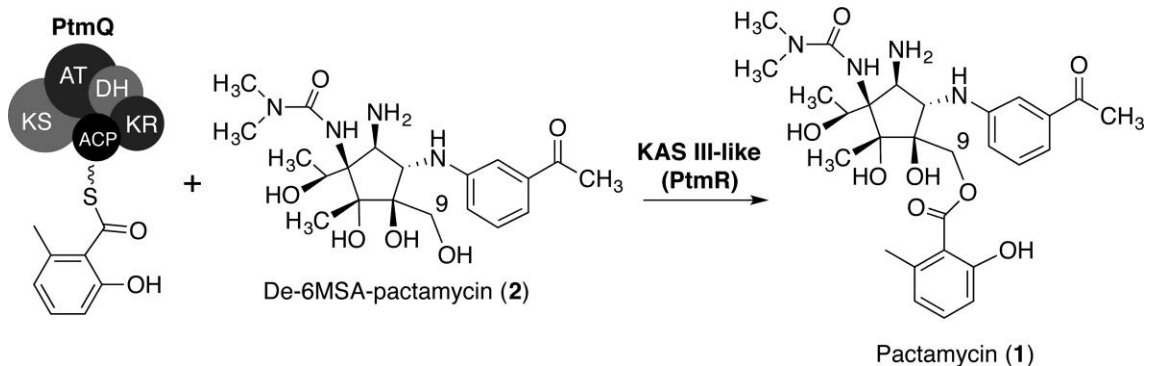


Figure 3.3. Proposed catalytic activity of PtmR.

The fact that PtmR not only processes de-6-MSApactamycin but also de-6-MSA-7-deoxypactamycin, de-6-MSA pactamycate, and TM-025 indicates that it has relaxed substrate specificity in regard to the aminocyclitol moiety. To explore if PtmR can also transfer acyl groups other than 6-MSA, we synthesized an additional 13 NAC thioesters with a variety of alkyl and aromatic features ranging from acetyl-SNAC to 3-aminobenzoyl-SNAC to cycloheptanecarbonyl SNAC (Table 1) and incubated them with TM-025 and a cell-free extract of *E. coli* containing PtmR. ESI-MS analysis of the enzymatic reactions revealed the ability of PtmR to use all 13 NAC thioesters, resulting in a suite of new pactamycin analogs with diverse functionalities (Table 3.1 and Figures S10, S15–S17). Parallel experiments with benzoyl-CoA, acetyl-CoA, propionyl-CoA, and butyryl-CoA did not give any products (Figure S18), indicating that PtmR does not recognize CoA esters as substrates. Scaled-up enzymatic reactions using 4-chlorobutyryl-SNAC furnished TM-107, whose complete chemical structure was determined by 1D and 2D NMR spectroscopic data (Figures S48–S52).

The ability of PtmR to utilize a broad range of substrates is somewhat surprising, as so far KAS III-like proteins, e.g., CloN2, ChIB6, CalO4, AviN, and EvrI, have only been associated with the transfer of an aryl or pyrrolylcarbonyl group to a sugar moiety. A phylogenetic analysis of PtmR and homologous proteins showed that PtmR falls within a clade of KAS III-like enzymes, but it forms a separate subclade together with a number of hypothetical proteins from *Streptomyces niveiscabiei* NRRL B-24457, *Streptomyces acidizcabies* 84–104, and *Streptomyces* sp. DSM 15324 (Figure S19). Genome mining studies revealed that these genes are part of gene clusters that resemble the pactamycin cluster of *S. pactum*. Similar to *ptmR*, they are also located next to a gene encoding an iterative type I PKS (6-MSA synthase). Therefore, we predict that the encoding proteins are also responsible for the attachment of 6-MSA or its analogs to the corresponding natural products.

In conclusion, the present work showed that a highly promiscuous KAS III-like enzyme is responsible for the attachment of 6-MSA directly from an iterative type I PKS to an aminocyclopentitol unit in pactamycin biosynthesis. The results also serve as a starting point for the development of KAS III-like proteins as versatile tools for creation of new libraries of complex natural products.

Table 3.1. Conversion of TM-025 to various pactamycin analogs

R	Product	HR ESI-MS (<i>m/z</i>)		Mol. Formula	Relative Conversion ^a
		Calcd	Observed		
	TM-026	529.2657 [M+H] ⁺	529.2664 [M+H] ⁺	C ₂₇ H ₃₆ N ₄ O ₇	100%
	TM-104	437.2395 [M+Na] ⁺	437.2396 M+Na] ⁺	C ₂₁ H ₃₂ N ₄ O ₆	71%
	TM-105	473.2371 [M+Na] ⁺	473.2383 [M+Na] ⁺	C ₂₂ H ₃₄ N ₄ O ₆	87%
	TM-106	465.2708 [M+H] ⁺	465.2718 [M+H] ⁺	C ₂₃ H ₃₆ N ₄ O ₆	91%
	TM-107	499.2318 [M+H] ⁺	499.2327 [M+H] ⁺	C ₂₃ H ₃₅ ClN ₄ O ₆	100%
	TM-108	465.2708 [M+H] ⁺	465.2718 [M+H] ⁺	C ₂₃ H ₃₆ N ₄ O ₆	83%
	TM-109	479.2864 [M+H] ⁺	479.2874 [M+H] ⁺	C ₂₄ H ₃₈ N ₄ O ₆	61%
	TM-110	505.3021 [M+H] ⁺	505.3025 [M+H] ⁺	C ₂₆ H ₄₀ N ₄ O ₆	44%
	TM-111	479.2864 [M+H] ⁺	479.2872 [M+H] ⁺	C ₂₄ H ₃₈ N ₄ O ₆	20%
	TM-112	499.2551 [M+H] ⁺	499.2558 [M+H] ⁺	C ₂₆ H ₃₄ N ₄ O ₆	43%
	TM-113	514.2660 [M+H] ⁺	514.2690 [M+H] ⁺	C ₂₆ H ₃₅ N ₅ O ₆	17%
	TM-114	513.2708 [M+H] ⁺	513.2738 [M+H] ⁺	C ₂₇ H ₃₆ N ₄ O ₆	95%
	TM-115	505.3021 [M+H] ⁺	505.3022 [M+H] ⁺	C ₂₆ H ₄₀ N ₄ O ₆	57%
	TM-116	519.3177 [M+H] ⁺	519.3182 [M+H] ⁺	C ₂₇ H ₄₂ N ₄ O ₆	87%

^aBased on relative intensity of (+)-ESI-MS substrate (*m/z* 395) and observed product peak.

METHODS

Construction of $\Delta ptmR$ and $\Delta ptmH/\Delta ptmR$ Mutant Strains. The target genes were inactivated using a gene in-frame deletion strategy (Figure S3). Two ~ 1 kb PCR fragments upstream (HindIII/EcoRI) and downstream (EcoRI/XbaI) of the *ptmR* gene were fused and cloned into the HindIII/XbaI site of pBluescript II SK(–) vector to generate pTMM056 (Table S2). The fused PCR fragment was excised and cloned into the HindIII/XbaI site of pTMN002 to generate pTMM057. The plasmid was then introduced into the wildtype, and the $\Delta ptmH$ mutant strains of *S. pactum* ATCC 27456 by conjugation using *E. coli* ET12567/pUZ8002 as a donor strain. Apramycin resistant strains representing single crossover mutants were obtained and grown on BTT [glucose (1%), yeast extract (0.1%), beef extract (0.1%), casein hydrolysate (0.2%), agar (1.5%), pH 7.4] agar plates containing apramycin ($50 \mu\text{g mL}^{-1}$). Subsequently, apramycin sensitive colonies were counter-selected by replica plating on BTT agar with and without apramycin ($50 \mu\text{g mL}^{-1}$). The resulting double crossover candidate strains were confirmed by PCR amplification with *ptmR*-F1 and *ptmR*-R2 primers (Table S3) flanking the respective targeted gene (Figure S3).

Complementation of $\Delta ptmH/\Delta ptmR$ Mutant. For complementation of the $\Delta ptmH/\Delta ptmR$ mutant, the *ptmR* gene was amplified by PCR using the primers *PtmR*-pET-F and *PtmR*-C-R (Table S3). The PCR products were digested with BglII and EcoRI and

ligated into the BamHI/EcoRI sites of the cloning vector pBluescript II SK(–) to generate pTMM058. DNA sequencing confirmed the correct sequence of the construct. The resulting plasmid was digested with NdeI/EcoRI, and the DNA fragment was ligated into the integration vector pTMW50, predigested with the same restriction enzymes, to generate pTMM059. The pTMM059 plasmid was then transferred into *E. coli* ET12567/pUZ8002, which was subsequently used to transform the $\Delta ptmH$ strain by conjugation.¹⁶ Selection of the exconjugants ($\Delta ptmH/\Delta ptmR$ mutants) was performed on BTT agar containing apramycin (50 $\mu\text{g mL}^{-1}$) and ampicillin (100 $\mu\text{g mL}^{-1}$).

Analysis of $\Delta ptmR$, $\Delta ptmH/\Delta ptmR$, and $\Delta ptmH/\Delta ptmR$ +pTMM059 Metabolic Profiles.

The $\Delta ptmR$, $\Delta ptmH/\Delta ptmR$, and $\Delta ptmH/\Delta ptmR$ +pTMM059 strains were grown on BTT agar at 30°C for 3 days. Single colonies were used to inoculate the BTT seed cultures [medium for $\Delta ptmH/\Delta ptmR$ + pTMM059 was supplemented with apramycin (10 $\mu\text{g mL}^{-1}$) and ampicillin (20 $\mu\text{g mL}^{-1}$)] and incubated at 30 °C for 2 days. Production cultures were prepared in modified Bennett's medium (50 mL)¹² and inoculated with seed cultures [10% (v/v)]. The production cultures were incubated at 30 °C for 5 days under vigorous shaking (200 rpm). The mycelia were centrifuged, and the supernatants were extracted twice with equal volumes of EtOAc followed by extraction with *n*-BuOH. The organic solvent from each extraction was evaporated *in vacuo* and the residues dissolved in MeOH and analyzed by reversed-phase HPLC and/or ESI-MS. Analysis of the metabolites of the mutants and those complemented with *ptmR* was carried out by reversed-

phase HPLC with a C-18 column (Supelcosil LC-18-DB 15 cm × 4.6 cm, 5 μ m) using H₂O [95% (v/v)] and CH₃CN [5% (v/v)] containing TFA [0.1% (v/v)] as a mobile phase at a 1 mL min⁻¹ flow rate.

Construction of $\Delta ptmI$, $\Delta ptmO$, and $\Delta ptmS$ Mutant Strains. The target genes were inactivated using a gene in-frame deletion strategy (Figure S3a).

Construction of $ptmK::aac(3)IV$ Mutant. The $ptmK$ gene (1.7kb) was inactivated using a gene disruption strategy (Figure S3b).

Feeding Experiments with 6-MSA to $\Delta ptmQ$ and $\Delta ptmH/\Delta ptmQ$ Mutants. The $\Delta ptmQ$ and $\Delta ptmH/\Delta ptmQ$ mutants were streaked on BTT agar [glucose (1% (w/v)), yeast extract (0.1% (w/v)), beef extract (0.1% (w/v)), casein hydrolysate (0.2% (w/v)), agar (1.5% (w/v)), pH 7.3] and incubated at 30 °C for 3 days. Spores of the $\Delta ptmQ$ and $\Delta ptmH/\Delta ptmQ$ mutants were individually grown in two Erlenmeyer flasks (125 mL) containing seed medium [glucose (1% (w/v)), yeast extract (0.1% (w/v)), beef extract (0.1% (w/v)), casein hydrolysate (0.2% (w/v)), pH 7.3; 50 mL] for 3 days at 30 °C and 200 rpm. Each of these seed cultures (10 mL) was used to inoculate four Erlenmeyer flasks (250 mL) containing modified Bennett's medium (100 mL). After incubation for 18 h under the same conditions, the cultures were grouped into two groups: the first group was supplemented with 6-MSA (5 mM, 250 μ L), and the second group was used as a control.

The feeding was repeated every 12 h for 2 days. All experiments were done in triplicate. After 5 days of incubation, the cultures were centrifuged. The metabolites of each group were extracted with ethyl acetate (2×100 mL). The organic solvent was evaporated using a rotary evaporator, and the products were analyzed by MS.

Coculture Experiments. For details on coculture experiments with $\Delta ptmJ$, $\Delta ptmI$, $\Delta ptmS$, and $\Delta ptmH/\Delta ptmQ$ mutants, see the Supporting Information.

Production of PtmR. The *ptmR* gene was amplified using primer pairs PtmR-pET-F and PtmR-pET-R (Table S3). High fidelity Taq DNA polymerase (Invitrogen) was used for PCR, and the resulting 1.0-kb PCR product was cloned into the pET-20b(+) vector (Novagen) to generate expression vector pTMM060, which was introduced into *E. coli* BL21(DE3) pLysS (Invitrogen). For protein production, the bacteria were grown in LB medium supplemented with ampicillin ($100 \mu\text{g mL}^{-1}$) and chloramphenicol ($25 \mu\text{g mL}^{-1}$) at 30°C with shaking at 250 rpm until an OD₆₀₀ of 0.8–1 was reached. The culture was shaken at 16°C for 1 h. Protein expression was induced by the addition of IPTG (0.5 mM) with further cultivation for 36 h. The cells were harvested by centrifugation and resuspended in sodium phosphate buffer (40 mM, pH 7.5) containing NaCl (300 mM) and imidazole (10 mM) and then disrupted by sonication. After centrifugation of the sample, the supernatant was directly loaded onto a Ni-NTA spin column (Qiagen). The recombinant PtmR was eluted using sodium phosphate buffer (40 mM, pH 7.5) containing NaCl (300 mM)

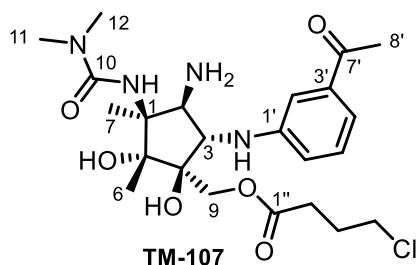
and imidazole (250 mM). The PtmR-containing fractions were dialyzed (3 times, 5 h each) in 1 L of solution containing sodium phosphate buffer (20 mM, pH 7), MgCl_2 (10 mM), glycerol (10% (w/v)), and dithiothreitol (0.5 mM) at 4 °C.

Acyltransferase Assay: The acyltransferase reaction was typically carried out in 50 μL mixtures containing TM-25 or de-6-MSApactamycin (1 mM), NAC thioester (2 mM), purified PtmR or a cell free extract of *E. coli* containing PtmR (47 μL), and MgCl_2 (10 mM) in sodium phosphate buffer (50 mM, pH 7.5). Boiled protein or cell free extract of empty pET-20b(+) was used as a negative control. The reaction was incubated at 30 °C. After 4 h, the reaction was quenched by the addition of one volume of MeOH, centrifuged at 14 000 rpm for 15 min, and the supernatants were analyzed by reversed-phase HPLC and/or ESI-MS.

Scaled-up Enzymatic Reaction and Isolation of TM-107: Scaled-up enzymatic reactions (100 $\mu\text{L} \times 100$, 10 mL total) were carried out using the cell free extract of *E. coli* containing PtmR in sodium phosphate buffer (40 mM, pH 7.5, contains 10 mM MgCl_2 and 10% (w/v) glycerol), TM-025 (1 mM), and 4-chlorobutyryl- SNAC (2 mM). The mixtures were incubated at 30 °C for 3 h. The reactions were then quenched by the addition of one volume of MeOH and centrifuged at 14 000 rpm for 15 min. The supernatants were pooled and subjected to rotary evaporator to remove MeOH, and the aqueous mixture was extracted twice with two volumes of EtOAc. The EtOAc extract was dried in vacuo, and the residue was dissolved in MeOH (400 μL) and subjected to reverse-phase HPLC (YMC-Pack ODS-A, 250 \times 10 mm I.D., 5 μm ; solvent gradient: $\text{CH}_3\text{CN-H}_2\text{O}$ (5:95) to

CH₃CN (100%) containing TFA [0.1% (v/v)] over 60 min, flow rate 4.7 mL min⁻¹, detection at 254 nm) to give TM-107 (1.2 mg). TM-107. A white powder, [α]_D = +37° (c 0.267, MeOH, 20 °C). UV (MeOH): λ max 240 nm (ε 1.6 × 10³), 264 nm (ε 4.65 × 10²), and 354 nm (ε 24.4). IR (KBr, MeOH): ν = 3359, 2919, 2856, 1679, 1536, 1483, 1206, and 1138 cm⁻¹. ¹H NMR (700 MHz, CD₃OD) ¹³CNMR (175 MHz, CD₃OD):

Table 3.2. ¹H NMR and ¹³C NMR shifts for TM107



position	δ _H (ppm) int., multipl. (Hz)	δ _C (ppm)
2'	7.36 (1H, m)	111.3
4'	7.32 (1H, m)	117.5
5'	7.29 (1H, t, 8)	129.0
6'	7.03 (1H, m)	118.0
NH	6.64 (1H, brs)	-
9	4.31 (2H, q, 12)	64.6
3	4.14 (1H, d, 9)	65.3
2	3.73 (1H, d, 9)	64.0
4''	3.45 (2H, m)	43.4
11, 12	2.98 (6H, s)	35.4
8'	2.59 (3H, s)	25.5
2''	2.22 (1H, m); 1.94 (1H, m)	30.3
3''	1.8 (2H, m)	27.2
7	1.66 (3H, s)	13.5
6	1.42 (3H, s)	14.9
7'	-	200.1
10	-	159.2
1''	-	172.8
3'	-	137.9
1'	-	149.0
5	-	81.3
4	-	82.1
1	-	65.1

Reference

1. A template search reveals mechanistic similarities and differences in beta-ketoacyl synthases (KAS) and related enzymes. Dawe, J. H., Porter, C. T., Thornton, J. M., Tabor, A. B. *Proteins: Struct., Funct., Genet.* **2003**, 52, 427–435.
2. Characterization of beta-ketoacyl-acyl carrier protein synthase III from *Streptomyces glaucescens* and its role in initiation of fatty acid biosynthesis: Han, L., Lobo, S., Reynolds, K. A. *J. Bacteriol.* **1998**, 180, 4481–4486.
3. CloN2, a novel acyltransferase involved in the attachment of the pyrrole-2-carboxyl moiety to the deoxysugar of clorobiocin: Xu, H., Kahlich, R., Kammerer, B., Heide, L., Li, S. M. *Microbiology* **2003**, 149, 2183–2191.
4. A ketosynthase homolog uses malonyl units to form esters in cervimycin biosynthesis: Bretschneider, T., Zocher, G., Unger, M., Scherlach, K., Stehle, T., Hertweck, C. *Nat. Chem. Biol.* **2012**, 8, 154–161.
5. Dissection of two acyl-transfer reactions centered on acyl-S-carrier protein intermediates for incorporating 5-chloro-6-methyl-O-methylsalicylic acid into chlorothricin: He, Q. L., Jia, X. Y., Tang, M. C., Tian, Z. H., Tang, G. L., Liu, W. *ChemBioChem*, **2009**, 10, 813–819.
6. Biosynthesis of the orthosomycin antibiotic avilamycin A: deductions from the molecular analysis of the avi biosynthetic gene cluster of *Streptomyces viridochromogenes* Tu57 and production of new antibiotics: Weitnauer, G., Muhlenweg, A., Trefzer, A., Hoffmeister, D., Sussmuth, R. D., Jung, G., Welzel, K., Vente, A., Girreser, U., Bechthold, A. *Chem. Biol.* **2006**, 8, 569–581.
7. Characterization of the biosynthetic gene cluster for the oligosaccharide antibiotic, Evernimicin, in *Micromonospora carbonacea* var. *africana* ATCC39149. Hosted, T. J., Wang, T. X., Alexander, D. C., Horan, A. C. *J. Ind. Microbiol. Biotechnol.* **2001** 27, 386–392.
8. The calicheamicin gene cluster and its iterative type I enediyne PKS. Ahlert, J., Shepard, E., Lomovskaya, N., Zazopoulos, E., Staffa, A., Bachmann, B. O., Huang, K., Fontstein, L., Csisny, A., Whitwam, R. E., Farnet, C. M., Thorson, J. S. *Science* **2002**, 297, 1173–1176.
9. Organisation of the biosynthetic gene cluster and tailoring enzymes in the biosynthesis of the tetracyclic quinone glycoside antibiotic polyketomycin. Daum, M., Peintner, I., Linnenbrink, A., Frerich, A., Weber, M., Paululat, T., Bechthold, A. *ChemBioChem* **2009**, 10, 1073–1083.
10. Characterization of tiacumicin B biosynthetic gene cluster affording diversified tiacumicin analogues and revealing a tailoring dihalogenase. Xiao, Y., Li, S., Niu, S., Ma, L., Zhang, G., Zhang, H., Zhang, G., Ju, J., Zhang, C. *J. Am. Chem. Soc.* **2011**, 133, 1092–1105.
11. Insights into a divergent phenazine biosynthetic pathway governed by a plasmid-born esmeraldin gene cluster. Rui, Z., Ye, M., Wang, S., Fujikawa, K., Akerele, B., Aung, M., Floss, H. G., Zhang, W., Yu, T. W. *Chem. Biol.* **2012**, 19, 1116–1125.

12. Deciphering pactamycin biosynthesis and engineered production of new pactamycin analogues. Ito, T., Roongsawang, N., Shirasaka, N., Lu, W., Flatt, P. M., Kasanah, N., Miranda, C., Mahmud, T. *ChemBioChem*, **2009**, 10, 2253–2265.
13. Interrogating the tailoring steps of pactamycin biosynthesis and accessing new pactamycin analogues. Abugrain, M. E., Lu, W., Li, Y., Serrill, J. D., Brumsted, C. J., Osborn, A. R., Alani, A., Ishmael, J. E., Kelly, J. X., Mahmud, T. *ChemBioChem* **2016**, 17, 1585–1588.
14. Biosynthetic studies and genetic engineering of pactamycin analogs with improved selectivity toward malarial parasites. Lu, W., Roongsawang, N., Mahmud, T. *Chem. Biol.* **2011**, 18, 425–431.
15. Cloning of the pactamycin biosynthetic gene cluster and characterization of a crucial glycosyltransferase prior to a unique cyclopentane ring formation. Kudo, F., Kasama, Y., Hirayama, T., Eguchi, T. *J. Antibiot.* **2007**, 60, 492–503.
16. Kieser, T., Bibb, M. J., Buttner, M. J., Chater, K. F., Hopwood, D. A. *Practical Streptomyces Genetics*, The John Innes Foundation, Norwich, England, **2000**.

SUPPORTING INFORMATION

A Highly Promiscuous β -Ketoacyl-ACP Synthase (KAS) III-like Protein is Involved in Pactamycin Biosynthesis

Mostafa E. Abugrain,[†] Corey J. Brumsted,[‡] Andrew R. Osborn,[†] Benjamin Philmus,[†] and Taifo Mahmud^{†,‡,*}

[†]Department of Pharmaceutical Sciences, Oregon State University Corvallis, Oregon 97331, United States

[‡]Department of Chemistry, Oregon State University, Corvallis, Oregon 97331, United States

Inventory of Supporting Items:

Supporting Methods

Supporting Tables

Table S1. Bacterial strains used in this study.

Table S2. Plasmids used in this study.

Table S3. Primers used in this study.

Table S4. Sources and accession numbers of KAS III homologues.

Table S5. ¹H and ¹³C NMR data for TM-107.

Supporting Figures

Figure S1. Distinct catalytic activities of KAS III and KAS III-like proteins.

Figure S2. Genetic organization of the pactamycin biosynthetic gene cluster.

Figure S3. Cloning strategies for in-frame and gene disruption mutations of *S. pactum*.

Figure S4. Genotypic confirmation of Δ ptmI, Δ ptmO, Δ ptmR, Δ ptmH/ Δ ptmR, and *ptmK::aac(3)IV* mutants by PCR.

Figure S5. ESI-MS analysis of Δ ptmI, Δ ptmO, and *ptmK::aac(3)IV* mutants.

Figure S6. HPLC analyses of Δ ptmR and Δ ptmH/ Δ ptmR mutant strains of *S. pactum*.

Figure S7. ESI-MS analysis of Δ ptmR mutant.

Figure S8. ESI-MS analysis of Δ ptmH/ Δ ptmR mutant.

Figure S9. SDS PAGE of purified PtmR.

Figure S10. ESI-MS spectra of de-6-MSA-pactamycin, de-6-MSA-pactamycate, and TM-025 incubated with cell free extracts of cultures of *E. coli* harboring empty vector pET-20b(+) and that harboring *ptmR* in the presence of 6-MSA-SNAC or acetyl-SNAC.

Figure S11. HPLC profile of PtmR enzymatic reaction using de-6-MSA-pactamycate and 6-MSA-SNAC.

Figure S12. Feeding experiments with 6-MSA to the Δ ptmQ and Δ ptmQ/ Δ ptmH strains of *S. pactum*.

Figure S13. Genotypic and phenotypic analyses of Δ ptmS.

Figure S14. ESI-MS analysis of co-culture products.

Figure S15. ESI-MS spectra of TM-025 incubated with cell free extracts of cultures of *E. coli* harboring empty vector pET-20b(+) and that harboring *ptmR* in the presence of propionyl-, butyryl-, chlorobutyryl-, or isobutyryl-SNAC.

Figure S16. ESI-MS spectra of TM-025 incubated with cell free extracts of cultures of *E. coli* harboring empty vector pET-20b(+) and that harboring *ptmR* in the presence of isovaleryl-, 2,4-dimethyl-2-pentenoyl-, 2-methylbutyryl-, or benzoyl-SNAC.

Figure S17. ESI-MS spectra of TM-025 incubated with cell free extracts of cultures of *E. coli* harboring empty vector pET-20b(+) and that harboring *ptmR* in the presence of 3-aminobenzoyl-, phenylacetyl-, cyclohexanecarbonyl-, or cycloheptanecarbonyl-SNAC.

Figure S18. ESI-MS spectra of TM-025 (*m/z* 395) incubated with cell free extracts of cultures of *E. coli* harboring empty vector pET-20b(+) and that harboring *ptmR* in the presence of NAC and CoA esters of acetate, propionate, butyrate, and benzoate.

Figure S19. Phylogenetic analysis of PtmR and homologous proteins.

Figure S20. ^1H NMR spectrum of 6-MSA-SNAC.

Figure S21. ^{13}C NMR spectrum of 6-MSA-SNAC.

Figure S22. ^1H NMR spectrum of acetyl-SNAC.

Figure S23. ^{13}C NMR spectrum of acetyl-SNAC.

Figure S24. ^1H NMR spectrum of propionyl-SNAC.

Figure S25. ^{13}C NMR spectrum of propionyl-SNAC.

Figure S26. ^1H NMR spectrum of butyryl-SNAC.

Figure S27. ^{13}C NMR spectrum of butyryl-SNAC.

Figure S28. ^1H NMR spectrum of 4-chlorobutyryl-SNAC.

Figure S29. ^{13}C NMR spectrum of 4-chlorobutyryl-SNAC.

Figure S30. ^1H NMR spectrum of isobutyryl-SNAC.

Figure S31. ^{13}C NMR spectrum of isobutyryl-SNAC.

Figure S32. ^1H NMR spectrum of isovaleryl-SNAC.

Figure S33. ^{13}C NMR spectrum of isovaleryl-SNAC.

Figure S34. ^1H NMR spectrum of 2,4-dimethyl-2-pentenoyl-SNAC.

Figure S35. ^{13}C NMR spectrum of 2,4-dimethyl-2-pentenoyl-SNAC.

Figure S36. ^1H NMR spectrum of 2-methylbutyryl-SNAC.

Figure S37. ^{13}C NMR spectrum of 2-methylbutyryl-SNAC.

Figure S38. ^1H NMR spectrum of benzoyl-SNAC.

Figure S39. ^{13}C NMR spectrum of benzoyl-SNAC.

Figure S40. ^1H NMR spectrum of 3-aminobenzoyl-SNAC.

Figure S41. ^{13}C NMR spectrum of 3-aminobenzoyl-SNAC.

Figure S42. ^1H NMR spectrum of phenylacetyl-SNAC.

Figure S43. ^{13}C NMR spectrum of phenylacetyl-SNAC.

Figure S44. ^1H NMR spectrum of cyclohexanecarbonyl-SNAC.

Figure S45. ^{13}C NMR spectrum of cyclohexanecarbonyl-SNAC.

Figure S46. ^1H NMR spectrum of cycloheptanecarbonyl-SNAC.

Figure S47. ^{13}C NMR spectrum of cycloheptanecarbonyl-SNAC.

Figure S48. ^1H NMR spectrum of TM-107.

Figure S49. ^{13}C NMR spectrum of TM-107.

Figure S50. HSQC spectrum of TM-107.

Figure S51. HMBC spectrum of TM-107.

Figure S52. ^1H - ^1H COSY spectrum of TM-107.

Supporting References

Supporting methods

General. All chemicals were obtained either from Sigma Aldrich, EMD, TCI, or Pharmacia. Analytical thin-layer chromatography (TLC) was performed using silica gel plates (60 Å), which were visualized using a UV lamp and ceric ammonium molybdate (CAM) solution. Chromatographic purification of products was performed on silica gel (60 Å, 72–230 mesh). NMR spectra were recorded on Bruker 400, 500, or 700 MHz spectrometers. Chemical shifts are reported in ppm (δ) relative to the residual solvent signals as the internal standard. Multiplicities in the ^1H NMR spectra are described as follows: s = singlet, bs = broad singlet, d = doublet, bd = broad doublet, t = triplet, bt = broad triplet, q = quartet, m = multiplet; coupling constants are reported in Hz. (ESI) mass spectra were recorded on a Thermo-Finnigan liquid chromatograph-ion trap mass spectrometer. High-resolution ESI mass spectra were recorded on a ThermoElectron LTQ-Orbitrap Discovery mass spectrometer with a dedicated Accela HPLC system.

General DNA manipulations. Genomic DNA of *S. pactum* ATCC 27456 was prepared by standard protocol¹ or using the DNeasy Tissue Kit (Qiagen). DNA fragments were recovered from an agarose gel by using the QIAquick Gel Extraction Kit (Qiagen). Restriction endonucleases were purchased from Invitrogen or Promega. Preparation of plasmid DNA was done by using a QIAprep Spin Miniprep Kit (Qiagen). All other DNA manipulations were performed according to standard protocols.^{1,2} PCR was performed in 30 cycles by using a Mastercycler gradient thermocycler (Eppendorf) and Platinum *Taq* high fidelity DNA polymerase (Invitrogen). Oligodeoxyribonucleotides for PCR primers were synthesized by Sigma-Genosys. The nucleotide sequences of the gene fragments were determined at the Center for Genome Research and Biocomputing (CGRB) Core Laboratories, Oregon State University. ORFs were analyzed by FramePlot3 analysis and BLAST program.⁴

Construction of $\Delta ptmI$, $\Delta ptmO$, and $\Delta ptmS$ mutant strains. The target genes were inactivated using a gene in-frame deletion strategy (Figure S3a). Two ~1 kb PCR fragments upstream (HindIII/EcoRI) and downstream (EcoRI/XbaI) of the *ptmI*, *ptmO* and *ptmS* genes were fused and cloned into the HindIII/XbaI site of pBluescript II SK(-) vector to generate pTMM051, pTMM007, and pTMM015, respectively. The PCR products of *ptmI* and *ptmO* were excised and cloned into the HindIII/XbaI site of pTMN002 to generate pTMM052, pTMM08, and pTMM016, respectively. All plasmids were then individually introduced into *S. pactum* ATCC 27456 strain by conjugation using the *E. coli* donor

strain ET12567/pUZ8002. Apramycin resistant strains representing single crossover mutants were obtained and subsequently grown on BTT agar plates containing apramycin ($50 \mu\text{g mL}^{-1}$). Apramycin sensitive colonies were counter-selected by replica plating on BTT agar with and without apramycin ($50 \mu\text{g mL}^{-1}$). The resulting double-crossover candidate strains were confirmed by PCR amplification with HindIII/XbaI primers flanking the respective targeted gene.

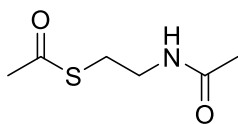
Construction of *ptmK::aac(3)IV* mutant. The *ptmK* gene (1.7 kb) was inactivated using a gene disruption strategy (Figure S3b). The internal fragment (0.88 kb) of *ptmK* was generated by PCR using a forward primer containing a HindIII site and a reverse primer containing an XbaI site and *S. pactum* genomic DNA as template. The PCR product was cloned into the HindIII/XbaI sites of pTMN002 to generate pTMM055. Plasmid pTMM055 was introduced into *S. pactum* strain by conjugation, as described in our previous publication.⁵ Briefly, the freshly harvested spores and the overnight-grown *Escherichia coli* ET12567/pUZ8002 containing plasmid pTMM055 were mixed and plated onto an MS agar plate containing 10 mM MgCl₂ (10 mM). After incubation at 30 °C for 18 h, the plate was overlaid with sterile water (1 mL) containing nalidixic acid (1mg mL^{-1}) and apramycin (1 mg mL^{-1}) and incubated at 30 °C for 5-7 days. The exconjugant (single crossover) colonies were purified by plating on BTT agar plates supplemented with apramycin ($50 \mu\text{g mL}^{-1}$). The disruption of *ptmK* was confirmed by PCR amplification (Figure S3).

Co-culture experiments. The $\Delta ptmJ$, $\Delta ptmI$, $\Delta ptmS$, and $\Delta ptmH/\Delta ptmQ$ mutants were streaked on BTT agar [glucose (1%), yeast extract (0.1%), beef extract (0.1%), casein hydrolysate (0.2%), agar (1.5%), pH 7.3] and incubated at 30 °C for 3 days. Spores of the $\Delta ptmJ$, $\Delta ptmI$, $\Delta ptmS$ and $\Delta ptmH/\Delta ptmQ$ mutants were individually grown in Erlenmeyer flasks (125 mL) containing seed medium [glucose (1%), yeast extract (0.1%), beef extract (0.1%), casein hydrolysate (0.2%), pH 7.3] (50 mL) for 3 days at 30 °C and 200 rpm. The seed culture of $\Delta ptmH/\Delta ptmQ$ mutant (5 mL each) was then transferred to 3 Erlenmeyer flasks (150 mL) containing modified Bennett's medium (50 mL), and to each of these cultures was added the seed culture (5 mL) of $\Delta ptmJ$, $\Delta ptmS$, or $\Delta ptmI$ individually and grown at 30 °C and 200 rpm. All experiments were done in triplicate. Each of the mutants was also grown individually in modified Bennett's medium (50 mL) as control. After five days of incubation, the cultures were centrifuged and the metabolites of each control and co-cultures were extracted from the broths with ethyl acetate (2 x 50 mL). The organic solvent was evaporated using rotary evaporator and the products were analyzed by ESI-MS.

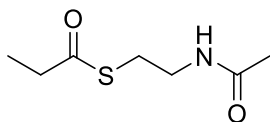
Chemical synthesis of NAC thioesters. *S*-(2-acetamidoethyl) 2-hydroxy-6-methylbenzothioate (6-MSA-SNAC): To 2-hydroxy-6-methyl-benzoic acid (100 mg, 0.66 mmol) in CH_2Cl_2 (10 mL) was added HOBT (1.05 eq, 0.69 mmol, 92 mg), EDCI (1.05 eq, 0.69 mmol, 131 mg), HSNAC (1.4 eq, 0.92 mmol, 110 mg), then triethylamine (2 eq, 1.32 mmol, 133 mg) at 0 °C and stirred 18 h gradually reaching room temperature. The reac-

tion was diluted with CH_2Cl_2 (20 mL) and washed successively with saturated aqueous NaHCO_3 solution (5 mL), H_2O (10 mL), 1M HCl (15 mL), then brine (5 mL). The organic fraction was then dried over Na_2SO_4 , filtered and the solvent removed *in vacuo*. The product was purified by flash column chromatography (Hexane – EtOAc = 6:1, 4:1) to give pure 6-MSA-SNAC (40 mg, 25%). ^1H NMR (500 MHz, CDCl_3) δ = 7.23 (br t, J = 8 Hz, 1H), 6.82 (d, J = 8 Hz, 1H), 6.74 (d, J = 8 Hz, 1H), 5.98 (brs, 1H), 3.58 (brq, J = 6 Hz, 2H), 3.24 (t, J = 6 Hz, 2H), 2.58 (s, 3H), 2.00 (s, 3H). ^{13}C NMR (125 MHz, CDCl_3) δ = 197.7, 170.9, 157.9, 137.9, 133.3, 123.5, 123.1, 115.7, 39.3, 29.8, 23.2, 22.8. HR ESI-MS: m/z 276.0667 $[\text{M}+\text{Na}]^+$, calculated for $\text{C}_{12}\text{H}_{15}\text{NO}_3\text{SNa}$ 276.0665.

Other NAC thioesters were synthesized using a standard procedure described above.

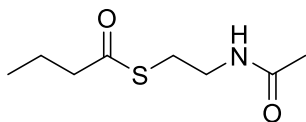


Acetyl-SNAC: ^1H NMR (700 MHz, CDCl_3) δ = 5.90 (s, 1H), 3.44 (brq, J = 6 Hz, 2H), 3.03 (t, J = 6 Hz, 2H), 2.36 (s, 3H), 1.98 (s, 3H). ^{13}C NMR (176 MHz, CDCl_3) δ = 196.4, 170.4, 39.7, 30.7, 28.8, 23.2. HR-ESI-MS: calculated for $\text{C}_5\text{H}_{11}\text{NO}_2\text{SNa}$ m/z 184.04027 $[\text{M}+\text{Na}]^+$, found m/z 184.04054.

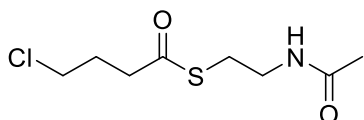


Propionyl-SNAC: ^1H NMR (500 MHz, CDCl_3) δ = 6.07 (s, 1H), 3.40 (td, J = 6 Hz, 2H), 3.00 (t, J = 6 Hz, 2H), 2.57 (q, J = 8 Hz, 2H), 1.94 (s, 3H), 1.15 (t, J = 7.5 Hz, 3H). ^{13}C NMR (126

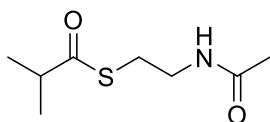
MHz, CDCl_3) δ = 200.8, 170.4, 39.7, 37.5, 28.4, 23.2, 9.6. HR-ESI-MS: calculated for $\text{C}_7\text{H}_{13}\text{NO}_2\text{SNa}$ m/z 198.05592 $[\text{M}+\text{Na}]^+$, found m/z 198.05628.



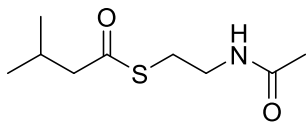
Butyryl-SNAC: ^1H NMR (500 MHz, CDCl_3) δ = 5.97 (brs, 1H), 3.41 (brq, J = 7 Hz, 2H), 3.00 (t, J = 7 Hz, 2H), 2.53 (t, J = 7 Hz, 2H), 1.94 (s, 3H), 1.67 (brh, J = 7 Hz, 2H), 0.93 (t, J = 7 Hz, 3H). ^{13}C NMR (126 MHz, CDCl_3) δ = 200.1, 170.3, 45.9, 39.8, 28.4, 23.2, 19.2, 13.5. ^1H -HR-ESI-MS: calculated for $\text{C}_8\text{H}_{15}\text{NO}_2\text{SNa}$ m/z 212.07157 $[\text{M}+\text{Na}]^+$, found m/z 212.07188.



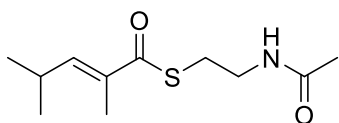
4-Chlorobutyryl-SNAC: ^1H NMR (700 MHz, CDCl_3) δ = 5.87 (s, 1H), 3.58 (t, J = 7 Hz, 2H), 3.44 (brq, 3J = 6 Hz, 2H), 3.05 (t, J = 6 Hz, 2H), 2.78 (t, J = 7.2 Hz, 2H), 2.17 – 2.02 (m, 2H), 1.98 (s, 3H). ^{13}C NMR (176 MHz, CDCl_3) δ = 198.8, 170.4, 43.8, 40.9, 39.6, 28.7, 28.0, 23.2. HR-ESI-MS: calculated for $\text{C}_8\text{H}_{14}\text{ClNO}_2\text{SNa}$ m/z 246.03260 $[\text{M}+\text{Na}]^+$, found m/z 246.03289.



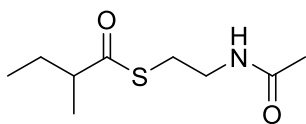
Isobutyryl-SNAC: ^1H NMR (500 MHz, CDCl_3) δ = 5.81 (s, 1H), 3.43 (brq, J = 6 Hz, 2H), 3.01 (t, J = 6 Hz, 2H), 2.76 (hept, J = 7 Hz, 1H), 1.96 (s, 3H), 1.20 (d, J = 7 Hz, 6H). ^{13}C NMR (126 MHz, CDCl_3) δ = 204.9, 170.3, 43.2, 39.8, 28.2, 23.2, 19.4. HR-ESI-MS: calcd for $\text{C}_8\text{H}_{15}\text{NO}_2\text{SNa}$ m/z 212.07157 $[\text{M}+\text{Na}]^+$, found m/z 212.07142.



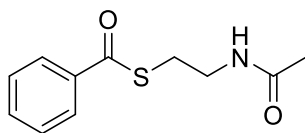
Isovaleryl-SNAC: ^1H NMR (700 MHz, CDCl_3) δ = 6.10 (brs, 1H), 3.45 (brq, J = 6 Hz, 2H), 3.04 (t, J = 6 Hz, 2H), 2.46 (d, J = 7 Hz, 2H), 2.20 – 2.12 (m, 1H), 2.00 (s, 3H), 0.96 (d, J = 7 Hz, 6H). ^{13}C NMR (176 MHz, CDCl_3) δ = 199.8, 170.7, 52.9, 40.1, 28.4, 26.5, 23.0, 22.3. HR-ESI-MS: calculated for $\text{C}_9\text{H}_{17}\text{NO}_2\text{SNa}$ m/z 226.08722 $[\text{M}+\text{Na}]^+$, found m/z 226.08683.



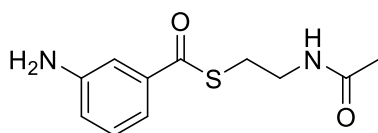
2,4-Dimethyl-2-pentenoyl-SNAC: ^1H NMR (700 MHz, CDCl_3) δ = 6.56 (dd, J = 10, 1 Hz, 1H), 6.03 (s, 1H), 3.54 – 3.35 (m, 2H), 3.16 – 2.92 (m, 2H), 2.77 – 2.58 (m, 1H), 1.98 – 1.97 (m, 2H), 1.87 (d, J = 1 Hz, 3H), 1.06 – 1.02 (m, 6H). ^{13}C NMR (176 MHz, CDCl_3) δ = 194.3, 170.4, 148.4, 133.7, 39.9, 28.4, 28.1, 23.2, 21.9, 12.4. HR-ESI-MS: calculated for $\text{C}_{11}\text{H}_{19}\text{NO}_2\text{SNa}$ m/z 252.10287 $[\text{M}+\text{Na}]^+$, found m/z 252.10215.



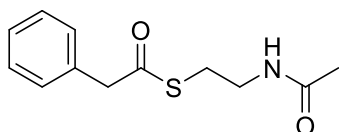
2-Methylbutyryl-SNAC: ^1H NMR (400 MHz, CDCl_3) δ = 5.92 (s, 1H), 3.4 (td, J = 7, 2 Hz, 2H), 3.02 (td, J = 7, 2 Hz, 2H), 2.70 – 2.43 (m, 1H), 1.97 (d, J = 2 Hz, 3H), 1.82 – 1.61 (m, 1H), 1.59 – 1.30 (m, 1H), 1.17 (dd, J = 7, 2 Hz, 3H), 0.91 (td, J = 7, 2 Hz, 3H). ^{13}C NMR (101 MHz, CDCl_3) δ = 204.6, 170.4, 170.1, 50.2, 39.9, 28.1, 27.2, 23.2, 17.2, 11.6. HR-ESI-MS: calculated for $\text{C}_9\text{H}_{17}\text{NO}_2\text{SNa}$ m/z 226.08722 $[\text{M}+\text{Na}]^+$, found m/z 226.08652.



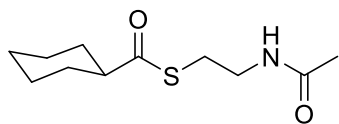
Benzoyl-SNAC: ^1H NMR (700 MHz, CDCl_3) δ = 8.12 – 7.86 (m, 2H), 7.71 – 7.55 (m, 1H), 7.52 – 7.40 (m, 2H), 6.03 (s, 1H), 3.55 (brq, J = 6 Hz, 2H), 3.24 (t, J = 6 Hz, 2H), 1.99 (s, 2H). ^{13}C NMR (176 MHz, CDCl_3) δ = 192.3, 170.5, 136.7, 133.8, 128.7, 127.3, 39.8, 28.6, 23.2. HR-ESI-MS: calculated for $\text{C}_{11}\text{H}_{13}\text{NO}_2\text{SNa}$ m/z 246.05592 $[\text{M}+\text{Na}]^+$, found m/z 246.05498.



3-Aminobenzoyl-SNAC: ^1H NMR (300 MHz, d_6 -DMSO) δ 8.05 (brs, 1H), 7.22 – 7.12 (m, 2H), 7.07 (d, J = 8 Hz, 1H), 6.85 (d, J = 8 Hz, 1H), 5.66 (brs, 1H), 3.24 (brq, J = 6 Hz, 2H), 3.05 (t, J = 6 Hz, 2H), 1.78 (s, 3H). ^{13}C NMR (75 MHz, d_6 -DMSO) δ = 191.2, 169.2, 148.5, 137.2, 129.4, 119.4, 114.6, 111.8, 38.2, 28.1, 22.5. HR-ESI-MS: calculated for $\text{C}_{11}\text{H}_{14}\text{N}_2\text{O}_2\text{SNa}$ m/z 261.06682 $[\text{M}+\text{Na}]^+$, found m/z 261.06675.

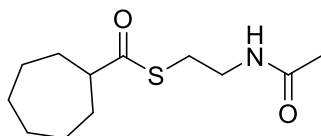


Phenylacetyl-SNAC: ^1H NMR (400 MHz, CDCl_3) δ = 7.55 – 7.01 (m, 1H), 5.80 (s, 1H), 3.84 (s, 2H), 3.41 (brq, J = 6 Hz, 2H), 3.01 (t, J = 6 Hz, 2H), 1.88 (s, 3H). ^{13}C NMR (101 MHz, CDCl_3) δ = 198.0, 170.3, 133.4, 129.5, 128.8, 127.6, 50.5, 39.5, 28.9, 23.1. HR-ESI-MS: calculated for $\text{C}_{12}\text{H}_{15}\text{NO}_2\text{SNa}$ m/z 260.07157 $[\text{M}+\text{Na}]^+$, found m/z 260.07188.



Cyclohexanecarboxylyl-SNAC: ^1H NMR (500 MHz, CDCl_3) δ = 5.79 (br s, 1H), 3.43 (brq, J = 6 Hz, 2H), 3.04 – 2.98 (m, 2H), 2.51 (t, J = 12, 4 Hz, 1H), 1.95 (s, 3H), 1.94-1.88 (m, 2H), 1.82-1.76 (m, 2H), 1.70 – 1.63 (m, 1H), 1.45 (ddd, J = 24, 12, 3 Hz, 2H), 1.34 – 1.16 (m, 3H). ^{13}C NMR (176 MHz, CDCl_3) δ = 204.5, 170.3, 54.5, 39.8, 31.3, 28.2, 28.1, 26.4, 23.2.

HR-ESI-MS: calculated for $\text{C}_{11}\text{H}_{19}\text{NO}_2\text{SNa}$ m/z 252.10287 $[\text{M}+\text{Na}]^+$, found m/z 252.10200.



Cycloheptanecarboxylyl-SNAC: ^1H NMR (500 MHz, CDCl_3) δ = 5.79 (brs, 1H), 3.43 (brq, J = 6 Hz, 2H), 3.00 (t, J = 6 Hz, 2H), 2.71 – 2.60 (m, 1H), 1.96 (s, 3H), 1.94 – 1.89 (m, 2H), 1.76-1.70 (m, 2H), 1.68 – 1.61 (m, 2H), 1.60-1.40 (m, 6H). ^{13}C NMR (126 MHz, CDCl_3) δ = 204.5, 170.3, 54.6, 39.9, 31.4, 28.2, 28.2, 26.4, 23.2. HR-ESI-MS: calculated for $\text{C}_{12}\text{H}_{21}\text{NO}_2\text{SNa}$ m/z 266.11852 $[\text{M}+\text{Na}]^+$, found m/z 266.11771.

Supporting Tables

Table S1. Bacterial strains used in this study

Strains	Relevant genotype/comments	Source/Ref
<i>Escherichia coli</i> DH10B	<i>F mcrA Δ(mrr-hsdRMS-mcrBC)φ80lacZΔM15 ΔlacX74 recA1 endA1 araD139 Δ(ara, leu)7697 galU galK λ⁻ rspL nupG</i>	GibcoBRL
<i>Escherichia coli</i> BL21(DE3) pLysS	<i>F ompT hsdS_B (r_B⁻ m_B⁻) gal dcm</i> (DE3) pLysS (CmR)	Promega
<i>E. coli</i> ET12567(pUZ8002)	<i>dam dcm hsdS</i> , pUZ8002	6
<i>Streptomyces pactum</i> ATCC 27456	Wild-type pactamycin producing strain	ATCC
<i>S. pactum</i> ΔptmH	<i>ptmH</i> in-frame deletion mutant	5
<i>S. pactum</i> ΔptmR	<i>ptmR</i> in-frame deletion mutant	This study
<i>S. pactum</i> ΔptmH/ΔptmR	in-frame deletion of <i>ptmR</i> in ΔptmH	This study
ΔptmH/ΔptmR/TMM058	ΔptmH/ΔptmR mutant complemented with pTMM058	This study
<i>S. pactum</i> ΔptmI	<i>ptmI</i> in-frame deletion mutant	This study
<i>S. pactum</i> ΔptmO	<i>ptmO</i> in-frame deletion mutant	This study
<i>S. pactum</i> <i>ptmK::aac(3)IV</i>	<i>ptmK</i> disruption mutant	This study
<i>S. pactum</i> ΔptmS	<i>ptmS</i> disruption mutant	This study

Table S2. Plasmids used in this study

Plasmid	Description	Source/Ref
pBlueScript II SK(-)	ColE1-based phagemid vector with f1 (-) and pUC origins; T3, T7 and lac promoters; <i>bla</i> .	Stratagene
pET-20b(+)	f1 (-) and pBR322 origins; <i>pelB</i> ; T7 promoter; <i>bla</i> ; C-terminal histag.	Novagen
pTMN002	pJTU1278+ derivative containing a 1 kb <i>aac(3)/IV</i> apramycin resistance cassette from pOJ446	7
pTMM007	Two 1 kb PCR fragments upstream and downstream of the <i>ptmO</i> gene in pBlueScript II SK(-)	This study
pTMW008	Two 1 kb PCR fragments upstream and downstream of the <i>ptmO</i> gene in pTMN002	This study
pTMW050	pTMX12b derivative containing <i>PerME*</i> promoter from pJTU695 and MCS	5
pTMM051	Two 1 kb PCR fragments upstream and downstream of the <i>ptmI</i> gene in pBlueScript II SK(-)	This study
pTMM052	Two 1 kb PCR fragments upstream and downstream of the <i>ptmI</i> gene in pTMN002	This study
pTMM015	Two 1 kb PCR fragments upstream and downstream of the <i>ptmS</i> gene in pBlueScript II SK(-)	This study
pTMM016	Two 1 kb PCR fragments upstream and downstream of the <i>ptmS</i> gene in pTMN002	This study
pTMM055	0.88 kb PCR fragment of the <i>ptmK</i> gene in pTMN002	This study
pTMM056	Two 1 kb PCR fragments upstream and downstream of the <i>ptmR</i> gene in pBlueScript II SK(-)	This study
pTMW057	Two 1 kb PCR fragments upstream and downstream of the <i>ptmR</i> gene in pTMN002	This study
pTMM058	pTMW050 containing complete structural gene of <i>ptmR</i>	This study
pTMN059	pBlueScrip II SK- containing complete structural gene of <i>ptmR</i>	This study
pTMN060	pET-20b(+) containing complete structural gene of <i>ptmR</i>	This study

Table S3. Primers used in this study

Primer	Sequence
<i>ptmI</i> -F1	5'-CCCAAGCTTGCTGCAGACCATGGACGAAT-3'
<i>ptmI</i> -R1	5'-CCGGAATTCGTCCATCGTGTCTCTCTCC-3'
<i>ptmI</i> -F2	5'-CCGGAATTCGTCCATCGTGTCTCTCTCC-3'
<i>ptmI</i> -R2	5'-GCTCTAGAAGGTGGTACGCGACCGTGTCCA-3'
<i>ptmR</i> -F1	5'-CCCAAGCTTACGCCTACGGGTTCTGGGCTGT-3'
<i>ptmR</i> -R1	5'-CCGGAATTCGTCTCTCACTCTTCCGATGT-3'
<i>ptmR</i> -F2	5'-CCGGAATTCGTGTGAGCGCGGCCAAGGAC-3'
<i>ptmR</i> -R2	5'-TGCTCTAGATCGGTACGGCCGTCCTGGCT-3'
<i>ptmR</i> -pET-F	5'-GAAGATCTACATATGGTGAGAACACCGGGCATTTCCT-3'
<i>ptmR</i> -pET-R	5'-CGCGGAATTCGCCACGCGCCGCTC-3'
<i>ptmR</i> -C-R	5'-CGCGGGAATTCTCACCACGCGCCGCTCCCT-3'
<i>ptmS</i> -F1	5'-CCCAAGCTTGTGTGGAGCAGGTCAGGTTC-3'
<i>ptmS</i> -R1	5'-CCGGAATTCGGCGGAGGTCATCCGAGTCC-3'
<i>ptmS</i> -F2	5'-CCGGAATTCCTGCTTCTGCGGGAGCGTCT-3'
<i>ptmS</i> -R2	5'-TGCTCTAGAGCCAGGTGGTCGAGGTGGATG-3'
<i>ptmO</i> -F1	5'-CCCAAGCTTGAGCTGCTGGCGGTGAACAT-3'
<i>ptmO</i> -R1	5'-CCGGAATTCGCCGAGGTCGTACGGTTCCT-3'
<i>ptmO</i> -F2	5'-CCGGAATTCGCTCCATCTGTTTCTGACTGG-3'
<i>ptmO</i> -R2	5'-TGCTCTAGAACTGCAGGGTCGCGGGTTGC-3'
<i>ptmK</i> -F1	5'-CCCAAGCTTGATGGTGGTCTGCGAGGT-3'
<i>ptmK</i> -F2	5'-TGCTCTAGAGTGACCGTGCACGTAGTCC-3'

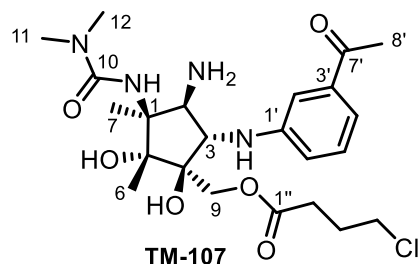
Bold letters represent restriction sites

Table S4. Sources and accession numbers of KAS III homologues

Species	Accession number	Protein
<i>Streptomyces pactum</i>	A8R0K3_9ACTO	KASIII/ACP-Shuttle AT-like, PtmR
<i>Streptomyces acidiscabies</i>	WP_010359166	KASIII/ACP-Shuttle AT-like
<i>Streptomyces niveiscabies</i> NRRL B-24457	WP_055718178.1	Hypothetical protein/FabH
<i>Streptomyces</i> sp. DSM 15324	WP_067252534.1	Hypothetical protein
<i>Streptomyces antibioticus</i>	AFB35630	KASIII/ACP-Shuttle AT-like, EsmD1
<i>Dactylosporangium aurantiacum</i> subsp. <i>hamdenensis</i>	ADU85987.1	ACP-Shuttle AT, TiaF
<i>Micromonospora echinospora</i>	AAM70354.1	ACP-Shuttle AT CalO4
<i>Nocardiopsis dassonvillei</i>	ZP_04334033.1	ACP-Shuttle AT
<i>Saccharopolyspora erythraea</i>	YP_001107471.1	ACP-Shuttle AT
<i>Stigmatella aurantiaca</i>	ZP_01462124.1	ACP-Shuttle AT
<i>Streptomyces antibioticus</i>	AAZ77676.1	ACP-Shuttle AT, ChlB3
<i>Streptomyces diastatochromogenes</i>	ACN64832.1	ACP-Shuttle AT
<i>Streptomyces rishiriensis</i>	AAG29787.2	ACP-Shuttle AT
<i>Streptomyces roseochromogenes</i>	AAN65231.1	ACP-Shuttle AT, CloN2
<i>Streptomyces</i> sp. Tü6071	ABB69750.1	ACP-Shuttle AT
<i>Streptomyces viridochromogenes</i> Tü57	AF333038_20	ACP-Shuttle AT, AviN
<i>Actinobacillus pleuropneumoniae</i>	ZP_00134992.2	FabB
<i>Citrobacter</i> sp. 30_2	ZP_04562837.1	FabB
<i>Escherichia coli</i>	NP_416826.1	FabB
<i>Shigella boydii</i>	YP_001881145.1	FabB
<i>Escherichia albertii</i>	ZP_02902779.1	FabF
<i>Escherichia coli</i>	NP_415613.1	FabF
<i>Staphylococcus aureus</i>	NP_645683.1	FabF
<i>Streptococcus pneumoniae</i>	NP_344945.1	FabF
<i>Thermus thermophilus</i>	YP_143679.1	FabF
<i>Streptomyces coelicolor</i>	NP_626634.1	KAS III
<i>Streptomyces echinatus</i>	AAV84077.1	KAS III
<i>Streptomyces glaucescens</i>	Q54206.1	KAS III
<i>Streptomyces griseus</i>	AAQ08929.1	KAS III
<i>Streptomyces griseus</i>	YP_001826619.1	KAS III
<i>Streptomyces roseofulvus</i>	AAC18104.1	KAS III
<i>Streptomyces</i> sp. A2991200	CAM58805.1	KAS III
<i>Streptomyces</i> sp. CM020	ACI88883.1	KAS III
<i>Streptomyces</i> sp. R1128	AAG30195.1	KAS III
<i>Streptomyces antibioticus</i>	AAZ77679.1	KAS III-like, ChlB6
<i>Streptomyces galilaeus</i>	AAF70109.1	KAS III-like
<i>Streptomyces galilaeus</i>	BAB72048.1	KAS III-like
<i>Streptomyces peucetius</i>	AAA65208.1	KAS III-like, EviR
<i>Streptomyces</i> sp. SPB74	WP_008748182.1	KAS III-like
<i>Streptomyces tendae</i>	AEI91069.1	KAS III -like, CerJ

<i>Escherichia coli</i>	NP_415610.1	Malonyl-CoA-(ACP)-AT
<i>Saccharopolyspora erythraea</i>	YP_001102990.1	Type I PKS
<i>Streptomyces antibioticus</i>	AAF82408.1	Type I PKS
<i>Streptomyces fradiae</i>	AAB66504.1	Type I PKS
<i>Streptomyces griseoruber</i>	AAP85336.1	Type I PKS
<i>Streptomyces nanchangensis</i>	AAP42874.1	Type I PKS
<i>Streptomyces</i> sp. 307-9	ADC79637.1	Type I PKS
<i>Streptomyces violaceusniger</i>	ABJ97437.1	Type I PKS

Table S5. ^1H NMR and ^{13}C NMR shifts for TM107



position	δ_{H} (ppm) int., multipl. (Hz)	δ_{C} (ppm)
2'	7.36 (1H, m)	111.3
4'	7.32 (1H, m)	117.5
5'	7.29 (1H, t, 8)	129.0
6'	7.03 (1H, m)	118.0
NH	6.64 (1H, brs)	-
9	4.31 (2H, q, 12)	64.6
3	4.14 (1H, d, 9)	65.3
2	3.73 (1H, d, 9)	64.0
4''	3.45 (2H, m)	43.4
11, 12	2.98 (6H, s)	35.4
8'	2.59 (3H, s)	25.5
2''	2.22 (1H, m); 1.94 (1H, m)	30.3
3''	1.8 (2H, m)	27.2
7	1.66 (3H, s)	13.5
6	1.42 (3H, s)	14.9
7'	-	200.1
10	-	159.2
1''	-	172.8
3'	-	137.9
1'	-	149.0
5	-	81.3
4	-	82.1
1	-	65.1

Supporting Figures

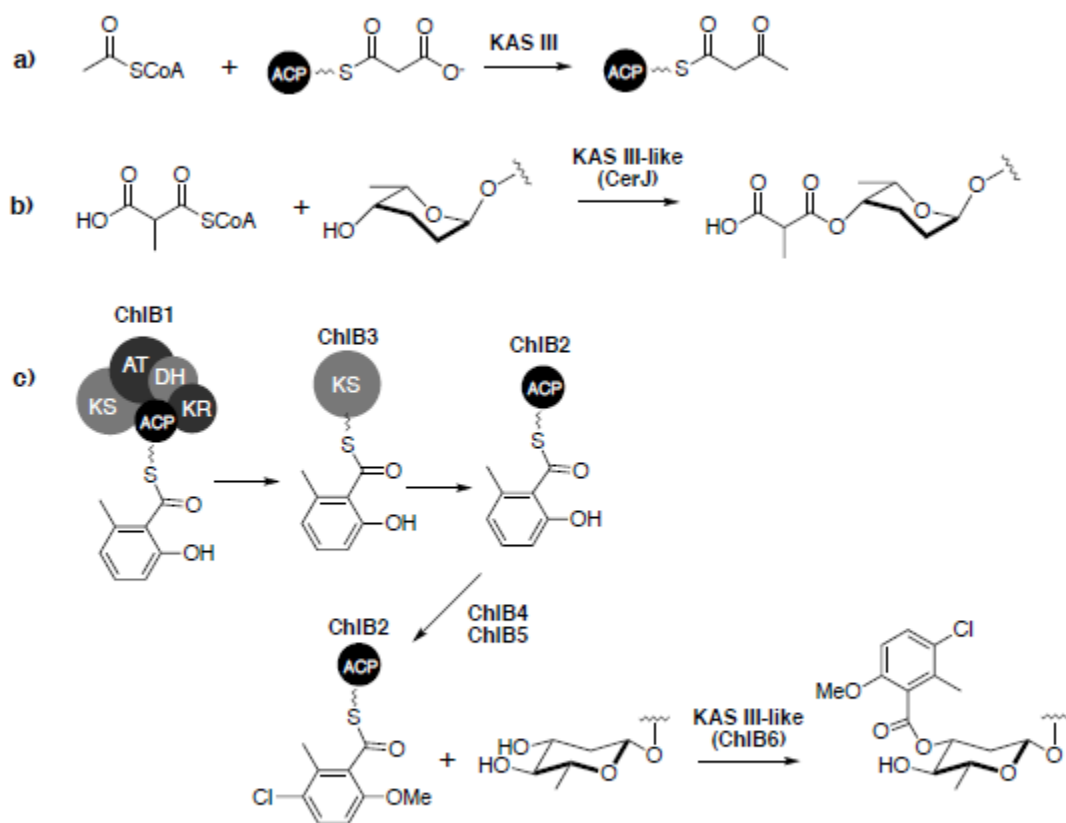


Figure S1. Distinct catalytic activities of KAS III and KAS III-like proteins. Only partial structures of the cervimycins and chlorothricin are shown.

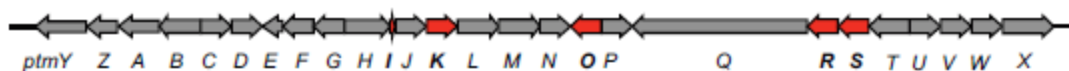


Figure S2. Genetic organization of the pactamycin biosynthetic gene cluster. *ptmI*, *ptmK*, *ptmO*, *ptmR*, and *ptmS* (red arrows) are genes being knocked out in this study.

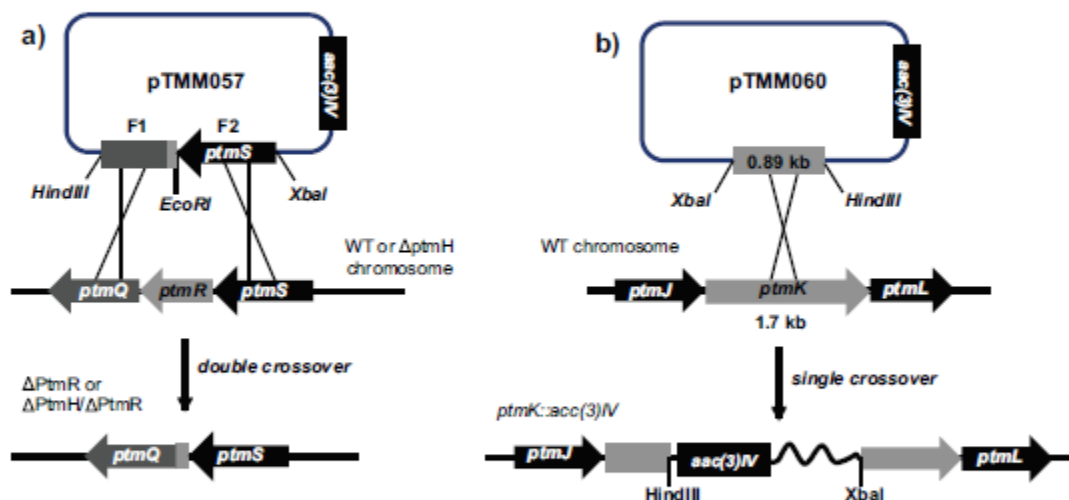


Figure S3. Cloning strategies for in-frame and gene disruption mutations of *S. pactum*. **a)** Double cross-over recombination strategy for the in-frame deletion of *ptmR* in *S. pactum* wild-type or in Δ *ptmH* mutant. Construction of Δ *ptmI*, Δ *ptmO*, and Δ *ptmS* adopted the same strategy. **b)** Single cross-over recombination strategy for the disruption of *ptmK* in *S. pactum*. A gene disruption method was pursued for *ptmK* because an in-frame deletion approach was not successful.

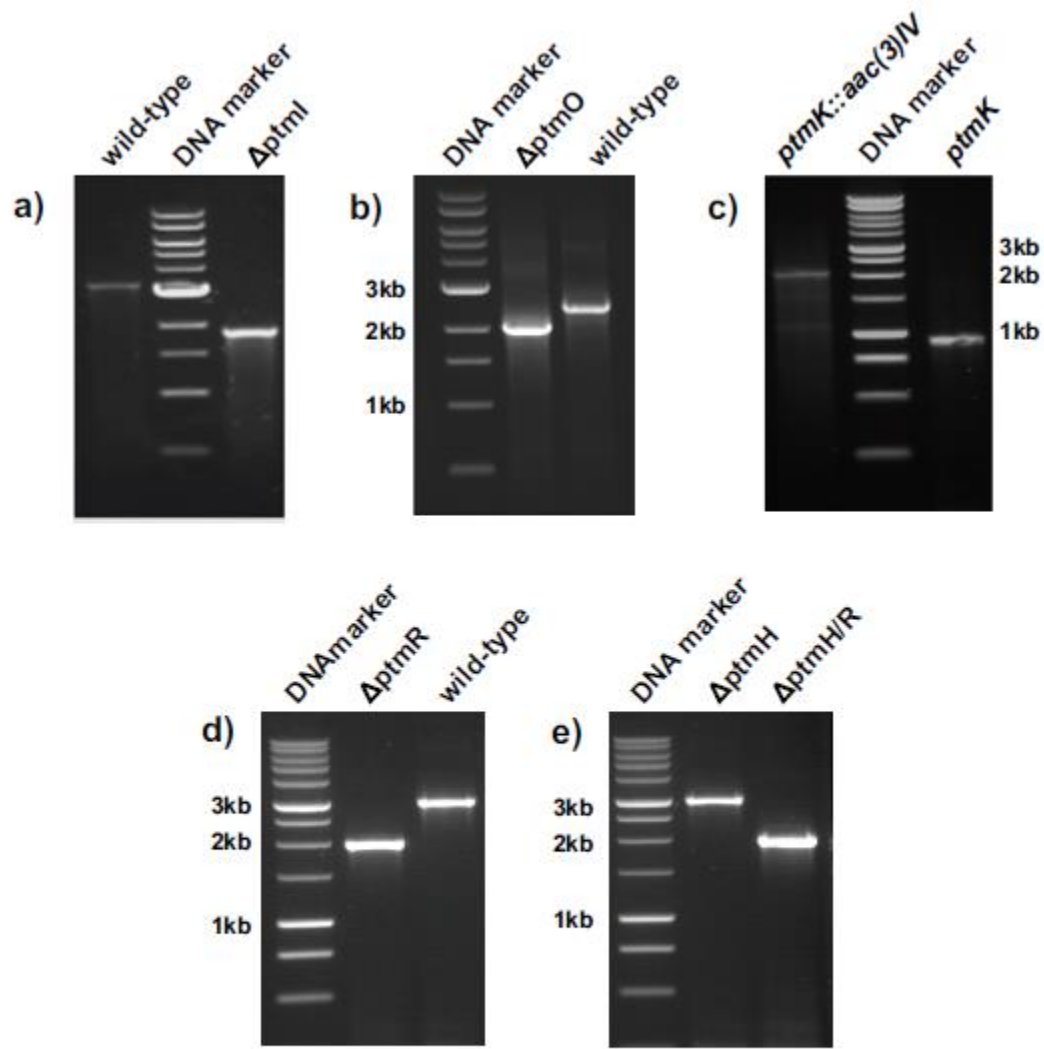


Figure S4. Genotypic confirmation of $\Delta ptmI$, $\Delta ptmO$, $\Delta ptmR$, $\Delta ptmH/\Delta ptmR$, and *ptmK::aac(3)/V* mutants by PCR. **a.** DNA gel electrophoresis of PCR product of $\Delta ptmI$. **b.** DNA gel electrophoresis of PCR product of $\Delta ptmO$. **c.** DNA gel electrophoresis of PCR product of *ptmK::aac(3)/V* mutant. **d.** DNA gel electrophoresis of PCR product of $\Delta ptmR$. **e.** DNA gel electrophoresis of PCR product of $\Delta ptmH/\Delta ptmR$.

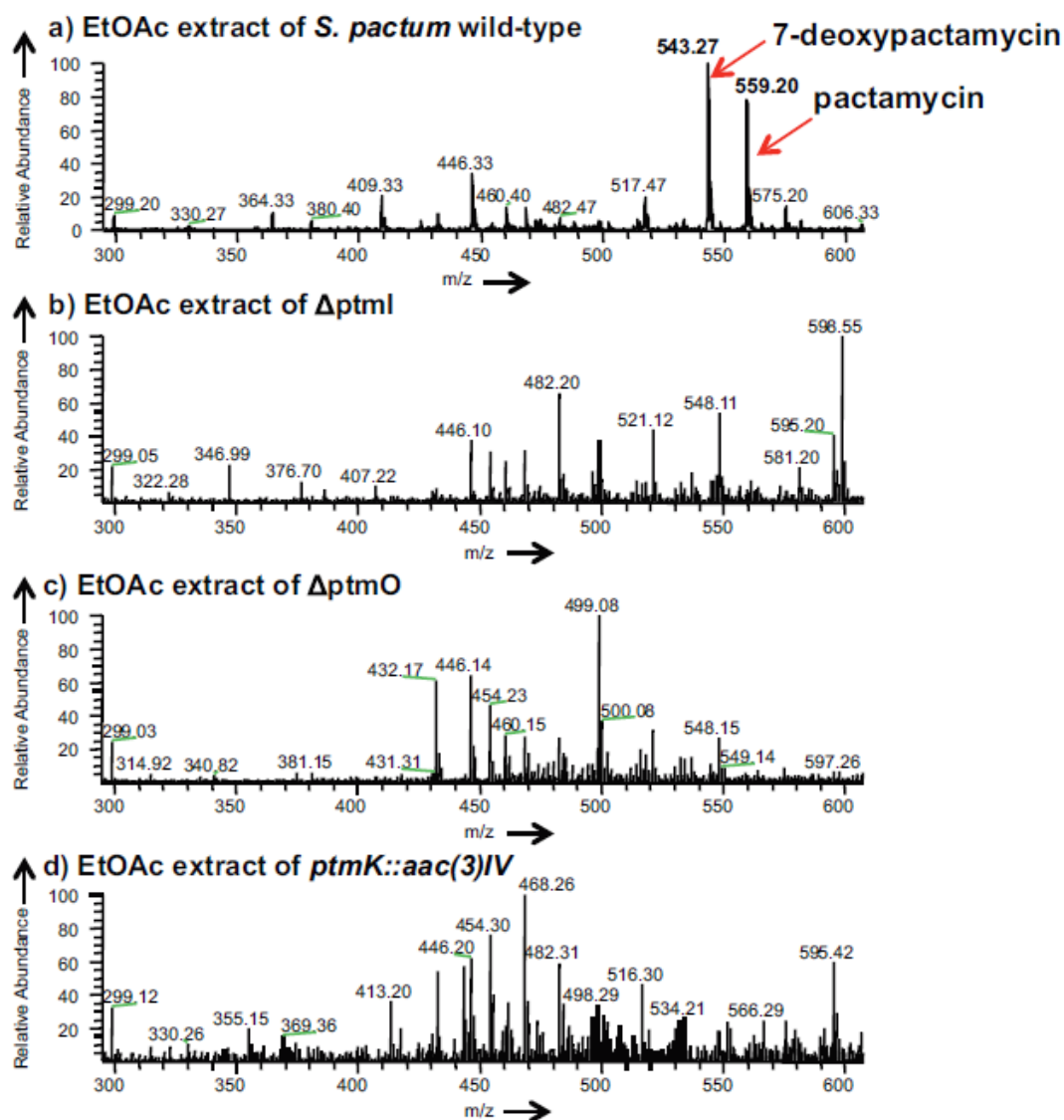


Figure S5. ESI-MS analysis of $\Delta ptmI$, $\Delta ptmO$, and *ptmK::aac(3)IV* mutants.

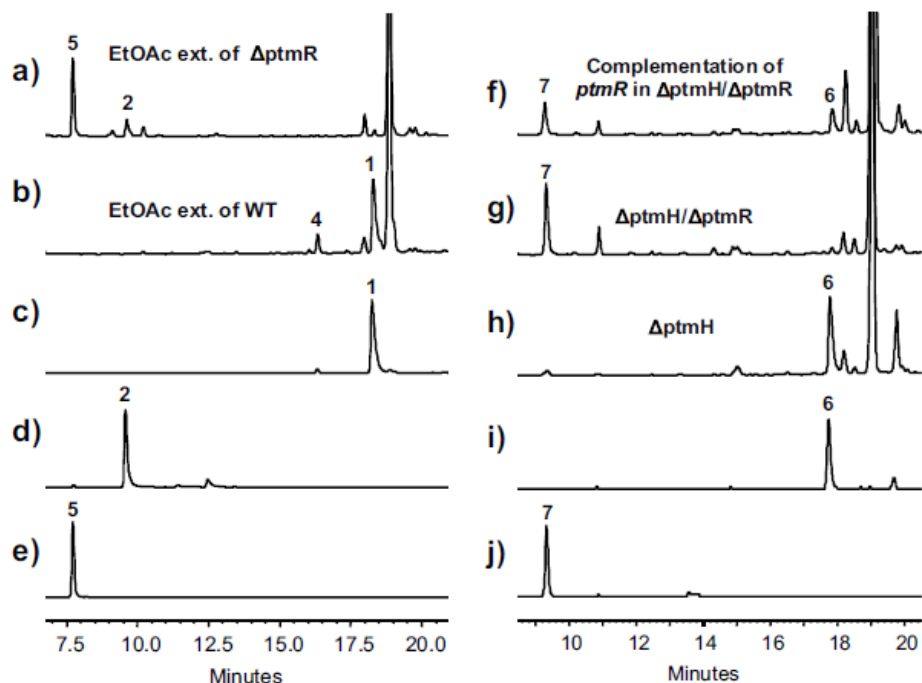


Figure S6. HPLC analyses of $\Delta ptmR$ and $\Delta ptmH/\Delta ptmR$ mutant strains of *S. pactum*. a, EtOAc extract of $\Delta ptmR$. b, EtOAc extract of wild-type. c, pactamycin standard. d, de-6MSA-pactamycin standard. e, de-6MSA-pactamycate standard. f, EtOAc extract of $\Delta ptmH/\Delta ptmR$ complemented with intact *ptmR*. g, EtOAc extract of $\Delta ptmH/\Delta ptmR$. h, EtOAc extract of $\Delta ptmH$. i, TM-026 standard. j, TM-025 standard.

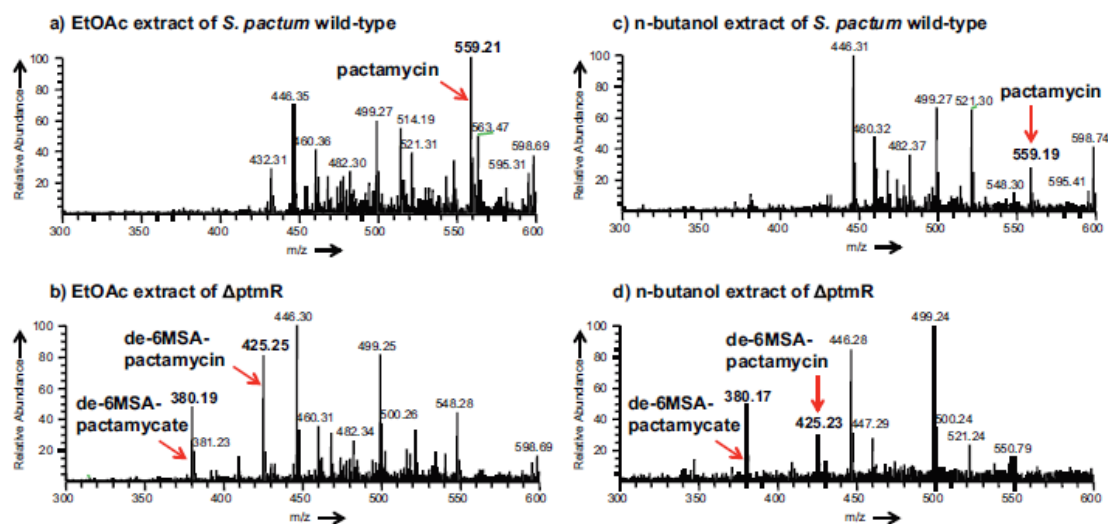


Figure S7. ESI-MS analysis of $\Delta ptmR$ mutant. a, EtOAc extract of a culture of *S. pactum* wild-type. b, EtOAc extract of a culture of $\Delta ptmR$ mutant. c, Butanol extract of a culture of *S. pactum* wild-type. d, Butanol extract of a culture of $\Delta ptmR$ mutant.

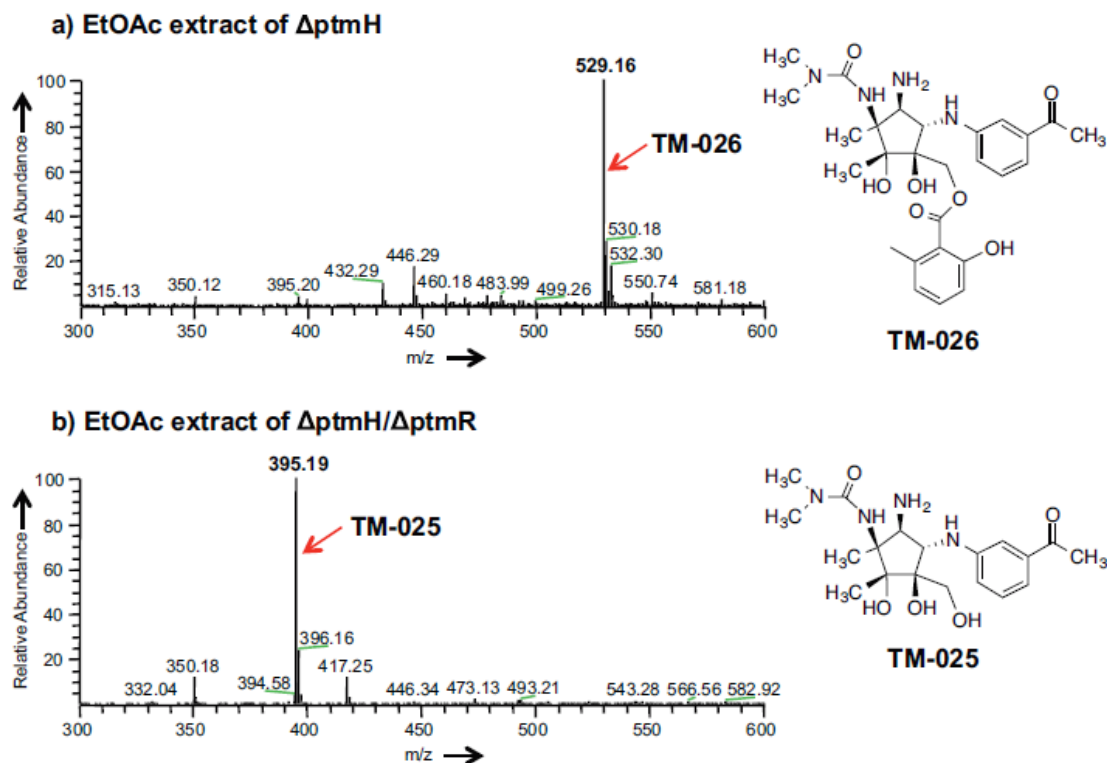


Figure S8. ESI-MS analysis of Δ ptmH/ Δ ptmR mutant. **a**, EtOAc extract of a culture of Δ ptmH mutant, which produces TM-026 (m/z 529). **b**, EtOAc extract of a culture of Δ ptmH/ Δ ptmR double mutant.

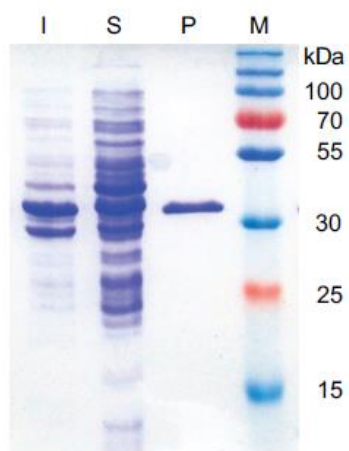


Figure S9. SDS PAGE of purified PtmR. I, insoluble proteins; S, soluble proteins (cell free extract); P, purified PtmR, M, protein marker.

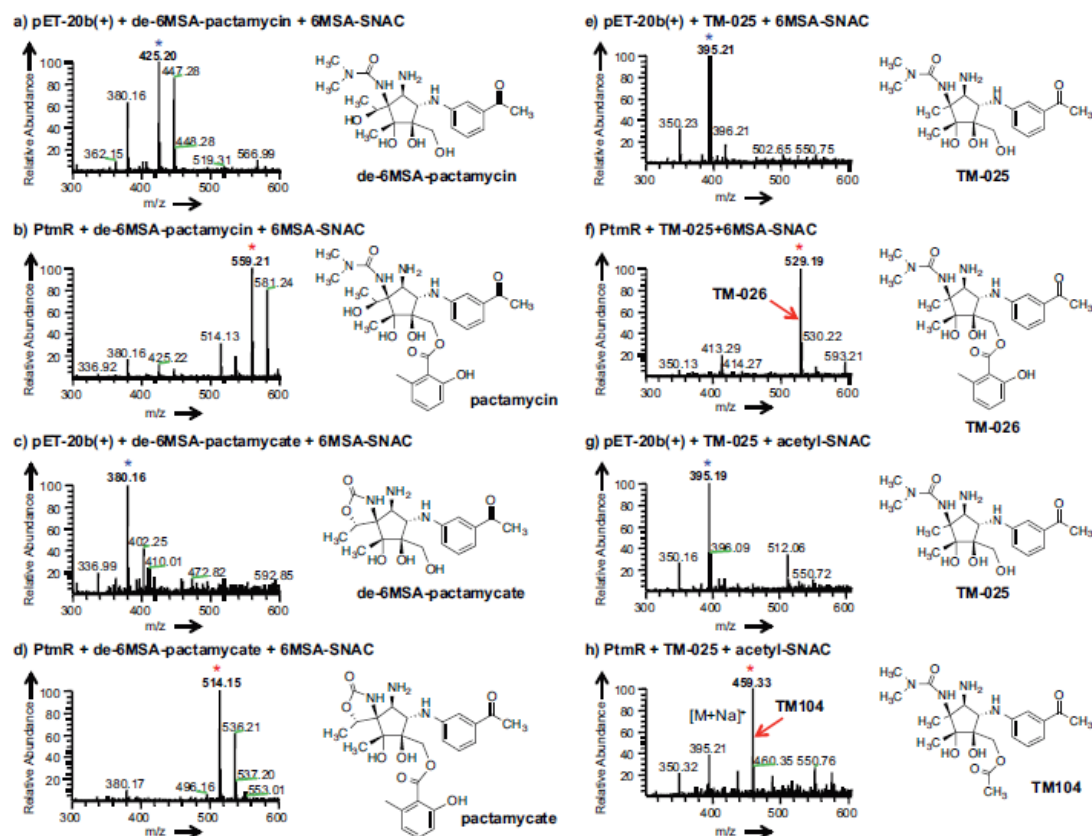


Figure S10. ESI-MS spectra of de-6MSA-pactamycin, de-6MSA-pactamycate, and TM-025 incubated with cell free extracts of cultures of *E. coli* harboring empty vector pET-20b(+) and that harboring *ptmR* in the presence of 6MSA-SNAC or acetyl-SNAC. Blue stars represent the substrates and red stars represent the products.

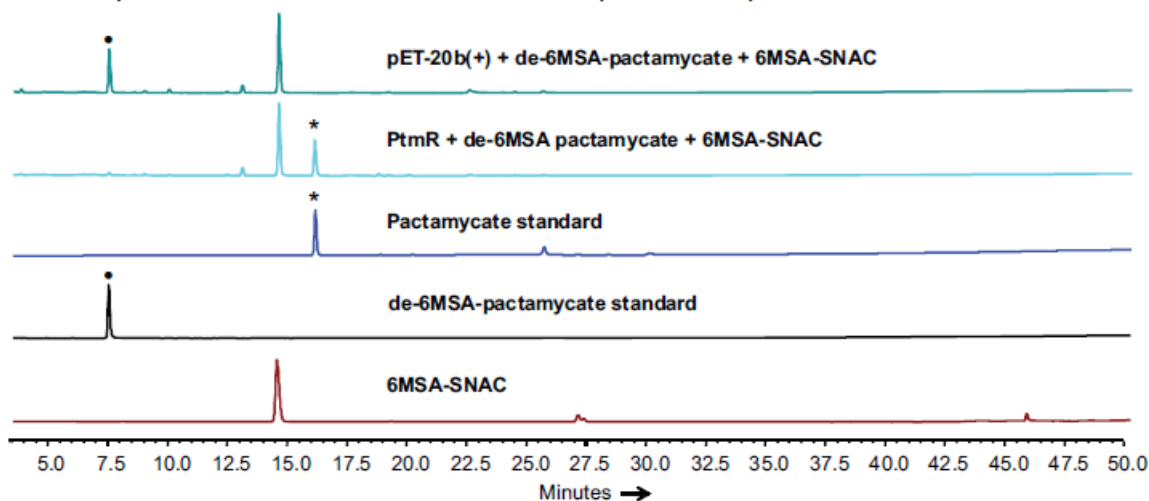


Figure S11. HPLC profile of PtMR enzymatic reaction using de-6MSA-pactamycate and 6MSA-SNAC. Filled circles represent de-6MSA-pactamycate and stars represent pactamycate.

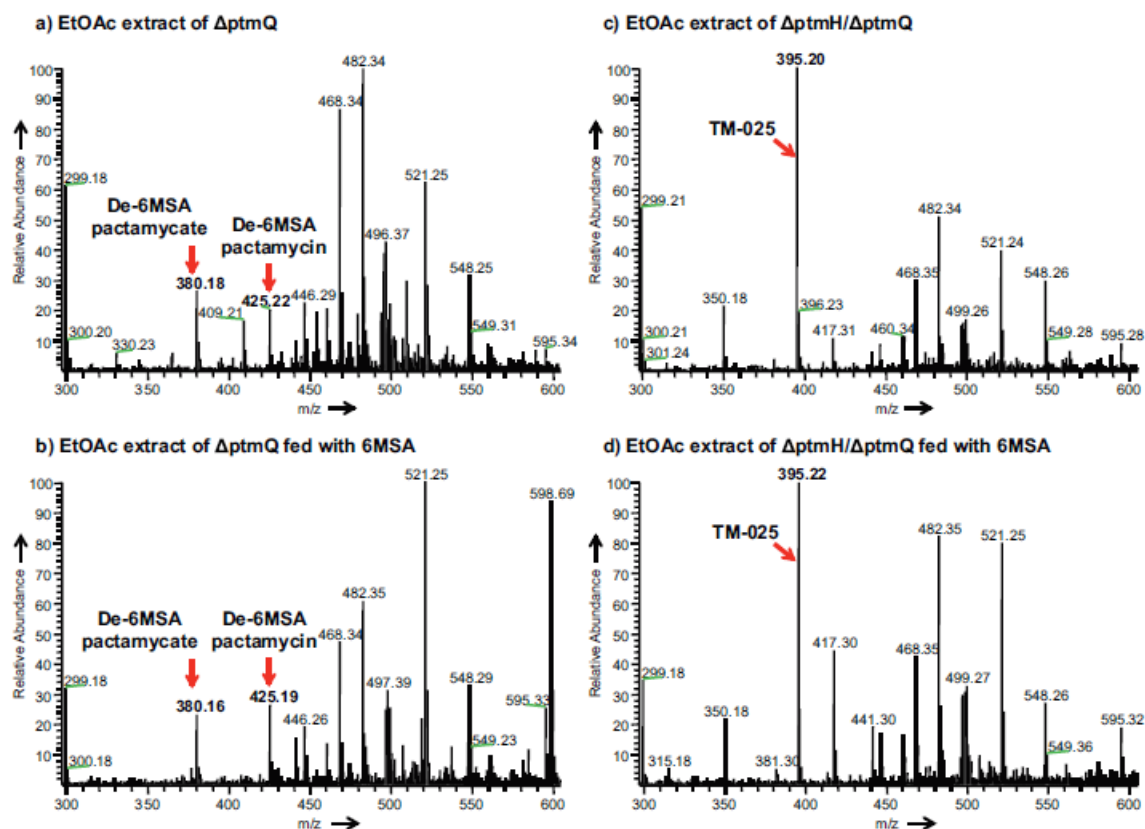


Figure S12. Feeding experiments with 6MSA to the Δ ptmQ and Δ ptmQ/ Δ ptmH strains of *S. pactum*. **a**, ESI-MS spectrum of EtOAc extract of Δ ptmQ. **b**, ESI-MS spectrum of EtOAc extract of Δ ptmQ fed with 6MSA. **c**, ESI-MS spectrum of EtOAc extract of Δ ptmQ/ Δ ptmH. **d**, ESI-MS spectrum of EtOAc extract of Δ ptmQ/ Δ ptmH fed with 6MSA.

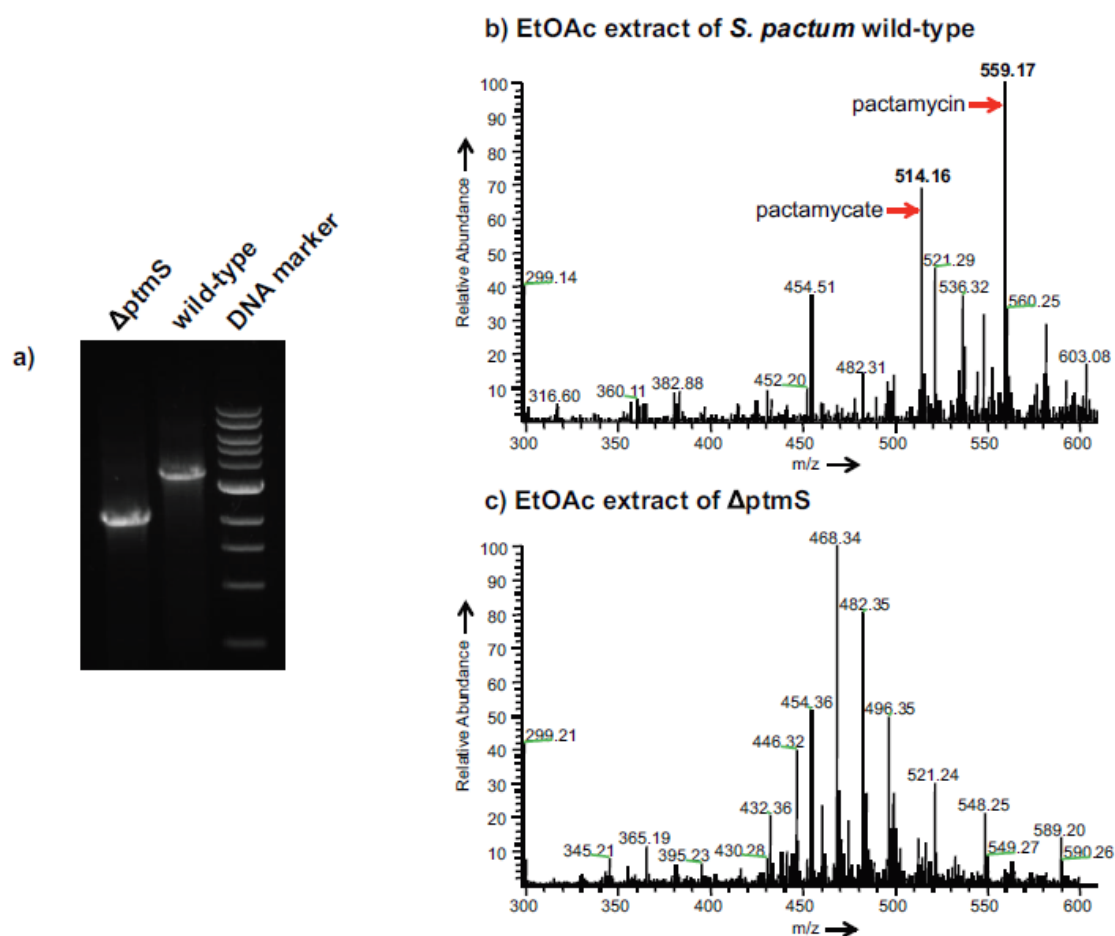


Figure S13. Genotypic and phenotypic analyses of Δ ptmS. **a**, DNA gel electrophoresis of PCR product of Δ ptmS. **b**, ESI-MS spectrum of EtOAc extract of *S. pactum* wild-type. **c**, ESI-MS spectrum of EtOAc extract of Δ ptmS.

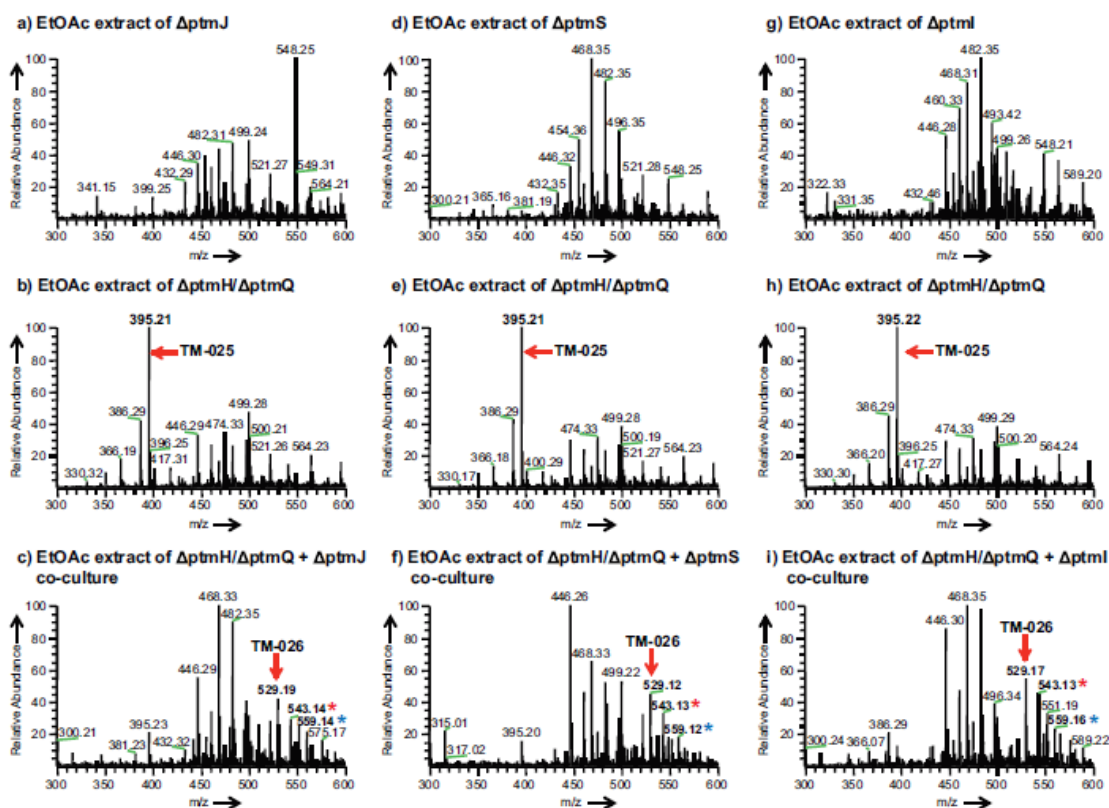


Figure S14. ESI-MS analysis of co-culture products. **a**, ESI-MS spectrum of EtOAc extract of $\Delta ptmJ$. **b**, ESI-MS spectrum of EtOAc extract of $\Delta ptmH/\Delta ptmQ$. **c**, ESI-MS spectrum of EtOAc extract of $\Delta ptmH/\Delta ptmQ$ + $\Delta ptmJ$ co-culture. **d**, ESI-MS spectrum of EtOAc extract of $\Delta ptmS$. **e**, ESI-MS spectrum of EtOAc extract of $\Delta ptmH/\Delta ptmQ$. **f**, ESI-MS spectrum of EtOAc extract of $\Delta ptmH/\Delta ptmQ$ + $\Delta ptmS$ co-culture. **g**, ESI-MS spectrum of EtOAc extract of $\Delta ptmI$. **h**, ESI-MS spectrum of EtOAc extract of $\Delta ptmH/\Delta ptmQ$. **i**, ESI-MS spectrum of EtOAc extract of $\Delta ptmH/\Delta ptmQ$ + $\Delta ptmI$ co-culture. Red star indicates 7-deoxypactamycin, blue star indicates pactamycin. The production of 7-deoxypactamycin and pactamycin suggests that to some extent TM-025 and/or TM-026 are also modified by a radical SAM-dependent methyltransferase and a hydroxylase in the $\Delta ptmJ$ strain.

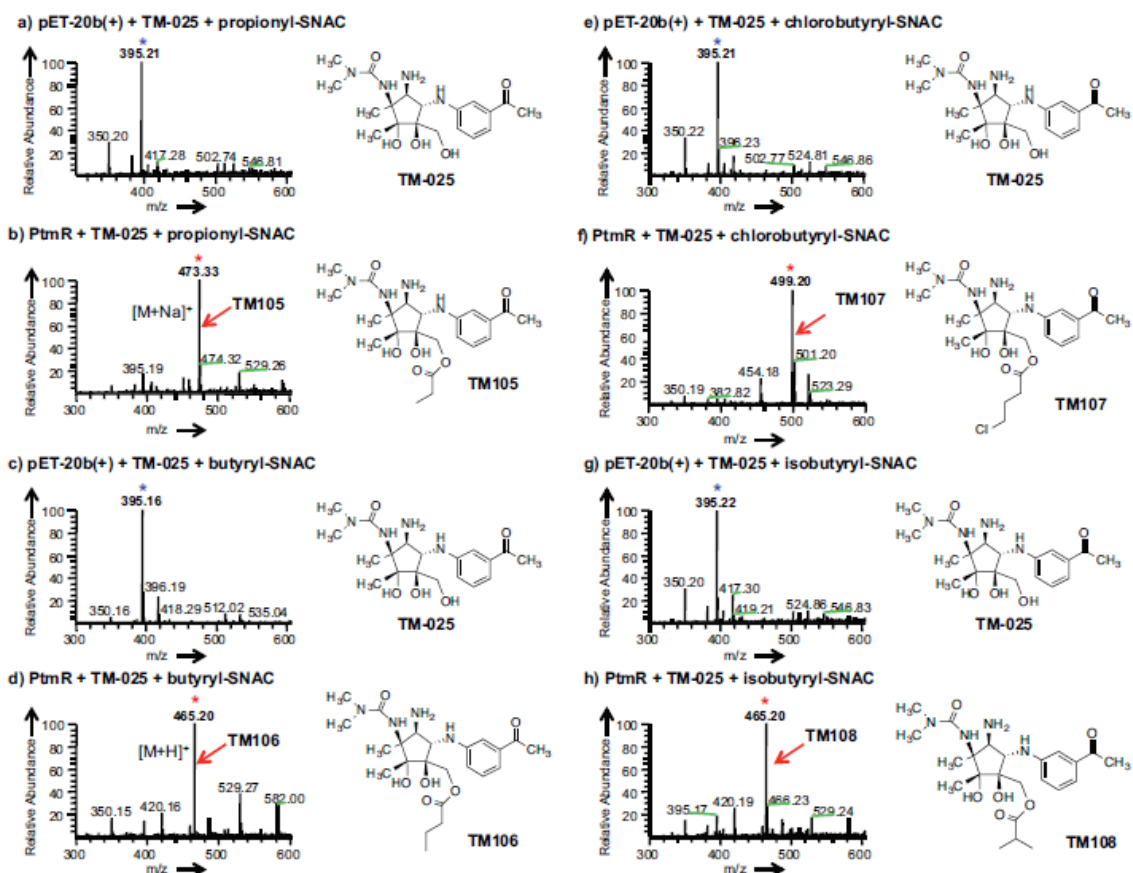


Figure S15. ESI-MS spectra of TM-025 incubated with cell free extracts of cultures of *E. coli* harboring empty vector pET-20b(+) and that harboring *ptmR* in the presence of propionyl-, butyryl-, chlorobutyryl-, or isobutyryl-SNAC. Blue stars represent the substrates and red stars represent the products.

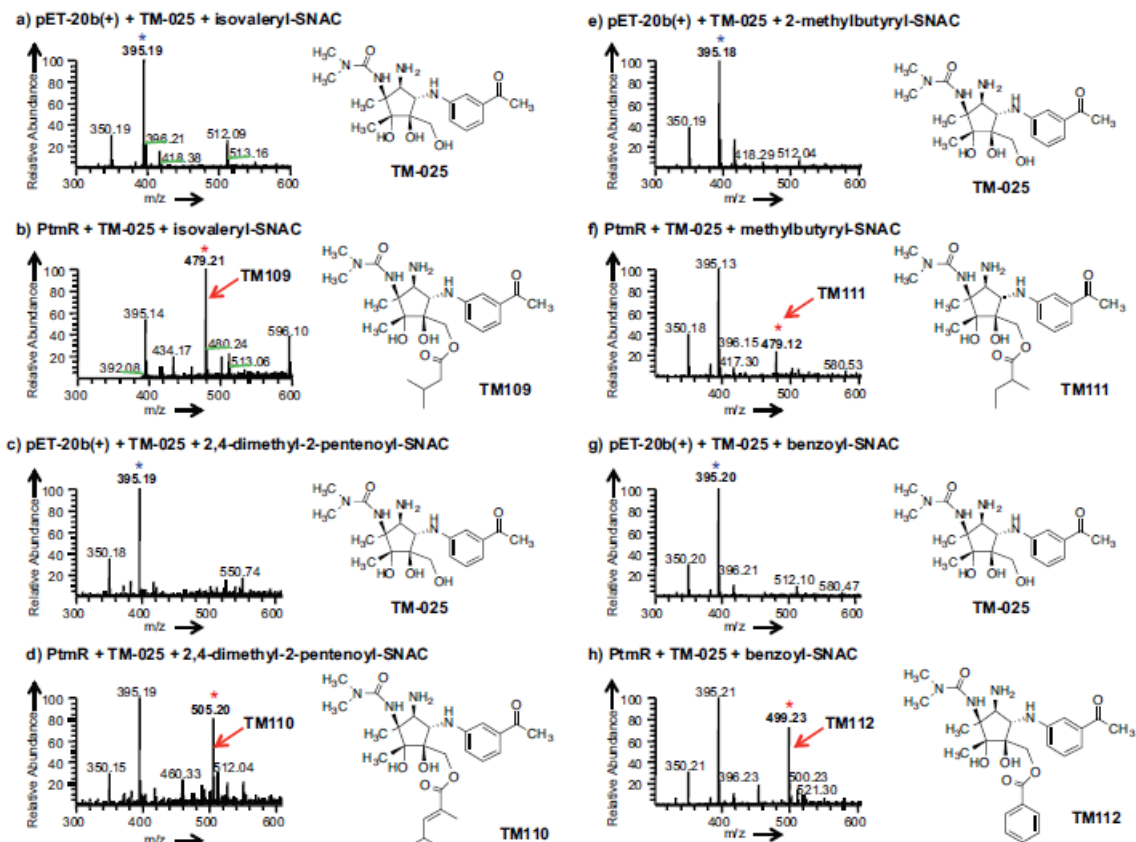


Figure S16. ESI-MS spectra of TM-025 incubated with cell free extracts of cultures of *E. coli* harboring empty vector pET-20b(+) and that harboring *ptmR* in the presence of isovaleryl-, 2,4-dimethyl-2-pentenyl-, 2-methylbutyryl-, or benzoyl-SNAC. Blue stars represent the substrates and red stars represent the products.

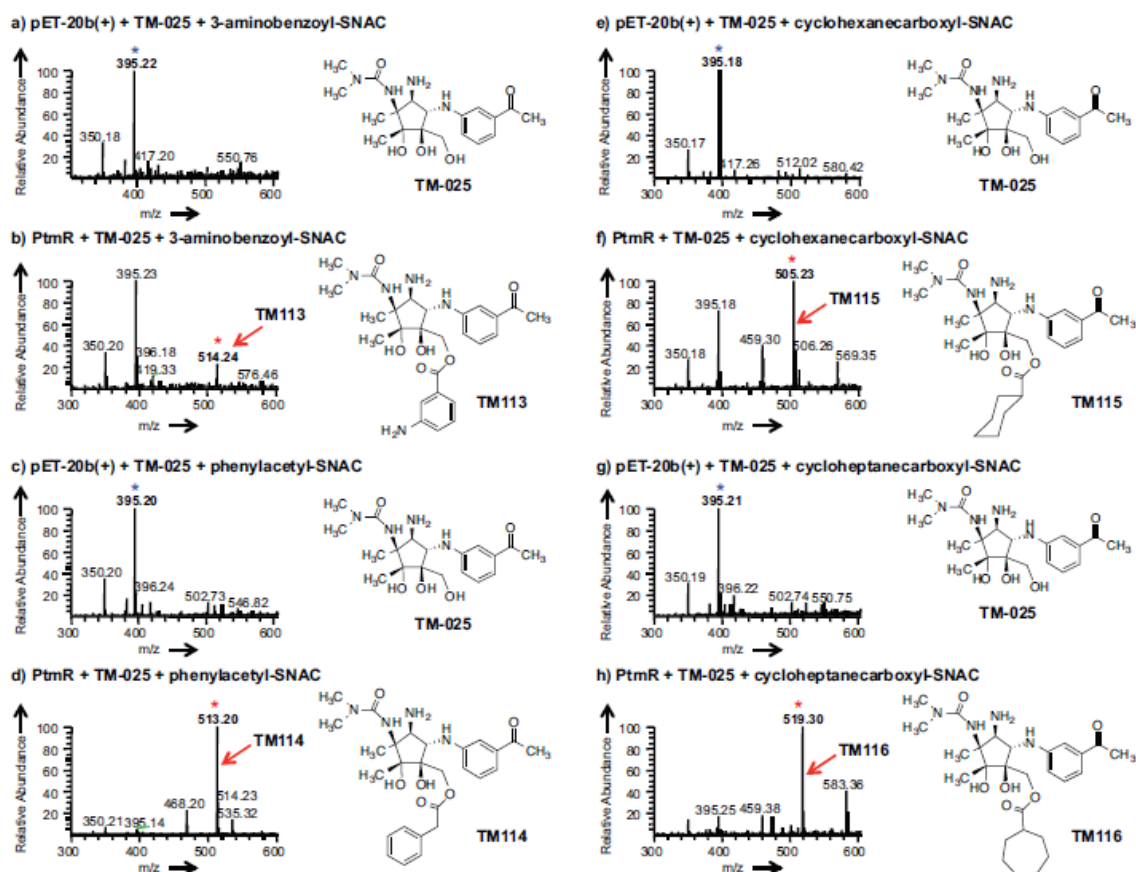


Figure S17. ESI-MS spectra of TM-025 incubated with cell free extracts of cultures of *E. coli* harboring empty vector pET-20b(+) and that harboring *ptmR* in the presence of 3-aminobenzoyl-, phenylacetyl-, cyclohexanecarboxyl-, or cycloheptanecarboxyl-SNAC. Blue stars represent the substrates and red stars represent the products.

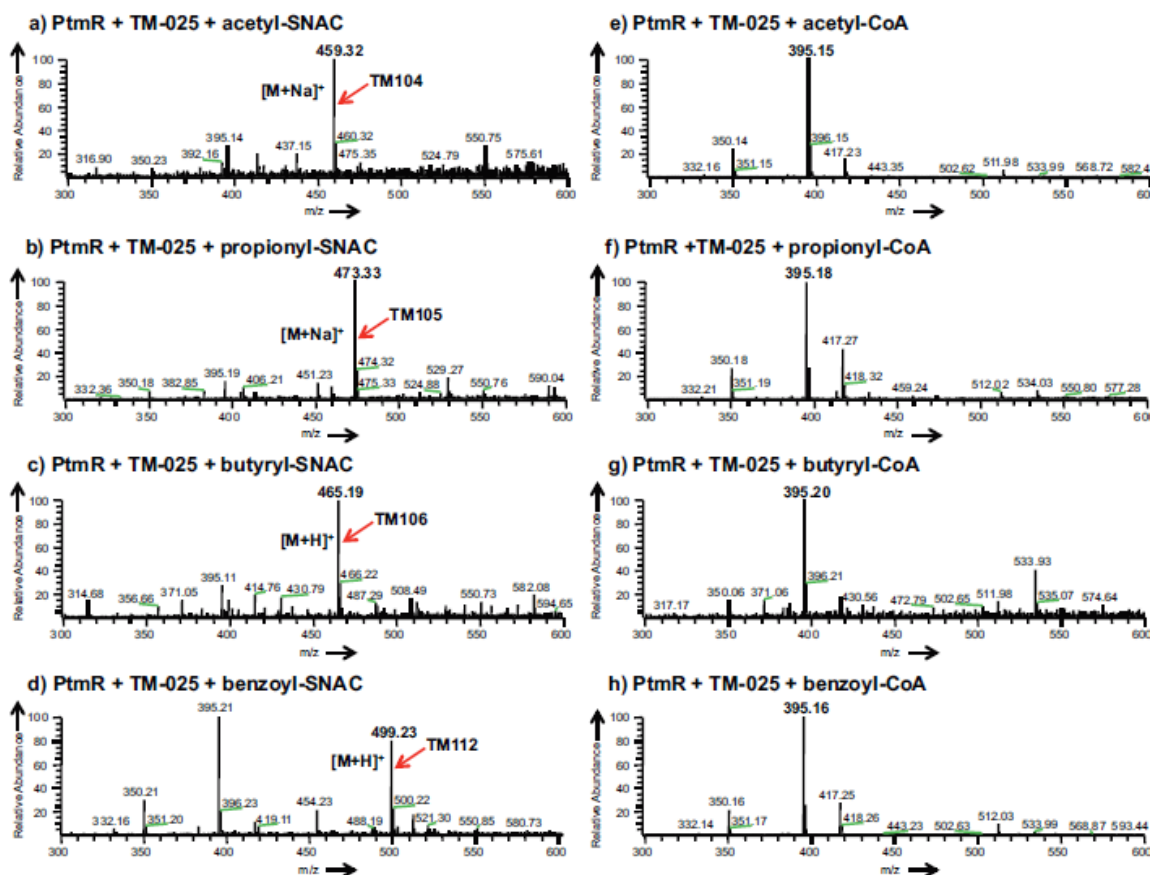


Figure S18. ESI-MS spectra of TM-025 (m/z 395) incubated with cell free extracts of cultures of *E. coli* harboring empty vector pET-20b(+) and that harboring *ptmR* in the presence of NAC and CoA esters of acetate, propionate, butyrate, and benzoate.

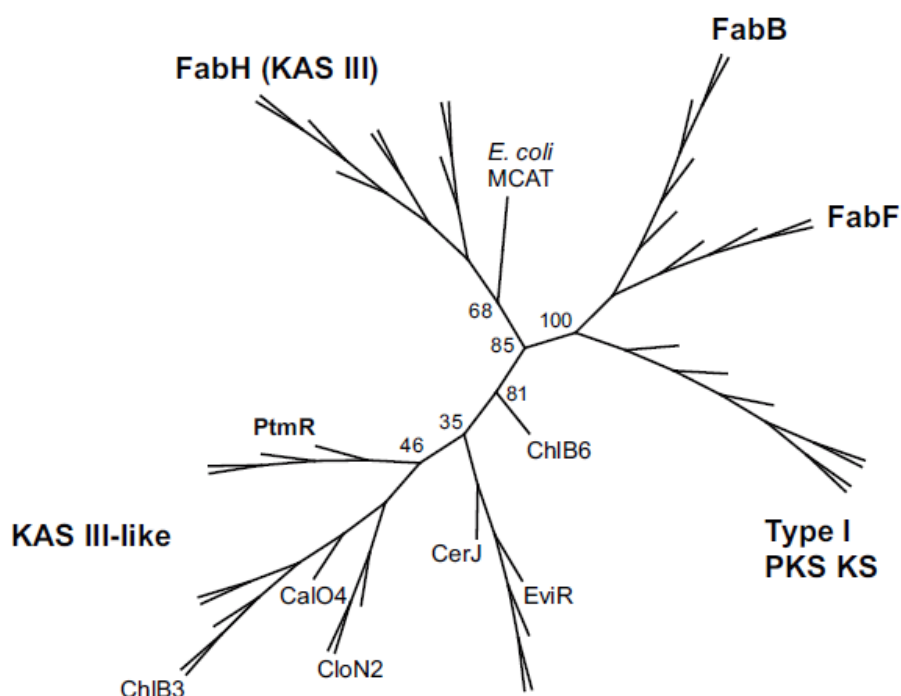


Figure S19. Phylogenetic analysis of PtmR and homologous proteins. Full-length amino acid sequences were aligned with MUSCLE and the best protein model was determined by RaxML (WAG+G).^{8, 9} RaxML was then used to build the phylogenetic tree. Computations were performed on the CGRB servers. The source and accession number of the proteins are listed in Table S4.

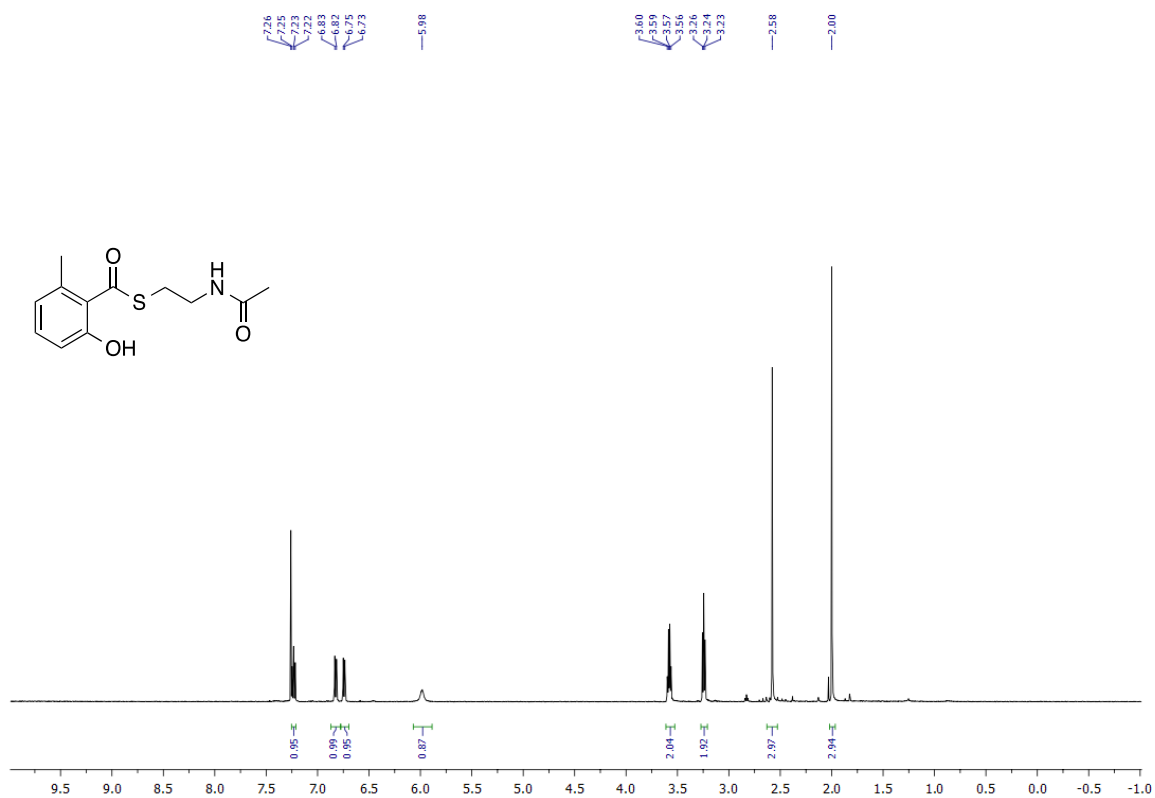
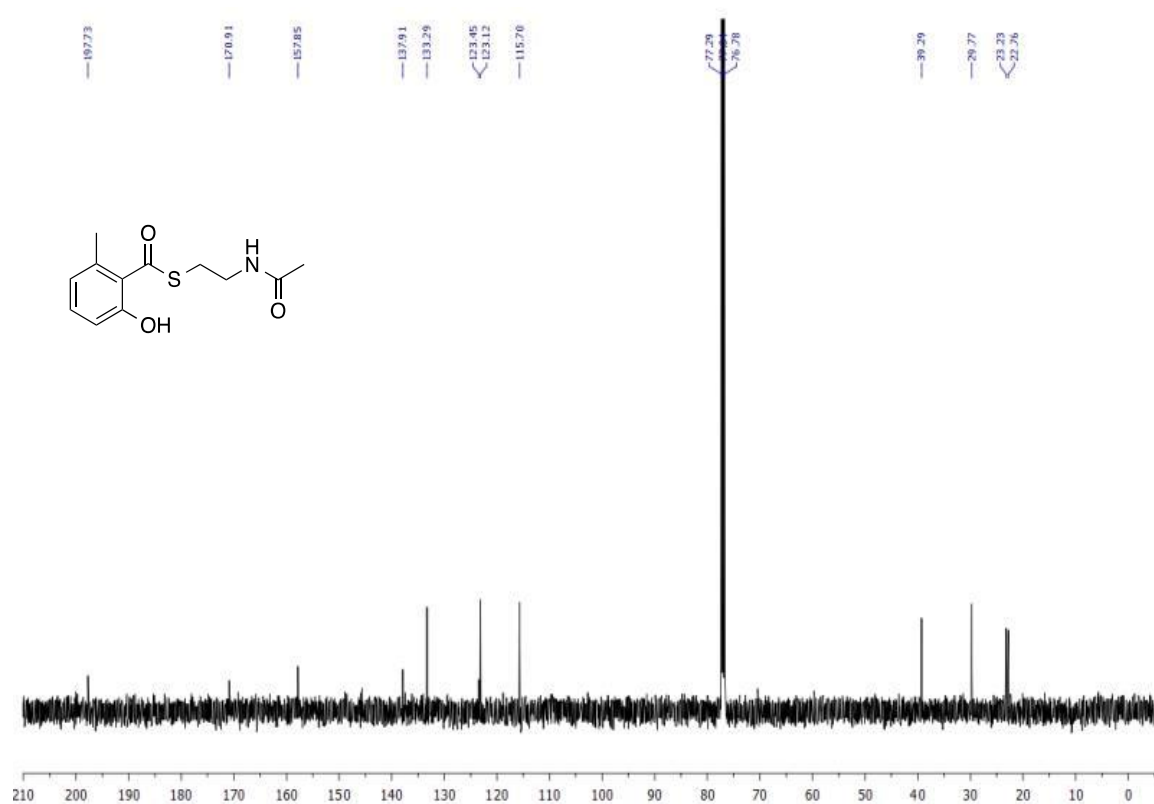
Figure S20. ^1H NMR Spectrum of 6-MSA-SNAC.

Figure S21. ^{13}C NMR Spectrum of 6-MSA-SNAC.

Figures S22–S47 (^1H and ^{13}C NMR data for SNAC compounds; See Appendix B page 212)

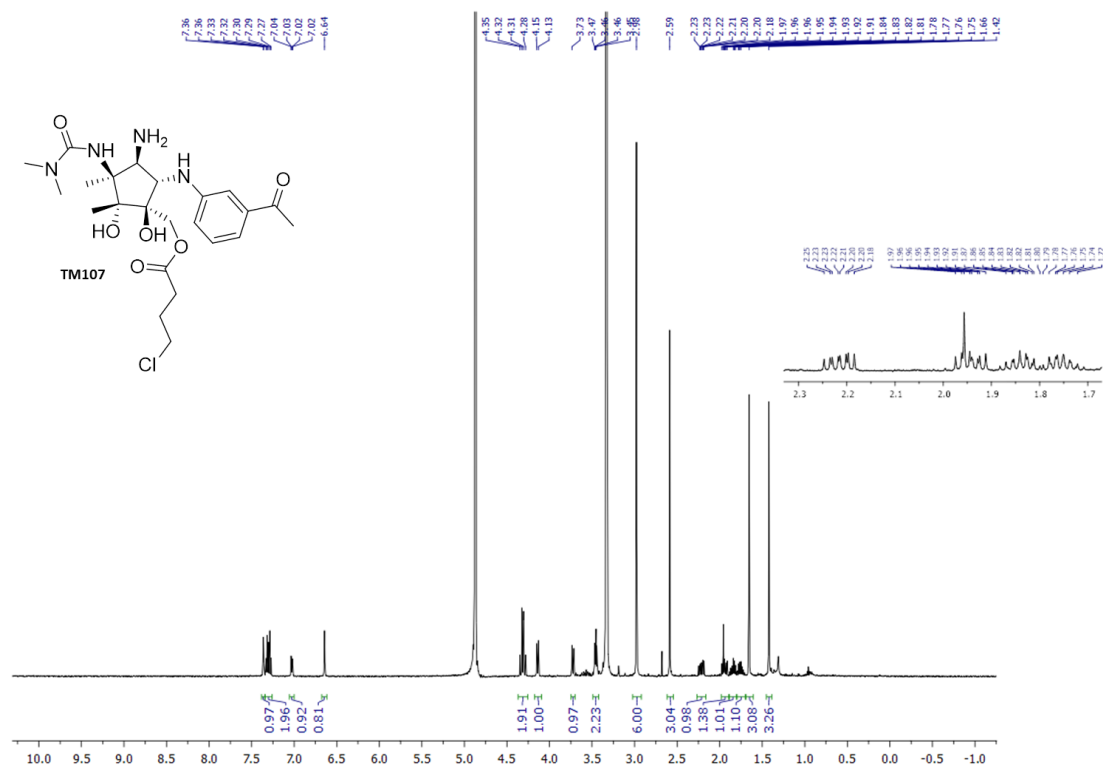
Figure S48. ^1H NMR (MeOD) spectrum of TM107

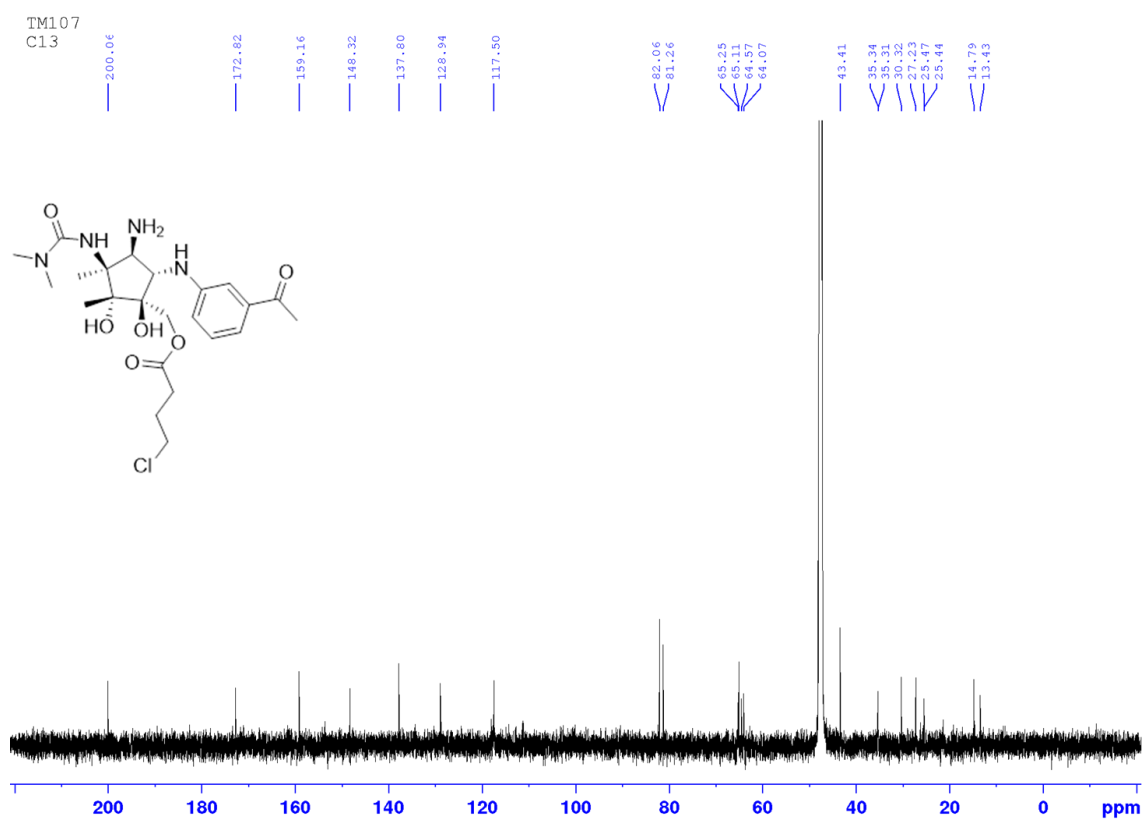
Figure S49. ^{13}C NMR (MeOD) spectrum TM107

Figure S50. HSQC (MeOD) spectrum of TM-107.

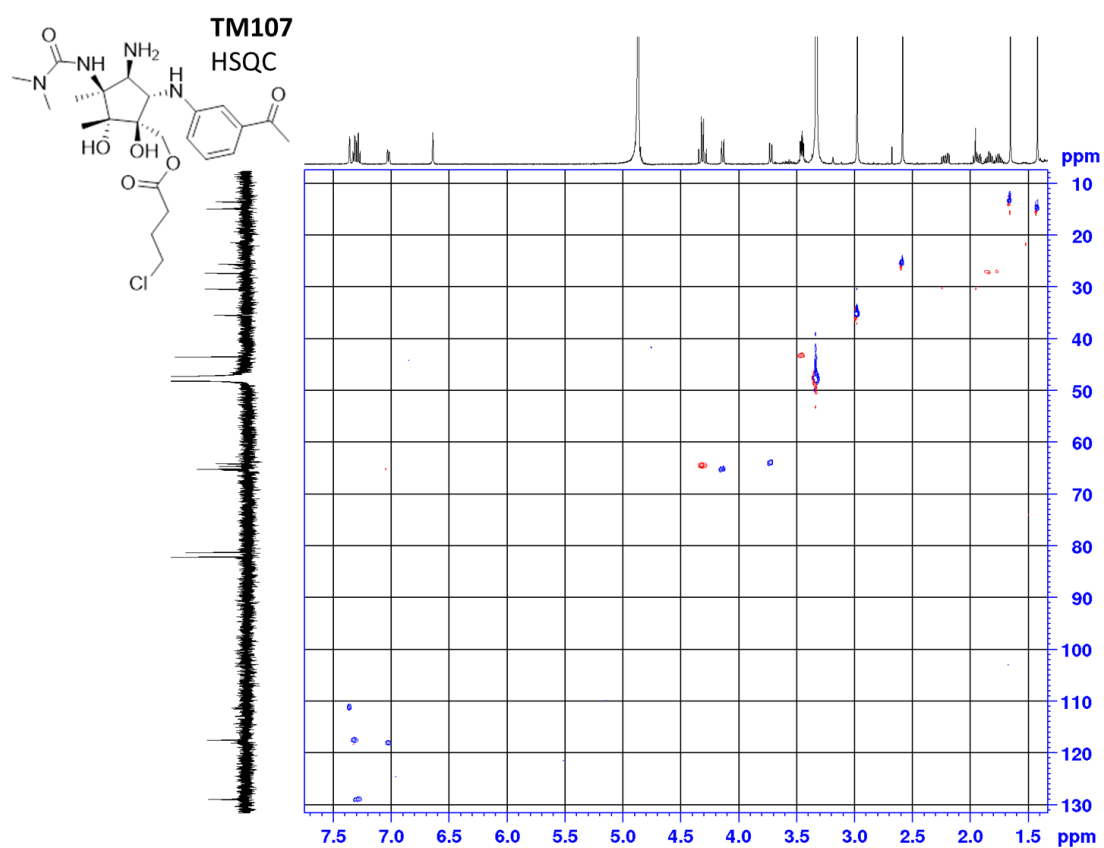


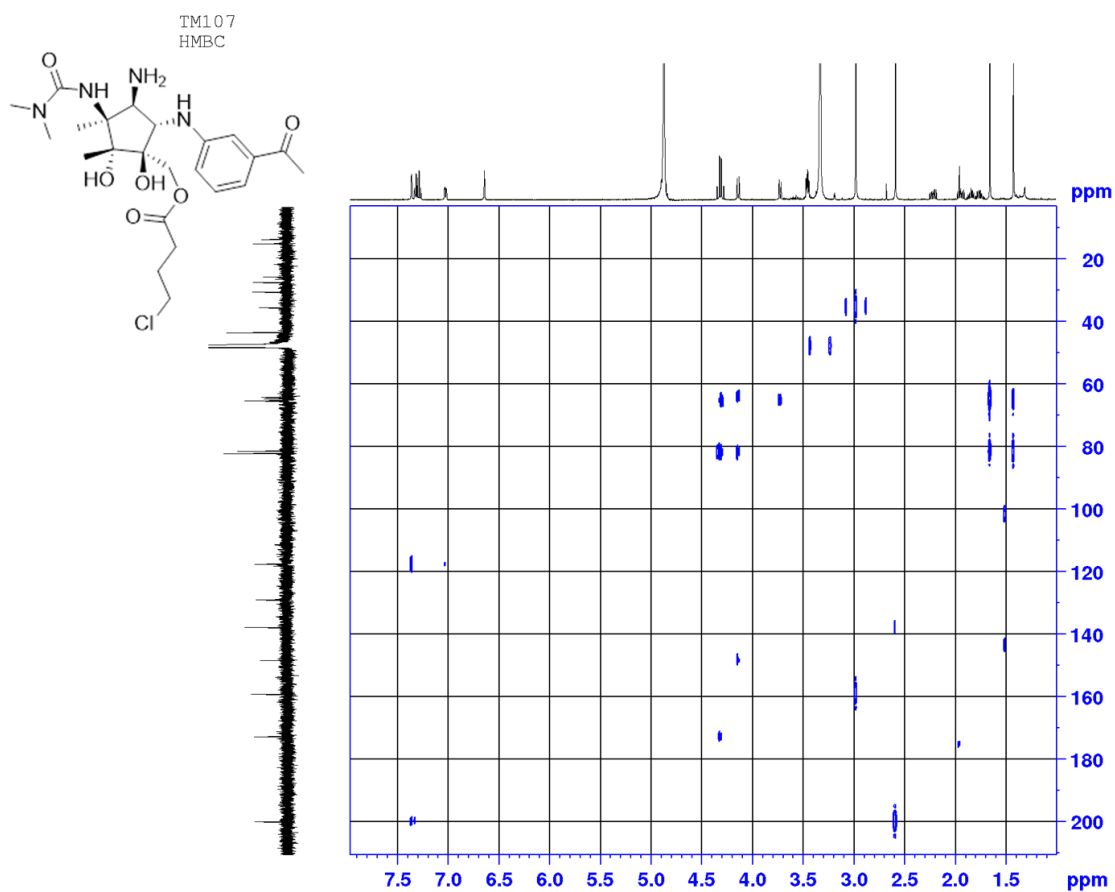
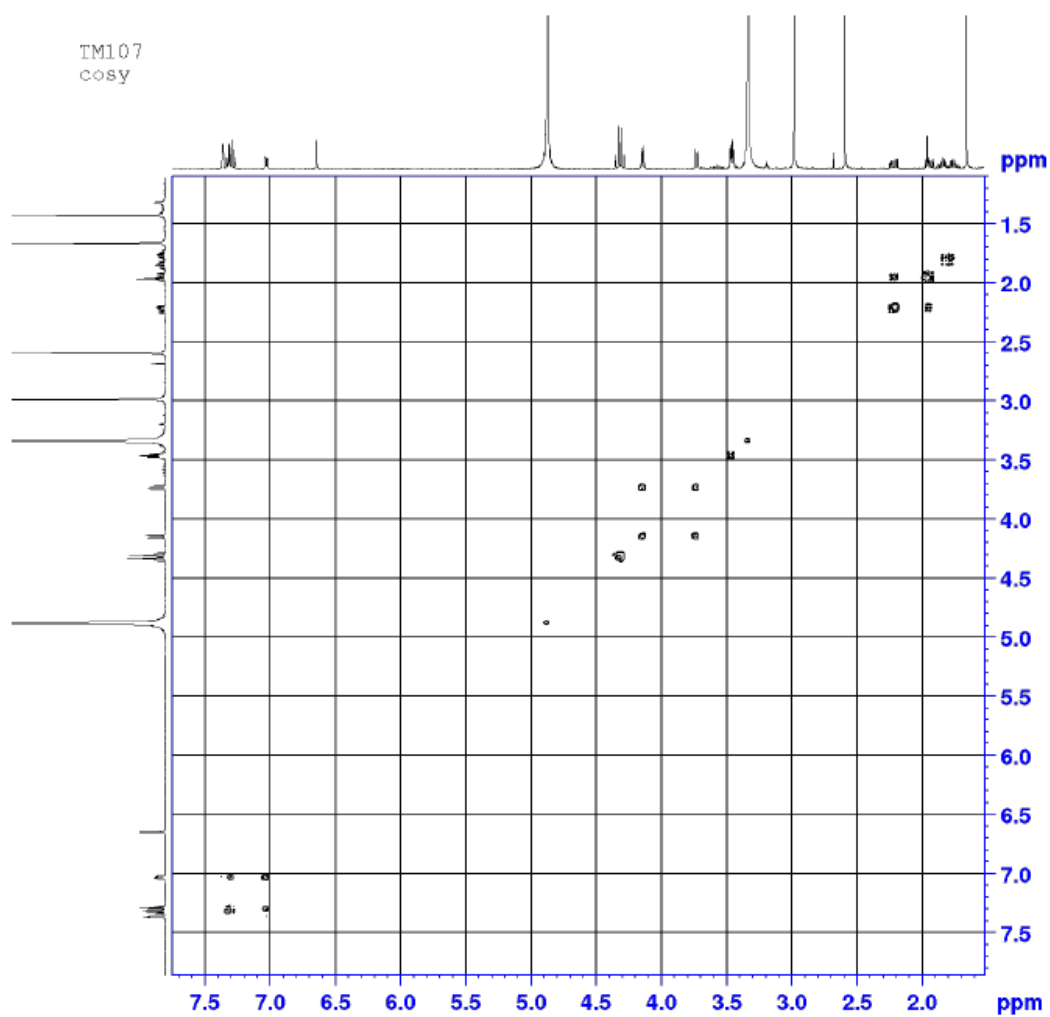
Figure S51. HMBC (MeOD) spectrum of TM-107.

Figure S52. COSY (MeOD) spectrum of TM-107.



Supporting References

1. Kieser, T., Bibb, M. J., Buttner, M. J., Chater, K. F., and Hopwood, D. A. 2000, "Practical Streptomyces Genetics", *The John Innes Foundation Norwich*, England.
2. Sambrook, J., and Russell, D. W. (2001) *Molecular Cloning. A Laboratory Manual*, 3rd ed., Cold Spring Harbor Laboratory Press, New York.
3. Ishikawa, J., and Hotta, K. (1999) FramePlot: a new implementation of the frame analysis for predicting protein-coding regions in bacterial DNA with a high G + C content, *FEMS Microbiol. Lett.* 174, 251-253.
4. Altschul, S. F., Gish, W., Miller, W., Myers, E. W., and Lipman, D. J. (1990) Basic local alignment search tool, *J. Mol. Biol.* 215, 403-410.
5. Lu, W., Roongsawang, N., and Mahmud, T. (2011) Biosynthetic studies and genetic engineering of pactamycin analogs with improved selectivity toward malarial parasites, *Chem. Biol.* 18, 425-431.
6. Paget, M. S., Chamberlin, L., Atrih, A., Foster, S. J., and Buttner, M. J. (1999) Evidence that the extracytoplasmic function sigma factor sigmaE is required for normal cell wall structure in *Streptomyces coelicolor* A3(2), *J. Bacteriol.* 181, 204.
7. Ito, T., Roongsawang, N., Shirasaka, N., Lu, W., Flatt, P. M., Kasanah, N., Miranda, C., and Mahmud, T. (2009) Deciphering pactamycin biosynthesis and engineered production of new pactamycin analogues, *ChemBioChem* 10, 2253-2265.
8. Stamatakis, A. (2014) RAxML version 8: a tool for phylogenetic analysis and postanalysis of large phylogenies, *Bioinformatics* 30, 1312-1313.
9. Edgar, R. C. (2004) MUSCLE: multiple sequence alignment with high accuracy and high throughput, *Nucleic Acids Res.* 32, 1792-1797.

**Chapter 4. Asymmetric Total Synthesis of a Pactamycin-Inspired
Aminocyclopentitol Using a Sml_2 Mediated Imino-Pinacol Coupling
Strategy**

Natural products continue to play a vital role in drug discovery. Approximately two-thirds of small molecule pharmaceuticals currently on the market are natural products or derived from natural product structures.¹ Pactamycin (**1**) is a potent antitumor antibiotic produced by the soil bacterium *Streptomyces pactum*, originally isolated in the 1960s.² The pronounced biological activity displayed by pactamycin

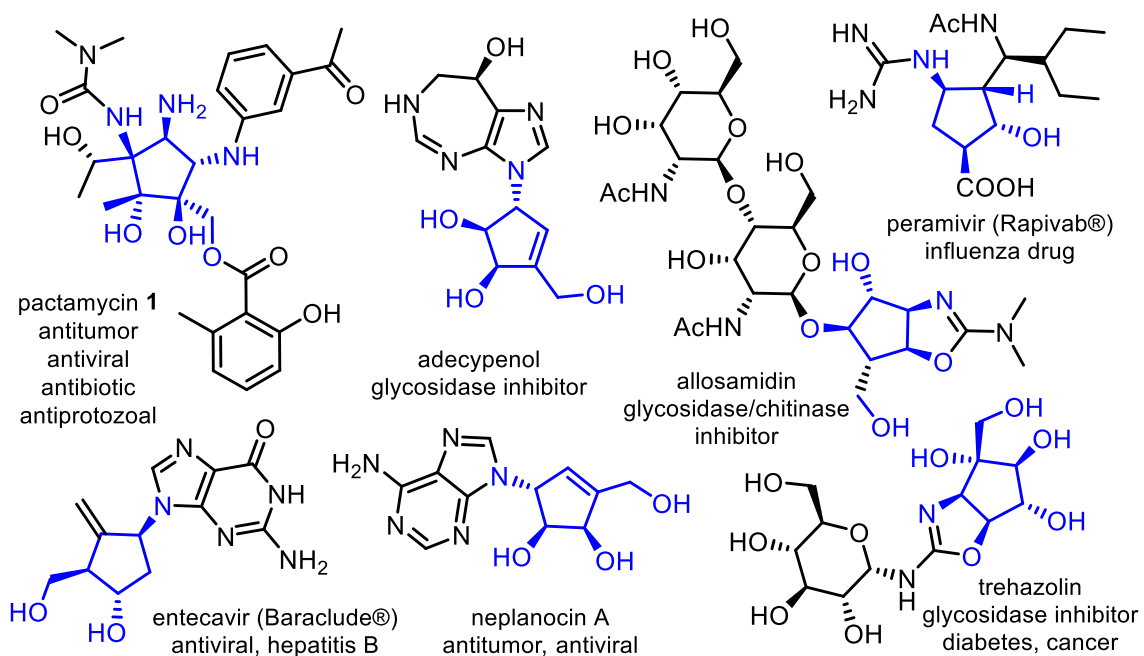


Figure 4.1. Bioactive aminocyclopentitol (blue) units in natural products and clinically used drugs

spans across all three phylogenetic domains.^{2,3,4,5} Pactamycin is an aminocyclopentitol natural product, a family of microbial secondary metabolites of rich bioactivity whose structures derive from carbohydrates (Figure 4.1).⁶ Aminocyclopentitols cover a broad swath of biological activity some of which include glycosidase inhibitors, antitumor, antibacterial and antiviral agents.

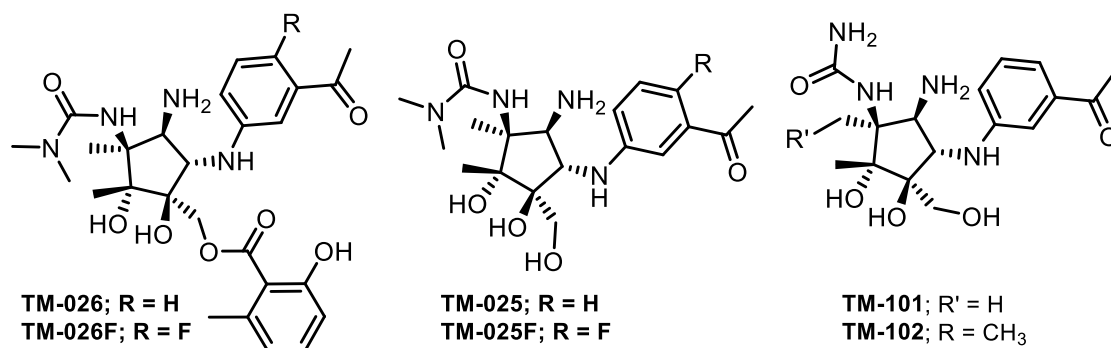


Figure 4.2. Biosynthetically modified pactamycin congeners

Unfortunately the indiscriminate cytotoxicity of pactamycin towards mammalian cells has suppressed its development toward therapeutic application. Nevertheless, we believe pactamycin is a wellspring of promising biological activity that is waiting to be harnessed. Accordingly, we have demonstrated, through biosynthetic manipulations, production of new pactamycin analogs with pronounced antimalarial activity, that lack significant antibacterial activity, and are about 10–30 times less toxic than pactamycin toward mammalian cells (Figure 4.2).^{7,8,9} Recently, we discovered that the acyltransferase (PtmR), used by *S. pactum* in the biosynthesis of pactamycin is capable of accepting a variety of substrates and developed a chemoenzymatic process to produce novel pactamycin analogs.¹⁰ Continuing our efforts to draw further on the bountiful activity of the aminocyclitol core of pactamycin, we have taken a third approach by synthesizing the core aminocyclopentitol ring which could open up a diverse library of biologically active compounds.

The intricate aminocyclopentitol structure of pactamycin, harboring 6-

contiguous stereocenters, has garnered considerable attention from the synthesis community over the years and only recently culminated in the landmark total synthesis by Hanessian in 2011 followed up by an elegant and efficient total synthesis by Johnson in 2013.^{11,12,13,14,15,16,17,18,19,20,21}

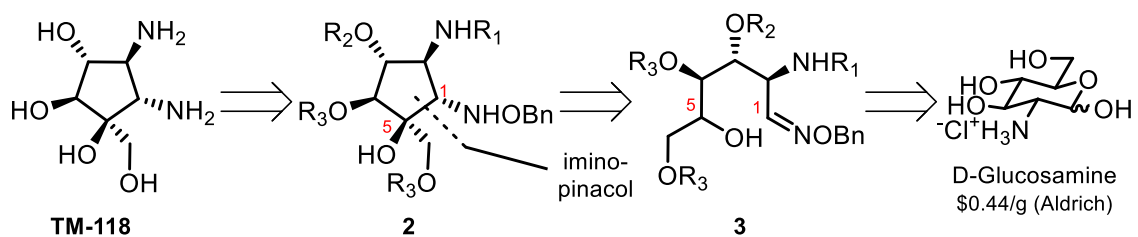


Figure 4.3. Retrosynthesis of **TM-118**.

The structurally complex aminocyclitol core is expected to be responsible for the bioactivity of pactamycin and its congeners. As such we set out to synthesize the aminocyclopentitol core lacking the aromatic rings, methyl groups and the *N,N*-dimethyl urea, all of which have been shown to affect the cytotoxicity of pactamycin or its analogs to some extent.^{8,9,22,23} The overarching goal would be to obtain modular access to a structurally unique aminocyclopentitol, that itself or a direct precursor could be derivatized to suit further SAR studies. To achieve the synthesis of the desired aminocyclopentitol ring, we surveyed general methods to synthesize highly functionalized cyclopentylamino alcohols.^{24,25,26,27} The most attractive in terms of starting material cost, flexibility and efficiency would be an intramolecular imino-pinacol coupling strategy starting from a suitable carbohydrate such as glucosamine (Figure 4.3).

Our retrosynthetic analysis to obtain the desired aminocyclopentitol starts with

deprotection of **2**. An orthogonally protected diamine (**2**) would allow further functionalization/derivatization at nearly any position imparting a high degree of synthetic flexibility to support future SAR studies. Diamine (**2**) could be constructed in a key imino-pinacol cyclization step from a 1, 5-keto-aldoxime ether, after oxidation of **3**.

Oxime ether (**3**) was chosen as oxime ethers are resistant to hydrolysis, tautomerization, as well as the reverse ring closing reaction to reform a pyranose ring, unlike

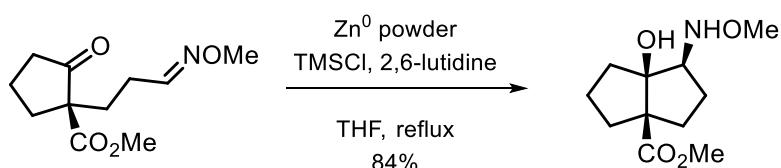


Figure 4.4. First reported keto aldoxime pinacol coupling.²⁹

their imine counterparts. Additionally oxime-ethers are good radical acceptors (approximately an order of magnitude faster than imines in 5-exo cyclizations) a requisite for the imino-pinacol coupling.²⁸ Reductive pinacol carbocyclizations between oxime ethers

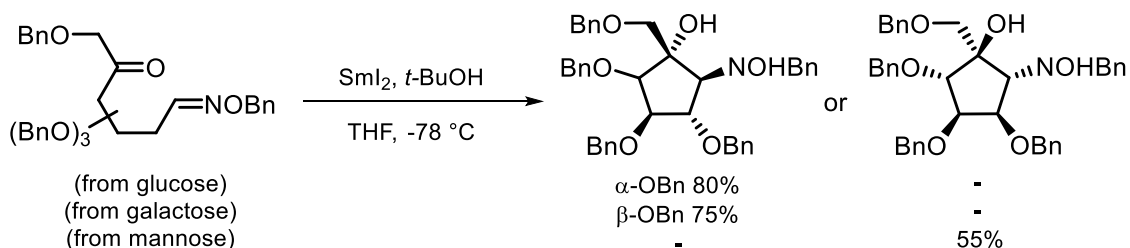


Figure 4.5. Imino pinacol coupling from carbohydrate precursors.³²⁻³⁵

and carbonyls were first demonstrated by Corey in 1983 using Zn^0/TMSCl (Figure 4.4).²⁹

Electro-reduction and tributyltin hydride were later revealed to also affect imino-pinacol

couplings.^{30,31} The scope and generality was greatly expanded to substrates derived from carbohydrates with the use of SmI_2 (Figure 4.5).^{32,33,34,35} The keto-oxime ether used in our study would come from a suitably protected carbohydrate derived from D-glucosamine. Aside from cost benefit, glucosamine had multiple advantages that we wished to exploit. Firstly, it contains most of the desired functionality, and 3 out of 5 of the necessary stereocenters in the product. Secondly, the stereochemistry at C-2 and C-4 of the carbohydrate was anticipated to be critical, based off of reported findings on similar systems, to obtain the desired diastereoselectivity in the key imino-pinacol coupling step. We based our strategy around the assumption that the undesired diastereomers resulting from configurations **A** and **C** (Figure 4.6) would be minimized due to the unfavorable stereoelectronic interactions. Configuration **C** is expected to

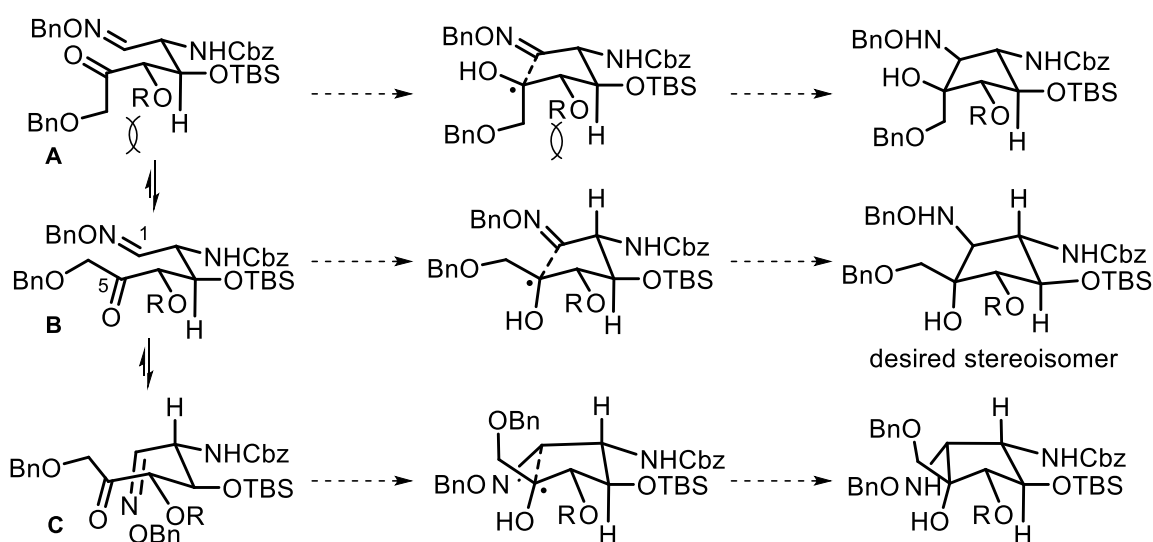


Figure 4.6. Substrate configurations that are expected to effect diastereoselection.

suffer from 1,3-allylic strain caused by the aldoxime double bond and the substituents at C2, and therefore not expected to contribute substantially to the final product. Configuration **A** is expected to experience considerable 1,3-diaxial interactions, as well as strong destabilizing electronic effects between the C5 oxygen and the negative charge developing at the N-OBn nitrogen in the transition state. While configuration **B** would lead to the product with the desired *all-trans* stereochemistry with the newly formed stereocenters at carbons 1 and 5. Unlike pinacol couplings between two carbonyls that both contain oxygen, SmI_2 induced coupling between ketones and aldoximes favor *trans* 1,5-products as coordination between the metal and the aldoxime heteroatoms is not favored. The opposite *trans*-coupled product, epimeric at C1 and C5 (not shown) is expected not to form as it would result from a configuration that encompasses all of the negative stereoelectronic contributions from both configurations **A** and **C**.^{31-35,36,37}

The forward synthesis (Figure 4.7) commenced with Cbz-protection of the glucosamine nitrogen under aqueous conditions, followed by benzylidene acetalization of the 4, 6-hydroxy groups, then bis-silylation of the remaining anomeric and the C-3 hydroxyls with 2 eq of TBSCl/imidazole providing the bis-TBS benzylidene acetal (**4**) as a single diastereomer in 53% yield over 3-steps. After considerable experimentation, screening a number of known methods, we had not found suitable conditions to affect the reductive benzylidene ring opening to expose the free C-6 hydroxyl.^{38,39} During our route scouting we identified $\text{Et}_3\text{SiH/TFA}$ as a high yielding reagent combination for this substrate that selectively exposes the C4-OH (**6**, Figure 4.7).

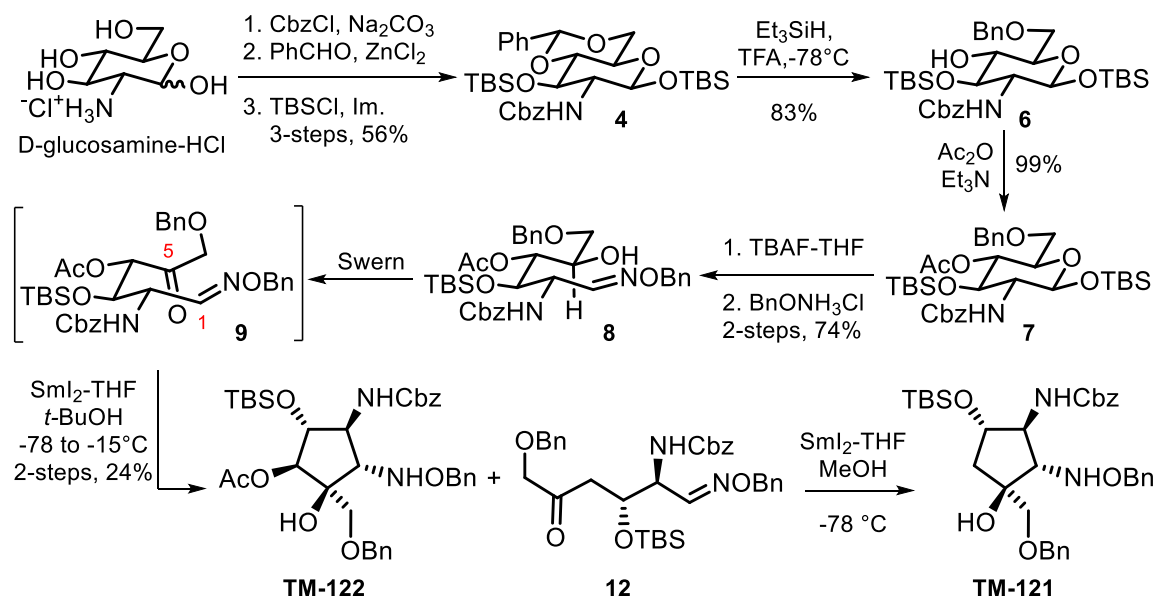


Figure 4.7. Synthesis scheme to aminocyclopentitols and deoxyaminocyclopentitols.

Although we later developed new conditions that exclusively provide the exposed C6-hydroxyl intermediate (**5**, Figure 4.10), our first attempts at synthesizing the aminocyclopentitol ring proceeded through the 4-OH intermediate (**6**, Figure 4.7).

Our initial efforts to a protected aminocyclopentitol (**2**, Figure 4.3) accessed the 4-OH glucopyranose intermediate (**6**) in good yield from reductive benzylidene ring opening of acetal (**4**) with $\text{Et}_3\text{SiH/TFA}$ (Figure 4.7). The C4 hydroxyl group on the pyranose ring proved particularly unreactive as a nucleophile. We found benzylation ineffective under a variety of conditions ($\text{Ag}_2\text{O/BnBr}$; NaH, BnBr NaH/PMBCl/NaI ; BaO/Ba(OH)_2 ; $\text{BnBr/NaI/DIPEA/130}^\circ\text{C}$; $\text{PMBCl/TBAI/DIPEA/130}^\circ\text{C}$), even *O*-acylation with benzoyl chloride and stoichiometric quantities of DMAP was challenging with this substrate.³⁹ However, acetylation ($\text{Ac}_2\text{O/DMAP/Et}_3\text{N}$) gave the 4-OAc compound in high yield. We

were aware this protecting group might be problematic during the imino-pinacol cyclization due to potential elimination of the alpha acetoxy group. Deoxygenation of alpha-acetoxy ketones with SmI_2 is a known and generally efficient reaction usually carried out in large volume excesses of MeOH, HMPA and/or ethylene glycol - mixtures that are known to strongly enhance the reduction potential of SmI_2 , so we were unsure at the time whether de-acetoxylation would compete with the intramolecular radical coupling in the absence of such excesses of these reagents.^{40,41} Despite the possible pitfalls, we decided to carry the 4-OAc substrate forward to the imino-pinacol coupling stage for several reasons. Firstly, while SmI_2 was our first choice to affect the reductive pinacol coupling reaction, other radical promotors (Mg^0/TMSCl , $\text{Bu}_3\text{SnH}/\text{AIBN}$, TTMSH/AIBN , $\text{Et}_3\text{B}/\text{O}_2$, $\text{NiCl}_2/\text{TMSCl}/\text{Mg}^0$) are capable of generating ketyl radicals and effective at promoting pinacol coupling reactions and could be attempted.^{29-31,42,43,44,45} Furthermore, SmI_2 is fairly unique in its ability to promote des-acetoxy eliminations. Secondly, we reasoned if deoxygenation were to occur, the linear deoxy-byproduct might undergo cyclization and produce a structurally unique mono-deoxy-aminocyclitol product that would be an interesting substrate for later SAR studies.

Eager to assess the cyclization, we carried the 4-OAc substrate (**7**) forward. A regioselective desilylation exposed the anomeric hydroxyl group in high yield providing both alpha and beta diastereomers which could be allowed to equilibrate to the alpha diastereomer, then subjected to dehydrative ring opening (BnONH_3Cl , pyridine) to form the 5-hydroxy aldoxime (**8**) in moderate yield. Oxidation to the 5-keto 1-aldoxime ether

would provide the imino-pinacol precursor. After screening a number of oxidation conditions (DMSO-Ac₂O, IBX, DMP, TPAP-NMO) we observed the desired 5-ketoaldoxime ether product, but the reactions were not clean. Additionally, we found the desired 5-ketoaldoxime ether product (**9**) to be thermally unstable, which would restrict our reagent choices for the oxidation and ultimately the imino-pinacol coupling conditions as well. We were pleased to find that a modified Swern oxidation [(COCl)₂, DMSO, THF, then DIPEA, -78 °C to -20 °C] successfully, and cleanly, delivered the 5-ketoaldoxime **9**.⁴⁶ As mention above, the instability of **9** would limit the reagent system that could be employed for the imino-pinacol cyclization to those capable of forming the requisite ketyl radical at low temperatures such as SmI₂ or Et₃B/O₂. Gratifyingly, a one-pot Swern oxidation/SmI₂ mediated reductive cyclization (SmI₂/THF/*t*-BuOH) produced the desired aminocyclopentitol TM-123, albeit in low yield (2 steps, 14%). The major reaction products in this 1-pot sequence were identified as the *N*-cyclized pyrrolidine aldoxime (**11** not shown, 14% yield) and the linear *des*-acetoxy ketone (**12**, 35% yield). We observed the *N*-cyclized compound, pyrrolidine **11**, was formed when the 5-ketoaldoxime **9** from the Swern step was warmed to room temperature. The pyrrolidine byproduct could be suppressed by keeping the Swern oxidation below -15 °C after addition of DIPEA, resulting in a modest increase in yield to 24%, however the linear *des*-acetoxy **12** product could not. Though, after isolation of the linear *des*-acetoxy **12** then re-subjecting it to the reductive cyclization conditions, provided the deoxy-aminocyclopentitol TM-122. Interestingly, we also found that the *des*-acetoxy-aminocyclopentitol TM-122 could be obtained

clean and directly from the Swern oxidation/ SmI_2 -reductive coupling sequence simply by switching the proton donor from *t*-BuOH to MeOH.⁴¹ This reaction sequence efficiently accesses the 4-deoxy-diaminocyclopentitol ring effectively, comprising of 3-steps in one pot: alcohol oxidation, elimination-deoxygenation, and C-C coupling. Though we were pleased to have successfully reached the protected diamino-cyclopentitol TM-122 as well as delivering a novel and efficient entry into deoxy-aminocyclopentitols such as TM-121, we sought a higher yield of the target compound. We had hoped to improve the Swern/reductive coupling steps by taking advantage of the tunability of SmI_2 by swapping proton donors, lone pair donors, metal halide additives etc., but this was overall unsuccessful. It became clear that a more robust protecting group at the 4-OH position of the pyranose was necessary.

We eventually obtained the liberated C-6 alcohol (**5**, Figure 4.10) through a regioselective reductive benzylidene ring opening. However, during the course of investigating suitable protecting groups for C4-hydroxyl in **6** and the C-6 hydroxyl in **5** we found that anionic benzylation (NaH, DMF) of **5** resulted not only in facile *N*-benzylation but also cyclization of the carbamate to the 2,3-oxazolidinone. Though we later discovered that with strict temperature control (-20° C to -15° C) both side reactions can be suppressed completely to give the desired 6-OBn **14**.

However, using the oxazolidinone intrigued us, because we reasoned that a fully protected imino-pinacol substrate (**15**), could be prepared very rapidly from **16** (Figure 4.8). Nevertheless, we were cognizant that the pinacol coupling proposed with this sub-

strate would be expected to yield a strained *trans*-fused bicyclo[3.3.0] octane-like ring system, which is rarely synthesized but not unprecedented; we felt that rapid access to the pinacol substrate (**15**) justified the effort.^{47,48}

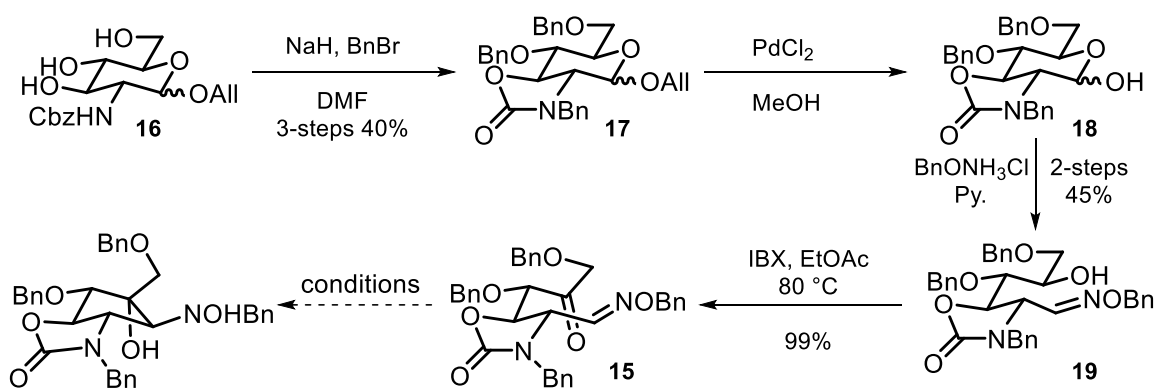


Figure 4.8. Synthesis scheme towards aminocyclopentitols via oxazolidinone route.

The synthesis of oxazolidinone aldoxime ether (**15**) commenced with anionic benzylation (NaH, DMF then BnBr) and *in-situ* carbamate cyclization of *N*-Cbz 1-allyl glucosamine **16** which afforded the orthogonally protected oxazolidinone (**17**, 3 steps; 50 %). Cleavage of the allyl ether (PdCl₂, 1 eq, MeOH, rt) at C-1 exposed the anomeric hydroxyl providing hemiacetal (**18**) which eluded characterization due to apparent palladium contamination evident by broadened ¹H NMR signals in the purified material. However, we found that using the Pd-contaminated hemi-acetal (**18**) in the subsequent dehydrative ring opening with *O*-Benzylhydroxyl amine still produced the desired 5-hydroxyaldoxime ether (**19**) in reasonable yield (2 steps, 45% yield). Oxidation (IBX, EtOAc, 75-80 °C) of the secondary alcohol, 5-hydroxyaldoxime ether (**19**), to the 5-ketoaldoxime ether (**15**) proceeded uneventfully in high yield (99%). As expected, the 5-

ketoaldoxime ether (**15**) is stable at room temperature unlike substrates with an exposed nitrogen (NHCbz). With the cyclization substrate (**15**) in hand, we proceeded to the imino-pinacol coupling. Remarkably, no reaction occurred in the presence of

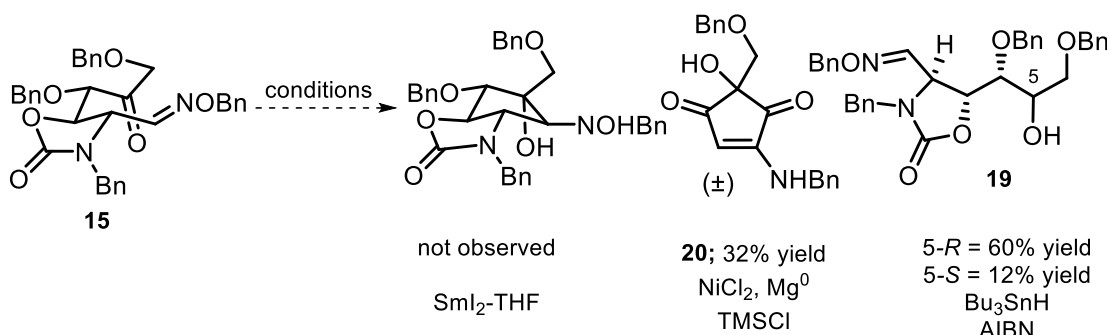


Figure 4.9. Summary of conditions and results for the oxazolidinone pinacol coupling.

Sml_2 in THF at room temperature. In fact it is completely inert to $\text{Sml}_2\text{-THF}$ with or without proton donors, organic amines or metal halides unless heat was applied. When heated at 50 °C for 5 min, a new TLC spot was observed at the expected *rf* range, the starting material was consumed, and mass spectrometry data from the reaction mixture indicated a product *m/z* value that matched the desired product. However, the TLC spot disappeared before the compound could be isolated, suggesting the *trans*-fused cyclopentane ring system likely formed but was unstable and short-lived. The experiment was repeated, and to our dismay produced the same result: formation of a single new spot with the expected *m/z* value followed by loss of the TLC spot prior to reaction workup. Surprisingly, we did not observe any of the 5-hydroxy reduction product (**19**) under these conditions. Other radical initiators capable of generating the necessary

ketyl radical from an aliphatic ketone were also screened in order to affect the cyclization of the 5-ketoaldoxime (**15**) to the desired aminocyclopentitol and the conditions leading to reduction products are summarized in Figure 4.9. Interestingly, tributyltin hydride/AIBN produced exclusively ca. 6:1 mixtures of the diastereomeric alcohols, while the Sml_2 conditions did not. When **15** was treated with Rieke nickel ($\text{NiCl}_2/\text{TMSCl}/\text{Mg}^0$)⁴⁵, a new spot had formed and upon isolation and characterized as the benzylamino-cyclopentene dione (**20**). However, **20** was found to be a racemic mixture and also missing key functional features, which unfortunately precludes the utility of this compound in our synthesis of the target molecule. Having attempted a number of conditions to obtain the desired aminocyclopentitol from two different ketoaldoximes (**15** and **9**) with limited success, we turned to aldoxime (**21**, Figure 4.10) that after oxidation would produce not only a less-strained pinacol product (than the oxazolidinone) but also utilizes the more robust (-OBn) protecting group at the C4-hydroxyl.

Turning our attention to aldoxime **21** (Figure 4.10), we screened several reported conditions to selectively open the benzylidene ring in **4** to provide **5**. One promising condition (cyanuric chloride, NaBH_4) provided the desired 4-OBn **5** selectively but suffered a low yield (10%). By switching from TFA- Et_3SiH in our first route (Figure 4.9) to a Lewis acid system, Bu_2BOTf - Et_3SiH (Figure 4.10), completely reversed the selectivity, favoring the desired, free C6 alcohol **5** in high yield (86%). To our knowledge, this reagent combination is new for this type of transformation and has not been reported.^{38,39}

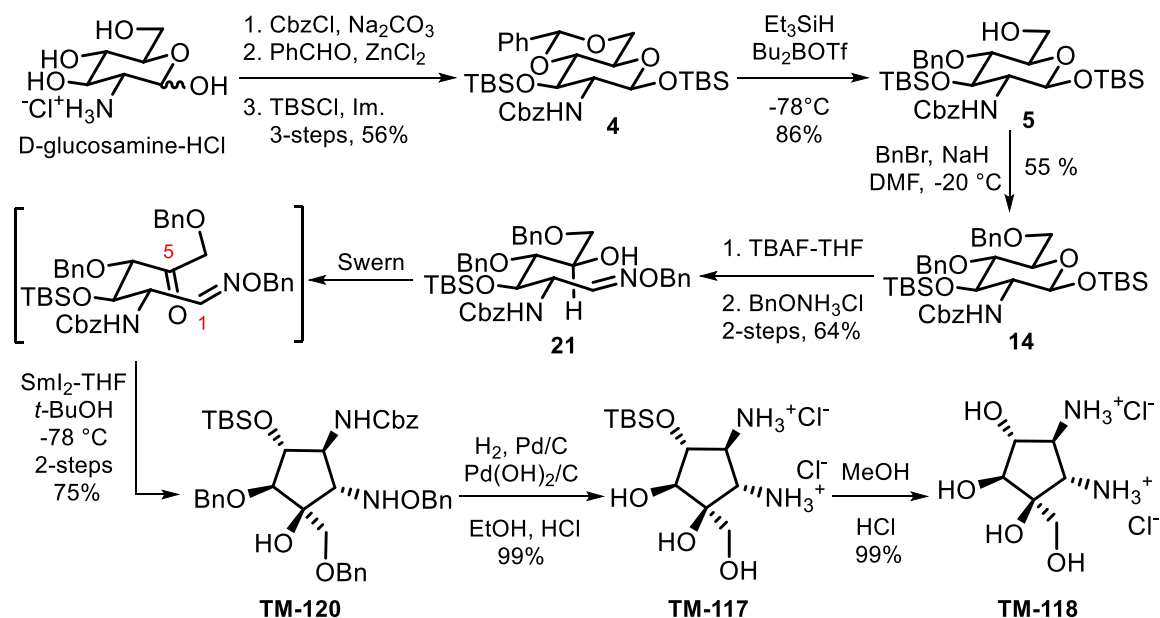


Figure 4.10. Total synthesis of aminocyclopentitol TM118.

Benzylation (NaH, BnBr, -20 °C) of the C-6 hydroxyl provided benzylated intermediate (**14**) in modest yield (55%), suffering from competitive *N*-benzylation of the 6-*O*-benzyl product (**14**) with *O*-benzylation of the starting material (**5**). *N*-Benzylation could be suppressed completely by keeping the reaction below -20 °C and quenching the reaction at 50% conversion. Selective removal of the anomeric-TBS group (TBAF, THF, 0 °C) afforded the corresponding free lactol. Literature methods for this transformation use AcOH-TBAF to buffer the basicity of the fluoride anion, but we found the reaction sluggish requiring over 48 h to reach completion.⁴⁹ By omitting AcOH, the reaction was complete within 10 m, selective and high yielding (90%). Dehydrative ring opening of the lactol, provided both *E/Z*-isomers of the 5-hydroxy-aldoxime ether **21** in 64% yield. After screening a number of oxidation conditions to obtain the 1,5-keto-aldoxime as the

imino-pinacol precursor, we settled on modified Swern conditions $[(\text{COCl})_2, \text{DMSO}, \text{DIPEA}, -78^\circ \text{C}]$ with the observation that the product ketone was unstable above 0°C .⁴⁶ As the reductive keto-aldoxime cyclization was expected to occur at low temperatures, we therefore attempted to telescope the Swern and imino-pinacol coupling steps to overcome the instability issue of the intermediate ketone.³² To our delight, the Swern/imino-pinacol coupling successfully produced the desired orthogonally protected aminocyclopentitol TM-120 as a mixture of two out of four possible diastereomers (Figure 4.10 and Figure 4.11, 75% yield).

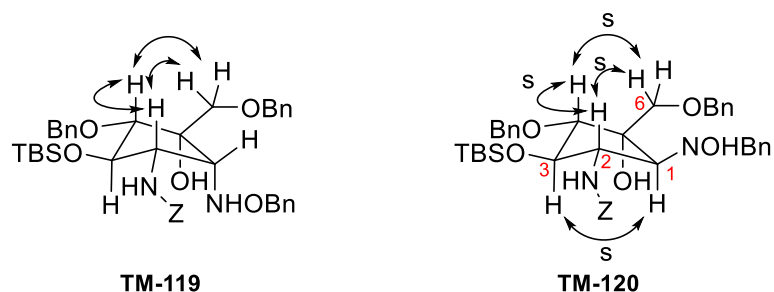


Figure 4.11. Key NOE correlations of the imino-pinacol products TM-119 and TM-120.

We have successfully repeated this two-step conversion on gram scale. Importantly, this strategy grants convenient access to differentially protected cyclopentyl diamines utilizing an imino-pinacol coupling strategy. Notably, Chiara and co-workers attempted similar imino-pinacol couplings with protected 2-amino-carbamate 1-aldoxime ethers but reportedly suffered from *N*-cyclization and a mixture of many products.⁵⁰ In our hands we found the *N*-cyclized compound was the major decomposition product from the ketone starting material if allowed to warm above 0°C .

While formation of the desired stereoisomer TM-120, can be rationalized by the stereoelectronic effects noted in figure 4.6, the formation of diastereomer TM-119 is less straightforward. Interestingly, a similar erosion of stereoinduction was reported in a series of otherwise completely diastereoselective imino-pinacol couplings. The anomalous result occurred with a substrate containing an *O*-acetate vicinal to the radical accepting aldoxime.⁵¹ As carbonyl oxygens are sometimes capable of directing SmI_2 mediated reactions,⁵² we hypothesize that coordination of an organosamarium with the *N*-carbobenzyloxy group is responsible for overriding the otherwise inherent stereoelectronic biases highlighted in figure 4.6, forming the diastereomer TM-119.

At this stage in the synthesis, the protected aminocyclopentitol TM-120 can be used as a branching point for derivatization/SAR studies, but for our immediate purposes we desired the free aminocyclopentitol TM-118. However, to our dismay, a number of hydrogenation conditions failed to deliver any desired product even with extended reaction times and higher temperatures. Interestingly, the one electron reductant, LiDBB, furnished the desired putative intermediate (TM-117; by MS and ^1H NMR) but left the highly water soluble aminocyclitol as an intractable mixture of mostly inorganic impurities after aqueous workup.³⁹ A number of non-aqueous workup/purification conditions also failed to provide TM-117. It is noteworthy, however, that LiDBB has not been previously demonstrated to cleave the N-O bond in hydroxylamines. Seeking alternate debenzoylation conditions, an intriguing paper caught our attention that reported a mixture of $\text{Pd}(\text{OH})_2/\text{C}$ and Pd/C affords “a more reactive hydrogenation catalyst than

either catalyst alone”.⁵³ Upon adaptation of their method, we were pleasantly surprised to find that the catalyst combination successfully debenzylated the aminocyclopentitol at 0 °C (H₂, EtOH, conc. HCl) in less than 3h to provide the desired TM-117 as the sole product (99% yield). Encouraged by this result, we hoped to debenzylate and remove the TBS group in 1-pot by switching from EtOH to MeOH as the hydrogenation solvent, however, this was unsuccessful.⁵⁴ We observed that after full conversion to TM-117, followed by a filtration and solvent exchange to MeOH, full desilylation had occurred providing the desired final product TM-118 in nearly quantitative yield (99%). With the desired product TM-118 and a number of novel aminocyclopentitols in hand from our synthetic routes, we were eager to test the bioactivity.

Biological Activity

Preliminary biological testing of TM-118, TM-117, and fully protected aminocyclopentitol TM-120 against four bacterial strains (two Gram-positive and two Gram-negative), indicated that TM-117 and TM-120 displayed modest activity against Gram-positive *Staphylococcus aureus*. While TM-120 also displayed modest inhibitory activity, similar to pactamycin, versus Gram-negative *Pseudomonas aeruginosa* (Figure 4.12). Importantly, further biological evaluation of some of the synthetic intermediates

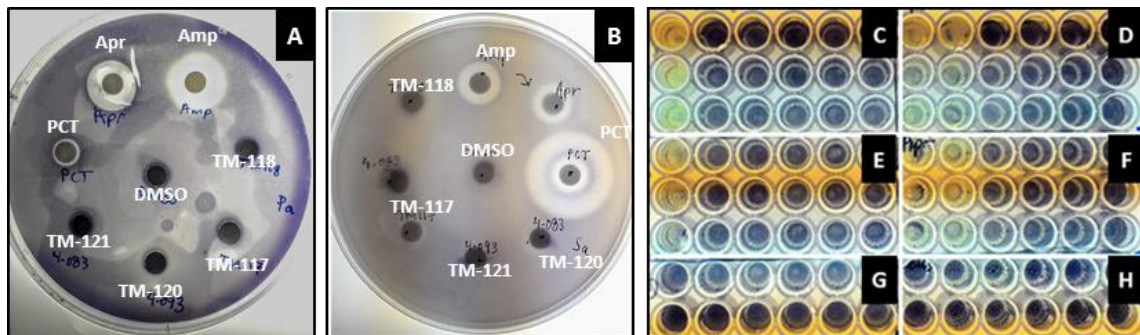


Figure 4.12. Antibacterial testing of pactamycin analogs. Agar diffusion assay of pactamycin analogs against *P. aeruginosa* (A) and *S. aureus* (B). PCT = pactamycin; Amp = ampicillin; Apra = apramycin; DMSO; 10 μ L of 10 mM each. Microdilution assay of TM-117 and other antibiotics *S. aureus* (C-F). (C) TM-117 (1mM to 1 nM); (D) pactamycin (1mM to 1 nM); (E) ampicillin (1mM to 1 nM); (F) apramycin (1mM to 1 nM); (G) DMSO; (H) cells.

containing the aminocyclopentitol ring revealed that deoxy-aminocyclopentitol TM-121 and acetate-TM-122 exhibited potent anticancer activity against melanoma (A375 cells, Figure 4.13). This result is on par with the anticancer activity observed with pactamycin derivative TM-026. These are important preliminary biological results and should be followed up with more rigorous studies to establish selectivity, toxicity and whether the mechanism of action is unique or similar to pactamycin.

In conclusion, we have developed an efficient asymmetric route to the aminocyclopentitol TM-118. Moreover, we have demonstrated that the synthetic precursors, TM-117 and aminocyclopentitol TM-120, are modestly active against Gram-positive bacteria. In addition, we have found that aminocyclopentitols TM-121 and TM-122 are also significantly bioactive molecules and display promising cancer cell toxicity.

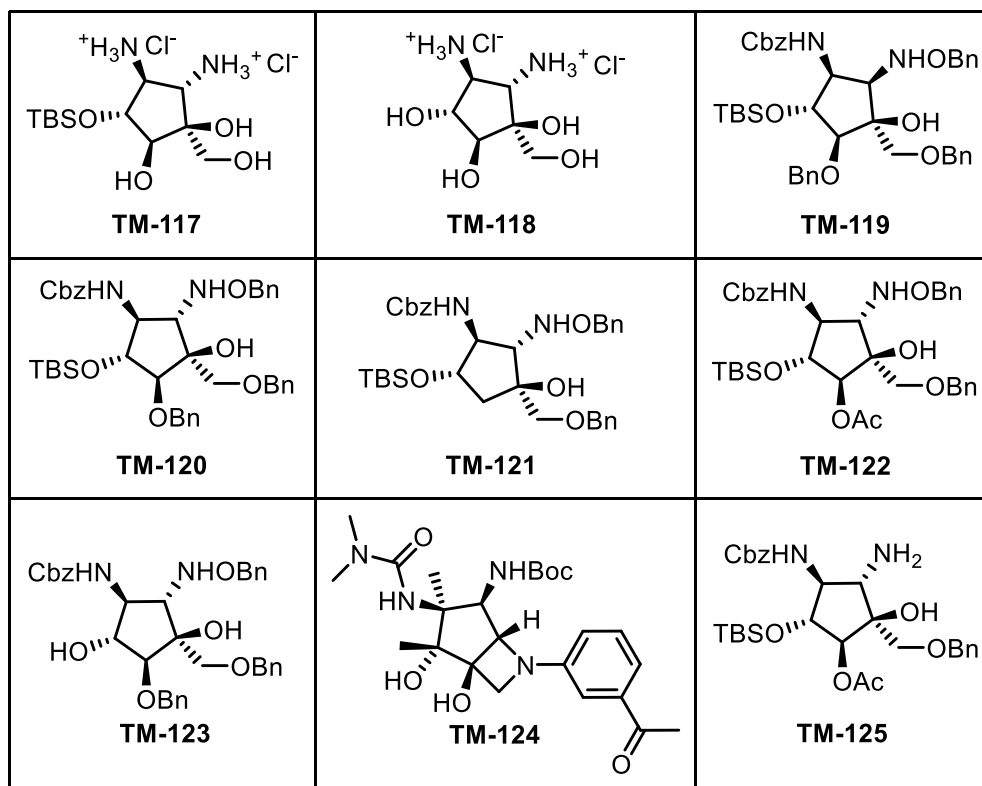
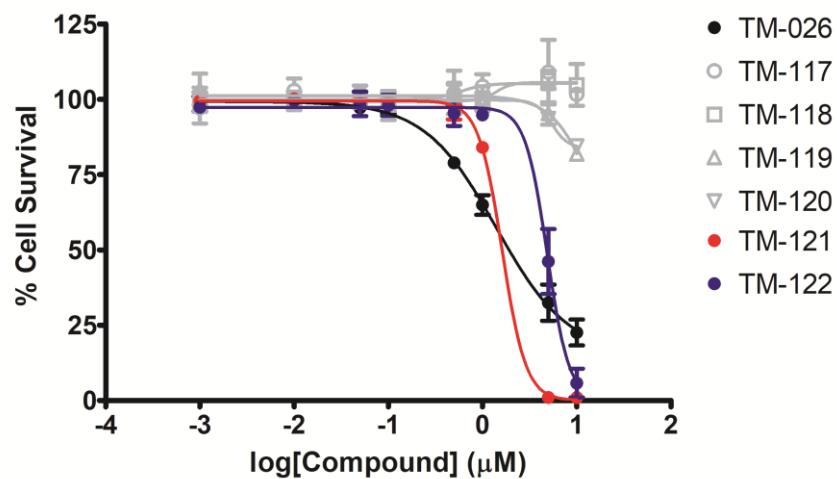
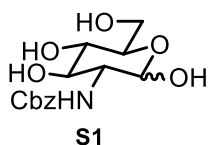


Figure 4.13. Antitumor activity of pactamycin analogs. Dose response curve (above) and structures of synthetic pactamycin analogs (below) screened against melanoma A375 cells.

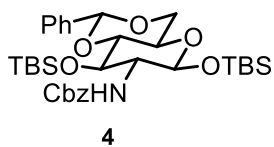
Supporting information

General: All reactions were carried out under an inert Argon atmosphere in oven-dried glassware unless indicated otherwise. Flash column chromatography was carried out with SiliaFlash P60, 60 Å silica gel. Reactions and column chromatography were monitored with EMD silica gel 60 F254 plates and visualized with potassium permanganate, ceric ammonium molybdate, iodine, or vanillin stains. Molecular sieves were pre-activated by heating for 2h at 200 °C under vacuum. Tetrahydrofuran (THF), and diethyl ether (Et₂O) were freshly distilled from a sodium benzophenone ketyl. Triethylamine (Et₃N), diisopropylethyl amine (DIPEA), pyridine (Py), dichloromethane (DCM) and acetonitrile (MeCN) were distilled over calcium hydride prior to use. DMSO and *t*-BuOH were stored over 3 Å molecular sieves. Sml₂ was freshly prepared using a modified version of Imamoto's method (reagent was heated only until color change occurred then cooled to room temperature and stirred a minimum of 18 h under an atmosphere of argon prior to use).⁵⁵ All syringes were purged with argon 3 x prior to use. All other reagents and solvents were used without further purification from commercial sources. Instrumentation: FT-IR spectra were obtained on NaCl plates with a PerkinElmer Spectrum Vision spectrometer. Proton and carbon NMR spectra (¹H NMR and ¹³C NMR) were recorded in deuterated chloroform (CDCl₃) unless otherwise noted on a Bruker 700 MHz Avance III Spectrometer with carbon-optimized cryoprobe and Bruker 400 MHz spectrometer and calibrated to residual solvent peaks. Multiplicities are abbreviated as fol-

lows: s = singlet, d = doublet, t = triplet, q = quartet, sept = septet, br = broad, m = multiplet.

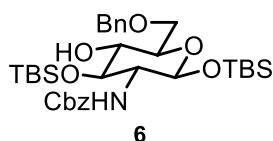


Synthesis of benzyl ((3*R*,4*R*,5*S*,6*R*)-2,4,5-trihydroxy-6-(hydroxymethyl)tetrahydro-2*H*-pyran-3-yl)carbamate (**S1**)⁵⁶: An aqueous solution of *D*-glucosamine·HCl (0.27 M, 0.163 mol, 35 g) was cooled in an ice-bath 15 m and added Na₂CO₃ (0.358 mol, 37.9 g, 2.2 eq), followed by a dropwise addition of benzylchloroformate (24.4 mL, 0.171 mol, 1.05 eq) at 0°C. The reaction was held at this temperature for 1h before slowly warming to room temperature and stirring 14h. TLC (EtOAc-MeOH = 9:1). indicated reaction completion. The product was collected by filtration and the solids were washed successively on the funnel with water (2 x 100 mL) on the filter, then toluene (2 x 50 mL) then CH₂Cl₂ (2 x 50 mL). The resulting solids were dried under vacuum on funnel (12 h), then transferred to a round bottom flask and any residual water was azeotropically removed by 2 cycles of addition and evaporation of toluene (2 x 300 mL) at 35 °C. Remaining volatiles were removed *in vacuo* and used in the next step without further purification.



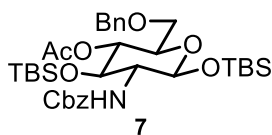
Synthesis of benzyl ((2*R*,4*aR*,6*S*,7*R*,8*R*,8*aR*)-6,8-bis((tert-butyldimethylsilyl)oxy)-2-phenylhexahydropyrano[3,2-*d*][1,3]dioxin-7-yl)carbamate (**4**): ZnCl₂ was fused prior to the reaction by adding ZnCl₂ to a dry preweighed round bottom flask and fused under vacuum with a flame until bubbling ceased. The flask was then allowed to cool to room temperature while under high vacuum. The flask containing fused ZnCl₂ (37.2 g, 0.243 mol, 2 eq) was backfilled with argon and added benzaldehyde (449 mL, 0.27 M) and stirred 10 min at room temperature. Starting material **S1** was then added at room temperature and stirred 24 h under argon. TLC indicated reaction completion (EtOAc-MeOH = 10:1). The reaction mixture was poured onto an equal volume of ice water, then warmed to room temperature and the crude product collected by filtration as an amorphous white solid. Successive washes with EtOAc, Hexanes then Et₂O on the filter to remove residual benzaldehyde, then the solids were dried by azeotropic distillation with toluene (2 x 250 mL) & volatiles were removed *in vacuo* (24 h). The resulting white solids (41.0 g, 0.102 mol) were dissolved in anhydrous DMF (157 mL, 0.65 M) and added TBSCl (33.9 g, 0.225 mol, 2.2 eq), then imidazole (20.87 g, 0.306 mmol, 3 eq) was added and stirred 24h at RT until reaction reached completion as indicated by TLC (Hexane-EtOAc = 4:1). The mixture was diluted with EtOAc (500 mL), and washed with 0.1 M HCl (2 x 250 mL), the aqueous extracted with EtOAc (3 x 500 mL), organics combined and washed with water (3 x 500 mL), brine (250 mL), dried (Na₂SO₄), filtered and volatiles removed *in vacuo*. The resulting gummy foam was purified by flash chromatography and eluted with Hexane-Et₂O = 10:1 to yield **4** (55 g, 55.5% yield). [α]_D = -29° (c 5.4, DMSO,

23 °C). IR (film): 3355, 3067, 3036, 2954, 2929, 1714 cm^{-1} . ^1H NMR (500 MHz, CDCl_3) δ 7.53 – 7.48 (m, 2H), 7.42 – 7.33 (m, 8H), 5.52 (s, 1H), 5.09 (brs, 1H), 5.06 (d, J = 7 Hz, 1H), 4.95 (d, J = 7 Hz, 1H), 4.32 – 4.28 (m, 1H), 4.21 (brs, 1H), 3.85 – 3.74 (m, 1H), 3.50 (d, J = 4 Hz, 2H), 3.18 (d, J = 8 Hz, 1H), 0.91 (s, 9H), 0.84 (s, 9H), 0.13 (s, 3H), 0.10 (s, 3H), 0.01 (s, 3H), -0.02 (s, 3H). ^{13}C NMR (126 MHz, CDCl_3) δ 155.4, 137.3, 136.3, 129.0, 128.5, 128.4, 128.1, 128.1, 126.3, 101.7, 95.7, 82.5, 71.1, 68.8, 66.7, 66.1, 62.0, 25.7, 25.5, 18.1, 17.9, -4.1, -4.2, -5.3. HR-ESI (+)-MS: Theoretical $\text{C}_{33}\text{H}_{52}\text{NO}_7\text{Si}_2$ $[\text{M}+\text{H}]^+ = m/z$ 630.32768; Observed $[\text{M}+\text{H}]^+ = m/z$ 630.32888.



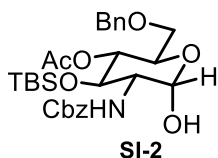
benzyl ((2*S*,3*R*,4*R*,5*R*,6*R*)-6-((benzyloxy)methyl)-2,4-bis((*tert*-butyldimethylsilyl)oxy)-5-hydroxytetrahydro-2*H*-pyran-3-yl)carbamate (**6**): Benzylidene **4** (7.9 mmol, 5 g) in anhydrous DCM (79.5 mL, 0.1 M) was added Et_3SiH (12.76 mL, 0.08 mol, 9.3 g) and 3 Å Mol sieves (beads) then cooled to 0°C and allowed to stir 1.5h at 0°C. Trifluoroacetic acid (6.03 mL, 8.99 g, 0.079 mol; freshly distilled from 0.1% TFAA; TFA Bp = 71°C) was added slowly over 15 m via syringe at 0°C. TLC (Hexane-EtOAc=4:1) indicated reaction completion. Reaction was quenched by dropwise addition of Et_3N (13 mL, 12eq, 0.095 mol) at 0°C. The quenched reaction was incubated 12h at -20°C, then filtered through 2 x 3 in. pad of SiO_2 , rinsed with 200 mL DCM, and the organics washed with NaHCO_3 , water (150 mL), brine (100 mL) and dried (Na_2SO_4), filtered and volatiles removed *in vacuo*. The re-

sulting pale yellow oil was purified by flash chromatography (Hexane-EtOAc = 100:20) to yield **6** (4.1 g, 83%). $[\alpha]_D = -5^\circ$ (c 20, DCM, 27 °C); IR (film) 3441, 2929, 2856, 1703, 1521 cm^{-1} . ^1H NMR (400 MHz, CDCl_3) δ 7.40 – 7.29 (m, 10H), 5.06 (s, 2H), 4.91 (d, $J = 6$ Hz, 1H), 4.79 (d, $J = 6$ Hz, 1H), 4.59 (d, $J = 12$ Hz, 1H), 4.64 (d, $J = 12$ Hz, 1H), 3.93 – 3.82 (m, 1H), 3.76 (m, 2H), 3.56 – 3.43 (m, 2H), 3.19 – 3.05 (m, 1H), 2.50 (d, $J = 2$ Hz, 1H), 0.89 – 0.86 (m, 18H), 0.19 – -0.05 (m, 12H). ^{13}C NMR (101 MHz, CDCl_3) δ 155.5, 137.6, 136.4, 128.5, 128.2, 128.1, 127.7, 127.7, 95.4, 74.7, 73.7, 73.7, 73.6, 70.7, 66.7, 60.7, 25.8, 25.6, 18.2, 17.9, -4.2, -4.9, -5.4. HR-ESI (+)-MS: Theoretical $\text{C}_{33}\text{H}_{53}\text{NO}_7\text{Si}_2$ $[\text{M}+\text{H}]^+ = m/z$ 632.34333; Observed $[\text{M}+\text{H}]^+ = m/z$ 632.34409.



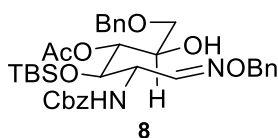
(2*R*,3*R*,4*R*,5*R*,6*S*)-5-(((benzyloxy)carbonyl)amino)-2-((benzyloxy)methyl)-4,6-bis((*tert*-butyldimethylsilyl)oxy)tetrahydro-2H-pyran-3-yl acetate (**7**): Alcohol **6** (4.73 g, 7.49 mmol) was dissolved in DCM (25 mL) and pyridine (12.6 mL), then DMAP (0.183 g, 1.49 mmol, 0.2 eq) followed by Ac_2O (1.23 mL, 1.33 g, 11.23 mmol, 1.5 eq) and stirred 24h at room temperature. TLC (Hexane-EtOAc = 4:1) indicated reaction completion. Reaction mixture was diluted with DCM, washed with water (2 x 500 mL), 0.1 M HCl (2 x 200 mL), water (2 x 500mL), dried over Na_2SO_4 , filtered and volatiles removed in vacuo. The resulting oil was purified by flash chromatography (Pet. Ether-EtOAc = 10:1) to yield **7** (5.045 g, 99% yield). $[\alpha]_D = +78^\circ$ (c 20, DCM, 27 °C); IR (film) 3355, 2930, 2857, 1749,

1717 cm^{-1} . ^1H NMR (700 MHz, CDCl_3) δ 7.39 – 7.30 (m, 10H), 5.10 – 5.03 (m, 2H), 4.91 (d, J = 7 Hz, 1H), 4.85 (t, J = 9 Hz, 1H), 4.54 (d, J = 12 Hz, 1H), 4.51 (d, J = 12 Hz, 1H), 4.21 (t, J = 9 Hz, 1H), 3.64 – 3.58 (m, 1H), 3.58 – 3.51 (m, 2H), 3.07 (m, 1H), 1.97 (s, 3H), 0.89 (s, 9H), 0.83 (s, 9H), 0.13 (s, 3H), 0.08 (s, 3H), 0.00 (s, 6H). ^{13}C NMR (176 MHz, CDCl_3) δ 170.0, 155.4, 138.1, 136.2, 128.5, 128.5, 128.3, 128.2, 127.7, 127.6, 94.7, 73.7, 73.5, 73.0, 71.5, 70.5, 66.8, 61.6, 25.6, 25.6, 21.3, 18.0, 17.9, -4.2, -4.5, -5.4 ppm.



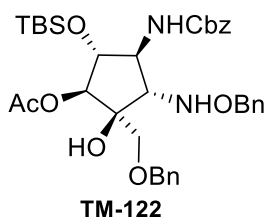
(2*R*,3*R*,4*R*,5*R*,6*S*)-5-(((benzyloxy)carbonyl)amino)-2-((benzyloxy)methyl)-4-((*tert*-butyldimethylsilyl)oxy)-6-hydroxytetrahydro-2H-pyran-3-yl acetate (**SI-2**): A solution of **7** (1 g, 1.49 mmol) in THF (5.95 mL) was cooled to 0 °C, then a solution of TBAF-THF (1.47 mL, 1.47 mmol, 0.99 eq, 1M in THF) was added slowly under argon. After 15 m stirring at this temperature, TLC (H-E = 2:1) indicated reaction completion. The mixture was diluted with TBME (200 mL) and washed with water (3 x 50mL), brine (1 x 50 mL), dried over Na_2SO_4 , filtered and volatiles removed *in vacuo*. The resulting waxy solids were purified by flash chromatography (Hexane-EtOAc = 20:10) to yield the α -diastereomer (824 mg, 99%). $[\alpha]_{\text{D}} = + 39^\circ$ (c 8, DCM, 27 °C); IR (film) 3419, 3350, 3032, 2928, 2856, 1739, 1722, 1516, 1230 cm^{-1} . ^1H NMR (700 MHz, CDCl_3) δ 7.40 – 7.29 (m, 10H), 5.24 (brs, 1H), 5.12 (d, J = 12 Hz, 1H), 5.08 (d, J = 12 Hz, 1H), 4.95 – 4.84 (m, 2H), 4.53 (m, 2H), 4.09 (m,

1H), 3.90 (m, 1H), 3.53 (m, 1H), 3.46 (m, 1H), 1.98 (s, 1H), 0.84 (s, 1H), 0.04 – 0.01 (m, 1H). ¹³C NMR (126 MHz, CDCl₃) δ 169.8, 155.8, 137.5, 136.2, 129.9, 128.5, 128.4, 128.4, 128.2, 128.1, 127.8, 92.3, 73.5, 72.7, 70.6, 69.8, 69.1, 67.1, 55.9, 25.6, 21.2, 17.8, -4.4, -4.5.



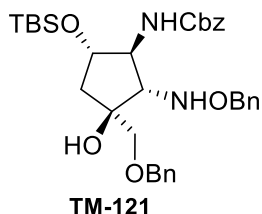
(2*R*,3*R*,4*R*,5*S*,*E*)-1-(benzyloxy)-5-(((benzyloxy)carbonyl)amino)-6-((benzyloxy)imino)-4-(((*tert*-butyldimethylsilyl)oxy)-2-hydroxyhexan-3-yl acetate (**8**): Lactol **SI-2** (2.49 g, 4.45 mmol) in DCM-Pyridine (1:1, 4.45 mL) and added BnONH₂·HCl (1.06g, 6.68 mmol, 1.5 eq) then stirred 48h when TLC (Hexane-EtOAc = 2:1) indicated reaction was essentially complete. Volatiles were removed *in vacuo*, and title compound was purified by flash chromatography (Hexane-EtOAc = 400:100) to yield 320 mg recovered starting material, a mixture of *E/Z*- diastereomers (305 mg, 10%) and pure *E*-diastereomer (1.89 g, 63%; or 83%-combined yield brsm). [α]_D = -25 ° (c 2.2, DCM, 24 °C); IR (film) 3425, 3089, 3065, 3032, 2954, 2930, 2858, 1730, 1498, 1455 cm⁻¹. ¹H NMR (400 MHz, CDCl₃) δ 7.62 (d, *J* = 2 Hz, 1H), 7.42 – 7.31 (m, 15H), 5.68 (d, *J* = 7 Hz, 1H), 5.19 (d, *J* = 12 Hz, 1H), 5.10 (d, *J* = 12 Hz, 1H), 5.08 – 4.99 (m, 3H), 4.64 – 4.46 (m, 4H), 3.95 – 3.85 (m, 1H), 3.50 (dd, *J* = 9, 3 Hz, 1H), 3.37 (dd, *J* = 9, 6 Hz, 1H), 2.47 (d, *J* = 6 Hz, 1H), 1.90 (s, 3H), 0.93 (s, 9H), 0.23 – 0.15 (m, 6H). ¹³C NMR (176 MHz, CDCl₃) δ 170.4, 155.9, 146.9, 137.5, 136.8, 136.2, 128.7, 128.5, 128.4, 128.1, 128.0, 127.9, 76.3, 73.5, 70.7, 70.4, 70.2, 67.9, 67.0, 53.3,

25.8, 20.8, 18.0, -4.7, -5.0. HR-ESI (+)-MS: Theoretical $C_{36}H_{48}N_2O_8Si$ $[M+H]^+ = m/z$ 665.32527; Observed $[M+H]^+ = m/z$ 665.32583.



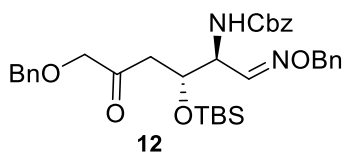
(1*S*,2*S*,3*S*,4*S*,5*R*)-3-((benzyloxy)amino)-4-(((benzyloxy)carbonyl)amino)-2-((benzyloxy)methyl)-5-((*tert*-butyldimethylsilyl)oxy)-2-hydroxycyclopentyl acetate (**TM-122**): Under argon, oxalyl chloride (0.051 mL, 76.4 mg, 0.602 mmol, 2 eq) was dissolved in dry THF (1.2 mL) and cooled to -78° C. A solution of DMSO-THF (0.4 mL, 3 M, 1.2 mmol, 4 eq) was added slowly at -78° C and allowed to stir 15m at -78 °C (bubbling had ceased). A solution of **8** in THF (2 mL, 0.301 mmol, 0.15 M) was slowly added at -78 °C and stirred at this temperature 15m, then warmed to -62 °C and stirred 15 m at this temperature. The reaction was cooled back to -78 °C and DIPEA (0.362 mL, 2.08 mmol, 5.95 eq) was added slowly. The reaction was stirred 1h at -78 °C, then warmed to -20 °C and stirred at this temperature 16 h when TLC (Hexane-EtOAc = 2:1) indicated reaction was complete. The reaction mixture was cooled to -78 °C and slowly diluted with THF (8.44 mL, [0.025M] final concentration) to avoid warming then subjected to 3 x freeze pump thaw cycles, and backfilled with argon. The resulting slurry was held at -78 °C for 15 m. A separate flask was evacuated and backfilled 3 times with argon, then dry degassed *t*-BuOH was added, cooled to 0 °C and added a solution of SmI_2 -THF (3 mL, 0.903

mmol, 0.1M) under argon and stirred 30 min at 0°C, then cooled to -78 °C. The Swern slurry was then transferred dropwise via cannula into the cold solution of Sml_2 -THF-*t*-BuOH. The reaction was incubated 12h at -78 °C then quenched by bubbling a stream of dry air at -30°C, then added a saturated solution of NaHCO_3 (6 mL), then EtOAc (30 mL) and warmed to room temperature. The mixture was stirred vigorously for 30 minutes. The organics were separated and extracted with EtOAc (3 x 30 mL), washed with 10% $\text{Na}_2\text{S}_2\text{O}_4$ (1 x 15 mL), brine (1 x 25 mL), dried over Na_2SO_4 , filtered and volatiles removed *in vacuo*. The resulting oil was purified by flash chromatography (Hexane-EtOAc = 5:1) to yield linear deoxy-**12** (TM-121, 65 mg, 35%); *N*-cyclized-**11** (14 mg, 7%) and TM-122 (32 mg, 16% yield, 2 steps). $[\alpha]_D = +12^\circ$ (c 1, DCM, 27 °C); IR (film) 3400, 2926, 1718, 1700 cm^{-1} . ^1H NMR (700 MHz, CDCl_3) δ 7.39 – 7.29 (m, 15H), 6.07 (brs, 1H), 5.14 (d, $J = 8$ Hz, 1H), 5.11 (s, 2H), 5.05 (d, $J = 9$ Hz, 1H), 4.69 (d, $J = 12$ Hz, 1H), 4.66 (d, $J = 12$ Hz, 1H), 4.53 (d, $J = 11$ Hz, 1H), 4.43 (d, $J = 11$ Hz, 1H), 4.30 (t, $J = 8$ Hz, 1H), 3.79 – 3.71 (m, 2H), 3.59 (d, $J = 10$ Hz, 1H), 3.42 (s, 1H), 3.30 (brs, 1H), 2.01 (s, 3H), 0.85 (s, 9H), 0.03 – -0.03 (m, 6H). ^{13}C NMR (176 MHz, CDCl_3) δ 170.0, 155.9, 137.5, 137.1, 136.1, 128.5, 128.3, 128.2, 128.2, 128.0, 128.0, 128.0, 127.9, 127.8, 127.7, 127.5, 126.8, 79.0, 77.4, 77.0, 76.2, 73.6, 72.2, 71.1, 66.8, 57.7, 25.4, 20.8, 17.7, -5.0. HR-ESI (+)-MS: Theoretical $\text{C}_{34}\text{H}_{46}\text{N}_2\text{O}_6\text{Si}$ $[\text{M}+\text{H}]^+ = m/z$ 665.32527; Observed $[\text{M}+\text{H}]^+ = m/z$ 665.32916

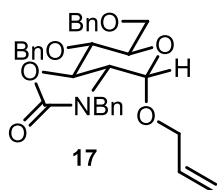


benzyl((1*S*,2*S*,3*S*,5*S*)-2-((benzyloxy)amino)-3-((benzyloxy)methyl)-5-((*tert*-butyldimethylsilyl)oxy)-3-hydroxycyclopentyl)carbamate (**TM-121**):

TM-121 was obtained using the same procedure as TM-122, except MeOH (0.018 mL, 0.45 mmol, 6 eq) was used in place of *t*-BuOH. TM-123 $[\alpha]_D = +10^\circ$ (c 1.4, DCM, 25 °C); IR (film) 3412, 3339, 3064, 3031, 2953, 2927, 2855, 1702, 1518, 1497 cm^{-1} . ^1H NMR (700 MHz, CDCl_3) δ 7.40 – 7.17 (m, 15H), 6.14 (brs, 1H), 5.14 (d, $J = 9$ Hz, 1H), 5.11 (s, 2H), 4.67 (d, $J = 11$ Hz, 1H), 4.64 (d, $J = 11$ Hz, 1H), 4.58 (d, $J = 12$ Hz, 1H), 4.53 (d, $J = 12$ Hz, 1H), 4.30 (dd, $J = 14, 7$ Hz, 1H), 3.82 (dd, $J = 14, 6$ Hz, 1H), 3.67 (d, $J = 9$ Hz, 1H), 3.51 (d, $J = 10$ Hz, 1H), 3.30 (d, $J = 5$ Hz, 1H), 3.23 (s, 1H), 2.04 (dd, $J = 13, 7$ Hz, 1H), 1.77 (dd, $J = 13, 8$ Hz, 1H), 0.87 (s, 9H), 0.04 (m, 6H). ^{13}C NMR (176 MHz, CDCl_3) δ 156.1, 137.8, 137.5, 136.4, 128.6, 128.5, 128.4, 128.2, 128.2, 127.9, 127.9, 79.2, 76.2, 75.1, 73.6, 73.5, 72.9, 66.8, 62.2, 43.7, 25.8, 18.0, -4.8. HR-ESI (+)-MS: Theoretical $\text{C}_{34}\text{H}_{46}\text{N}_2\text{O}_6\text{Si}$ $[\text{M}+\text{H}]^+ = m/z$ 607.31979; Observed $[\text{M}+\text{H}]^+ = m/z$ 607.32047.

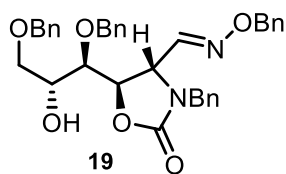


benzyl ((5*S*,6*R*,*E*)-6-(3-(benzyloxy)-2-oxopropyl)-8,8,9,9-tetramethyl-1-phenyl-2,7-dioxasila-3-aza-8-siladec-3-en-5-yl)carbamate (**12**): $[\alpha]_D = -19^\circ$ (c 2, DCM, 27 °C); IR (film): 3432, 3064, 3032, 2952, 2928, 2856, 1723, 1497 cm^{-1} . ^1H NMR (700 MHz, CDCl_3) δ 7.49 (d, $J = 3.3$ Hz, 1H), 7.38 – 7.28 (m, 15H), 5.47 (d, $J = 8$ Hz, 1H), 5.14 – 5.04 (m, 4H), 4.63 – 4.49 (m, 3H), 4.48 – 4.41 (m, 1H), 3.99 (s, 1H), 2.56 (dd, $J = 17$, 5 Hz, 1H), 2.47 (dd, $J = 17$, 7 Hz, 1H), 0.86 – 0.82 (m, 9H), 0.13 – -0.10 (m, 6H). ^{13}C NMR (176 MHz, CDCl_3) δ 206.2, 156.0, 147.4, 137.2, 137.1, 136.2, 128.6, 128.6, 128.5, 128.4, 128.3, 128.1, 128.1, 128.0, 127.9, 127.7, 127.7, 127.5, 76.4, 75.5, 73.4, 68.6, 67.2, 54.8, 42.4, 25.8, 25.7, 17.9, -4.8. HR-ESI (+)-MS: Theoretical $[\text{M}+\text{H}]^+ = m/z$ 605.30414 Observed $[\text{M}+\text{H}]^+ = m/z$ 605.30474.



(3*aR*,4*S*,6*R*,7*S*,7*aR*)-4-(allyloxy)-3-benzyl-7-(benzyloxy)-6-((benzyloxy)methyl)tetrahydro-4H-pyrano[3,4-*d*]oxazol-2(3H)-one (**17**): To a dry flask under argon, NaH (60% mineral oil suspension, 4.08 g, 84.5 mmol, 5 eq) was added, then washed with hexanes (2 x 10 mL) under argon. DMF (120 mL) was transferred to the flask containing NaH via cannula and cooled to 5°C. A solution of **16** in DMF (48 mL, 16.9 mmol, 0.35M) was transferred dropwise via cannula to the cold solution of NaH-DMF. The mixture was stirred 15 m then warmed slowly to room temperature and stirred for 4h at this temperature. Then BnBr (9.97 mL, 14.36 g, 5 eq) was added dropwise (exotherm) and stirred at ambient

temperature 4h. After reaction completion as judged by TLC, the mixture was quenched by pouring into ice water (500 mL) then extracted with EtOAc (2 x 200 mL), washed with 1M HCl (1 x 100 mL) then water (4 x 500 mL), saturated NaHCO₃ (1 x 100 mL), brine (1 x 50 mL), dried over Na₂SO₄, filtered and volatiles removed *in vacuo*. The title compound was obtained after purification by flash chromatography (Hexane-EtOAc = 2:1) to yield **17** (4.7 g, 54% yield). $[\alpha]_D = +38^\circ$ (c 0.5, DCM, 25 °C); IR (film): 3031, 2917, 2869, 1765 cm⁻¹. ¹H NMR (700 MHz, CDCl₃) δ 7.44 – 7.30 (m, 13H), 7.27 – 7.21 (m, 2H), 5.76 (ddd, $J = 16, 11, 6$ Hz, 1H), 5.26 (d, $J = 17$ Hz, 1H), 5.21 (d, $J = 11$ Hz, 2H), 4.88 (d, $J = 11$ Hz, 1H), 4.77 (d, $J = 3$ Hz, 1H), 4.70 (dd, $J = 12, 10$ Hz, 1H), 4.64 – 4.48 (m, 4H), 4.45 (s, 2H), 4.02 (dd, $J = 13, 5$ Hz, 1H), 3.94 (t, $J = 9$ Hz, 1H), 3.76 – 3.70 (m, 2H), 3.67 (dd, $J = 12, 6$ Hz, 1H), 3.64 – 3.61 (m, 1H), 3.35 (dd, $J = 12, 3$ Hz, 1H). ¹³C NMR (176 MHz, CDCl₃) δ 159.1, 137.8, 137.5, 135.3, 133.1, 128.8, 128.8, 128.7, 128.5, 128.5, 128.4, 128.4, 128.4, 128.2, 128.1, 128.0, 127.9, 127.9, 127.8, 127.8, 127.7, 118.2, 94.4, 77.4, 77.2, 77.0, 76.8, 74.9, 73.5, 73.0, 72.6, 68.9, 67.7, 61.1, 48.7.



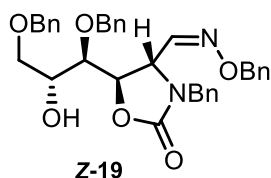
(*E*)-3-benzyl-5-((1*R*,2*R*)-1,3-bis(benzyloxy)-2-hydroxypropyl)-2-oxooxazolidine-4-carbaldehyde *O*-benzyl oxime (**19**): The crude lactol (500 mg, 1.05 mmol) from the previous step, in pyridine (5 mL) was added BnONH₃Cl (427 mg, 2.683 mmol, 2.55 eq) under

argon and stirred 8h. TLC (H-E=2:1) indicated complete consumption starting material.

Volatiles were removed *in vacuo* and purified by flash chromatography (Pet. ether-

EtOAc = 5:1) to yield 260 mg, 45% 2-steps (combined *E/Z* isomers), *E*-isomer (160 mg):

$[\alpha]_D = -35^\circ$ (c 7.5, DCM, 25 °C); IR (film) 3437, 3091, 3031, 2925, 2858, 1756, 1495, 1454 cm^{-1} ; ^1H NMR (700 MHz, CDCl_3) δ 7.43 – 7.26 (m, 12H), 7.25 – 7.20 (m, 2H), 7.16 (t, $J = 8$ Hz, 2H), 7.10 (d, $J = 7$ Hz, 2H), 7.04 (d, $J = 6$ Hz, 2H), 5.11 – 5.06 (m, 2H), 4.67 (dd, $J = 7, 2$ Hz, 1H), 4.64 (d, $J = 15$ Hz, 1H), 4.55 (d, $J = 12$ Hz, 1H), 4.53 – 4.48 (m, 2H), 4.42 (d, $J = 11$ Hz, 1H), 4.12 – 4.07 (m, 1H), 4.04 – 3.99 (m, 1H), 3.98 (t, $J = 10$ Hz, 1H), 3.71 – 3.61 (m, 2H), 3.50 (dd, $J = 8, 2$ Hz, 1H), 2.48 (d, $J = 7$ Hz, 1H). ^{13}C NMR (176 MHz, CDCl_3) δ 157.2, 146.7, 137.5, 137.2, 137.1, 135.2, 128.7, 128.6, 128.6, 128.5, 128.5, 128.4, 128.2, 128.0, 128.0, 127.9, 127.8, 127.7, 77.3, 76.5, 76.4, 74.2, 73.5, 70.3, 69.8, 56.1, 46.5.



(*Z*)-3-benzyl-5-((1*R*,2*R*)-1,3-bis(benzyloxy)-2-hydroxypropyl)-2-oxooxazolidine-4-

carbaldehyde *O*-benzyl oxime (**Z-19**): *Z*-isomer (75 mg): $[\alpha]_D = -46^\circ$ (c 2.9, DCM, 27 °C); IR

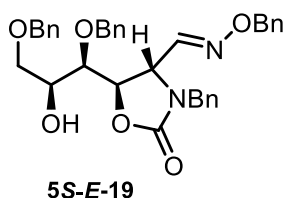
(film) 3437, 3091, 3031, 2923, 2867, 1755, 1496, 1454 cm^{-1} . ^1H NMR (700 MHz, CDCl_3) δ

7.39 – 7.24 (m, 16H), 7.22 (t, $J = 7$ Hz, 1H), 7.17 (d, $J = 7$ Hz, 2H), 7.13 (t, $J = 8$ Hz, 2H),

6.96 (d, $J = 7$ Hz, 2H), 6.71 (d, $J = 6$ Hz, 1H), 5.06 (d, $J = 12$ Hz, 1H), 5.02 (d, $J = 12$ Hz, 1H),

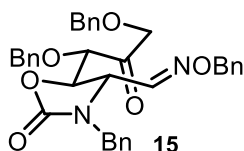
4.65 (t, $J = 6$ Hz, 1H), 4.60 (dd, $J = 6, 1$ Hz, 1H), 4.55 – 4.46 (m, 3H), 4.36 (d, $J = 12$ Hz, 1H),

4.24 (d, $J = 12$ Hz, 1H), 4.17 (d, $J = 15$ Hz, 1H), 4.01 – 3.96 (m, 1H), 3.63 (dd, $J = 10, 3$ Hz, 1H), 3.57 – 3.54 (m, 2H), 2.32 (d, $J = 7$ Hz, 1H). ^{13}C NMR (176 MHz, CDCl_3) δ 157.5, 149.4, 137.6, 137.6, 136.5, 135.2, 128.7, 128.7, 128.7, 128.6, 128.6, 128.5, 128.5, 128.5, 128.4, 128.4, 128.4, 128.2, 128.0, 128.0, 128.0, 128.0, 128.0, 127.9, 127.8, 127.7, 127.7, 127.4, 78.4, 76.5, 76.4, 74.1, 73.4, 70.4, 69.7, 52.6, 47.3.



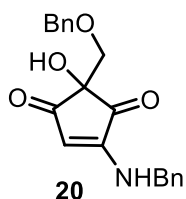
(*E*)-3-benzyl-5-((1*R*,2*S*)-1,3-bis(benzyloxy)-2-hydroxypropyl)-2-oxo oxazolidine-4-carbaldehyde *O*-benzyl oxime (**5S-E-19**): A solution of ketone-**15** in benzene (50 mg, 0.087mmol, 1.75 mL, 0.05M) was added AIBN (3.8 mg, 0.27 eq) and degassed by 3x freeze-pump-thaw cycles), backfilled with argon and heated at reflux 4h. A separate flask containing a solution of Bu_3SnH -benzene (0.750 mL, 0.092 mmol, 0.12 M, 1.07 eq) was added AIBN (2.4 mg, 0.014 mmol) and carefully degassed (3 x freeze-pump-thaw cycles and backfilled with argon) then added dropwise over 1h via syringe. After 15h, TLC indicated reaction complete. The reaction was cooled to room temperature, then diluted with CH_3CN (3 mL) and washed with hexanes (1 x 30 mL), the CH_3CN layer was separated and the volatiles were removed *in vacuo*. Flash chromatography (Hexane-EtOAc = 2:1) provided pure **5R-E-19** (30 mg, 60 % yield) and **5S E-19** (6 mg, 12 % yield); $[\alpha]_{\text{D}} = -41^\circ$ (c 0.4, DCM, 27 °C); IR (film) 3437, 3091, 3031, 2925, 2858, 1755, 1495, 1454

cm^{-1} . ^1H NMR (700 MHz, CDCl_3) δ 7.41 – 7.23 (m, 19H), 7.19 (d, J = 8 Hz, 1H), 7.17 (dd, J = 6, 3 Hz, 2H), 7.13 (d, J = 7 Hz, 2H), 4.68 – 4.61 (m, 2H), 4.56 (d, J = 11 Hz, 1H), 4.53 (dd, J = 7, 5 Hz, 1H), 4.50 (d, J = 12 Hz, 1H), 4.49 (d, J = 12 Hz, 1H), 4.10 (t, J = 7 Hz, 1H), 4.01 (d, J = 15 Hz, 1H), 3.95 – 3.91 (m, 1H), 3.58 – 3.56 (m, 1H), 3.56 – 3.53 (m, 2H), 2.21 (d, J = 6 Hz, 1H). ^{13}C NMR (176 MHz, CDCl_3) δ 174.2, 156.4, 146.7, 128.7, 128.5, 128.5, 128.2, 128.0, 77.7, 76.5, 76.3, 74.4, 73.4, 70.7, 69.1, 56.5, 46.5.



(*E*)-3-benzyl-5-((*S*)-1,3-bis(benzyloxy)-2-oxopropyl)-2-oxooxazolidine-4-carbaldehyde *O*-benzyl oxime(**15**): Aldoxime *E*-**19** (500 mg, 0.86 mmol) was dissolved in EtOAc (8.33 mL, 0.103 M) and added IBX (615.4 mg, 2.20 mmol, 2.55 eq). The resulting suspension was heated 6 h at 75 - 80 °C when TLC (Hexane-EtOAc = 2:1) indicated the reaction was complete. The reaction was cooled to room temperature, diluted with 1 mL EtOAc and the IBX & IBA-byproduct(s) were filtered off through 1 inch of silica gel topped with celite and washed with EtOAc (3 x 1 mL). The volatiles were removed *in vacuo* resulting in pure *E*-**15** as a colorless oil (490 mg, 98% yield). $[\alpha]_{\text{D}} = -53^\circ$ (c 2.5, DCM, 25 °C); IR (film) 3064, 3031, 2927, 2871, 1761, 1737, 1496, 1454, 1416 cm^{-1} . ^1H NMR (400 MHz, CDCl_3) δ 7.45 – 7.17 (m, 17H), 7.12 (d, J = 7 Hz, 2H), 7.00 – 6.94 (m, 1H), 5.10 – 5.02 (m, 2H), 4.71 (d, J = 15 Hz, 1H), 4.64 – 4.57 (m, 2H), 4.53 – 4.43 (m, 3H), 4.37 – 4.28 (m, 2H), 4.06 – 4.01 (m, 1H), 3.92 (d, J = 15 Hz, 1H), 3.88 (d, J = 2 Hz, 1H). ^{13}C NMR (101 MHz,

CDCl₃) δ 206.3, 156.4, 145.8, 136.9, 136.9, 135.5, 134.9, 128.7, 128.7, 128.6, 128.6, 128.5, 128.4, 128.3, 128.1, 128.1, 81.3, 77.2, 76.6, 76.3, 74.2, 73.5, 55.6, 46.5. HR-ESI (+)-MS: Theoretical C₂₀H₁₉NO₄ [M+H]⁺ = m/z 338.13868; Observed [M+H]⁺ = m/z 338.13890.



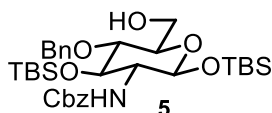
(±)-4-(benzylamino)-2-((benzyloxy)methyl)-2-hydroxycyclopent-4-ene-1,3-dione (**20**): A dry flask containing Mg turnings (2.4 mg, 0.1 mmol, 2 eq) was subjected to 3 x evacuate/backfill cycles with argon and stirred vigorously for 1.5 h to activate. Then anhydrous NiCl₂ (1.3 mg, 0.01 mmol, 0.2 eq) was added under argon followed by **15** as a THF solution (0.250 mL, 0.050 mmol, 0.2M) and TMSCl (0.038 mL, 32 mg, 0.3 mmol, 6 eq). The mixture was stirred 4h at room temperature then heated at reflux 12h. TLC (Hexane-EtOAc = 3:2) indicated reaction complete. The reaction was cooled to room temperature and added 1M HCl (1 mL) and extracted with EtOAc (3 x 5 mL), organics washed with saturated aqueous NaHCO₃ (2 x 2 mL), washed with brine and dried over Na₂SO₄ filtered and volatiles removed *in vacuo*. The title compound was obtained pure after flash chromatography (Hexane-EtOAc = 2:1) to provide **20** (5.5 mg, 32% yield). [α]_D = 0° (c 1.0, DCM, 25 °C); IR (film) 3366, 3306, 2919, 2851, 1751, 1682, 1608 cm⁻¹. ¹H NMR (700 MHz, CDCl₃) δ 7.42 – 7.21 (m, 10 H), 6.00 (s, 1H), 5.85 (brs, 1 H), 4.55 – 4.48

(m, 1H), 4.47 – 4.40 (m, 1H), 3.75 (d, $J = 9$ Hz, 1 H), 3.73 (d, $J = 9$ Hz, 1 H), 2.92 (brs, 1H).

^{13}C NMR (176 MHz, CDCl_3) δ 197.7, 196.3, 158.2, 137.2, 135.1, 129.2, 128.5, 128.4,

127.8, 127.6, 127.5, 110.5, 73.8, 73.7, 71.0, 48.2. HR-ESI (+)-MS: Theoretical $\text{C}_{20}\text{H}_{19}\text{NO}_4$

$[\text{M}+\text{H}]^+ = m/z$ 338.13868; Observed $[\text{M}+\text{H}]^+ = m/z$ 338.13890.



Synthesis of benzyl ((2*S*,3*R*,4*R*,5*R*,6*R*)-5-(benzyloxy)-2,4-bis((tert-butyldimethylsilyl)oxy)-

6-(hydroxymethyl)tetrahydro-2*H*-pyran-3-yl)carbamate (**5**): Benzylidene **4** (20 g, 31.78

mmol) was dissolved in dry DCM (252.7 mL, 0.125 M) under argon and cooled to -78°C .

Et_3SiH (15.2 mL, 11.1 g, 95.3 mmol) was then added under argon followed by a dropwise

addition of a solution of 1M Bu_2BOTf –DCM (65.1 mL, 65.1 mmol, 1M, 2.05 eq). The re-

action was stirred 3.5 h at -78°C when TLC (Hexane-EtOAc = 4:1) indicated reaction

complete. The reaction was quenched at -78°C with Et_3N (61 mL, 45 g, 444 mmol, 14

eq), then dropwise added MeOH (61 mL). The reaction mixture was allowed to warm

slowly to -20°C over 12 h, then warmed to room temperature and filtered through a 2 x

2 inch pad of SiO_2 and the volatiles were removed *in vacuo*. MeOH (3 x 100mL) was

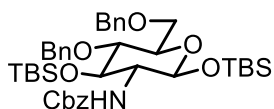
added and evaporated by rotovapor to remove any boron adducts. The residue was

chromatographed over SiO_2 , (Hexane- Et_2O = 100:0; 5:1, 2:1) to provide pure **5** (15.7 g,

87% yield). $[\alpha]_D = -4^\circ$ (c 8.7, DMSO, 24°C). IR (film): cm^{-1} 3349, 3033, 2954, 2929, 2884,

2856, 1709; ^1H NMR (400 MHz, CDCl_3) δ 7.40 – 7.27 (m, 10H), 5.05 (s, 2H), 4.90 (brd, $J =$

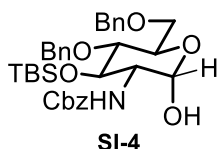
8 Hz, 1H), 4.81 (d, $J = 12$ Hz, 1H), 4.74 (brd, $J = 9$ Hz, 1H), 4.61 (d, $J = 12$ Hz, 1H), 3.95 (m, 1H), 3.79 (d, $J = 12$ Hz, 1H), 3.63 (brd, $J = 11$ Hz, 1H), 3.44 – 3.36 (m, 2H), 3.26 – 3.13 (m, 1H), 0.89 – 0.83 (m, 18H), 0.11 – -0.03 (m, 12H). ^{13}C NMR (101 MHz, CDCl_3) δ 155.5, 138.1, 136.2, 128.4, 128.4, 128.3, 128.1, 127.6, 127.3, 95.4, 79.3, 75.0, 74.5, 73.9, 66.7, 62.2, 61.2, 25.8, 25.5, 18.0, 17.8, -4.0, -4.1, -4.5, -5.3. HR-ESI (+) MS: Theoretical $\text{C}_{33}\text{H}_{54}\text{NO}_7\text{Si}_2$ $[\text{M}+\text{H}]^+ = m/z$ 632.3433; Observed $[\text{M}+\text{H}]^+ = m/z$ 632.33078.



6

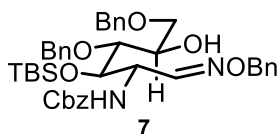
Synthesis of benzyl ((2*S*,3*R*,4*R*,5*R*,6*R*)-5-(benzyloxy)-6-((benzyloxy)methyl)-2,4-bis((*tert*-butyldimethylsilyl)oxy)tetrahydro-2*H*-pyran-3-yl)carbamate (**6**): Sodium hydride (4.06 g, 0.102 mol, 4.75 eq, 60% in min. oil) in a dry 3-neck flask under argon equipped with a thermometer, was washed with dry hexanes (1 x 30 mL) to remove the mineral oil. Anhydrous DMF (43 mL) was added and the mixture was cooled to -45 °C. A separate flask containing **5** (13.5 g, 0.021 mol) under argon was dissolved in THF (65 mL) then *slowly* transferred into NaH-DMF at -45 °C such that the internal temperature remained stable between -45 °C and -40 °C. Additional anhydrous THF (20 mL) was used to transfer the residual **5** into the NaH-DMF. BnBr was then added slowly under argon at this temperature (no exotherm was observed). Reaction was warmed to -25 °C and mild gas evolution was apparent. The reaction was incubated at -25 °C to -20 °C for 4h and quenched

with a saturated solution of NaHCO_3 (100 mL) at $-20\text{ }^\circ\text{C}$ and warmed to room temperature with vigorous stirring. The mixture was extracted with EtOAc (2 x 300 mL), the organic layers combined and washed with water (5 x 500 mL), brine (1 x 75 mL), dried over Na_2SO_4 , filtered and the volatiles removed *in vacuo*. The residue was pure by flash chromatography (H-E=100:0; 20:1) to yield pure **6** (8.5 g, 55% yield); $[\alpha]_D = +9^\circ$ (c 1.65, DMSO, $24\text{ }^\circ\text{C}$). IR (film): 3349, 3065, 3032, 2952, 2928, 2887, 2856, 1709 cm^{-1} ; ^1H NMR (500 MHz, CDCl_3) δ 7.40 – 7.23 (m, 15H), 5.07 (brs, 2H), 4.88 (brd, $J = 7\text{ Hz}$, 1H), 4.83 – 4.74 (m, 2H), 4.63 (d, $J = 12\text{ Hz}$, 1H), 4.59 (d, $J = 12\text{ Hz}$, 1H), 4.56 (d, $J = 12\text{ Hz}$, 1H), 3.95 (m, 1H), 3.69 (brs, 2H), 3.54 – 3.47 (m, 2H), 3.32 – 3.19 (m, 1H), 0.93 – 0.83 (m, 18H), 0.18 – -0.04 (m, 12H). ^{13}C NMR (126 MHz, CDCl_3) δ 155.5, 138.3, 136.4, 128.4, 128.3, 128.3, 128.2, 128.1, 127.5, 127.4, 127.3, 127.2, 95.4, 79.4, 74.7, 74.2, 74.1, 73.3, 69.1, 66.6, 61.0, 25.8, 25.62, 18.0, 17.9, -4.0, -4.1, -4.6, -5.3; HR-ESI (+)-MS: Theoretical $\text{C}_{40}\text{H}_{60}\text{NO}_7\text{Si}_2^+$ $[\text{M}+\text{H}]^+ = m/z\ 722.39028$; Observed $[\text{M}+\text{H}]^+ = m/z\ 722.39292$. The pure over-alkylated side product **SI-3** was also obtained 6 g, 34% yield. **SI-3** HR-ESI (+)-MS: Theoretical $\text{C}_{47}\text{H}_{66}\text{NO}_7\text{Si}_2^+$ $[\text{M}+\text{H}]^+ = m/z\ 812.43723$; Observed $[\text{M}+\text{H}]^+ = m/z\ 812.43836$.



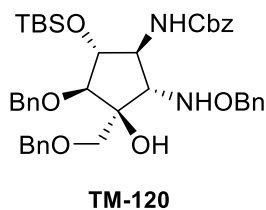
Synthesis of benzyl ((3*R*,4*R*,5*R*,6*R*)-5-(benzyloxy)-6-((benzyloxy)methyl)-4-((tert-butylidimethylsilyl)oxy)-2-hydroxytetrahydro-2H-pyran-3-yl)carbamate (**SI-4**): Under ar-

gon, **6** (7 g, 9.7 mmol) was dissolved in dry THF (39 mL) and cooled to 0 °C, stirred 20 m at this temperature, then a 1M solution of TBAF-THF (9.6 mL, 9.6 mmol, 0.98 eq) was slowly added and the reaction stirred 15 m at 0 °C. TLC (Hexane-EtOAc = 2 : 1) indicated reaction complete. The reaction was diluted with Et₂O (300 mL), then washed with water (3 x 300 mL), dried over Na₂SO₄, and solvents removed *in vacuo*. Crude (5.3 g) can be carried into the next reaction without further purification, or pure lactol can be obtained by flash chromatography (Hexane-EtOAc = 4:1, 2:1). IR (film): 3410, 3035, 2929, 2859, 1698 cm⁻¹; ¹H NMR (500 MHz, CDCl₃) δ 7.43 – 7.15 (m, 16H), 5.23 (brs, 1H), 5.14 (d, *J* = 12 Hz, 1H), 5.09 (d, *J* = 12 Hz, 1H), 4.94 (brd, *J* = 10 Hz, 1H), 4.82 (d, *J* = 12 Hz, 1H), 4.57 – 4.48 (m, 3H), 4.08 – 4.00 (m, 1H), 3.92 – 3.86 (m, 2H), 3.67 – 3.60 (m, 2H), 3.48 – 3.42 (m, 1H), 3.03 (brs, 1H), 0.92 – 0.83 (m, 9H), 0.10 – -0.02 (m, 6H). ¹³C NMR (176 MHz, CDCl₃) δ 155.8, 138.0, 137.8, 136.2, 128.5, 128.4, 128.3, 128.3, 128.2, 127.8, 127.7, 127.5, 127.4, 92.5, 79.1, 74.7, 73.4, 72.6, 71.2, 69.0, 67.0, 55.8, 25.8, 17.8, -4.0, -4.2; ESI (+)-MS: Theoretical C₃₄H₄₆NO₇SiNa⁺ [M+Na]⁺ = *m/z* 630.28575; Observed [M+H]⁺ = *m/z* 630.28560.



Synthesis of benzyl ((5*S*,6*R*,*E*)-6-((1*R*,2*R*)-1,3-bis(benzyloxy)-2-hydroxypropyl)-8,8,9,9-tetramethyl-1-phenyl-2,7-dioxa-3-aza-8-siladec-3-en-5-yl)carbamate (**7**): A suspension of

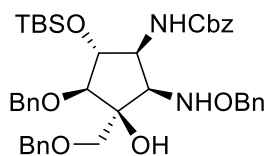
BnONH₃Cl (2.77 g, 17.5 mmol, 2.0 eq) in pyridine (50 mL) was added lactol **SI-4** (5.3 g, 8.73 mmol), then stirred at room temperature 48 h. The reaction was diluted with Et₂O (300 mL), washed with 0.1M HCl (2 x 350 mL), water (3 x 350 mL), saturated NaHCO₃ (50 mL), water (1 x 100 mL), brine (50 mL) and dried over Na₂SO₄, filtered and volatiles removed *in vacuo*. The title compound was obtained pure after flash chromatography (Hexane-EtOAc = 100:0, 100:10, 80:10) as a mixture of *E/Z*-isomers (ratio 7:3) **7** (4 g, 64% yield). $[\alpha]_D = +1^\circ$ (c 10, DMSO, 24 °C); IR (film): 3434, 3065, 3032, 2953, 2929, 2884, 2857, 1725 cm⁻¹. ¹H NMR (500 MHz, CDCl₃) δ 7.61 (d, *J* = 3 Hz, 1H), 7.45 – 7.12 (m, 20H), 5.66 (d, *J* = 7 Hz, 1H), 5.21 – 5.05 (m, 3H), 5.02 (d, *J* = 12 Hz, 1H), 4.94 (d, *J* = 12 Hz, 1H), 4.67 – 4.61 (m, 1H), 4.60 – 4.36 (m, 5H), 4.32 (brs, 1H), 3.98 – 3.87 (m, 1H), 3.69 – 3.53 (m, 3H), 2.66 (brs, 1H), 0.92 – 0.79 (m, 9H), 0.35 – -0.41 (m, 6H). ¹³C NMR (126 MHz, CDCl₃) δ 156.0, 152.8, 148.5, 138.2, 137.9, 137.4, 137.0, 136.4, 136.3, 128.5, 128.5, 128.4, 128.4, 128.3, 128.2, 128.2, 128.0, 127.9, 127.9, 127.8, 127.7, 127.7, 127.6, 127.5, 127.4, 79.2, 77.7, 73.4, 73.3, 72.9, 72.6, 71.4, 70.9, 70.5, 67.0, 66.9, 53.1, 49.9, 25.9, 18.0, -4.6. HR-ESI (+)-MS: Theoretical C₄₁H₅₃N₂O₇Si⁺ [M+H]⁺ = *m/z* 713.36165 Observed [M+H]⁺ = *m/z* 713.36285.



Synthesis of benzyl ((1*S*,2*S*,3*S*,4*S*,5*R*)-4-(benzyloxy)-2-((benzyloxy)amino)-3-

((benzyloxy)methyl)-5-((tert-butyldimethylsilyl)oxy)-3-hydroxycyclopentyl)carbamate (TM-120): Oxalyl chloride (0.241 mL, 0.356 g, 2.8 mmol, 2 eq) was added to a flame dried round bottom flask under argon, then THF (5.4 mL) was added and cooled to -78 °C then stirred 15 min at this temperature. A solution of DMSO (0.40 mL, 5.6 mmol, 4 eq) in THF (2.4 mL) was slowly added under argon at -78 °C, stirred 15 min at this temperature, then the alcohol **7** (1 g, 1.4 mmol) in THF (7 mL, 0.2M) was slowly added and stirred 30 min before warming to -60 °C and stirring at this temperature for another 30 min. The reaction was added DIPEA (1.4 mL, 8 mmol, 5.7 eq). The reaction was warmed to -35 °C and stirred 1 h at this temperature. Additional DIPEA (1.4 mL, 8 mmol, 5.7 eq) added and reaction stirred at -20 °C for 45 h. TLC (Hexane-EtOAc = 3:1) indicated reaction completion. The mixture was diluted with THF (38 mL, 0.025 M) and was then degassed thoroughly via 3- freeze-pump-thaw cycles and stirred at -78 °C under argon. To a separate oven dried flask was added *t*-BuOH (0.671 mL, 7.018 mmol, 5 eq) and sparged with argon for 2 min then added to a flask containing freshly prepared SmI_2 -THF (0.1M, 49.1 mL, 4.91 mmol, 3.5 eq) at 0 °C stirred 15 min at this temperature, then cooled to -78 °C. The Swern suspension was cannula transferred slowly into the SmI_2 -*t*-BuOH –THF solution at -78 °C warmed slowly to -20 °C over 12 h. TLC (Hexane-EtOAc – 3:1) indicated reaction complete (the reaction remained dark blue-green). The reaction was quenched at -50 °C by passing dry air into the reaction mixture and the color changed from dark blue-green to yellow. The reaction stirred 20 min, then warmed to -20 °C and added a 1:1 ratio of saturated solution of Rochelle's salt- NaHCO_3 (pH = 8.5; 57 mL, 1:1, *40 mL/mmol sub-

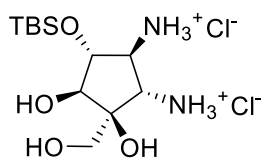
strate) and warmed to room temperature. The organics were separated and the aqueous was extracted with Et₂O (2 x 150mL), until TLC indicated no organic products remained. Organics were combined and washed with 10% Na₂S₂O₃ (1 x 100 mL) then brine (20 mL), dried (Na₂SO₄), filtered, and volatiles removed *in vacuo*. The residue was purified by flash chromatography (Hexane-EtOAc = 100:0; 50:10, 40:10) to provide TM-120 (400 mg); [α]_D = -7° (c 1, DMSO, 24 °C); IR (film) 3328, 3065, 3031, 2927, 2855, 1703 cm⁻¹; ¹H NMR (500 MHz, CDCl₃) δ 7.43 – 7.19 (m, 20H), 6.21 (brs, 1H), 5.12 (m, 2H), 4.94 (d, *J* = 9 Hz, 2H), 4.72 (d, *J* = 12 Hz, 1H), 4.71 (d, *J* = 11 Hz, 1H), 4.65 (d, *J* = 12 Hz, 1H), 4.56 (d, *J* = 11 Hz, 1H), 4.53 (d, *J* = 12 Hz, 1H), 4.41 (d, *J* = 12 Hz, 1H), 4.09 (t, *J* = 7 Hz, 1H), 3.86 (dd, *J* = 16, 7 Hz, 1H), 3.76 (d, *J* = 7 Hz, 1H), 3.56 (dd, *J* = 10 Hz, 1H), 3.44 (d, *J* = 10 Hz, 1H), 3.26 (d, *J* = 7 Hz, 1H), 3.13 (s, 1H), 0.91 (s, 9H), 0.09 (s, 3H), 0.07 (s, 3H). ¹³C NMR (126 MHz, CDCl₃) δ 155.9, 137.7, 137.7, 137.6, 136.4, 128.6, 128.4, 128.4, 128.4, 128.3, 128.2, 128.1, 128.1, 128.0, 127.9, 127.8, 127.7, 127.1, 85.0, 79.7, 76.3, 74.1, 73.7, 72.3, 71.6, 66.8, 57.3, 25.7, 17.9, -4.5, -4.6. HR-ESI (+)-MS: Theoretical C₄₁H₅₃N₂O₇Si⁺ [M+H]⁺ = *m/z* 713.36165 Observed [M+H]⁺ = *m/z* 713.36215.



TM-119

TM-119 (350 mg) [α]_D = -6° (c 1, DMSO, 24 °C); IR (film) 3414, 3089, 3064, 3031, 2952, 2928, 2884, 2856, 1726 cm⁻¹; ¹H NMR (500 MHz, CDCl₃) δ 7.42 – 7.17 (m, 20H), 5.98

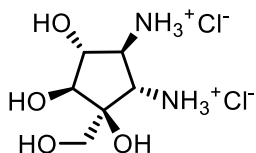
(brs, 1H), 5.26 (d, $J = 10$ Hz, 1H), 5.08 (dd, $J = 12$ Hz, 1H), 5.02 (dd, $J = 12$ Hz, 1H), 4.77 – 4.56 (m, 4H), 4.50 (d, $J = 11$ Hz, 1H), 4.47 (d, $J = 11$ Hz, 1H), 4.26 (td, $J = 10, 5$ Hz, 1H), 3.98 (dd, $J = 7, 5$ Hz, 1H), 3.80 – 3.72 (m, 2H), 3.70 (d, $J = 9$ Hz, 1H), 3.59 (d, $J = 9$ Hz, 1H), 2.85 – 2.58 (m, 1H), 0.87 (s, 9H), 0.22 – -0.24 (m, 6H). ^{13}C NMR (176 MHz, CDCl_3) δ 155.8, 138.4, 136.7, 128.7, 128.4, 128.3, 128.3, 128.3, 128.2, 128.1, 128.0, 127.9, 127.6, 127.5, 88.8, 81.6, 80.9, 77.2, 77.0, 76.8, 75.9, 74.1, 73.0, 69.3, 66.4, 65.8, 56.3, 25.7, 17.9, -4.7, -4.9. HR-ESI (+)-MS: Theoretical $\text{C}_{41}\text{H}_{53}\text{N}_2\text{O}_7\text{Si}^+$ $[\text{M}+\text{H}]^+ = m/z$ 713.36165; Observed $[\text{M}+\text{H}]^+ = 713.36201$.



TM-117

Synthesis of (1S,2S,3R,4S,5S)-4,5-diamino-3-((tert-butyldimethylsilyl)oxy)-1-(hydroxymethyl)cyclopentane-1,2-diol - dihydrochloride salt (TM-117): A solution of **8** (8 mg, 0.0112 mmol) in EtOH (0.200 mL, 0.056 M) was cooled in an ice-bath and stirred 10 min. Concentrated HCl (0.005 mL, 0.058 mmol, 5.2 eq) was added followed by 10 % Pd/C (8 mg) then 10% $\text{Pd}(\text{OH})_2/\text{C}$ (8 mg). The flask was evacuated and back-filled 2x with H_2 gas from a balloon (double) and stirred 3h at 0°C. Consumption of starting material was monitored by TLC (Hexane-EtOAc=3:2) and ESI(+) MS. Filtered through celite (2 cm x 0.5 cm) and volatiles were removed *in vacuo* to provide TM-117 (4.05 mg 99%). $[\alpha]_{\text{D}} =$

+26° (c 0.1, DMSO, 24 °C); IR (film) 3420, 3000, 2910, 1020 cm^{-1} ; ^1H NMR (500 MHz, D_2O - CD_3OD = 5:1) δ 4.16 (t, J = 7 Hz, 1H), 3.75 (d, J = 7 Hz, 1H), 3.65 (s, 2H), 3.61 (d, J = 8 Hz, 1H), 3.48 (t, J = 8 Hz, 1H), 0.80 (s, 9H), 0.08 (s, 3H), 0.07 (s, 3H). ^{13}C NMR (126 MHz, D_2O - CD_3OD = 5:1) δ 77.2, 76.2, 74.9, 61.9, 58.4, 56.5, 24.9, 17.1, -5.1, -5.7. HR-ESI-MS (+): Theoretical $\text{C}_{12}\text{H}_{29}\text{N}_2\text{O}_4\text{Si}$ $[\text{M}+\text{H}]^+ = m/z$ 293.18911; Observed $[\text{M}+\text{H}]^+ = m/z$ 293.18958.



TM118

Synthesis of (1*S*, 2*S*, 3*R*, 4*S*, 5*S*)-4,5-diamino-1-(hydroxymethyl)cyclopentane-1,2,3-triol (**TM-118**): A dry flask containing TM-117 (4.07 mg, 0.0112 mmol) was dissolved in MeOH (0.100 mL) under argon, cooled to 0 °C then stirred 10 min under argon. Concentrated HCl (0.035 mL, 0.407 mmol, 36 eq) was added at 0 °C and warmed to RT. Starting material was completely consumed as monitored by ESI(+) MS (48h). Volatiles were removed *in vacuo* at 0 °C to provide TM-118 as the dihydrochloride salt (2.77 mg, 99%). $[\alpha]_{\text{D}} = +53^\circ$ (c 0.1, DMSO, 24 °C); IR (film) 3424, 3000, 2915, 1023 cm^{-1} ; ^1H NMR (500 MHz, D_2O) δ 4.15 (t, J = 9 Hz, 1H), 3.86 (d, J = 9 Hz, 1H), 3.73 (d, J = 12 Hz, 1H), 3.68 (d, J = 8 Hz, 1H), 3.67 (d, J = 12 Hz, 1H), 3.50 (t, J = 8 Hz, 1H). ^{13}C NMR (126 MHz, D_2O) δ 75.9, 74.9, 73.8, 61.8, 58.3, 55.4. HR-ESI (+)-MS: Theoretical $\text{C}_6\text{H}_{14}\text{N}_2\text{O}_4$: $[\text{M}+\text{H}]^+ = m/z$ 179.10263; Observed $[\text{M}+\text{H}]^+ = m/z$ 179.10250.

Cell Culture

A375 (CRL-1619) melanoma cells were obtained from ATCC. Cells were monolayer cultured in DMEM (Invitrogen) supplemented with 10% FBS (Atlanta Biologicals) and 1% penicillin/ streptomycin (Cellgro). Cells were maintained in 75 cm² flasks (Greiner Bio-One) in a humidified atmosphere with 5% CO₂ at 37 °C. Experiments were performed in white, opaque 96 well plates (Greiner Bio-One) and incubated under the same conditions. Cells did not exceed passage number 30.

Dose Response Curves

A375 melanoma cells (7000 cell/well in 200 µL culture medium in a 96-well plate) were treated with pactamycin analogs at different doses (10, 5, 1, 0.5, 0.1, 0.05, 0.01, and 0.001 µM) in triplicate for 48h. Percent viability relative to DMSO vehicle control was quantified using the CellTiter-Glo® 2.0 Assay (Promega) according to the manufacturer's protocol. Data were fit to a 4-parameter variable slope IC₅₀ curve using GraphPad Prism 5.0 software.

Figure 4.14. ^1H NMR data for TM-118 (D_2O).

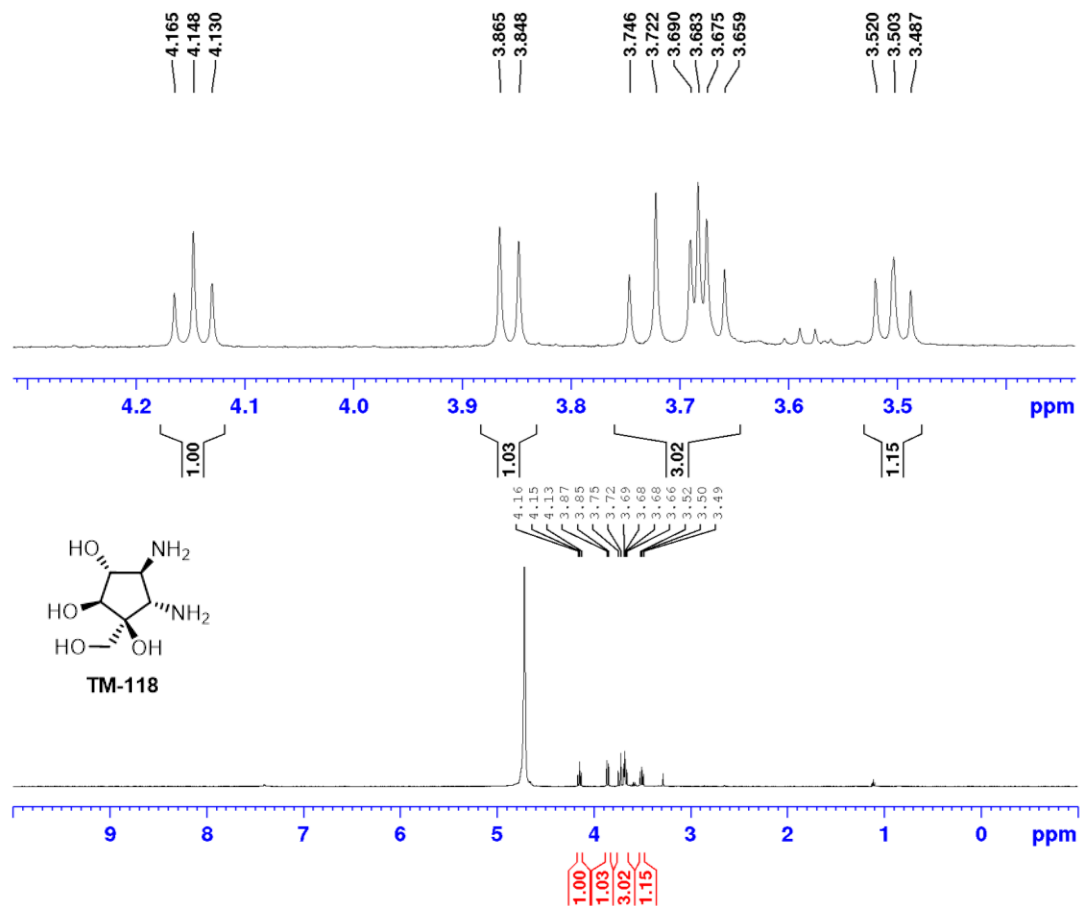
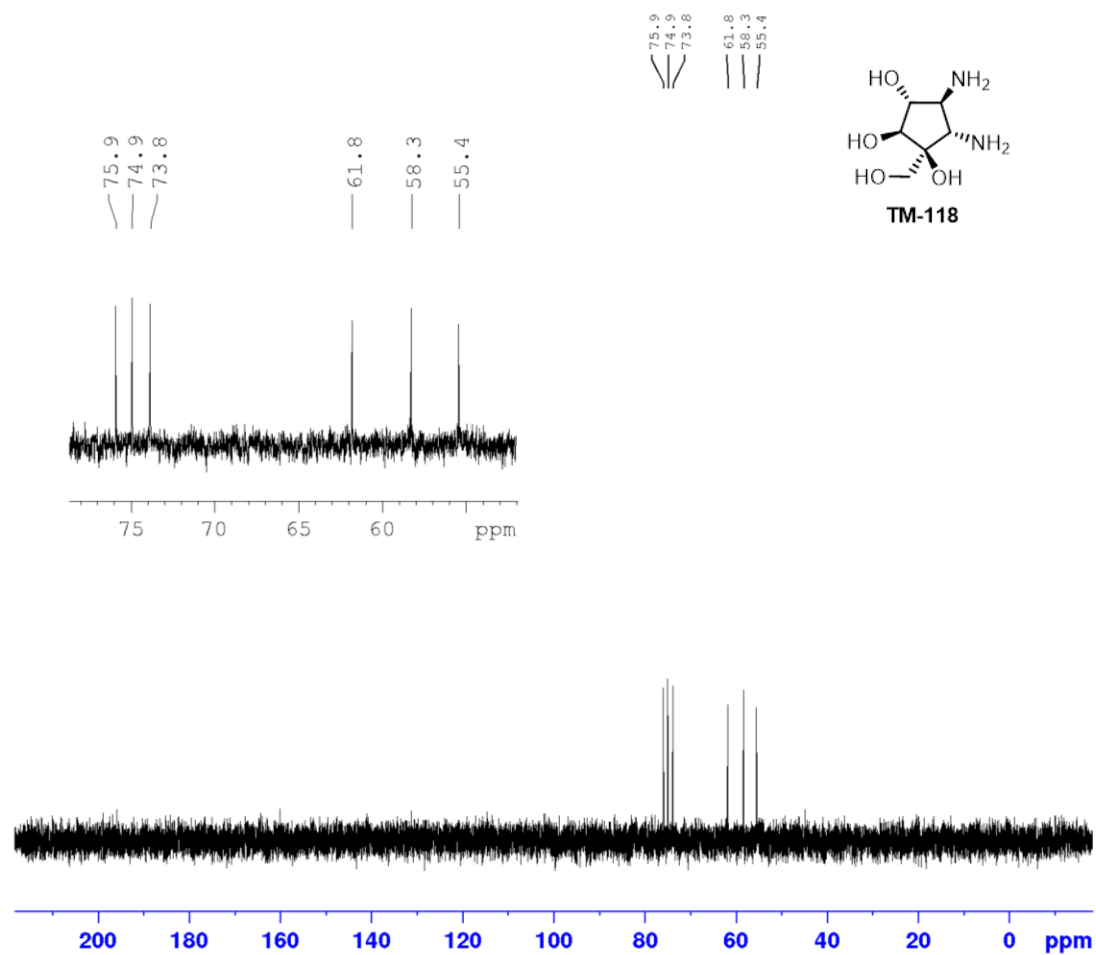


Figure 4.15. ^{13}C NMR of TM-118 (D_2O)

For accompanying NMR data See Appendix C (page 242)

References:

1. Newman, D. J., Cragg, G. M. *J. Nat. Prod.* **2016**, 79, 629.
2. Bhuyan, B. K. *Appl. Microbiol.* **1962**, 10, 302.
3. White, F. R. *Cancer Chemother. Rep.* **1962**, 24, 75.
4. Taber, R.; Rekosh, D.; Baltimore, D. *J. Virol.* 1971, 8, 395.
5. Ootoguro, K.; Iwatsuki, M.; Ishiyama, A.; Namatame, M.; Nishihara-Tukashima, A.; Shibahara, S.; Kondo, S.; Yamada, H.; Omura, S. *J. Antibiot. (Tokyo)* **2010**, 63, 381.
6. Mahmud, T., Flatt, P. M., Wu, X. *J. Nat. Prod.* **2007**, 70, 1384.
7. Lu, W., Roongsawang, N., Mahmud, T. *Chemistry & Biology* **2011**, 18, 425.
8. Almabruk, K. H., Lu, W., Li, Y., Abugreen, M., Kelly, J. X., Mahmud, T. *Org. Lett.* **2013**, 15, 1678.
9. Abugrain, M.E.; Lu, W.; Li, Y.; Serrill, J. D.; Brumsted, C. J.; Osborn, A. R.; Alani, A.; Ishmael, J. E.; Kelly, J. X.; Mahmud, T. *ChemBioChem* **2016**, 17, 1585.
10. Abugrain, M.E.; Brumsted, C.J.; Osborn, A. R.; Philmus, B.; Mahmud, T. *ACS Chem. Biol.* **2017**, 12, 362.
11. S. Hanessian, R. R. Vakiti, S. Dorich, S. Banerjee, F. Lecomte, J. R. DelValle, J. Zhang, B. Deschênes-Simard, *Angew. Chem. Int. Ed.* **2011**, 50, 3497.
12. Hanessian, S. Vakiti, R. R., Dorich, S., Banerjee, S. Deschênes-Simard, B. *J. Org. Chem.* **2012**, 77, 9458.
13. Malinowski, J. T., Sharpe, R. J., Johnson, J. S. *Science* **2013**, 340, 180
14. Sharpe, R. J., Malinowski, J. T., Johnson, J. S. *J. Am. Chem. Soc.* **2013**, 135, 17990.
- Synthesis studies towards pactamycin (15-21):*
15. Tsujimoto, T., Nishikawa, T., Urabe, D., Isobe, M. *Synlett* **2005**, 2005, 433.
16. Knapp, S., Yu, Y. *Org. Lett.* **2007**, 9, 1359.
17. Haussener, T. J., Looper, R. E. *Org. Lett.* **2012**, 14, 3632.
18. Matsumoto, N., Tsujimoto, T., Nakazaki, A. Isobe, M. Nishikawa, T. *RSC Adv.* **2012**, 2, 9448.
19. Malinowski, J. T., McCarver, S. J., Johnson, J. S. *Org. Lett.* **2012**, 14, 2878.
20. Yamaguchi, M., Hayashi, M. Hamada, Y. Nemoto, T. *Org. Lett.* **2016**, 18, 2347.
21. Gerstner, N. C., Adams, C. S., Grigg, R. D., Tretbar, M., Rigoli, J. W. Schomaker, J. M. *Org. Lett.* **2016**, 18, 284.
22. Sharpe, R. J.; Malinowski, J. T.; Sorana, F.; Luft, J. C.; Bowerman, C. J.; DeSimone, J. M.; Johnson, J. S., *Bioorganic & Medicinal Chemistry* **2015**, 23, 1849.
23. Hanessian, S., Vakiti, R. R., Chattopadhyay, A. K., Dorich, S., Lavallée, C. *Bioorganic & Medicinal Chemistry* **2013**, 21, 1775.
- Reviews on the Synthesis of Aminocyclopentitols (references 24-27):*
24. Delgado, A. *Eur. J. Org. Chem.* **2008**, 2008, 3893.
25. Ferrier, R. J.; S. Middleton, S. *Chem. Rev.* **1993**, 93, 2779.

-
26. Bereubar, A.; Grandjean, C.; Siriwardena, A. *Chem. Rev.* **1999**, 99, 779
 27. Arjona, O.; Gómez, A. M.; López, J. C.; Plumet, J. *Chem. Rev.* **2007**, 107, 1919.
 28. Liebman, J.; Rappoport Z. *The Chemistry of Hydroxylamines, Oximes and Hydroxamic acids*. John Wiley and Sons, Ltd., West Sussex PO19 8SQ, England, **2008**, part I.
 29. Corey, E. J.; Pyne, S. G. *Tetrahedron Lett.* **1983**, 24, 2821.
 30. Shono, T.; Kise, N.; Fujimoto, T. *Tetrahedron Lett.* **1991**, 32, 525.
 31. Naito, T.; Tajiri, K.; Harimoto, T.; Ninomiya, I.; Kiguchi, T. *Tetrahedron Lett.* **1994**, 35, 2205.
 32. Chiara, J. L.; Marco-Contelles, J.; Khair, N.; Gallego, P.; Destabel, C.; Bernabé, M. J. *Org. Chem.* **1995**, 60, 6010.
 33. Marco-Contelles, J.; Gallego, P.; Rodríguez-Fernández, M.; Khair, N.; Destabel, C.; Bernabé, M.; Martínez-Grau, A.; Chiara, J. L. *J. Org. Chem.* **1997**, 62, 7397.
 34. Storch de Gracia, I.; Dietrich, H.; Bobo, S.; Chiara, J. L. *J. Org. Chem.* **1998**, 63, 5883.
 35. Garcia, J., Chiara, J. L., *Synlett.* **2005**, 17, 2607.
 36. Hoffmann, R.W., *Chem. Rev.* **1989**, 89, 1841-1860.
 37. Boiron, A.; Zillig, P.; Faber, D.; Giese B. *J. Org. Chem.* **1998**, 63, 5877-5882
 38. Ohlin, M.; Johnsson, R.; Ellervik, U. *Carbohydrate Research* **2011**, 346, 12, 1358.
 39. Greene's protective groups in organic synthesis. **2014**. John Wiley & Sons, 5th ed. Wuts, P.G.M.
 40. Molander, G. A., Hahn, G., *J. Org. Chem.* **1986**, 51, 11.
 41. Procter, D.J.; Flowers, R.A. II; Skrydstrup, T.; *Organic Synthesis Using Samarium Diodide, A Practical Guide.* **2010**, The Royal Society of Chemistry, Cambridge, UK.
 42. Hutton, T. K.; Muir, K. W.; Procter, D. J. *Org. Lett.* **2003**, 5, 4811-4814.
 43. Suzuki, K.; Tamiya, M. *Comprehensive Organic Synthesis: Pinacol Coupling Reactions*. Elsevier Science. **2014**, 580-620.
 44. Gansauer, A.; Bluhm, H. *Chem. Rev.* **2000**, 100, 2771-2788.
 45. Shi, L.; Fan, C.-A.; Tu, Y.-Q.; Wang, M.; Zhang, F.-M. *Tetrahedron* **2004**, 60, 2851.
 46. Mancuso, A. J.; Swern, D. *Synthesis* **1981**, 165.
 47. Van Hijfte, L.; Little, R. D.; Petersen, J. L.; Moeller, K. D. *J. Org. Chem.* **1987**, 52, 4647.
 48. Lautens, M.; Lough, A.; Tam, W. *Acta Cryst.* **1995**, C51, 1944-1946
 49. Lu, Y.; Krische, M. J. *Org. Lett.* **2009**, 11, 3108.
 50. Chiara, J. L.; García, Á.; Cristóbal-Lumbroso, G. *J. Org. Chem.* **2005**, 70, 4142.
 51. Bobo, S.; Gracia, I. S. de; Chiara, J. L. *Synlett* **1999**, 10, 1551-1554.
 52. Matsuda, F.; Kawatsura, M.; Hosaka, K.; Shirahama, H. *Chem. Eur. J.* **1999**, 5, 3252
 53. Li, Y.; Manickam, G.; Ghoshal, A.; Subramaniam, P. *Synth. Comm.* **2006**, 36, 925.
 54. Ikawa, T.; Hattori, K.; Sajiki, H.; Hirota, K. *Tetrahedron* **2004**, 60, 6901.
 55. Imamoto, T.; Ono, M. *Chem. Lett.* **1987**, 16, 501.
 56. Walvoort, M. T. C.; Volbeda, A. G.; Reintjens, N. R. M.; van den Elst, H.; Plante, O. J.; Overkleeft, H. S.; van der Marel, G. A.; Codée, J. D. C. *Org. Lett.* **2012**, 14, 3776.

Chapter 5. Conclusion

Pactamycin is a structurally complex aminocyclopentitol natural product that displays a range of diverse biological activities. Despite a basic understanding of its biosynthetic origin, details of the mode of formation of this unique natural product were still elusive. To decipher the biosynthetic pathway to pactamycin in *S. pactum* we used genetic, chemical complementation, isotopic labeling, and biochemical studies. In chapter 2 we demonstrated that 3ABA is processed by a set of discrete polyketide synthase proteins, i.e. an AMP-forming acyl-CoA synthetase (PtmS), an acyl carrier protein (ACP) (PtmI), and a β -ketoacyl-ACP synthase (PtmK), to give 3-[3-aminophenyl]3-oxopropionyl-ACP, which is then glycosylated by a broad spectrum *N*-glycosyltransferase, PtmJ. This is the first example of glycosylation of an ACP-bound polyketide intermediate in natural product biosynthesis. Additionally, we demonstrate that PtmO is a hydrolase that is responsible for the release of the glycosylated β -ketoacid product from the ACP, and the free β -ketoacid product subsequently undergoes non-enzymatic decarboxylation.

While the marked biological activity displayed by pactamycin traverses all three phylogenetic domains, the unfortunate and indiscriminate cytotoxicity towards mammalian cells has hampered its therapeutic development. Nonetheless, pactamycin is a bountiful resource of biological activity awaiting to be channeled.

In chapter 3, we report the *in vivo* and *in vitro* characterization of a KAS III-like protein (PtmR), which directly transfers a 6-MSA unit from an iterative type I polyketide synthase to the aminocyclopentitol component in pactamycin biosynthesis. We have

demonstrated here that PtmR has a very relaxed substrate specificity capable of recognizing a wide array of *S*-acyl-*N*-acetylcysteamines as substrates, and we developed a chemoenzymatic process to produce a library of pactamycin analogs with diverse alkyl and aromatic features. Our results suggest that KAS III-like proteins have great potential as tools for modifying complex natural products for drug discovery.

Continuing our efforts to draw further on the bountiful activity of the aminocyclitol core of pactamycin, we have undertaken a *de novo* synthesis of the core aminocyclopentitol-ring. Our successful synthesis of this aminocyclitol could open up a diverse library of biologically active compounds. We have now demonstrated an efficient, asymmetric synthesis of several aminocyclopentitol compounds resembling the pactamycin pharmacophore believed responsible for its biological activity. As a result of our synthetic endeavor in chapter 4, we have produced four novel and biologically active aminocyclopentitols. Two of these synthetic congeners display potent anticancer activity against melanoma A375 cells.

This study not only illuminated fundamental details about the biosynthesis of an intriguing natural product, pactamycin, but also utilized that knowledge to the construction of a diverse array of new medically relevant compounds. Furthermore, we have employed the mechanistic tools inspired by those that nature uses to build complex molecules, to synthetically construct more accessible and also significantly bioactive molecules exemplified by TM-122 and TM-123.

Bibliography

Reference-Chapter 1

1. Dewick, P.M., *Medicinal Natural Products*. 2002 John Wiley & Sons, Ltd, Baffins Lane, Chichester, West Sussex, England.
2. Albuquerque, E.X.; Daly, J.W.; Witkop, B.; *Science*, **1971**, 172, 995.
3. Daly, J. W. *Proc. Natl. Acad. Sci. USA*, **1995**, 92, 9-13.
4. Osborn, A. R.; Amabruk, K. H.; Holzwarth, G.; Asamizu, S.; LaDu, J.; Kean, K. M.; Karplus, A.; Tanguay, R. L.; Bakalinsky, A. T.; Mahmud, T. *eLife*, **2015**;4:e05919.
5. McGraw, K. J.; Hill, G. E.; Stradi, R.; Parker, R. S. *Physiological and Biochemical Zoology* **2001**, 74, 843–852.
6. Butler, S. M. *J. Nat. Prod.* **2004**, 67, 2141-2153.
7. Newman, D. J.; Cragg, G. M. *J. Nat. Prod.* **2016**, 79, 629–661.
8. Ojima, I. *J. Med. Chem.* **2008**, 51, 2587–2588.
9. Newman, D. J. *J. Med. Chem.* **2008**, 51, 2589.
10. Li, J. W.-H.; Vederas, J. C. *Science* **2009**, 325, 161–165.
11. Wiffen, P. J.; Wee, B.; Moore, R. A., *Cochrane Database of Systematic Reviews*; John Wiley & Sons, Ltd, **2016**.
12. *WHO Model List of Essential Medicines* (19th List). World Health Organization. April 2015.
13. American Chemical Society International Historic Chemical Landmarks. Discovery and Development of Penicillin. <http://www.acs.org/content/acs/en/education/whatischemistry/landmarks/flemingpenicillin.html> (accessed May 27, 2017).
14. Shen, B. *Cell* **2015**, 163, 1297.
15. The Nobel Prize in Physiology or Medicine 2015. *Nobelprize.org*. Nobel Media AB 2014. Web.(Accessed July 3 2017)http://www.nobelprize.org/nobel_prizes/medicine/laureates/2015/
16. Rohmer, M.; Seemann, M.; Horbach, S.; Bringer-Meyer, S.; Sahm, H. *J. Am. Chem. Soc.* **1996**, 118, 2564.
17. Kuzuyama, T., Seto, H. *Proc. Jpn. Acad., Ser. B* **88** **2012**.
18. Augustin, M. M.; Ruzicka, D. R.; Shukla, A. K.; Augustin, J. M.; Starks, C. M.; O’Neil-Johnson, M.; McKain, M. R.; Evans, B. S.; Barrett, M. D.; Smithson, A.; Wong, G. K.-S.; Deyholos, M. K.; Edger, P. P.; Pires, J. C.; Leebens-Mack, J. H.; Mann, D. A.; Kutchan, T. M. *Plant J* **2015**, 82, 991–1003.
19. Pu, J.-Y.; Peng, C.; Tang, M.-C.; Zhang, Y.; Guo, J.-P.; Song, L.-Q.; Hua, Q.; Tang, G.-L. *Org. Lett.* **2013**, 15 (14), 3674–3677.
20. Payne, J. A. E.; Schoppet, M.; Hansen, M. H.; Cryle, M. J. *Mol. BioSyst.* **2016**, 13, 9.
21. Fischbach, M. A.; Walsh, C. T. *Chem. Rev.* **2006**, 106, 3468–3496.
22. Izumikawa, M.; Cheng, Q.; Moore, B. S. *J. Am. Chem. Soc.* **2006**, 128, 1428–1429.
23. Felnagle, E. A.; Jackson, E. E.; Chan, Y. A.; Podevels, A. M.; Berti, A. D.; McMahon, M. D.; Thomas, M. G. *Mol. Pharmaceutics* **2008**, 5, 191–211.
24. Gay, D., You, Y-k, Keatinge-Clay, A., Cane D.E.; *Biochemistry* **2013**, 52, 8916–8928.

25. Hopwood, D.A. *Chem. Rev.* **1997**, 97, 2465-2497.
26. Mahmud, T. *Nat. Prod. Rep.* **2003**, 20, 137–166.
27. Mahmud, T.; Flatt, P. M.; Wu, X. *J. Nat. Prod.* **2007**, 70, 1384–1391.
28. Blaser, A., Reymond, J.L. *Org. Lett.* **2000**, 2, 1733.
29. Smith, B. J.; McKimm-Breshkin, J. L.; McDonald, M.; Fernley, R. T.; Varghese, J. N.; Colman, P. M. *J. Med. Chem.* **2002**, 45, 2207–2212.
30. McElroy, W. T.; Seganish, W.M.; Herr, J.R.; Harding, J.; Yang, J.; Yet, L.; Komanduri, V.; Prakash, K. C.; Lavey, B.; Tulshian, D.; Greenlee, W. J.; Sondey, C.; Fischmann, T. O.; Niu, X. *Bioorg & Med Chem Lett* **2015**, 25, 1836–1841.
31. Bhuyan, B. K., Dietz, A. & Smith, C. G. *Antimicrob. Agents Chemother.* **1961**, 184, 1050–1056.
32. Taber, R., Rekosh, D., Baltimore, D. *J Virol* **1971**, 8, 395-401
33. Otoguro, K., Iwatsuki, M., Ishiyama, A., Namatame, M., Nishihara-Tukashima, A., Shibahara, S., Kondo, S., Yamada, H., and Omura, S. *The Journal of Antibiotics* **2010**, 63, 381-384.
34. Sakuda, S.; Sugiyama, Y.; Zhou, Z.-Y.; Takao, H.; Ikeda, H.; Kakinuma, K.; Yamada, Y.; Nagasawa, H. *J. Org. Chem.* **2001**, 66, 3356–3361.
35. Kudo F, Kasama Y, Hirayama T, Eguchi T *J Antibiot (Tokyo)* **2007**, 60, 492-503.
36. Kudo, F.; Hoshi, S.; Kawashima, T.; Kamachi, T.; Eguchi, T. *J. Am. Chem. Soc.* **2014**, 136, 13909–13915.
37. Sakuda, S.; Sugiyama, Y.; Zhou, Z.-Y.; Takao, H.; Ikeda, H.; Kakinuma, K.; Yamada, Y.; Nagasawa, H. *J. Org. Chem.* **2001**, 66, 3356–3361.
38. Ito, T.; Roongsawang, N.; Shirasaka, N.; Lu, W.; Flatt, P. M.; Kasanah, N.; Miranda, C.; Mahmud, T. *ChemBioChem* **2009**, 10, 2253–2265.
39. P. F. Wiley, H. K. Jahnke, F. MacKellar, R. B. Kelly, A. D. Argoudelis, *J. Org. Chem.* **1970**, 35, 1420 – 1425.
40. D. J. Duchamp, Abstracts J. Am. Crystal. Assoc. Winter Meeting. Albuquerque, **1972**, April, p. 23.
41. D. D. Weller, A. Haber, K. L. Rinehart, Jr., P. F. Wiley, *J. Antibiot.* **1978**, 31, 997 – 1006.
42. Egebjerg, J.; Garrett, R. A. *Biochimie* **1991**, 73, 1145–1149.
43. G. Dinos, D. N. Wilson, Y. Teraoka, W. Szaflarski, P. Fucini, D. Kalpaxis, K. H. Nierhaus, *Mol. Cell* **2004**, 13, 113
44. Tourigny, D. S.; Fernández, I. S.; Kelley, A. C.; Vakiti, R. R.; Chattopadhyay, A. K.; Dorich, S.; Hanessian, S.; Ramakrishnan, V. *J. of Mol. Bio.* **2013**, 425, 3907–3910.
45. Lu, W.; Roongsawang, N.; Mahmud, T. *Chemistry & Biology* **2011**, 18, 425–431.
46. Hanessian, S.; Vakiti, R. R.; Chattopadhyay, A. K.; Dorich, S.; Lavallée, C. *Bioorganic & Medicinal Chemistry* **2013**, 21, 1775–1786.
47. Ito, T.; Roongsawang, N.; Shirasaka, N.; Lu, W.; Flatt, P. M.; Kasanah, N.; Miranda, C.; Mahmud, T. *ChemBioChem* **2009**, 10, 2253–2265.
48. Otoguro, K.; Iwatsuki, M.; Ishiyama, A.; Namatame, M.; Nishihara-Tukashima, A.; Shibahara, S.; Kondo, S.; Yamada, H.; Ōmura, S. *J Antibiot* **2010**, 63, 381–384.

49. Almabruk, K. H.; Lu, W.; Li, Y.; Abugreen, M.; Kelly, J. X.; Mahmud, T. *Org. Lett.* **2013**, *15*, 1678–1681.
50. Sharpe, R. J.; Malinowski, J. T.; Johnson, J. S. *J. Am. Chem. Soc.* **2013**, *135*, 17990–17998.
51. Sharpe, R. J.; Malinowski, J. T.; Sorana, F.; Luft, J. C.; Bowerman, C. J.; DeSimone, J. M.; Johnson, J. S. *Bioorganic & Medicinal Chemistry* **2015**, *23*, 1849–1857.
52. Abugrain, M. E.; Lu, W.; Li, Y.; Serrill, J. D.; Brumsted, C. J.; Osborn, A. R.; Alani, A.; Ishmael, J. E.; Kelly, J. X.; Mahmud, T. *ChemBioChem* **2016**, *17* (17), 1585–1588.
53. Abugrain, M. E.; Brumsted, C. J.; Osborn, A. R.; Philmus, B.; Mahmud, T. *ACS Chem. Biol.* **2017**, *12*, 362–366.
54. Tsujimoto, T.; Nishikawa, T.; Urabe, D.; Isobe, M. *Synlett* **2005**, 2005, 433.
55. Knapp, S.; Yu, Y. *Org. Lett.* **2007**, *9*, 1359.
56. Haussener, T. J.; Looper, R. E. *Org. Lett.* **2012**, *14*, 3632.
57. Malinowski, J. T.; McCarver, S. J.; Johnson, J. S. *Org. Lett.* **2012**, *14*, 2878.
58. Matsumoto, N.; Tsujimoto, T.; Nakazaki, A.; Isobe, M.; Nishikawa, T. *RSC Adv.* **2012**, *2*, 9448.
59. Yamaguchi, M.; Hayashi, M.; Hamada, Y.; Nemoto, T. *Org. Lett.* **2016**, *18*, 2347.
60. Gerstner, N. C.; Adams, C. S.; Grigg, R. D.; Tretbar, M.; Rigoli, J. W.; Schomaker, J. M. *Org. Lett.* **2016**, *18*, 284.
61. S. Hanessian, R. R. Vakiti, S. Dorich, S. Banerjee, F. Lecomte, J. R. DelValle, J. Zhang, B. Deschênes-Simard, *Angew. Chem. Int. Ed.* **2011**, *50*, 3497.
62. Hanessian, S. Vakiti, R. R., Dorich, S., Banerjee, S. Deschênes-Simard, B. *J. Org. Chem.* **2012**, *77*, 9458.
63. Malinowski, J. T.; Sharpe, R. J.; Johnson, J. S. *Science* **2013**, *340*, 180.
64. Sharpe, R. J.; Malinowski, J. T.; Johnson, J. S. *J. Am. Chem. Soc.* **2013**, *135*, 17990.
65. Weller, D. D.; Rinehart, K. L. *J. Am. Chem. Soc.* **1978**, *100*, 6757–6760.
66. Rinehart, K. L., Jr.; Weller, D. D.; Pearce, C. J. *J. Nat. Prod.* **1980**, *43*, 1–20.
67. Rinehart, K. L.; Potgieter, M.; Delaware, D. L.; Seto, H. *J. Am. Chem. Soc.* **1981**, *103*, 2099–2101.
68. Kudo, F.; Kasama, Y.; Hirayama, T.; Eguchi, T. *J Antibiot (Tokyo)* **2007**, *60*, 492–503.
69. Ito, T.; Roongsawang, N.; Shirasaka, N.; Lu, W.; Flatt, P. M.; Kasanah, N.; Miranda, C.; Mahmud, T. *Chembiochem* **2009**, *10*, 2253–2265.
70. Hirayama, A.; Eguchi, T.; Kudo, F. *Chembiochem* **2013**, *14*, 1198–1203.
71. Rinehart, K. L., Jr. *Jpn J Antibiot* **1979**, *32 Suppl*, S32–46.
72. Averill, B. A.; Herskovitz, T.; Holm, R. H.; Ibers, J. A. *J. Am. Chem. Soc.* **1973**, *95*, 3523–3534.
73. Inoue, H.; Fujimoto, N.; Imoto, E. *J. Chem. Soc., Chem. Commun.* **1977**, *0*, 412–413.
74. Inoue, H.; Suzuki, M.; Fujimoto, N. *J. Org. Chem.* **1979**, *44*, 1722–1724.
75. Kudo, F.; Hoshi, S.; Kawashima, T.; Kamachi, T.; Eguchi, T. *J. Am. Chem. Soc.* **2014**, *136*, 13909–13915.

Reference-Chapter 2

1. Rinehart, K. L., Jr.; Weller, D. D.; Pearce, C. J. *J. Nat. Prod.* **1980**, 43, 1-20.
2. Almabruk, K. H.; Lu, W.; Li, Y.; Abugreen, M.; Kelly, J. X.; Mahmud, T. *Org Lett* **2013**, 15, 1678-1681.
3. Hirayama, A.; Eguchi, T.; Kudo, F. *Chembiochem* **2013**, 14, 1198-1203.
4. Rinehart, K. L., Jr. *Jpn J Antibiot* **1979**, 32 Suppl, S32-46.
5. Ito, T.; Roongsawang, N.; Shirasaka, N.; Lu, W.; Flatt, P. M.; Kasanah, N.; Miranda, C.; Mahmud, T. *Chembiochem* **2009**, 10, 2253-2265.
6. Kudo, F.; Kasama, Y.; Hirayama, T.; Eguchi, T. *J Antibiot (Tokyo)* **2007**, 60, 492-503.
7. Bibb, M. J.; Sherman, D. H.; Omura, S.; Hopwood, D. A. *Gene* **1994**, 142, 31-39.
8. Ahlert, J.; Shepard, E.; Lomovskaya, N.; Zazopoulos, E.; Staffa, A.; Bachmann, B. O.; Huang, K.; Fonstein, L.; Csisny, A.; Whitwam, R. E.; Farnet, C. M.; Thorson, J. S. *Science* **2002**, 297, 1173-1176.
9. Mao, Y.; Varoglu, M.; Sherman, D. H. *Chem Biol* **1999**, 6, 251-263.
10. Mao, Y.; Varoglu, M.; Sherman, D. H. *J Bacteriol* **1999**, 181, 2199-2208.
11. Abugrain, M. E.; Brumsted, C. J.; Osborn, A. R.; Philmus, B.; Mahmud, T. *ACS Chem Biol* **2017**, 12, 362-366.
12. Lu, W.; Roongsawang, N.; Mahmud, T. *Chem Biol* **2011**, 18, 425-431.
13. Adams, E. S.; Rinehart, K. L. *J Antibiot (Tokyo)* **1994**, 47, 1456-1465.
14. August, P. R.; Tang, L.; Yoon, Y. J.; Ning, S.; Muller, R.; Yu, T. W.; Taylor, M.; Hoffmann, D.; Kim, C. G.; Zhang, X.; Hutchinson, C. R.; Floss, H. G. *Chem Biol* **1998**, 5, 69-79.
15. Yu, T. W.; Bai, L.; Clade, D.; Hoffmann, D.; Toelzer, S.; Trinh, K. Q.; Xu, J.; Moss, S. J.; Leistner, E.; Floss, H. G. *Proc. Natl. Acad. Sci. U S A* **2002**, 99, 7968-7973.
16. Admiraal, S. J.; Khosla, C.; Walsh, C. T. *J. Am. Chem. Soc.* **2003**, 125, 13664-13665.
17. Kao, C. L.; Borisova, S. A.; Kim, H. J.; Liu, H. W. *J Am Chem Soc* **2006**, 128, 5606-5607.
18. Sweet, C. R.; Ribeiro, A. A.; Raetz, C. R. *J Biol Chem* **2004**, 279, 25400-25410.
19. Gilbert, I. H.; Ginty, M.; O'Neill, J. A.; Simpson, T. J.; Staunton, J.; Willis, C. L. *Bioorg. Med. Chem. Lett.* **1995**, 5, 1587-1590.
20. Gilbert, I. H.; Ginty, M.; O'Neill, J. A.; Simpson, T. J.; Staunton, J.; Willis, C. L. *Bioorganic & Medicinal Chemistry Letters* **1995**, 5, 1587-1590.
21. Higher yields were obtained when Meldrum's acid was recrystallized (acetone-water) immediately prior to use.
22. Ferdani, R.; Pajewski, R.; Djedović, N.; Pajewska, J.; Schlesinger, P. H.; Gokel, G. W. *New J. Chem.* **2005**, 29, 673-680.

Reference-Chapter 3

1. A template search reveals mechanistic similarities and differences in beta-ketoacyl synthases (KAS) and related enzymes. Dawe, J. H., Porter, C. T., Thornton, J. M., and Tabor, A. B. *Proteins: Struct., Funct., Genet.* **2003**, 52, 427–435.
2. Characterization of beta-ketoacyl-acyl carrier protein synthase III from *Streptomyces glaucescens* and its role in initiation of fatty acid biosynthesis: Han, L., Lobo, S., and Reynolds, K. A. *J. Bacteriol.* **1998**, 180, 4481–4486.
3. CloN2, a novel acyltransferase involved in the attachment of the pyrrole-2-carboxyl moiety to the deoxysugar of clorobiocin: Xu, H., Kahlich, R., Kammerer, B., Heide, L., and Li, S. M. *Microbiology* **2003**, 149, 2183–2191.
4. A ketosynthase homolog uses malonyl units to form esters in cervimycin biosynthesis: Bretschneider, T., Zocher, G., Unger, M., Scherlach, K., Stehle, T., and Hertweck, C. *Nat. Chem. Biol.* **2012**, 8, 154–161.
5. Dissection of two acyl-transfer reactions centered on acyl-S-carrier protein intermediates for incorporating 5-chloro-6-methyl-O-methylsalicylic acid into chlorothricin: He, Q. L., Jia, X. Y., Tang, M. C., Tian, Z. H., Tang, G. L., and Liu, W. *ChemBioChem*, **2009**, 10, 813–819.
6. Biosynthesis of the orthosomycin antibiotic avilamycin A: deductions from the molecular analysis of the avi biosynthetic gene cluster of *Streptomyces viridochromogenes* Tu57 and production of new antibiotics: Weitnauer, G., Muhlenweg, A., Trefzer, A., Hoffmeister, D., Sussmuth, R. D., Jung, G., Welzel, K., Vente, A., Girreser, U., and Bechthold, A. *Chem. Biol.* **2006**, 8, 569–581.
7. Characterization of the biosynthetic gene cluster for the oligosaccharide antibiotic, Evernimicin, in *Micromonospora carbonacea* var. africana ATCC39149. Hosted, T. J., Wang, T. X., Alexander, D. C., and Horan, A. C. *J. Ind. Microbiol. Biotechnol.* **2001**, 27, 386–392.
8. The calicheamicin gene cluster and its iterative type I enediyne PKS. Ahlert, J., Shepard, E., Lomovskaya, N., Zazopoulos, E., Staffa, A., Bachmann, B. O., Huang, K., Fontstein, L., Csisny, A., Whitwam, R. E., Farnet, C. M., and Thorson, J. S. *Science* **2002**, 297, 1173–1176.
9. Organisation of the biosynthetic gene cluster and tailoring enzymes in the biosynthesis of the tetracyclic quinone glycoside antibiotic polyketomycin. Daum, M., Peintner, I., Linnenbrink, A., Frerich, A., Weber, M., Paululat, T., and Bechthold, A. *ChemBioChem* **2009**, 10, 1073–1083.
10. Characterization of tiacumicin B biosynthetic gene cluster affording diversified tiacumicin analogues and revealing a tailoring dihalogenase. Xiao, Y., Li, S., Niu, S., Ma, L., Zhang, G., Zhang, H., Zhang, G., Ju, J., and Zhang, C. *J. Am. Chem. Soc.* **2011**, 133, 1092–1105.

11. Insights into a divergent phenazine biosynthetic pathway governed by a plasmid-born esmeraldin gene cluster. Rui, Z., Ye, M., Wang, S., Fujikawa, K., Akerele, B., Aung, M., Floss, H. G., Zhang, W., and Yu, T. W. *Chem. Biol.* **2012**, 19, 1116–1125.
12. Deciphering pactamycin biosynthesis and engineered production of new pactamycin analogues. Ito, T., Roongsawang, N., Shirasaka, N., Lu, W., Flatt, P. M., Kasanah, N., Miranda, C., and Mahmud, T. *ChemBioChem*, **2009**, 10, 2253–2265.
13. Interrogating the tailoring steps of pactamycin biosynthesis and accessing new pactamycin analogues. Abugrain, M. E., Lu, W., Li, Y., Serrill, J. D., Brumsted, C. J., Osborn, A. R., Alani, A., Ishmael, J. E., Kelly, J. X., and Mahmud, T. *ChemBioChem* **2016**, 17, 1585–1588.
14. Biosynthetic studies and genetic engineering of pactamycin analogs with improved selectivity toward malarial parasites. Lu, W., Roongsawang, N., and Mahmud, T. *Chem. Biol.* **2011**, 18, 425–431.
15. Cloning of the pactamycin biosynthetic gene cluster and characterization of a crucial glycosyltransferase prior to a unique cyclopentane ring formation. Kudo, F., Kasama, Y., Hirayama, T., and Eguchi, T. *J. Antibiot.* **2007**, 60, 492–503.
16. Kieser, T., Bibb, M. J., Buttner, M. J., Chater, K. F., and Hopwood, D. A. *Practical Streptomyces Genetics*, The John Innes Foundation, Norwich, England, **2000**.

References-Chapter 4

1. Newman, D. J., Cragg, G. M. *J. Nat. Prod.* **2016**, 79, 629.
2. Bhuyan, B. K. *Appl. Microbiol.* **1962**, 10, 302.
3. White, F. R. *Cancer Chemother. Rep.* **1962**, 24, 75.
4. Taber, R.; Rekosh, D.; Baltimore, D. *J. Virol.* 1971, 8, 395.
5. Otoguro, K.; Iwatsuki, M.; Ishiyama, A.; Namatame, M.; Nishihara-Tukashima, A.; Shibahara, S.; Kondo, S.; Yamada, H.; Omura, S. *J. Antibiot. (Tokyo)* **2010**, 63, 381.
6. Mahmud, T., Flatt, P. M., Wu, X. *J. Nat. Prod.* **2007**, 70, 1384.
7. Lu, W., Roongsawang, N., Mahmud, T. *Chemistry & Biology* **2011**, 18, 425.
8. Almabruk, K. H, Lu, W., Li, Y., Abugreen, M., Kelly, J. X., Mahmud, T. *Org. Lett.* **2013**, 15, 1678.
9. Abugrain, M.E.; Lu, W.; Li, Y.; Serrill, J. D.; Brumsted, C. J.; Osborn, A. R.; Alani, A.; Ishmael, J. E.; Kelly, J. X.; Mahmud, T. *ChemBioChem* **2016**, 17, 1585.
10. Abugrain, M.E.; Brumsted, C.J.; Osborn, A. R.; Philmus, B.; Mahmud, T. *ACS Chem. Biol.* **2017**, 12, 362.
11. S. Hanessian, R. R. Vakiti, S. Dorich, S. Banerjee, F. Lecomte, J. R. DelValle, J. Zhang, B. Deschênes-Simard, *Angew. Chem. Int. Ed.* **2011**, 50, 3497.
12. Hanessian, S. Vakiti, R. R., Dorich, S., Banerjee, S. Deschênes-Simard, B. *J. Org. Chem.* **2012**, 77, 9458.
13. Malinowski, J. T., Sharpe, R. J., Johnson, J. S. *Science* **2013**, 340, 180
14. Sharpe, R. J., Malinowski, J. T., Johnson, J. S. *J. Am. Chem. Soc.* **2013**, 135, 17990.

Synthesis studies towards pactamycin (15-21):

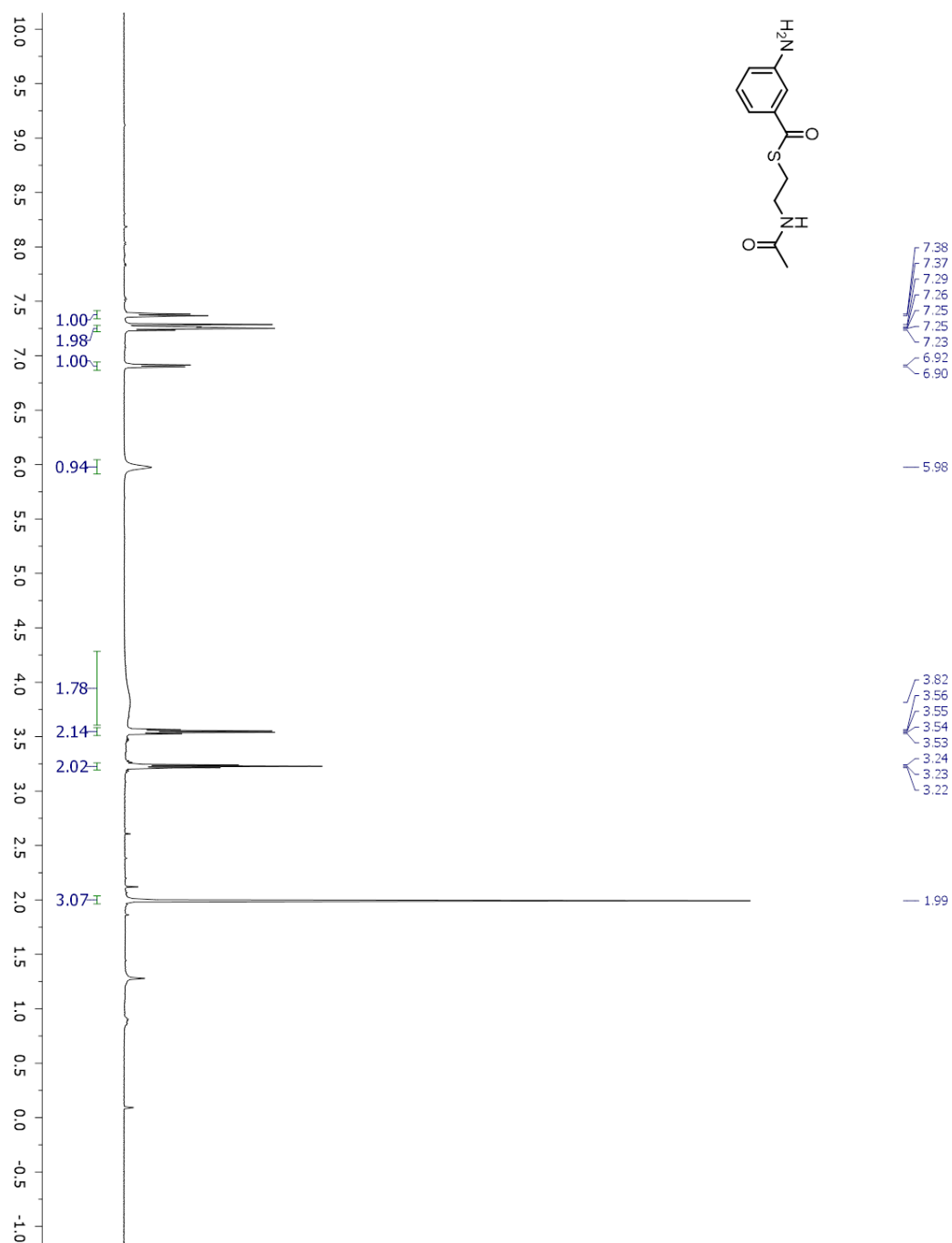
15. Tsujimoto, T., Nishikawa, T., Urabe, D., Isobe, M. *Synlett* **2005**, 2005, 433.
16. Knapp, S., Yu, Y. *Org. Lett.* **2007**, 9, 1359.
17. Haussener, T. J., Looper, R. E. *Org. Lett.* **2012**, 14, 3632.
18. Matsumoto, N., Tsujimoto, T., Nakazaki, A. Isobe, M. Nishikawa, T. *RSC Adv.* **2012**, 2, 9448.
19. Malinowski, J. T., McCarver, S. J., Johnson, J. S. *Org. Lett.* **2012**, 14, 2878.
20. Yamaguchi, M., Hayashi, M. Hamada, Y. Nemoto, T. *Org. Lett.* **2016**, 18, 2347.
21. Gerstner, N. C., Adams, C. S., Grigg, R. D., Tretbar, M., Rigoli, J. W. Schomaker, J. M. *Org. Lett.* **2016**, 18, 284.
22. Sharpe, R. J.; Malinowski, J. T.; Sorana, F.; Luft, J. C.; Bowerman, C. J.; DeSimone, J. M.; Johnson, J. S., *Bioorganic & Medicinal Chemistry* **2015**, 23, 1849.
23. Hanessian, S., Vakiti, R. R., Chattopadhyay, A. K., Dorich, S., Lavallée, C. *Bioorganic & Medicinal Chemistry* **2013**, 21, 1775.

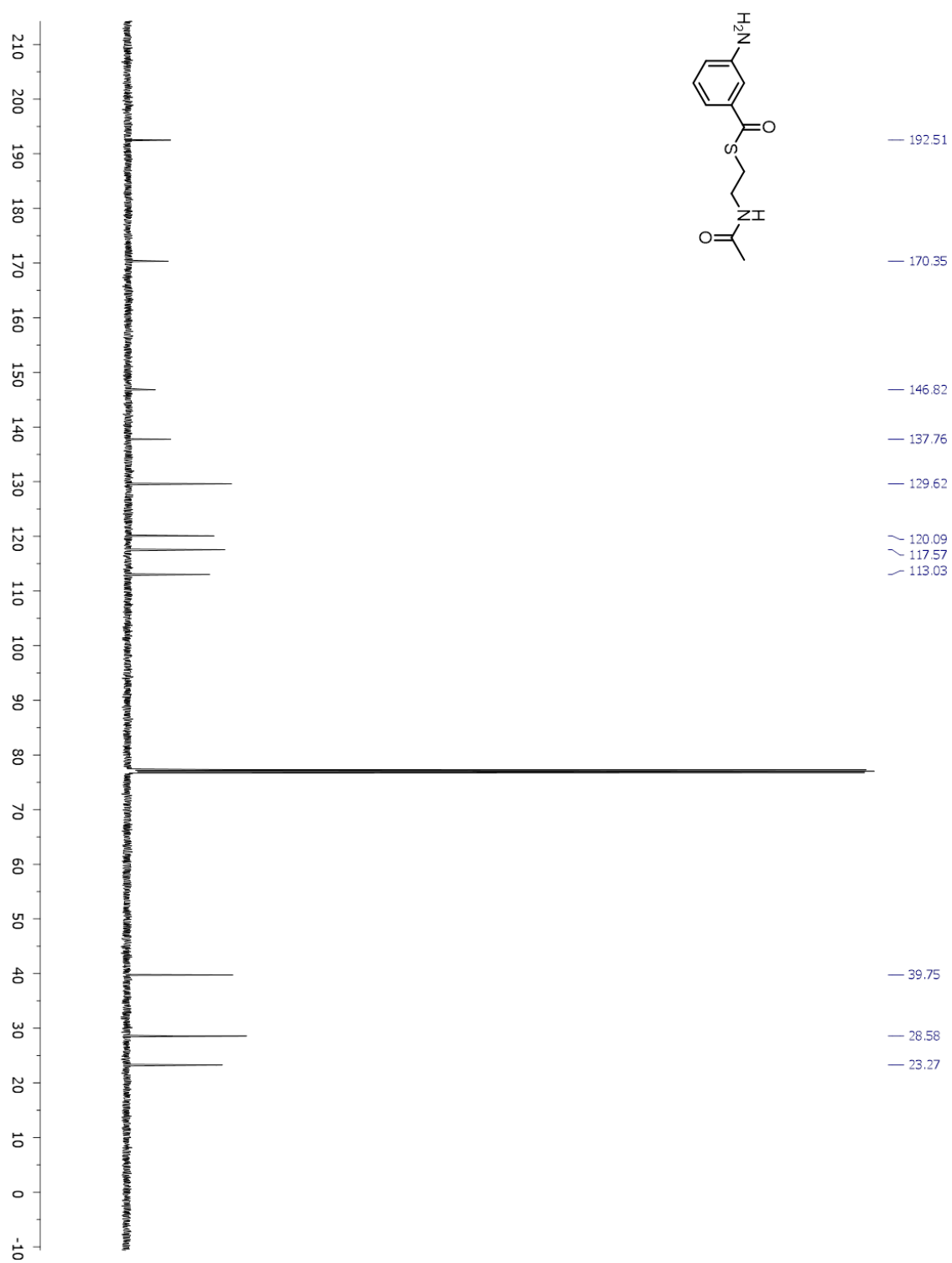
Reviews on the Synthesis of Aminocyclopentitols (references 24-27):

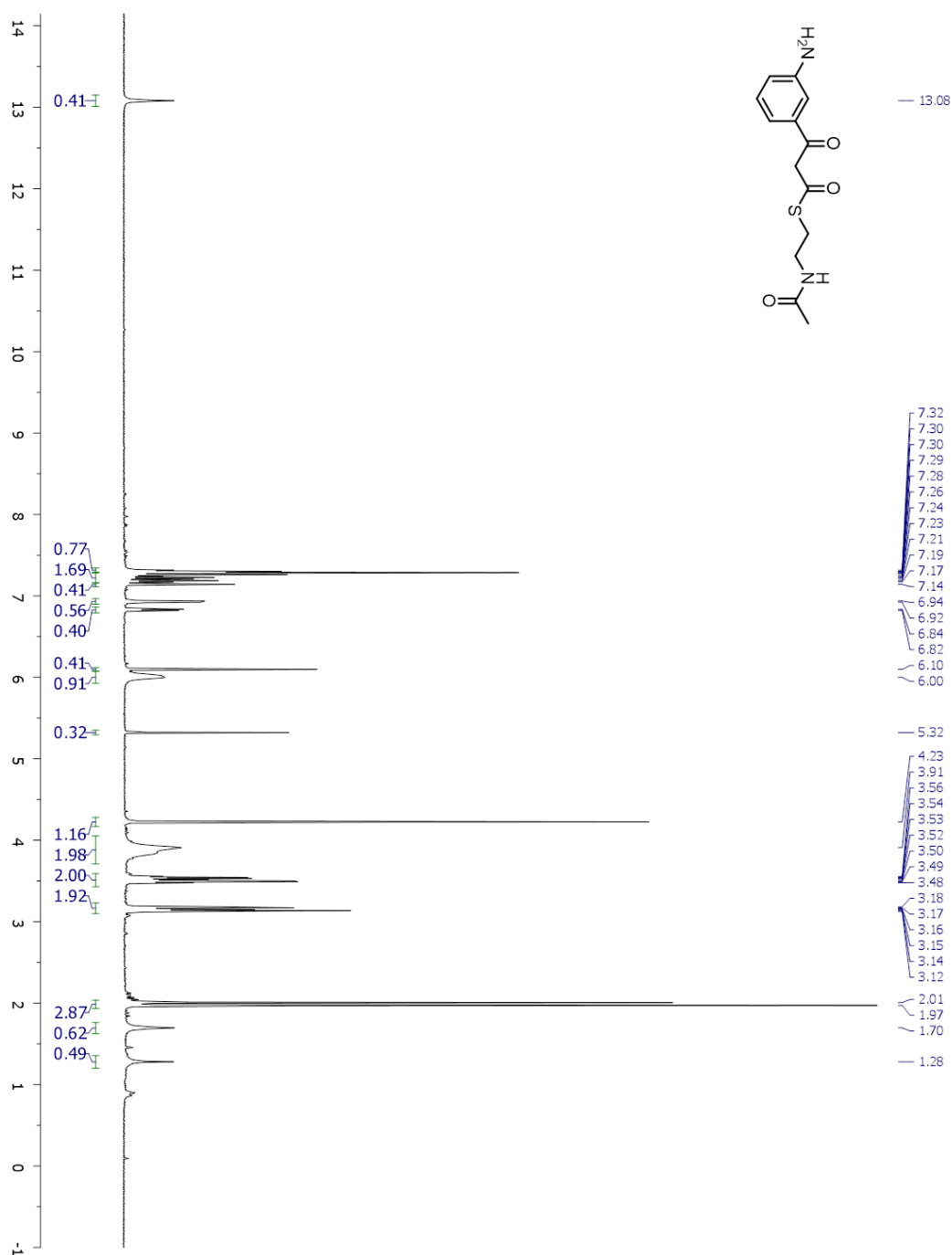
24. Delgado, A. *Eur. J. Org. Chem.* **2008**, 2008, 3893.
25. Ferrier, R. J.; S. Middleton, S. *Chem. Rev.* **1993**, 93, 2779.
26. Bereubar, A.; Grandjean, C.; Siriwardena, A. *Chem. Rev.* **1999**, 99, 779
27. Arjona, O.; Gómez, A. M.; López, J. C.; Plumet, J. *Chem. Rev.* **2007**, 107, 1919.
28. Liebman, J.; Rappoport Z. *The Chemistry of Hydroxylamines, Oximes and Hydroxamic acids*. John Wiley and Sons, Ltd., West Sussex PO19 8SQ, England, **2008**, part I.
29. Corey, E. J.; Pyne, S. G. *Tetrahedron Lett.* **1983**, 24, 2821.
30. Shono, T.; Kise, N.; Fujimoto, T. *Tetrahedron Lett.* **1991**, 32, 525.
31. Naito, T.; Tajiri, K.; Harimoto, T.; Ninomiya, I.; Kiguchi, T. *Tetrahedron Lett.* **1994**, 35, 2205.
32. Chiara, J. L.; Marco-Contelles, J.; Khiar, N.; Gallego, P.; Destabel, C.; Bernabé, M. J. *Org. Chem.* **1995**, 60, 6010.
33. Marco-Contelles, J.; Gallego, P.; Rodríguez-Fernández, M.; Khiar, N.; Destabel, C.; Bernabé, M.; Martínez-Grau, A.; Chiara, J. L. *J. Org. Chem.* **1997**, 62, 7397.
34. Storch de Gracia, I.; Dietrich, H.; Bobo, S.; Chiara, J. L. *J. Org. Chem.* **1998**, 63, 5883.
35. Garcia, J., Chiara, J. L., *Synlett.* **2005**, 17, 2607.
36. Hoffmann, R.W., *Chem. Rev.* **1989**, 89, 1841-1860.
37. Boiron, A.; Zillig, P.; Faber, D.; Giese B. J. *Org. Chem.* **1998**, 63, 5877-5882
38. Ohlin, M.; Johnsson, R.; Ellervik, U. *Carbohydrate Research* **2011**, 346, 12, 1358.
39. Greene's protective groups in organic synthesis. **2014**. John Wiley & Sons, Inc., 5th ed. Wuts, P.G.M.
40. Molander, G. A., Hahn, G., *J. Org. Chem.*, **1986**, 51, 1135
41. Procter, D.J.; Flowers, R.A. II; Skrydstrup, T.; *Organic Synthesis Using Samarium Diodide, A Practical Guide.* **2010**, The Royal Society of Chemistry, Cambridge CB4 0WF, UK.
42. Suzuki, K.; Tamiya, M. *Comprehensive Organic Synthesis: Pinacol Coupling Reactions.* Elsevier Science. **2014**, 580-620.

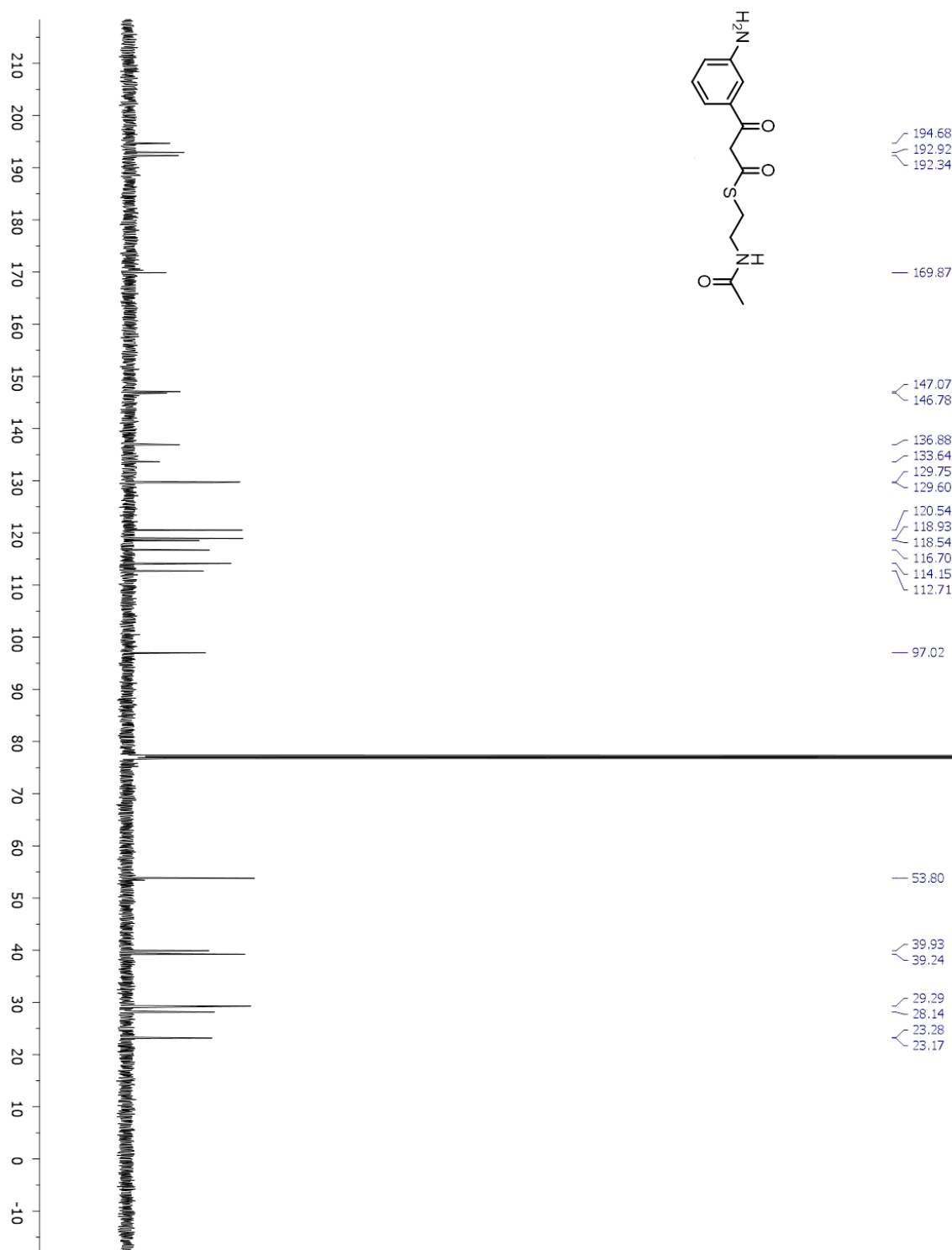
43. Gansauer, A; Bluhm, H. *Chem. Rev.* **2000**, 100, 2771-2788
44. Shi, L.; Fan, C.-A.; Tu, Y.-Q.; Wang, M.; Zhang, F.-M. *Tetrahedron* **2004**, 60, 2851–2855.
45. Mancuso, A. J.; Swern, D. *Synthesis* **1981**, 165.
46. Lu, Y.; Krische, M. J. *Org. Lett.* **2009**, 11, 3108.
47. Chiara, J. L.; García, Á.; Cristóbal-Lumbroso, G. *J. Org. Chem.* **2005**, 70, 4142.
48. Li, Y.; Manickam, G.; Atanu Ghoshal; Subramaniam, P. *Synth. Comm.* **2006**, 36, 925.
49. Ikawa, T.; Hattori, K.; Sajiki, H.; Hirota, K. *Tetrahedron* **2004**, 60, 6901.
50. Imamoto, T.; Ono, M. *Chem. Lett.* **1987**, 16, 501.
51. Walvoort, M. T. C.; Volbeda, A. G.; Reintjens, N. R. M.; van den Elst, H.; Plante, O. J.; Overkleeft, H. S.; van der Marel, G. A.; Codée, J. D. C. *Org. Lett.* **2012**, 14, 3776.

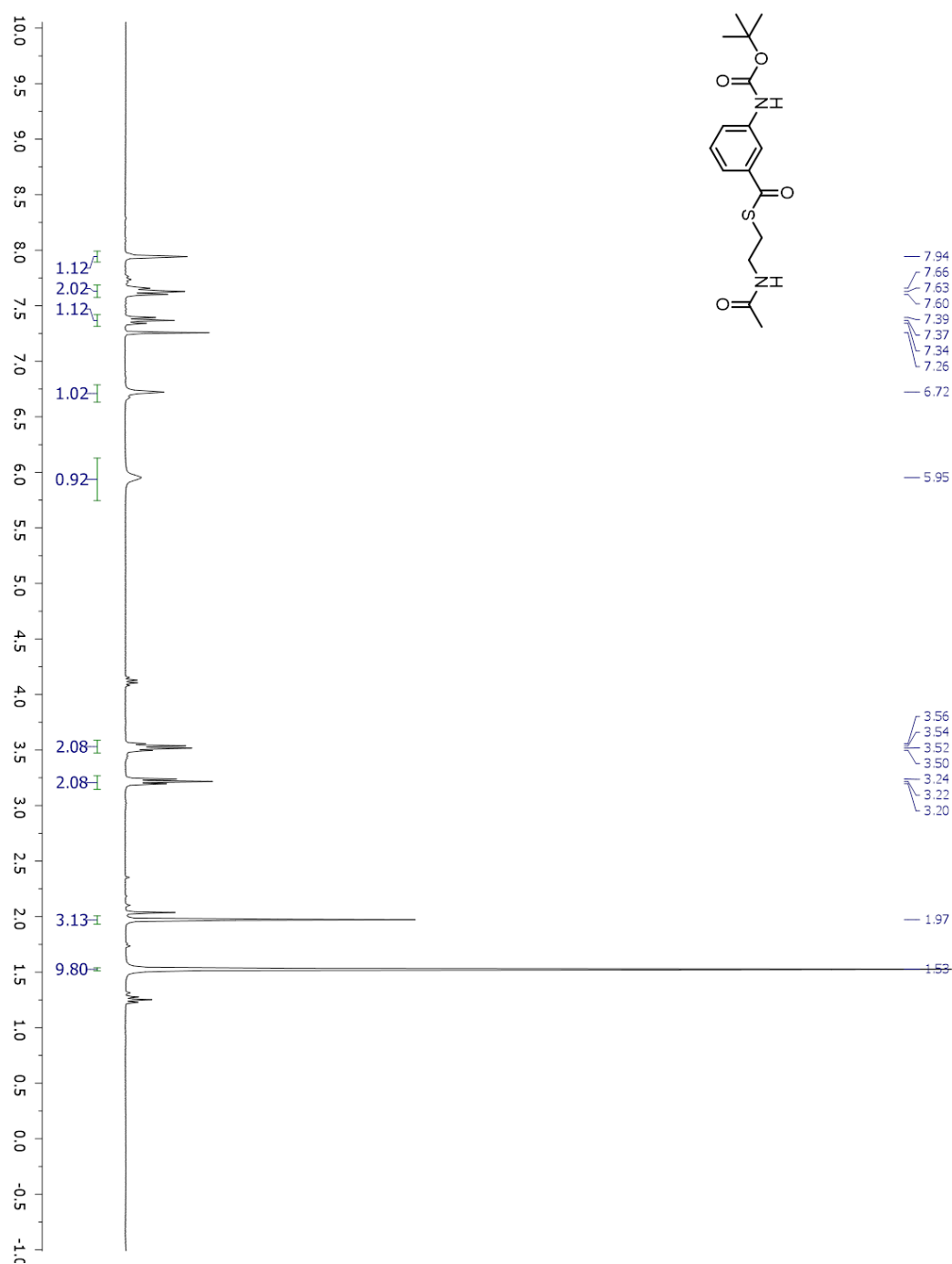
6. Appendix A. Chapter 2 NMR Data

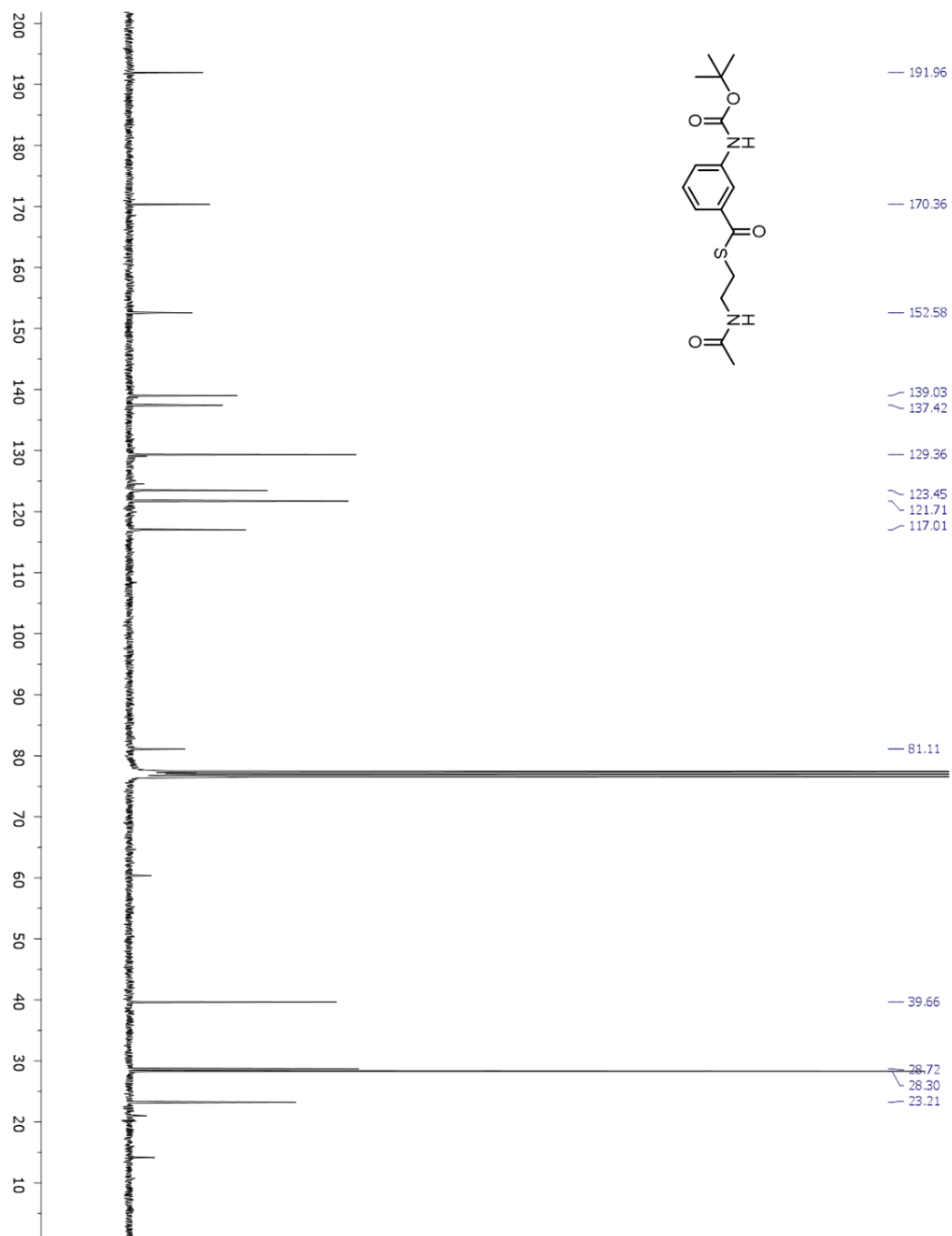
Appendix Figure 6.1. ^1H NMR (CDCl_3) spectrum of 3ABA-SNAC

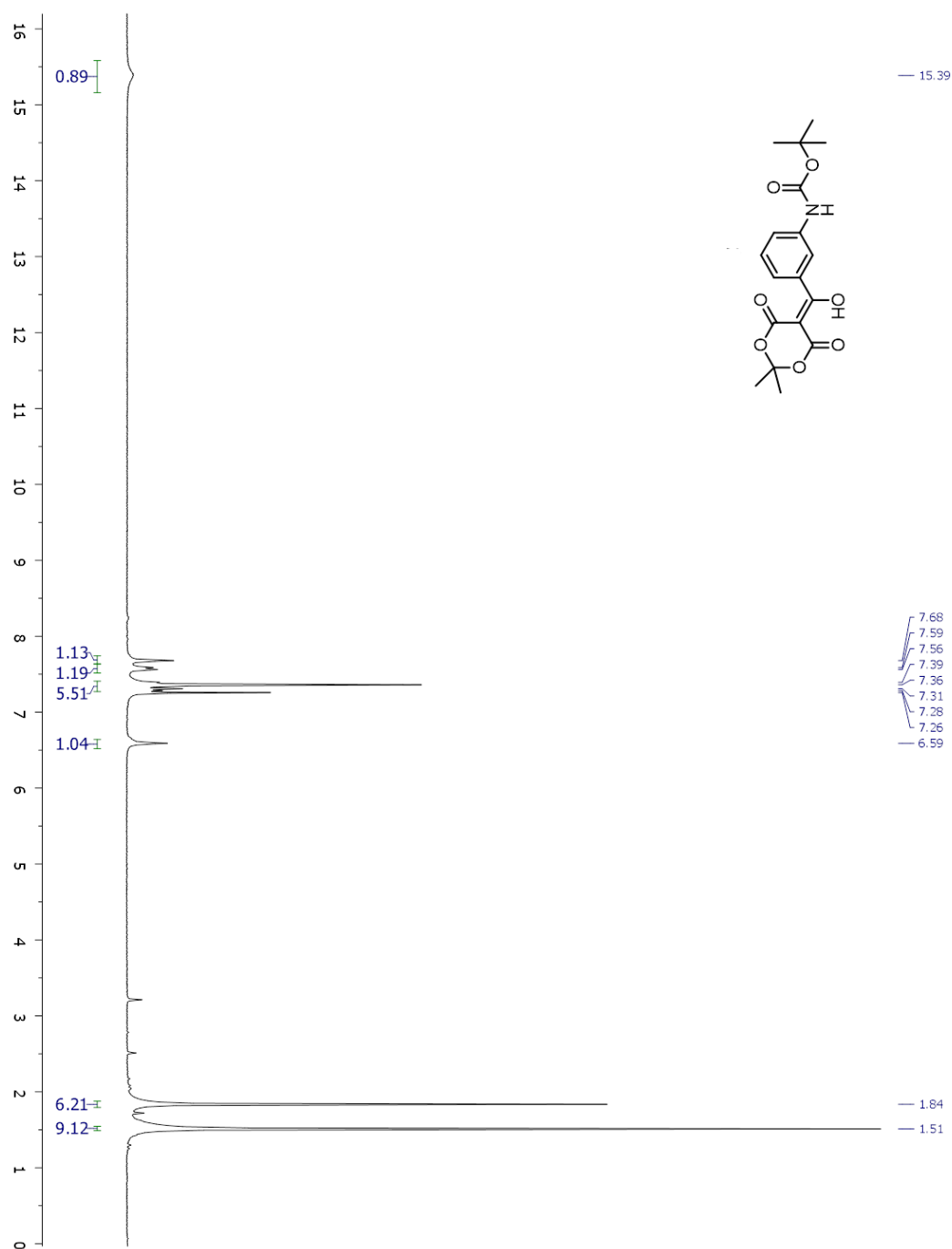
Appendix Figure 6.2. ^{13}C NMR (CDCl_3) spectrum of 3ABA-SNAC

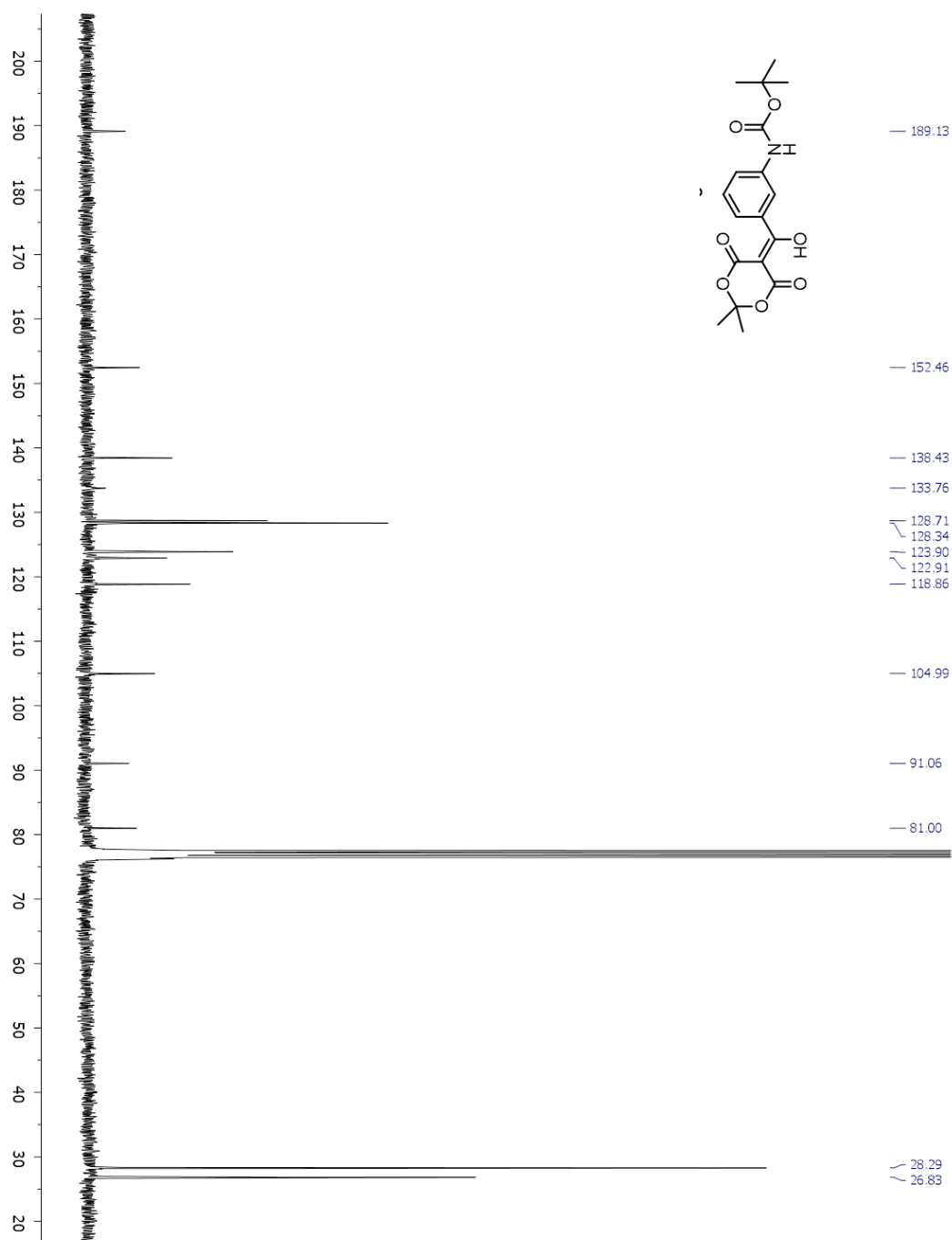
Appendix Figure 6.3. ^1H NMR (CDCl_3) spectrum of 3AP-3OP-SNAC

Appendix Figure 6.4. ^{13}C NMR (CDCl_3) spectrum of 3AP-3OP-SNAC

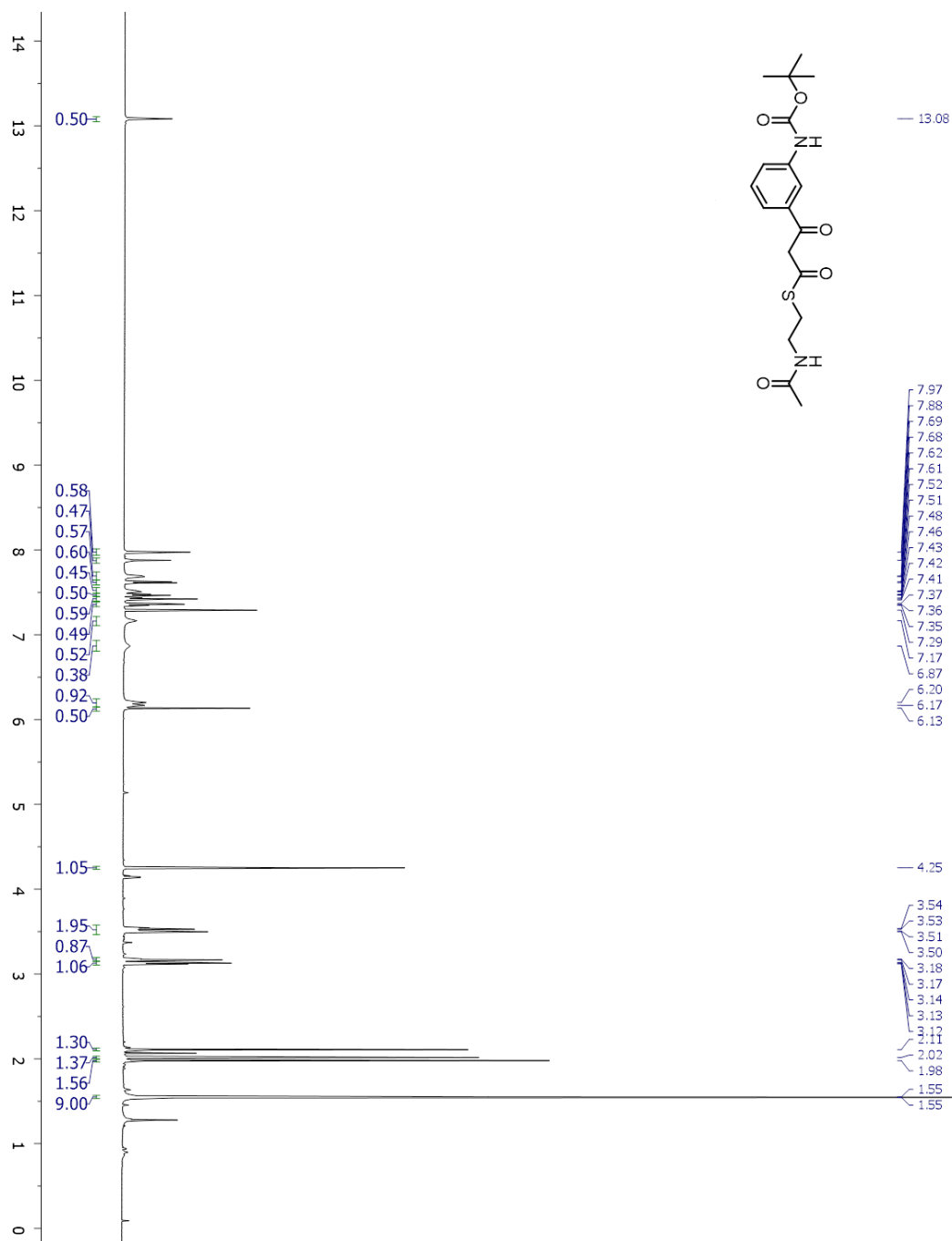
Appendix Figure 6.5. ^1H NMR (CDCl_3) spectrum of BOC-3ABA-SNAC

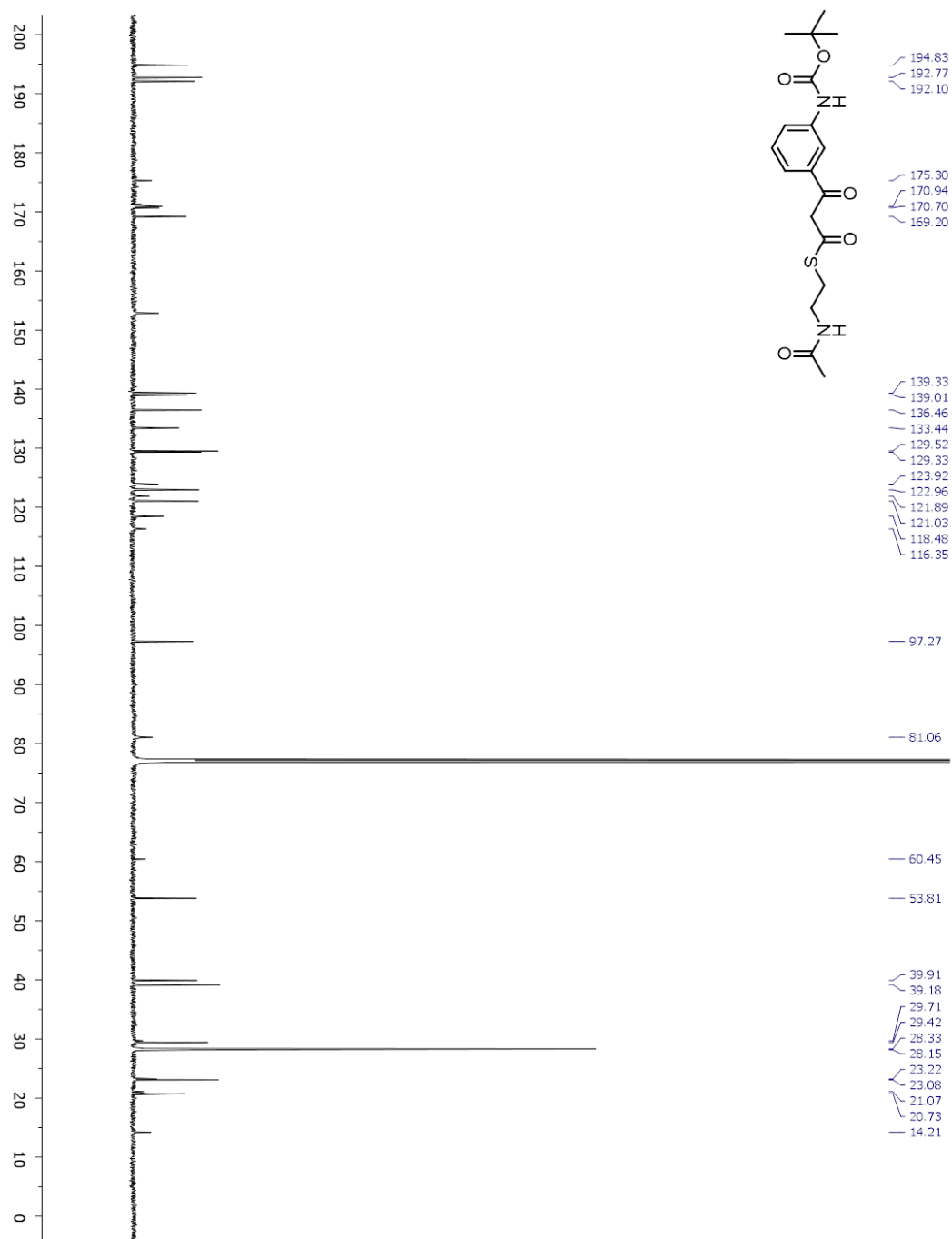
Appendix Figure 6.6. ^{13}C NMR (CDCl_3) spectrum of BOC ABA-SNAC

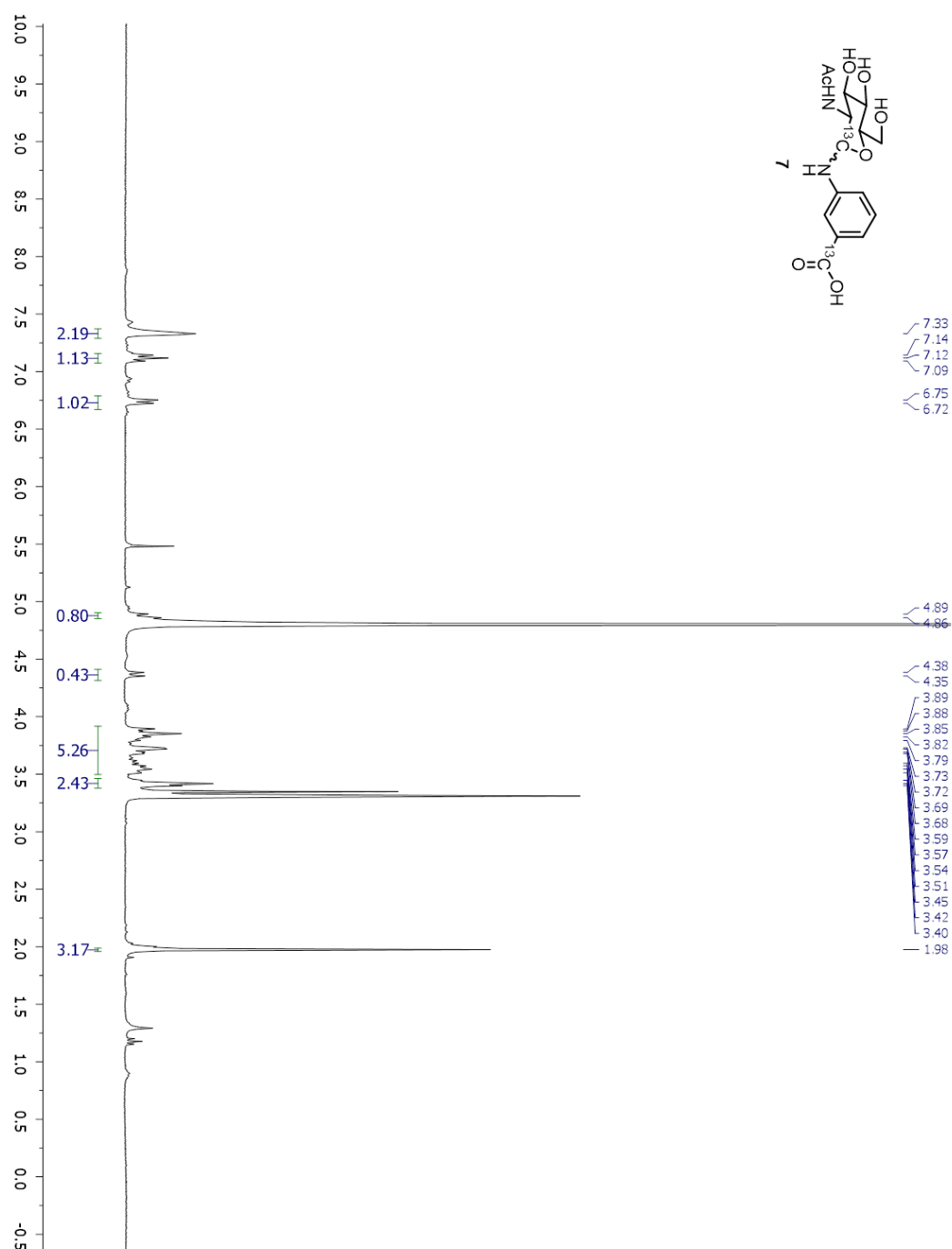
Appendix Figure 6.7. ^1H NMR (CDCl_3) spectrum of Meldrum's adduct **SI-2**

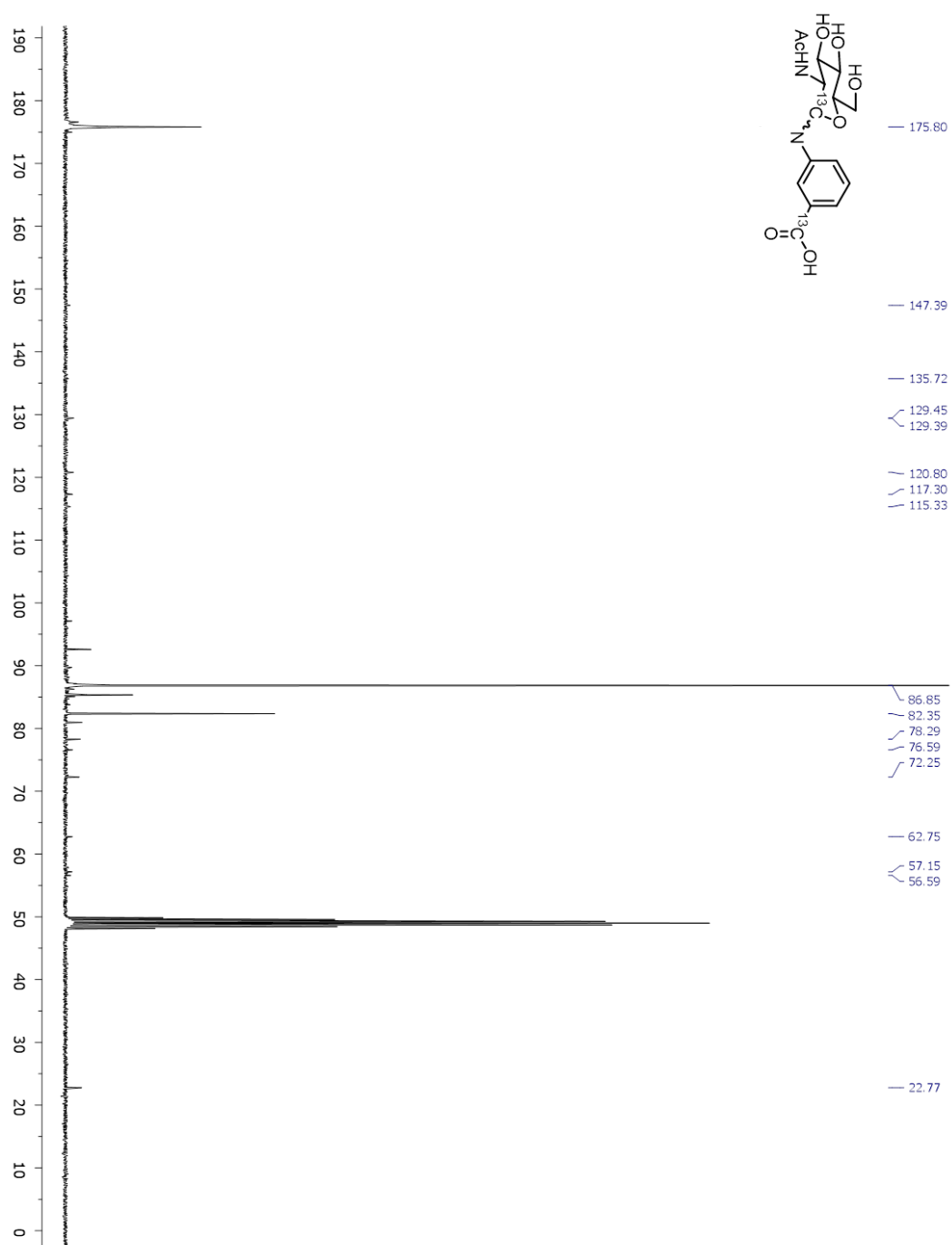
Appendix Figure 6.8. ^{13}C NMR (CDCl_3) spectrum of Meldrum's adduct **SI-2**

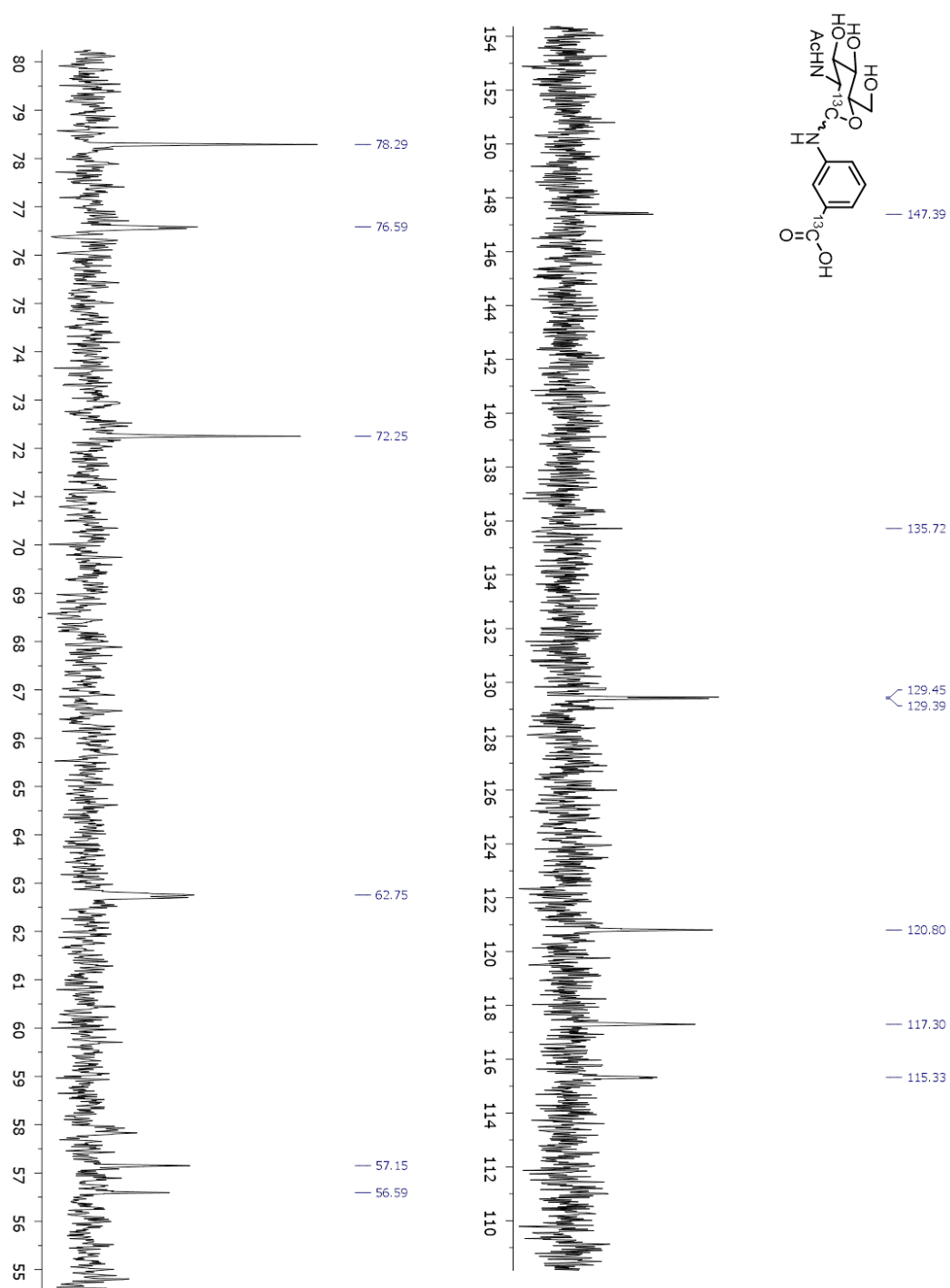
Appendix Figure 6.9. ^{13}C NMR (MeOD) spectrum of Meldrum's adduct SI-2

Appendix Figure 6.10. ^1H NMR (CDCl_3) spectrum of BOC-3AP-3OP-SNAC.

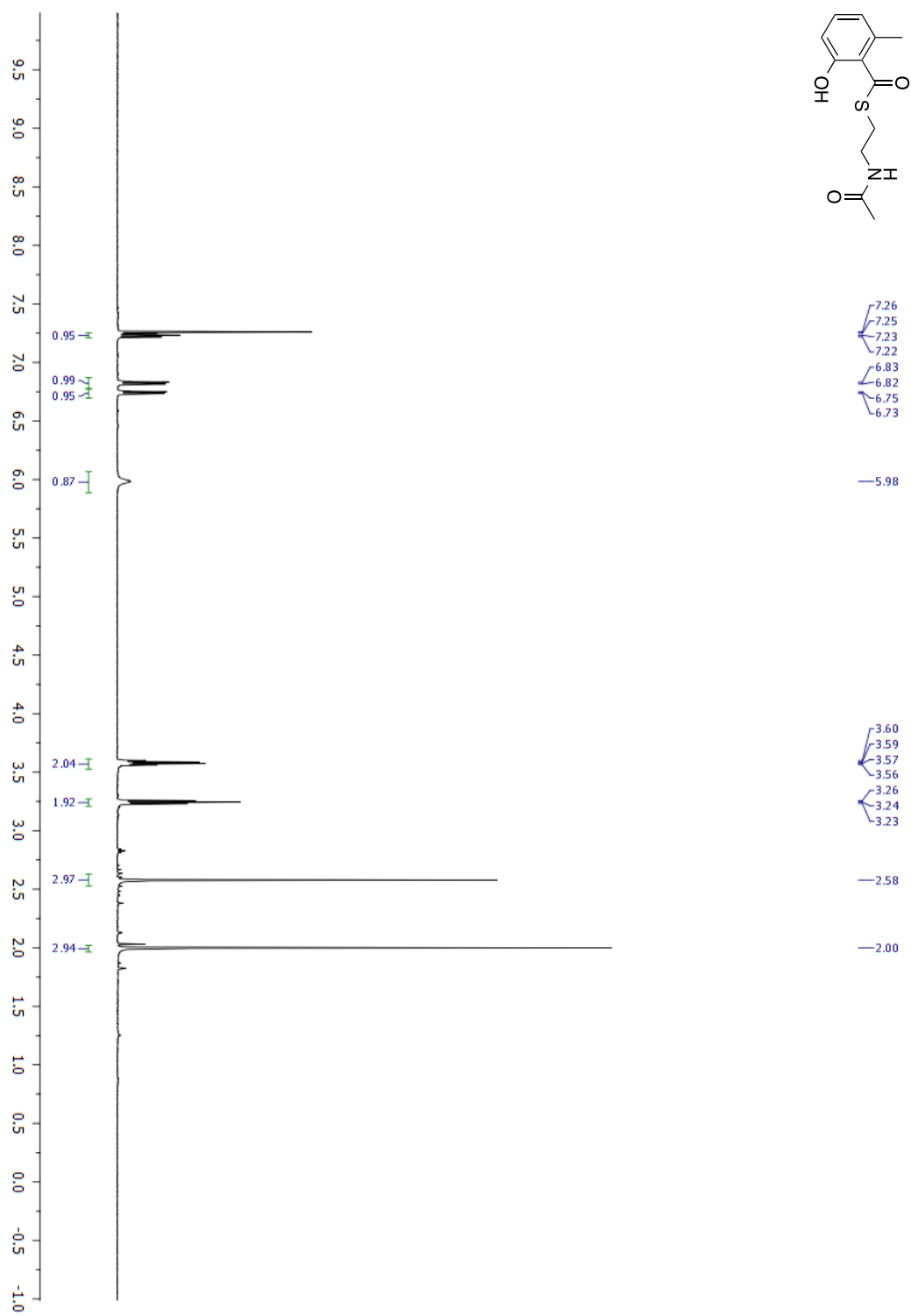
Appendix Figure 6.11. ^{13}C NMR (CDCl_3) spectrum of 3AP-3OP-SNAC.

Appendix Figure 6.12. ^1H NMR (D_2O -MeOD) spectrum of $[\text{}^{13}\text{C}]\text{GlcNAc}-[\text{}^{13}\text{C}]\text{3ABA}$ 

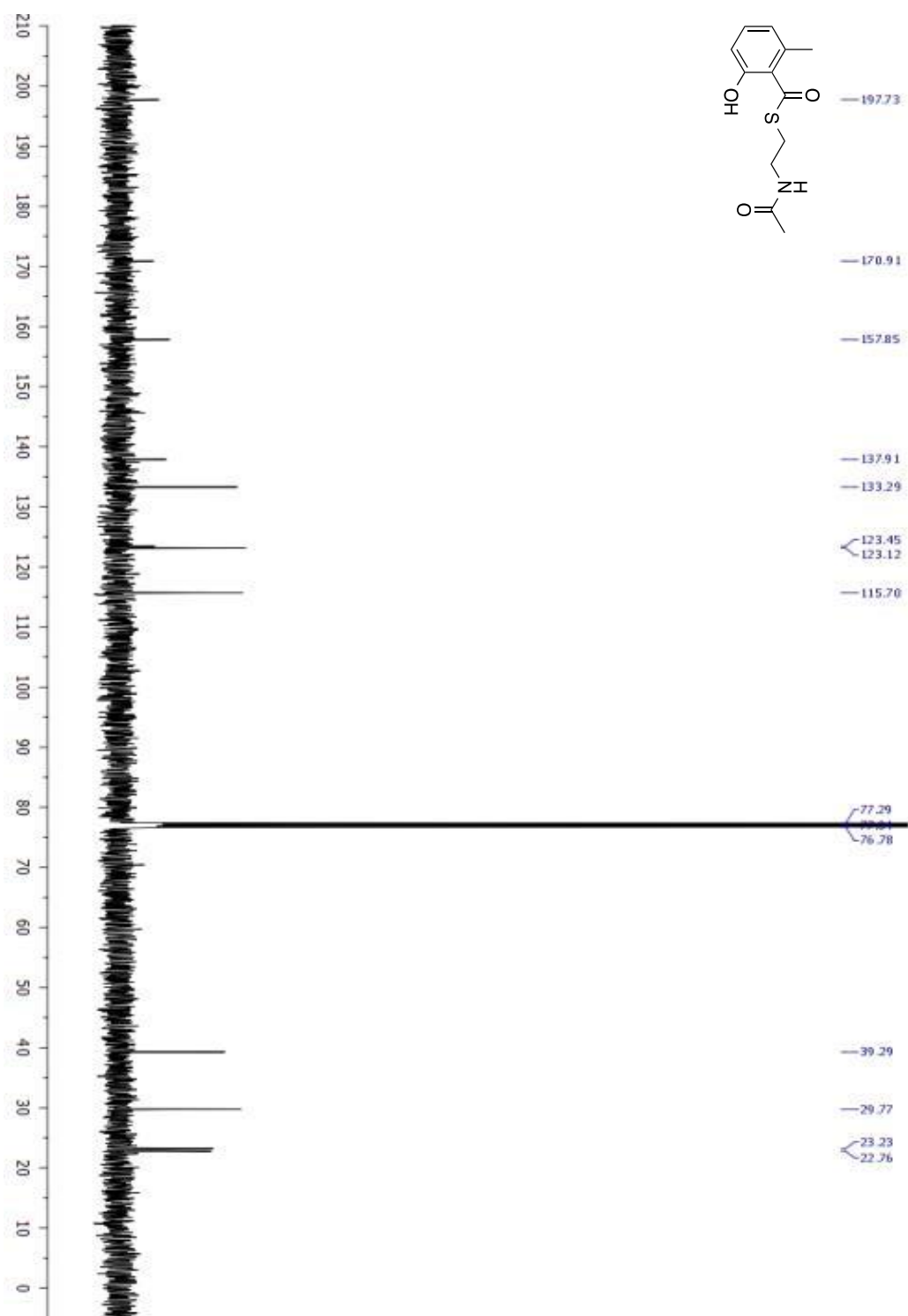
Appendix Figure 6.13. ^{13}C NMR (D_2O -MeOD) spectrum of $[^{13}\text{C}]\text{GlcNAc}$ - $[^{13}\text{C}]\text{3ABA}$ 

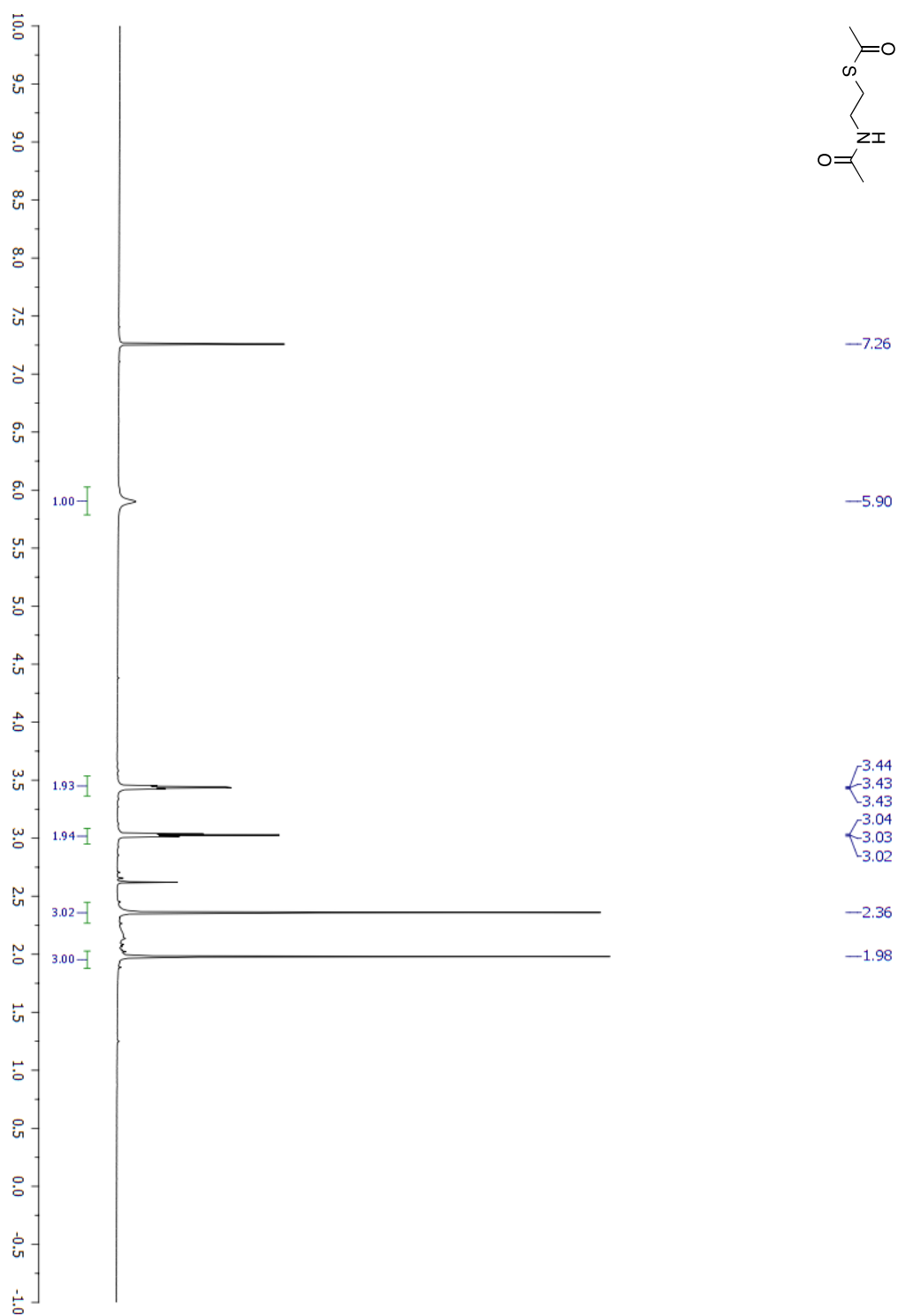
Appendix Figure 6.14. ^{13}C NMR (D_2O -MeOD) spectrum of $[^{13}\text{C}]\text{GlcNAc}$ - $[^{13}\text{C}]\text{3ABA}$ 

6.2 Appendix B: Chapter 3 NMR Data

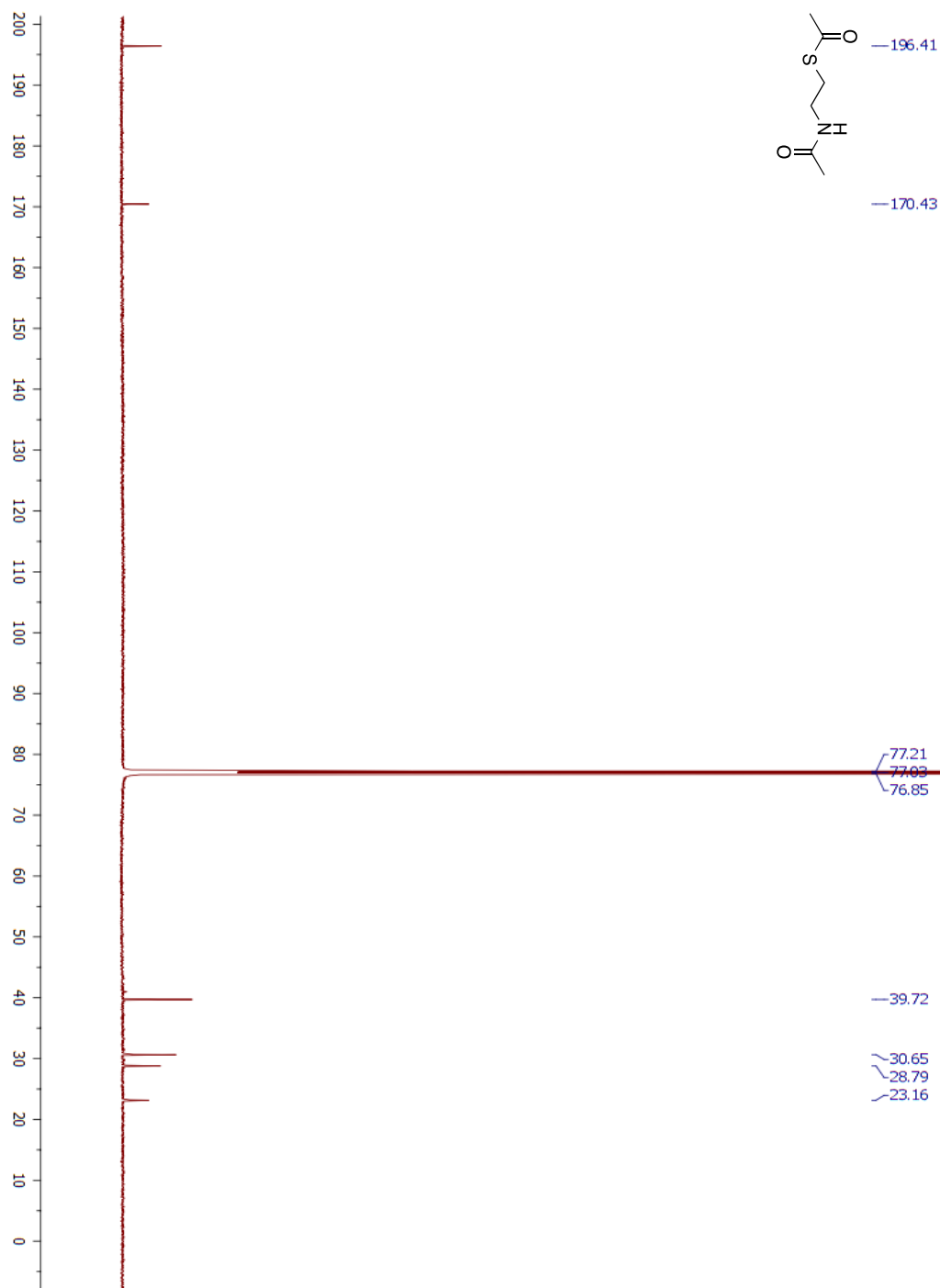
Appendix Figure 6.15. ^1H NMR (CDCl_3) spectrum of 6-MSA-SNAC.

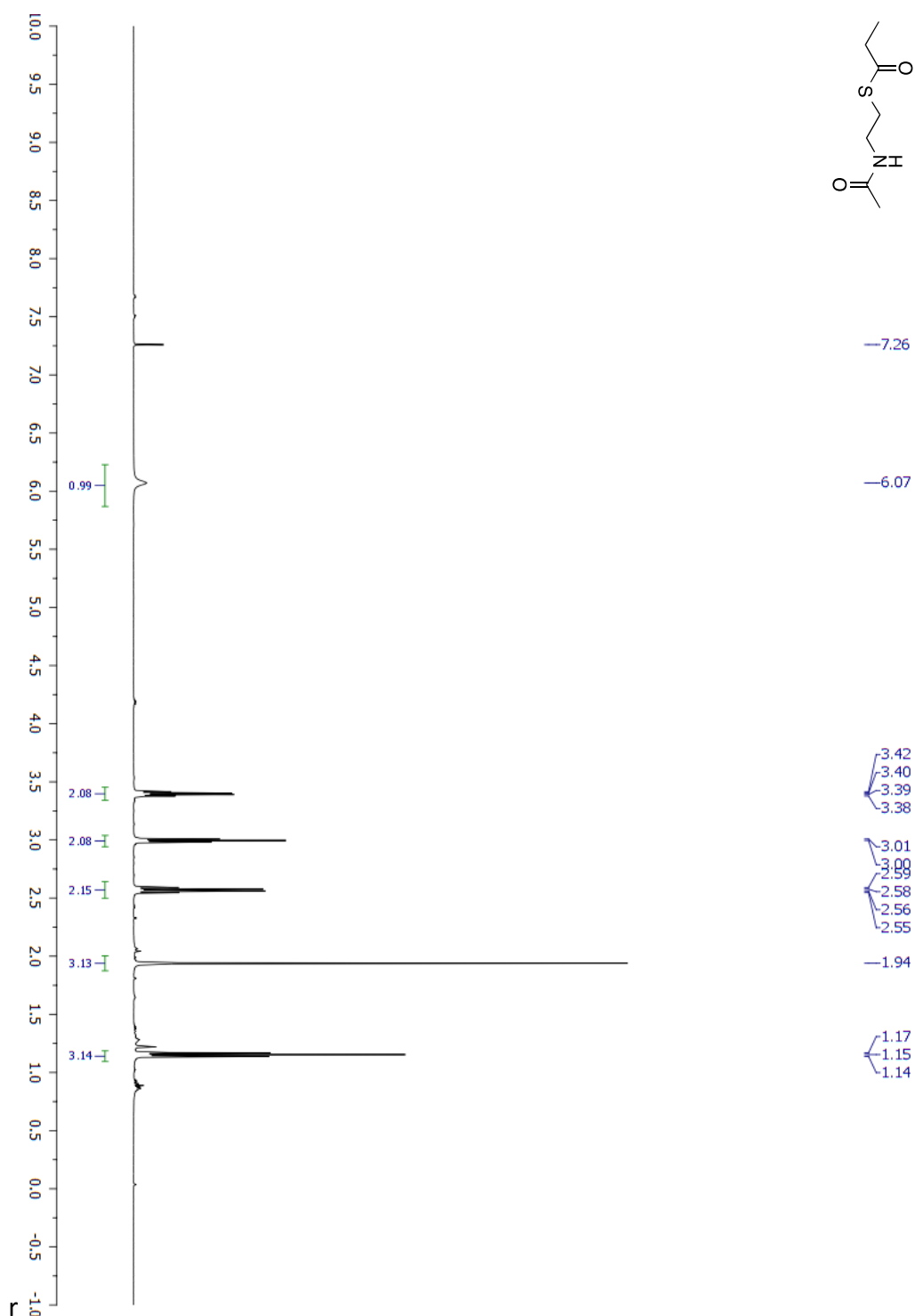
Appendix Figure 6.16. ^{13}C NMR (CDCl_3) spectrum of 6-MSA-SNAC



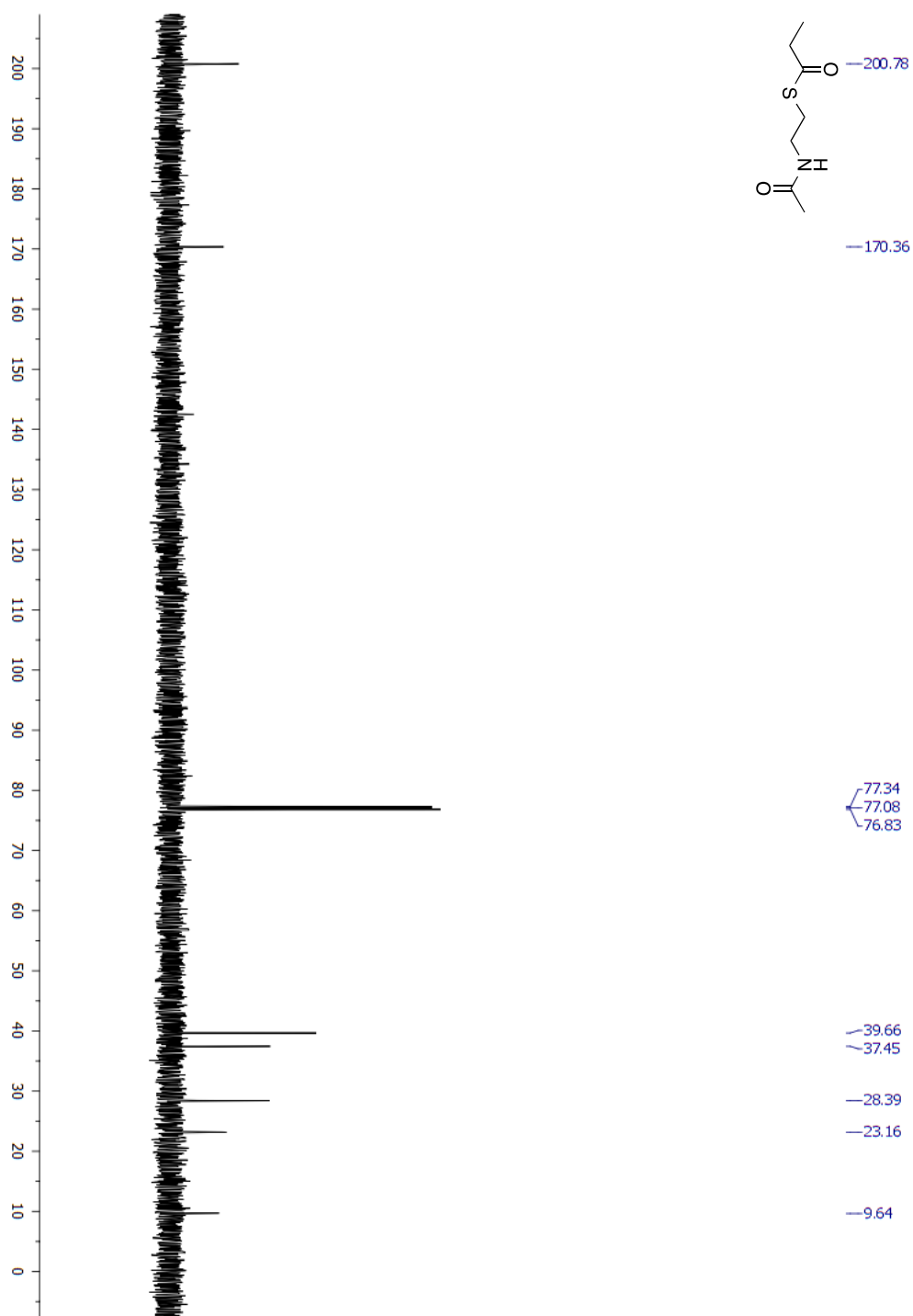
Appendix Figure 6.17. ^1H NMR (CDCl_3) spectrum of Acetyl-SNAC.

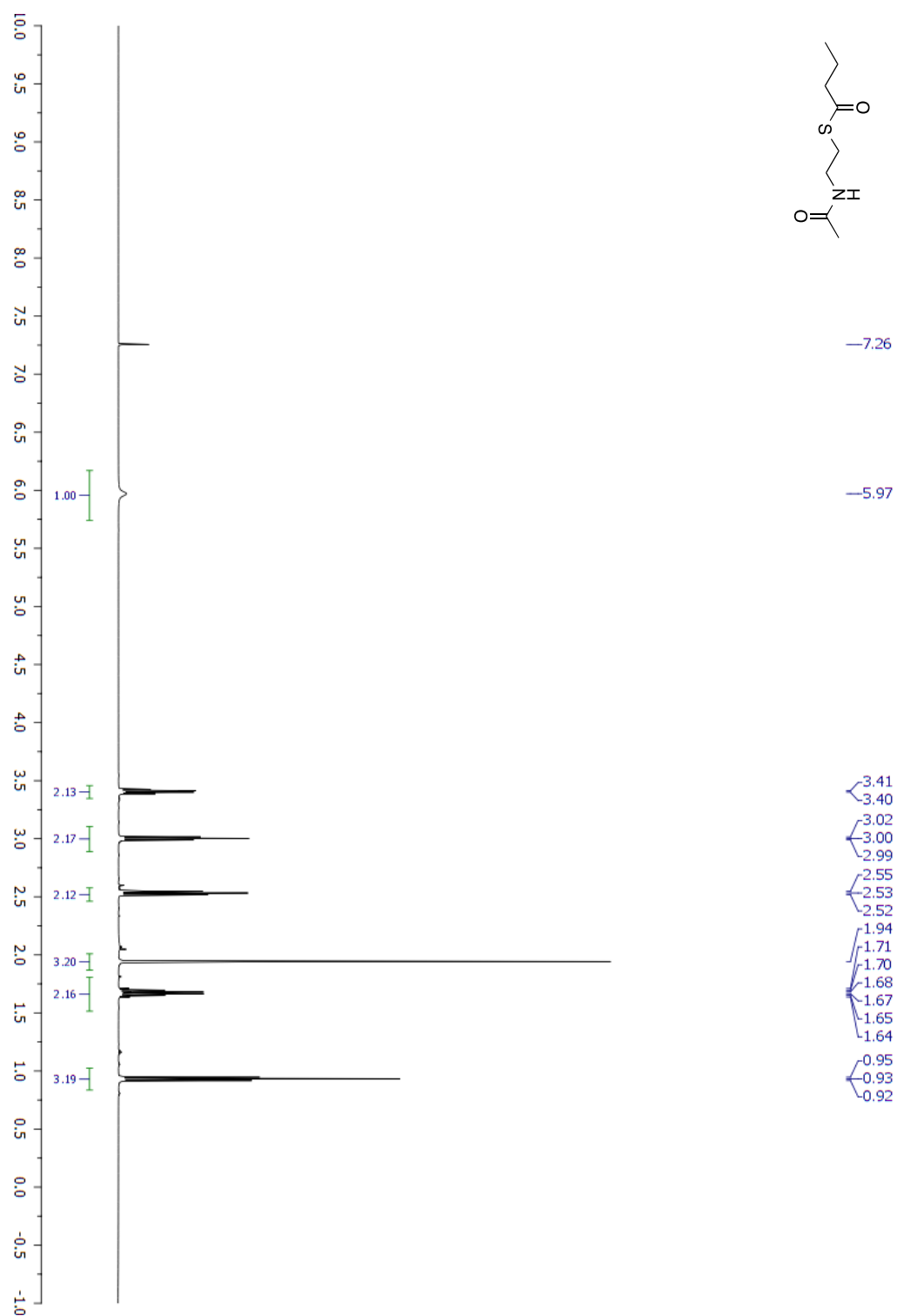
Appendix Figure 6.18. ^{13}C NMR (CDCl_3) spectrum of Acetyl-SNAC.

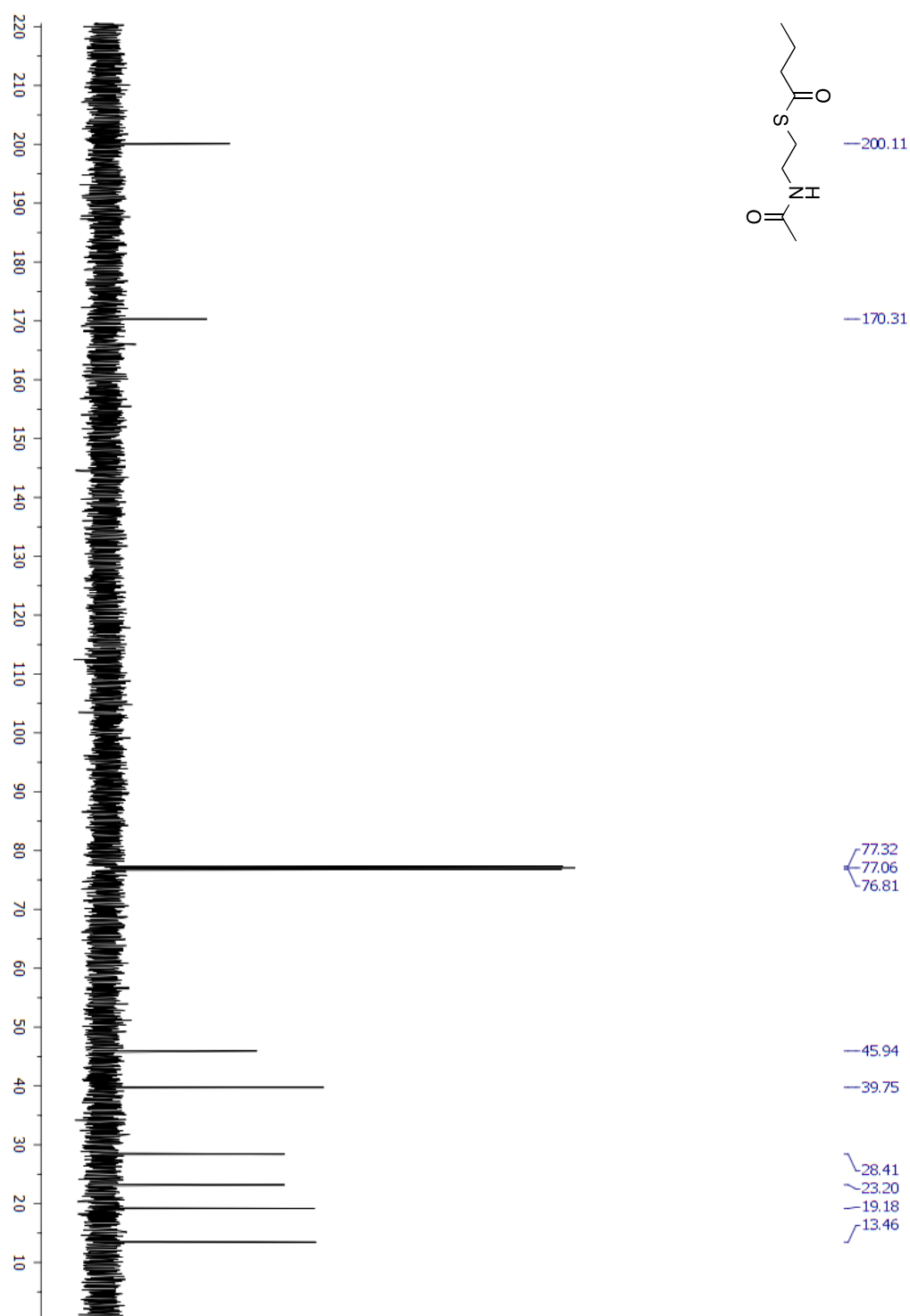


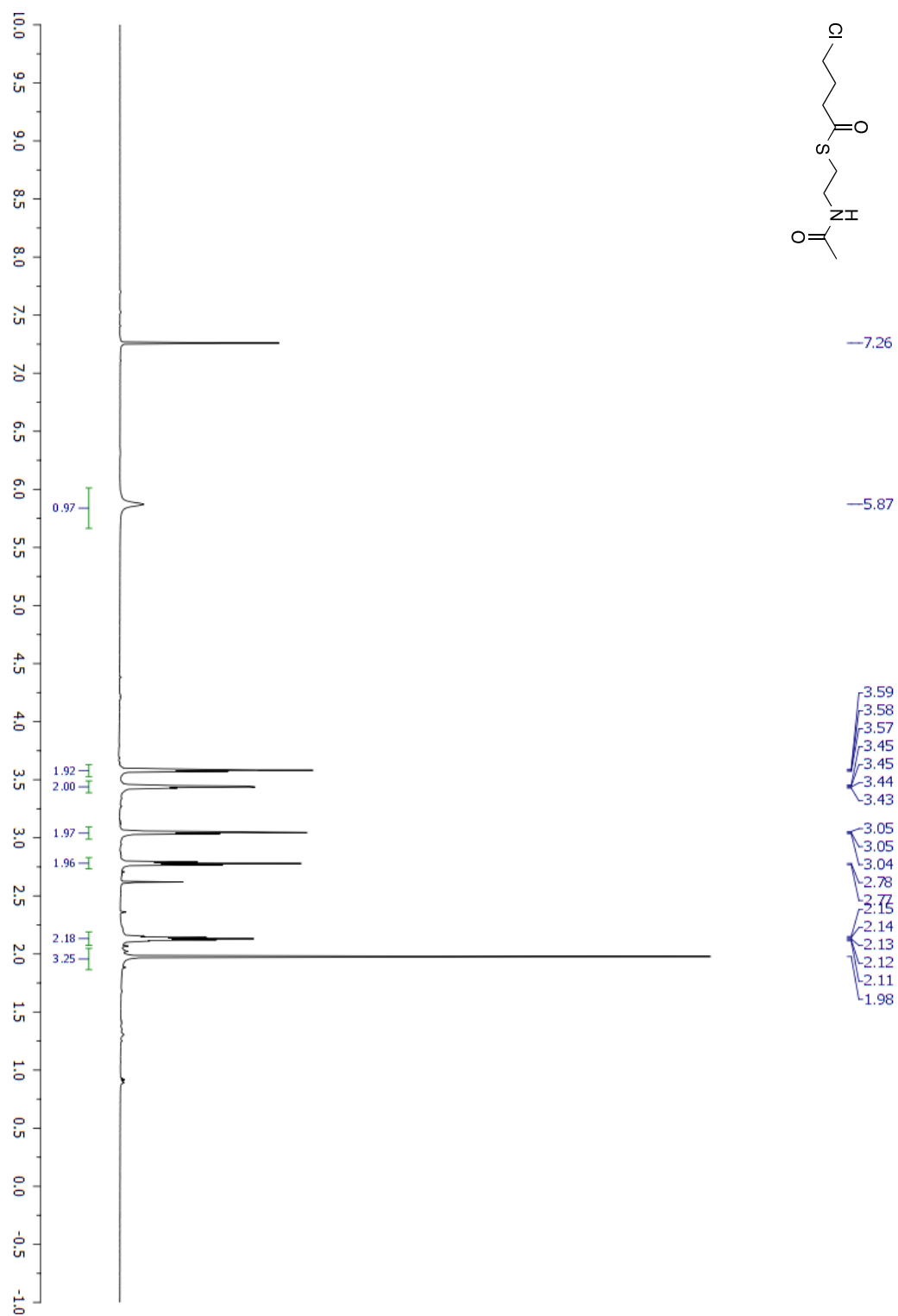
Appendix Figure 6.19.. ^1H NMR (CDCl_3) spectrum of propionyl-SNAC.

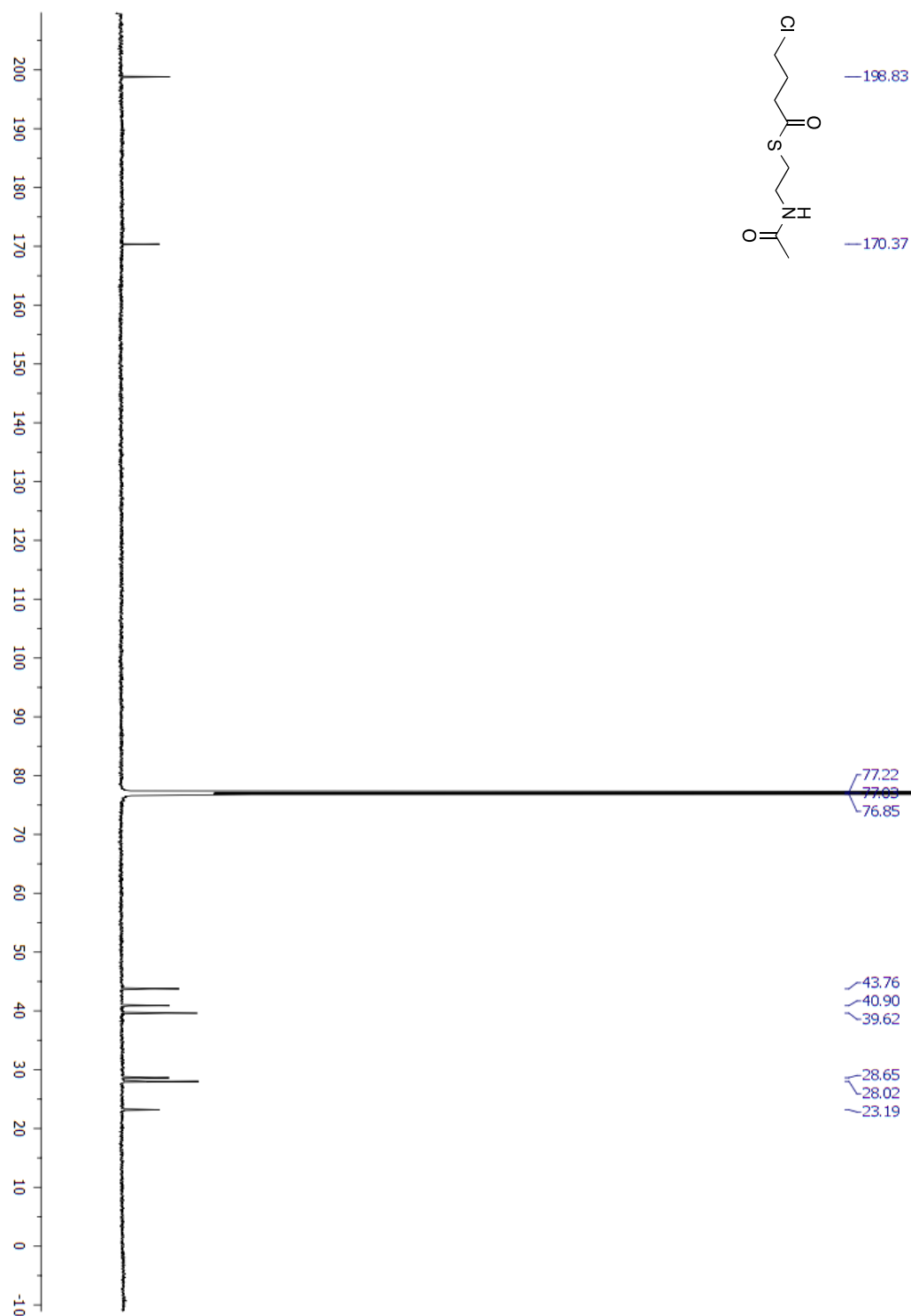
Appendix Figure 6.20. ^{13}C NMR (CDCl_3) spectrum of propionyl-SNAC.

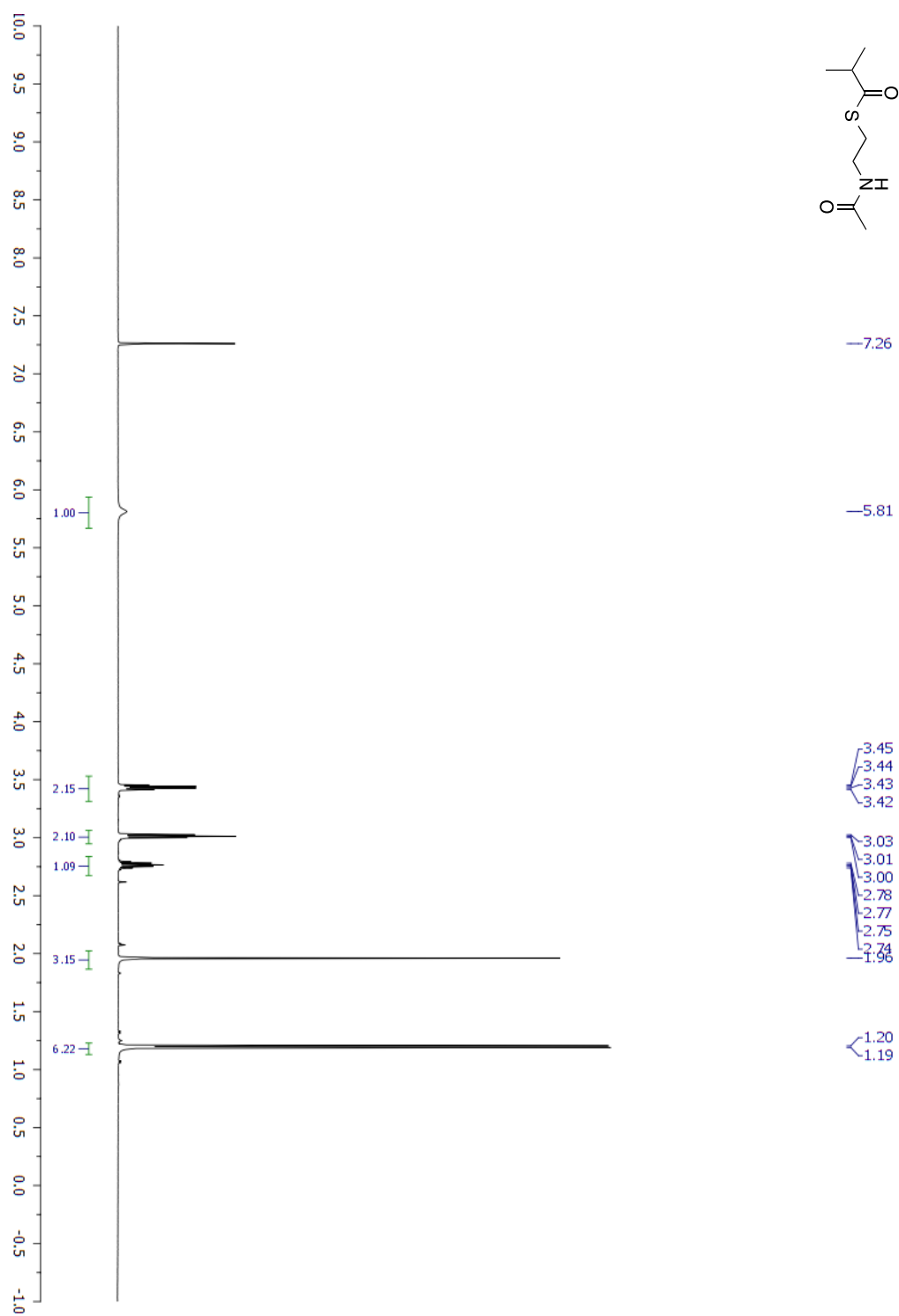


Appendix Figure 6.21. ^1H NMR (CDCl_3) spectrum of butyryl-SNAC.

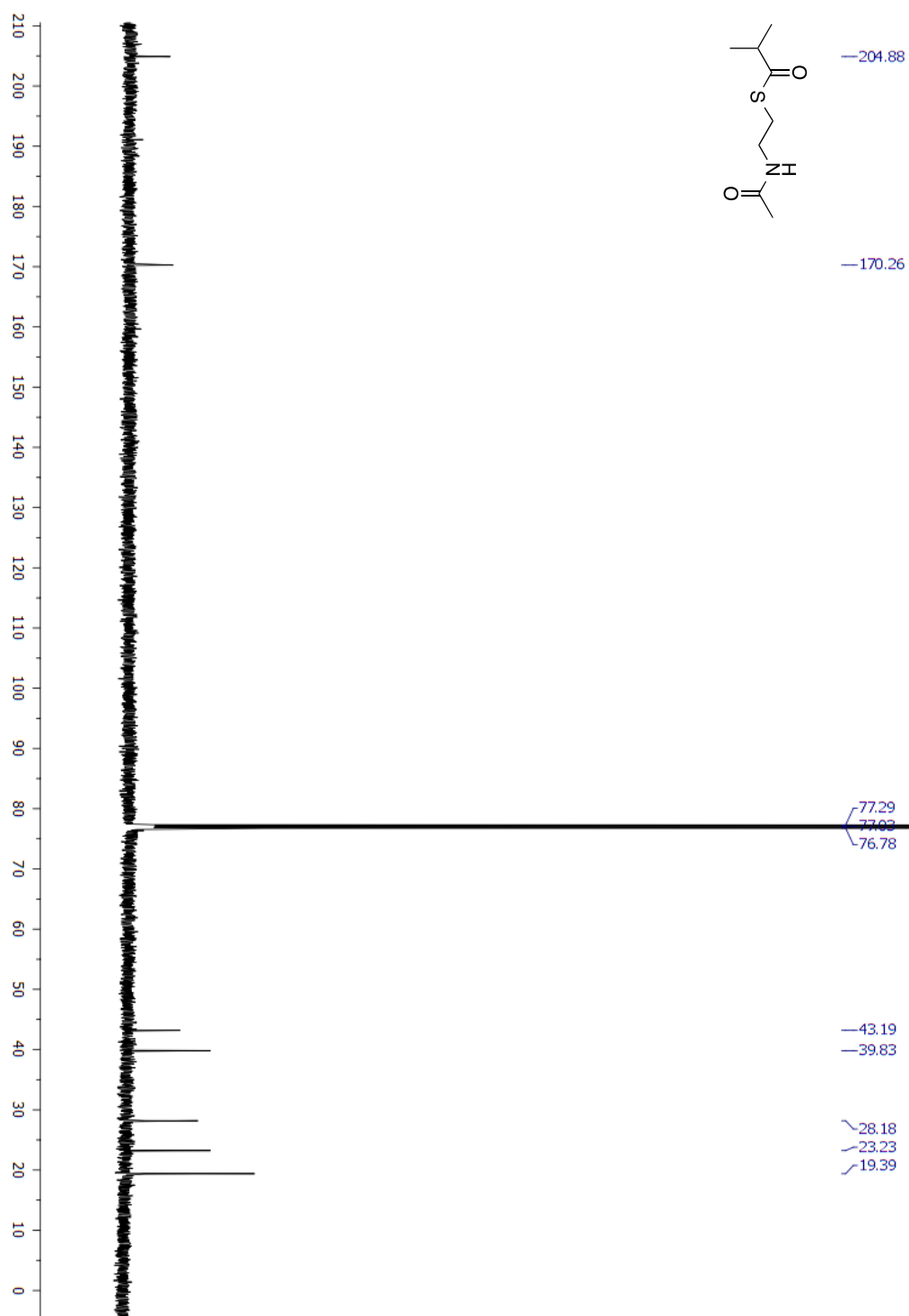
Appendix Figure 6.22. ^{13}C NMR (CDCl_3) spectrum of butyryl-SNAC.

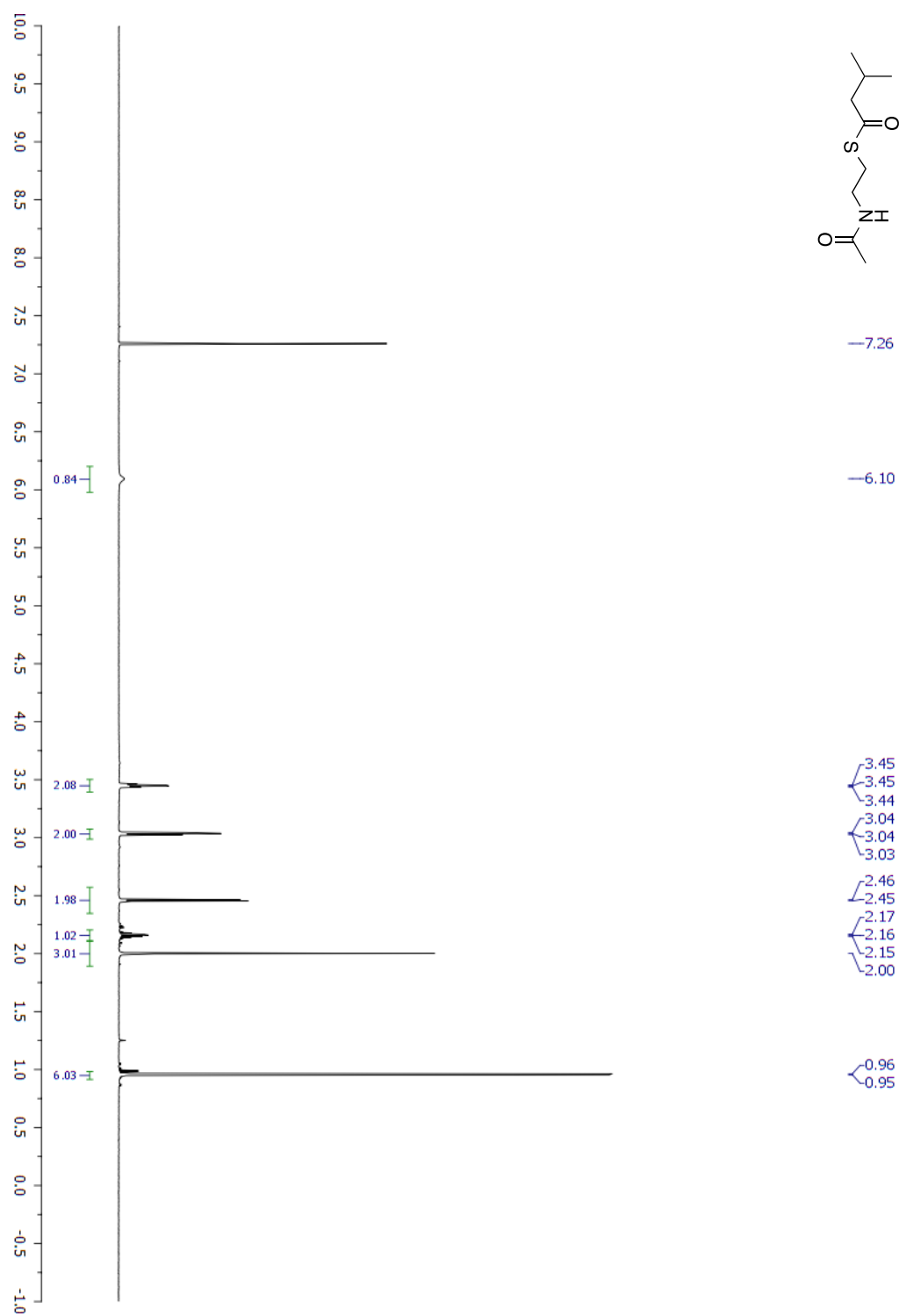
Appendix Figure 6.23 ^1H NMR (CDCl_3) spectrum of 4-chlorobutyl-SNAC

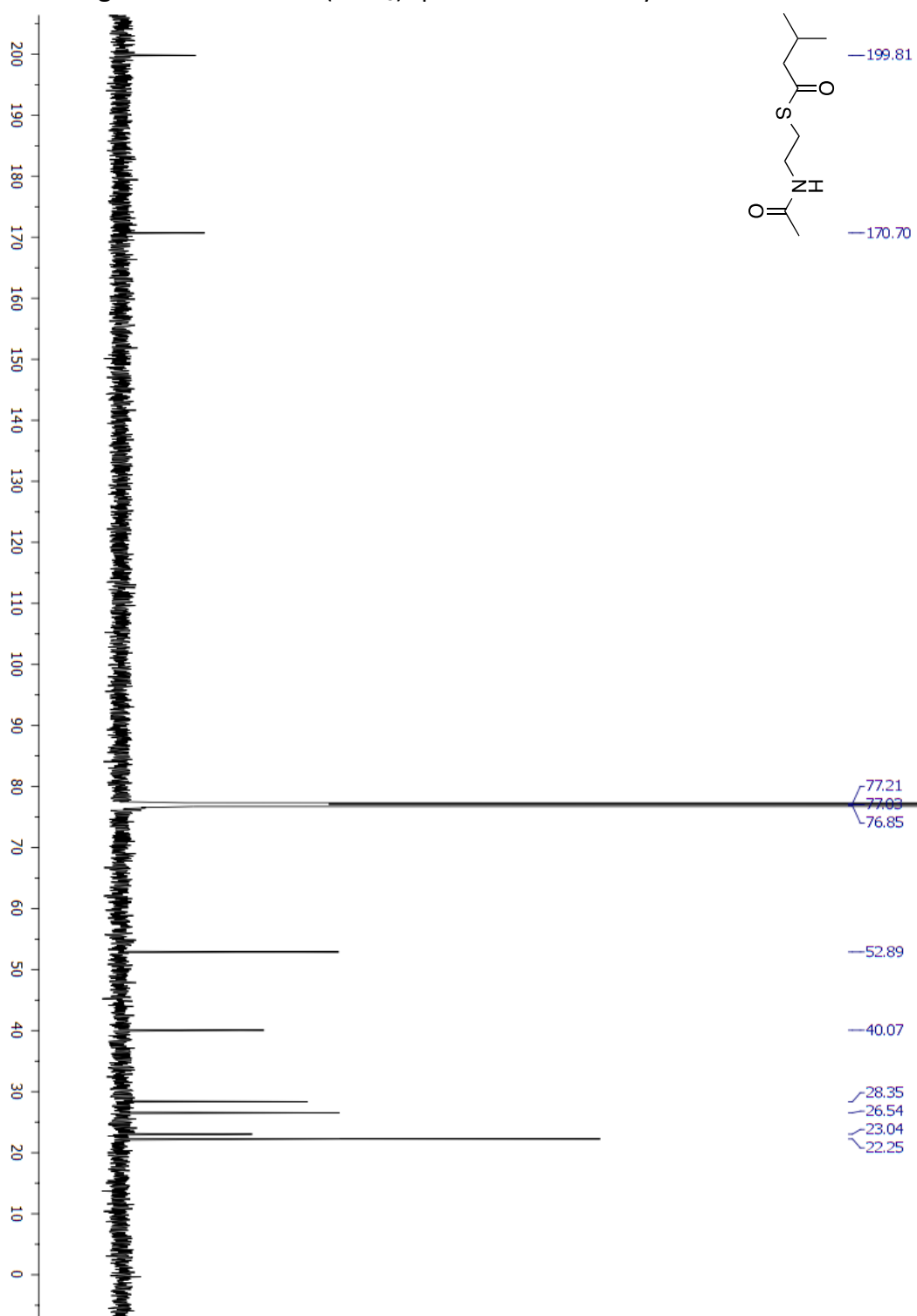
Appendix Figure 6.24. ^{13}C NMR (CDCl_3) spectrum of 4-chlorobutyryl-SNAC

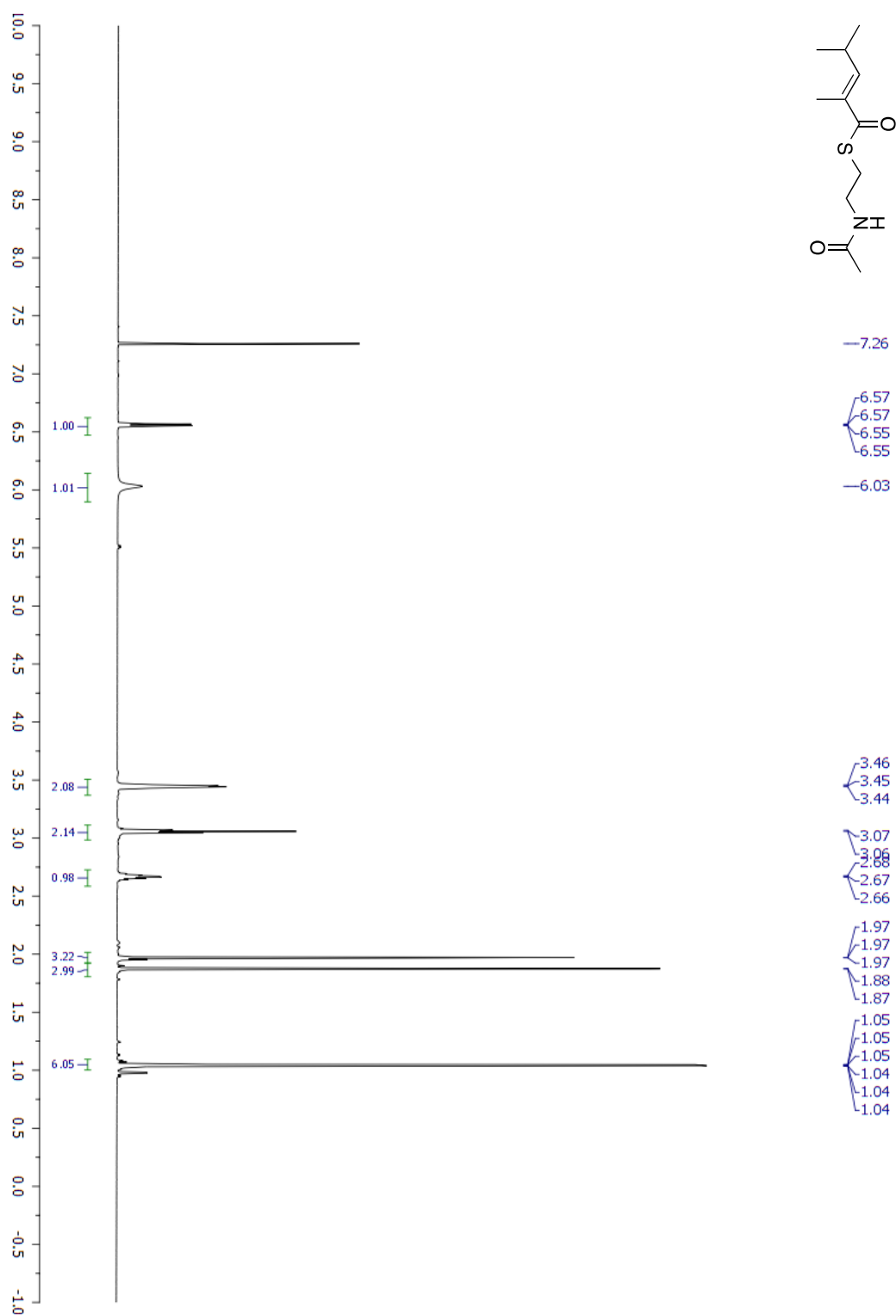
Appendix Figure 6.25. ^1H NMR (CDCl_3) spectrum of isobutyryl-SNAC

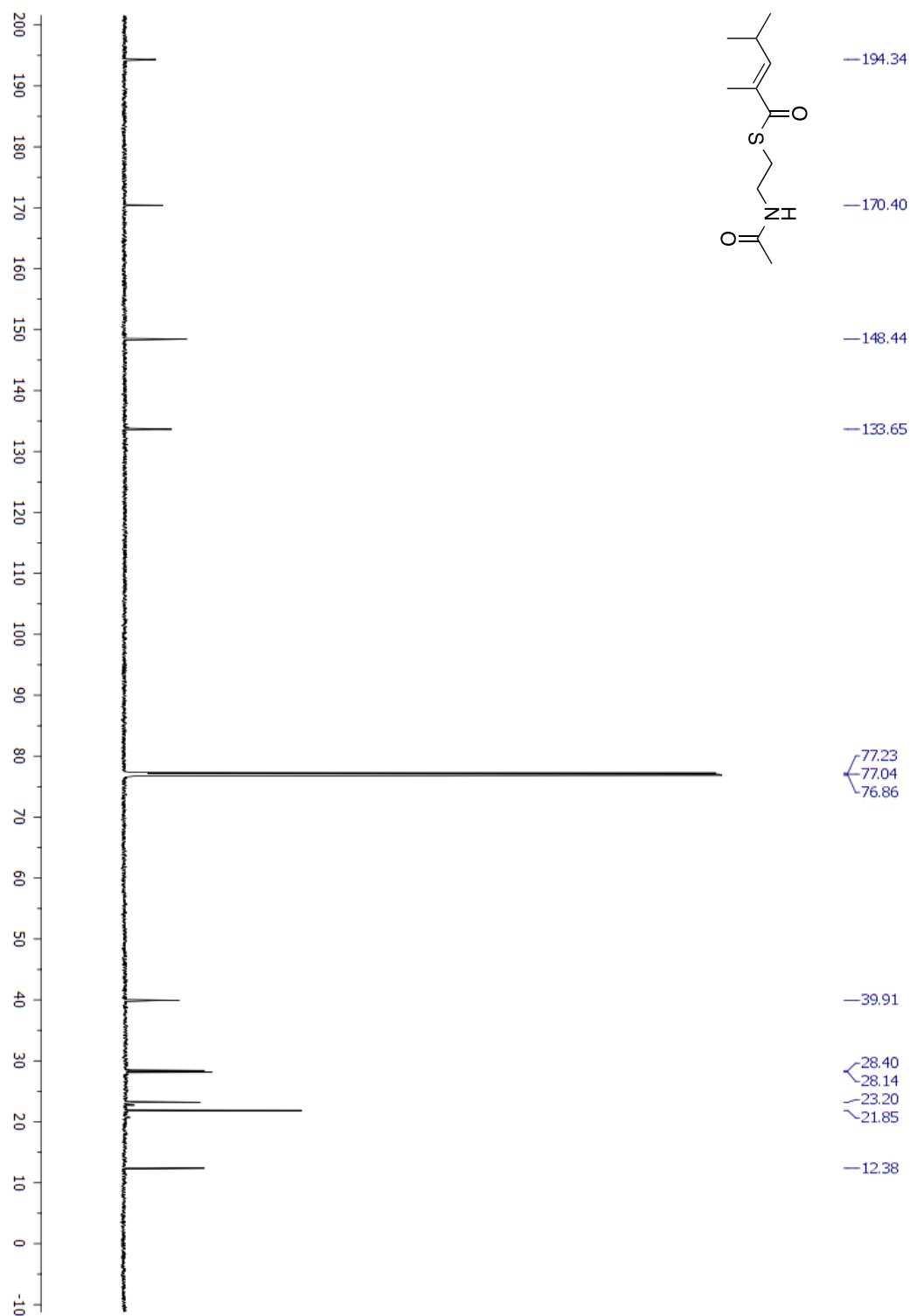
Appendix Figure 6.26. ^{13}C NMR (CDCl_3) spectrum of isobutyryl-SNAC.

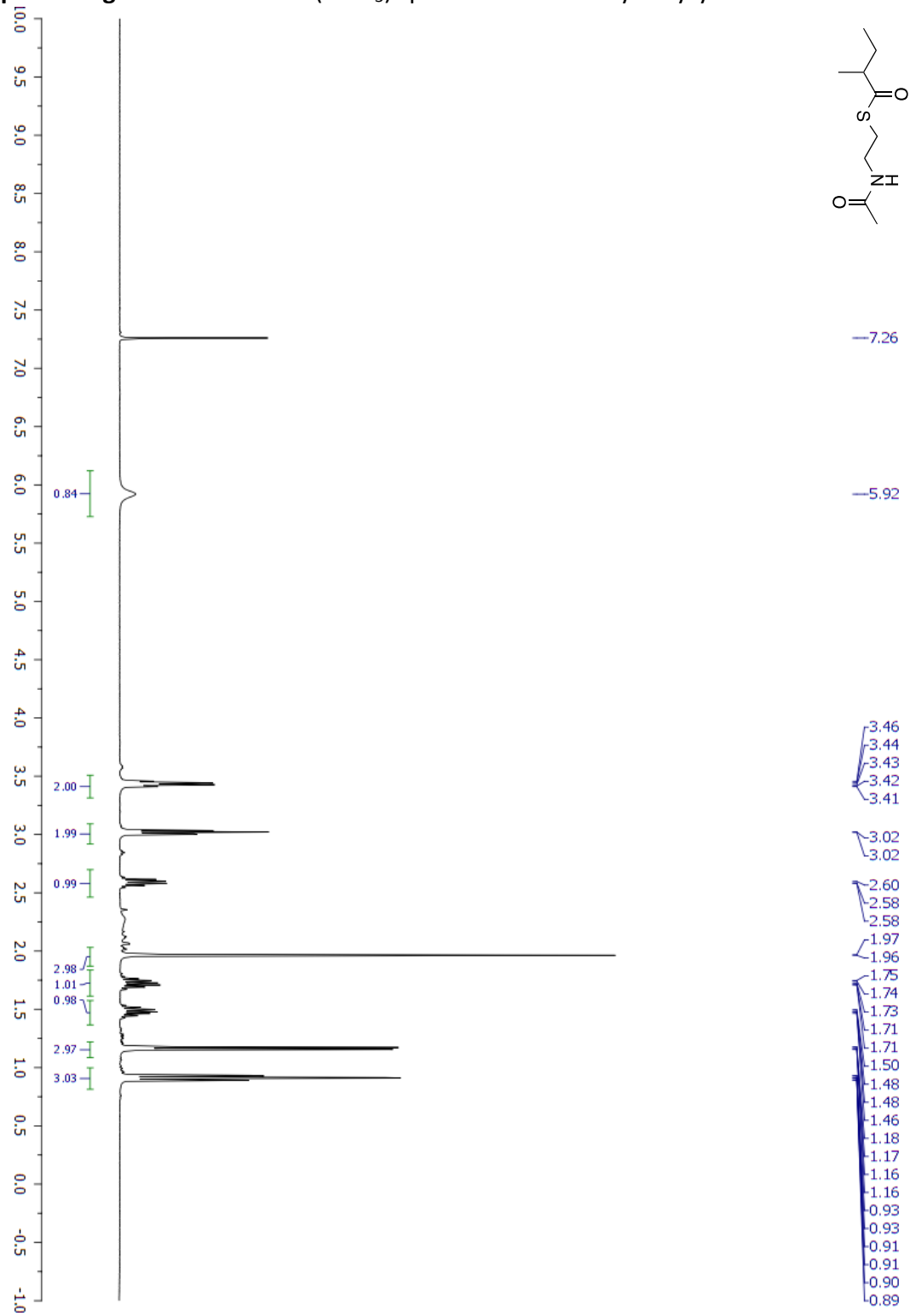


Appendix Figure 6.27. ^1H NMR (CDCl_3) spectrum of isovaleryl-SNAC.

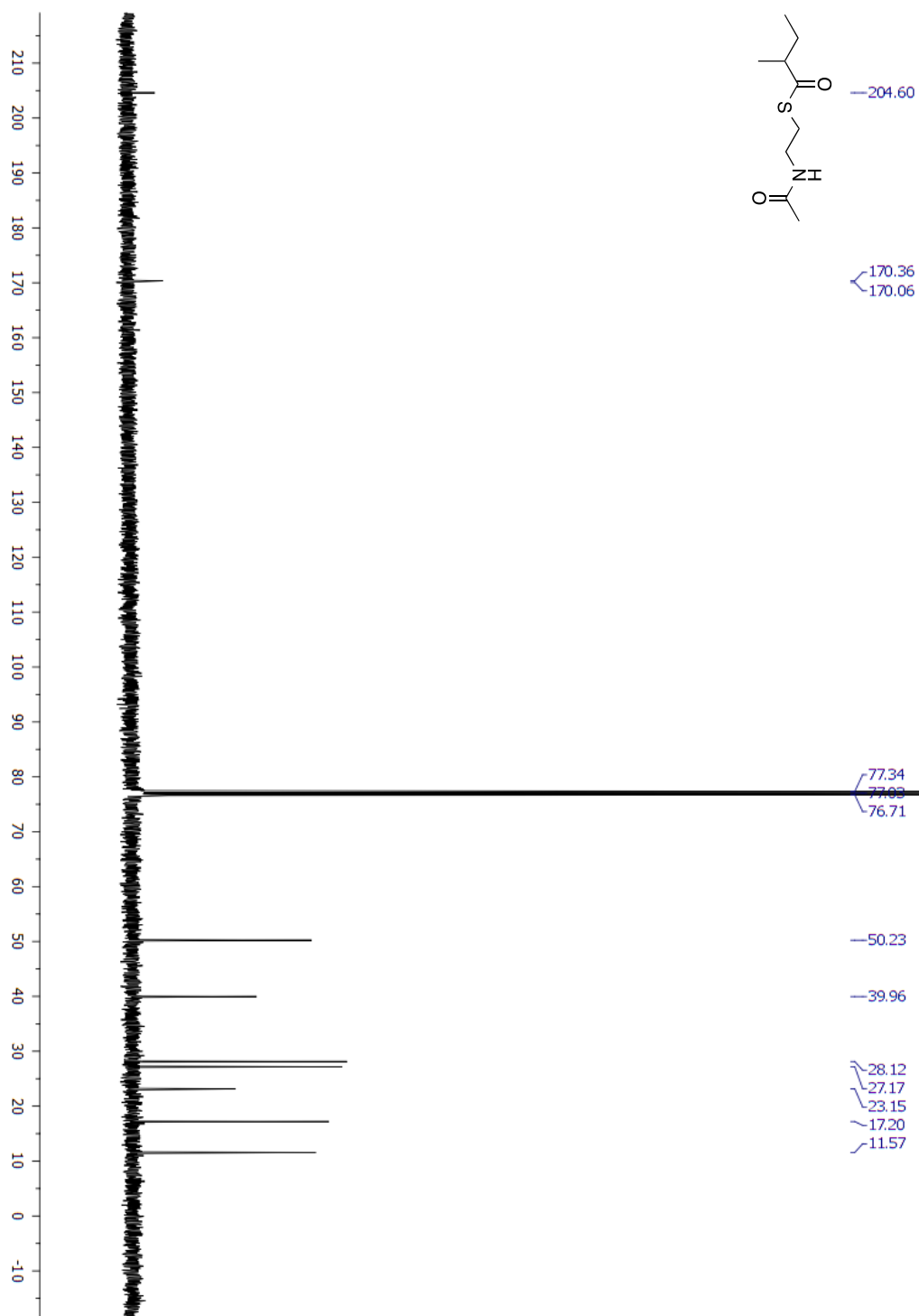
Appendix Figure 6.28. ^{13}C NMR (CDCl_3) spectrum of isovaleryl-SNAC

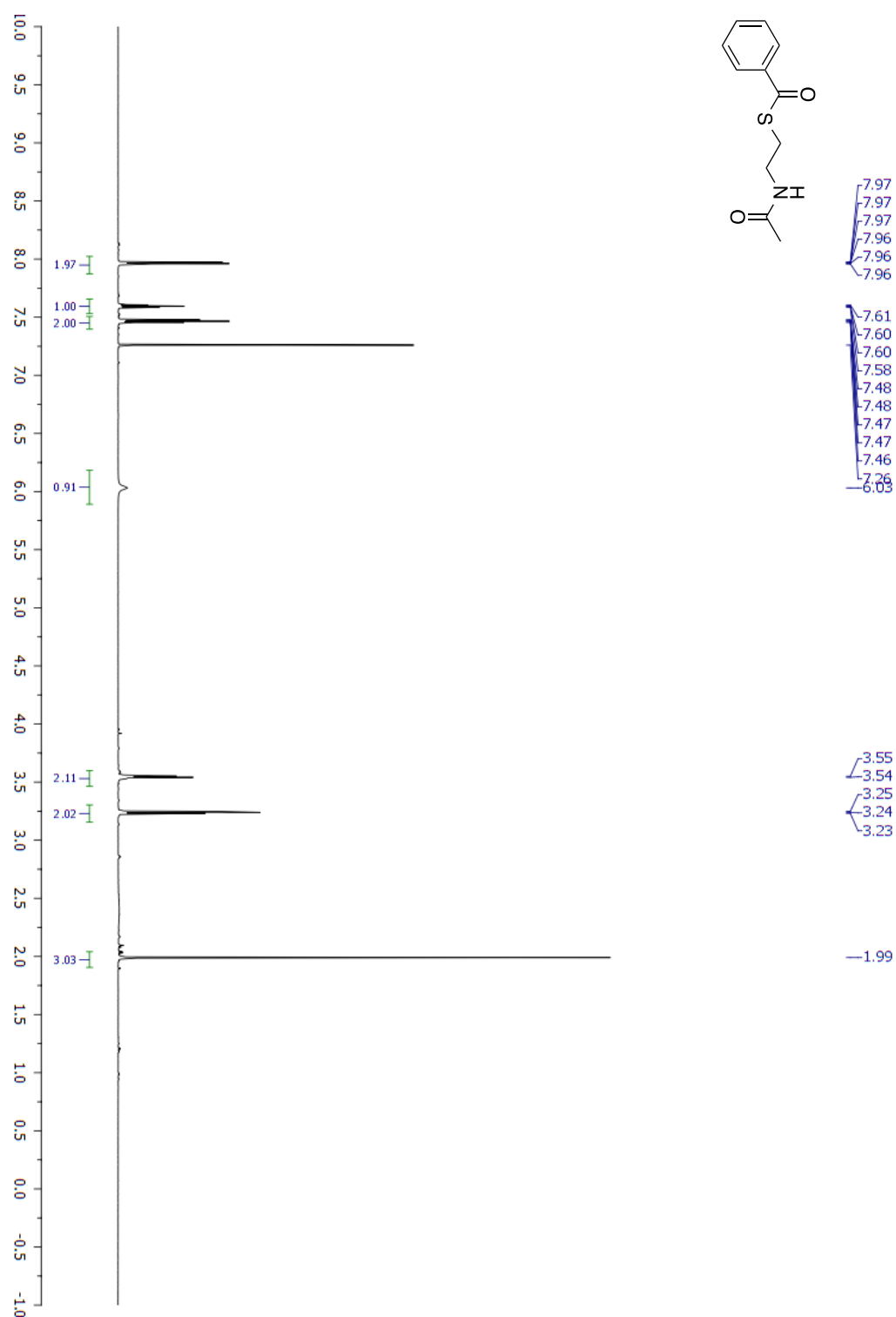
Appendix Figure 6.29. ^1H NMR (CDCl_3) spectrum of 2,4-dimethyl-2-pentenoyl-SNAC

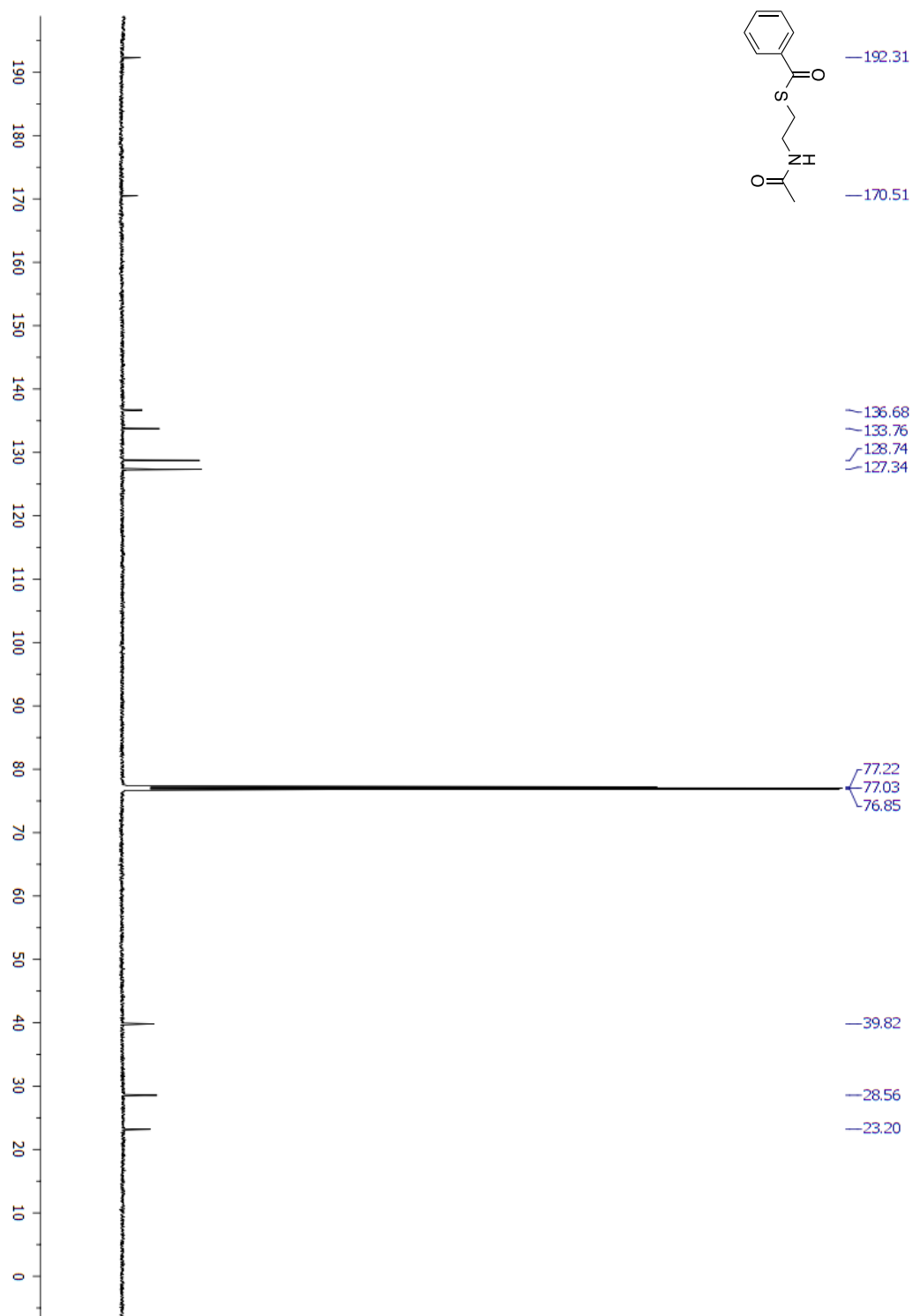
Appendix Figure 6.30. ^{13}C NMR (CDCl_3) spectrum of 2,4-dimethyl-2-pentenoyl-SNAC.

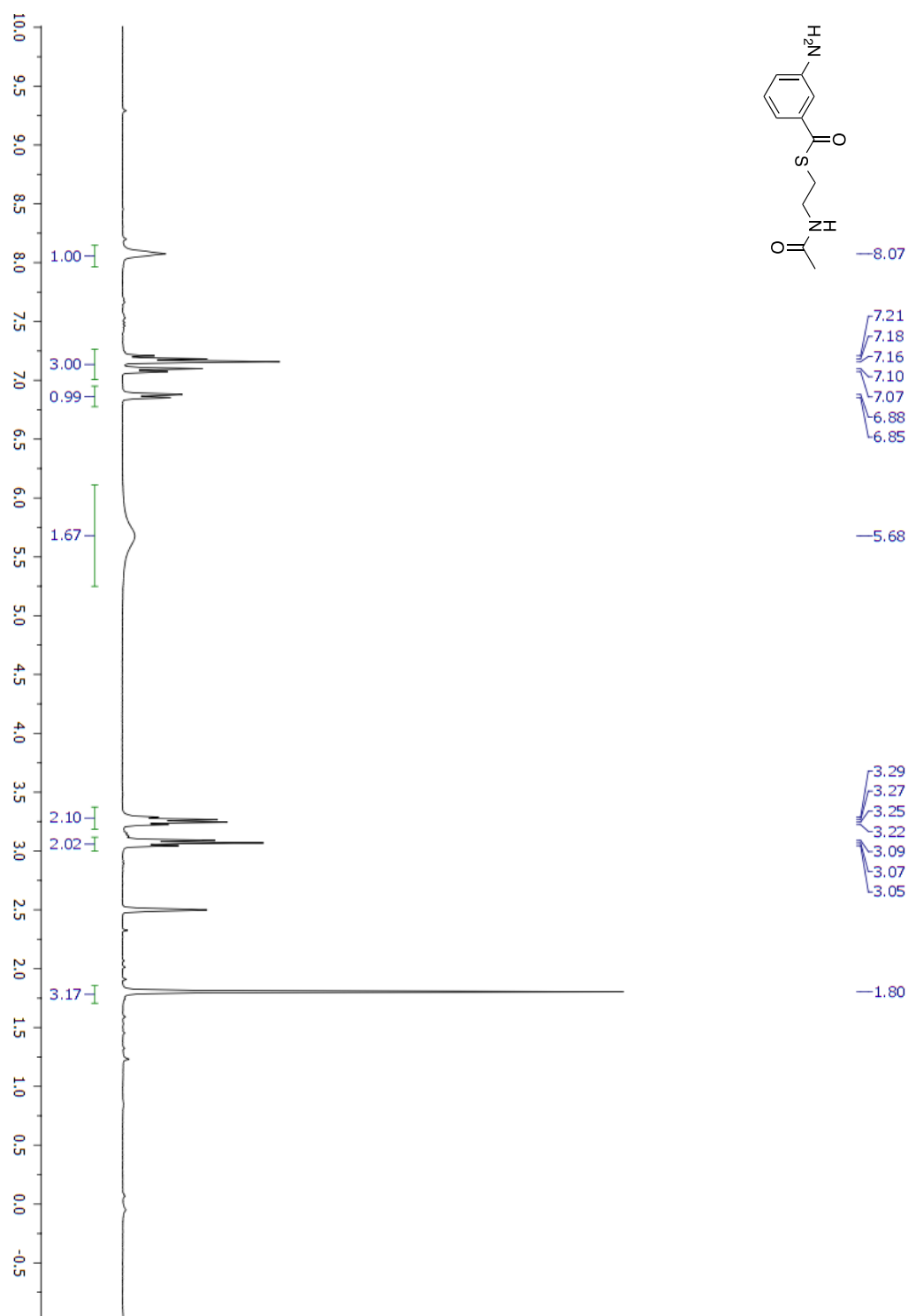
Appendix Figure 6.31. ^1H NMR (CDCl_3) spectrum of 2-methylbutyryl-SNAC

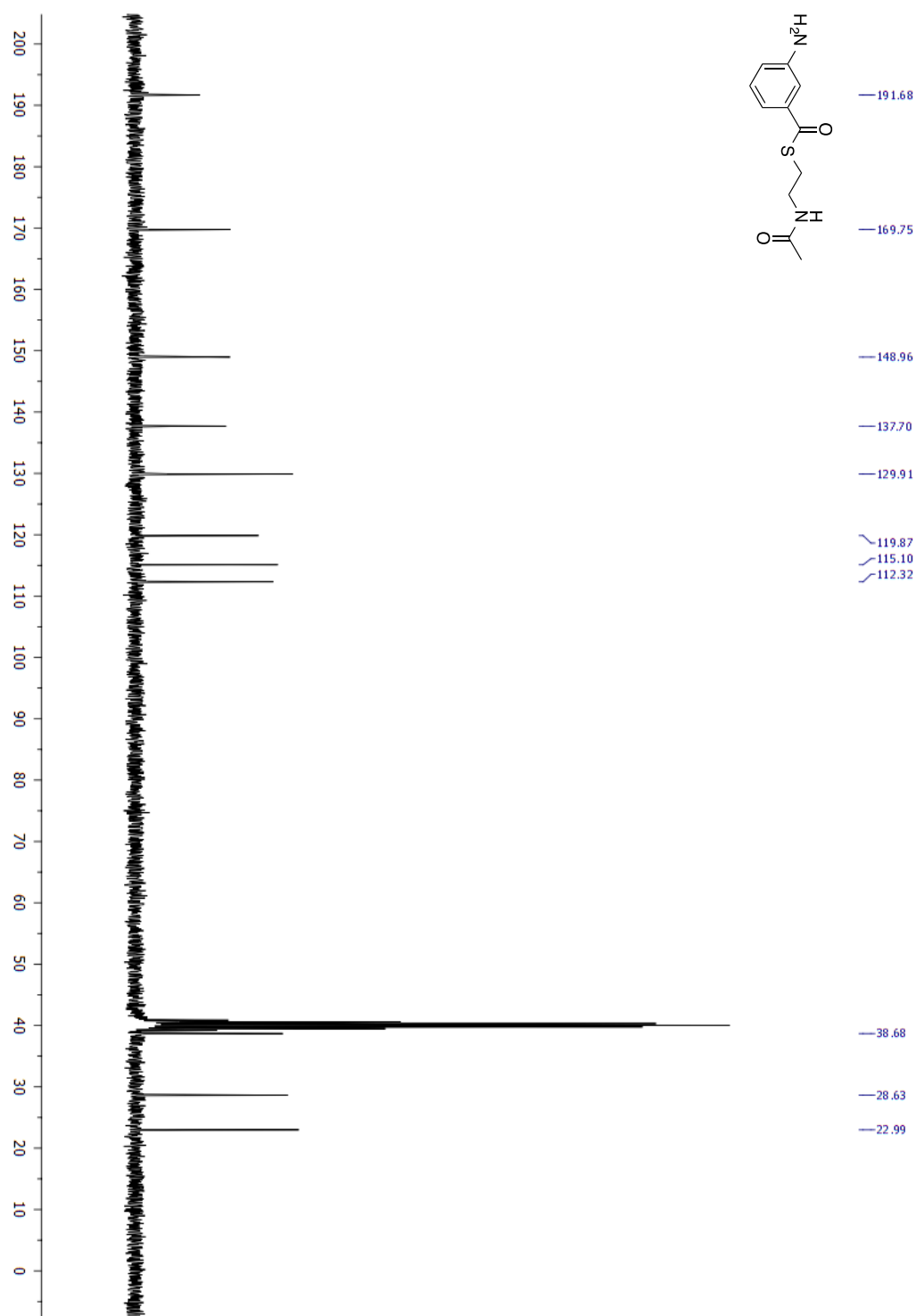
Appendix Figure 6.32. ^{13}C NMR (CDCl_3) spectrum of 2-methylbutyryl-SNAC.

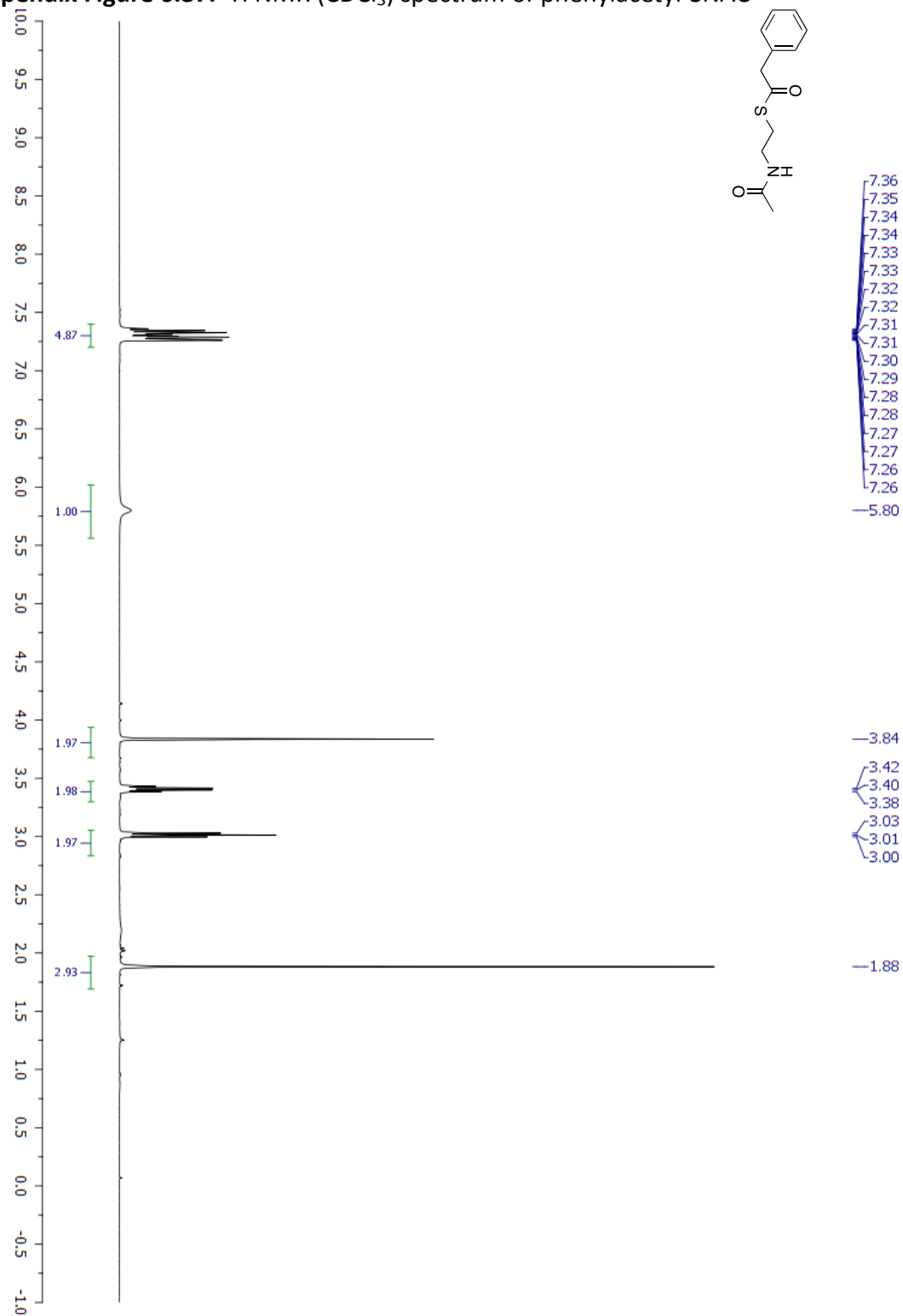


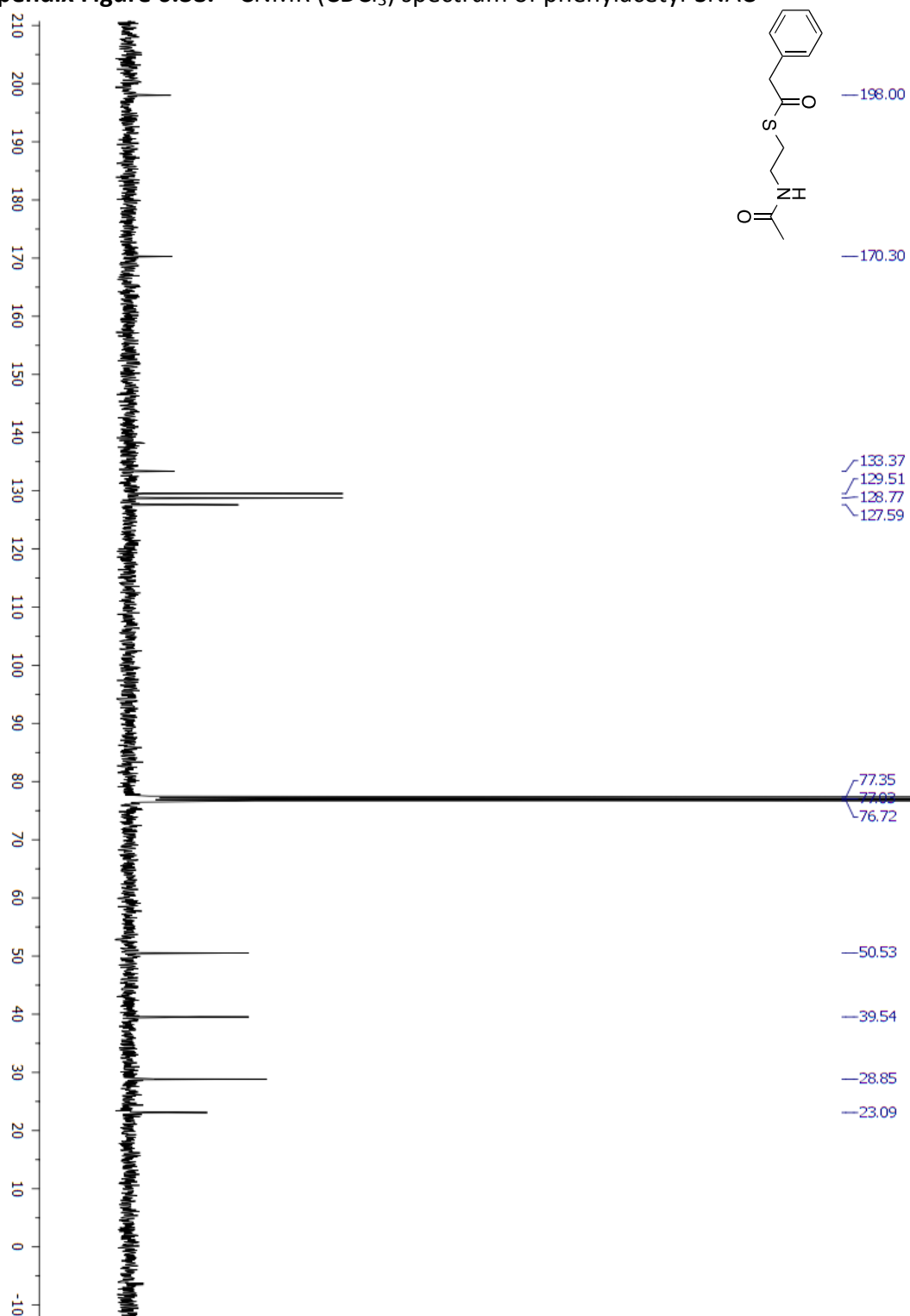
Appendix Figure 6.33. ^1H NMR (CDCl_3) spectrum of benzoyl-SNAC.

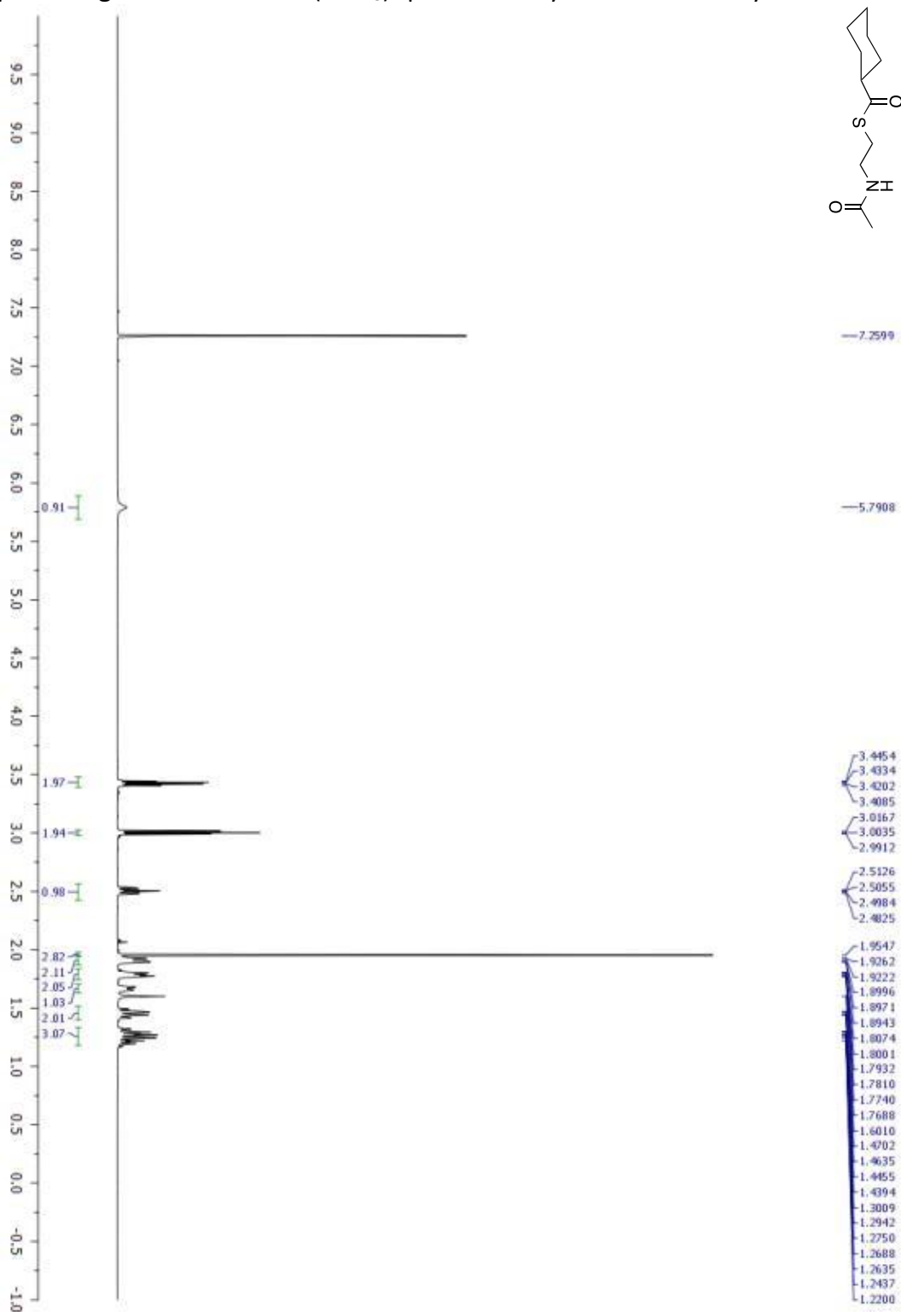
Appendix Figure 6.34. ^{13}C NMR (CDCl_3) spectrum of benzoyl-SNAC

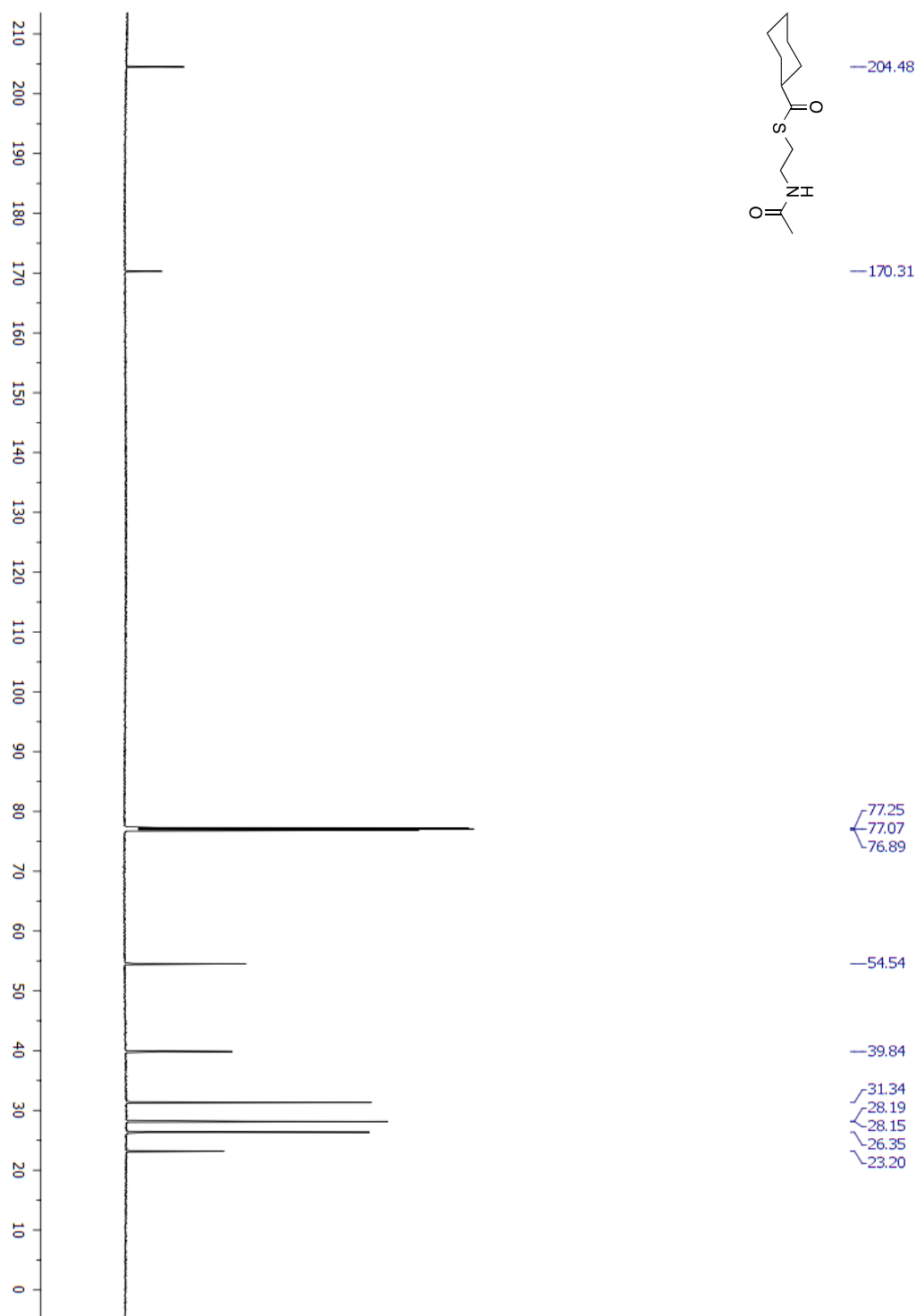
Appendix Figure 6.35. ^1H NMR (CDCl_3) spectrum of 3-aminobenzoyl-SNAC.

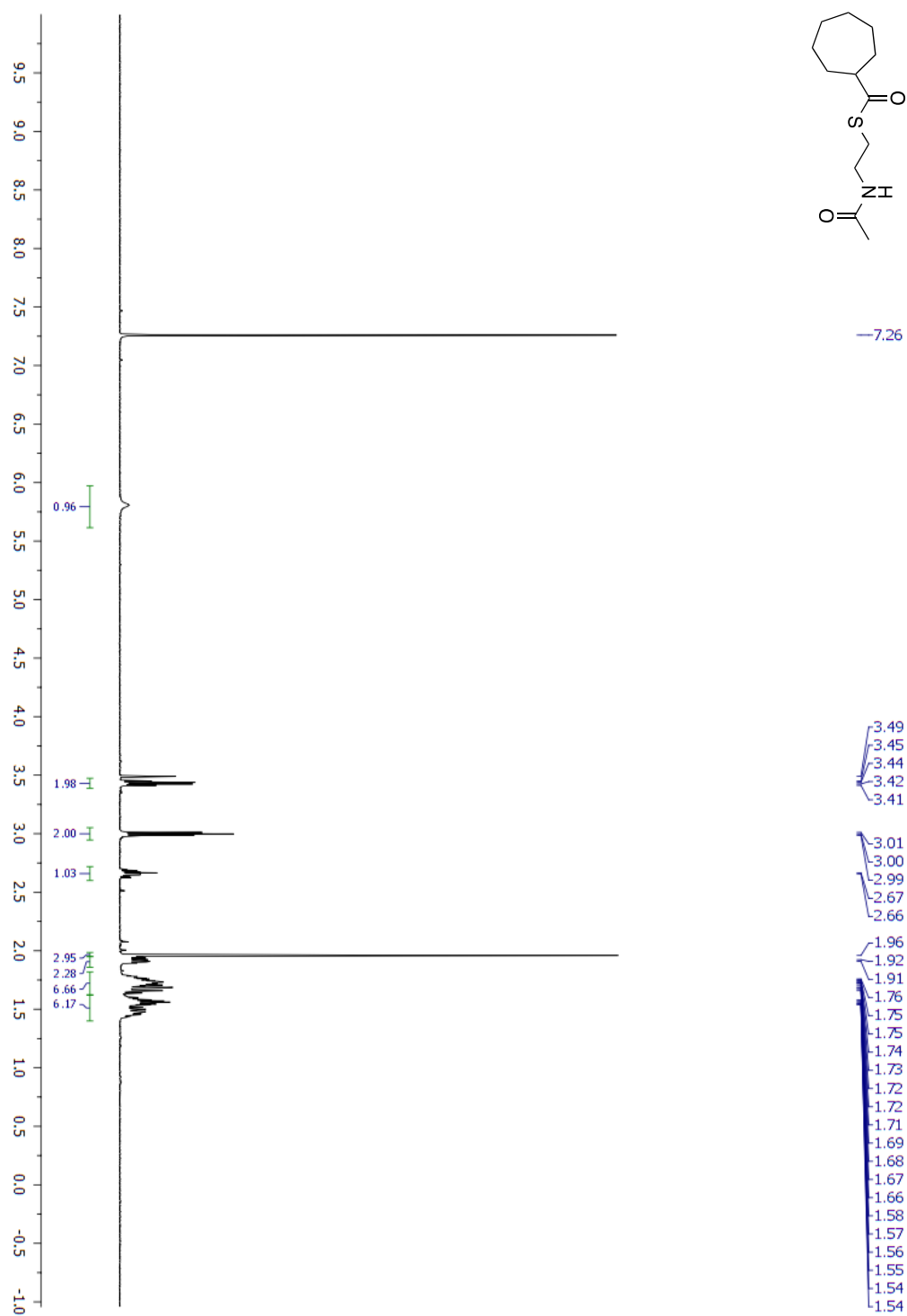
Appendix Figure 6.36. ^{13}C NMR (CDCl_3) spectrum of 3-aminobenzoyl-SNAC

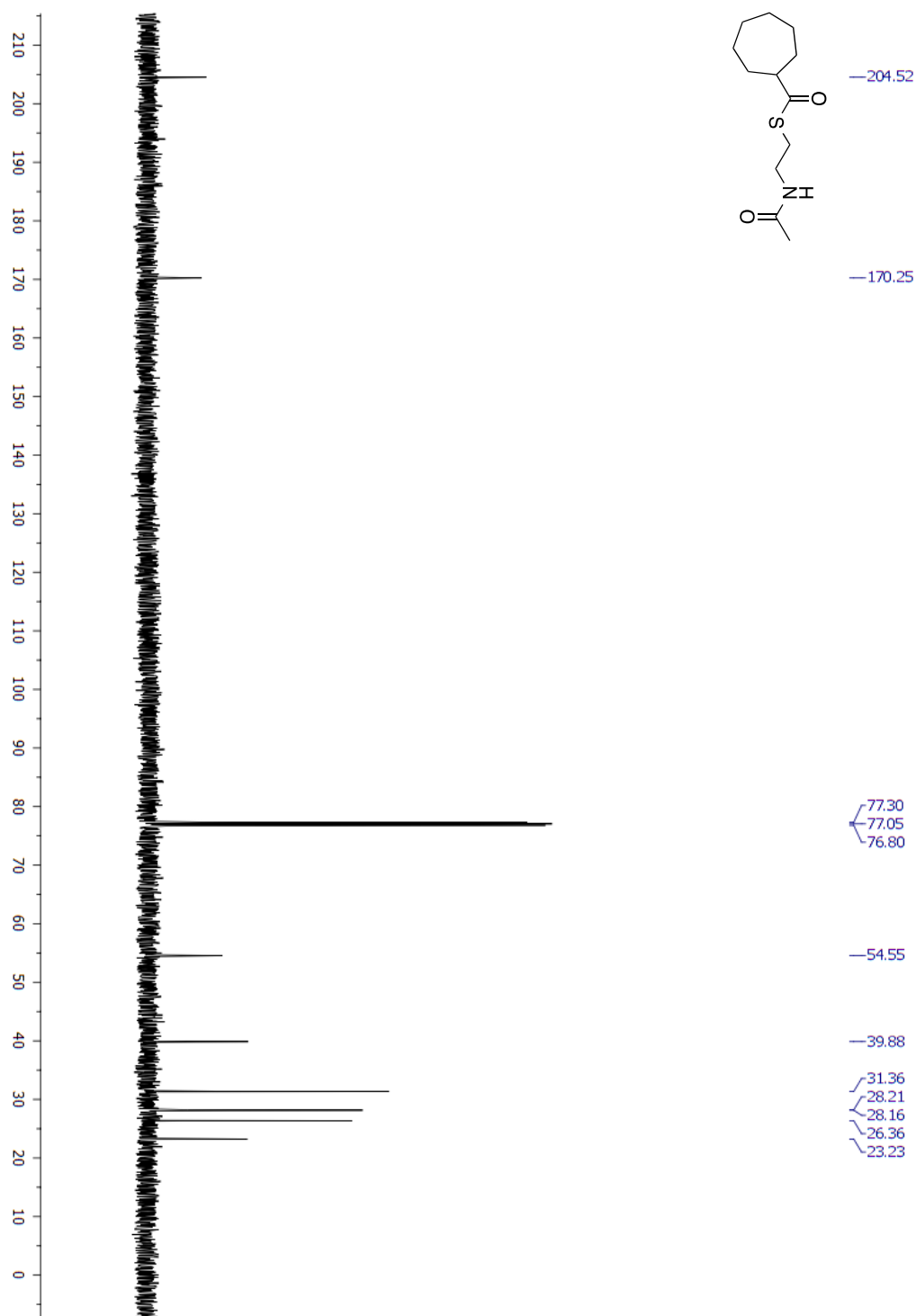
Appendix Figure 6.37. ^1H NMR (CDCl_3) spectrum of phenylacetyl-SNAC

Appendix Figure 6.38. ^{13}C NMR (CDCl_3) spectrum of phenylacetyl-SNAC

Appendix Figure 6.39. ^1H NMR (CDCl_3) spectrum of cyclohexanecarbonyl-SNAC

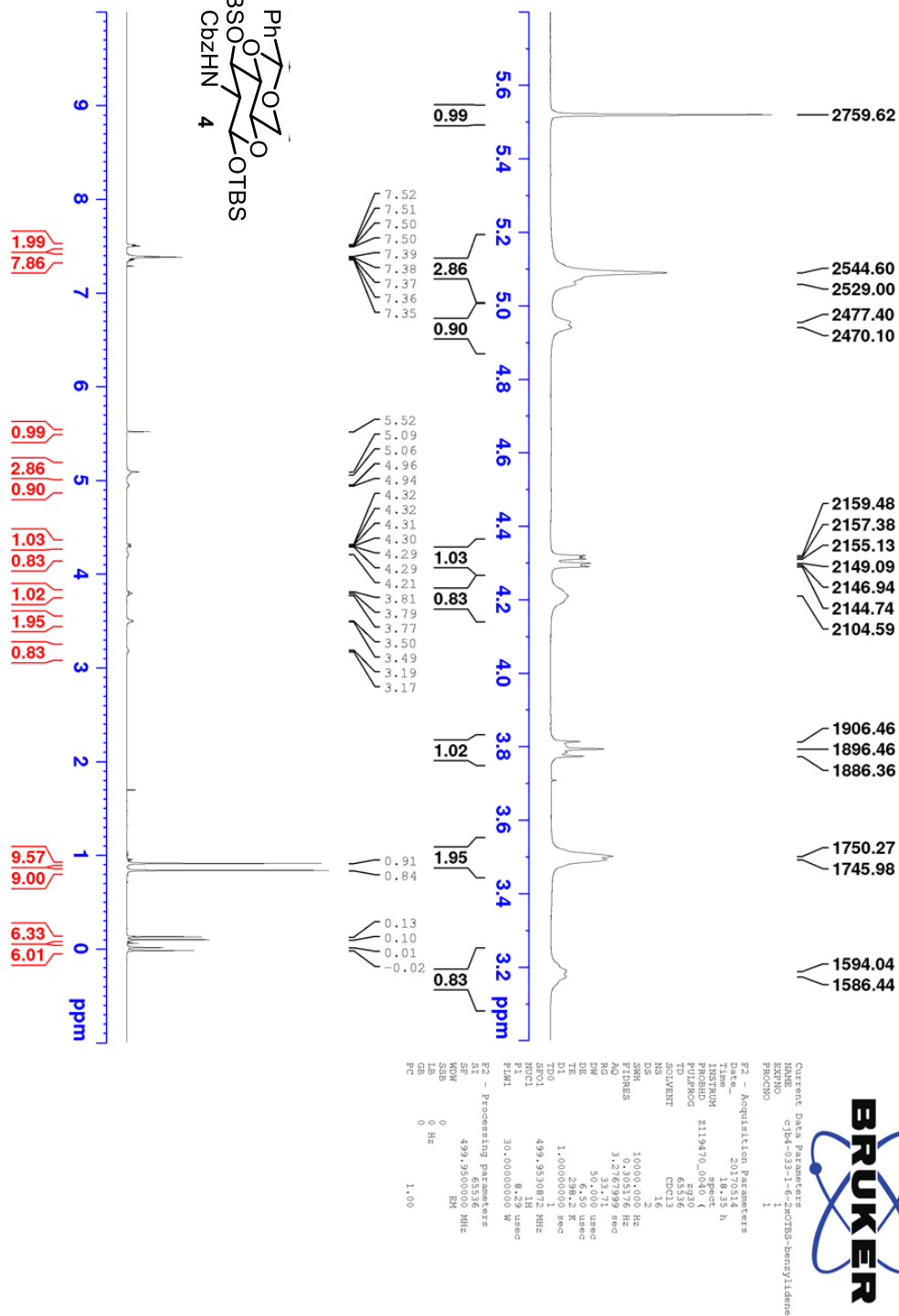
Appendix Figure 6.40. ^{13}C NMR (CDCl_3) spectrum of cyclohexanecarbonyl-SNAC.

Appendix Figure 6.41. ^1H NMR (CDCl_3) spectrum of cycloheptanecarbonyl-SNAC

Appendix Figure 6.42. ^{13}C NMR (CDCl_3) spectrum of cycloheptanecarbonyl-SNAC

6.3 Appendix C: Chapter 4 NMR Data

Chemical structure of compound **4** is shown, featuring a bicyclic core with a phenyl group (Ph) and a tert-butyldimethylsilyl (TBSO) group on one ring, and a tert-butyldimethylsilyl (OTBS) group and a chiral auxiliary (CbzHN) on the other ring.



95.7

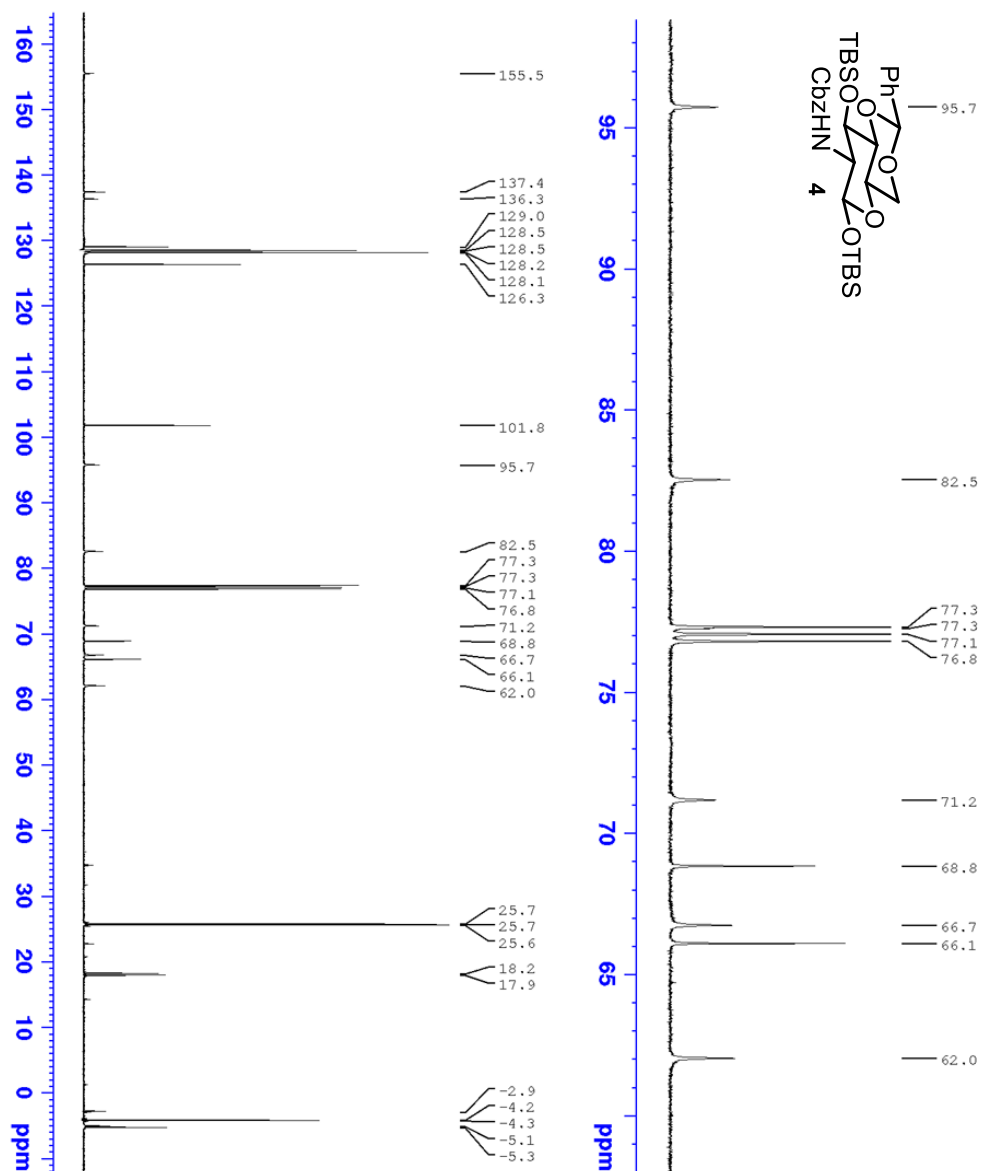
Ph

OTBS

OTBS

CbzHN

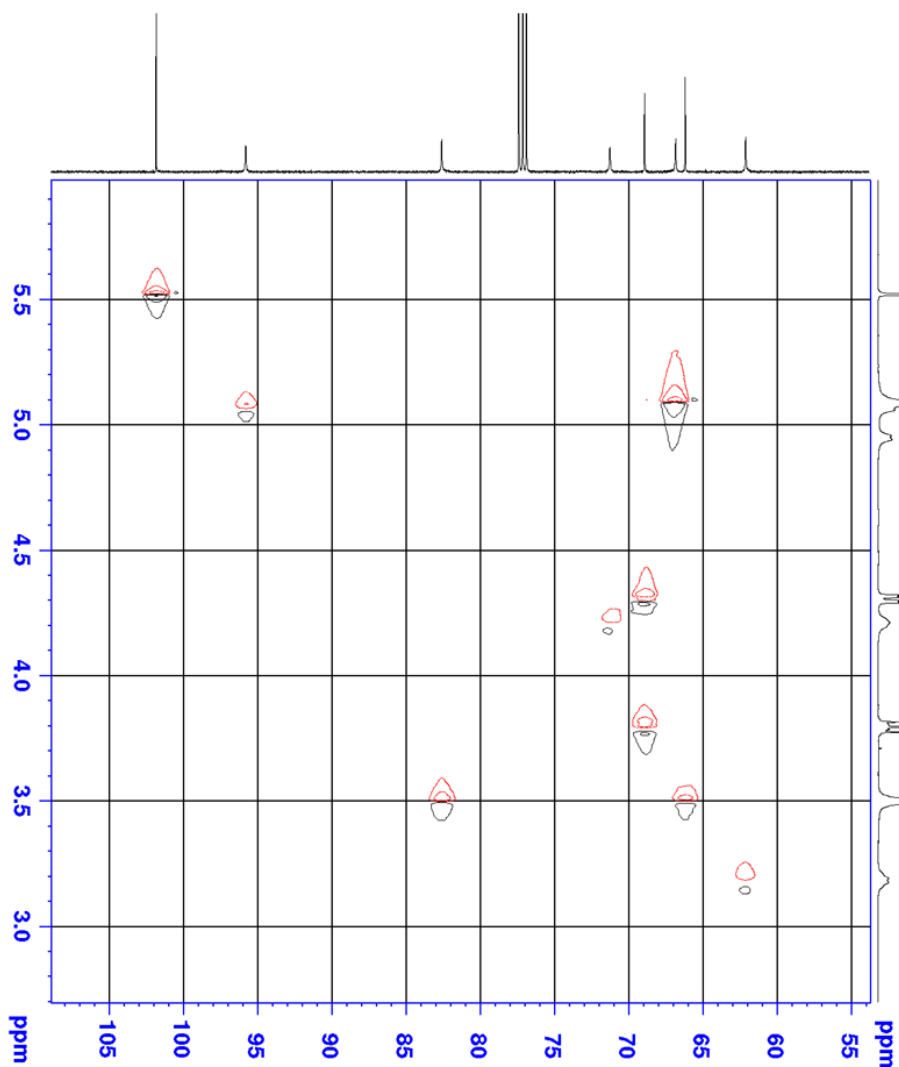
4



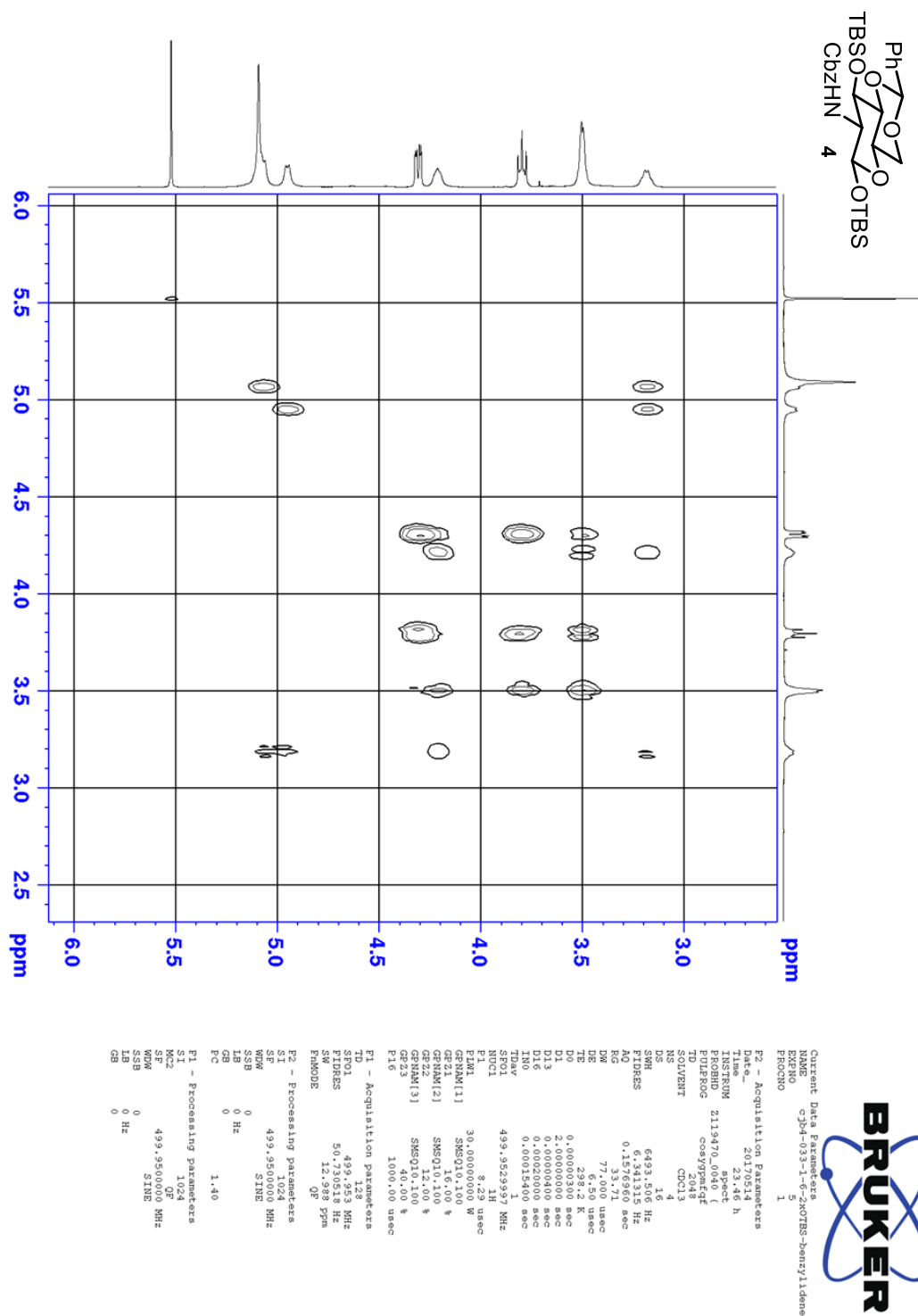
```

Current Data Parameters
=====
EXNO      C704-0351-6-2-NOTES-benzylidene
PROCMO    1
F2 - Acquisition Parameters
=====
Date_      20170514
Time       22:21 h
INSTRUM    spect
PULPROG    zgpg30
TD          65536
SOLVENT     CDCl3
NS          4004
DS          4
SWH         29761.904 Hz
FIDRES      0.206261 Hz
RG          1.190.98
RW          16.780 usec
DE          8.50 usec
TE          300.2 K
D1          2.00000000 sec
D11         0.03000000 sec
TD0         1
TDO         1
NUC1        13C
NUC2        13C
P1          125.725091 Hz
F1          100.62000000 W
F1A1        499.353121 Hz
DEPRGPRG2  waltz16
PCPD2       30.000000 usec
PCPD3       0.32514001 W
P1A12       0.15204900 W
P1A13       0
F2 - Processing Parameters
=====
SI          32768
SF          125.718275 MHz
WDW         EM
SSB          0
LB           0 Hz
GB           0
PC           1.40

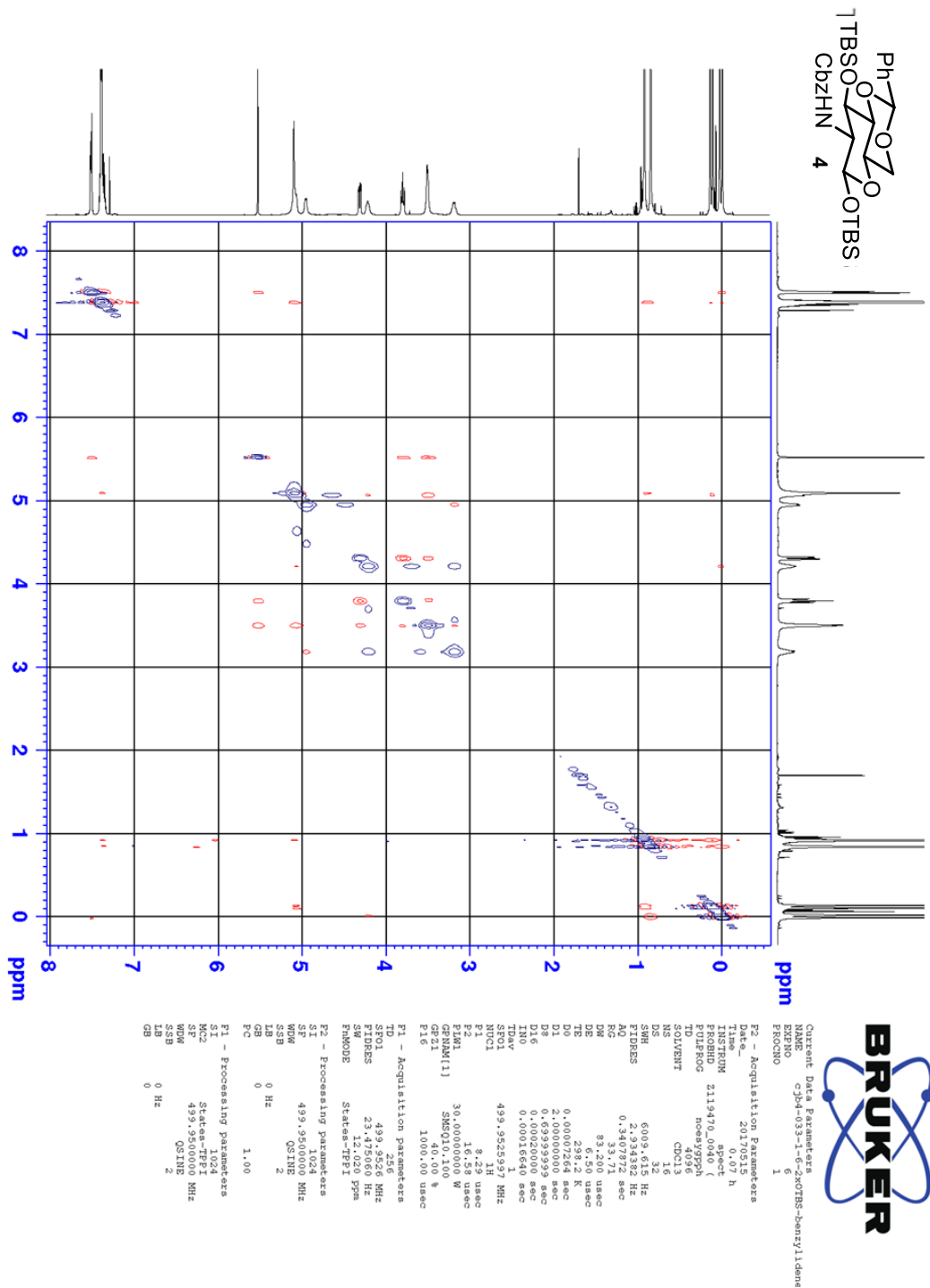
```



Current Data		Current Data		Current Data	
NAME	VALUE	NAME	VALUE	NAME	VALUE
PROGNO	1	PROGNO	1	PROGNO	1
F2 - Acquisition Parameters					
DATE	20170514	DATE	20170514	DATE	20170514
INSTRUM	SP100	INSTRUM	SP100	INSTRUM	SP100
PROGNO	2119470.0040	PROGNO	2119470.0040	PROGNO	2119470.0040
PROGNO	7048	PROGNO	7048	PROGNO	7048
ID	0000000000	ID	0000000000	ID	0000000000
NAME	SOLOVENT	NAME	SOLOVENT	NAME	SOLOVENT
D1	0.0000000000	D1	0.0000000000	D1	0.0000000000
D2	0.0000000000	D2	0.0000000000	D2	0.0000000000
D3	0.0000000000	D3	0.0000000000	D3	0.0000000000
D4	0.0000000000	D4	0.0000000000	D4	0.0000000000
D5	0.0000000000	D5	0.0000000000	D5	0.0000000000
D6	0.0000000000	D6	0.0000000000	D6	0.0000000000
D7	0.0000000000	D7	0.0000000000	D7	0.0000000000
D8	0.0000000000	D8	0.0000000000	D8	0.0000000000
D9	0.0000000000	D9	0.0000000000	D9	0.0000000000
D10	0.0000000000	D10	0.0000000000	D10	0.0000000000
D11	0.0000000000	D11	0.0000000000	D11	0.0000000000
D12	0.0000000000	D12	0.0000000000	D12	0.0000000000
D13	0.0000000000	D13	0.0000000000	D13	0.0000000000
D14	0.0000000000	D14	0.0000000000	D14	0.0000000000
D15	0.0000000000	D15	0.0000000000	D15	0.0000000000
D16	0.0000000000	D16	0.0000000000	D16	0.0000000000
D17	0.0000000000	D17	0.0000000000	D17	0.0000000000
D18	0.0000000000	D18	0.0000000000	D18	0.0000000000
D19	0.0000000000	D19	0.0000000000	D19	0.0000000000
D20	0.0000000000	D20	0.0000000000	D20	0.0000000000
D21	0.0000000000	D21	0.0000000000	D21	0.0000000000
D22	0.0000000000	D22	0.0000000000	D22	0.0000000000
D23	0.0000000000	D23	0.0000000000	D23	0.0000000000
D24	0.0000000000	D24	0.0000000000	D24	0.0000000000
D25	0.0000000000	D25	0.0000000000	D25	0.0000000000
D26	0.0000000000	D26	0.0000000000	D26	0.0000000000
D27	0.0000000000	D27	0.0000000000	D27	0.0000000000
D28	0.0000000000	D28	0.0000000000	D28	0.0000000000
D29	0.0000000000	D29	0.0000000000	D29	0.0000000000
D30	0.0000000000	D30	0.0000000000	D30	0.0000000000
D31	0.0000000000	D31	0.0000000000	D31	0.0000000000
D32	0.0000000000	D32	0.0000000000	D32	0.0000000000
D33	0.0000000000	D33	0.0000000000	D33	0.0000000000
D34	0.0000000000	D34	0.0000000000	D34	0.0000000000
D35	0.0000000000	D35	0.0000000000	D35	0.0000000000
D36	0.0000000000	D36	0.0000000000	D36	0.0000000000
D37	0.0000000000	D37	0.0000000000	D37	0.0000000000
D38	0.0000000000	D38	0.0000000000	D38	0.0000000000
D39	0.0000000000	D39	0.0000000000	D39	0.0000000000
D40	0.0000000000	D40	0.0000000000	D40	0.0000000000
D41	0.0000000000	D41	0.0000000000	D41	0.0000000000
D42	0.0000000000	D42	0.00		

Appendix Figure 6.47: COSY of (CDCl₃) spectrum of compound 4

Appendix Figure 6.48: NOESY (CDCl₃) spectrum of compound 4



```

Current Data Parameters
NAME      cjb2-104-22
EXPNO     1
PROCNO    1

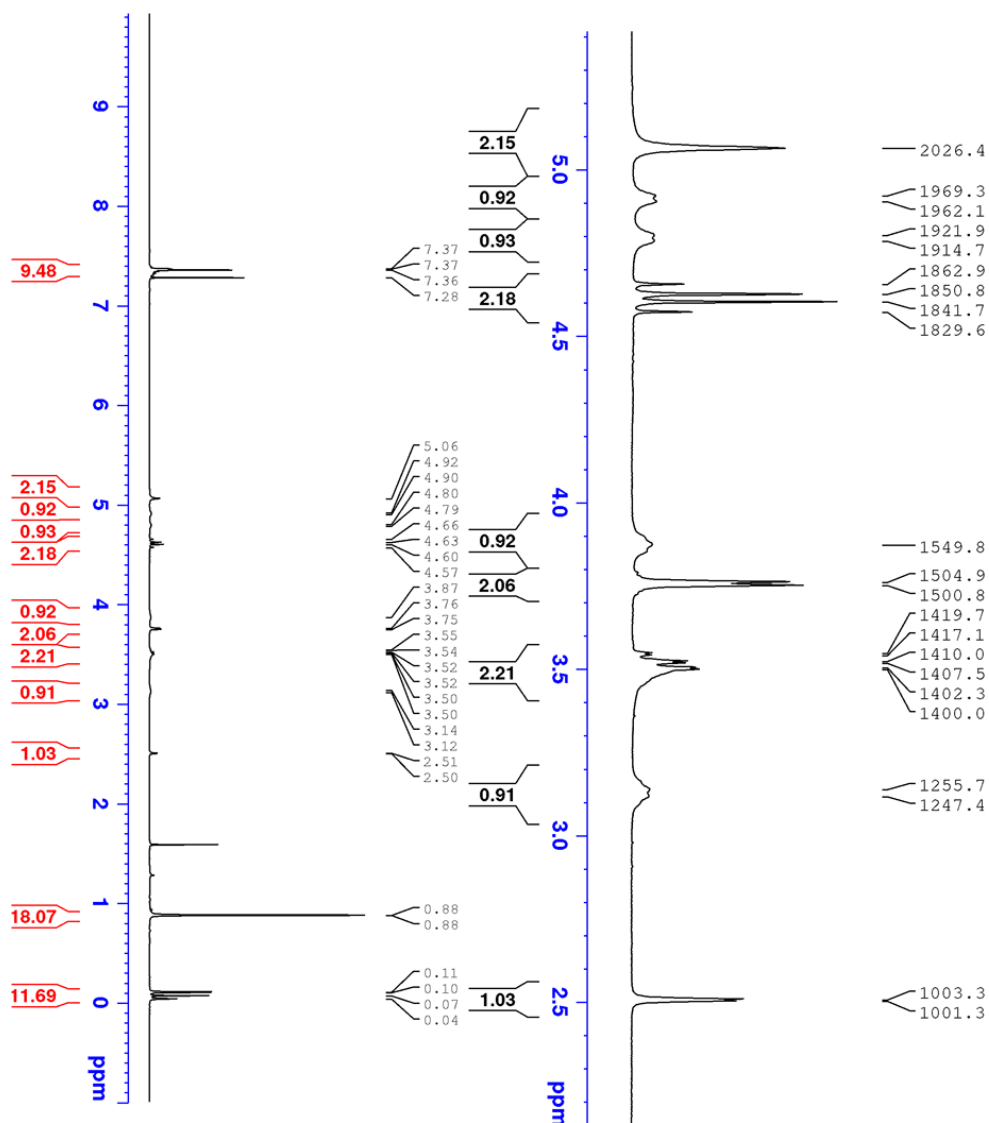
F2 - Acquisition Parameters
Date_     2014.10.23
Time      18.51
INSTRUM   robinson
PROBHD    5 mm PABBO BB-
PULPROG   zg30
TD         32768
SOLVENT   CDCl3
NS         32
DS         2
SWH        7183.908 Hz
AQ         0.21935 Hz
FIDRES     2.2806828 sec
RG         181
WDW         69.60 usec
SSB         0
DE         6.50 usec
TE         298.2 K
D1         2.00000000 sec
TD0         1

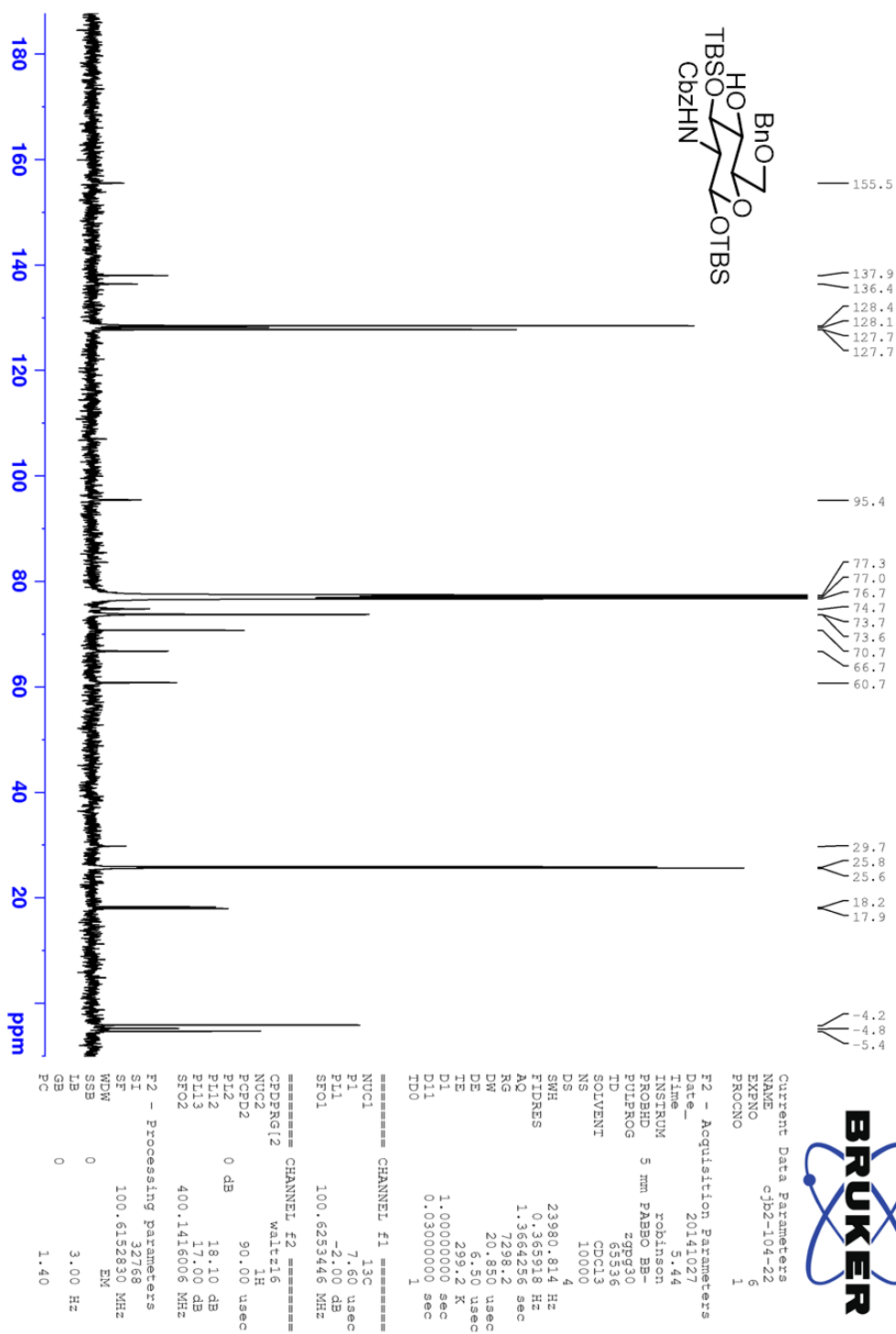
===== CHANNEL f1 =====
NUC1       CHANNEL f1
P1         1H
PL1        0 dB
SFO1       400.1428010 MHz

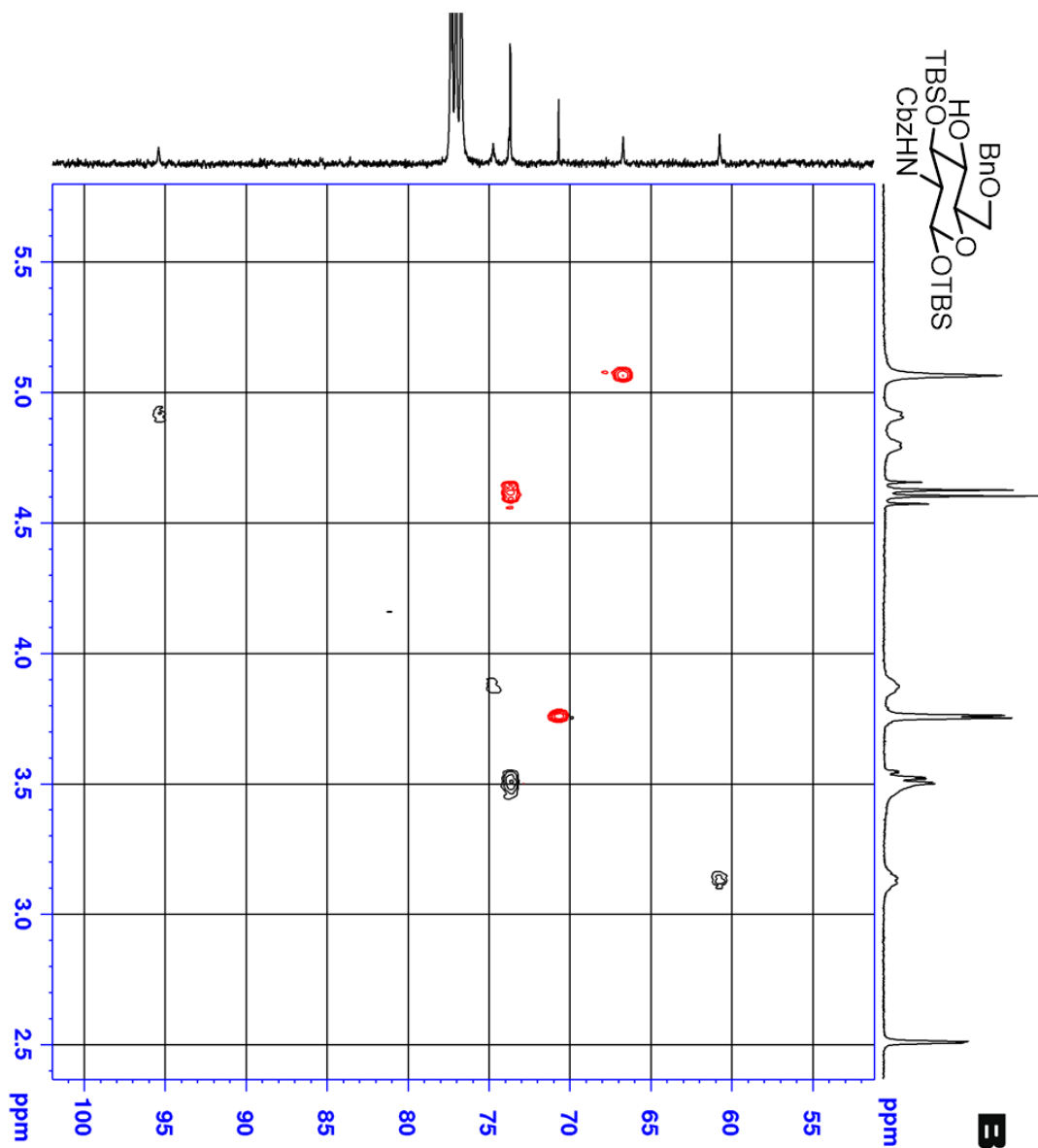
F2 - Processing parameters
SI         16384
SF         400.1400000 MHz
WOW        EM
SSB        0
LB         0.30 Hz
GB         0
PC         1.00

O=[N+]([O-])c1ccc(O)cc1
TBSO
CbZHN

```

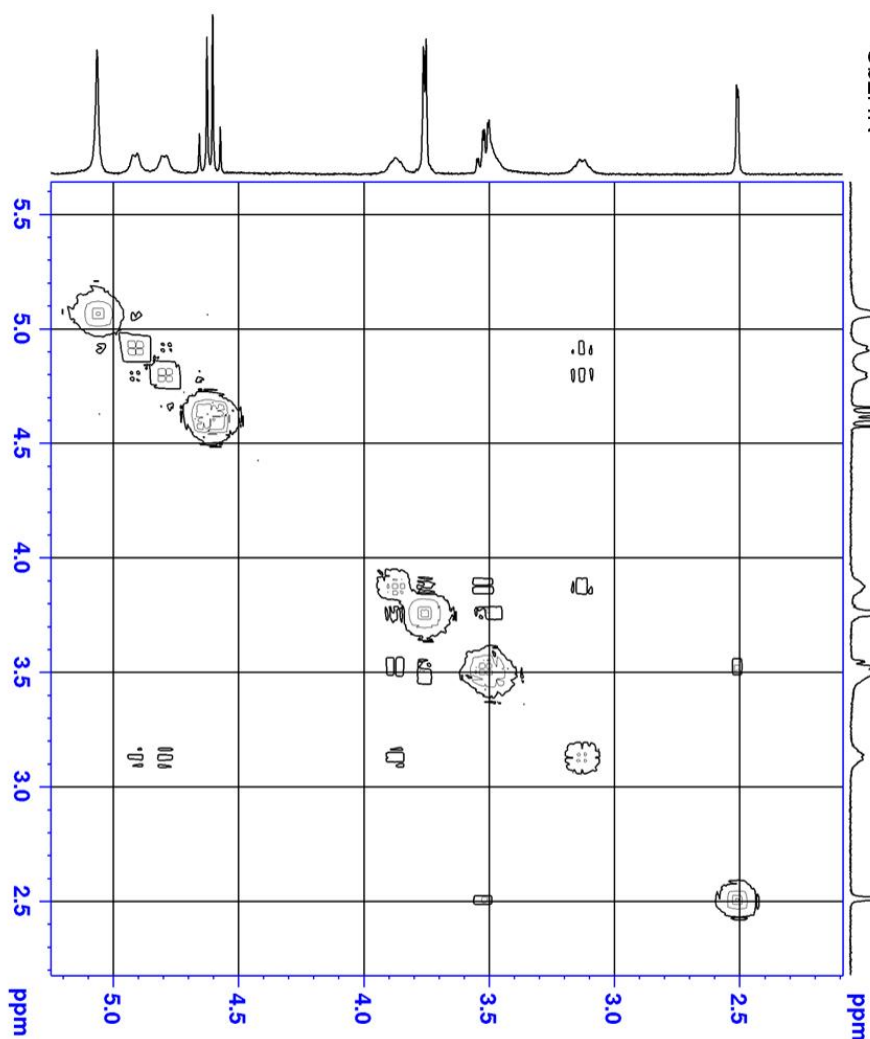


Appendix Figure 6.50: ^{13}C NMR (CDCl_3) spectrum of 6

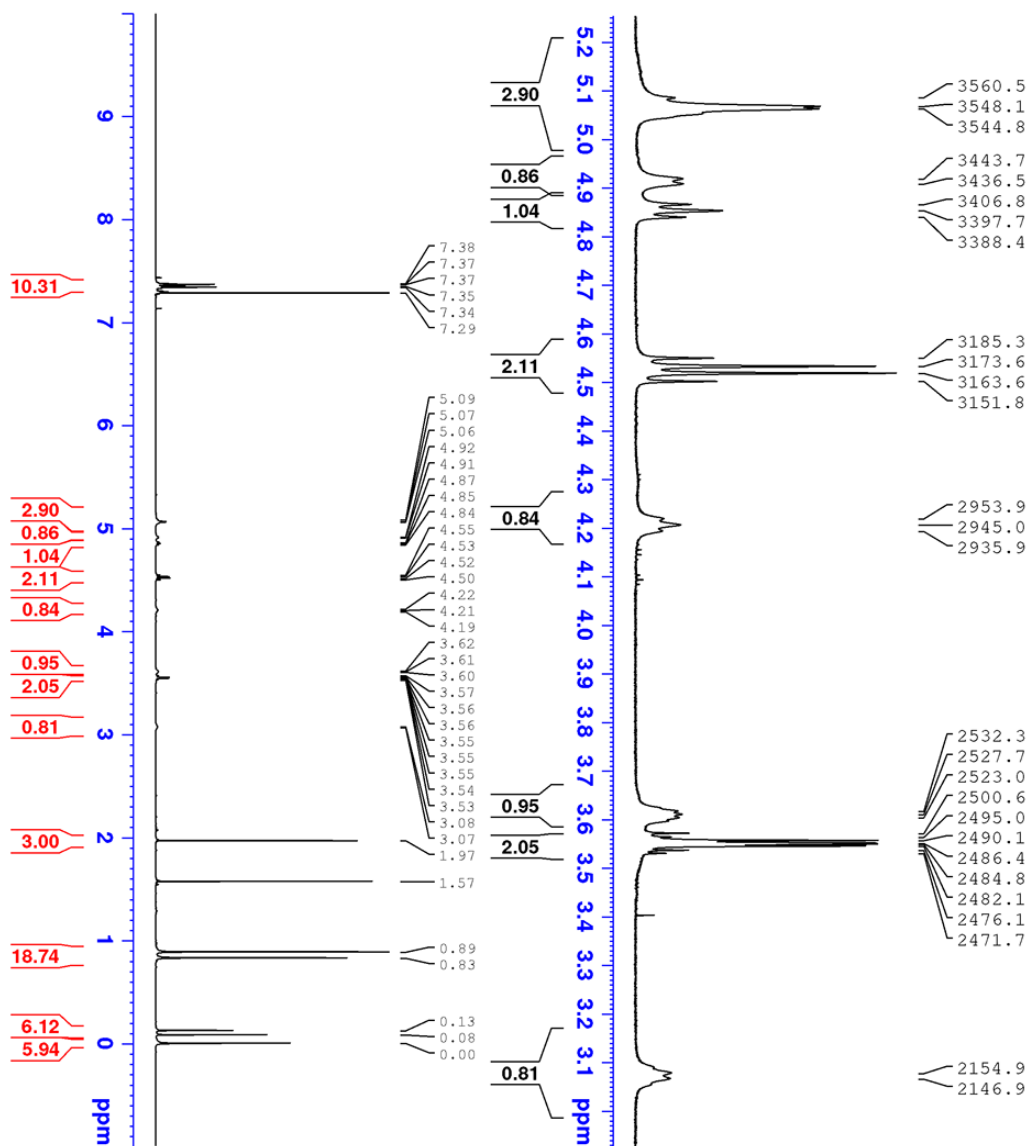
[illegible]



BRUKER



NAME	-----	DATE	-----
EXNO	CJ26-104-22		
PROCN0	7		
	1		
F2 - Acquisition Parameters			
Date--	201407		
INSTRUM	BBIO		
PROBHD	5 mm Rubbo Bb-		
PULPROG	zgpg30		
TD	2048		
SOLVENT	CDC13		
DS	4		
SWH	4139.073 Hz		
FIDRES	2.021032 Hz		
AQ	0.2473994 sec		
RG	326		
RG	120.900 usec		
RG	28.2 K		
TE	298.2 K		
D1	0.0000300 sec		
D2	2.00000000 sec		
D13	0.0000400 sec		
D16	0.0002000 sec		
IN0	0.00024240 sec		
CHANNEL f1			
NUC1	1H		
P0	11.20 usec		
P1	11.20 usec		
P1	0 dB		
SFO1	400.115653 MHz		
GRABINT CHANNEL			
GP2N1[1]	SINE,100		
P16	80.00 %		
	1000.00 usec		
F1 - Acquisition parameters			
SFO1	400.145 MHz		
TD	73		
FIDRES	56.113912 Hz		
SW	10.310 Ppm		
FMNOE	QF		
F2 - Processing parameters			
SF	2048		
SI	400.140000 MHz		
WDW	SINE		
SSB	0		
GB	0 Hz		
PC	1.40		
F1 - Processing parameters			
SF	208		
SI	400.140000 MHz		
WDW	SINE		
SSB	0		
GB	0 Hz		



```

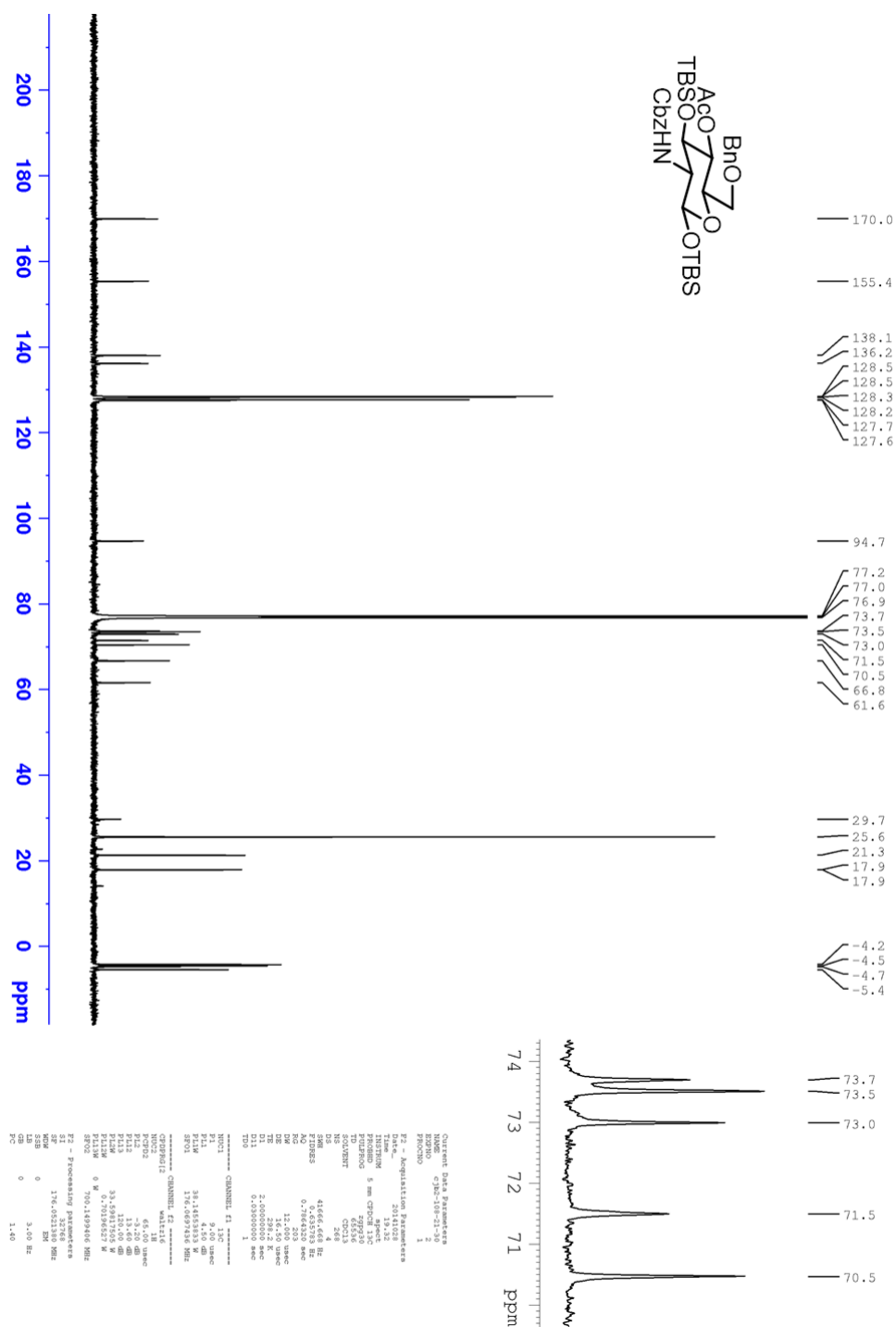
Current Data Parameters
NAME                cjb2-116-4-11
EXPNO                1
PROCNO               1

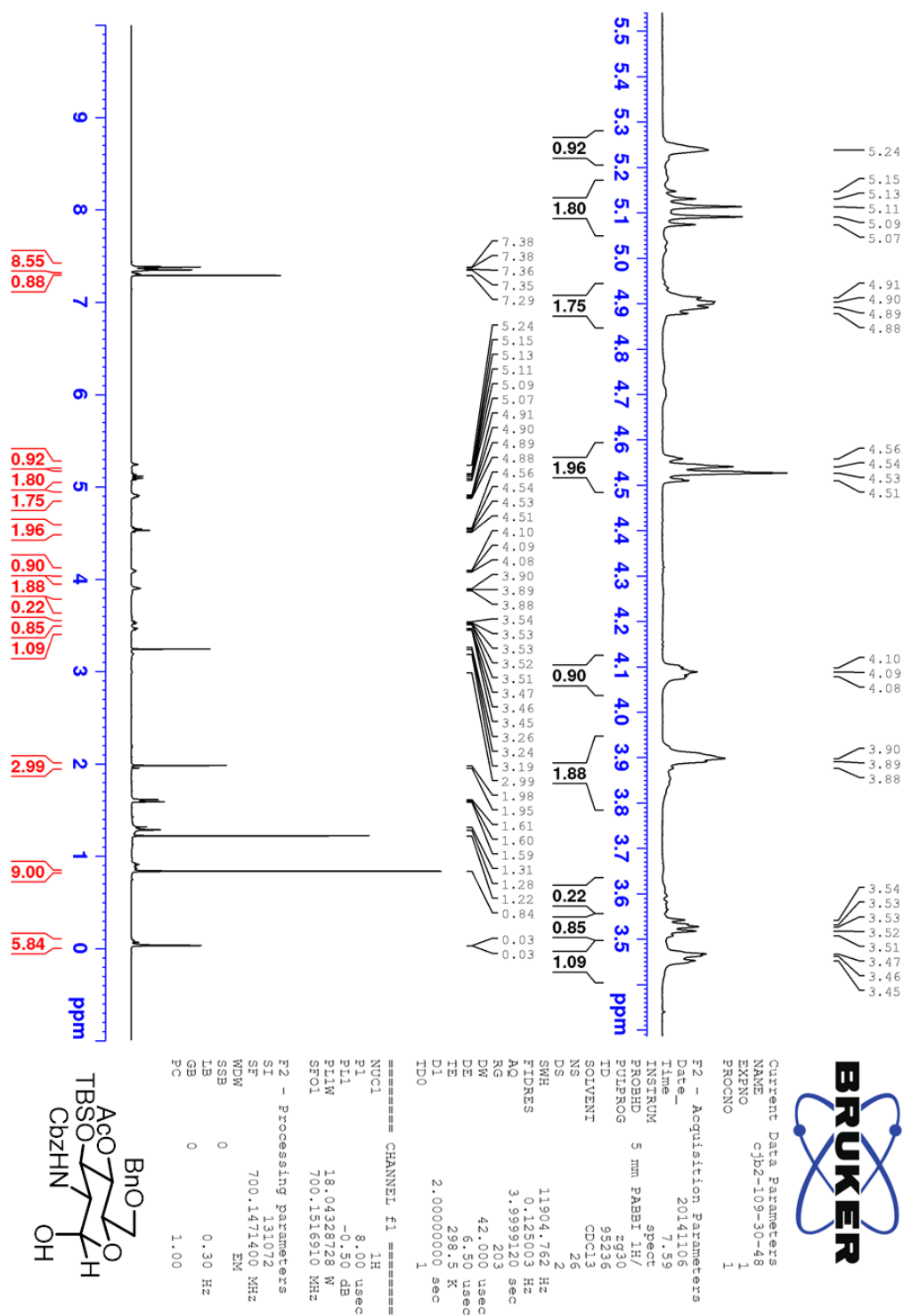
F2 - Acquisition Parameters
Date_                20141117
Time                 21:26
INSTRUM              spect
PROBHD               5 mm CPDCH-13C
PULPROG              zgpg30
FIDRES               0.130
AQ                   3.999120 sec
RG                   18
DM                   42.00 usec
DE                   6.50 usec
TE                   298.2 K
D1                   2.00000000 sec
TD                   1

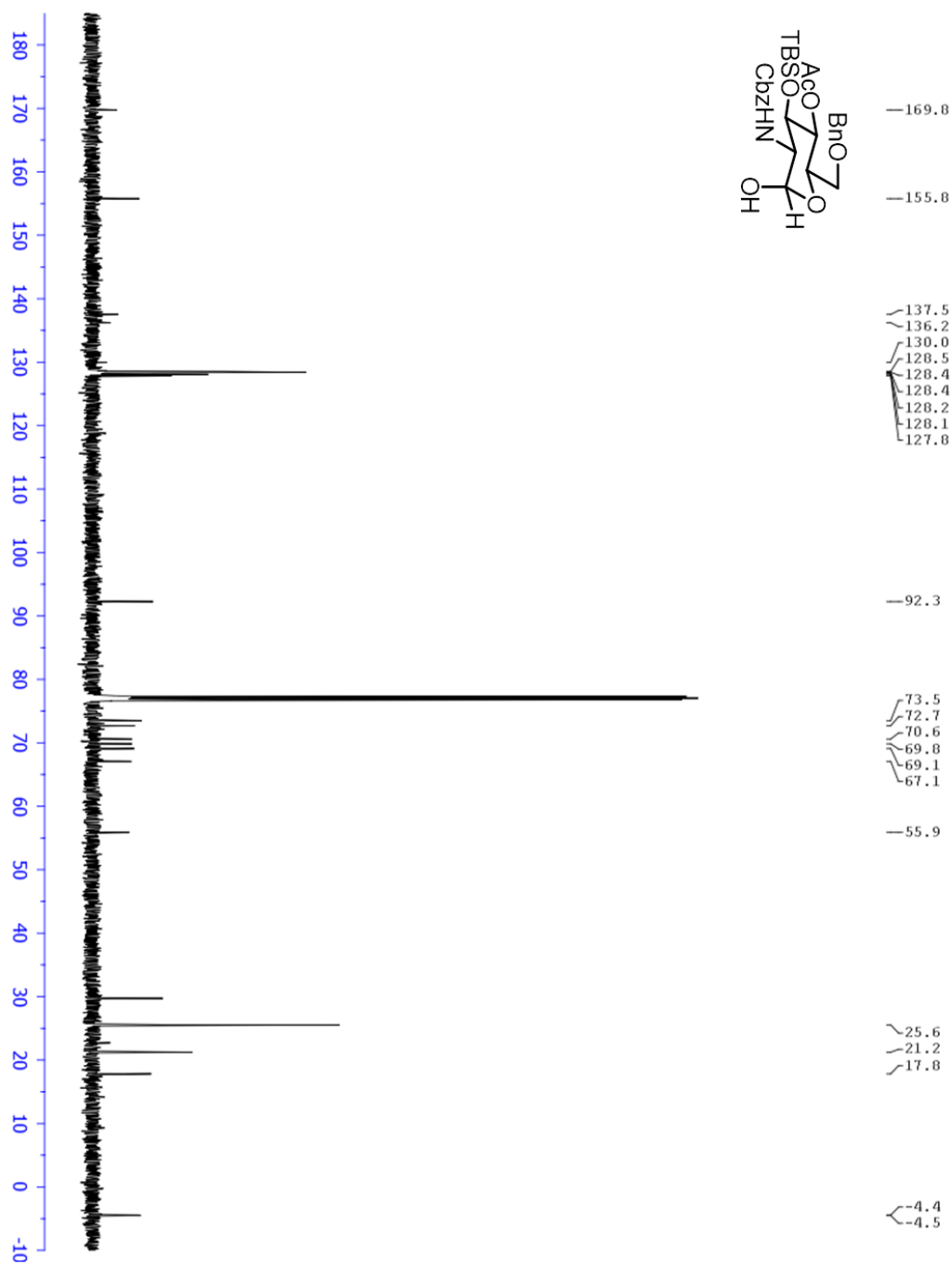
===== CHANNEL f1 =====
NUC1                 1H
P1                   9.40 usec
PL1                  -3.20 dB
PILW                 33.59817505 W
SFO1                 700.1515910 MHz

F2 - Processing parameters
SF                   700.1471400 MHz
SF                     130072
MNM                  EM
SSB                   0
GB                   0 Hz
PC                   1.00

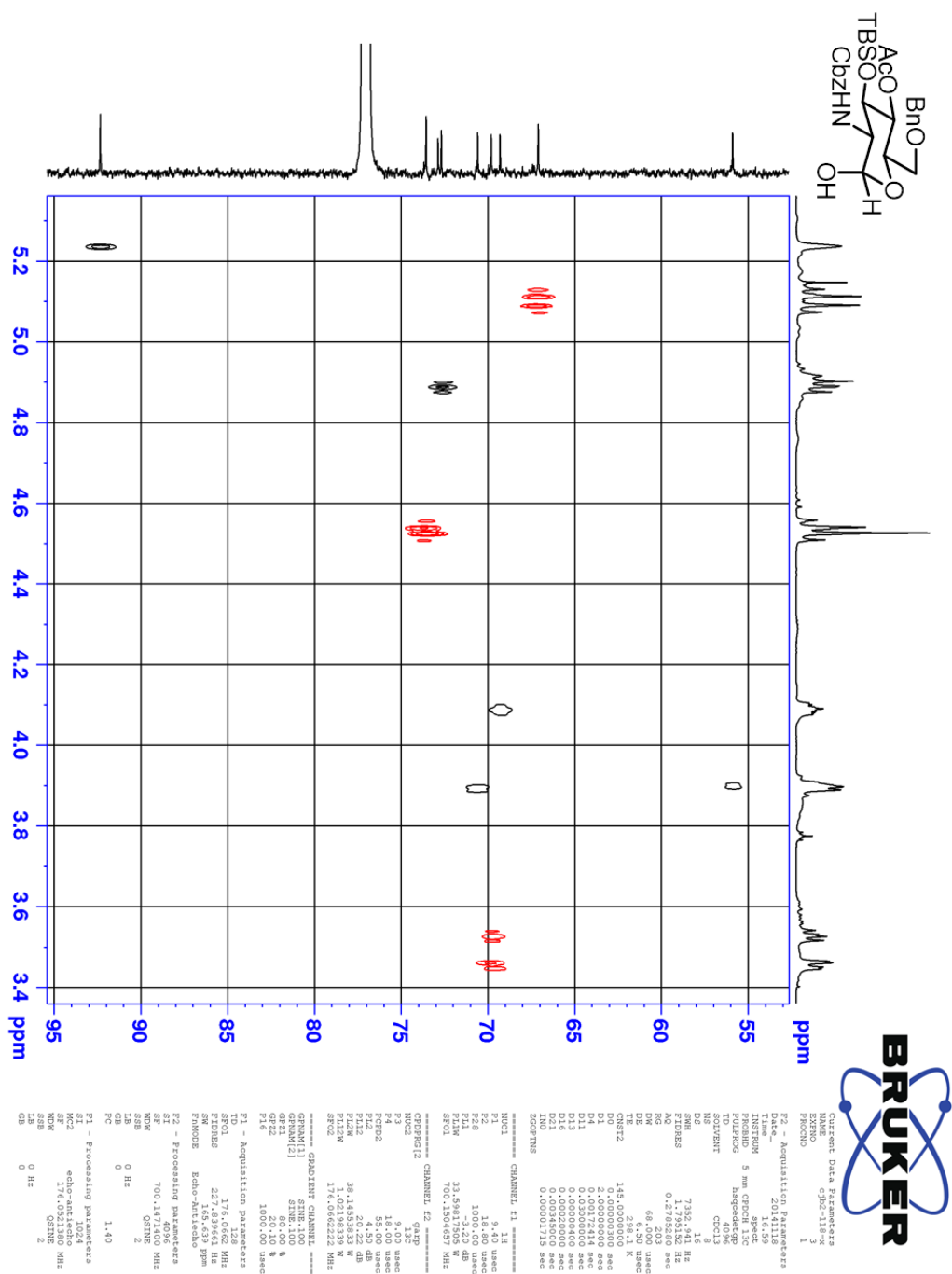
```

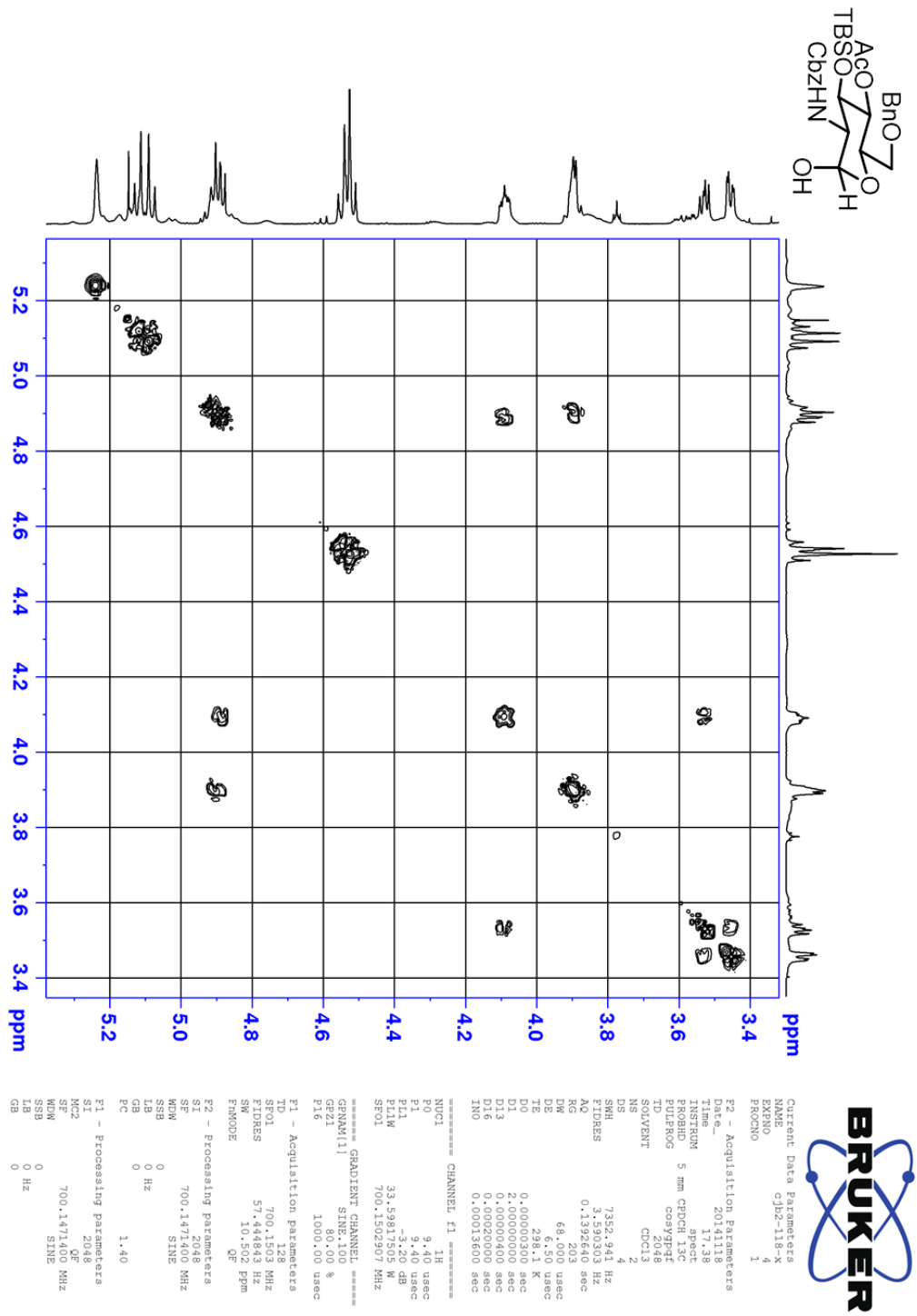
Appendix Figure 6.57: ^1H NMR (CDCl_3) spectrum of lactol SI-2

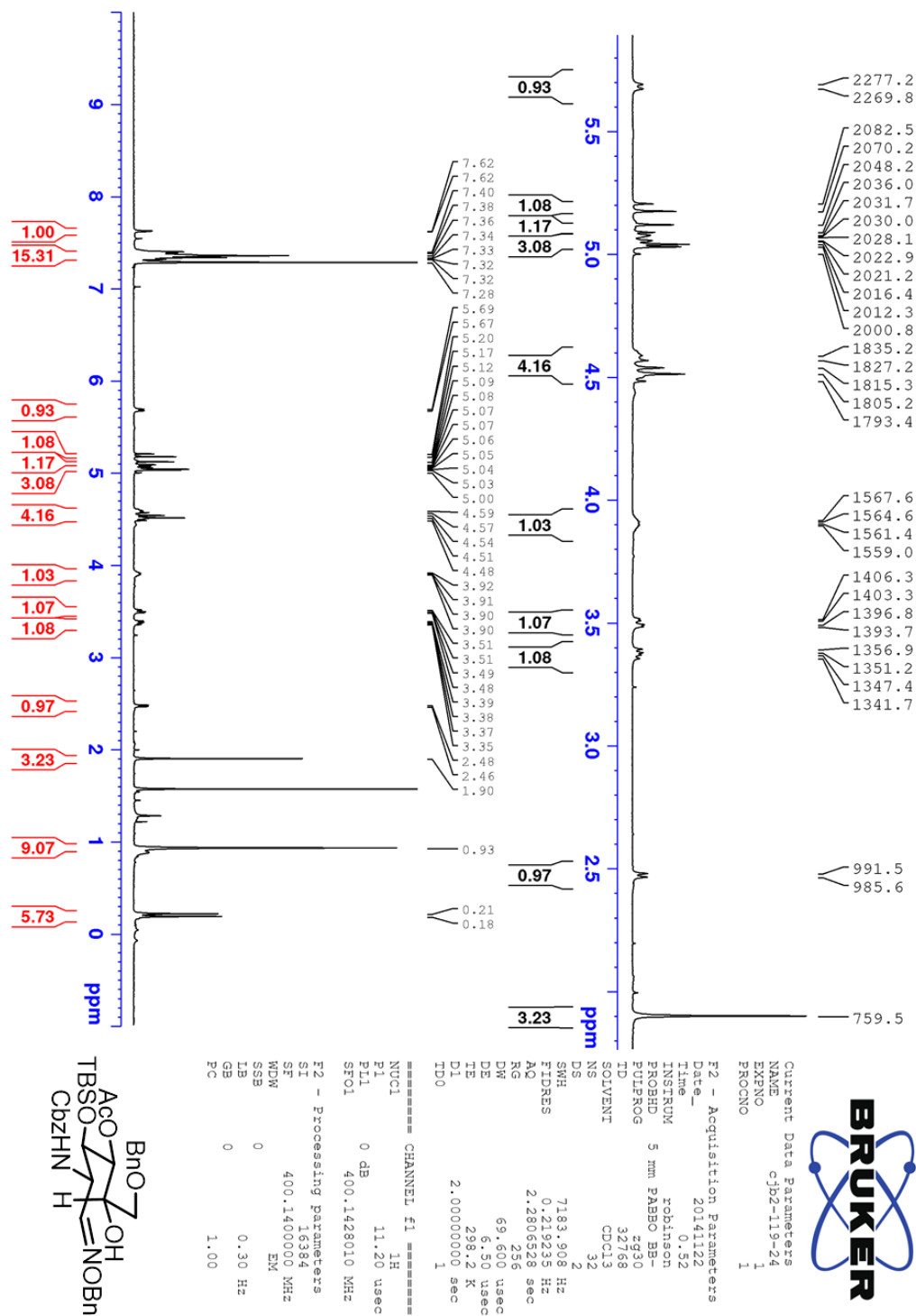
Appendix Figure 6.58: ^{13}C NMR (CDCl_3) spectrum of lactol **SI-2**

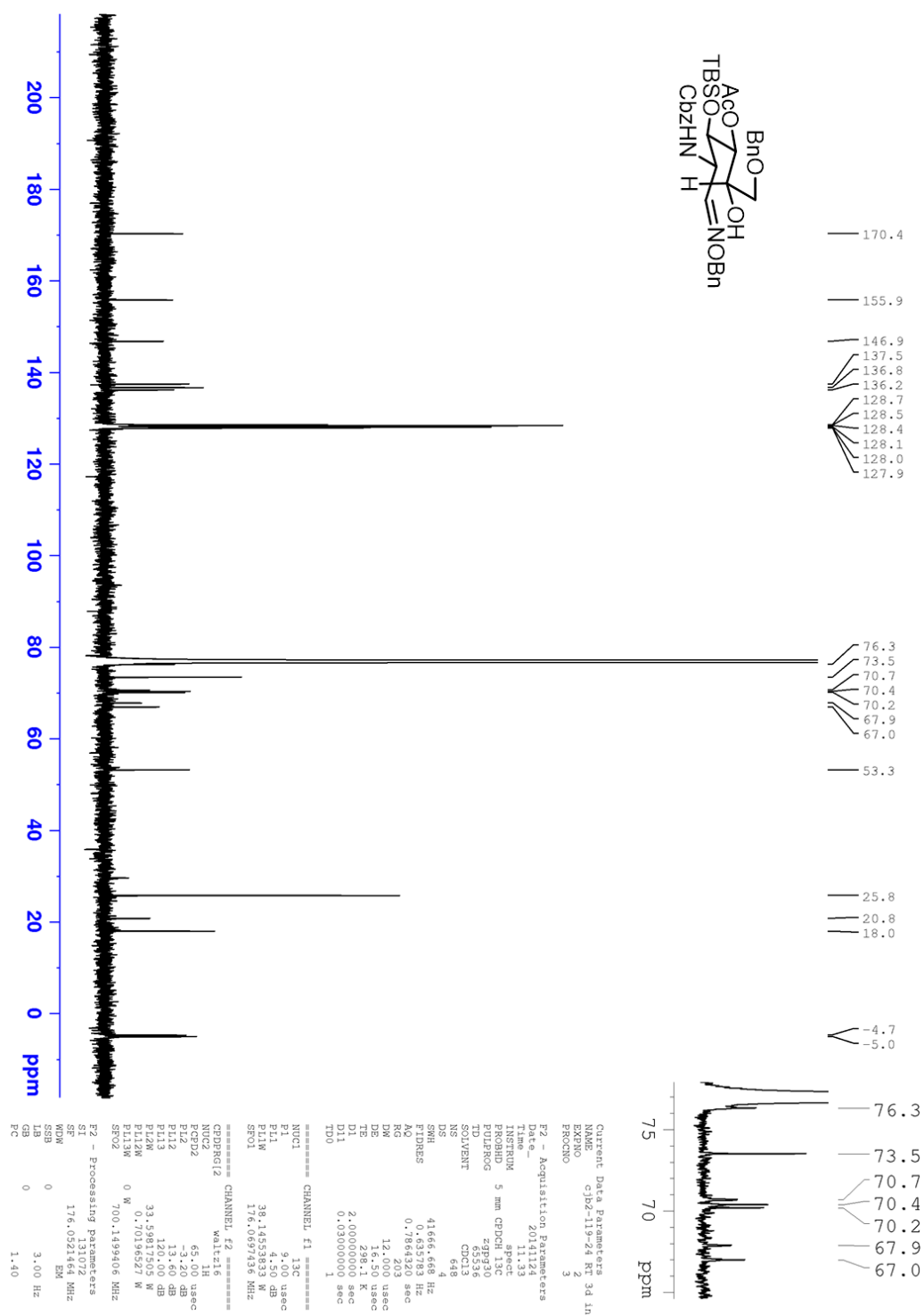
Appendix Figure 6.59: HSQC (CDCl_3) spectrum of lactol **SI-2**

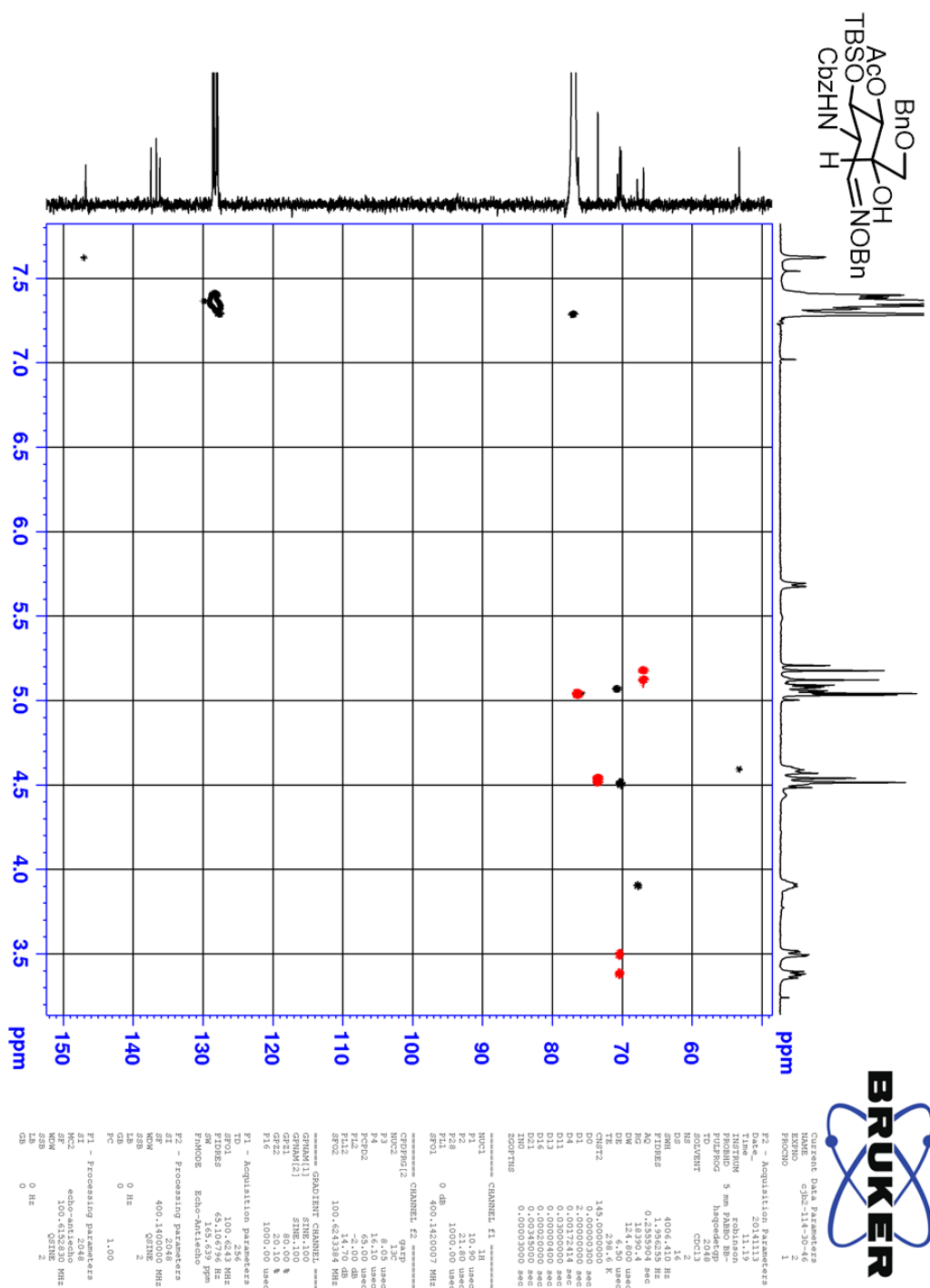


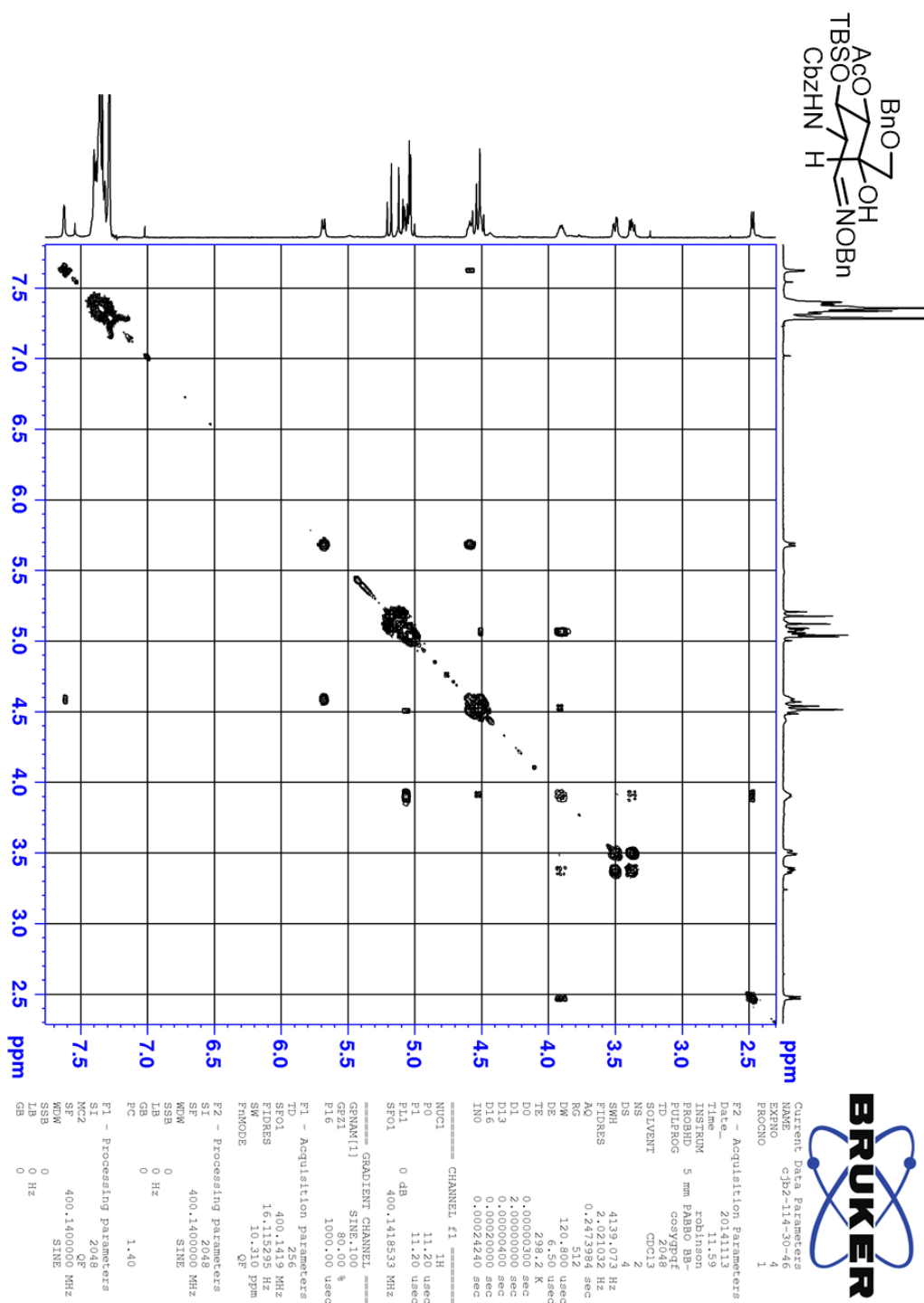
Appendix Figure 6.60: COSY (CDCl₃) spectrum of lactol SI-2

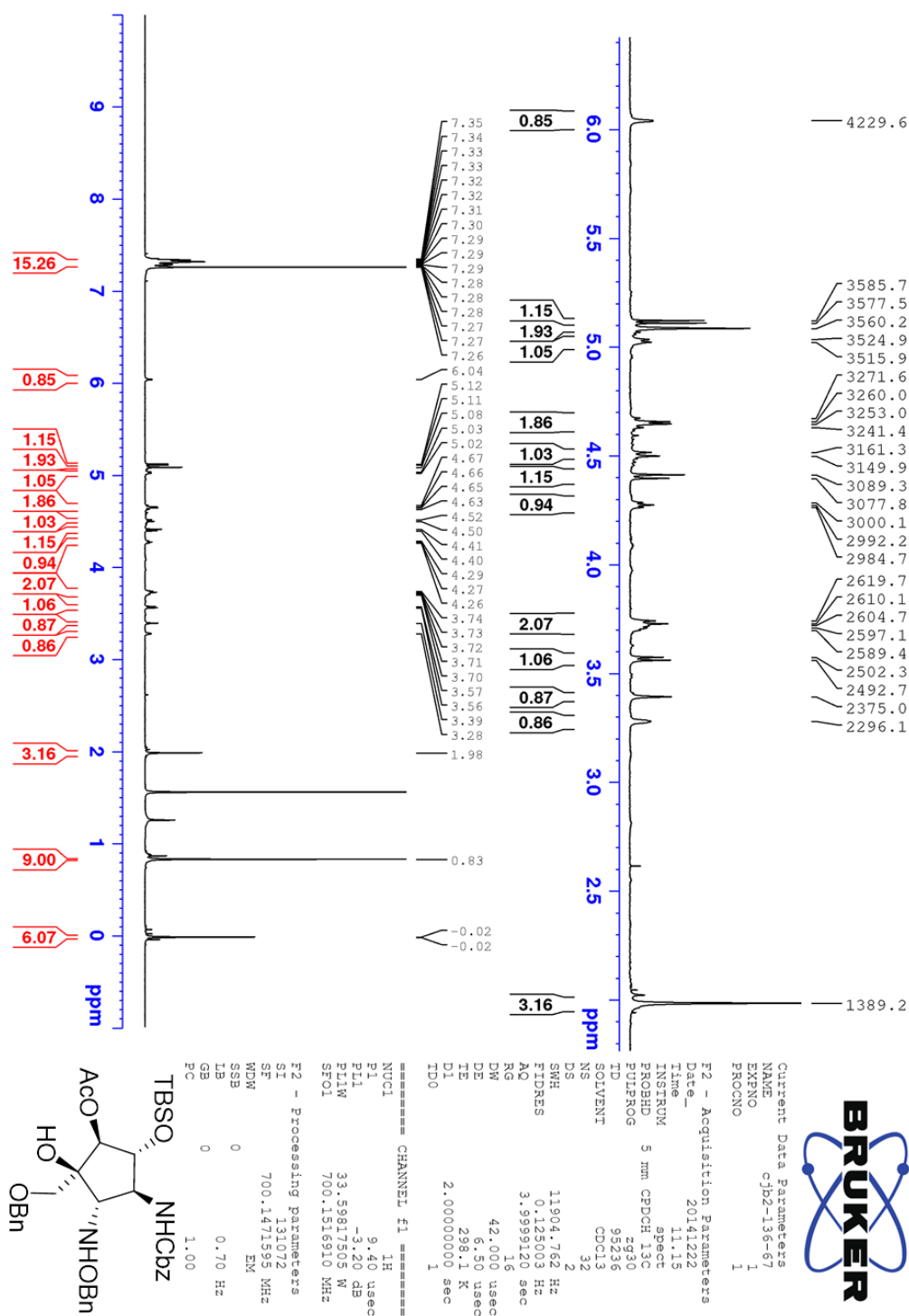


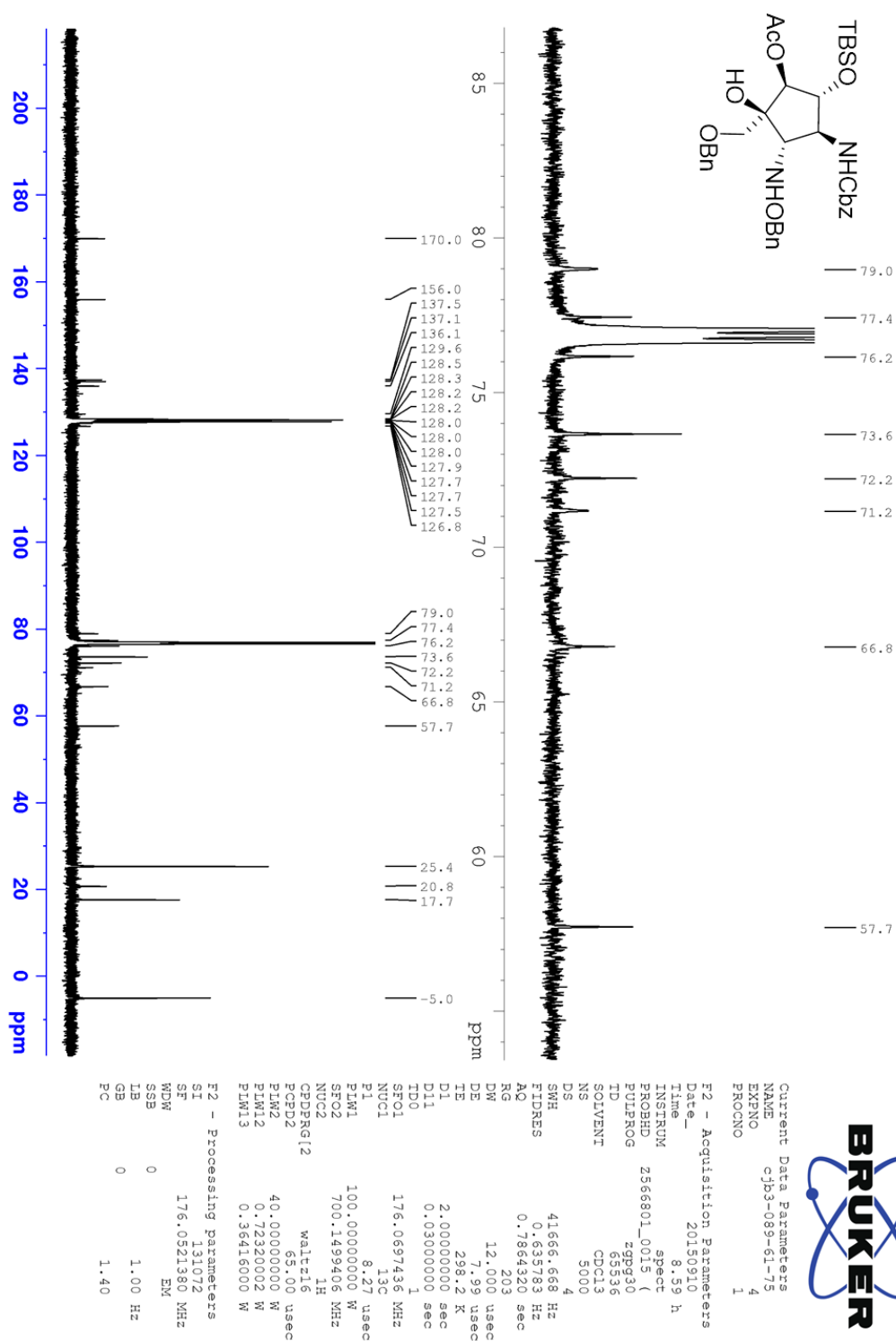
Appendix Figure 6.61: ^1H NMR (CDCl_3) spectrum of **8**

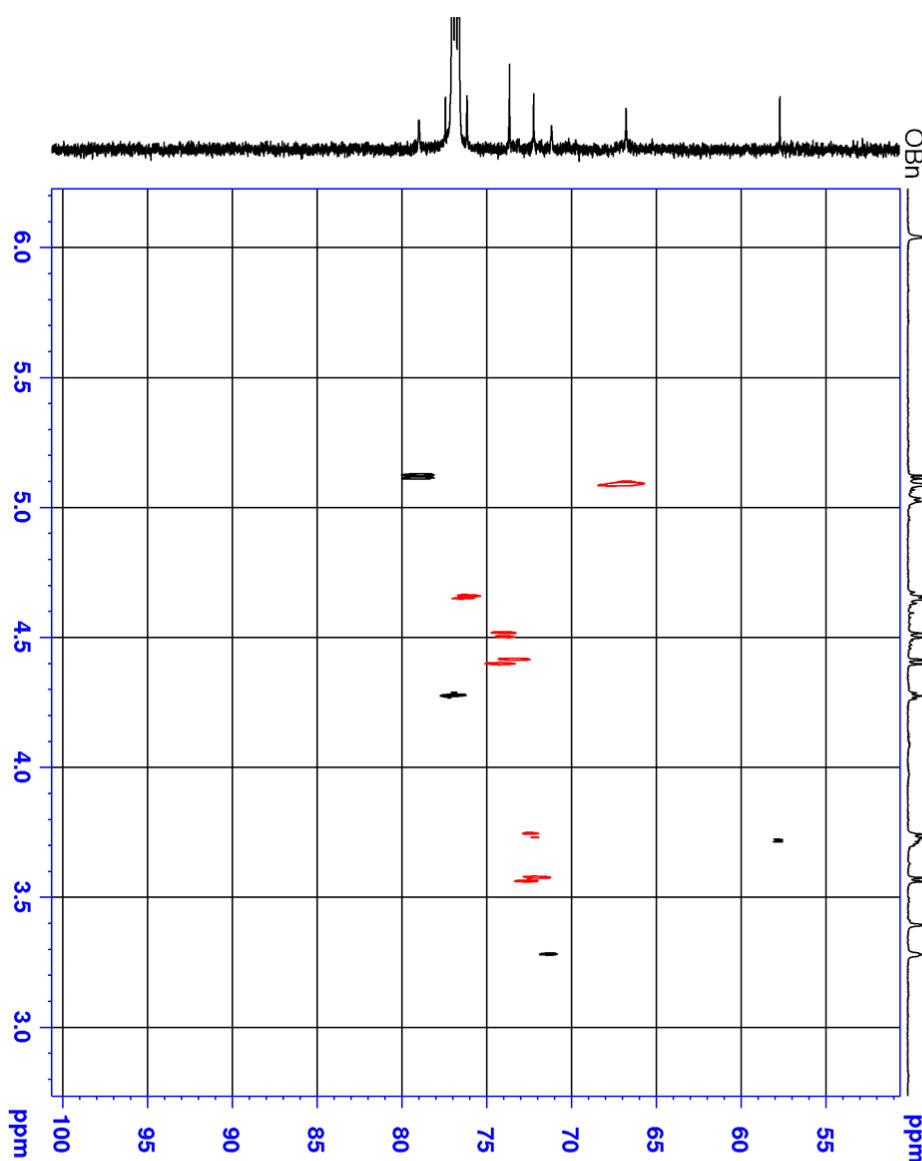
Appendix Figure 6.62: ^{13}C NMR (CDCl_3) spectrum of **8**

Appendix Figure 6.63: HSQC (CDCl₃) spectrum of 8

Appendix Figure 6.64: COSY (CDCl₃) spectrum of 8

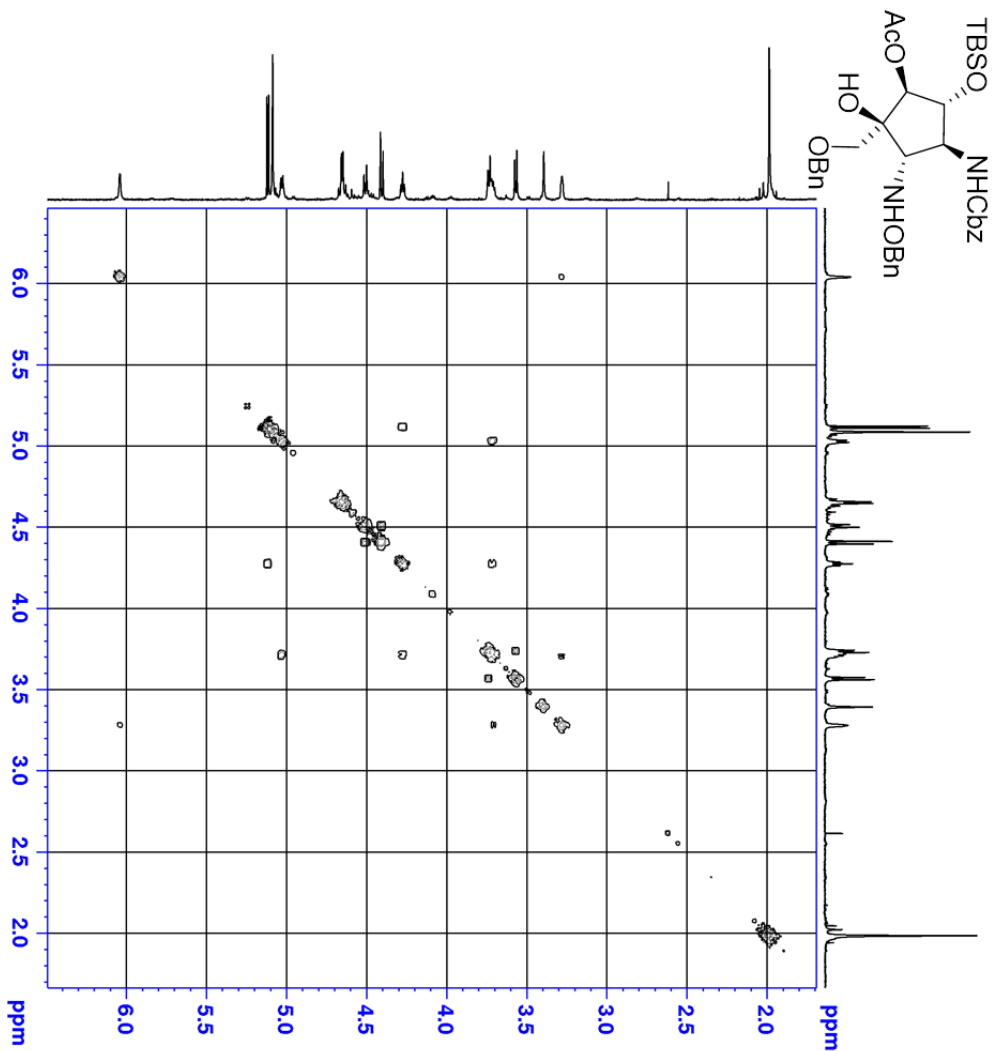
Appendix Figure 6.65: ^1H NMR (CDCl_3) spectrum of TM-122

Appendix Figure 6.66: ^{13}C NMR (CDCl_3) spectrum of TM-122

CCOC(=O)[C@H]1[C@@H](O)[C@H](Nc2ccccc2)[C@@H](O[C@@H]3CCCC[C@H]3OC(=O)c4ccccc4)[C@H]1O

	F2 - Acquisition Parameters	F1 - Processing parameters
Date_	20141227	
Time	16:18:29	
PROBHD	5 mm CUPCO JAC	
INSTRUM	spect	
PULPROG	zgpg30	
TD	4096	
SOLVENT	DMSO-d ₆	
DS	1	
DE	7.55, -1.6 Hz	
PRBS	1	
AQ	0.2789580 sec	
TE	300.2 K	
DE	6.50 usec	
DELTA	145.0000000 sec	
CH1C2	0.00000000 sec	
D0	0.00000000 sec	
D1	0.00000000 sec	
D2	0.00000000 sec	
D3	0.00000000 sec	
D4	0.00000000 sec	
D5	0.00000000 sec	
D6	0.00000000 sec	
D7	0.00000000 sec	
D8	0.00000000 sec	
D9	0.00000000 sec	
D10	0.00000000 sec	
D11	0.00000000 sec	
D12	0.00000000 sec	
D13	0.00000000 sec	
D14	0.00000000 sec	
D15	0.00000000 sec	
D16	0.00000000 sec	
D17	0.00000000 sec	
D18	0.00000000 sec	
D19	0.00000000 sec	
D20	0.00000000 sec	
D21	0.00000000 sec	
D22	0.00000000 sec	
D23	0.00000000 sec	
D24	0.00000000 sec	
D25	0.00000000 sec	
D26	0.00000000 sec	
D27	0.00000000 sec	
D28	0.00000000 sec	
D29	0.00000000 sec	
D30	0.00000000 sec	
D31	0.00000000 sec	
D32	0.00000000 sec	
D33	0.00000000 sec	
D34	0.00000000 sec	
D35	0.00000000 sec	
D36	0.00000000 sec	
D37	0.00000000 sec	
D38	0.00000000 sec	
D39	0.00000000 sec	
D40	0.00000000 sec	
D41	0.00000000 sec	
D42	0.00000000 sec	
D43	0.00000000 sec	
D44	0.00000000 sec	
D45	0.00000000 sec	
D46	0.00000000 sec	
D47	0.00000000 sec	
D48	0.00000000 sec	
D49	0.00000000 sec	
D50	0.00000000 sec	
D51	0.00000000 sec	
D52	0.00000000 sec	
D53	0.00000000 sec	
D54	0.00000000 sec	
D55	0.00000000 sec	
D56	0.00000000 sec	
D57	0.00000000 sec	
D58	0.00000000 sec	
D59	0.00000000 sec	
D60	0.00000000 sec	
D61	0.00000000 sec	
D62	0.00000000 sec	
D63	0.00000000 sec	
D64	0.00000000 sec	
D65	0.00000000 sec	
D66	0.00000000 sec	
D67	0.00000000 sec	
D68	0.00000000 sec	
D69	0.00000000 sec	
D70	0.00000000 sec	
D71	0.00000000 sec	
D72	0.00000000 sec	
D73	0.00000000 sec	
D74	0.00000000 sec	
D75	0.00000000 sec	
D76	0.00000000 sec	
D77	0.00000000 sec	
D78	0.00000000 sec	
D79	0.00000000 sec	
D80	0.00000000 sec	
D81	0.00000000 sec	
D82	0.00000000 sec	
D83	0.00000000 sec	
D84	0.00000000 sec	
D85	0.00000000 sec	
D86	0.00000000 sec	
D87	0.00000000 sec	
D88	0.00000000 sec	
D89	0.00000000 sec	
D90	0.00000000 sec	
D91	0.00000000 sec	
D92	0.00000000 sec	
D93	0.00000000 sec	
D94	0.00000000 sec	
D95	0.00000000 sec	
D96	0.00000000 sec	
D97	0.00000000 sec	
D98	0.00000000 sec	
D99	0.00000000 sec	
D100	0.00000000 sec	
D101	0.00000000 sec	
D102	0.00000000 sec	
D103	0.00000000 sec	
D104	0.00000000 sec	
D105	0.00000000 sec	
D106	0.00000000 sec	
D107	0.00000000 sec	
D108	0.00000000 sec	
D109	0.00000000 sec	

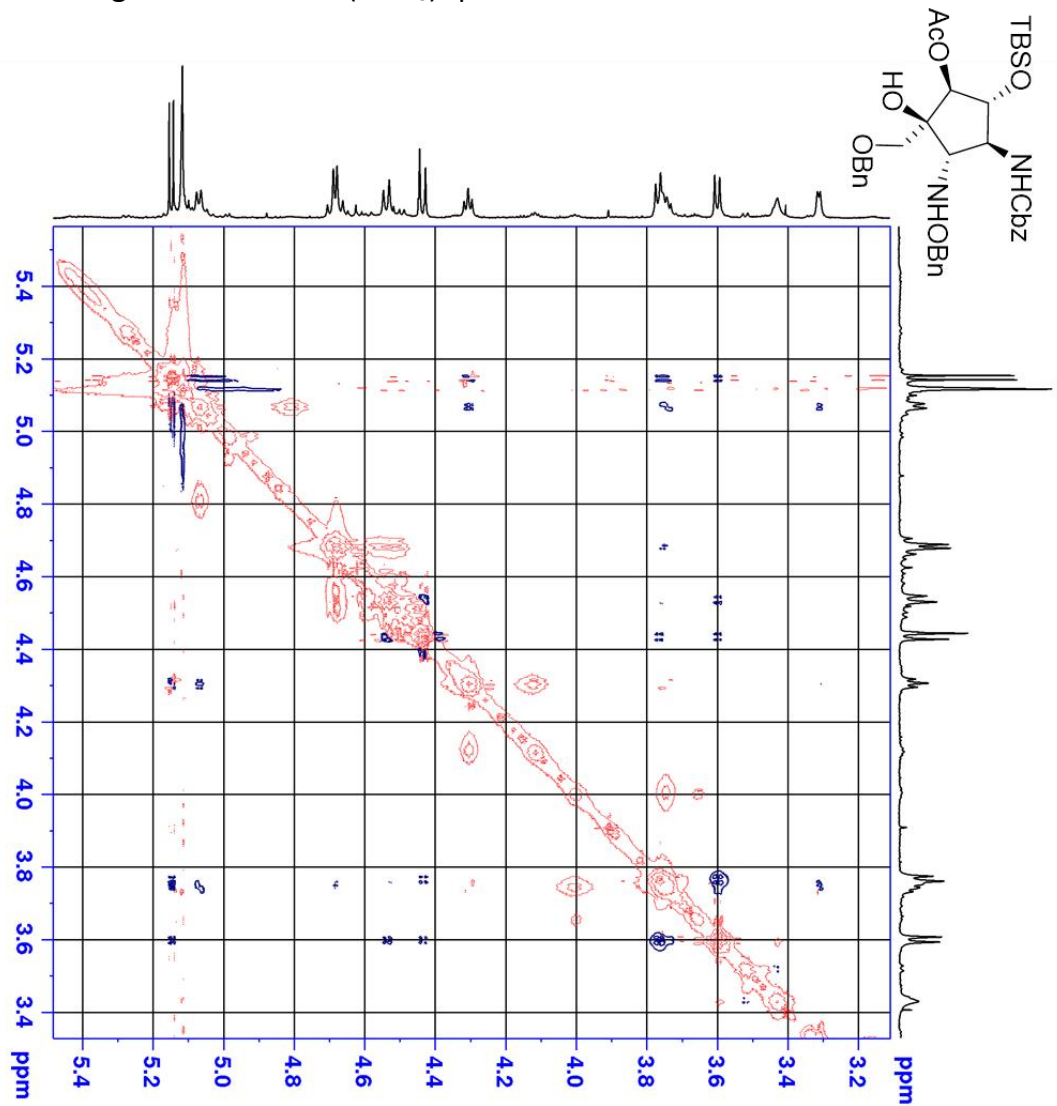
Appendix Figure 6.69: COSY (CDCl₃) spectrum of TM-122



Current Data Parameters
NAME cjh2-136-67
EXPNO 3
PROCNO 1
F2 - Acquisition Parameters
Date_ 20141222
Time 11.33
INSTRUM spect
PROBHD 5 mm CPDCH 13C
PULPROG zgpg30
TD 65536
SOLVENT CDCl3
NS 2
DS 4
SWH 7352.941 Hz
FIDRES 0.132640 Hz
AQ 0.132640 sec
RG 203
DW 68.000 usec
DE 2.500 usec
TE 300.2 K
D1 0.00000300 sec
D13 2.00000000 sec
D16 0.00000400 sec
D18 0.00020000 sec
IN0 0.00013600 sec
===== CHANNEL f1 =====
NUC1 1H
P1 9.40 usec
PL1 -3.40 dB
PL1W 33.59817505 W
SE01 700.1502907 MHz
===== CHANNEL f2 =====
GRADIENT CHANNEL
GPR1 31.000 %
GPR2 80.00 %
P16 1000.00 usec
===== F1 - Acquisition parameters =====
SI 1024
SF 700.1502907 MHz
FIDRES 57.444843 Hz
SW 10.502 PPM
F2 - Processing parameters
SI 1024
SF 700.1471587 MHz
WDW SINE
SSB 0 Hz
GB 0
PC 1.40
===== F1 - Processing parameters =====
SI 1024
SF 700.1471587 MHz
WDW SINE
SSB 0 Hz
GB 0
PC 1.40

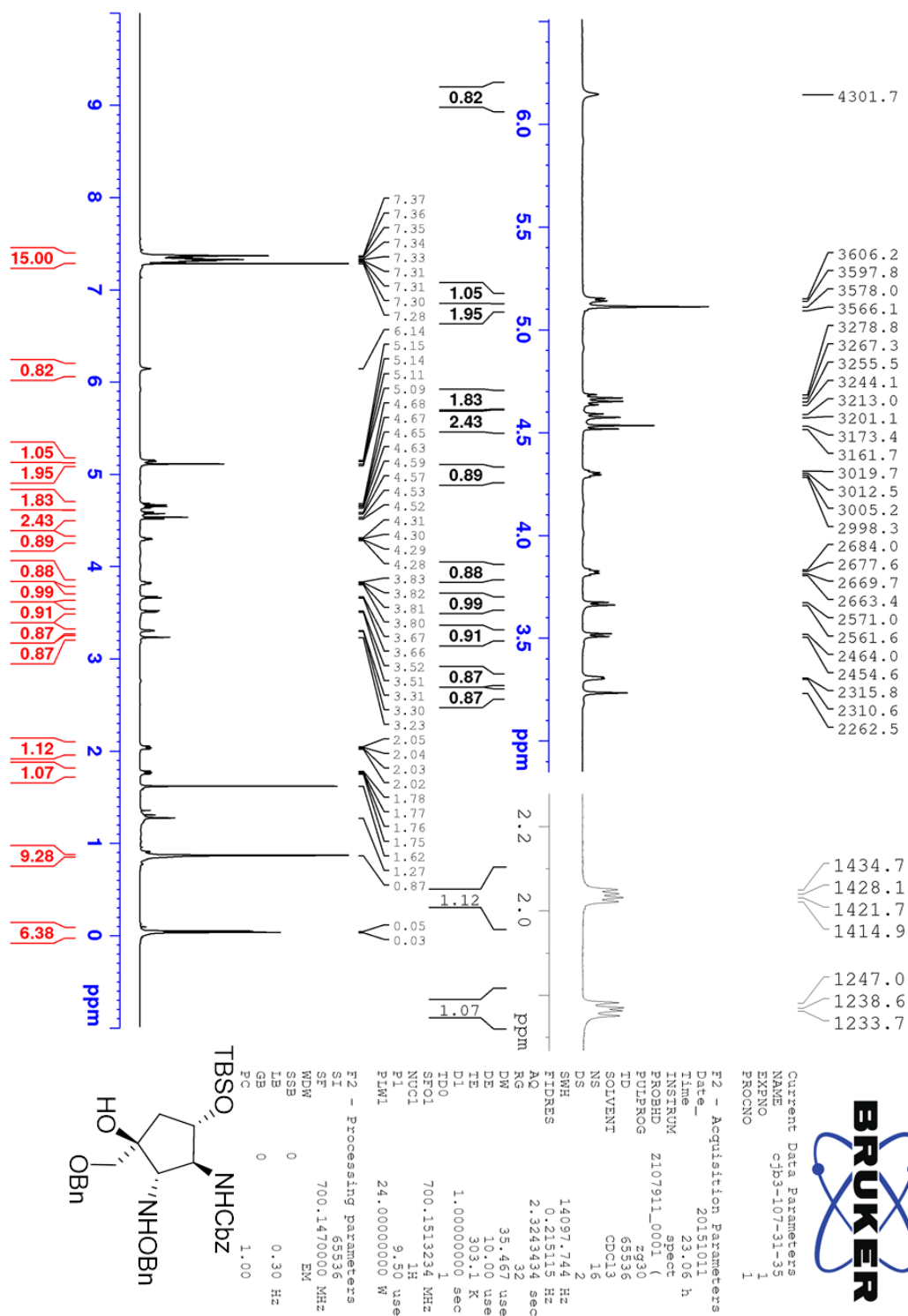


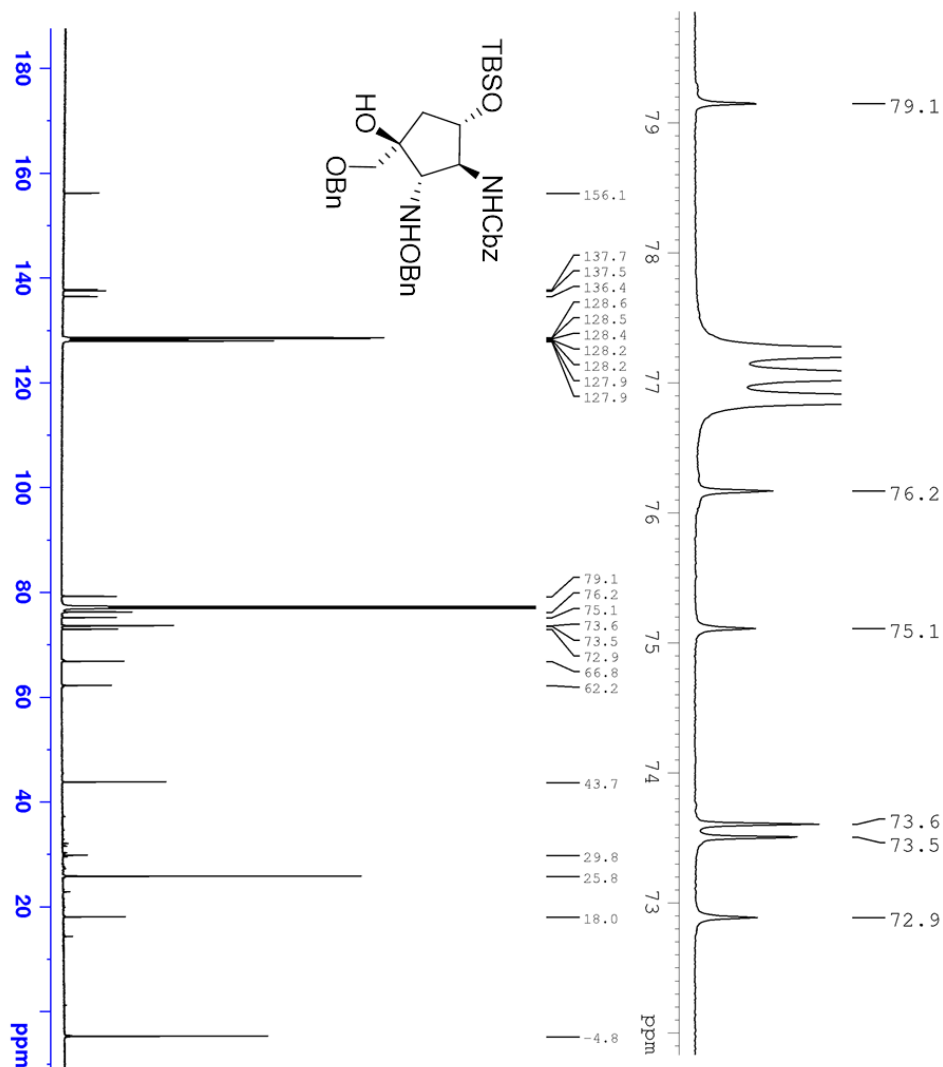
Appendix Figure 6.70: NOESY (CDCl₃) spectrum of TM-122



Current Data Parameters
NAME cjb2-136-61-71
EXNO 3
PROCNO 1
F2 - Acquisition Parameters
Date_ 20141222
Time 20.56
INSTRUM spect
PROBHD 5 mm CPDCH 13C
PULPROG zgpg30
TD 65536
SOLVENT CDCl3
NS 4
DS 4
SWH 7352.941 Hz
FIDRES 0.5714 Hz
AQ 0.5570560 sec
RG 128
DE 68.000 usec
TE 298.1 K
D1 0.00000000 sec
D16 0.00000000 sec
D8 0.50000000 sec
D16 0.00020000 sec
IN0 0.00013600 sec
F1 - Acquisition Parameters
TD 65536
SFO 700.140 MHz
WDW EM
SSB 0
LB 0 Hz
GB 0
PC 1.40
F1 - Processing parameters
SI 2048
MC2 States-TPII
SFO 700.140 MHz
WDW EM
SSB 0
LB 0 Hz
GB 0

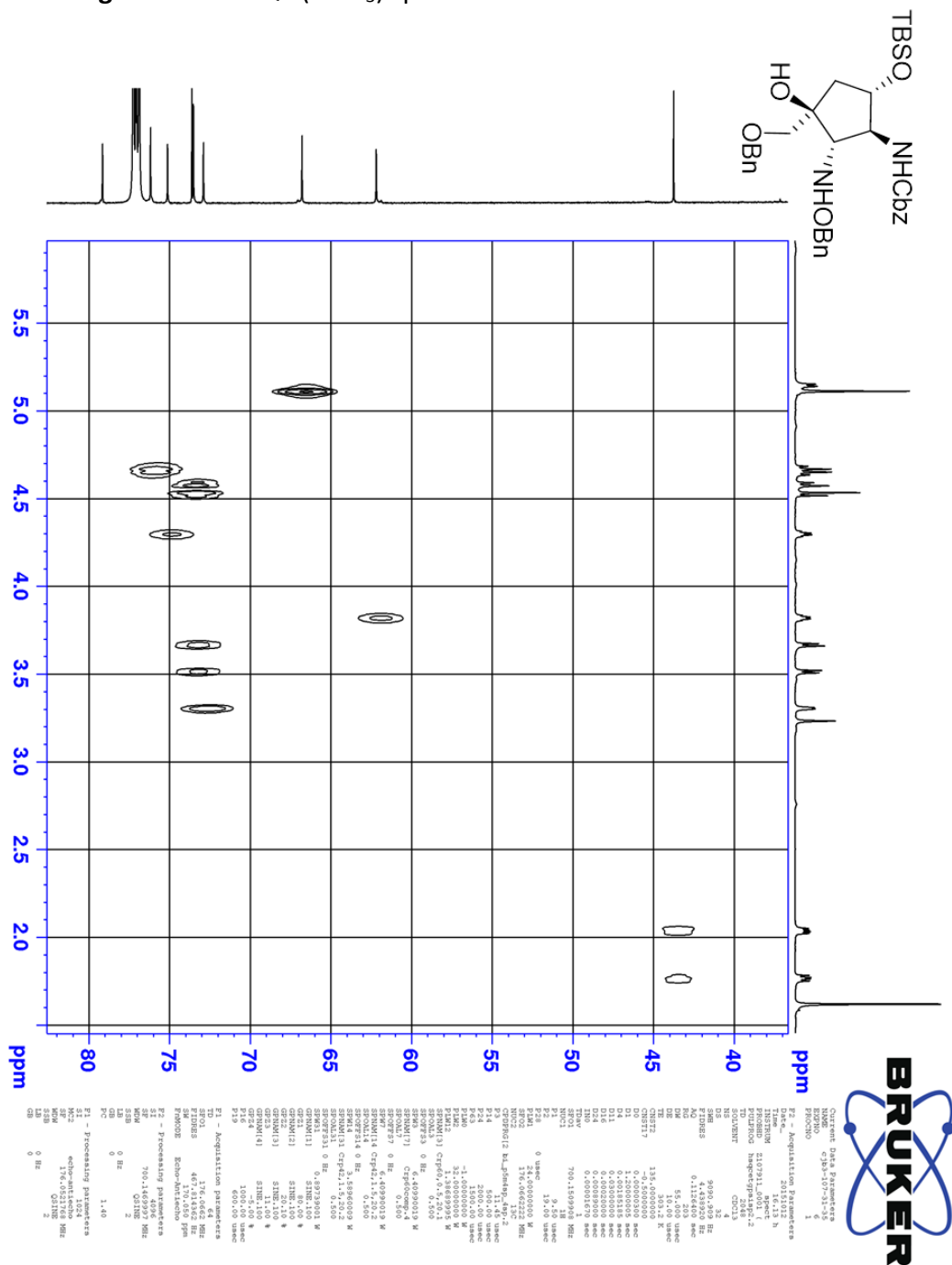


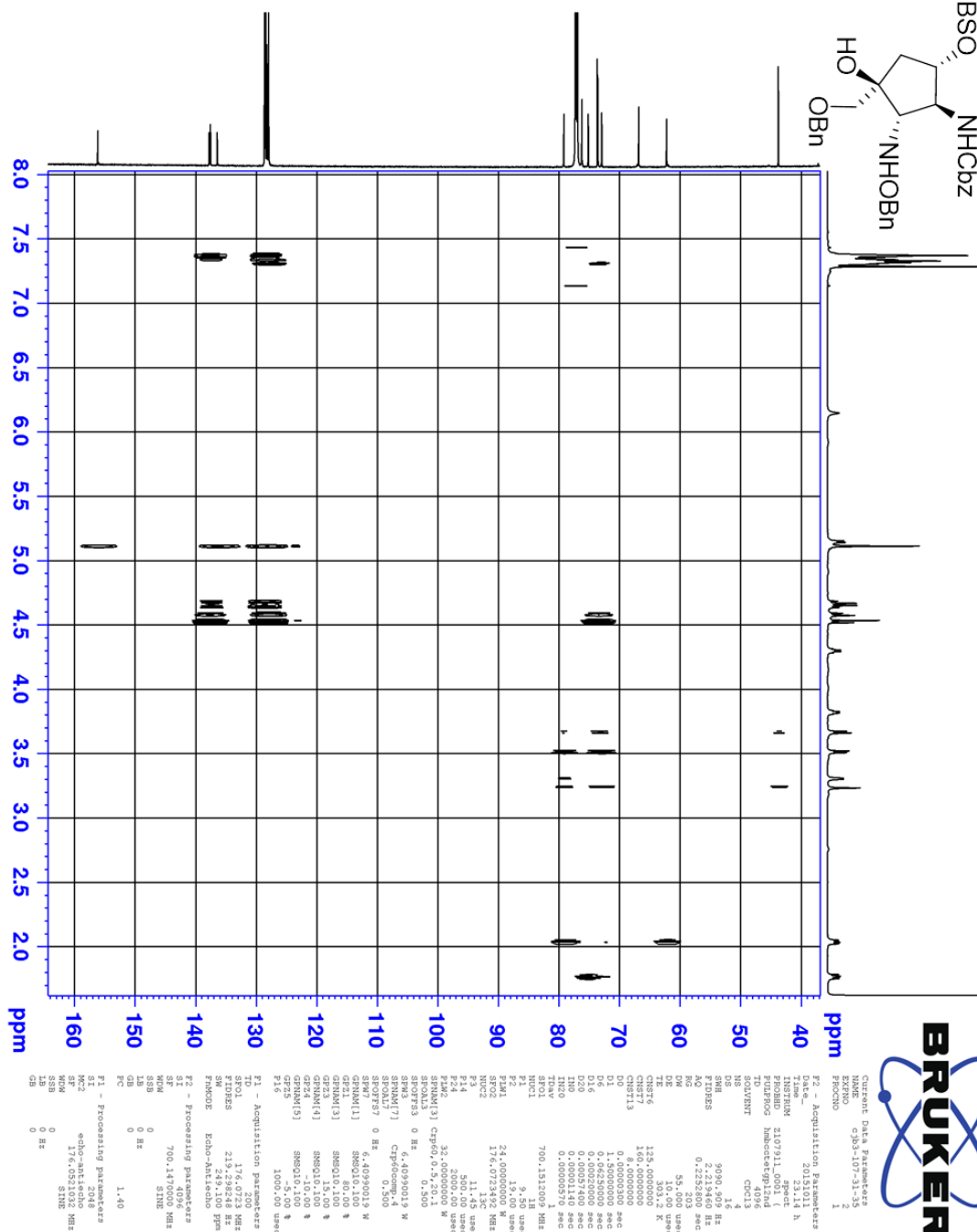
Appendix Figure 6.71: ^1H NMR (CDCl_3) spectrum of TM-121

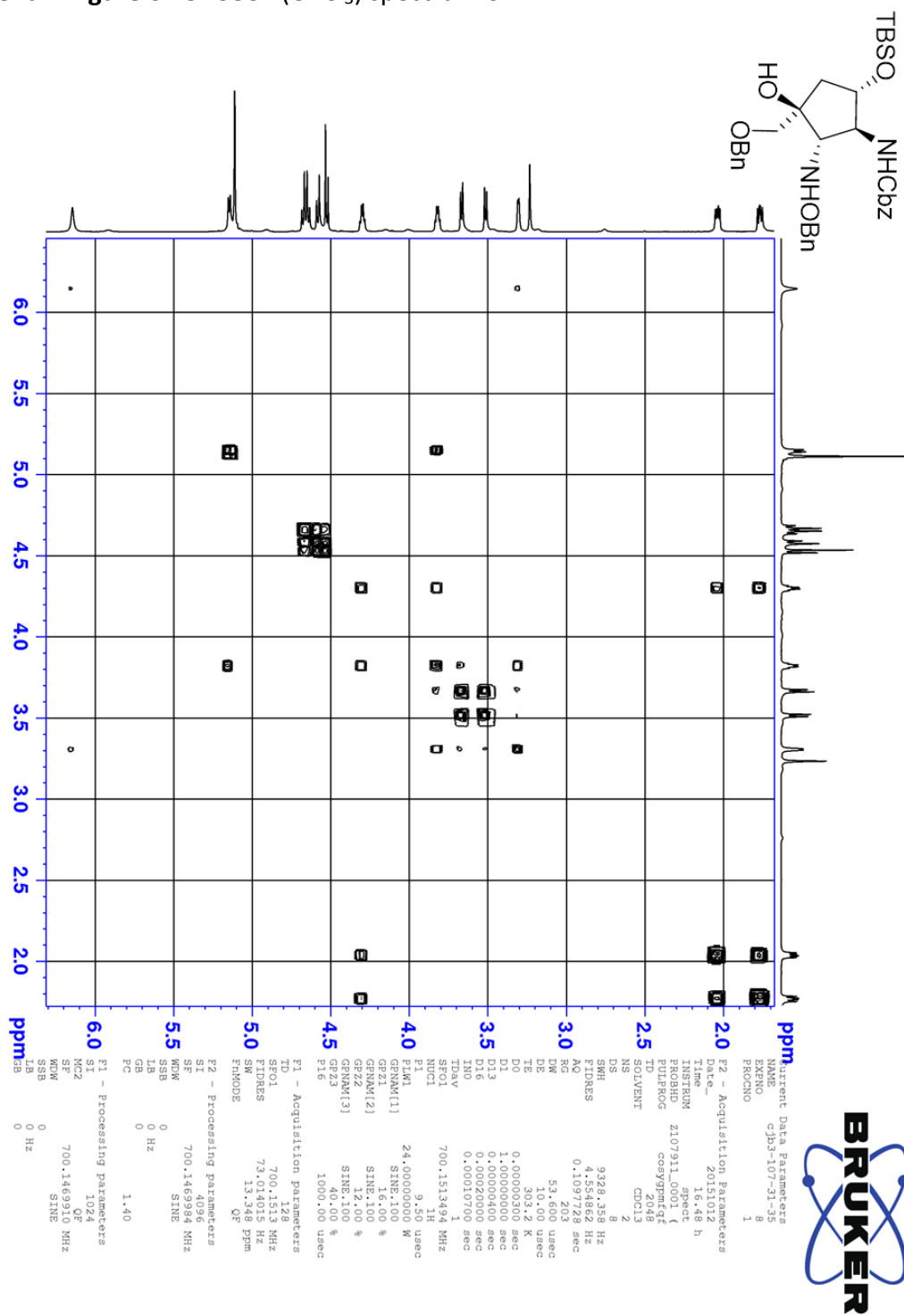


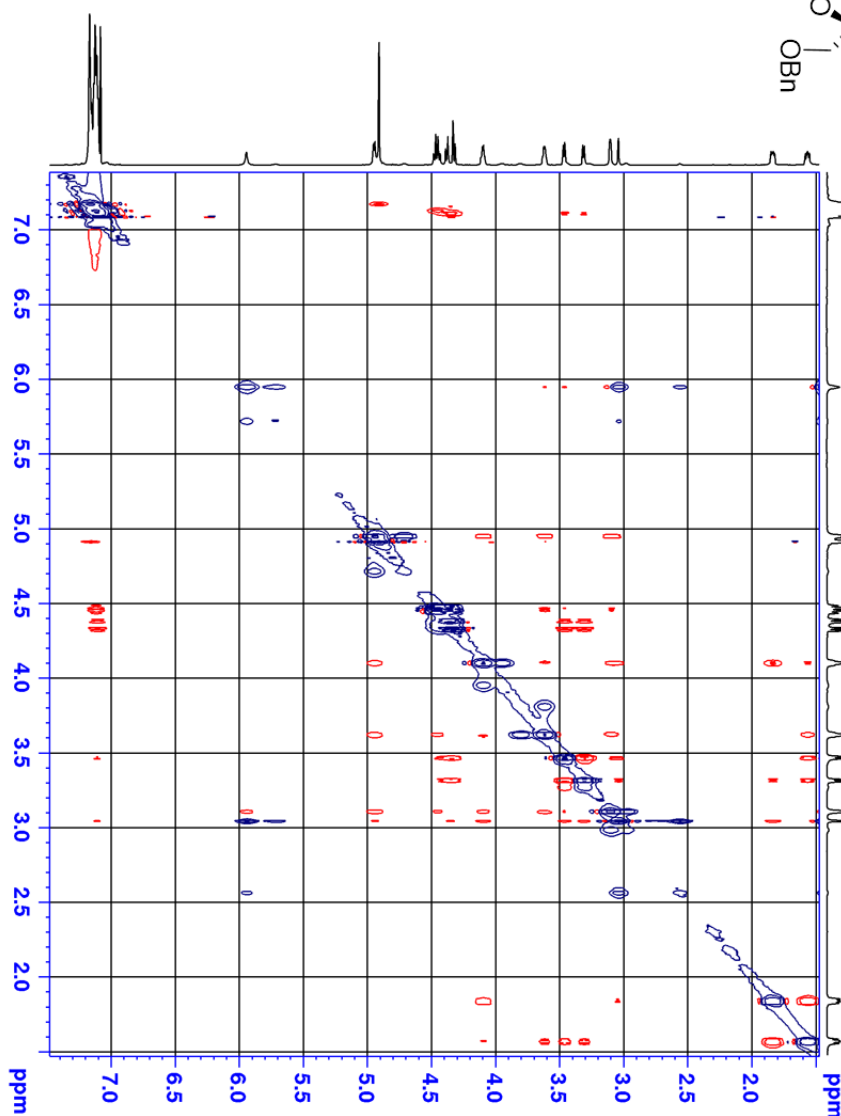
Current Data Parameters		F2 - Acquisition Parameters	
NAME	cj3-107-31-35	Date_____	2015012
EXPNO	1	Time_____	7.56 h
PROCNO	1	INSTRUM	2107911_0001
		PULPROG	zgpg30
		TD	65336
		SOLVENT	CDCl3
		NS	6000
		DS	4
		SWH	42613.637 Hz
		FIDRES	0.65023 Hz
		RG	0.766847 sec
		DE	11.733 usec
		TE	18.00 usec
		D1	33.2 K
		D11	2.0000000 sec
		TD0	0.0300000 sec
		NUC1	1
		PI	11.45 usec
		PI1	33.0000000 W
		SFO2	700.149806 MHz
		NUC2	1H
		CPDPRG2	waltz16
		PCPD2	45700 usec
		PI1M2	24.0000000 W
		PI1M2	0.51265003 W
		PI1M3	0.25615001 W
F2 - Processing parameters			
		SI	32768
		WDW	176.0521032 MHz
		SSB	EM
		GB	0
		PC	1.00 Hz
		RB	0
		LB	1.40
		CB	

Appendix Figure 6.73: HSQC (CDCl₃) spectrum of TM-121

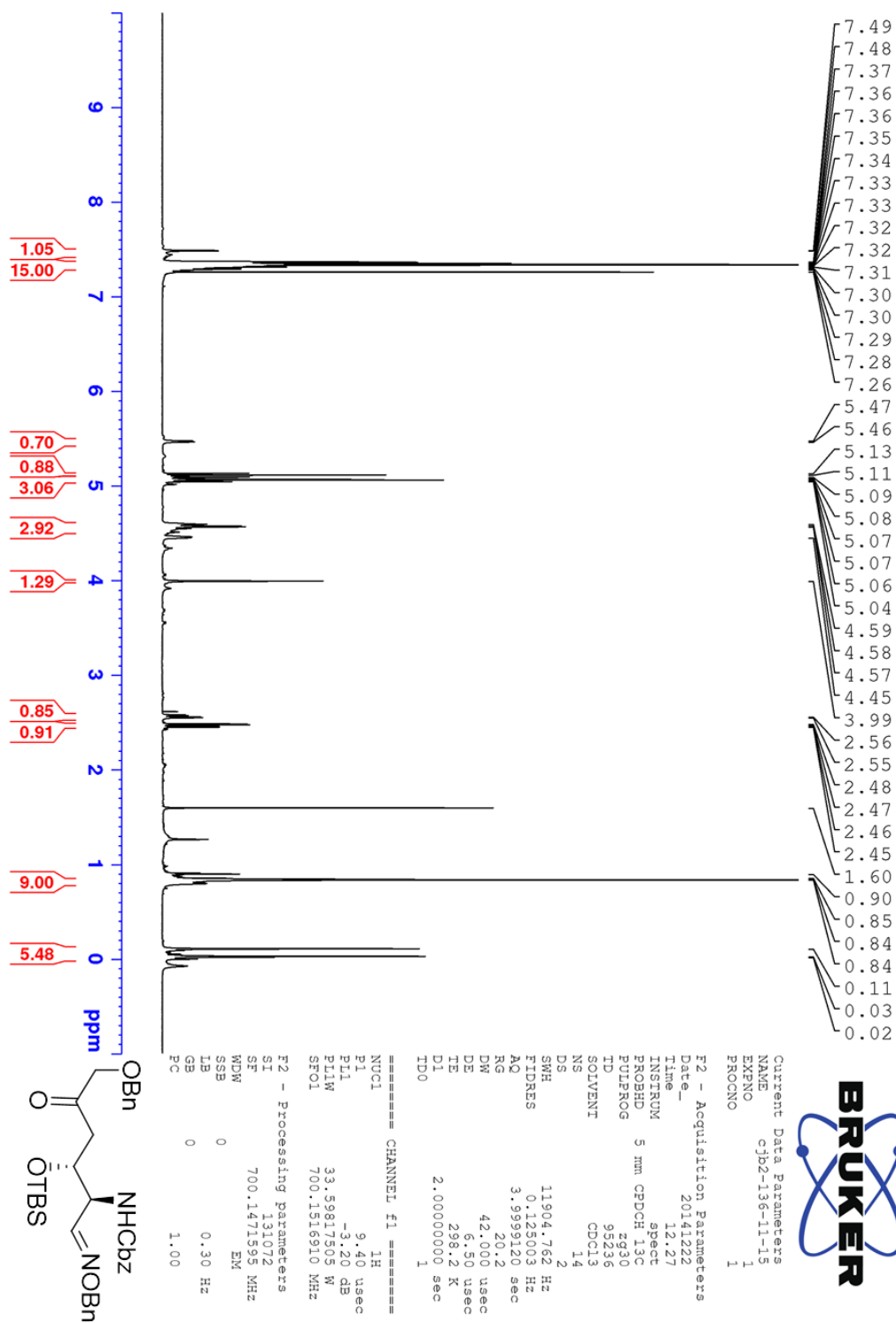


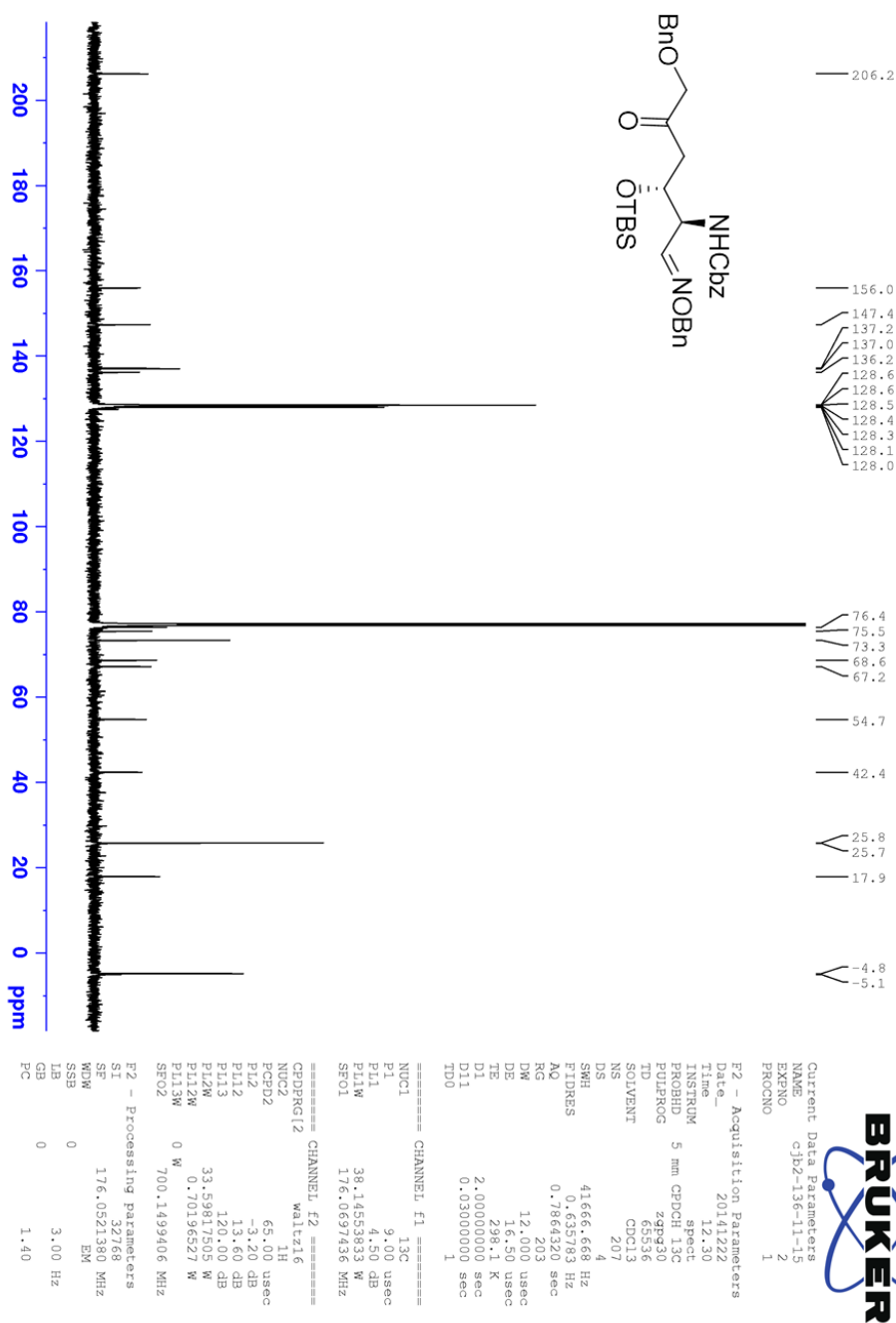


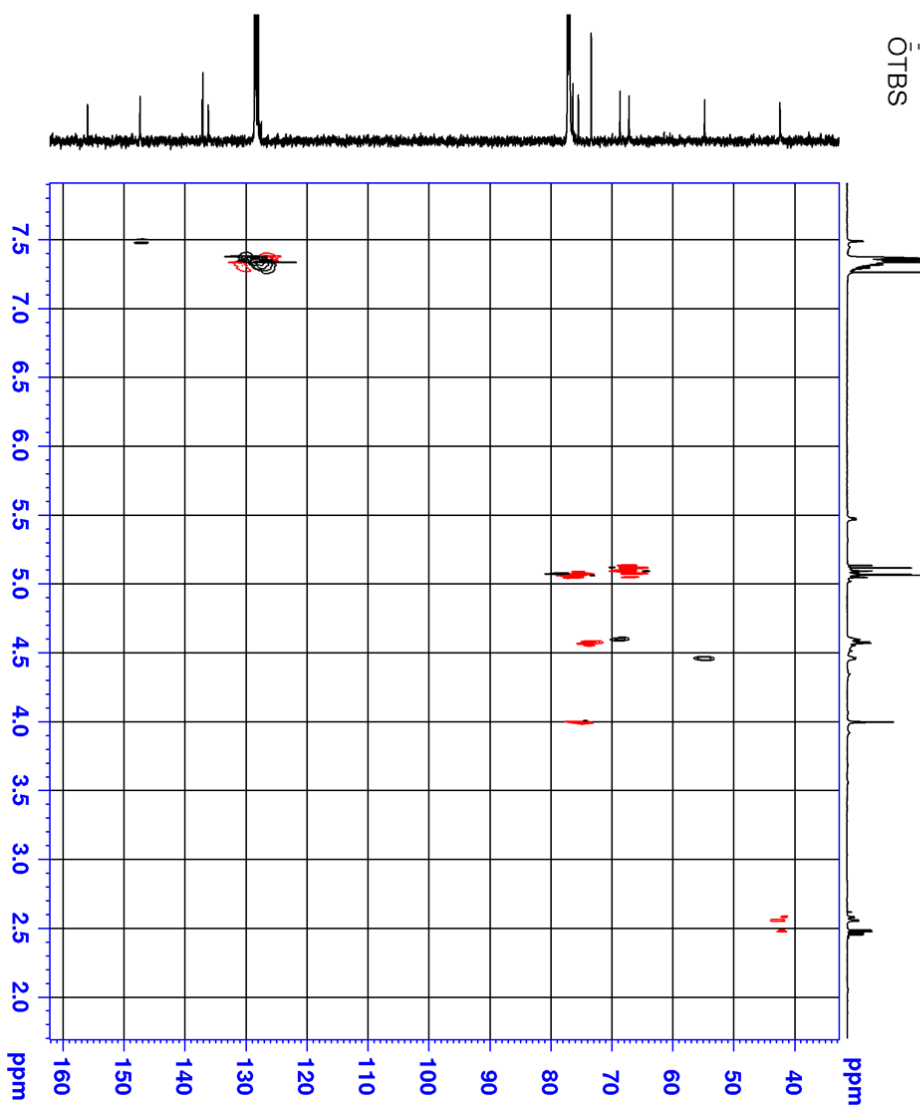
Appendix Figure 6.75: COSY (CDCl_3) spectrum of TM-121

CC1(C)C(C(C1)O)C(C(C(C1)C(C1)OC(=O)C)C(C1)OC(=O)C)C(C(C1)C(C1)OC(=O)C)C(C1)OC(=O)C

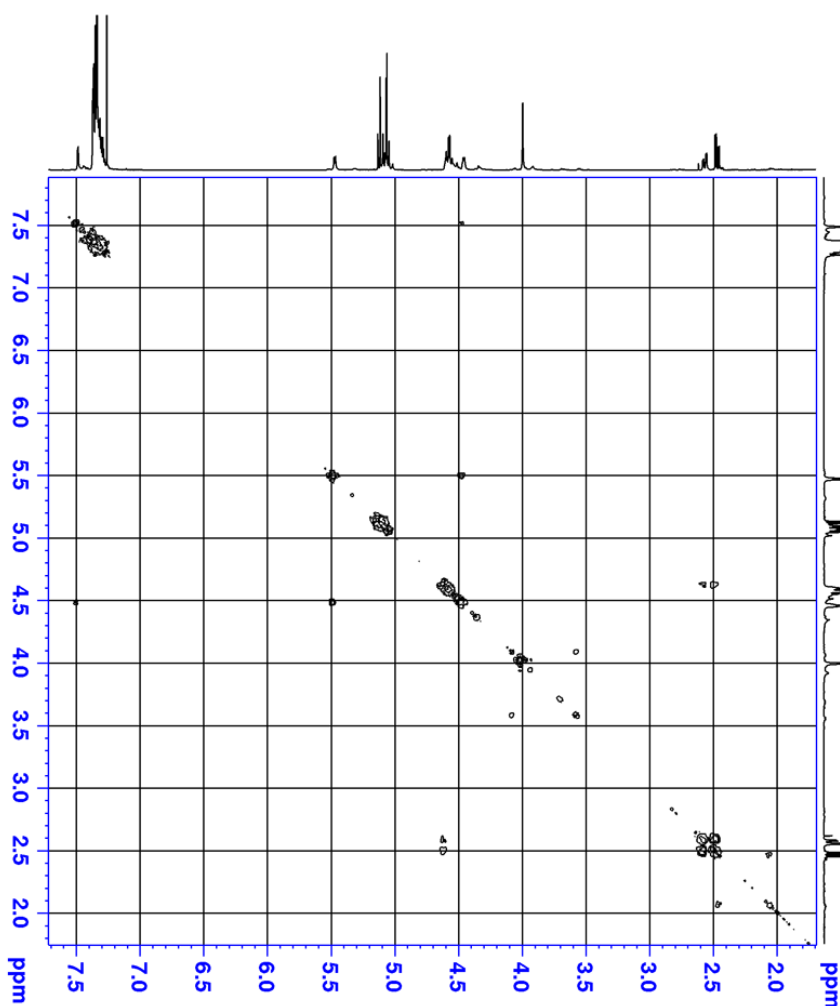
Current: Data Parameters		
NAME	cjbs-107-31-35	
EXNO	1	
FXNO	3	
F2 - Acquisition Parameters		
Date--	20151011	
Time	23.50	
INSTRUM	210791L0001	spec
PROBHD	10001	
TD	4056	noisy
SOLVENT	CDCl3	
NS	16	
DS	16	
SWH	7692.308	Hz
NUC1	13	
NUC2	1	
NUC3	0.662400	sec
RG	7.12	
DE	65.000	usecs
DW	10.00	usecs
TE	303.2	K
TD	2	
DE	0.000035280	sec
D8	0.6599999	sec
D16	0.00020000	sec
IND0	0.00012980	sec
TDV0	1	
SEF01	700.1504307	MHz
P1	9.50	usecs
P2	19.00	usecs
PW1	24.0000000	W
GPW1	40.00	%
GENP1{1}	STN: 10	
P16	1000.00	usecs
F1 - Acquisition Parameters		
TD	256	
SEF01	700.1504	MHz
F1FIRMS	30.094376	Hz
SW	11.004	ppm
F2 - Processing Parameters		
SE	4056	
SE	700.1471400	MHz
SSB	0	Hz
GB	0	
PC	1.00	
F1 - Processing parameters		
SI	2018	
SI2	700.1471400	MHz
MDW	0	Hz
SSB	2	
GB	0	Hz
PC	1.00	

Appendix Figure 6.77: ^1H NMR (CDCl_3) spectrum of **12**

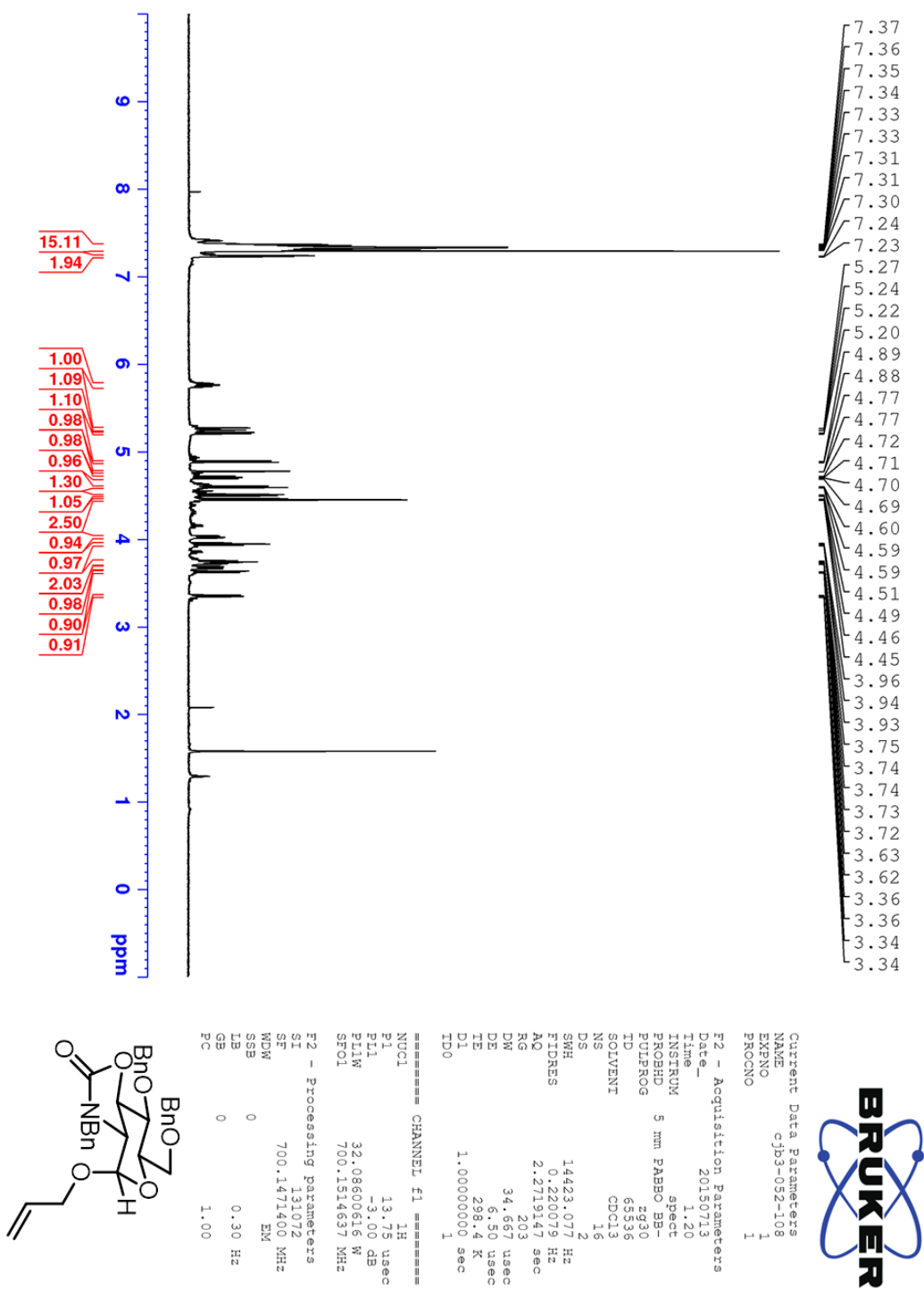
Appendix Figure 6.78: ^{13}C NMR (CDCl_3) spectrum of **12**

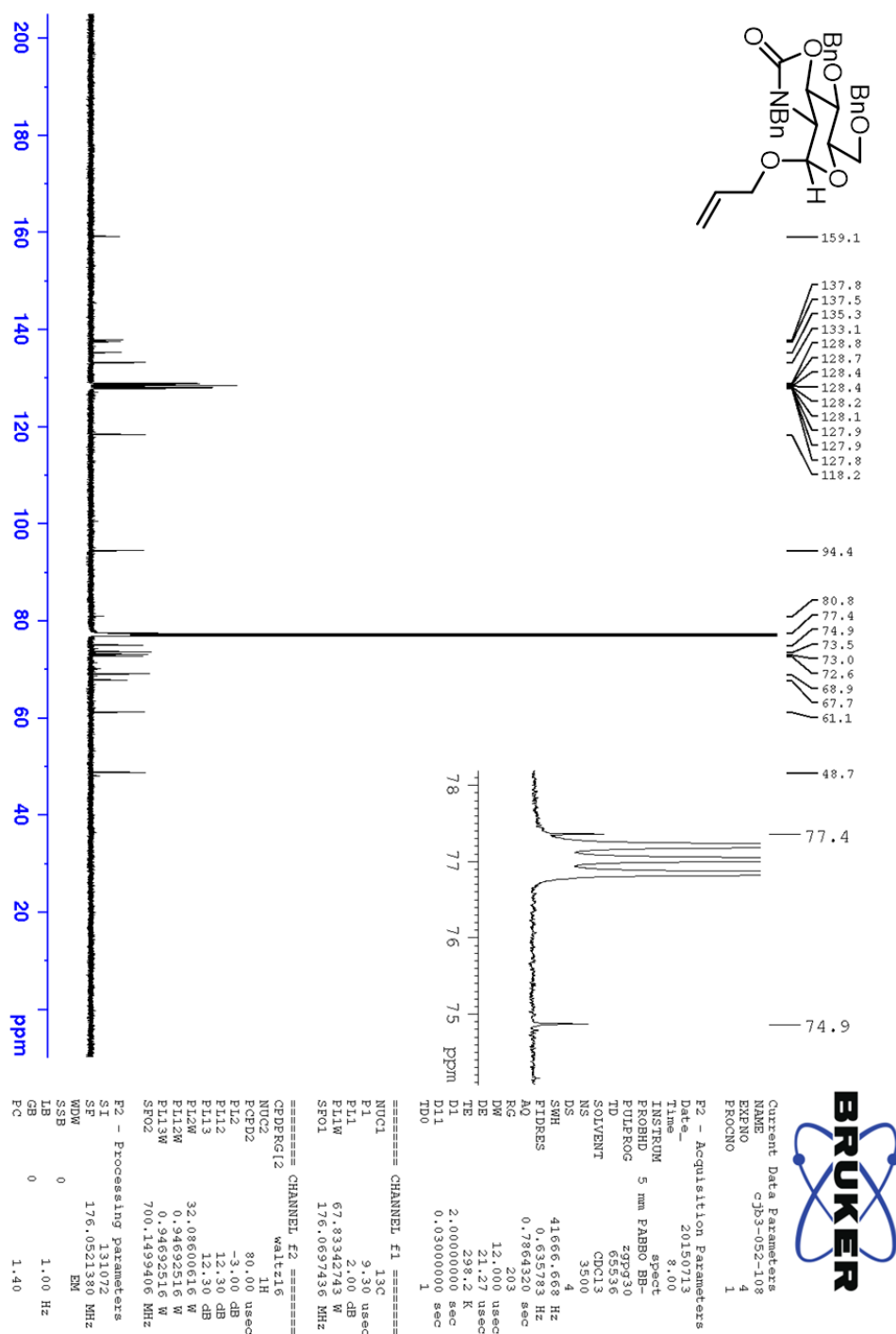
CCOC(=O)CC[C@H](C=C[C@@H](C)C(=O)O[Si](C)(C)C)C(=O)O[Si](C)(C)C

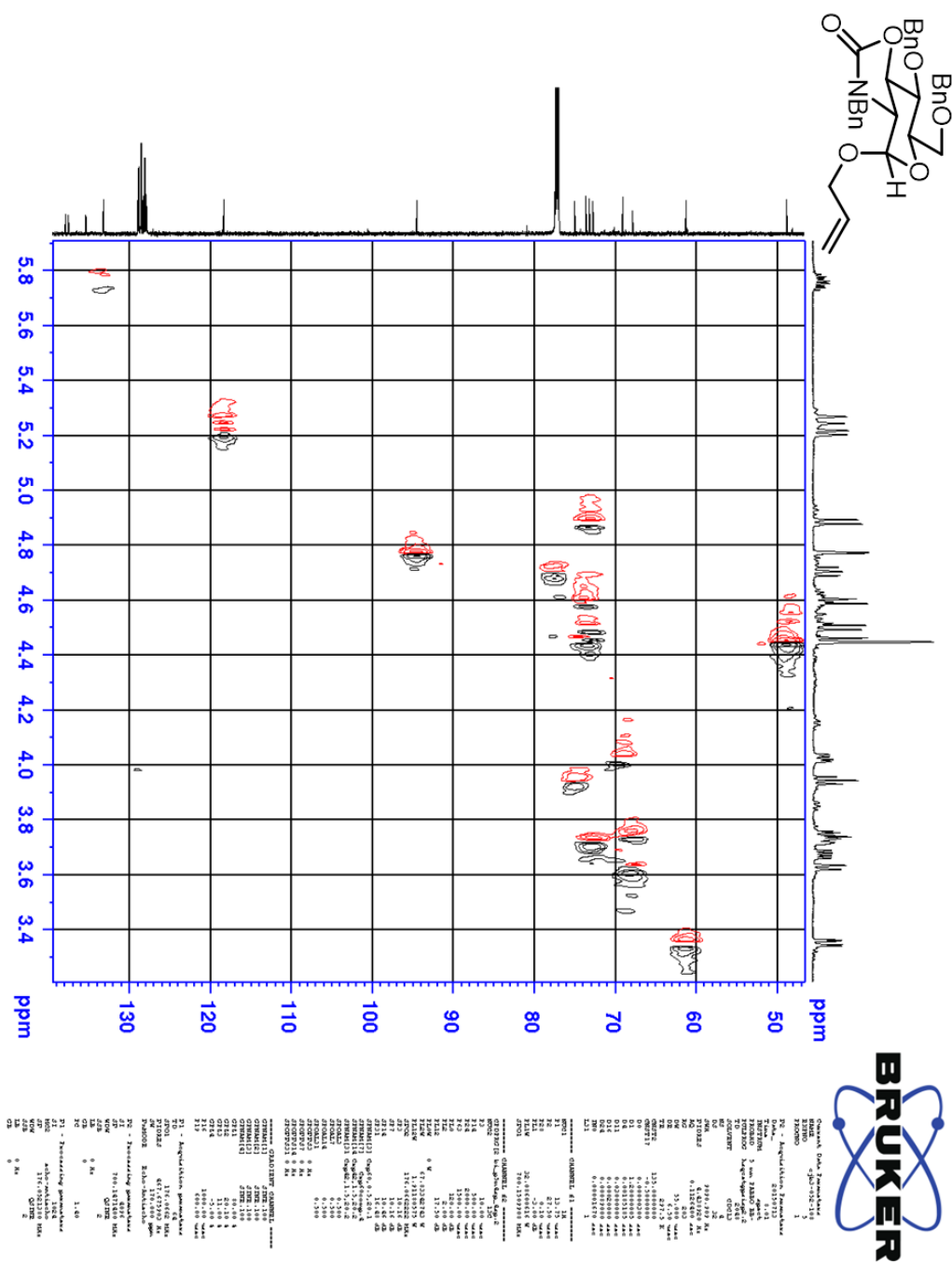
Current Data Parameters		F1 - Acquisition Parameters		F2 - Acquisition Parameters	
NAME	CurrentData	NAME	20111222	NAME	20111222
EXPNO	1	EXPNO	1	EXPNO	1
PROCNO	1	PROCNO	1	PROCNO	1
INSTRUM	5 mm CPMAS 13C	INSTRUM	5 mm CPMAS 13C	INSTRUM	5 mm CPMAS 13C
PROBHD	5 mm CPMAS 13C	PROBHD	5 mm CPMAS 13C	PROBHD	5 mm CPMAS 13C
TD	4096	TD	4096	TD	4096
RG	3.00	RG	3.00	RG	3.00
SD	0.00	SD	0.00	SD	0.00
DS	1.00	DS	1.00	DS	1.00
SS	1.00	SS	1.00	SS	1.00
SB	0	SB	0	SB	0
PC	1.40	PC	1.40	PC	1.40
WDW	EM	WDW	EM	WDW	EM
SSB	0	SSB	0	SSB	0
GB	0	GB	0	GB	0
MC	0	MC	0	MC	0
LB	0	LB	0	LB	0
GB	0	GB	0	GB	0
DB	0	DB	0	DB	0
SR	176.023180 MHz	SR	176.023180 MHz	SR	176.023180 MHz
OR	0.0000000 sec	OR	0.0000000 sec	OR	0.0000000 sec
RG	0.0000000 sec	RG	0.0000000 sec	RG	0.0000000 sec
DS	0.0000000 sec	DS	0.0000000 sec	DS	0.0000000 sec
SS	0.0000000 sec	SS	0.0000000 sec	SS	0.0000000 sec
SB	0.0000000 sec	SB	0.0000000 sec	SB	0.0000000 sec
PC	0.0000000 sec	PC	0.0000000 sec	PC	0.0000000 sec
WDW	EM	WDW	EM	WDW	EM
SSB	0	SSB	0	SSB	0
GB	0	GB	0	GB	0
MC	0	MC	0	MC	0
LB	0	LB	0	LB	0
GB	0	GB	0	GB	0
DB	0	DB	0	DB	0
SR	176.023180 MHz	SR	176.023180 MHz	SR	176.023180 MHz
OR	0.0000000 sec	OR	0.0000000 sec	OR	0.0000000 sec
RG	0.0000000 sec	RG	0.0000000 sec	RG	0.0000000 sec
DS	0.0000000 sec	DS	0.0000000 sec	DS	0.0000000 sec
SS	0.0000000 sec	SS	0.0000000 sec	SS	0.0000000 sec
SB	0.0000000 sec	SB	0.0000000 sec	SB	0.0000000 sec
PC	0.0000000 sec	PC	0.0000000 sec	PC	0.0000000 sec
WDW	EM	WDW	EM	WDW	EM
SSB	0	SSB	0	SSB	0
GB	0	GB	0	GB	0
MC	0	MC	0	MC	0
LB	0	LB	0	LB	0
GB	0	GB	0	GB	0
DB	0	DB	0	DB	0
SR	176.023180 MHz	SR	176.023180 MHz	SR	176.023180 MHz
OR	0.0000000 sec	OR	0.0000000 sec	OR	0.0000000 sec
RG	0.0000000 sec	RG	0.0000000 sec	RG	0.0000000 sec
DS	0.0000000 sec	DS	0.0000000 sec	DS	0.0000000 sec
SS	0.0000000 sec	SS	0.0000000 sec	SS	0.0000000 sec
SB	0.0000000 sec	SB	0.0000000 sec	SB	0.0000000 sec
PC	0.0000000 sec	PC	0.0000000 sec	PC	0.0000000 sec
WDW	EM	WDW	EM	WDW	EM
SSB	0	SSB	0	SSB	0
GB	0	GB	0	GB	0
MC	0	MC	0	MC	0
LB	0	LB	0	LB	0
GB	0	GB	0	GB	0
DB	0	DB	0	DB	0
SR	176.023180 MHz	SR	176.023180 MHz	SR	176.023180 MHz
OR	0.0000000 sec	OR	0.0000000 sec	OR	0.0000000 sec
RG	0.0000000 sec	RG	0.0000000 sec	RG	0.0000000 sec
DS	0.0000000 sec	DS	0.0000000 sec	DS	0.0000000 sec

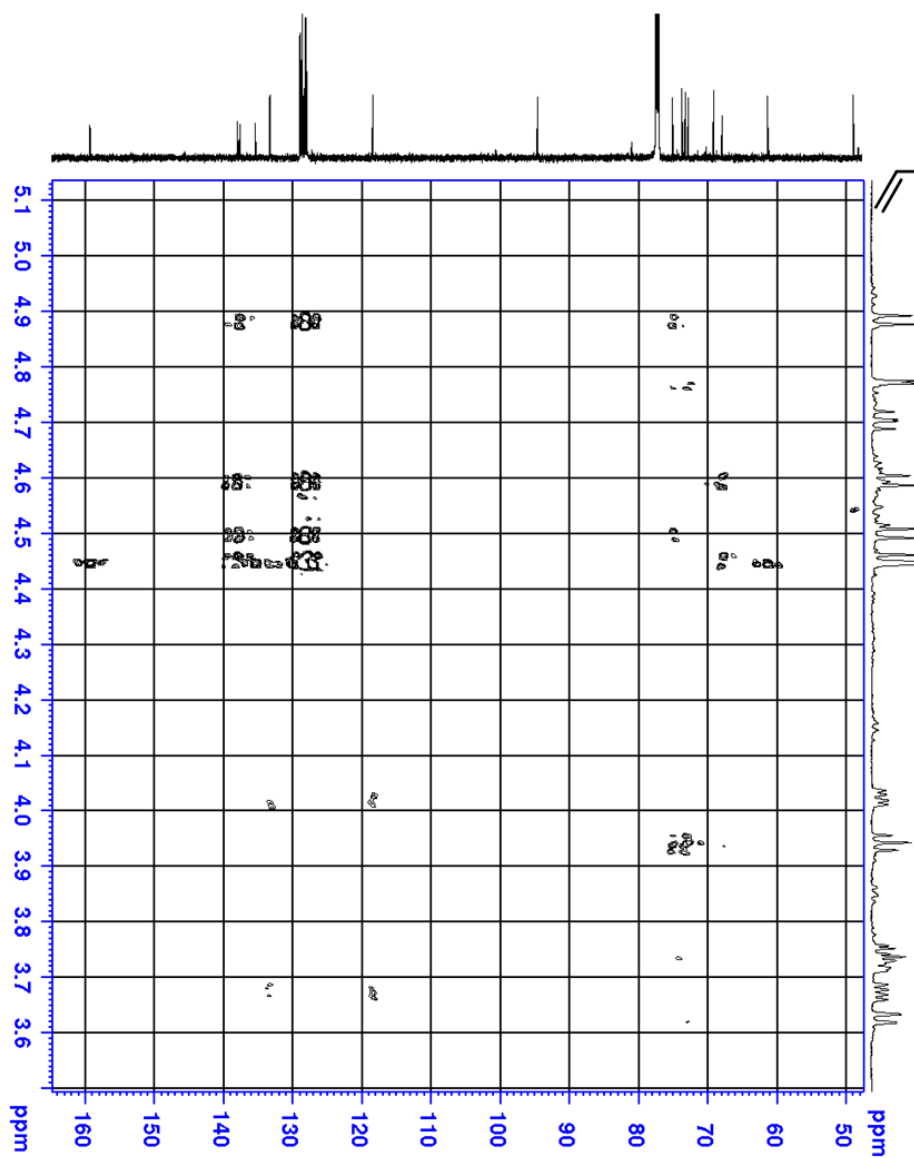
CC(=O)CC[C@H](C=C[N+](=O)[O-])C[C@@H](C)C(=O)O[Si](C)(C)C

Current Data Parameters					
NAME	C:\bz-136-f1-15				
EXPNO	4				
F2 - Acquisition Parameters					
Date_	20141222				
Time	13:01				
PROBHD	5 mm CPDPC				
PULPROG	zgpgmt				
ID	2048				
SOLVENT	CDCI3				
DS	2				
NS	2				
SRHS	7350.94 Hz				
FIRRS	3.590303 Hz				
AQ	0.1392640 sec				
Rg	2.03				
RG	3264				
TE	298.1 K				
TD	66.000 usec				
DE	298.1 K				
D0	0.00000300 sec				
D1	2.00000000 sec				
D13	0.00000400 sec				
IN6	0.00013600 sec				
CHANNEL f1					
NUC1	1H				
P1	9.40 usec				
P2	3.10 usec				
P11	-3.20 dB				
PLW	33.59817505 W				
SFO1	700.1502907 MHz				
GRADIENT CHANNEL f1					
GPRN11	SHINE				
GPR1	80.00 %				
P16	1000.00 usec				
f1 - Acquisition parameters					
SFO1	700.1503 MHz				
FIRRS	61.7899410 Hz				
SW	10.502 ppm				
FHMODE	GF				
f2 - Processing parameters					
SF	700.147100 MHz				
SI	SINE				
WDW					
SSB	0 Hz				
GB	0				
f1 - Processing parameters					
SF2	700.147100 MHz				
SI2	ZG48				
WDW					
SSB	0 Hz				
GB	0				

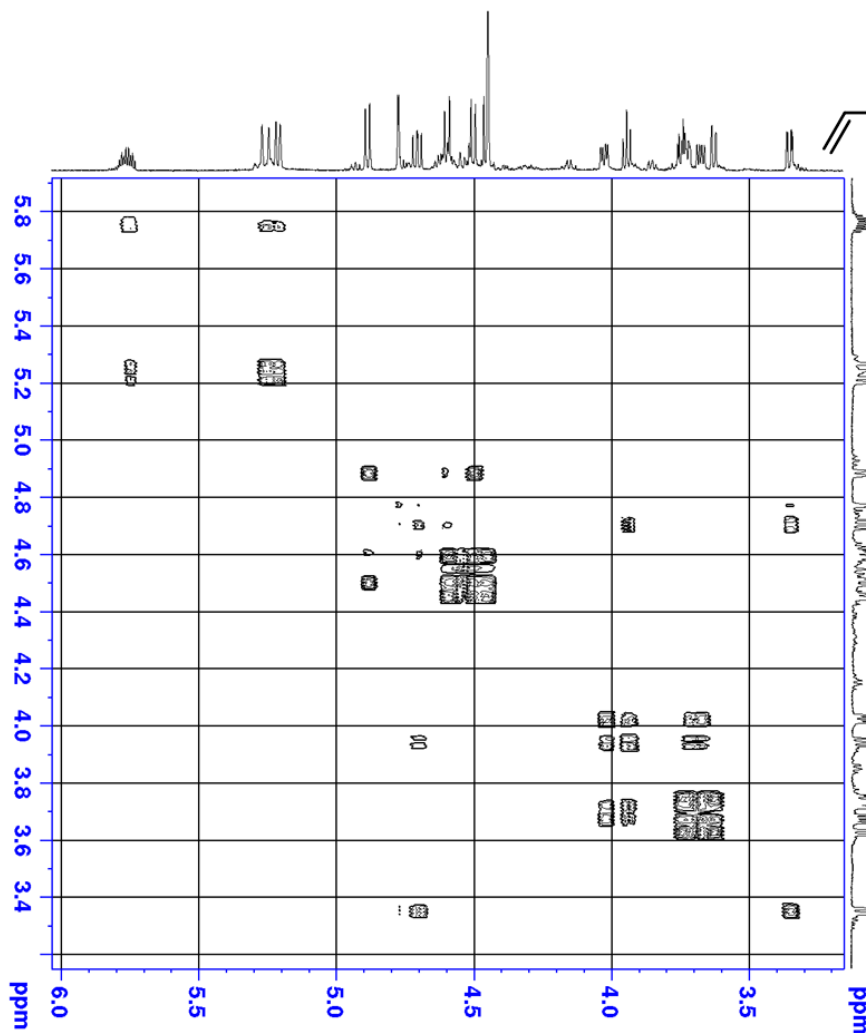
Appendix Figure 6.81: ^1H NMR (CDCl_3) spectrum of **17**

Appendix Figure 6.82: ^{13}C NMR (CDCl_3) spectrum of **17**

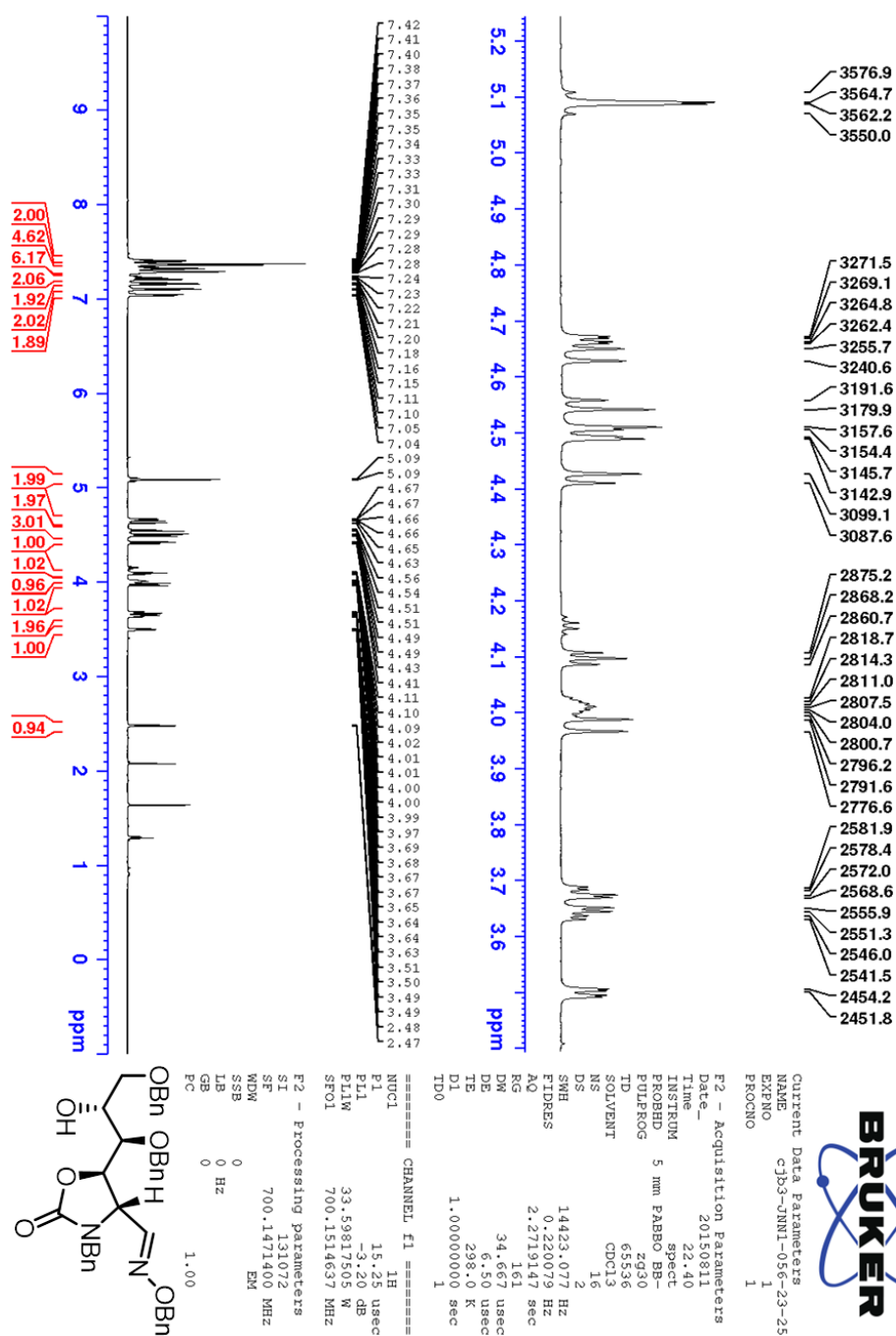
Appendix Figure 6.83: HSQC (CDCl_3) spectrum of **17**

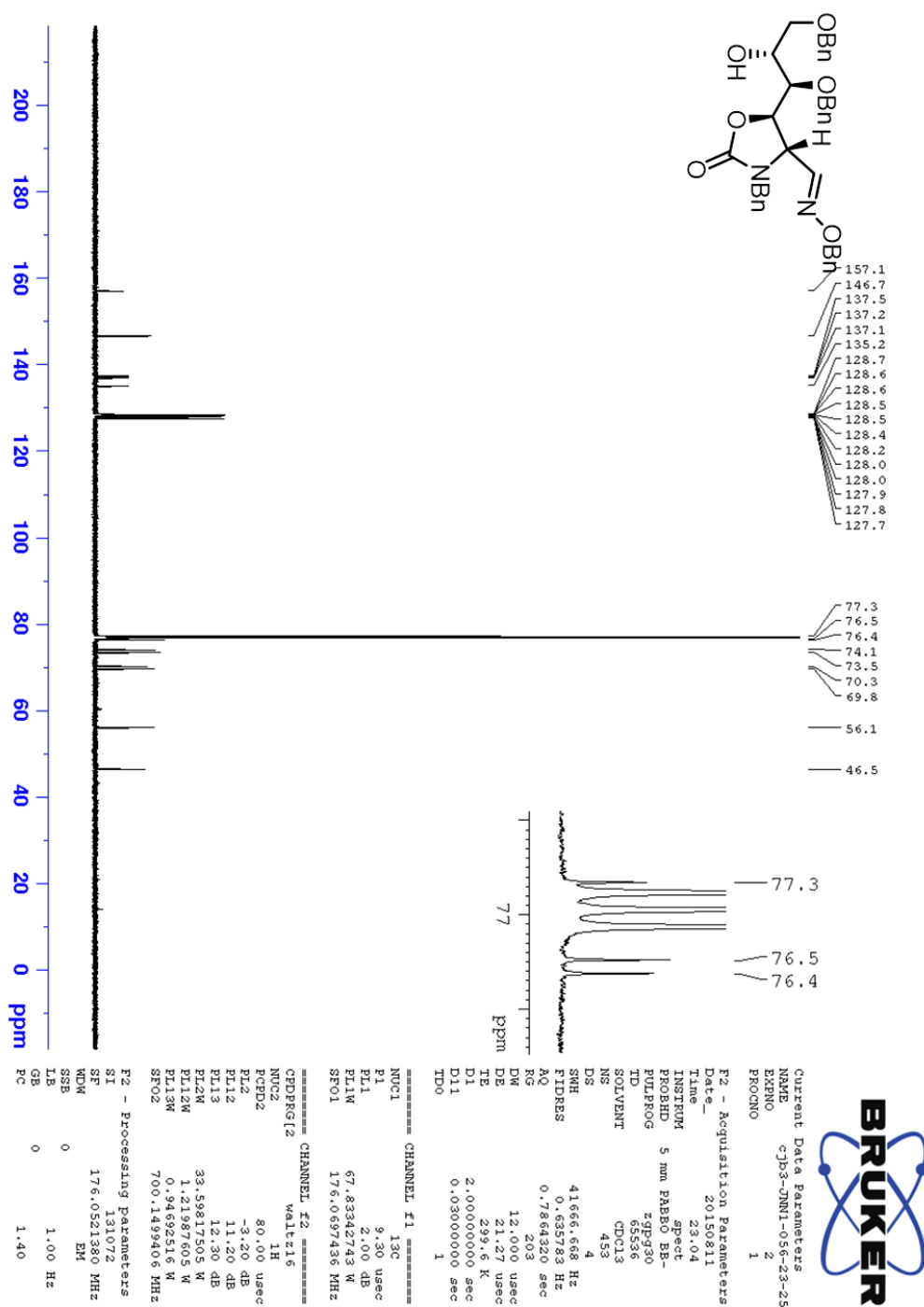
[illegible]

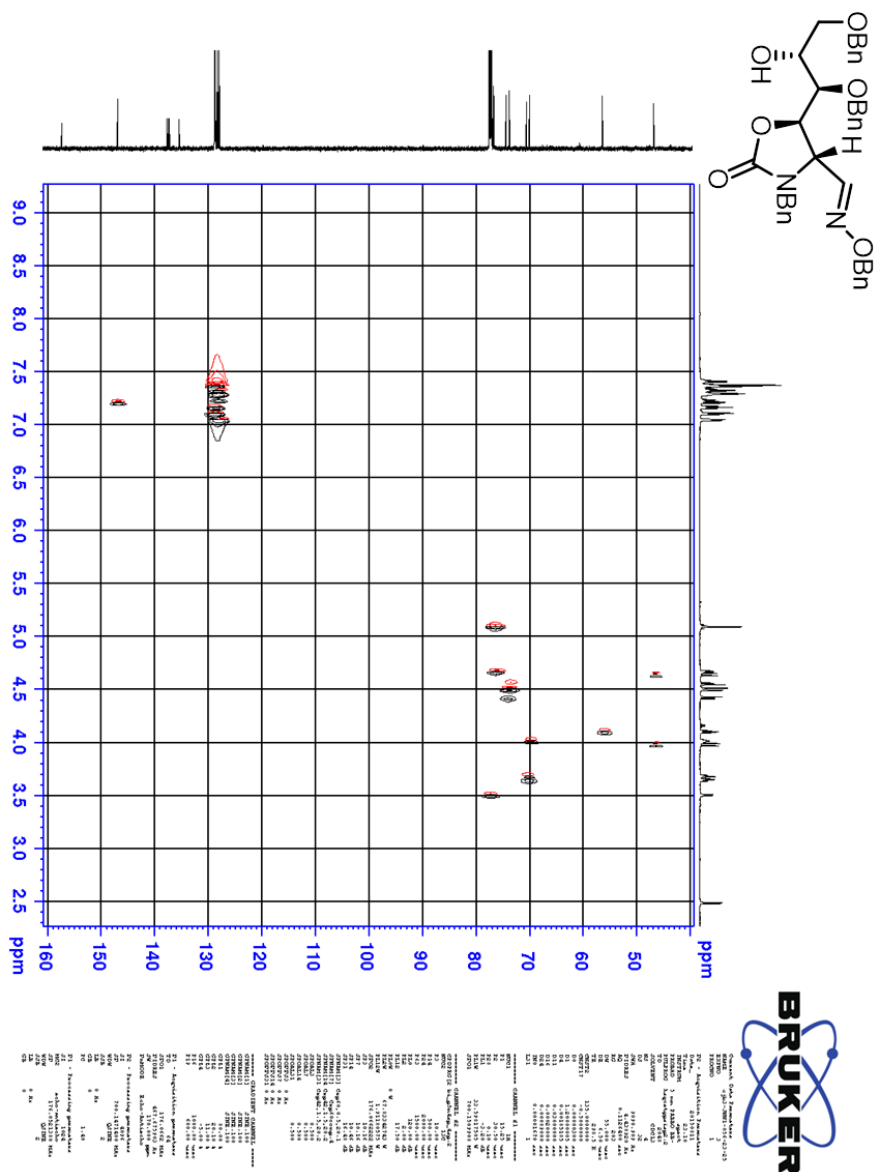
Chemical structure of compound 10: A bicyclic molecule featuring a benzylidene-protected diol and a benzyl carbamate group. The structure is shown in a chair conformation with the benzylidene group in the endo position and the benzyl carbamate group in the exo position.



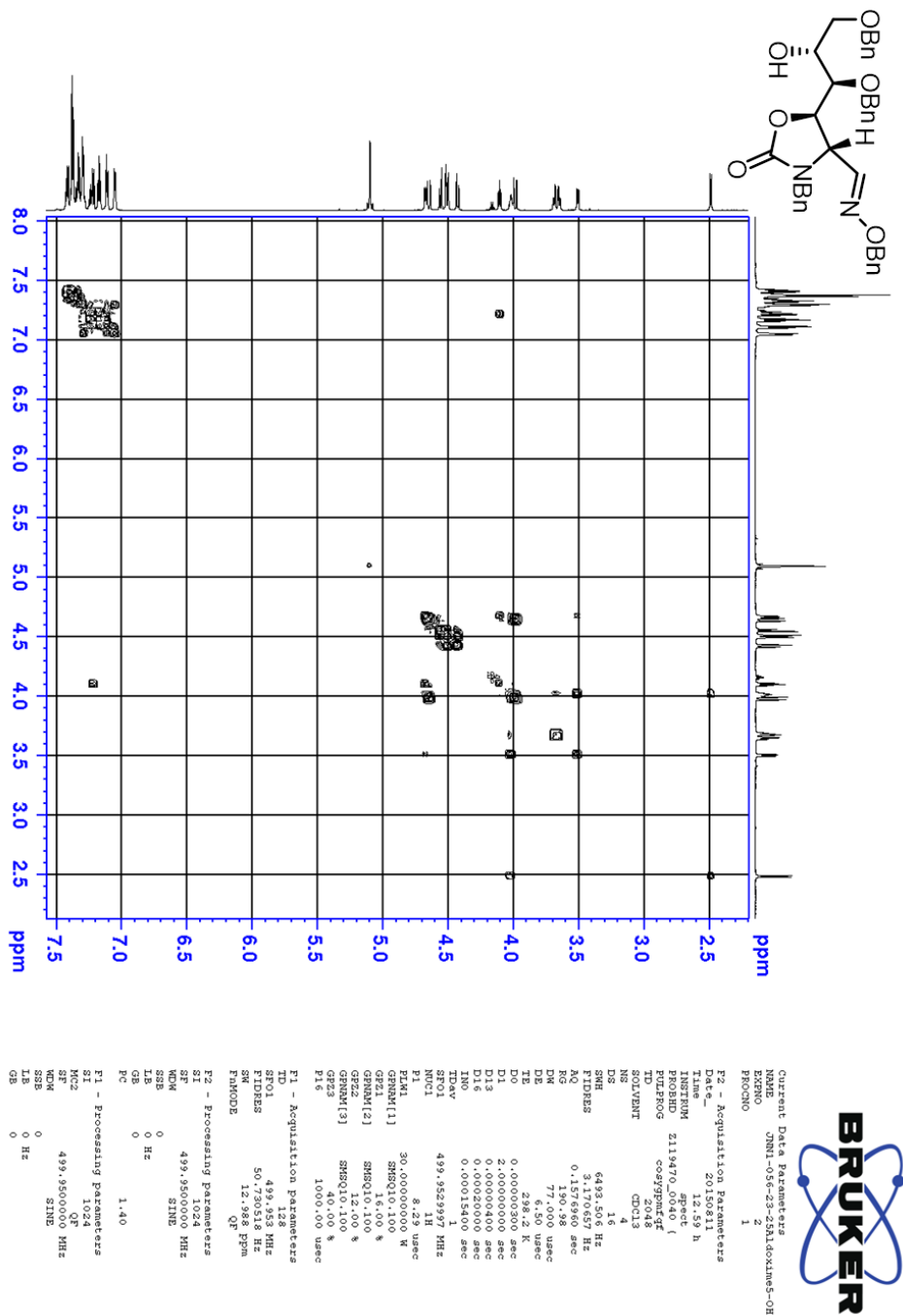
Current Data Parameters	
NAME	c3b5-052-108
PROBHD	5
PROBHD	1
Date - Acquisition Parameters	
Date	20150713
Time	0:08
PROBHD	5 mm PABBO BB-
PULPROG	zgpg30
TD	2048
SOLVENT	
SOLVENT	CDC13
DS	2
SWH	9348.38 Hz
FIDRES	4.558682 Hz
AQ	0.197928 sec
RG	53.205 usec
TE	298.2 K
D1	0.00000300 sec
D1.3	1.00000000 sec
D1.2	0.00000000 sec
D1.6	0.00020000 sec
IN0	0.00010700 sec
CHANNEL f1	
NUC1	¹³ C
P1	13.75 usec
PL1	-3.00 dB
FLW	32.08060616 W
RF01	700.1519440 MHz
GRADIENT CHANNEL	
GRANA11	LINE:100
GRANA12	LINE:100
GRANA13	LINE:100
GR21	16.00 *
GR22	16.00 *
GR23	16.00 *
P16	1000.00 usec
F1 - Acquisition parameters	
TD	700.1528 MHz
FIDRES	73.021339 Hz
SW	13.350 ppm
FMHRC	OF
F2 - Processing parameters	
SI	700.1471400 MHz
SE	700.1471400 MHz
WDW	SINE
SSB	0
GB	0 Hz
PC	1.00
F1 - Processing parameters	
SI	700.1471400 MHz
SE	700.1471400 MHz
WDW	SINE
SSB	0
GB	0 Hz

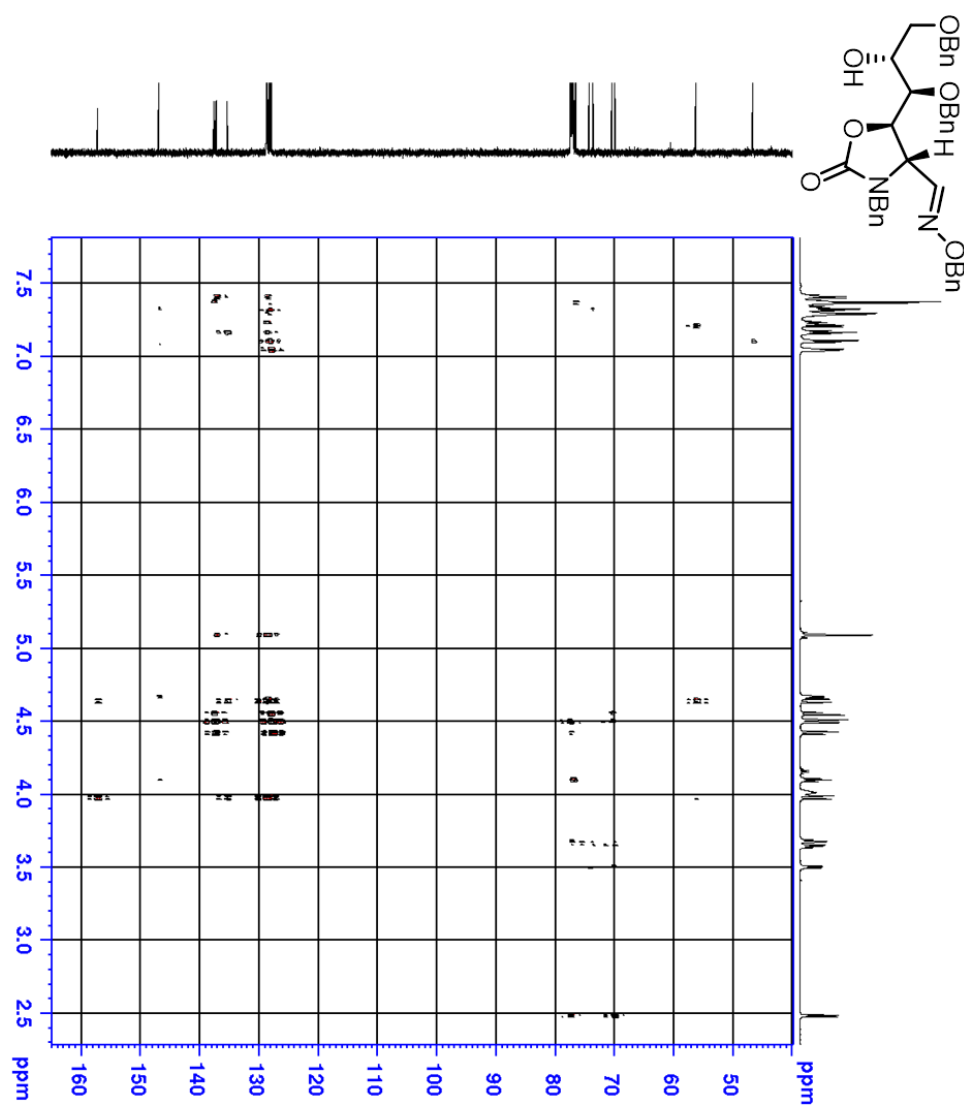
Appendix Figure 6.86: ^1H NMR (CDCl_3) spectrum of *E*-19

Appendix Figure 6.87: ^{13}C NMR (CDCl_3) spectrum of *E*-19

Appendix Figure 6.88: HSQC (CDCl₃) spectrum of *E*-19

Appendix Figure 6.89: COSY (CDCl₃) spectrum of *E*-19



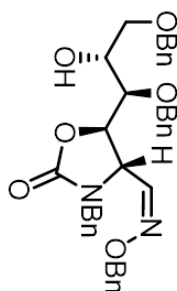
Appendix Figure 6.90: HMBC (CDCl₃) spectrum of **E-19**

BRUKER

NAME: c203-nmr1-054-23-23
PROCNO: 1
F2 - Acquisition Parameters
Date_: 20151111
Time: 14:45:42
INSTRUM: spect
PROBHD: 5 mm BBO-1H/13C
PULPROG: zgpg30
SOLVENT: CDCl3
D1: 2.00
D11: 0.05000000
D12: 0.05000000
D13: 0.05000000
D14: 0.05000000
D15: 0.05000000
D16: 0.05000000
D17: 0.05000000
D18: 0.05000000
D19: 0.05000000
D20: 0.05000000
D21: 0.05000000
D22: 0.05000000
D23: 0.05000000
D24: 0.05000000
D25: 0.05000000
D26: 0.05000000
D27: 0.05000000
D28: 0.05000000
D29: 0.05000000
D30: 0.05000000
D31: 0.05000000
D32: 0.05000000
D33: 0.05000000
D34: 0.05000000
D35: 0.05000000
D36: 0.05000000
D37: 0.05000000
D38: 0.05000000
D39: 0.05000000
D40: 0.05000000
D41: 0.05000000
D42: 0.05000000
D43: 0.05000000
D44: 0.05000000
D45: 0.05000000
D46: 0.05000000
D47: 0.05000000
D48: 0.05000000
D49: 0.05000000
D50: 0.05000000
D51: 0.05000000
D52: 0.05000000
D53: 0.05000000
D54: 0.05000000
D55: 0.05000000
D56: 0.05000000
D57: 0.05000000
D58: 0.05000000
D59: 0.05000000
D60: 0.05000000
D61: 0.05000000
D62: 0.05000000
D63: 0.05000000
D64: 0.05000000
D65: 0.05000000
D66: 0.05000000
D67: 0.05000000
D68: 0.05000000
D69: 0.05000000
D70: 0.05000000
D71: 0.05000000
D72: 0.05000000
D73: 0.05000000
D74: 0.05000000
D75: 0.05000000
D76: 0.05000000
D77: 0.05000000
D78: 0.05000000
D79: 0.05000000
D80: 0.05000000
D81: 0.05000000
D82: 0.05000000
D83: 0.05000000
D84: 0.05000000
D85: 0.05000000
D86: 0.05000000
D87: 0.05000000
D88: 0.05000000
D89: 0.05000000
D90: 0.05000000
D91: 0.05000000
D92: 0.05000000
D93: 0.05000000
D94: 0.05000000
D95: 0.05000000
D96: 0.05000000
D97: 0.05000000
D98: 0.05000000
D99: 0.05000000
D100: 0.05000000

¹H NMR spectrum of compound 10 in CDCl₃. The spectrum shows peaks from 0 to 10 ppm. Key features include a triplet at ~0.9 ppm (3H), a multiplet at ~1.2-1.6 ppm (12H), a multiplet at ~2.3-2.6 ppm (4H), a multiplet at ~3.3-3.7 ppm (4H), a multiplet at ~3.9-4.1 ppm (2H), a multiplet at ~4.5-4.7 ppm (2H), a multiplet at ~4.9-5.1 ppm (2H), a multiplet at ~6.7-7.4 ppm (10H), and a multiplet at ~7.1-7.4 ppm (10H). Integration values are provided for several peaks.

Chemical Shift (ppm)	Integration
0.92	0.99
1.06	2.00
1.08	1.08
1.10	1.01
1.12	3.05
1.14	0.98
1.16	0.97
1.18	0.97
1.20	1.01
1.22	1.02
1.24	1.94
2.32	0.99
2.34	0.92
2.36	0.92
2.38	0.92
2.40	0.92
2.42	0.92
2.44	0.92
2.46	0.92
2.48	0.92
2.50	0.92
2.52	0.92
2.54	0.92
2.56	0.92
2.58	0.92
2.60	0.92
2.62	0.92
2.64	0.92
2.66	0.92
2.68	0.92
2.70	0.92
2.72	0.92
2.74	0.92
2.76	0.92
2.78	0.92
2.80	0.92
2.82	0.92
2.84	0.92
2.86	0.92
2.88	0.92
2.90	0.92
2.92	0.92
2.94	0.92
2.96	0.92
2.98	0.92
3.00	0.92
3.02	0.92
3.04	0.92
3.06	0.92
3.08	0.92
3.10	0.92
3.12	0.92
3.14	0.92
3.16	0.92
3.18	0.92
3.20	0.92
3.22	0.92
3.24	0.92
3.26	0.92
3.28	0.92
3.30	0.92
3.32	0.92
3.34	0.92
3.36	0.92
3.38	0.92
3.40	0.92
3.42	0.92
3.44	0.92
3.46	0.92
3.48	0.92
3.50	0.92
3.52	0.92
3.54	0.92
3.56	0.92
3.58	0.92
3.60	0.92
3.62	0.92
3.64	0.92
3.66	0.92
3.68	0.92
3.70	0.92
3.72	0.92
3.74	0.92
3.76	0.92
3.78	0.92
3.80	0.92
3.82	0.92
3.84	0.92
3.86	0.92
3.88	0.92
3.90	0.92
3.92	0.92
3.94	0.92
3.96	0.92
3.98	0.92
4.00	0.92
4.02	0.92
4.04	0.92
4.06	0.92
4.08	0.92
4.10	0.92
4.12	0.92
4.14	0.92
4.16	0.92
4.18	0.92
4.20	0.92
4.22	0.92
4.24	0.92
4.26	0.92
4.28	0.92
4.30	0.92
4.32	0.92
4.34	0.92
4.36	0.92
4.38	0.92
4.40	0.92
4.42	0.92
4.44	0.92
4.46	0.92
4.48	0.92
4.50	0.92
4.52	0.92
4.54	0.92
4.56	0.92
4.58	0.92
4.60	0.92
4.62	0.92
4.64	0.92
4.66	0.92
4.68	0.92
4.70	0.92
4.72	0.92
4.74	0.92
4.76	0.92
4.78	0.92
4.8	



```

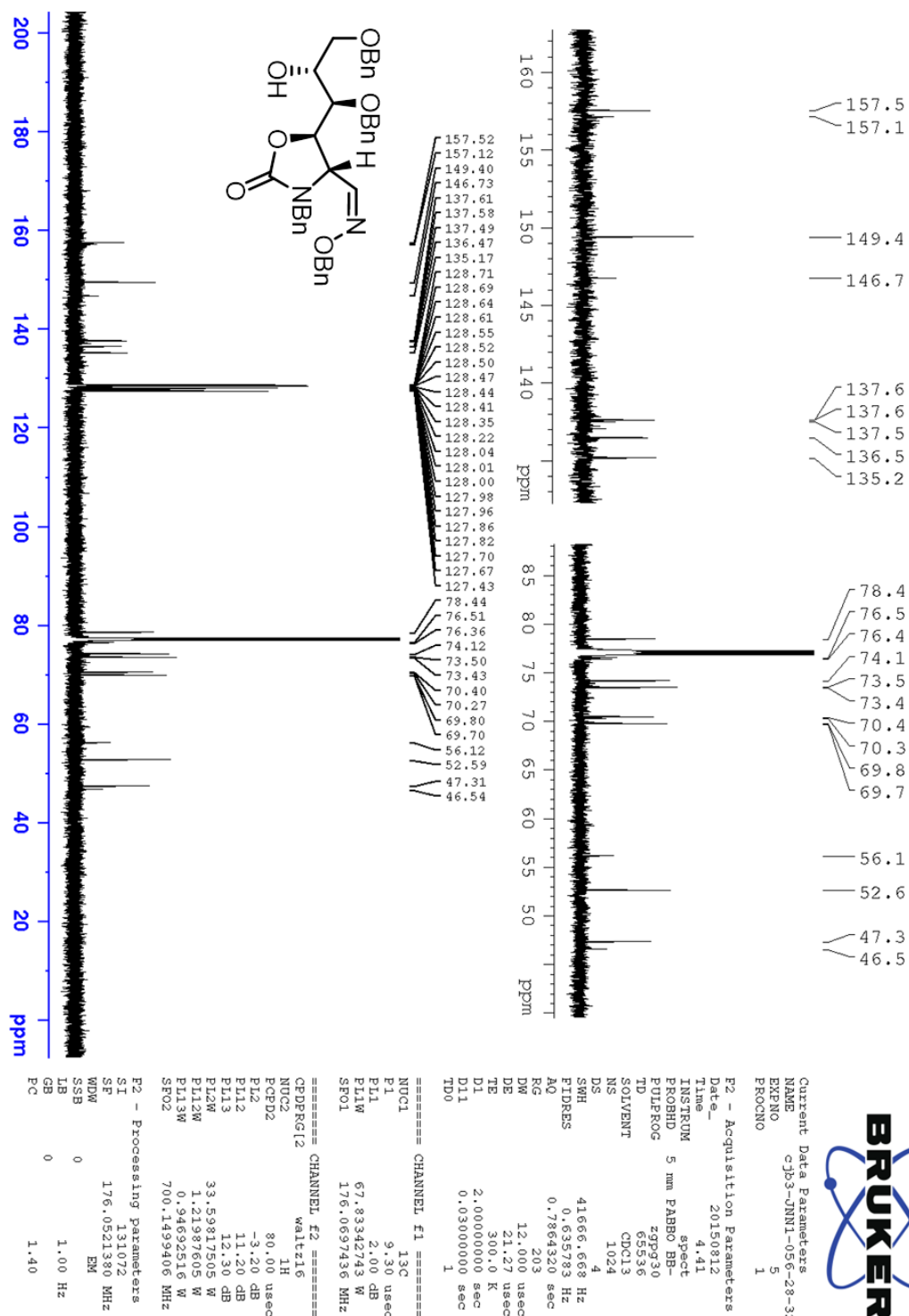
Current Data Parameters
NAME      cjd3-jnn1-056-28-33
EXPNO     1
PROCNO    1

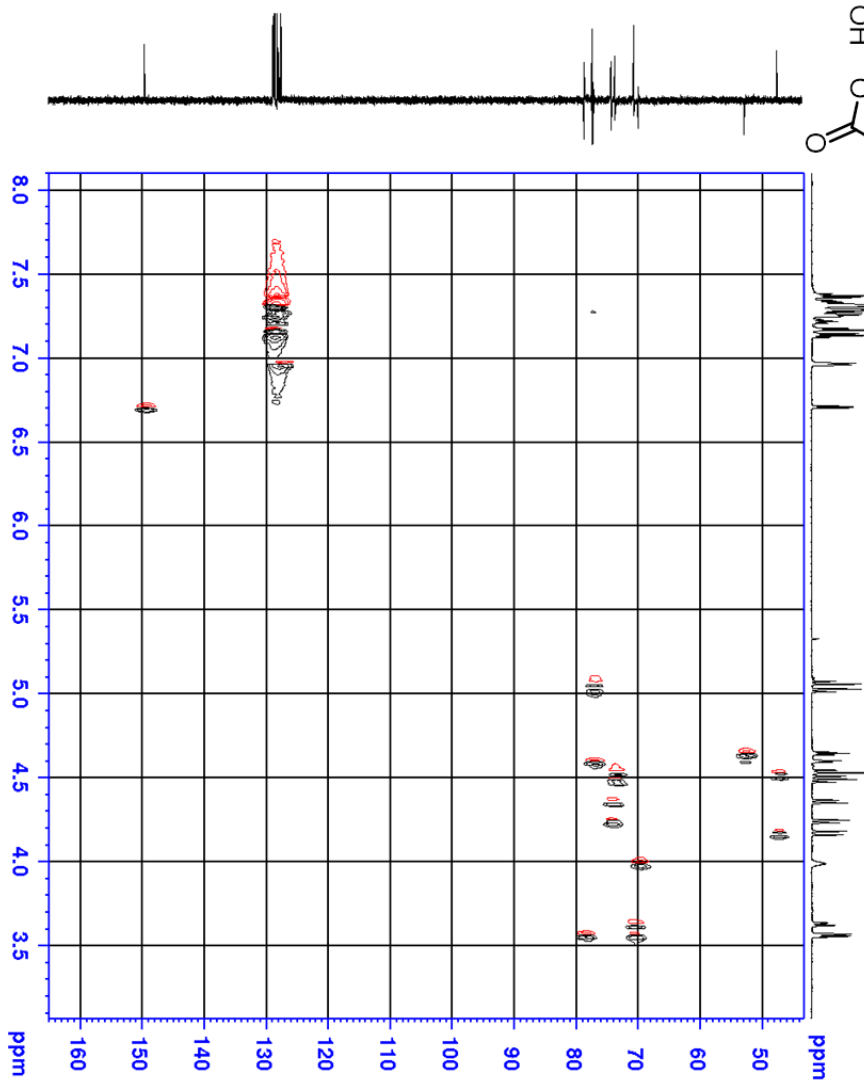
F2 - Acquisition Parameters
Date_     20150811
Time      23.52
INSTRUM   spect
PROBHD    5 mm PABBO-BB-
PULPROG   zgpg30
TD         65536
FIDRES    0.22079 Hz
RG         2.719147 sec
Rg         203
DE         34.667 usec
DE         6.50 usec
TE         298.1 K
D1         1.00000000 sec
TD0        1

===== CHANNEL f1 =====
NUC1       1H
P1         9.40 usec
PL1        -3.20 dB
PL1W       33.5981705 W
SFO1       700.151637 MHz

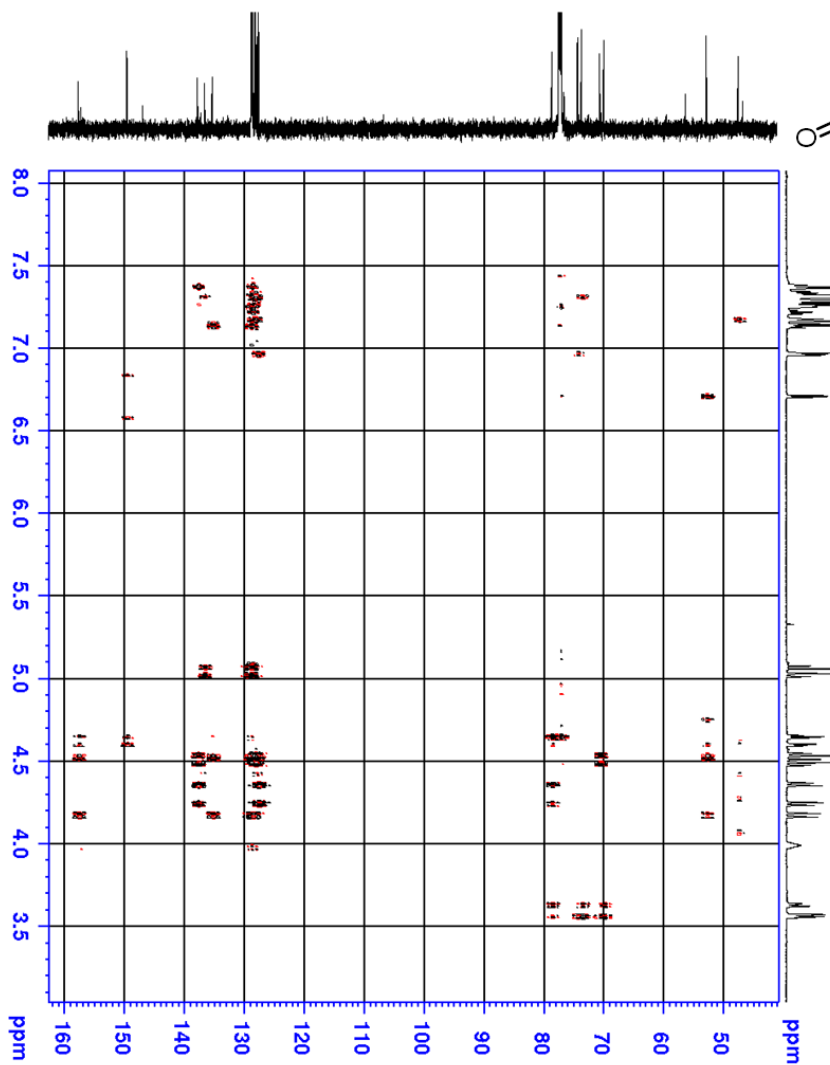
F2 - Processing parameters
SI         131072
SF         700.1471400 MHz
WDW        EM
SSB        0
EB         0.30 Hz
GB         0
EC         1.00

```

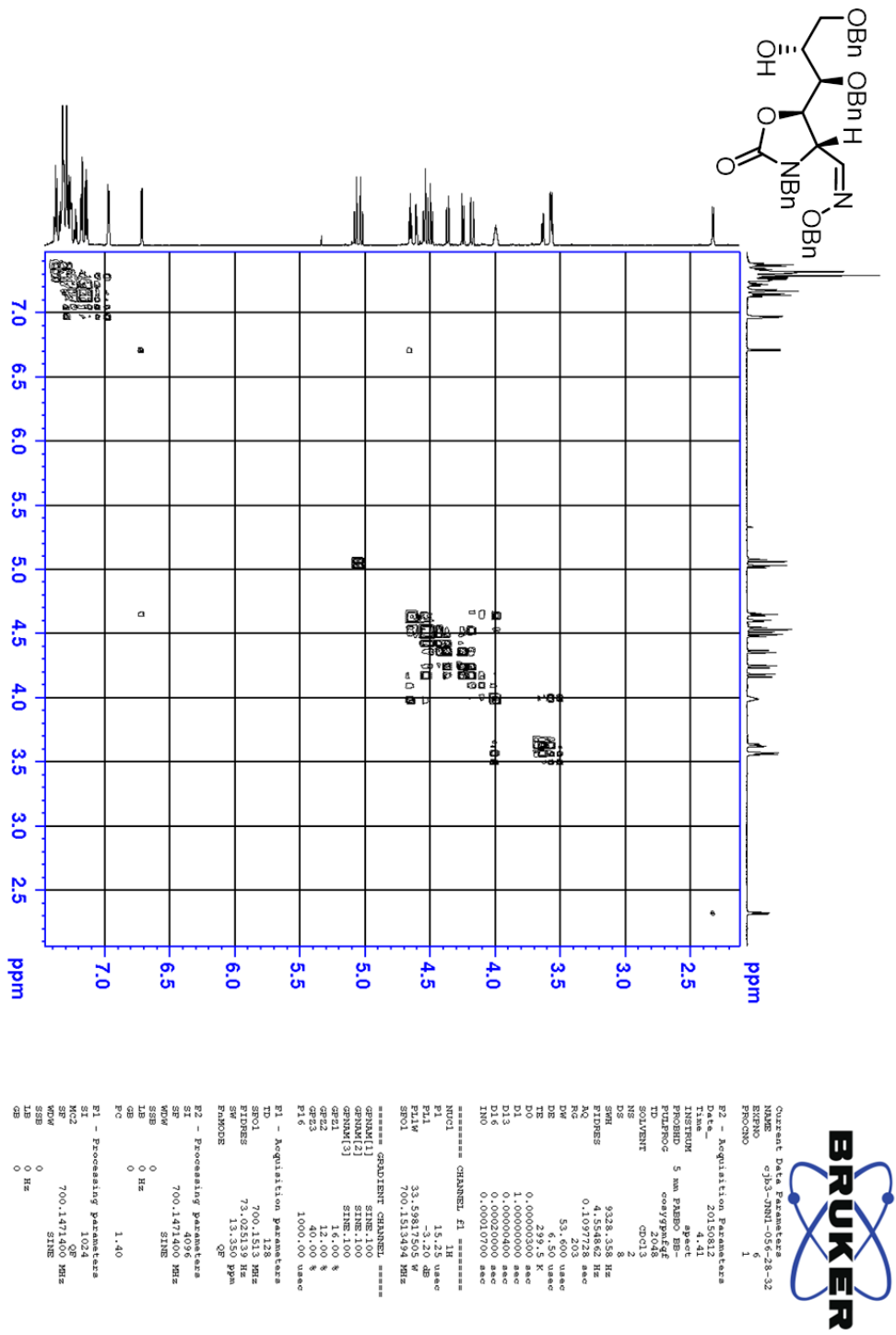
Appendix Figure 6.92: ^{13}C NMR (CDCl_3) spectrum of Z-19

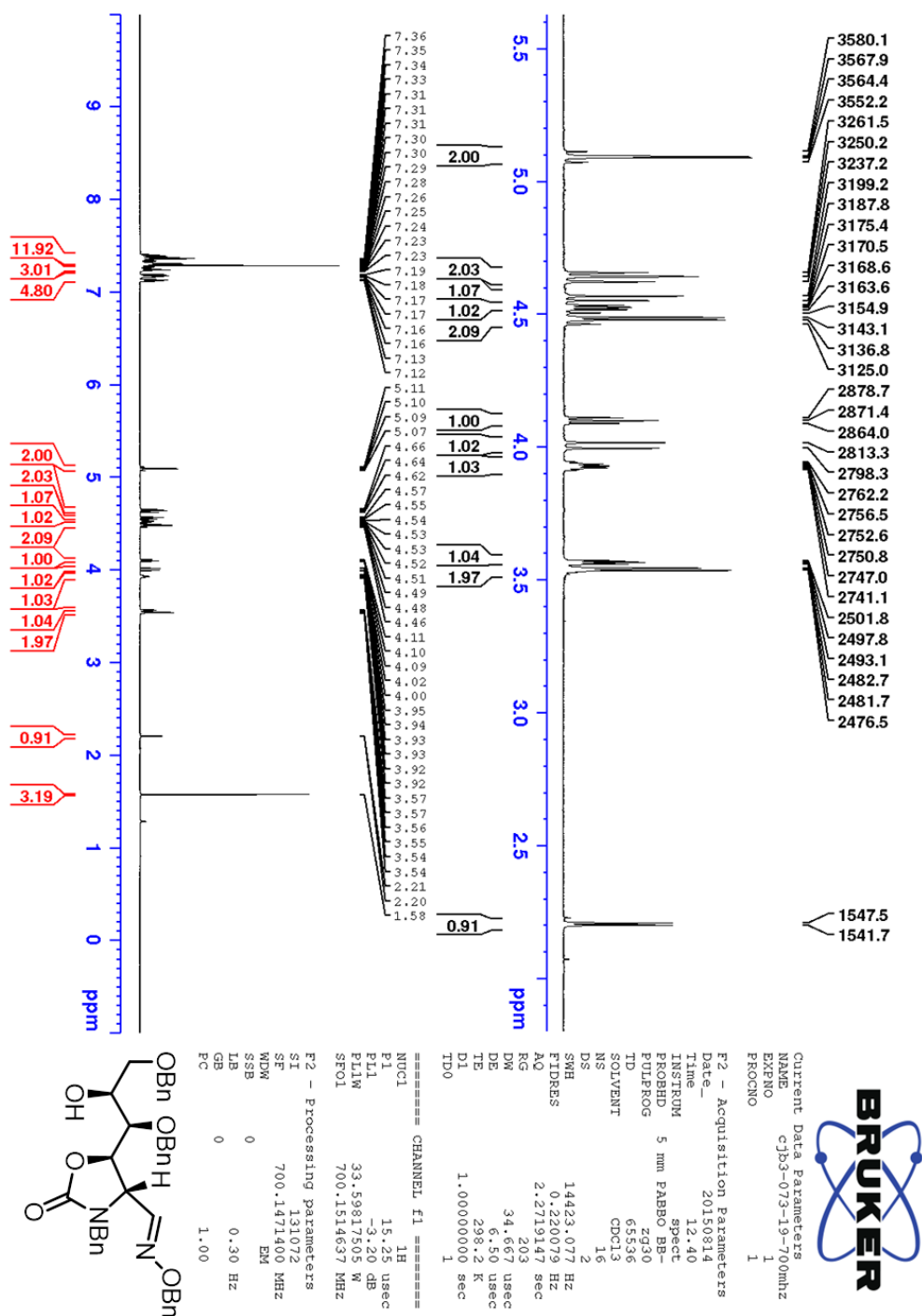
[illegible][illegible]

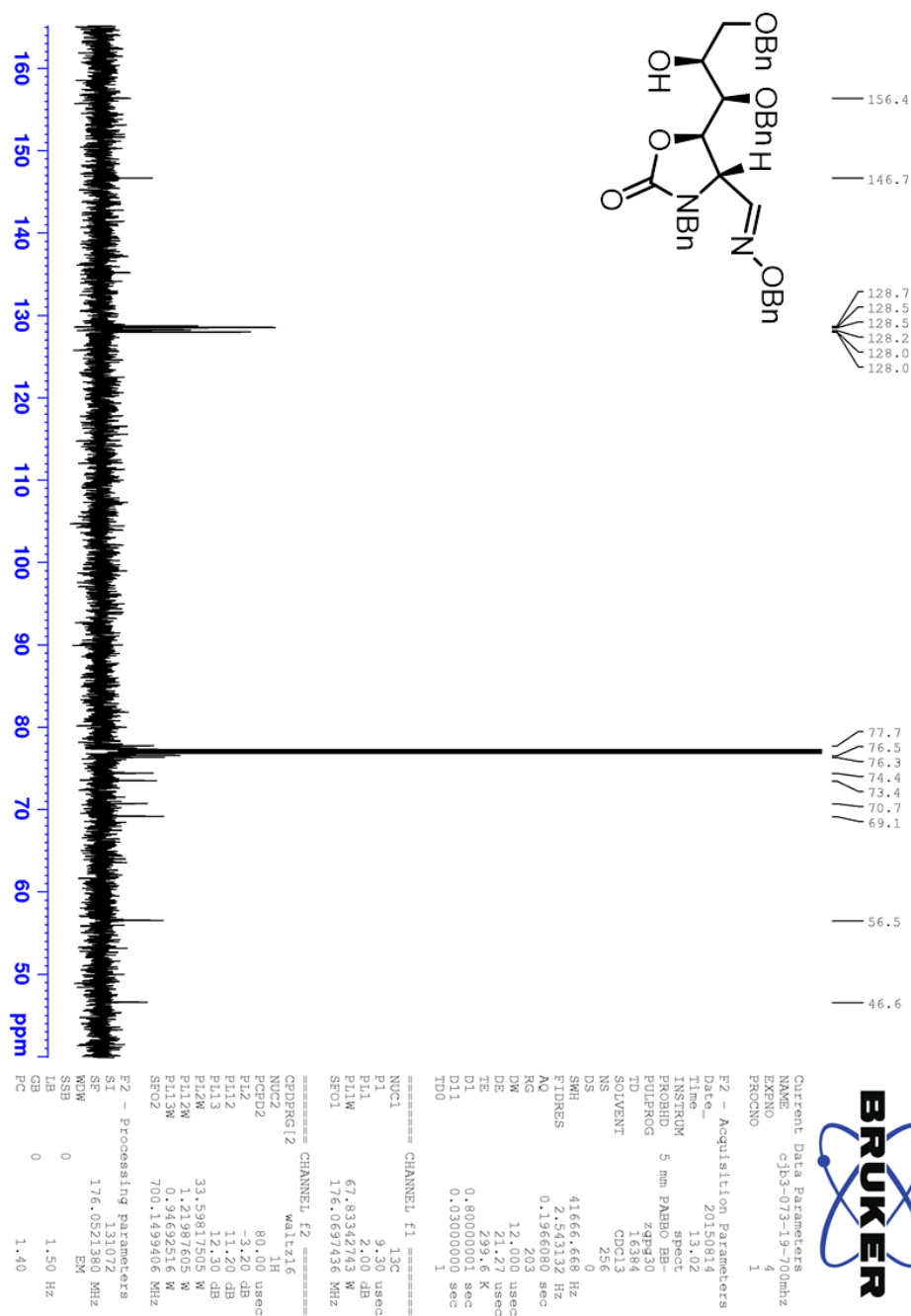
Chemical structure of compound 10, a complex bicyclic molecule with multiple OBn and H substituents.

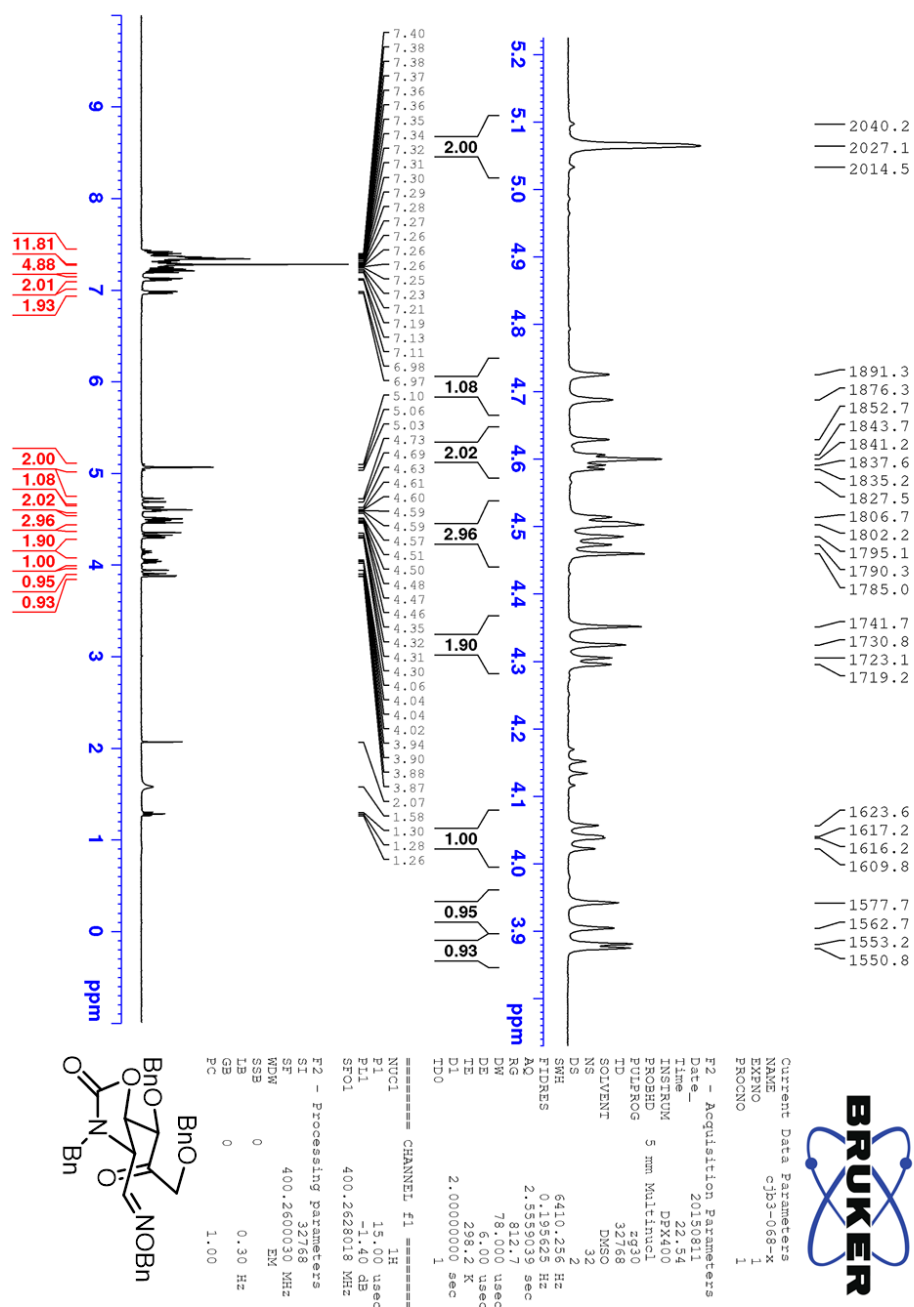
[illegible]

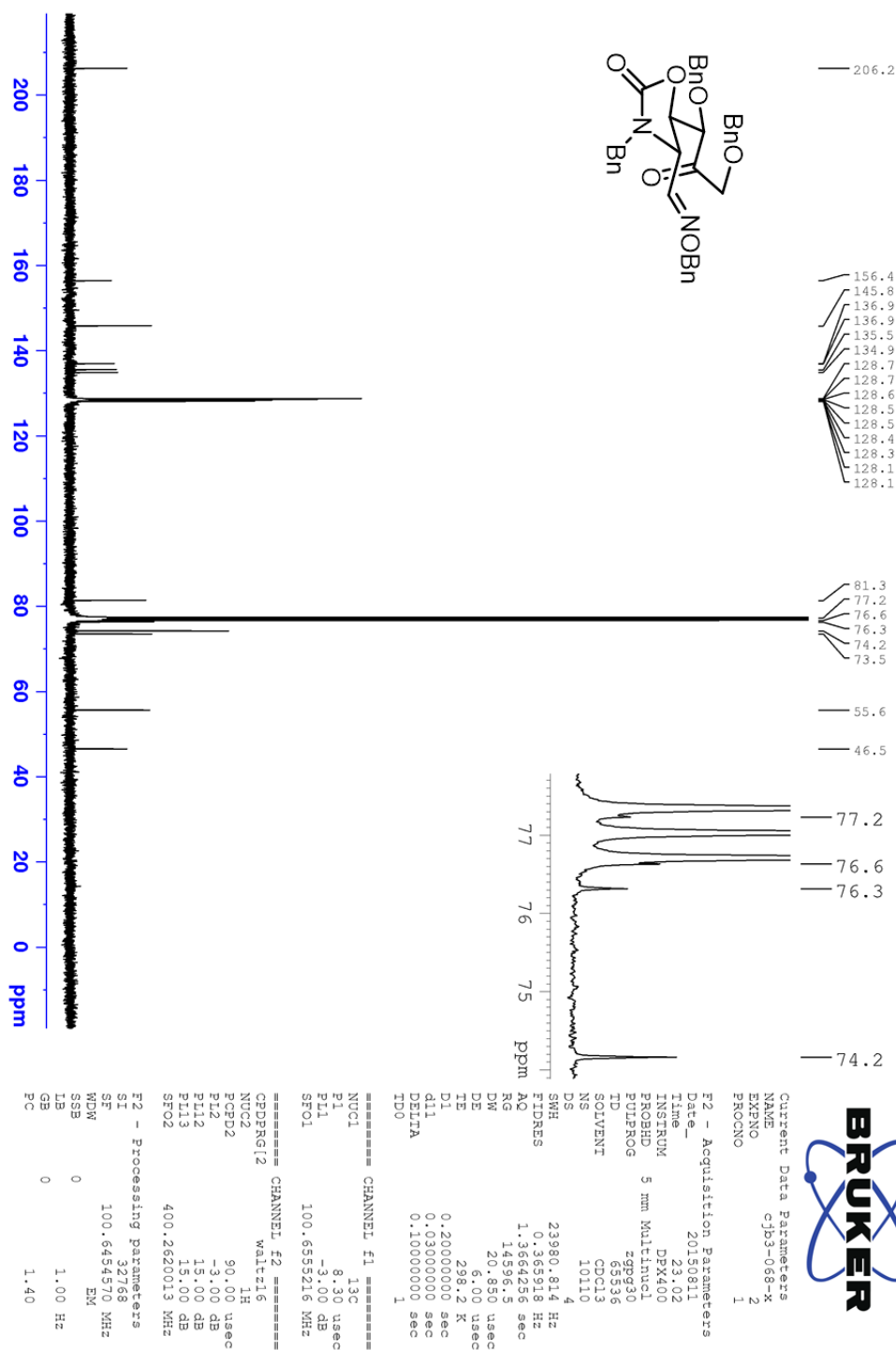
Appendix Figure 6.95: COSY (CDCl₃) spectrum of Z-19



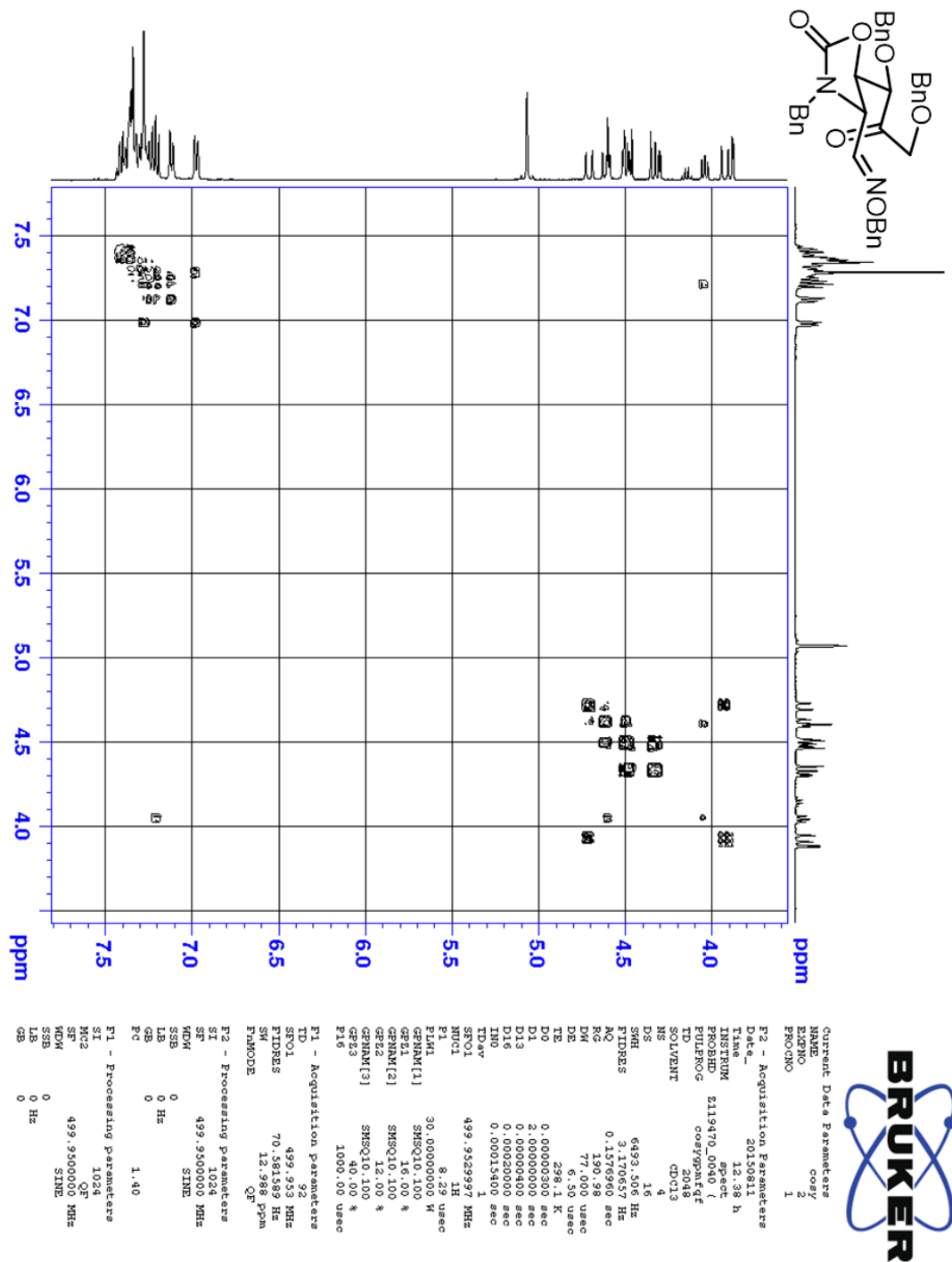
Appendix Figure 6.96: ^1H NMR (CDCl_3) spectrum of **55-E-19**

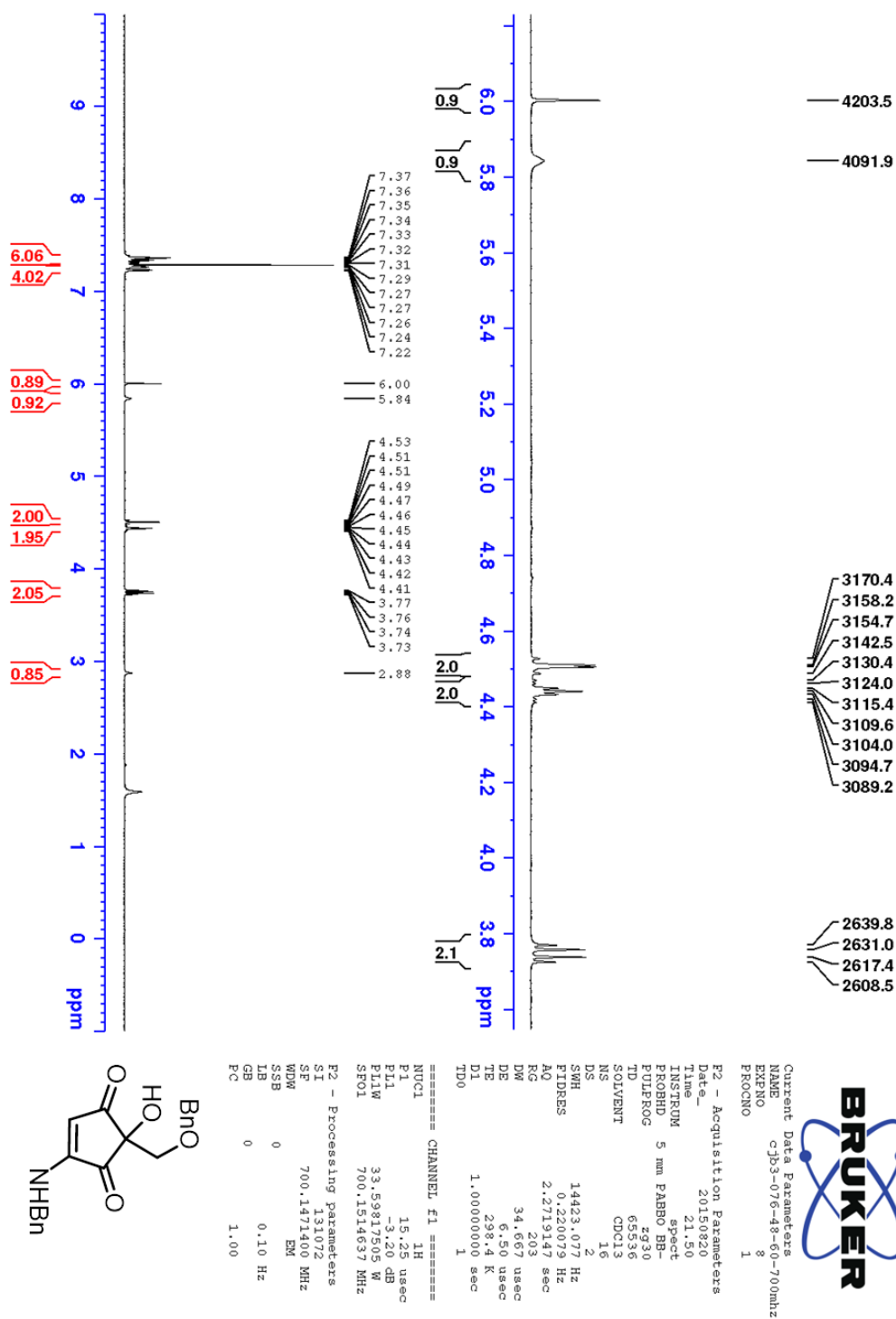
Appendix Figure 6.97: ^{13}C NMR (CDCl_3) spectrum of **5S-E-19**

Appendix Figure 6.98: ^1H NMR (CDCl_3) spectrum of **15**

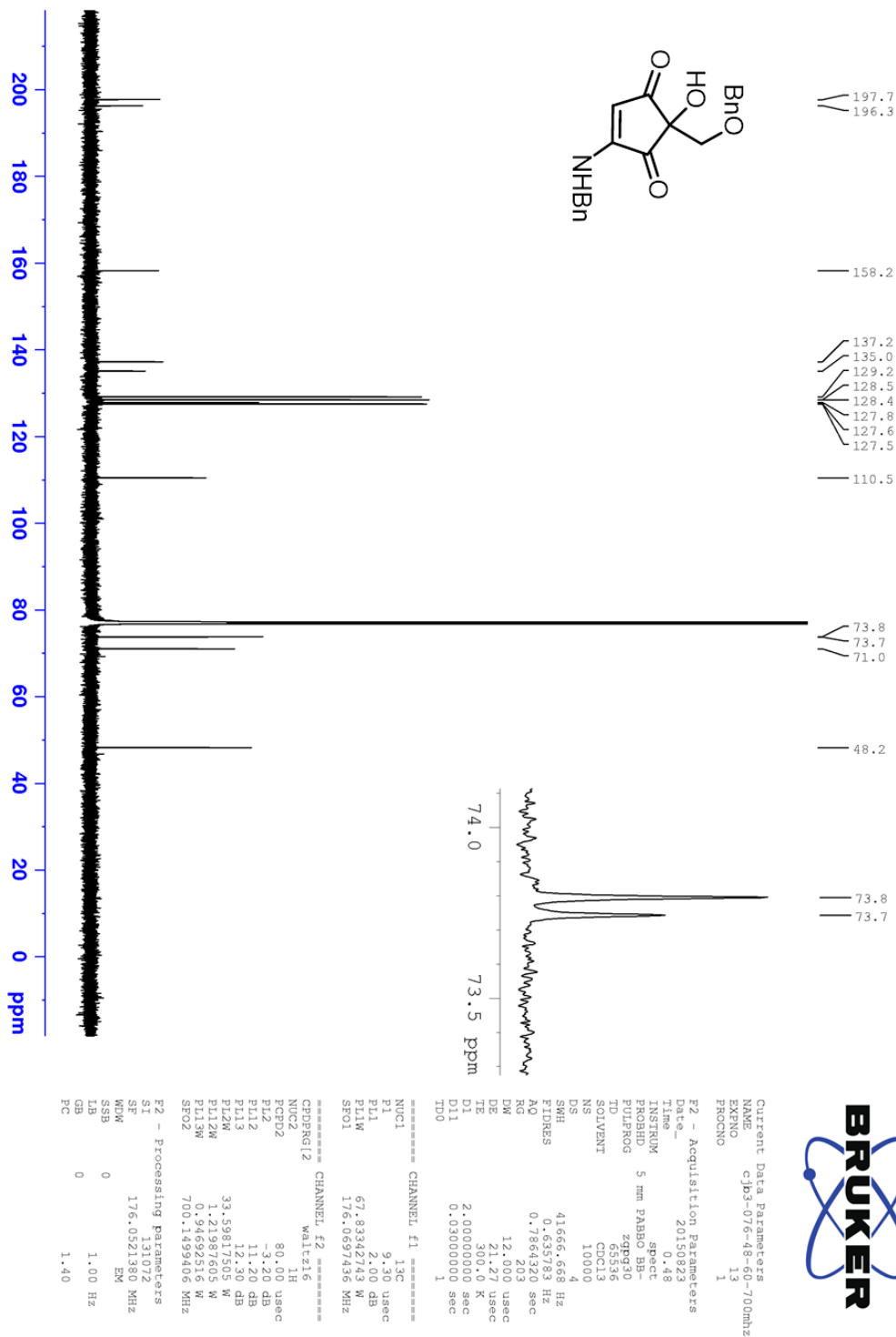
Appendix Figure 6.99: ^{13}C NMR (CDCl_3) spectrum of **15**

Appendix Figure 6.100: COSY (CDCl₃) spectrum of 15

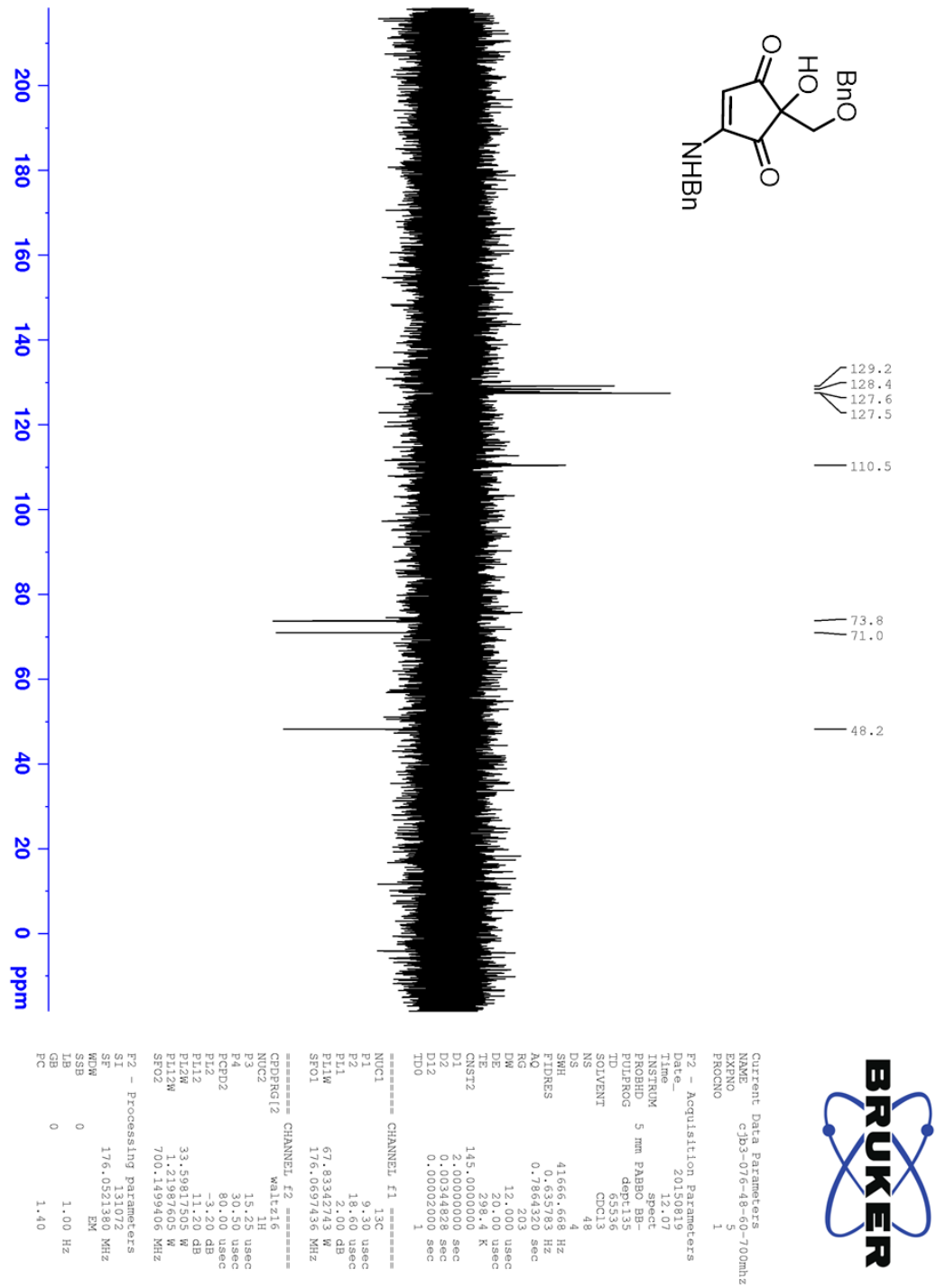


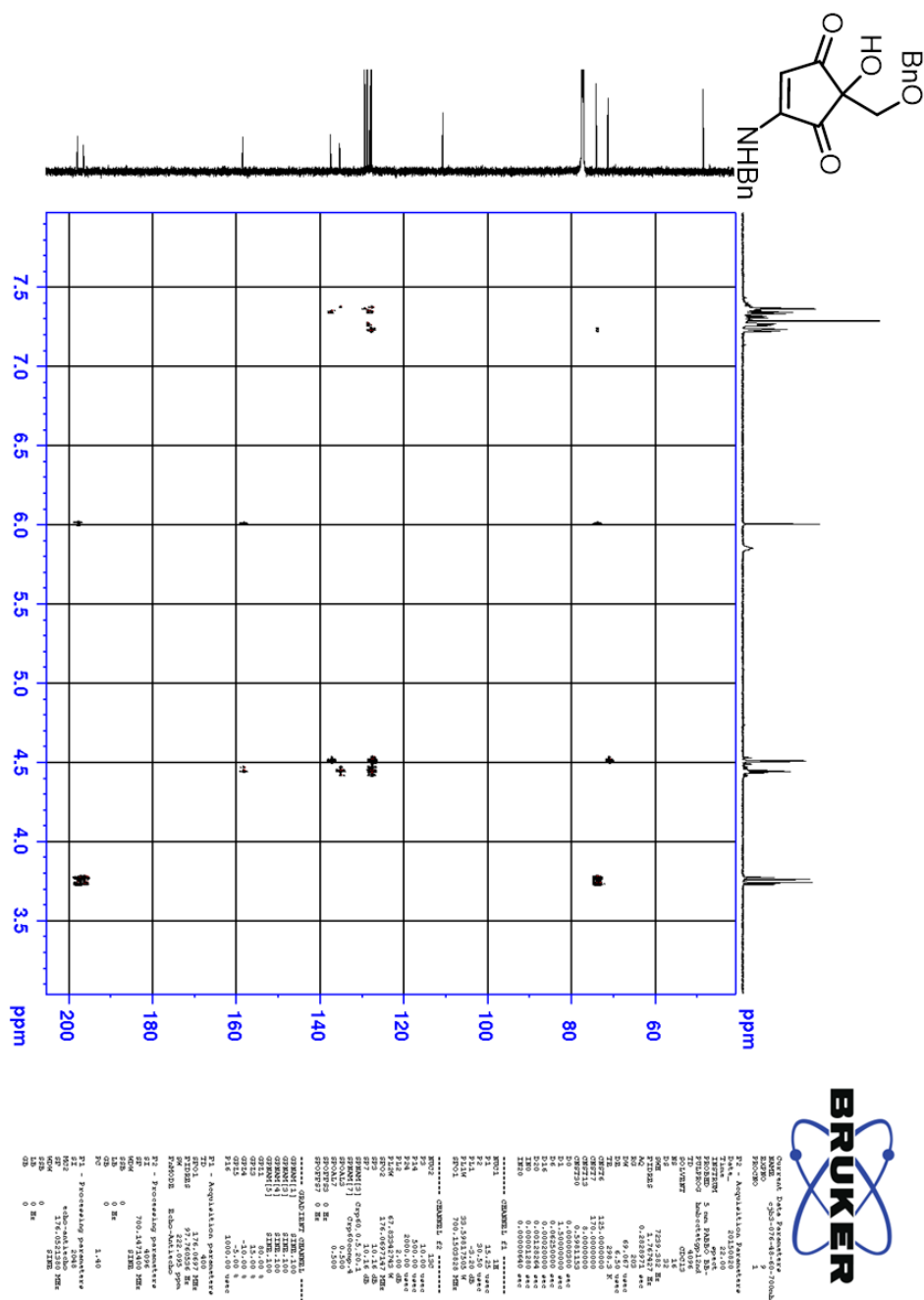
Appendix Figure 6.101: ^1H NMR (CDCl_3) spectrum of **20**

Appendix Figure 6.102: ^{13}C NMR (CDCl_3) spectrum of **20**

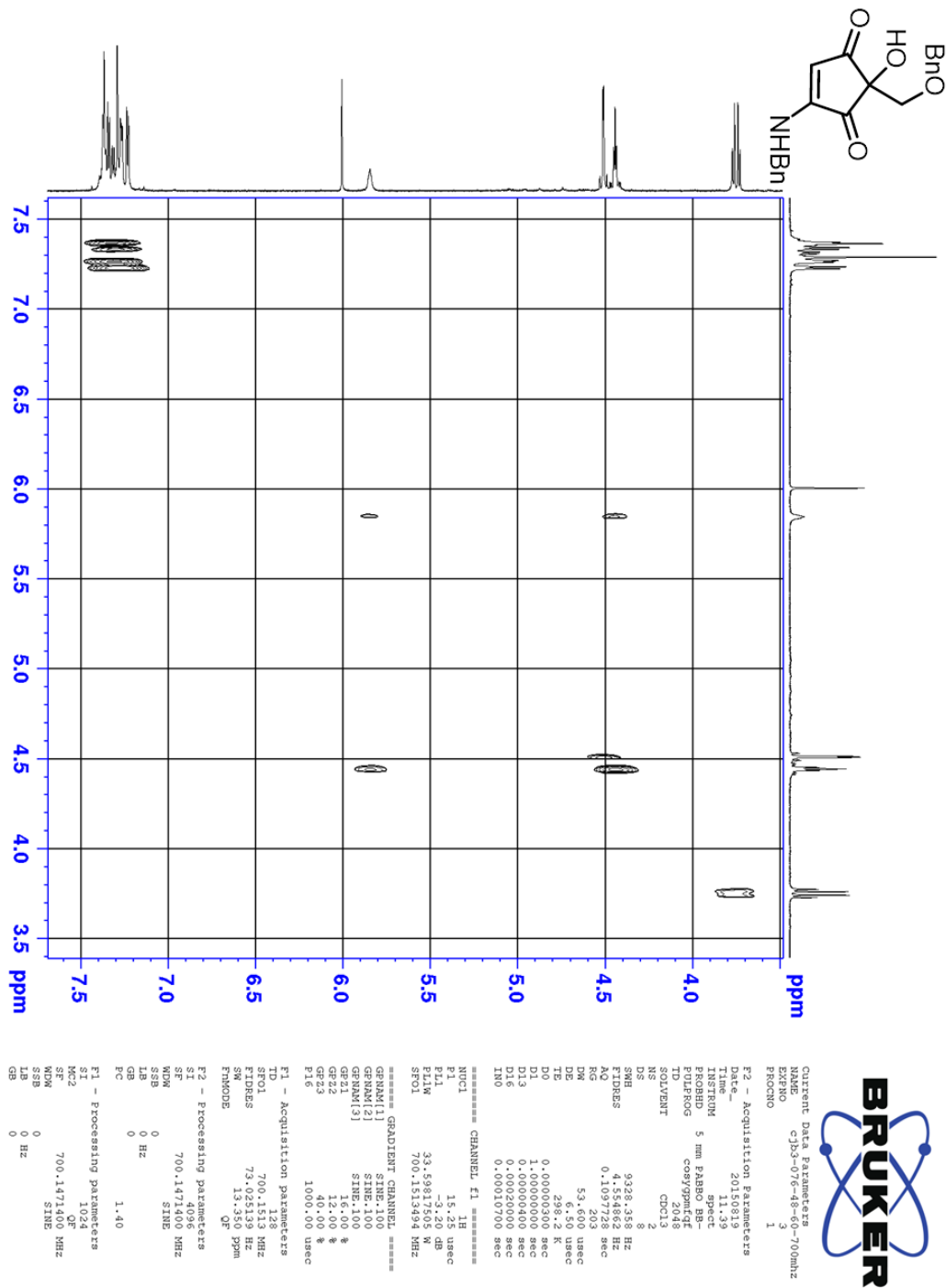


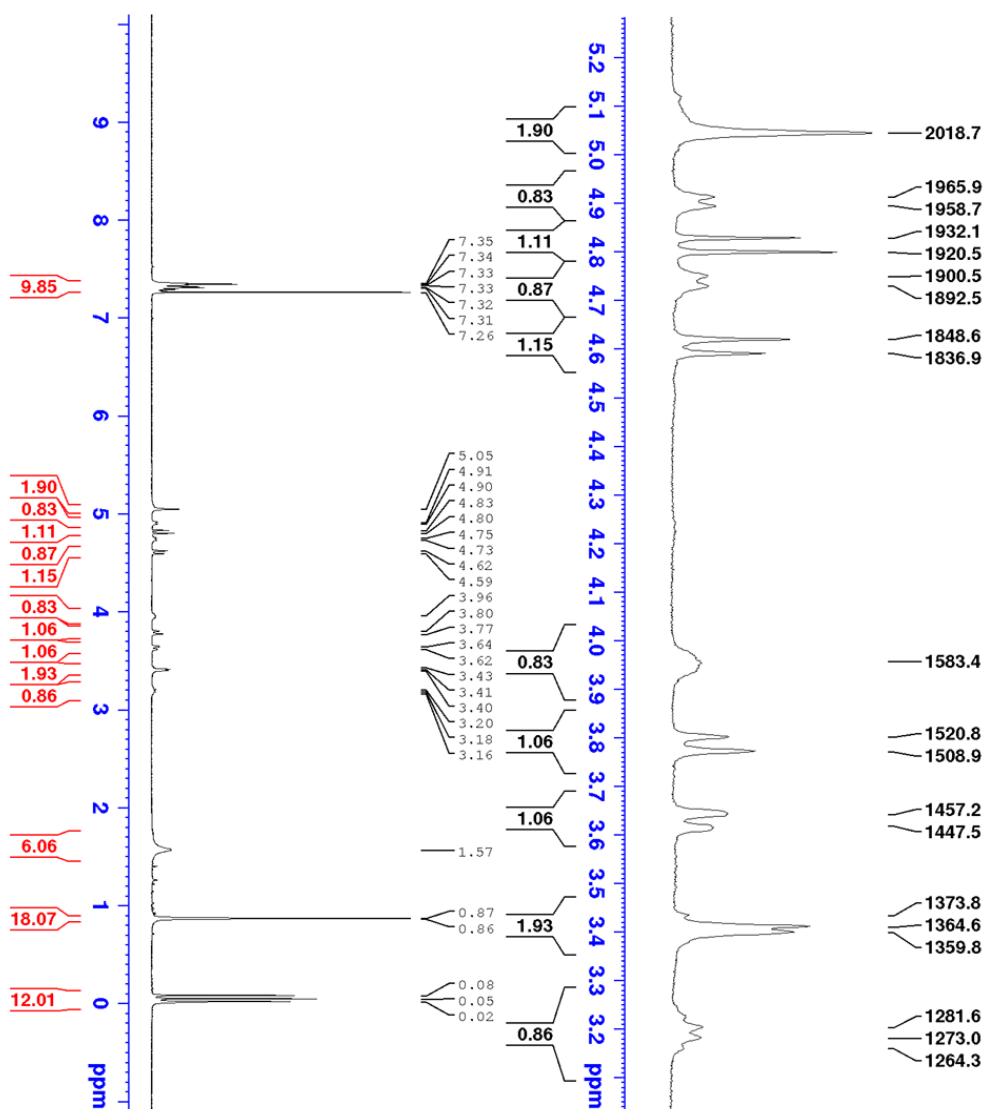
Appendix Figure 6.103: DEPT135 (CDCl₃) spectrum of **20**

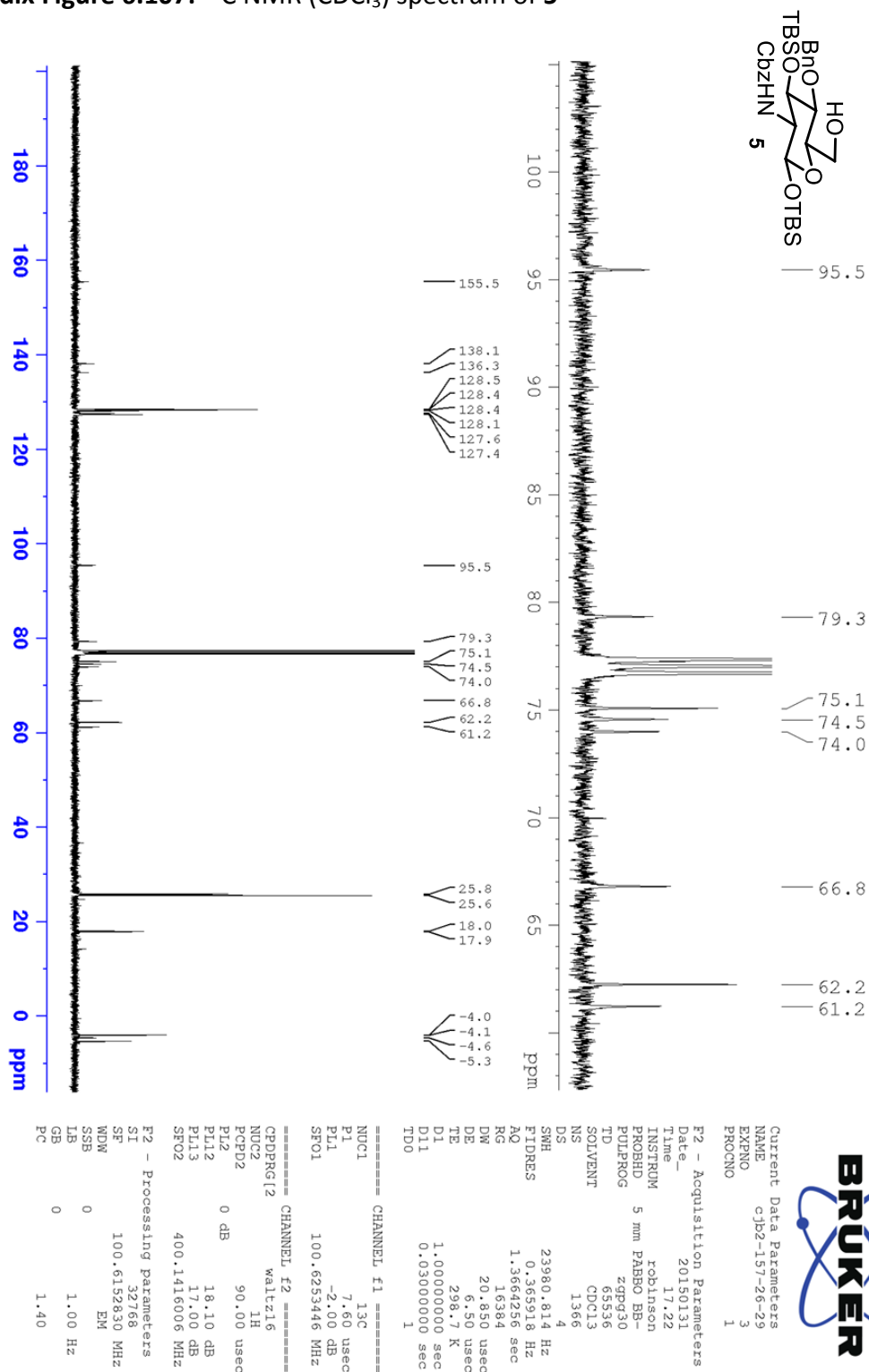


Appendix Figure 6.104: HMBC (CDCl₃) spectrum of **20**

Appendix Figure 6.105: COSY (CDCl₃) spectrum of **20**

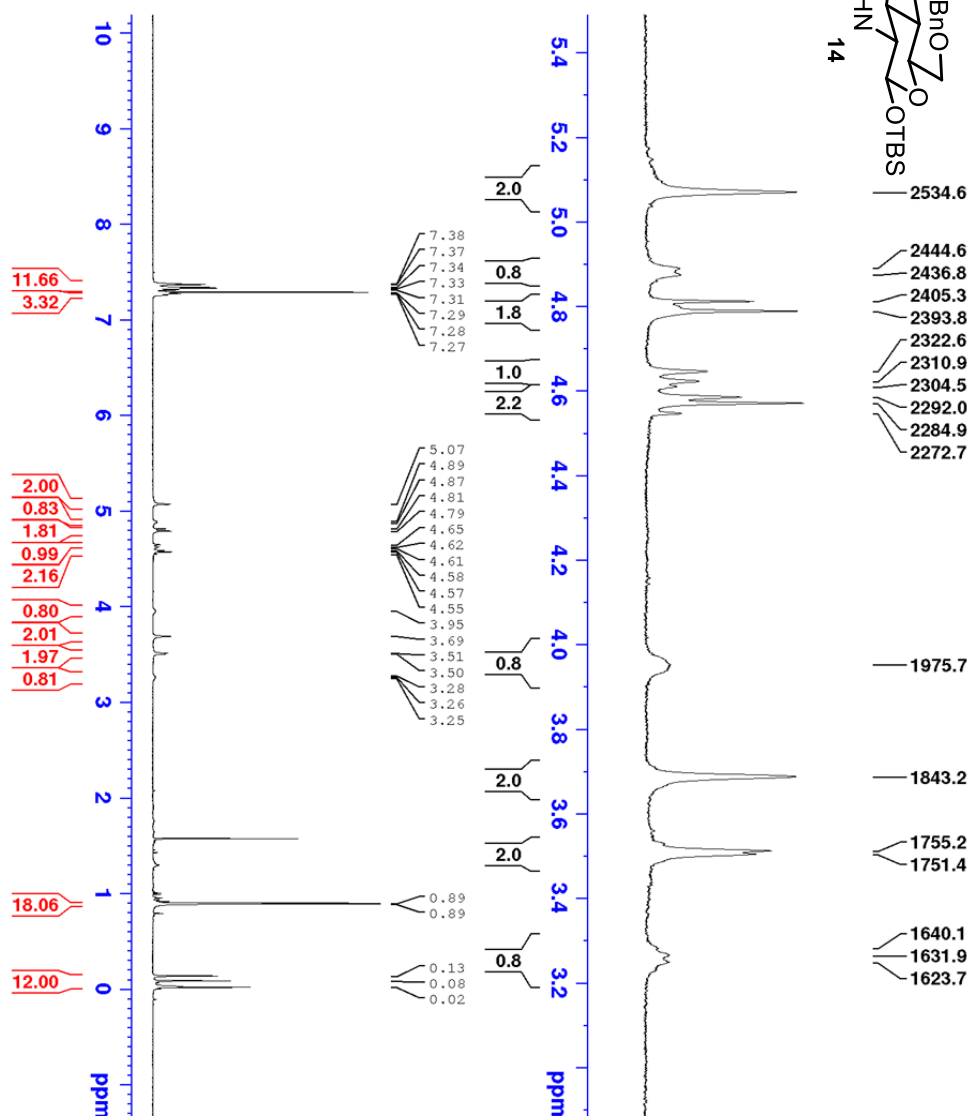




Appendix Figure 6.107: ^{13}C NMR (CDCl_3) spectrum of 5

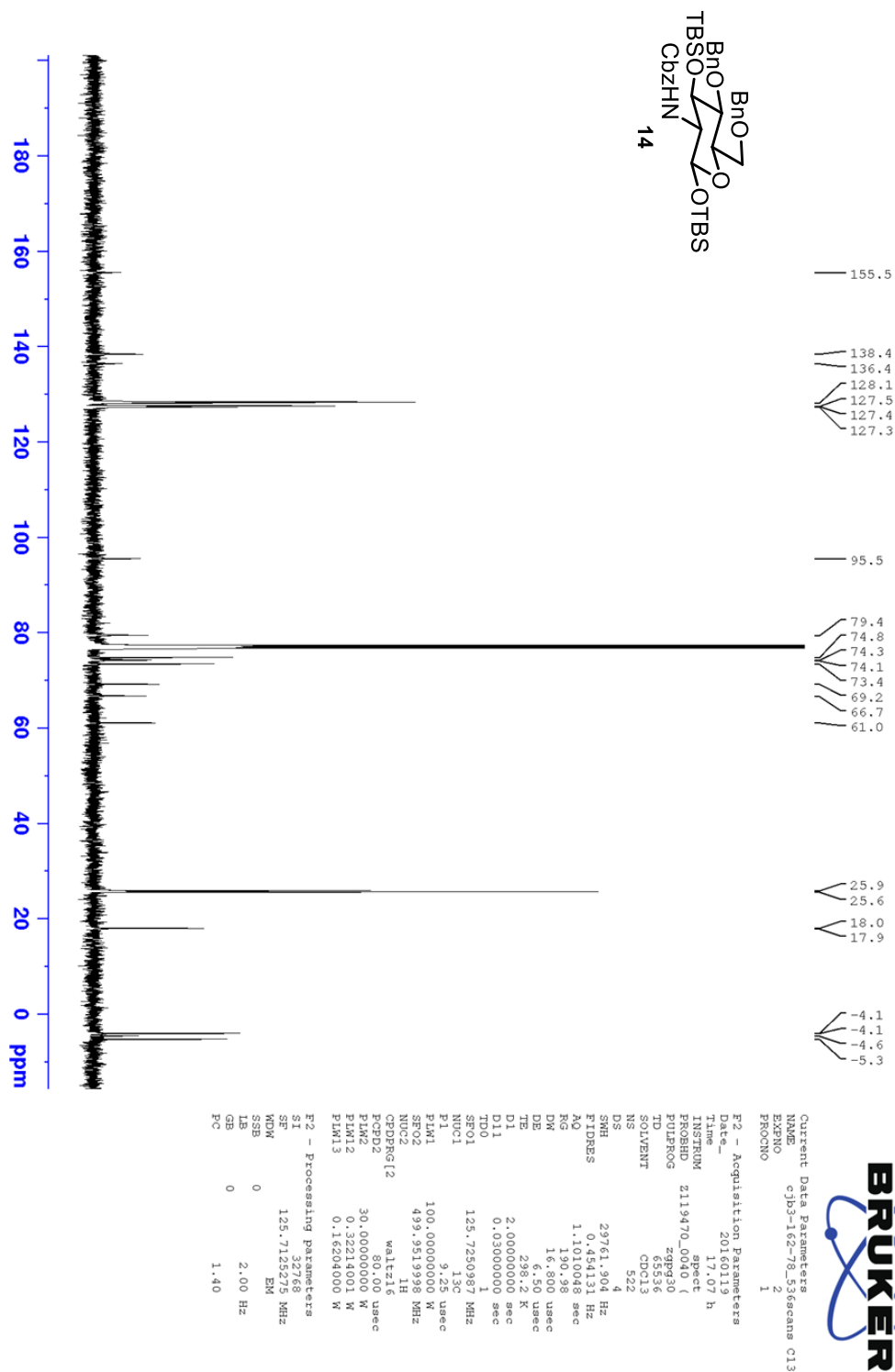


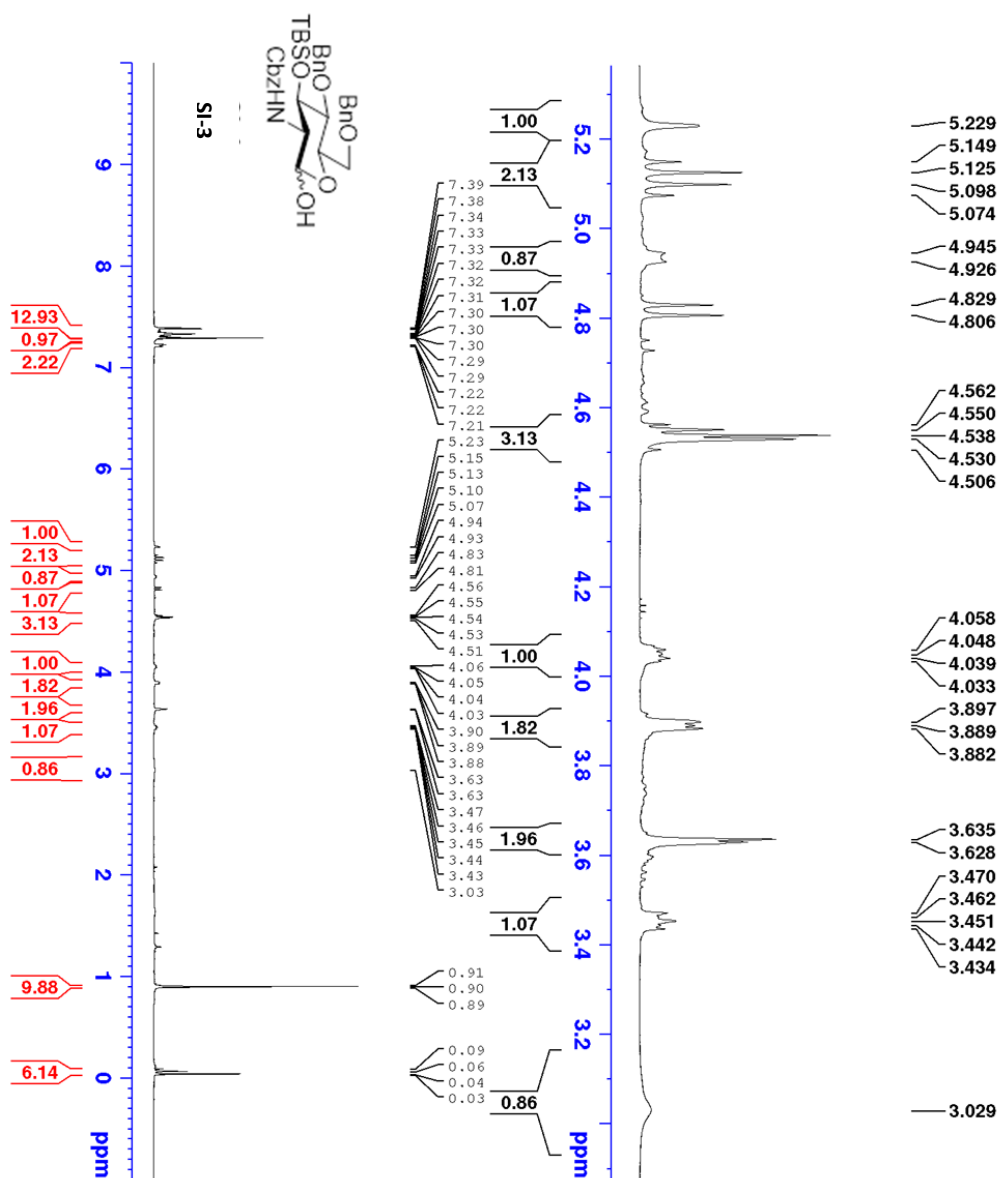
BRUKER



Current Data Parameters		
NAME	cjb4-043-fcc2-13-21	
EXPO		
PROGNO	1	
F2 - Acquisition Parameters		
Time	20160928	
Date	9.17 h	
INSTRUM		
PROBHD	2119470.0040 (spect
PULPROG	zg30	
	65536	
SOLVENT	CDCl3	
NS	13	
DS	2	
SM	10000.000	Hz
FIDRES	0.305176	Hz
AQ	3.276199	sec
RG	131.79	
DW	50.000	usec
DE	6.50	usec
TE	298.1	K
D1	1.0000000	sec
TD0	1	
SFO1	499.9530872	MHz
NUC1	1H	
P1	8.28	usec
PLM1	30.00000000	W
F2 - Processing Parameters		
SF	499.9500000	MHz
MDW		EM
SSB	0	
LB	0.30	Hz
GB	0	
PC	1.00	

Appendix Figure 6.109: ^{13}C NMR (CDCl_3) spectrum of **14**



Appendix Figure 6.110: ^1H NMR lactol SI-3

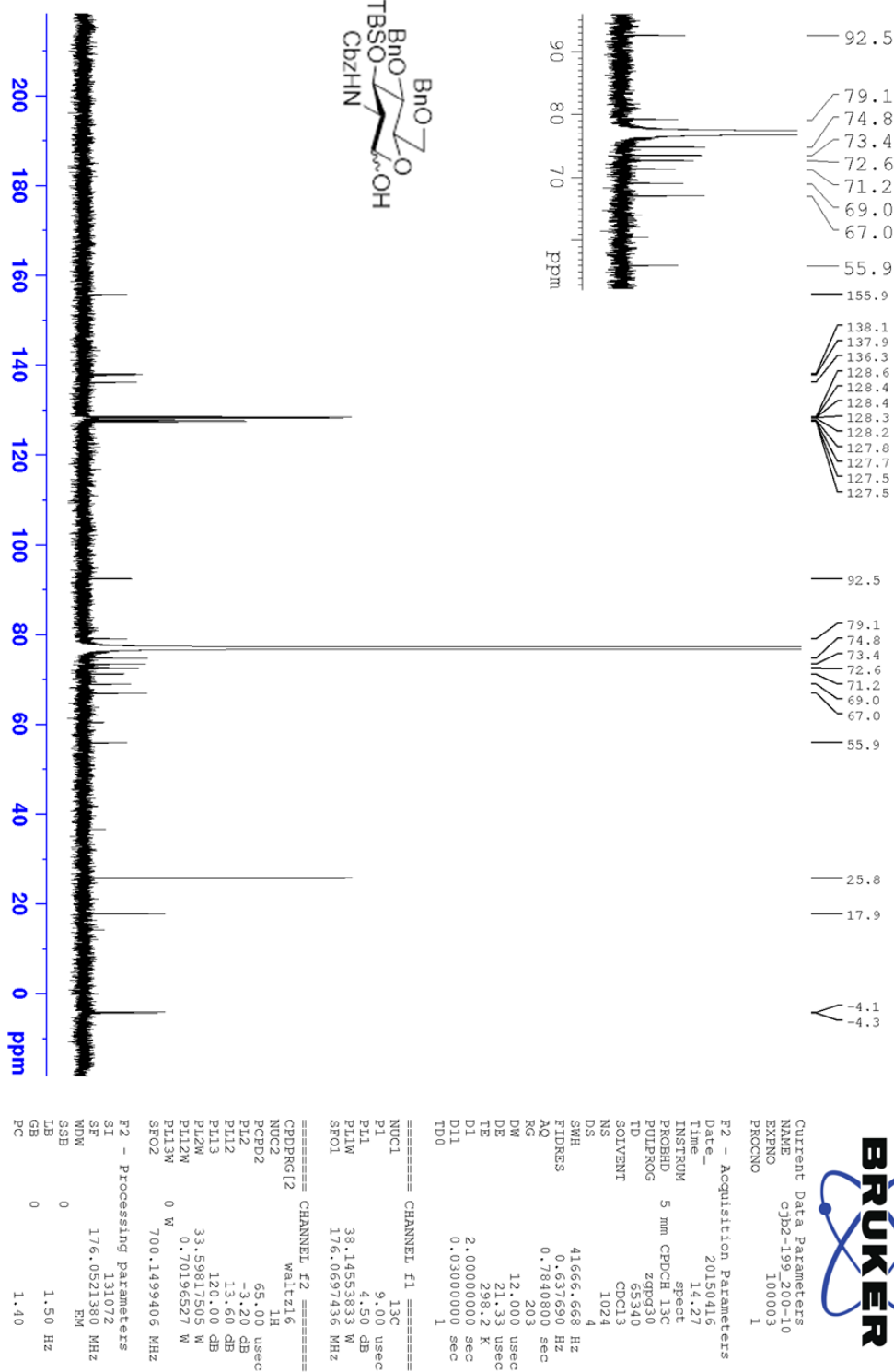
Current Data Parameters
 NAME cjb2-199_200-11-20
 EXPNO 1
 PROCNO 1

F2 - Acquisition Parameters
 Date_ 20150417
 Time 13.25
 INSTRUM spect
 PROBD 5 mm PATXI 1H/
 PULPROG zg30
 TD 65536
 SOLVENT CDCl3
 NS 71
 DS 2
 SWH 10000.000 Hz
 FIDRES 0.152588 Hz
 AQ 3.276799 sec
 RG 33.71
 DW 50.000 usec
 DE 6.50 usec
 TE 298.2 K
 D1 1.00000000 sec
 TDO 1

===== CHANNEL f1 =====
 SFO1 499.9530674 MHz
 NUCL 1H
 P1 8.00 usec
 PLW1 12.0059957 W

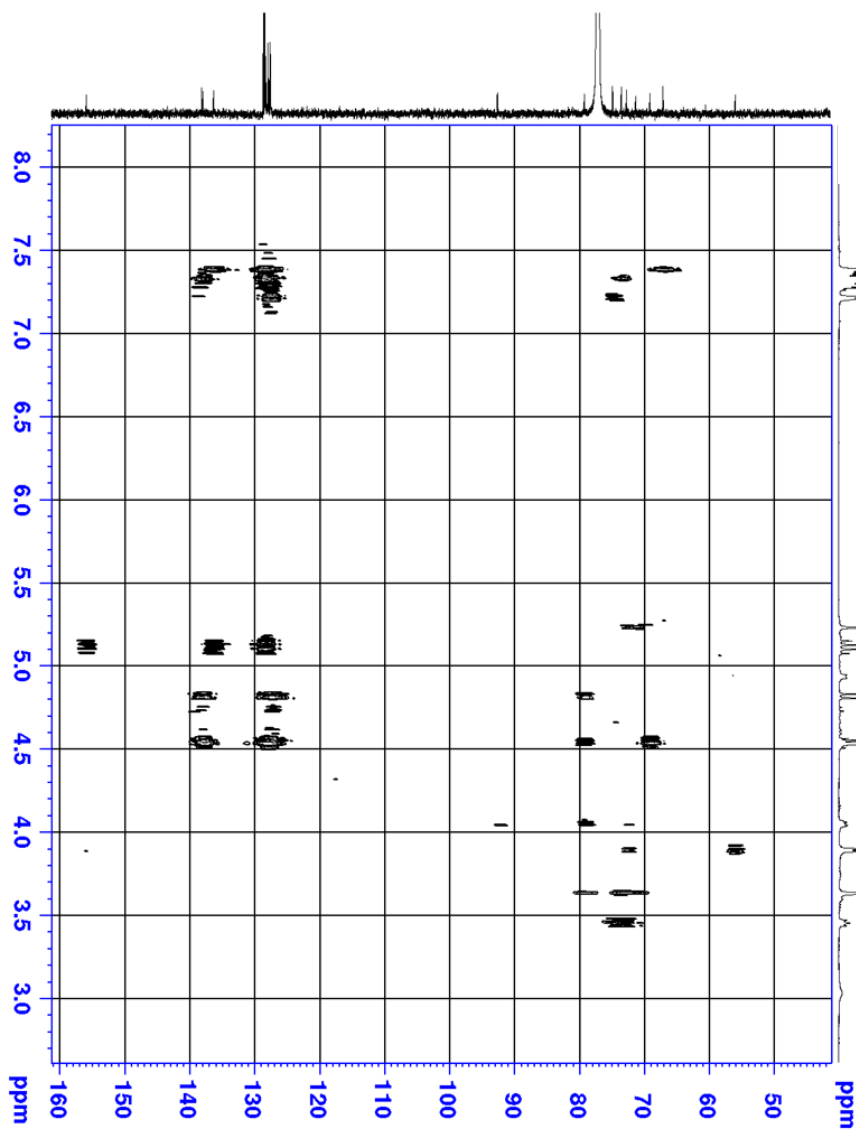
F2 - Processing parameters
 SI 131072
 SF 499.950000 MHz
 WDW EM
 SSB 0
 LB 0 Hz
 GB 0
 PC 1.00



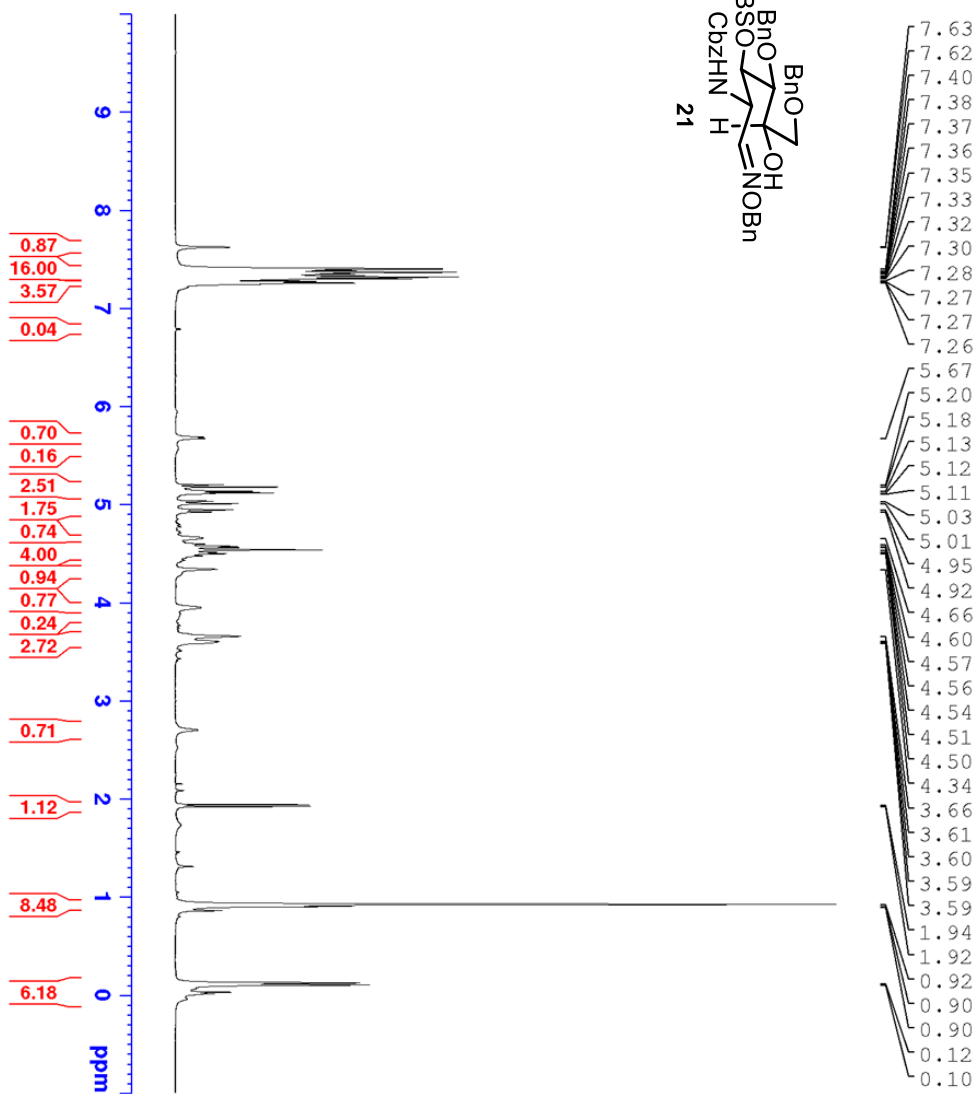




BRUKER
Current Data Parameters

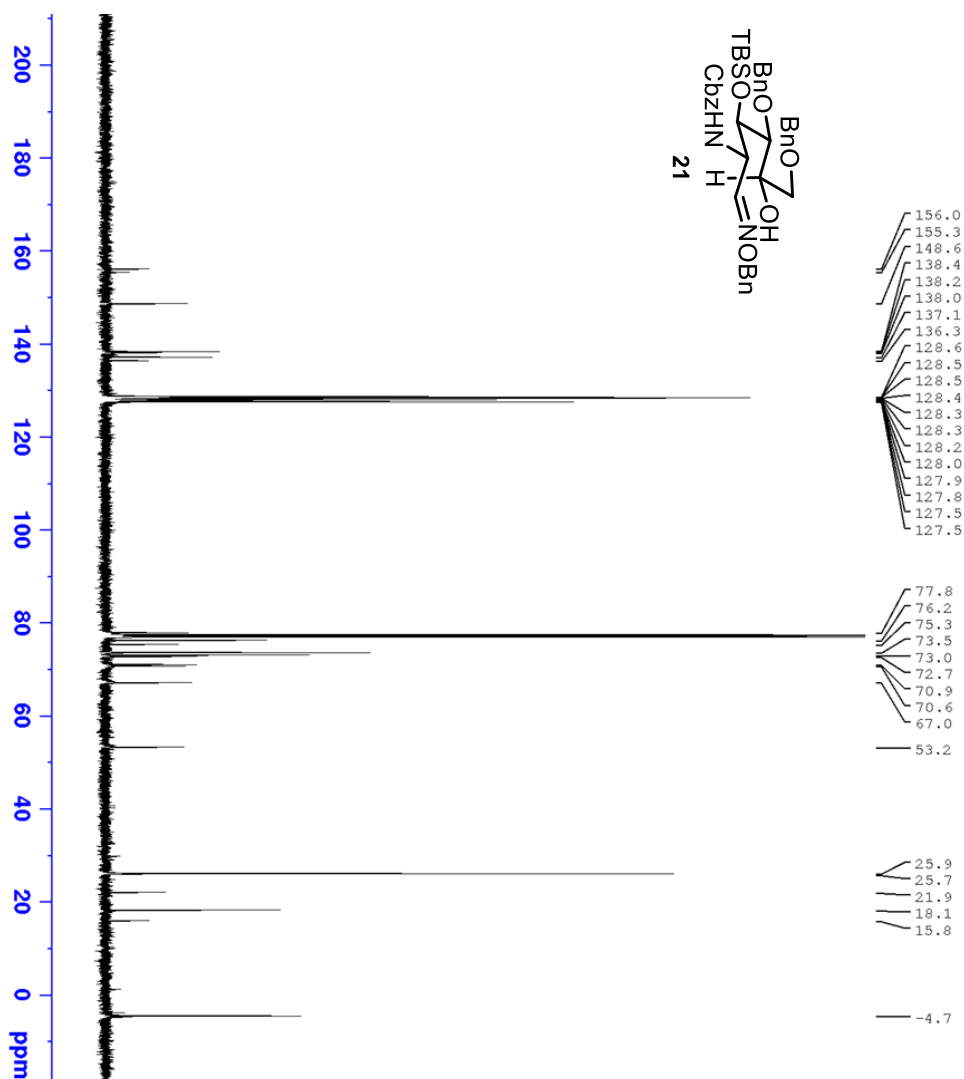
[illegible]

21



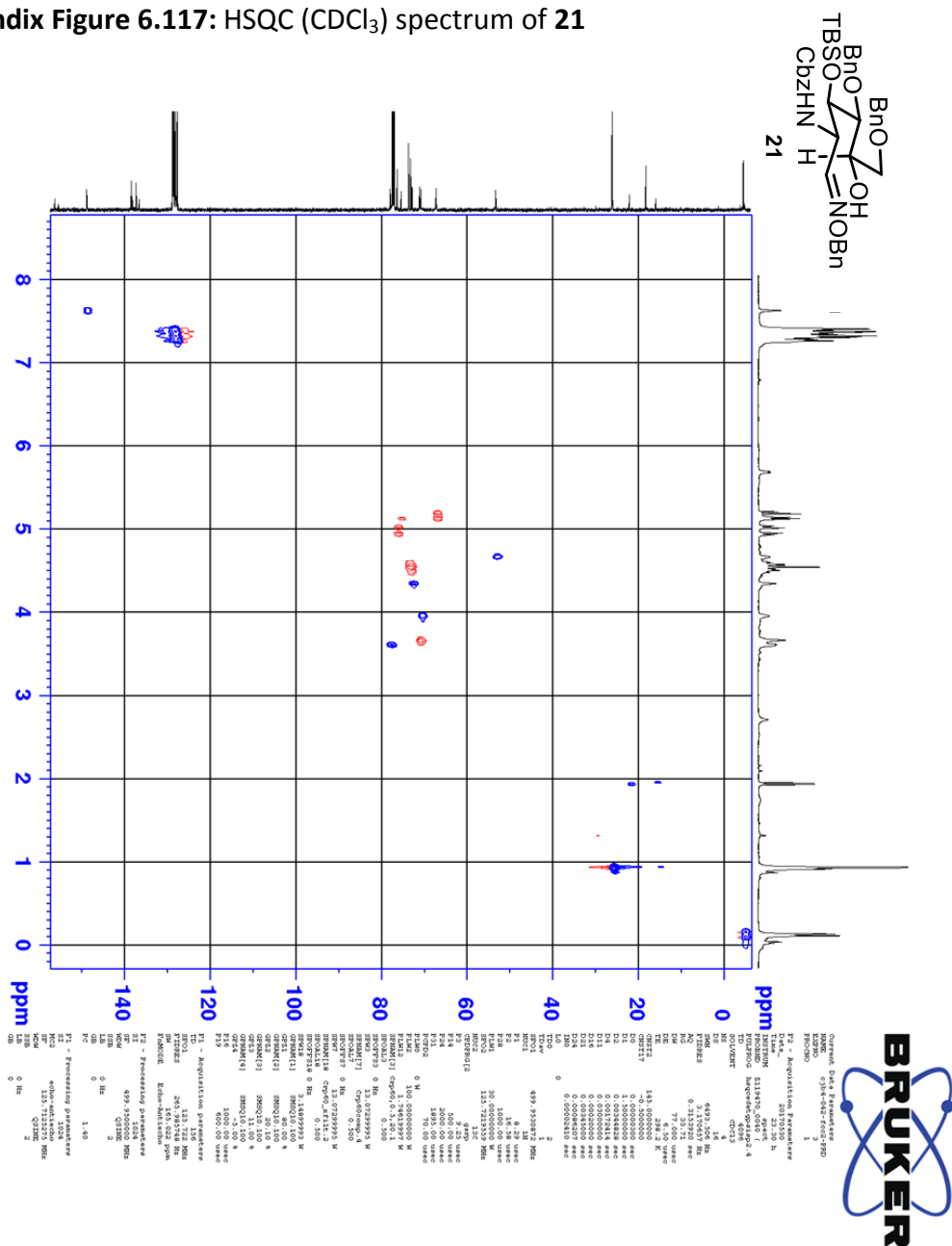
Current Data Parameters	
NAME	cjb4-042-fcc2-PND
EXPNO	1
PROCNO	1
F2 - Acquisition Parameters	
Date_	20170530
Time	23.01 h
INSTRUM	
PROBHD	2119470_0040 {
PULPROG	zg30
TD	65536
SOLVENT	CDCl3
DS	16
SWH	10000.000 Hz
FIDRES	0.305176 Hz
AQ	3.276199 sec
RG	33.71
DM	50.000 usec
DE	6.50 usec
TE	298.1 K
D1	1.00000000 sec
TD0	1
SFO1	499.9530872 MHz
NUC1	1H
P1	8.29 usec
PLM1	30.00000000 W
F2 - Processing Parameters	
SI	65536
SF	499.9500000 MHz
WDW	EM
SSB	0
LB	0 Hz
GB	0
PC	1.00

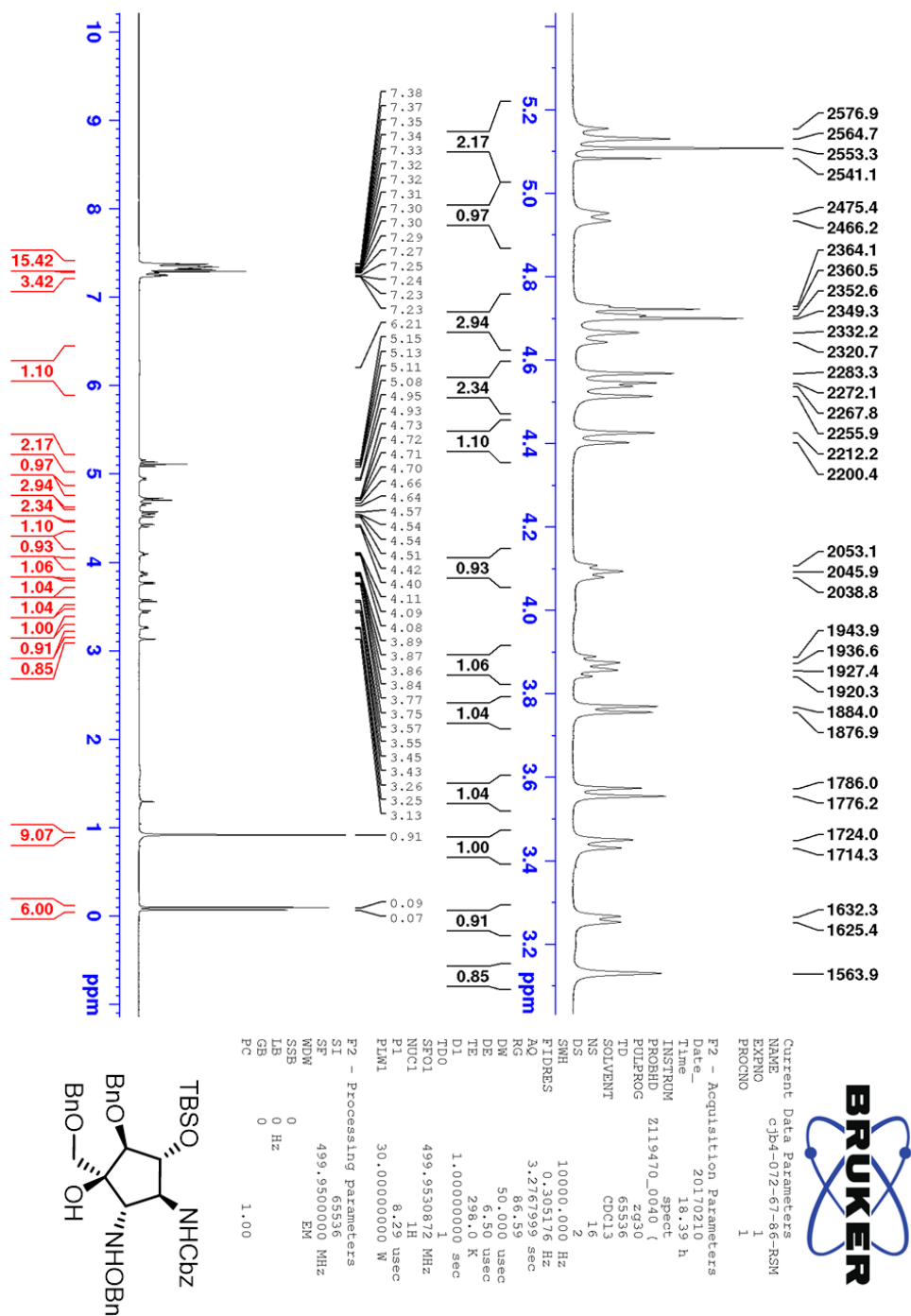
21

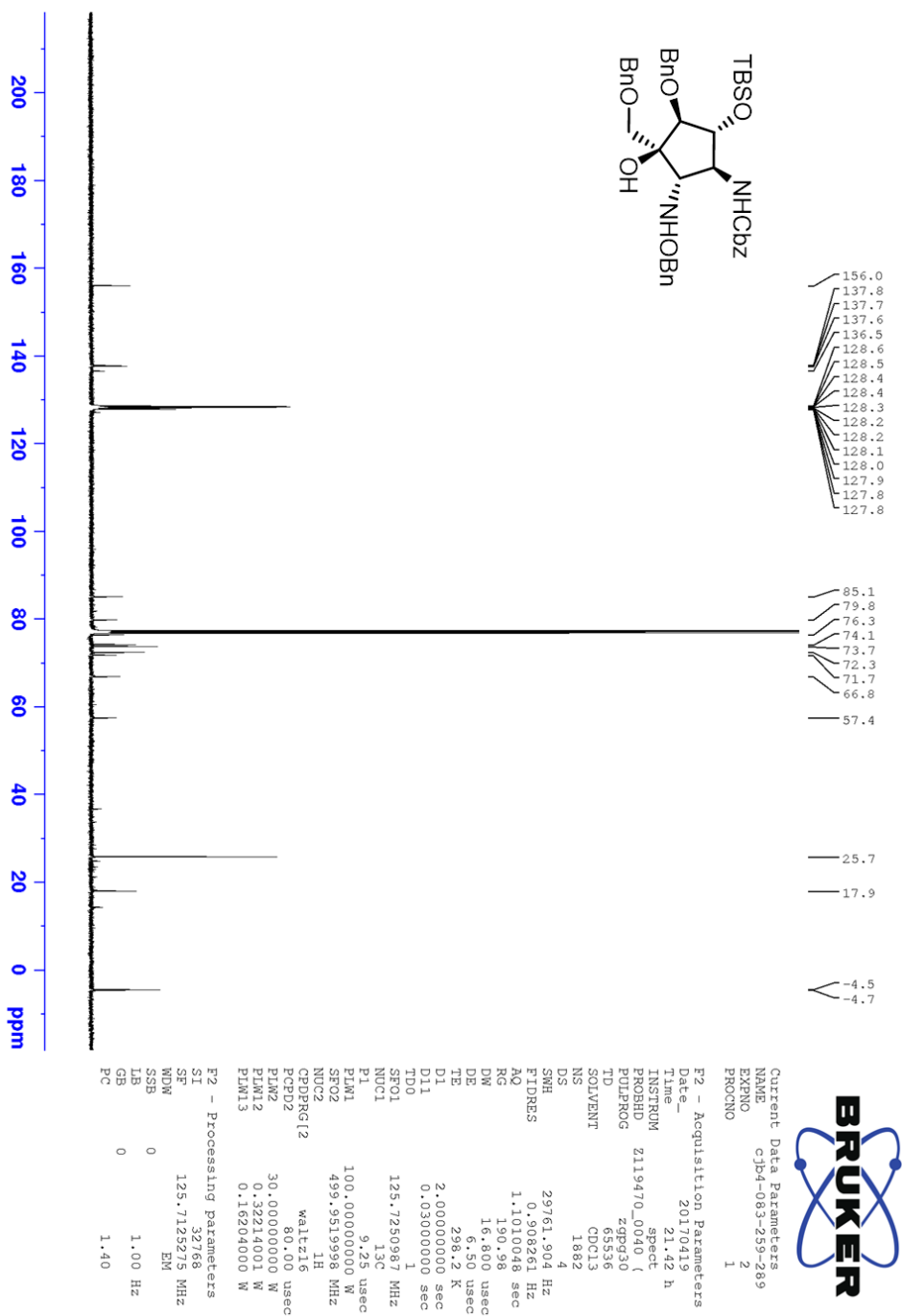


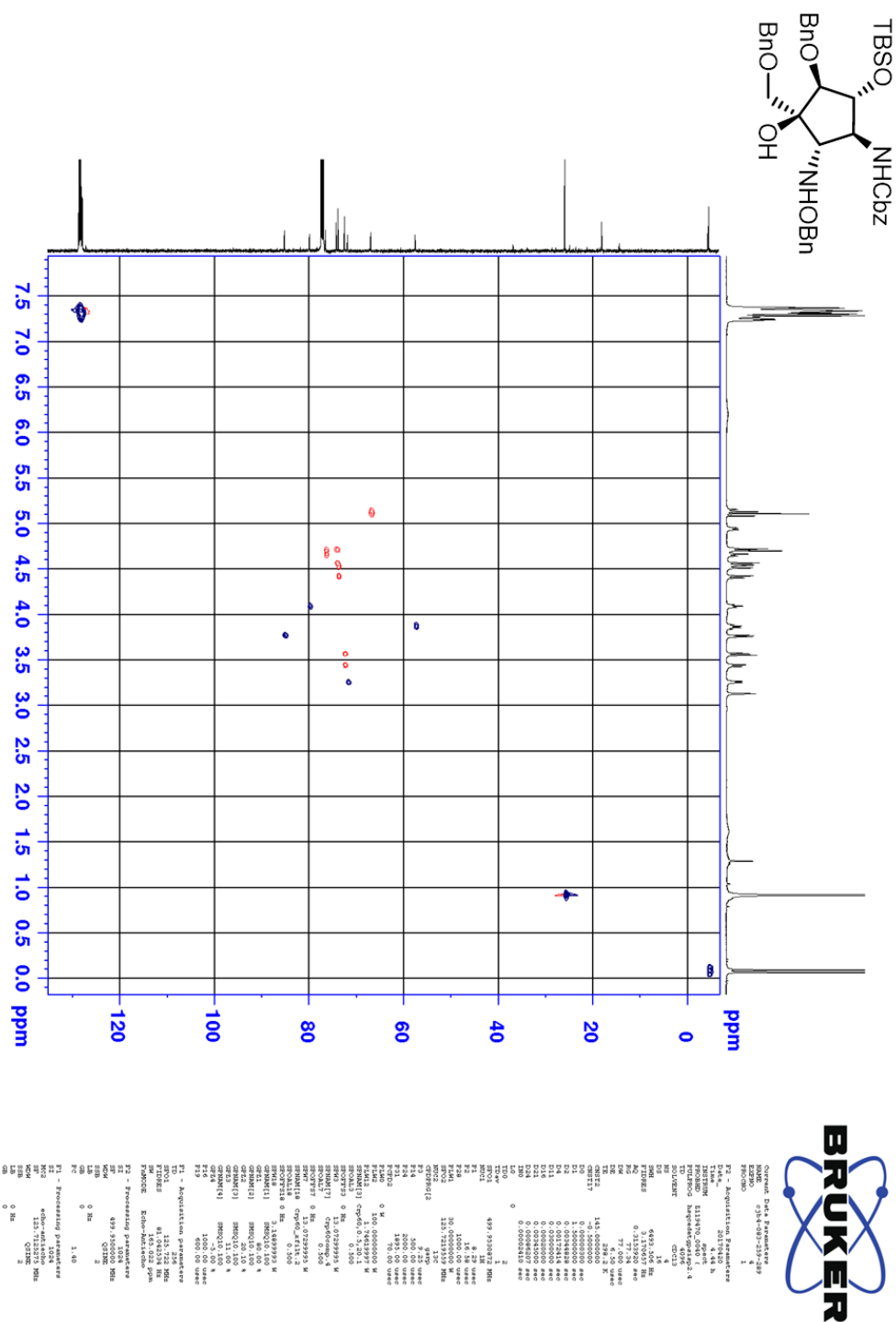
Current Data Parameters		cjb4-042-ficc-PND	
NAME	EXPNO	PROCNO	1
F2 - Acquisition Parameters			
Time	20170530	23.25	h
INSTRUM			
PROBHD	2119470.0040		spec
FIDPROC	zpgpg30		
TD	65336		
SOLVENT	CDCl3		
DS	3711		4
SMH	29761.904		Hz
FIDERS	0.908261		Hz
AQ	1.1010048		sec
RG	190.08		
DW	16.800		usec
DE	6.50		usec
TE	298.2		K
D1	2.00000000		sec
D11	0.03000000		sec
TDO			1
SFO1	125.7250987		MHz
NUC1	13C		
P1	9.25		usec
FLM1	100.00000000		W
SFO2	499.9519998		MHz
NUC2	1H		
CDPRG12	waltz16		
PCPD2	80.00		usec
PLM2	30.00000000		W
PLM12	0.3214001		W
PLM13	0.16204000		W
F2 - Processing parameters			
SI	32768		
SF	125.71125275		MHz
MDW	EM		
SSB	0		
LB	1.00		Hz
GB	0		
CB	1.40		

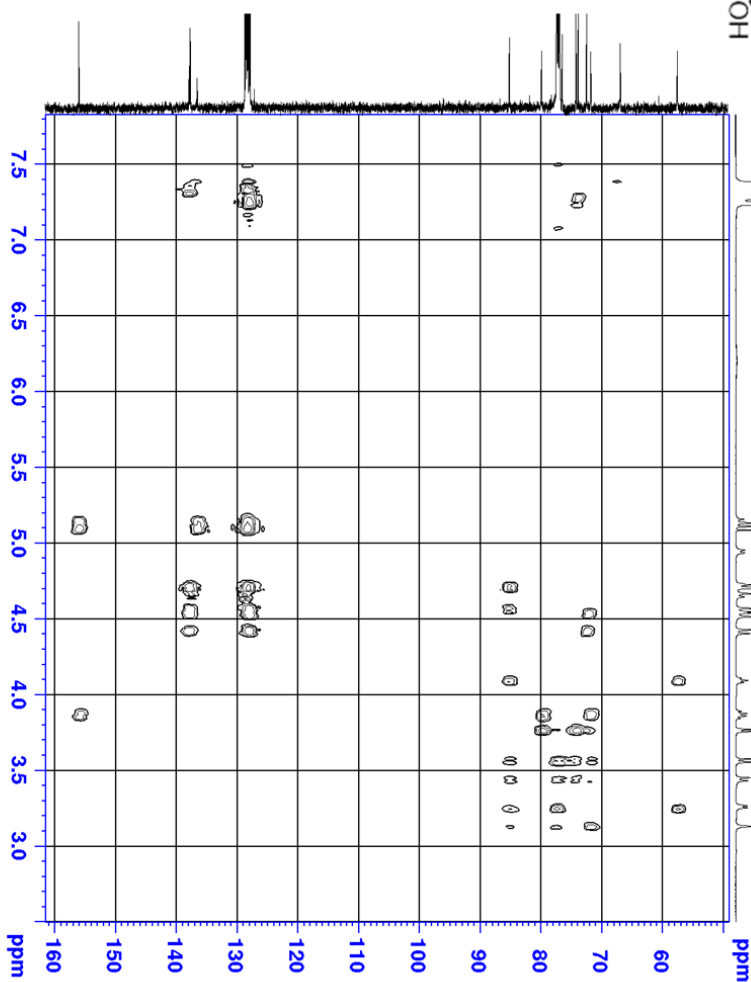
Appendix Figure 6.117: HSQC (CDCl₃) spectrum of **21**



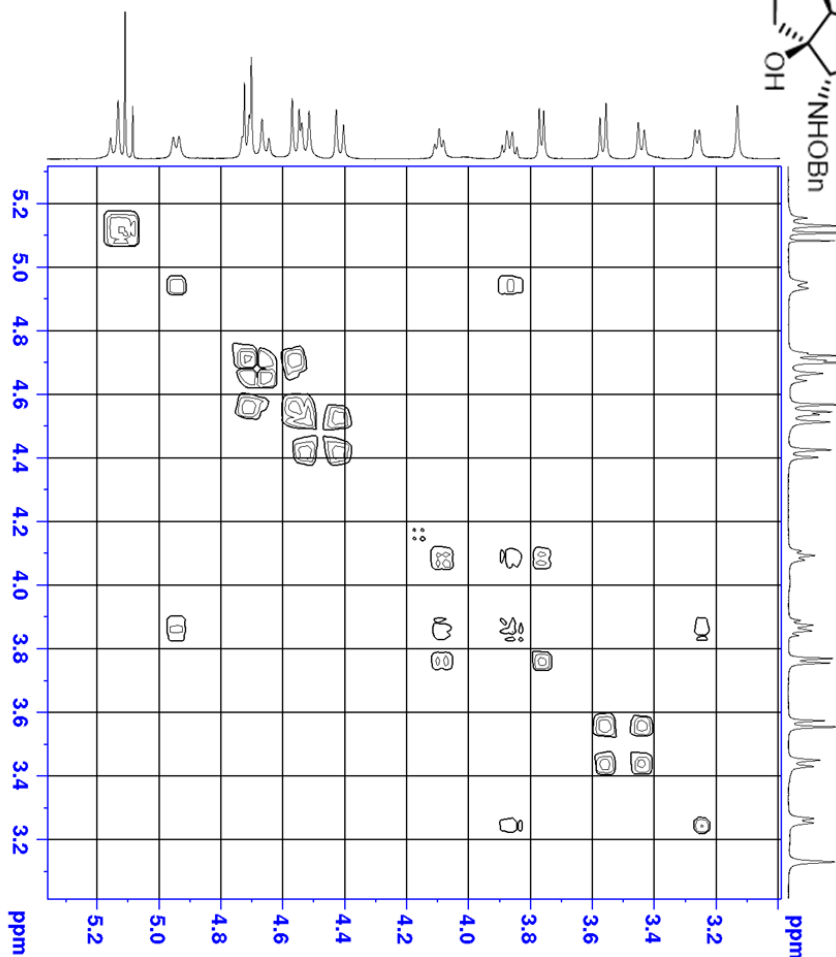
Appendix Figure 6.118: ^1H NMR (CDCl_3) spectrum of TM-120

Appendix Figure 6.119: ^{13}C NMR (CDCl_3) spectrum of TM-120

Appendix Figure 6.120: HSQC (CDCl₃) spectrum of TM-120

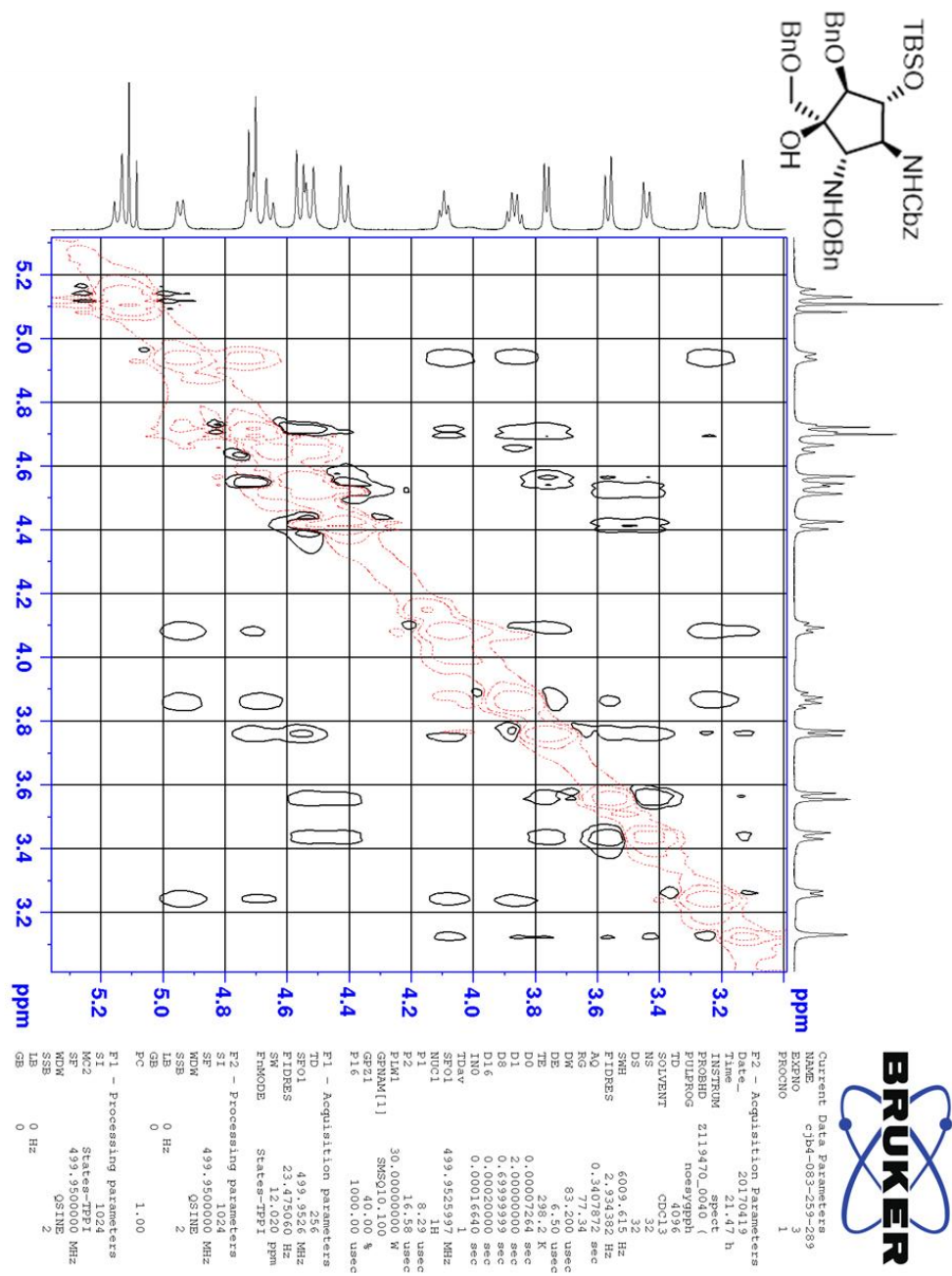
CC1(C)C(C(C1)OC(=O)N)OC(=O)N

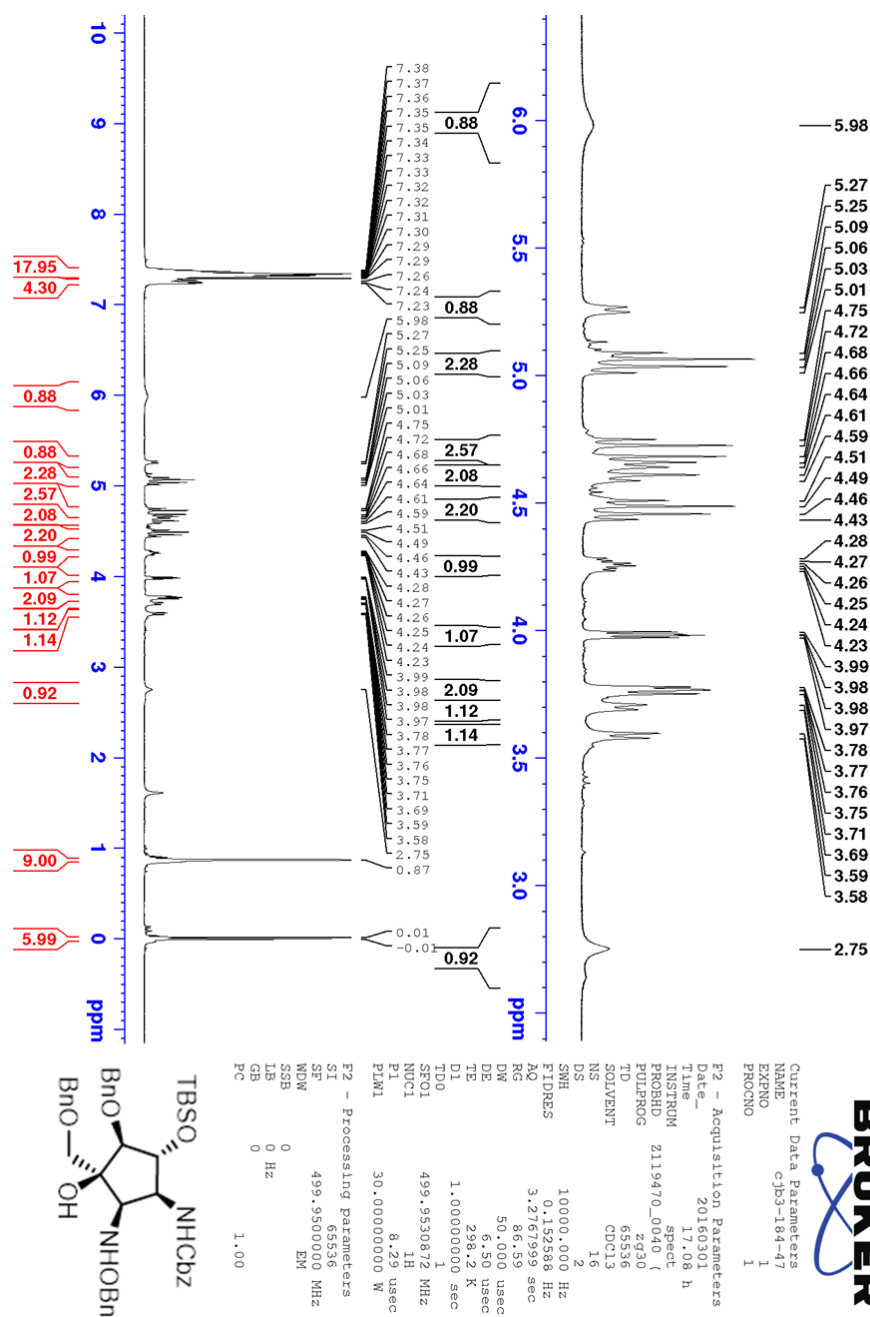
Current Data Parameters		F2 - Acquisition Parameters	
NAME	C94-015-2589	NAME	20170420
EXPNO	5	TIME	5.1 h
PROCNO	1	PROBHD	Z11470.0400 ()
		NUC1	13C
		NUC2	13C
		NUC3	13C
		NUC4	13C
		NUC5	13C
		NUC6	13C
		NUC7	13C
		NUC8	13C
		NUC9	13C
		NUC10	13C
		NUC11	13C
		NUC12	13C
		NUC13	13C
		NUC14	13C
		NUC15	13C
		NUC16	13C
		NUC17	13C
		NUC18	13C
		NUC19	13C
		NUC20	13C
		NUC21	13C
		NUC22	13C
		NUC23	13C
		NUC24	13C
		NUC25	13C
		NUC26	13C
		NUC27	13C
		NUC28	13C
		NUC29	13C
		NUC30	13C
		NUC31	13C
		NUC32	13C
		NUC33	13C
		NUC34	13C
		NUC35	13C
		NUC36	13C
		NUC37	13C
		NUC38	13C
		NUC39	13C
		NUC40	13C
		NUC41	13C
		NUC42	13C
		NUC43	13C
		NUC44	13C
		NUC45	13C
		NUC46	13C
		NUC47	13C
		NUC48	13C
		NUC49	13C
		NUC50	13C
		NUC51	13C
		NUC52	13C
		NUC53	13C
		NUC54	13C
		NUC55	13C
		NUC56	13C
		NUC57	13C
		NUC58	13C
		NUC59	13C
		NUC60	13C
		NUC61	13C
		NUC62	13C
		NUC63	13C
		NUC64	13C
		NUC65	13C
		NUC66	13C
		NUC67	13C
		NUC68	13C
		NUC69	13C
		NUC70	13C
		NUC71	13C
		NUC72	13C
		NUC73	13C
		NUC74	13C
		NUC75	13C
		NUC76	13C
		NUC77	13C
		NUC78	13C
		NUC79	13C
		NUC80	13C
		NUC81	13C
		NUC82	13C
		NUC83	13C
		NUC84	13C
		NUC85	13C
		NUC86	13C
		NUC87	13C
		NUC88	13C
		NUC89	13C
		NUC90	13C
		NUC91	13C
		NUC92	13C
		NUC93	13C
		NUC94	13C
		NUC95	13C
		NUC96	13C
		NUC97	13C
		NUC98	13C
		NUC99	13C
		NUC100	13C
		NUC101	13C
		NUC102	13C
		NUC103	13C
		NUC104	13C
		NUC105	13C
		NUC106	13C
		NUC107	13C
		NUC108	13C
		NUC109	13C
		NUC110	13C
		NUC111	13C
		NUC112	13C
		NUC113	13C
		NUC114	13C
		NUC115	13C

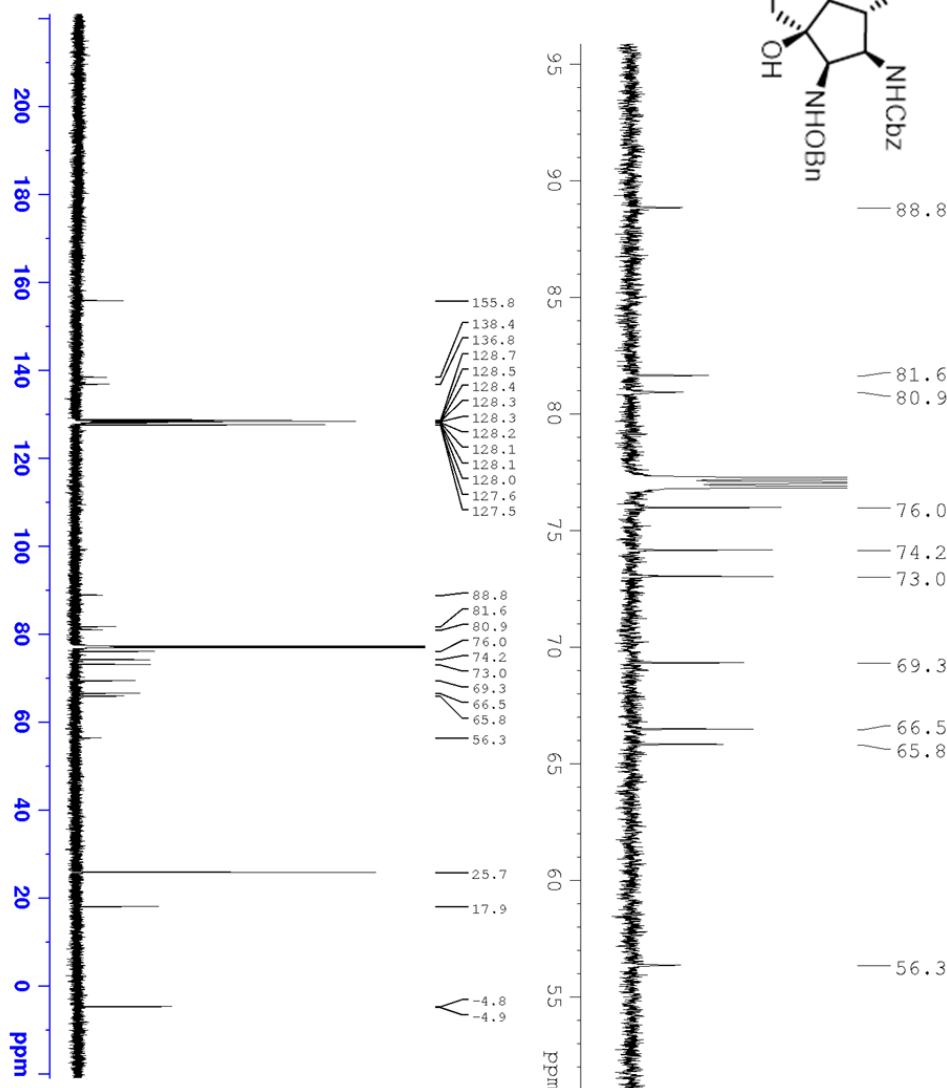
CN(C)C[C@H]1[C@@H](OC(=O)C)C[C@H](OC(=O)C)[C@H]1OC(=O)C

Current Data Parameters		NAME		C7H4-083-259-289	
PROCNM		PROBHD		2119470.0040	
TIME		INSTRUM		spect	
20.00		5.49 h			
F2 - Acquisition Parameters		PULPROG		cosymprdr	
NUC1		SOLVENT		CDCl3	
13		NS		16	
DE		DS		4	
FIDRES		AQ		0.1573916 Hz	
5.643 MHz		RG		77.34	
1.63618 Hz		DR		77.000 usec	
TE		DE		298.2 K	
283.2 K		TD		1	
DE		F1		499.952399 MHz	
0.00000300 sec		P1		8.29 usec	
2.00000000 sec		PR		30.00000000 W	
0.00000000 sec		GPMAN[1]		0.00000000	
0.00000000 sec		GPMAN[2]		0.00000000	
0.00000000 sec		GPMAN[3]		0.00000000	
0.00015400 sec		GE2S		12.00	
0.00015400 sec		GE2S		12.00	
0.00015400 sec		P2		1000.00 usec	
0.00015400 sec		F1 - Acquisition Parameters			
0.00015400 sec		F1		499.952399 MHz	
0.00015400 sec		P1		8.29 usec	
0.00015400 sec		PR		30.00000000 W	
0.00015400 sec		GPMAN[1]		0.00000000	
0.00015400 sec		GPMAN[2]		0.00000000	
0.00015400 sec		GPMAN[3]		0.00000000	
0.00015400 sec		GE2S		12.00	
0.00015400 sec		GE2S		12.00	
0.00015400 sec		P2		1000.00 usec	
0.00015400 sec		F2 - Processing Parameters			
0.00015400 sec		F2		499.9500000 MHz	
0.00015400 sec		P1		1024	
0.00015400 sec		PR		12.986 ppm	
0.00015400 sec		GPMAN[1]		0.00000000	
0.00015400 sec		GPMAN[2]		0.00000000	
0.00015400 sec		GPMAN[3]		0.00000000	
0.00015400 sec		GE2S		12.00	
0.00015400 sec		GE2S		12.00	
0.00015400 sec		P2		1000.00 usec	
0.00015400 sec		F3 - Processing Parameters			
0.00015400 sec		F3		499.9500000 MHz	
0.00015400 sec		P1		1024	
0.00015400 sec		PR		12.986 ppm	
0.00015400 sec		GPMAN[1]		0.00000000	
0.00015400 sec		GPMAN[2]		0.00000000	
0.00015400 sec		GPMAN[3]		0.00000000	
0.00015400 sec		GE2S		12.00	
0.00015400 sec		GE2S		12.00	
0.00015400 sec		P2		1000.00 usec	
0.00015400 sec		F4 - Processing Parameters			
0.00015400 sec		F4		499.9500000 MHz	
0.00015400 sec		P1		1024	
0.00015400 sec		PR		12.986 ppm	
0.00015400 sec		GPMAN[1]		0.00000000	
0.00015400 sec		GPMAN[2]		0.00000000	
0.00015400 sec		GPMAN[3]		0.00000000	
0.00015400 sec		GE2S		12.00	
0.00015400 sec		GE2S		12.00	
0.00015400 sec		P2		1000.00 usec	

Appendix Figure 6.123: NOESY (CDCl₃) spectrum of TM-120

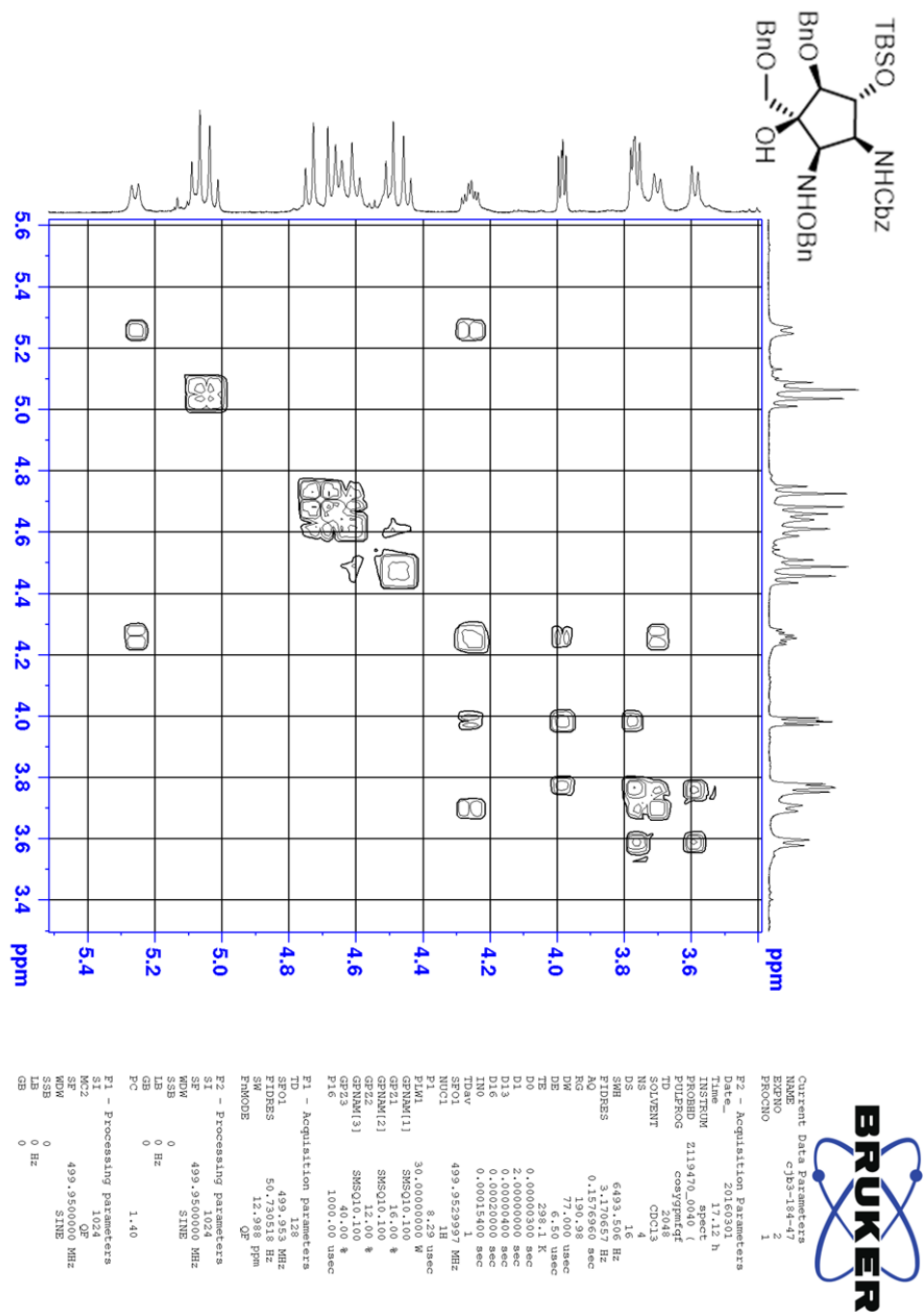


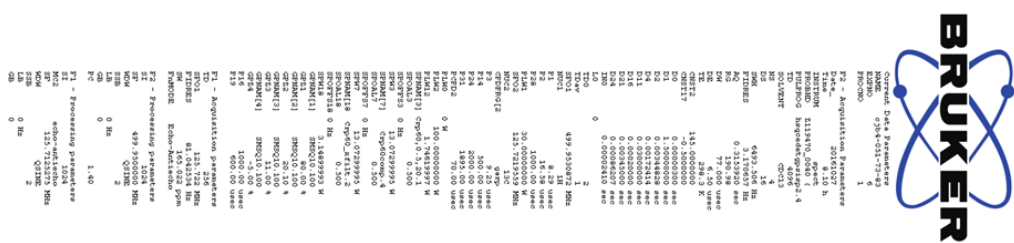
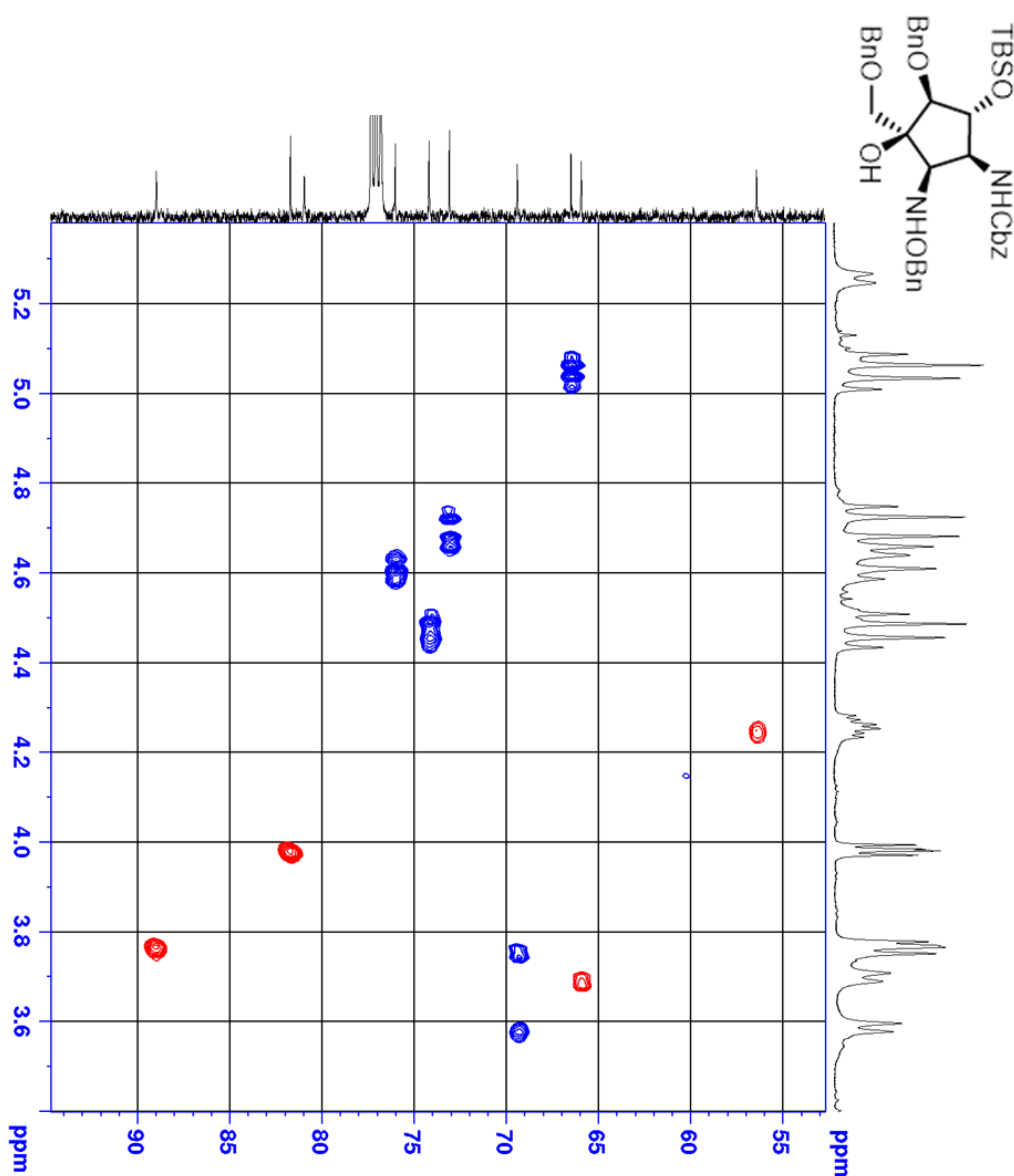
Appendix Figure 6.124: ^1H NMR (CDCl_3) spectrum of TM-119

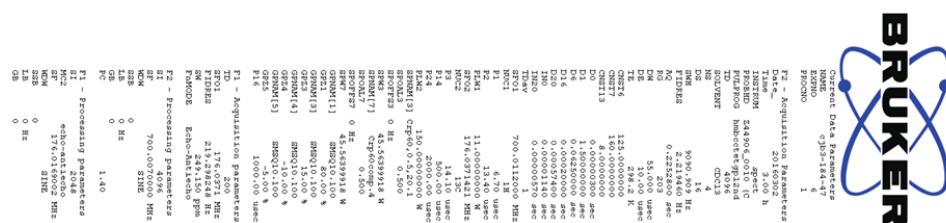


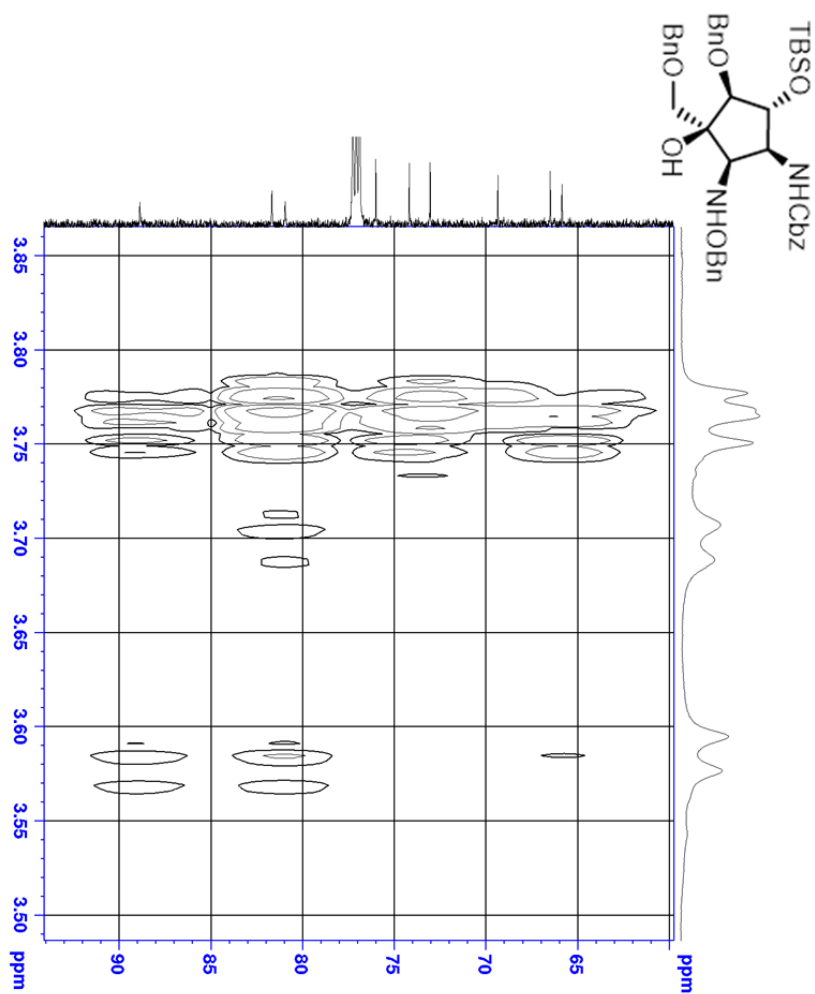
Current	Data Parameters	
NAME	cjb3-184-47	
EXPNO	1	
PROCNO	4	
F2 - Acquisition Parameters		
Time	20160302	
Date_	0.33 h	
INSTRUM	244906.0010	spec
PROBHD	0.10	13C
PULPROG	zgpg30	
TD	65356	
SOLVENT	CDCl3	
NS	1024	
DS	4	
SWH	42613.637	Hz
FIDRES	0.652023	Hz
AQ	0.7668437	sec
RG	203	
DW	11.733	usec
DE	18.00	usec
TE	298.2	K
D1	2.00000000	sec
D11	0.03000000	sec
TDO	1	
SFO1	176.0345018	MHz
NUC1	13C	
P1	14.10	usec
PLM1	150.0000000	W
SFO2	700.0098000	MHz
NUC2	1H	
CPDPRG2	waltz16	
PCPD2	65.00	usec
PLM2	11.00000000	W
PLM3	0.11687000	W
PLM3	0.05865100	W
F2 - Processing parameters		
SI	32768	
SF	176.0165002	MHz
WDW	EM	
SGB	0	
GB	1.00	Hz
PC	1.40	

Appendix Figure 6.126: COSY (CDCl₃) spectrum of TM-119

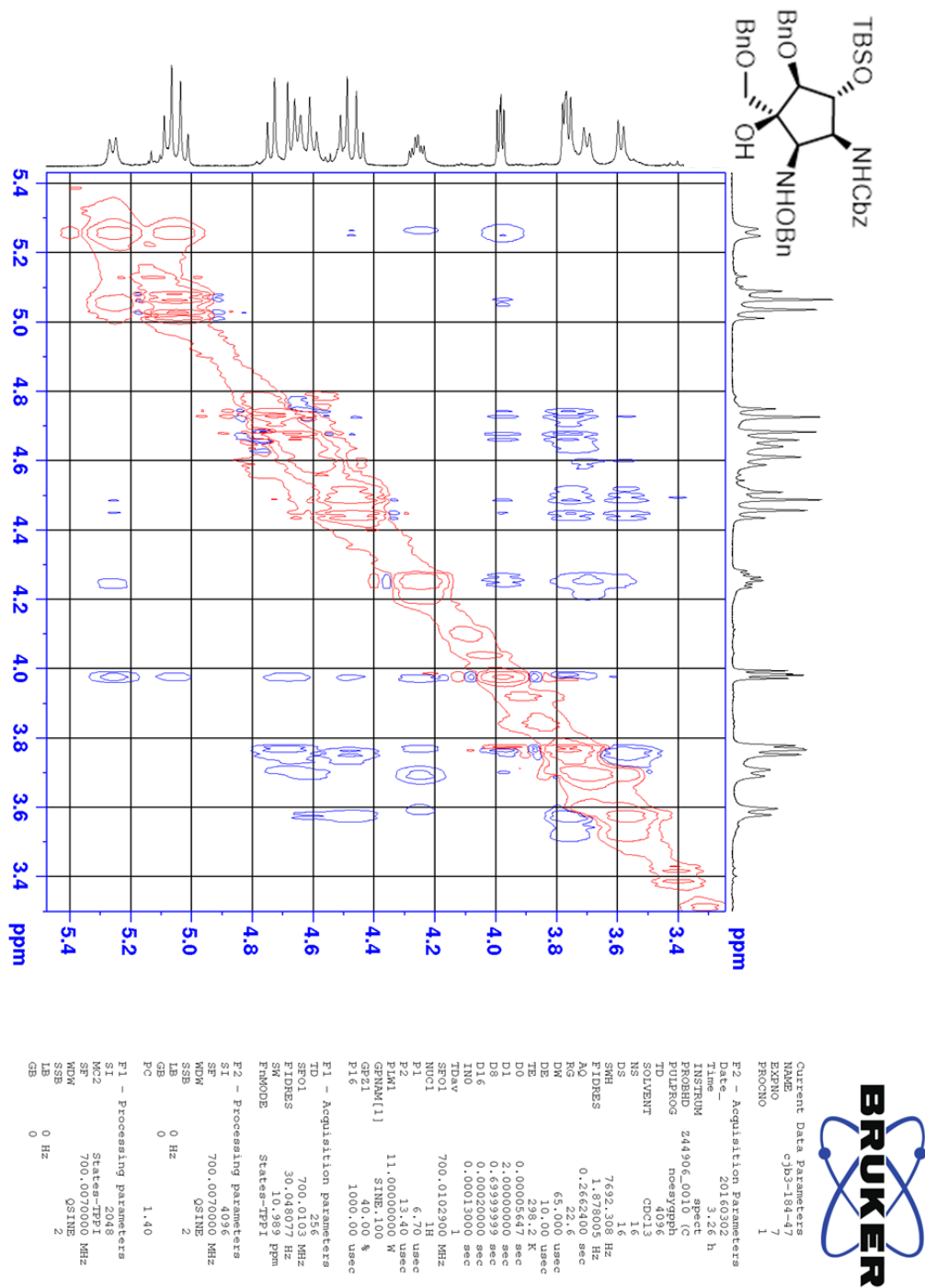


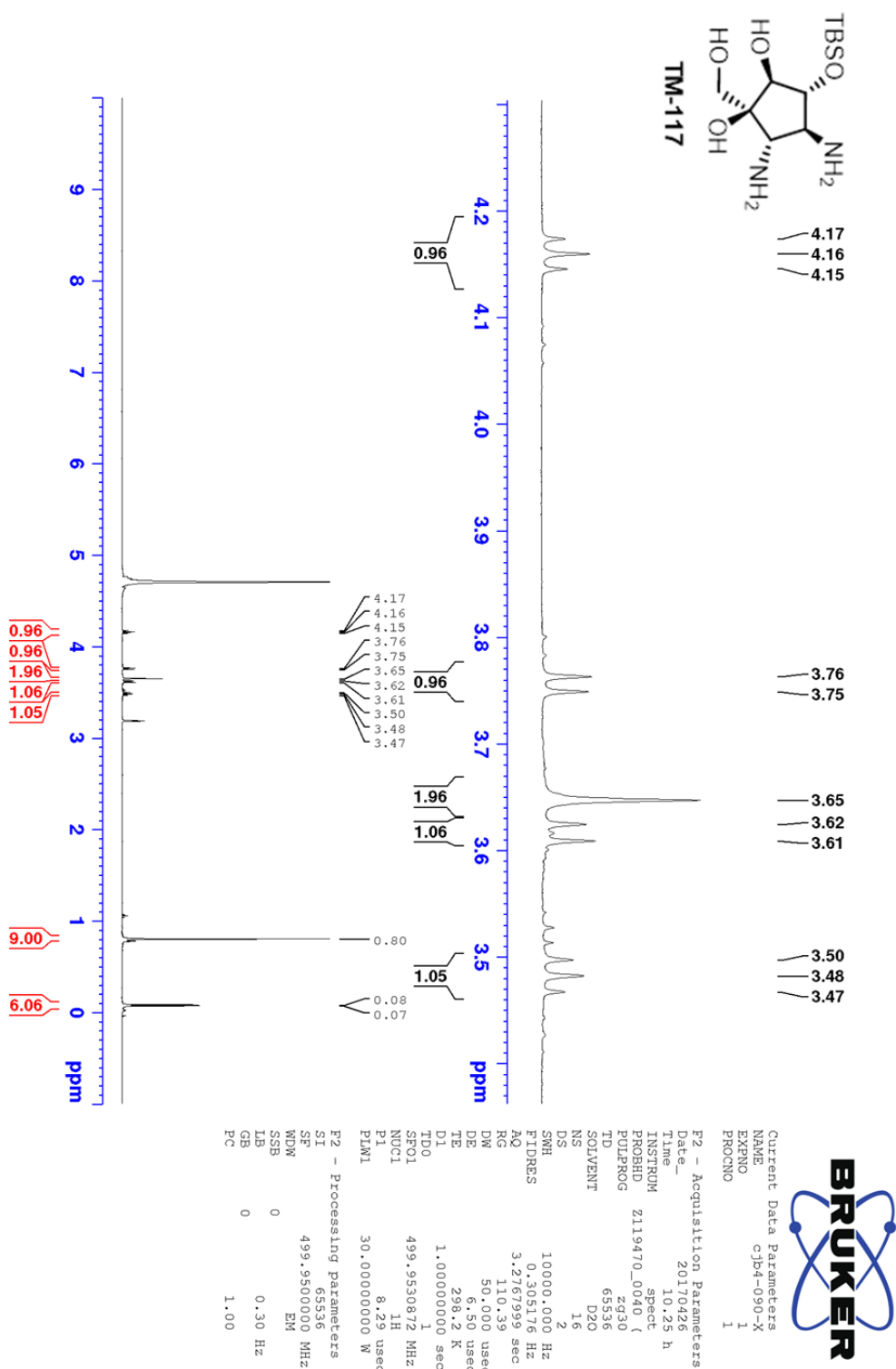
Appendix Figure 6.127: HSQC (CDCl_3) spectrum of TM-119

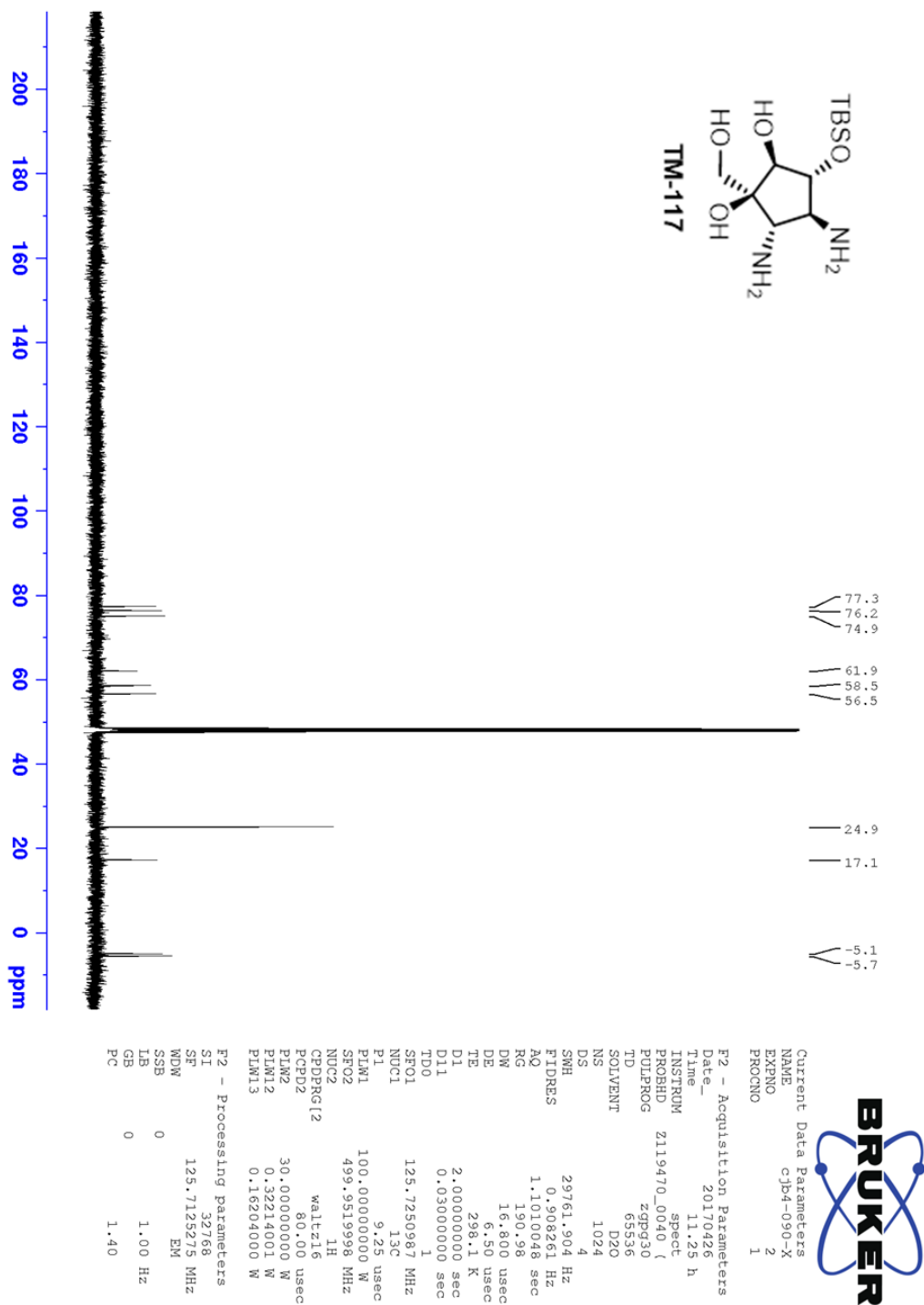


Appendix Figure 6.129: HMBC (CDCl_3) spectrum of TM-119

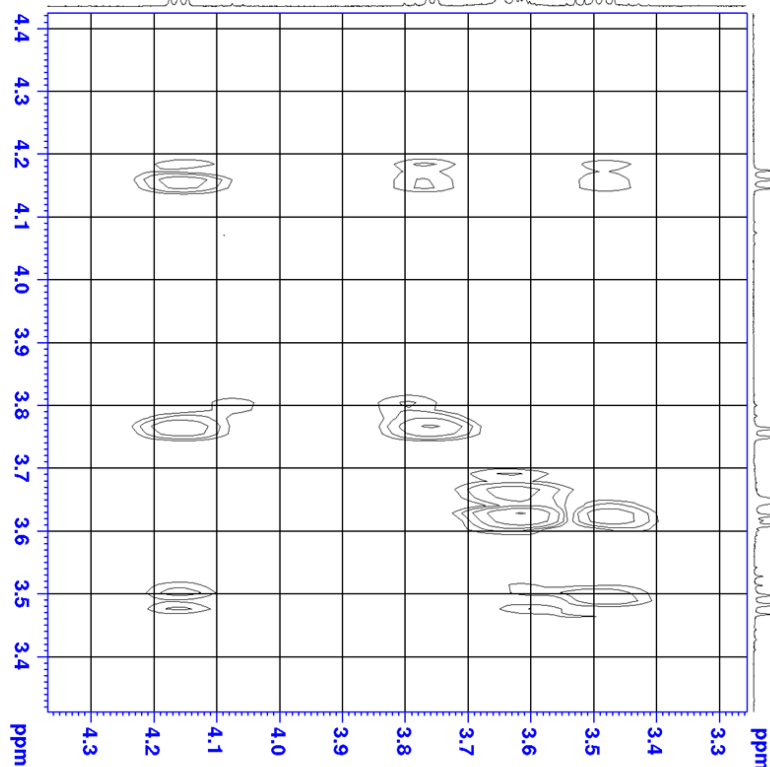
Appendix Figure 6.130: NOESY (CDCl₃) spectrum of TM-119



Appendix Figure 6.131: ^1H NMR (D_2O -MeOD) spectrum of TM-117

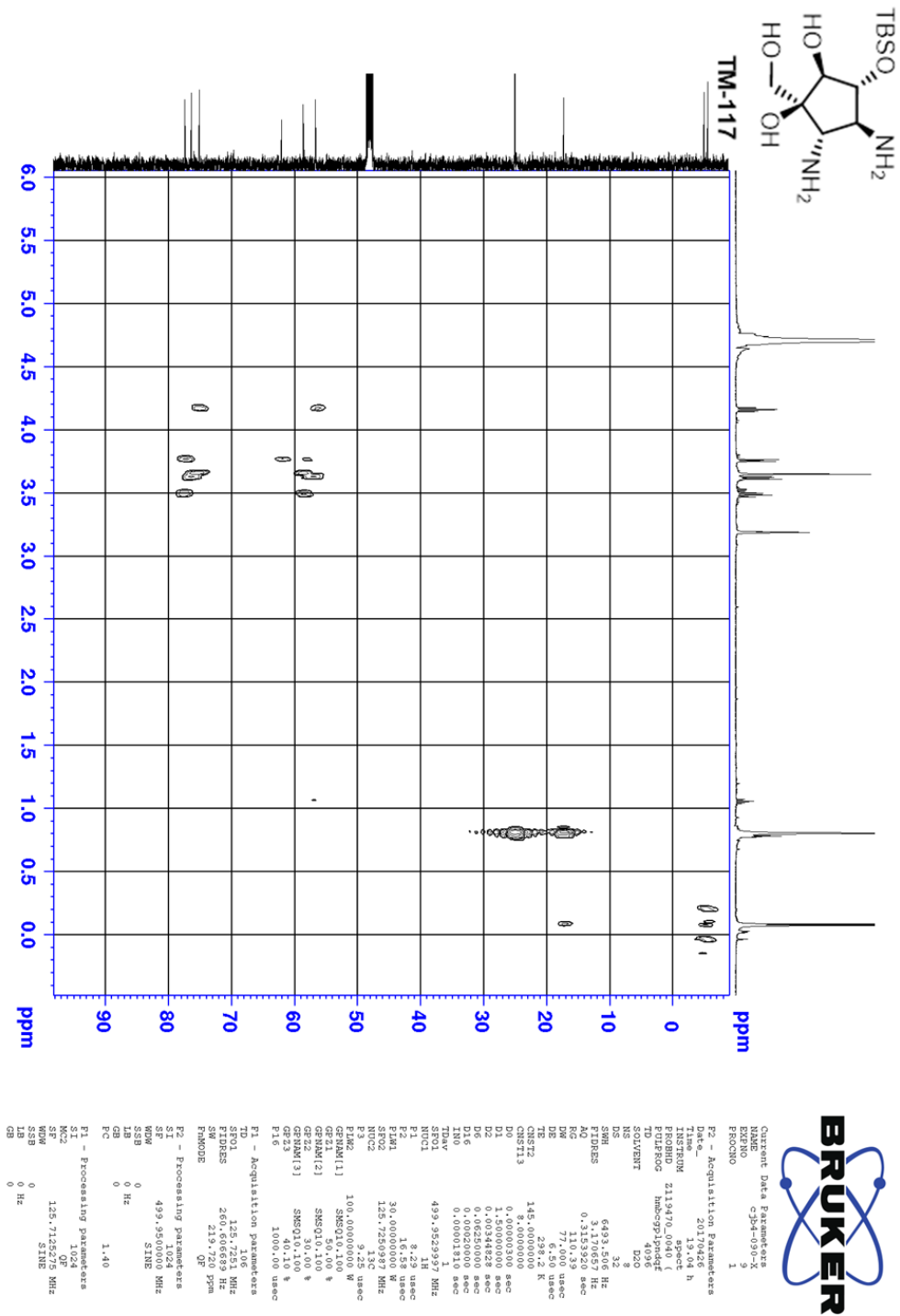
Appendix Figure 6.132: ^{13}C NMR (D_2O -MeOD) spectrum of TM-117

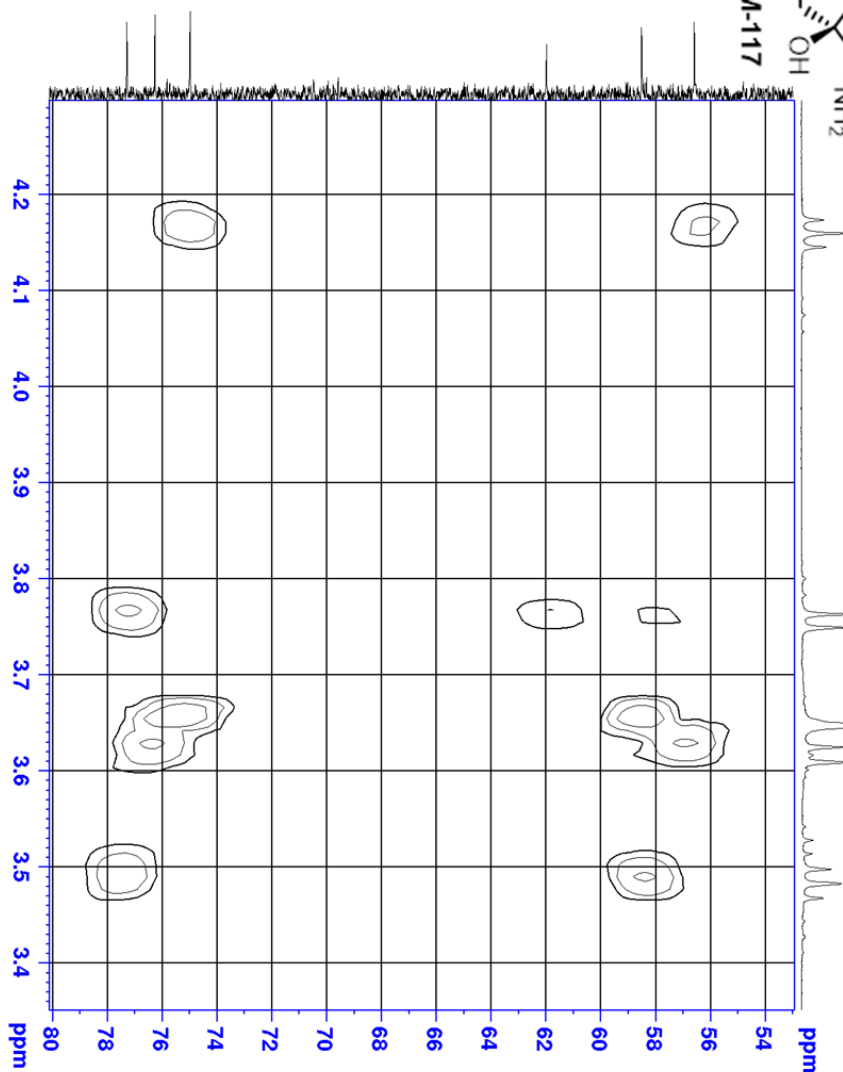
TM-117



Current Data Parameters		P1 - Acquisition Parameters	
EXPNO	0146-0930	EXPNO	11
PROCNO	1	PROCNO	1
Date_		Date_	20100426
Time		Time	23:04 h
INSTRUM	spect	INSTRUM	spect
PROBHD	131.970 mm	PROBHD	cryopmpd
PULPROG	zgpg30	PULPROG	zgpg30
TD	2048	TD	2048
SOLVENT	D2O	SOLVENT	D2O
DS	16	DS	16
SWH	6493.306 Hz	SWH	6493.306 Hz
F2FIDRES	0.474131 Hz	F2FIDRES	0.474131 Hz
RG	0.110 39	RG	0.110 39
DE	77.000 usec	DE	77.000 usec
TE	6.50 usec	TE	6.50 usec
DM	2.00000000 sec	DM	2.00000000 sec
D1	0.00000000 sec	D1	0.00000000 sec
D2	0.00000000 sec	D2	0.00000000 sec
D3	0.00000000 sec	D3	0.00000000 sec
INQ	0.00015000 sec	INQ	0.00015000 sec
TDV	499.9529991 MHz	TDV	499.9529991 MHz
NUC1	1H	NUC1	1H
NUC2	1H	NUC2	1H
FLN	8.29 usec	FLN	8.29 usec
PL1	36.00000000 W	PL1	36.00000000 W
PRQ1	0.100 usec	PRQ1	0.100 usec
GRPM121	SMOUL0.100	GRPM121	SMOUL0.100
GR22	12.00 usec	GR22	12.00 usec
GRPM23	SMOUL0.100	GRPM23	SMOUL0.100
P16	1000.000 usec	P16	1000.000 usec
P1 - Acquisition Parameters			
SEPI	499.958 MHz	SEPI	499.958 MHz
FIDRES	56.170318 Hz	FIDRES	56.170318 Hz
PRQ2	12.00 usec	PRQ2	12.00 usec
PRQ3	12.00 usec	PRQ3	12.00 usec
PRQ4	12.00 usec	PRQ4	12.00 usec
PRQ5	12.00 usec	PRQ5	12.00 usec
PRQ6	12.00 usec	PRQ6	12.00 usec
P2 - Processing Parameters			
WDW	499.9500000 MHz	WDW	499.9500000 MHz
SF	500.136052 MHz	SF	500.136052 MHz
GB	0	GB	0
PC	1.40	PC	1.40
P3 - Processing Parameters			
SI	1024	SI	1024
ME2	499.9500000 MHz	ME2	499.9500000 MHz
SF	500.136052 MHz	SF	500.136052 MHz
SF8	500.136052 MHz	SF8	500.136052 MHz
GB	0	GB	0
SB	0 Hz	SB	0 Hz

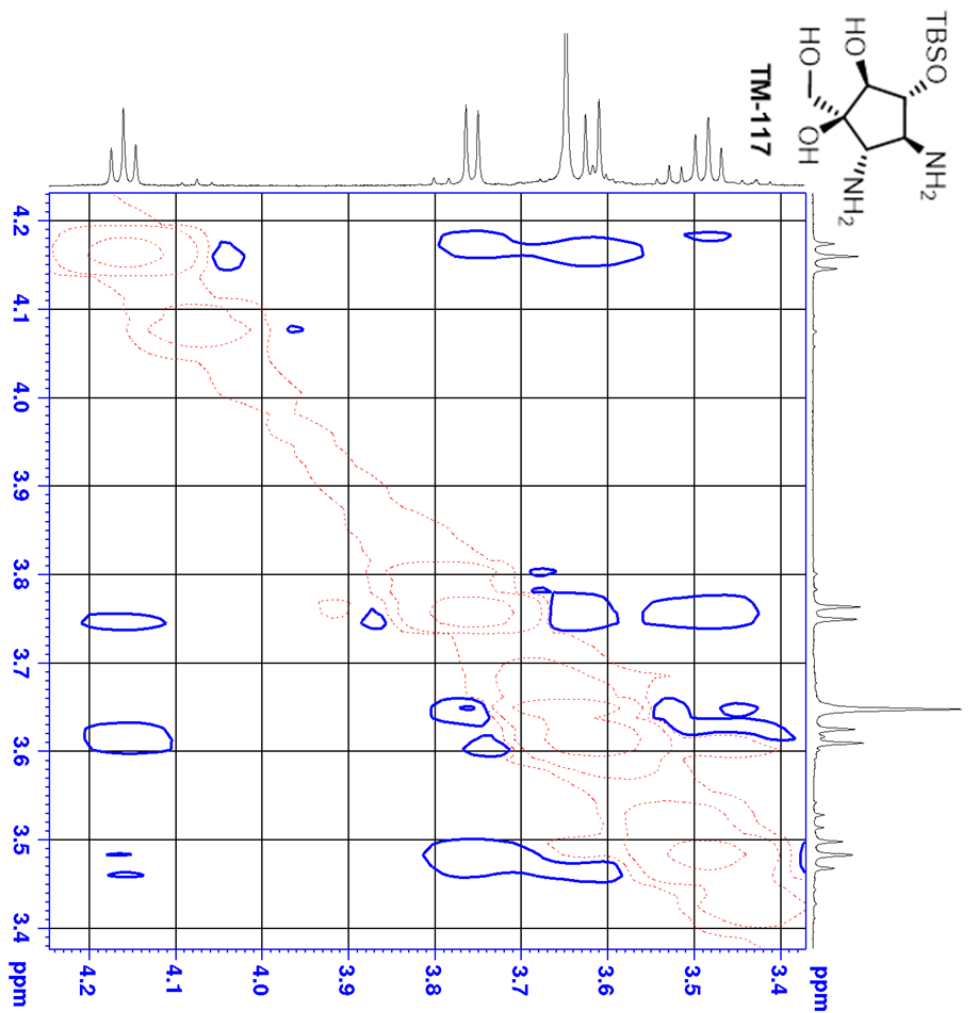
Appendix Figure 6.135: HMBC (D₂O-MeOD) spectrum of TM-117



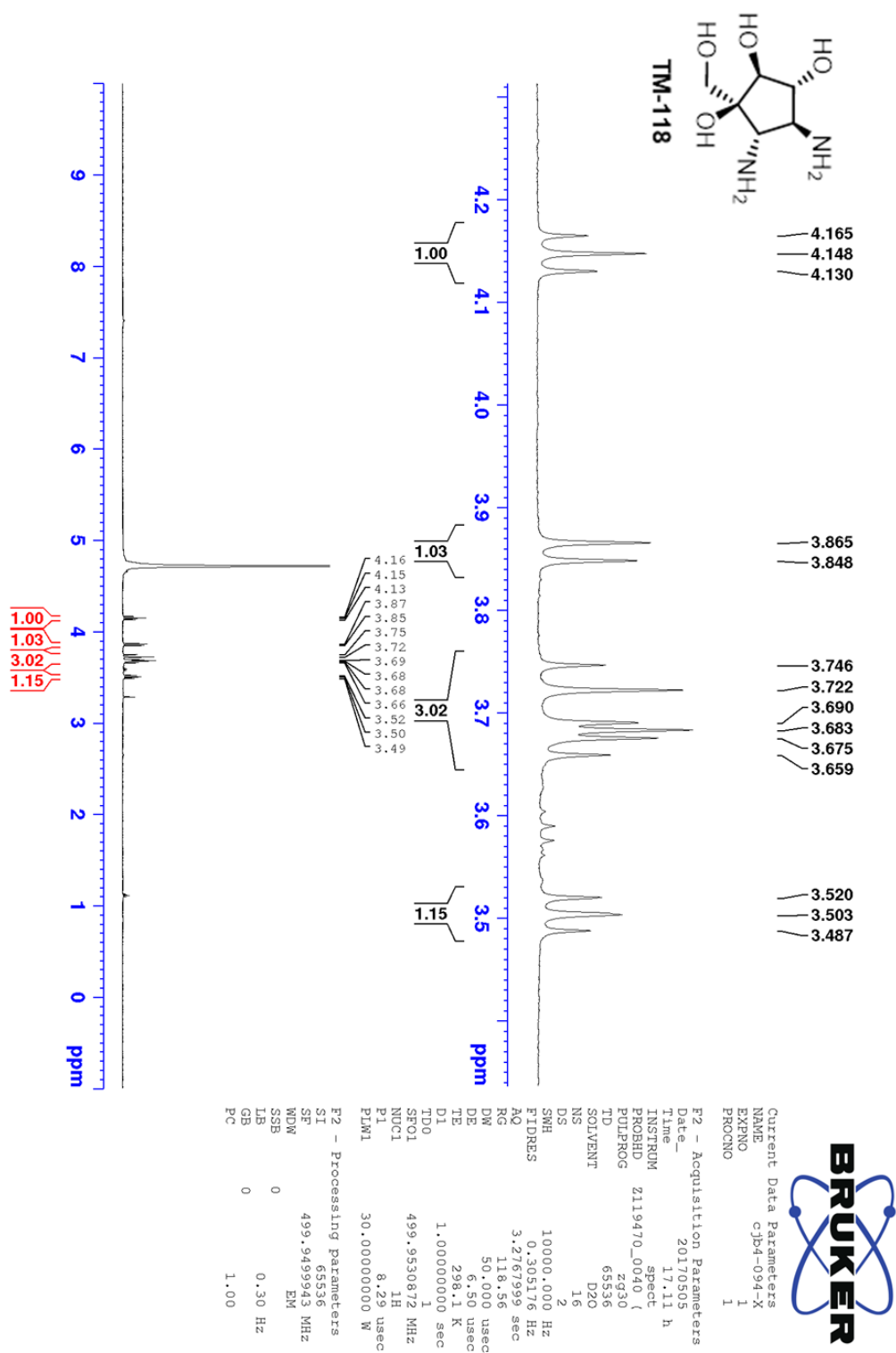
C[Si](C)(C)OC[C@H]1O[C@@H](CO)[C@H](N)[C@@H](N)[C@H]1O

P1 - Processing parameters		P2 - Acquisition Parameters	
SI	499.9600000 Mhz	Date_	20170426
SR	1024	Time	14h 45
SB	SINE	INSTRUM	nmbrspc
LB	0 Hz	PROBHD	2139470.0400 (
P2	0	PULPROG	nmbrspc
	1.40	PCPDPR	nmbrspc
		PCPDPR2	nmbrspc
		PCPDPR3	nmbrspc
		PCPDPR4	nmbrspc
		PCPDPR5	nmbrspc
		PCPDPR6	nmbrspc
		PCPDPR7	nmbrspc
		PCPDPR8	nmbrspc
		PCPDPR9	nmbrspc
		PCPDPR10	nmbrspc
		PCPDPR11	nmbrspc
		PCPDPR12	nmbrspc
		PCPDPR13	nmbrspc
		PCPDPR14	nmbrspc
		PCPDPR15	nmbrspc
		PCPDPR16	nmbrspc
		PCPDPR17	nmbrspc
		PCPDPR18	nmbrspc
		PCPDPR19	nmbrspc
		PCPDPR20	nmbrspc
		PCPDPR21	nmbrspc
		PCPDPR22	nmbrspc
		PCPDPR23	nmbrspc
		PCPDPR24	nmbrspc
		PCPDPR25	nmbrspc
		PCPDPR26	nmbrspc
		PCPDPR27	nmbrspc
		PCPDPR28	nmbrspc
		PCPDPR29	nmbrspc
		PCPDPR30	nmbrspc
		PCPDPR31	nmbrspc
		PCPDPR32	nmbrspc
		PCPDPR33	nmbrspc
		PCPDPR34	nmbrspc
		PCPDPR35	nmbrspc
		PCPDPR36	nmbrspc
		PCPDPR37	nmbrspc
		PCPDPR38	nmbrspc
		PCPDPR39	nmbrspc
		PCPDPR40	nmbrspc
		PCPDPR41	nmbrspc
		PCPDPR42	nmbrspc
		PCPDPR43	nmbrspc
		PCPDPR44	nmbrspc
		PCPDPR45	nmbrspc
		PCPDPR46	nmbrspc
		PCPDPR47	nmbrspc
		PCPDPR48	nmbrspc
		PCPDPR49	nmbrspc
		PCPDPR50	nmbrspc
		PCPDPR51	nmbrspc
		PCPDPR52	nmbrspc
		PCPDPR53	nmbrspc
		PCPDPR54	nmbrspc
		PCPDPR55	nmbrspc
		PCPDPR56	nmbrspc
		PCPDPR57	nmbrspc
		PCPDPR58	nmbrspc
		PCPDPR59	nmbrspc
		PCPDPR60	nmbrspc
		PCPDPR61	nmbrspc
		PCPDPR62	nmbrspc
		PCPDPR63	nmbrspc
		PCPDPR64	nmbrspc
		PCPDPR65	nmbrspc
		PCPDPR66	nmbrspc
		PCPDPR67	nmbrspc
		PCPDPR68	nmbrspc
		PCPDPR69	nmbrspc
		PCPDPR70	nmbrspc
		PCPDPR71	nmbrspc
		PCPDPR72	nmbrspc
		PCPDPR73	nmbrspc
		PCPDPR74	nmbrspc
		PCPDPR75	nmbrspc
		PCPDPR76	nmbrspc
		PCPDPR77	nmbrspc
		PCPDPR78	nmbrspc
		PCPDPR79	nmbrspc
		PCPDPR80	nmbrspc
		PCPDPR81	nmbrspc
		PCPDPR82	nmbrspc
		PCPDPR83	nmbrspc
		PCPDPR84	nmbrspc
		PCPDPR85	nmbrspc
		PCPDPR86	nmbrspc
		PCPDPR87	nmbrspc
		PCPDPR88	nmbrspc
		PCPDPR89	nmbrspc
		PCPDPR90	nmbrspc
		PCPDPR91	nmbrspc
		PCPDPR92	nmbrspc
		PCPDPR93	nmbrspc
		PCPDPR94	nmbrspc
		PCPDPR95	nmbrspc
		PCPDPR96	nmbrspc
		PCPDPR97	nmbrspc
		PCPDPR98	nmbrspc
		PCPDPR99	nmbrspc
		PCPDPR100	nmbrspc

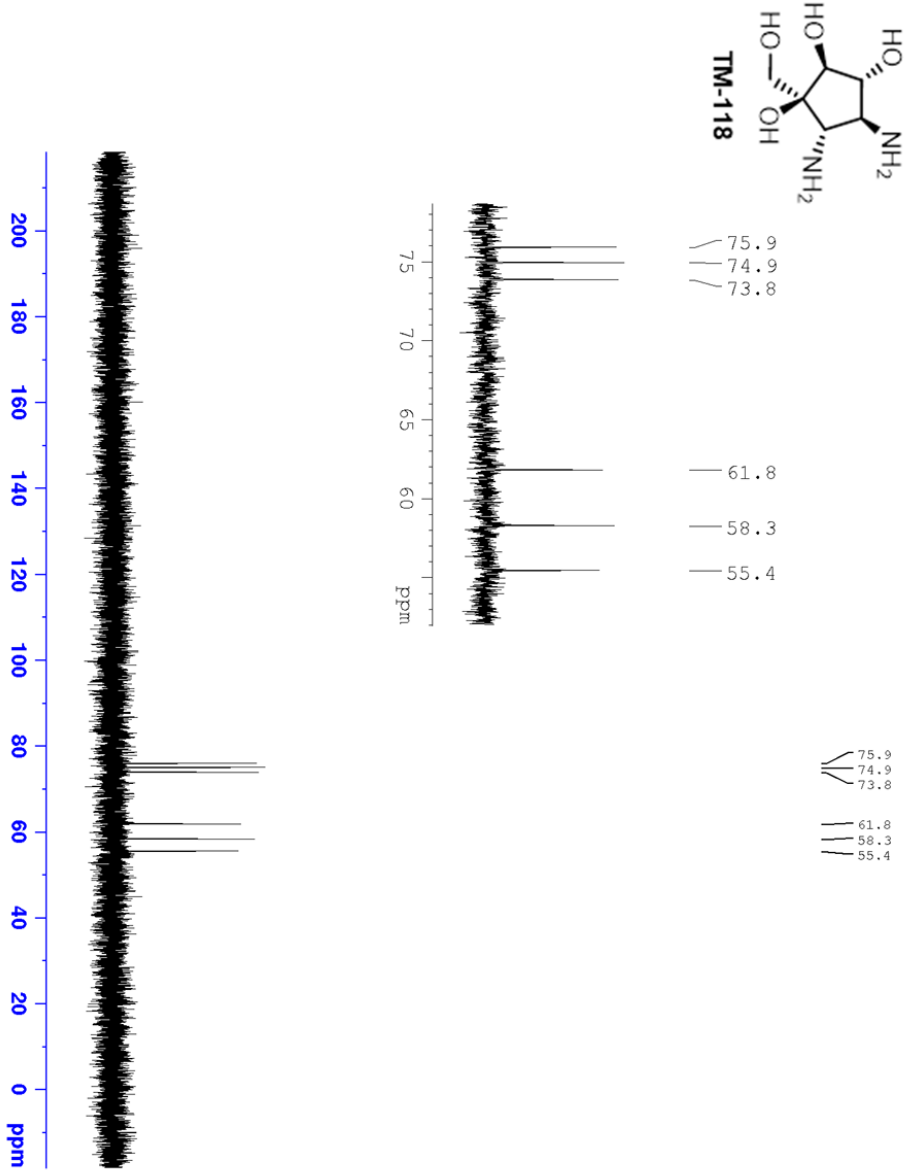
Appendix Figure 6.137: NOESY (D₂O-MeOD) spectrum of TM-117



Current Data Parameters
NAME cjb4-090-X
EXPNO 10
PROCNO 1
F2 - Acquisition Parameters
Date_ 20170426
Time 13:36
INSTRUM spect
PROBHD 211470.0040 (PULPROG noesypph
TD 4096
SOLVENT D2O
NS 16
DS 16
SWH 6003.615 Hz
FIDRES 2.934382 Hz
AQ 0.3407872 sec
RG 110.39
DW 83.200 usec
DE 6.50 usec
TE 293.2 K
D0 0.00007264 sec
D1 2.00000000 sec
D8 0.69999999 sec
D16 0.00020000 sec
IN0 0.00016640 sec
TDav 499.9525931 MHz
SFO1 499.9525931 MHz
NUC1 1H
P1 8.29 usec
P2 16.58 usec
PLM1 30.00000000 W
GPNRM[1] SWSO10.100
GP21 40.00 %
P16 1000.00 usec
F1 - Acquisition parameters
TD 256
SFO1 499.9526 MHz
FIDRES 23.475060 Hz
SR 12.020 ppm
FMODE States-TFPI
F2 - Processing parameters
SI 1024
SF 499.950000 MHz
WDW QSHINE
SSB 2
LB 0 Hz
GB 0
PC 1.00
F1 - Processing parameters
SI 1024
MC2 States-TFPI
SF 499.950000 MHz
WDW QSHINE
SSB 2
LB 0 Hz
GB 0

Appendix Figure 6.138: ^1H NMR (D_2O) spectrum of TM-118

Appendix Figure 6.139: ^{13}C NMR (D_2O) spectrum of TM-118



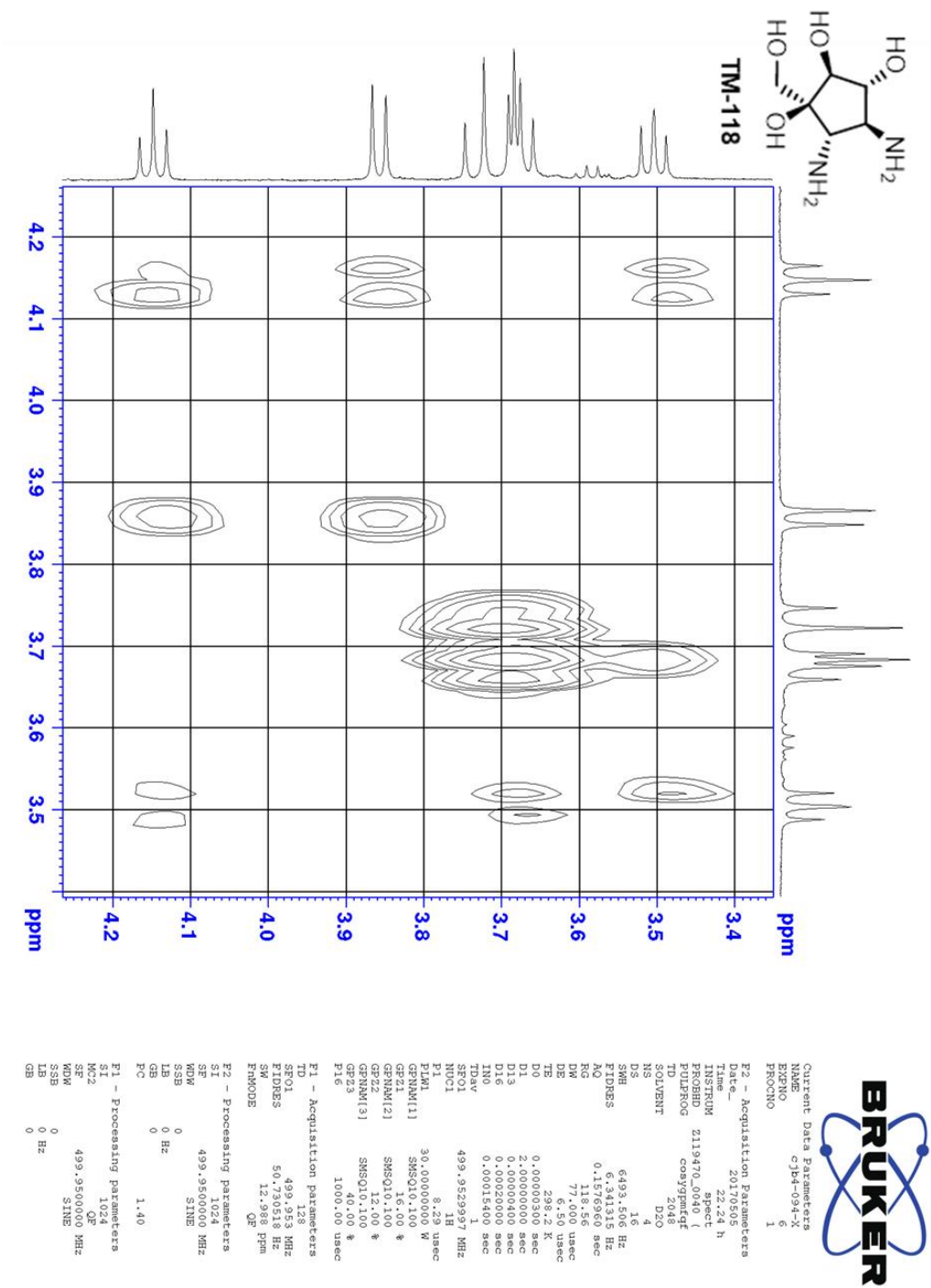
BRUKER

Current Data Parameters
NAME cjb4-094-X
EXPNO 2
PROCNO 1

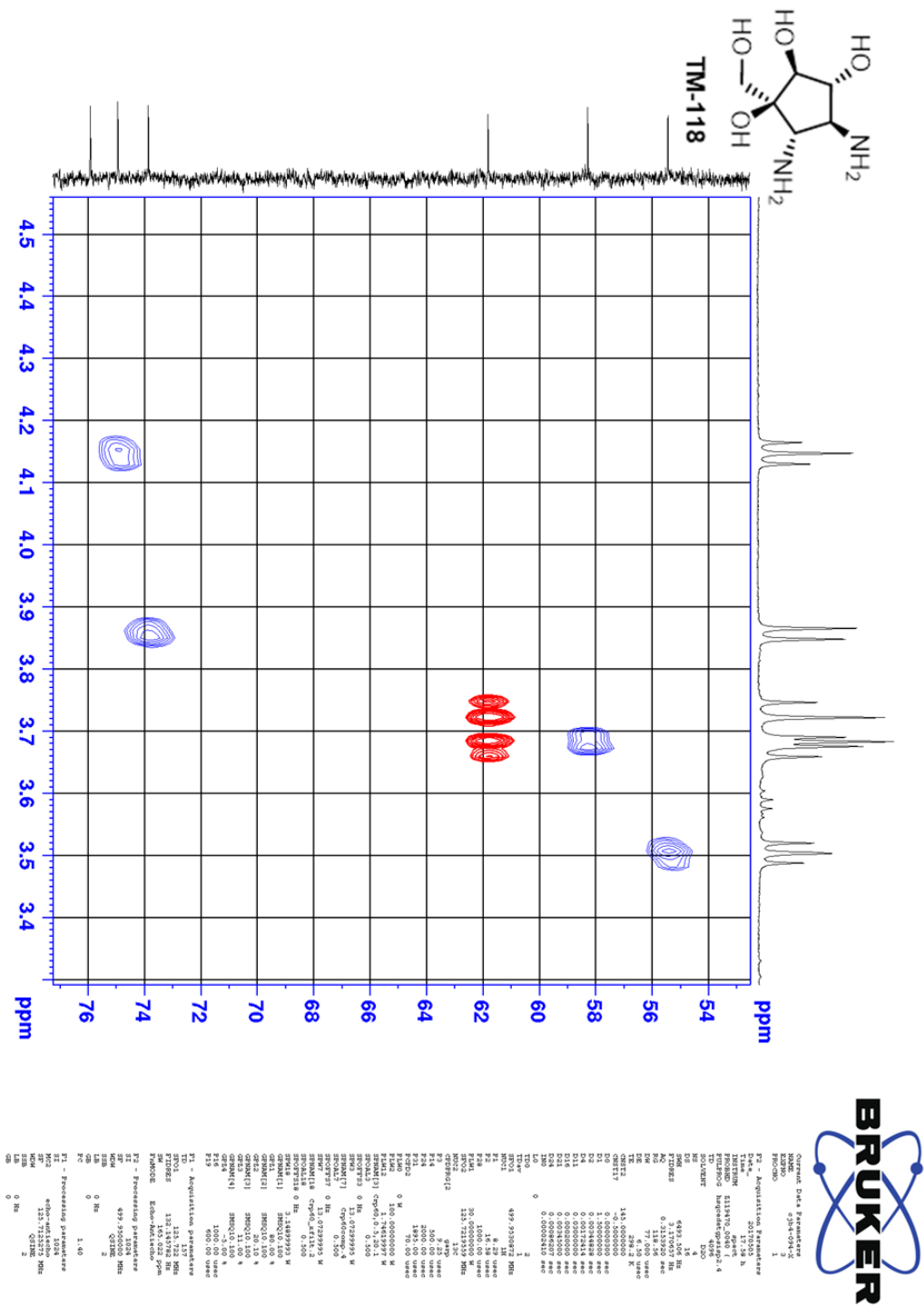
F2 - Acquisition Parameters
Date_ 20170505
Time 17.57 h
INSTRUM spect
PROBHD 2119470_0040 (zpg30)
PULPROG zgpg30
TD 65536
SOLVENT D2O
NS 753
DS 4
SWH 29761.904 Hz
FIDRES 0.908261 Hz
AQ 1.1010048 sec
RG 190.98
DW 16.800 usec
DE 6.50 usec
TE 298.2 K
D1 2.00000000 sec
D11 0.03000000 sec
TD0 1
SF01 125.7250967 MHz
NUC1 13C
P1 9.25 usec
PLW1 100.00000000 W
SF02 499.9519998 MHz
NUC2 1H
CPCPRG12 waitz16
PCPD2 80.00 usec
PLW2 30.00000000 W
PLW12 0.32214001 W
PLW13 0.16204000 W

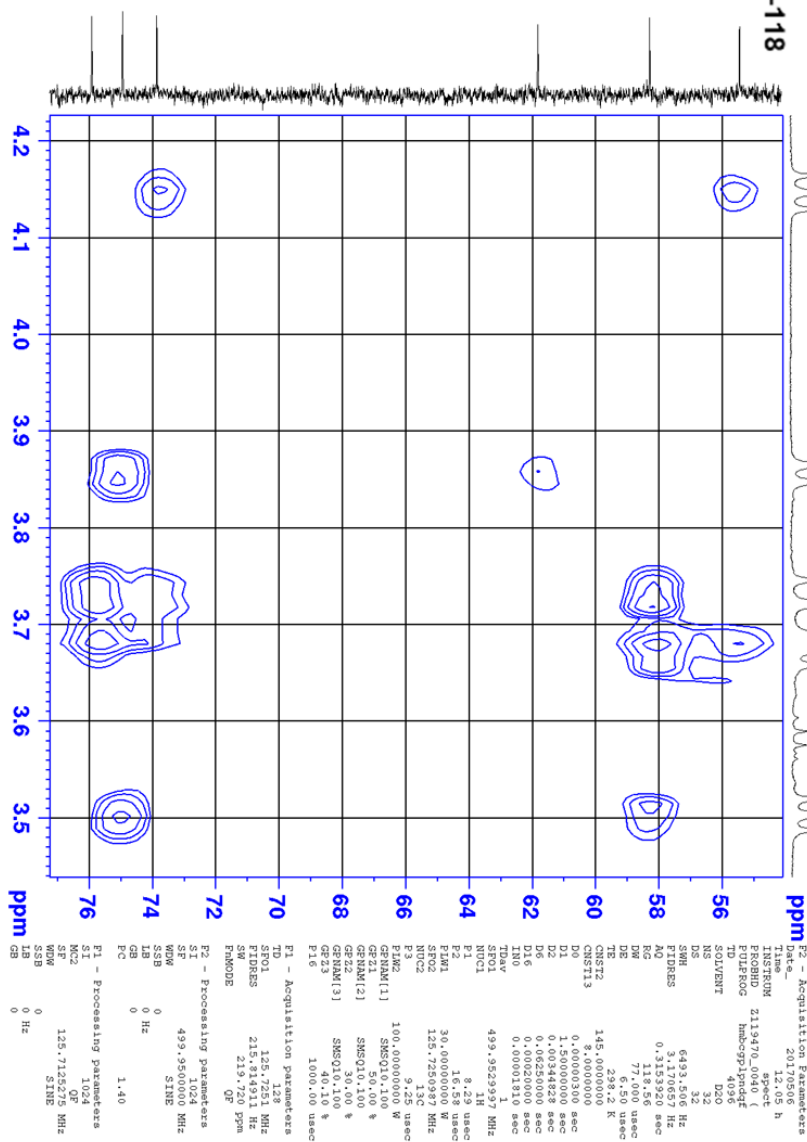
F2 - Processing parameters
SI 32768
SF 125.7125275 MHz
WDW EM
SSB 0
LB 1.00 Hz
GB 0
PC 1.40

Appendix Figure 6.140: COSY (D₂O) spectrum of TM-118



Appendix Figure 6.141: HSQC (D₂O) spectrum of TM-118



N[C@@H]1[C@H](O)[C@H](O)[C@@H](O)[C@H]1O

Appendix Figure 6.143: NOESY (D₂O) spectrum of TM-118

